Dissertation zur Erlangung des Doktorgrades
der Fakultät für Chemie und Pharmazie
der Ludwig-Maximilians-Universität München

Development and Characterization of Universal and Modular Bispecific Immune Cell Engagers for Cancer Immunotherapy

Marlena Katarzyna Surówka

aus
Gliwice, Polen

2024

Erklärung

Diese Dissertation wurde im Sinne von § 7 der Promotionsordnung vom 28. November 2011 von Herrn PD Dr. Christian Klein betreut.

Eidesstattliche Versicherung

Diese Dissertation wurde eigenständig und ohne unerlaubte Hilfe erarbeitet.

Zürich, 27.11.2024

_____

Marlena Katarzyna Surówka

Dissertation eingereicht am	4.12.2024
1. Gutachter:	PD Dr. Christian Klein
2. Gutachter:	Prof. Dr. Karl-Peter Hopfner
Mündliche Prüfung am	30.01.2025

Table of contents

1. Publications, conference presentations, patents and awards

1.1. List of publications

Literature Reviews (published, 2 first author manuscripts)

- **M. Surowka** and C. Klein. (2024) '*A pivotal decade for bispecific antibodies?*', mAbs, 16(1).

- **M. Surowka**, W. Schaefer, C. Klein. (2021) '*Ten years in the making: application of CrossMab technology for the development of therapeutic bispecific antibodies and antibody fusion proteins*', mAbs, 13(1).

Original Research Publications (in preparation, 3 first author manuscripts, 3 co-author manuscripts)

- **M. Surowka**, D. Darowski, I. Hutter-Karakoc, C. Claud, C. Ferrara-Koller, A. Freimoser-Grundschober, T. Hofer, A. Sobieniecki, D. Assisi, R. Gianotti, C. Spick, J. Sam, S. Leclair, M. Amann, E. Moessner, P. Umana, and C. Klein. *P329G-Engager: A Novel Universal Antibody-based Adaptor Platform For Cancer Immunotherapy*

- **M. Surowka,** D. Darowski, M. Spaeni, E. Moessner, and C. Klein. *Universal Protease-Activatable Cancer Immunotherapy Using Target-Agnostic Antibodies Engaging T cells or Innate Cells*

- **M. Surowka**, A. Ricci, M. Wichert, J. Benz, A. Ehler, T. Kober, J. Bonfilgio, D. Matscheko, R. Gianotti, R. Buser, A. Varol, J. Torres Barajas, M. Richards, V. Nicolini, P. Umana, D. Venetz, and C. Klein. *DOTAM-TCB: Universal Small Molecule-Guided Hapten- And T Cell Bispecific Antibodies For Cancer Immunotherapy*

- Z. Riester, **M. Surowka**, N. Seifert, D. Darowski, A. Ghosh, P.Spieler, J.Weber, R. Gianotti, T. Lother, T. Nerreter, E. Gerhard-Hartmann, M. Sauer, E. Moessner, H. Einsele, C. Ferrara Koller, C. Klein, M. Hudecek, and S. Danhof. *Multi-antigen redirection of anti-lymphoma CAR T cells via co-expression of an adapter CAR*

- I. Hutter-Karakoc, **M. Surowka**, D. Darowski, C. Claud, C. Ferrara-Koller, T. Hofer, A. Freimoser-Grundschober, E. Moessner, S. Leclair, P. Umana, C. Munz, M. Amann, and C. Klein. *Recruiting Innate Immune Cells Universally: Development Of A Novel Universal Innate Cell Engager For Cancer Immunotherapy*

- S. Stock, T. Strzalkowski, A. Gottschlich, L. Rohrbacher, L. Fertig, V. Menkhoff**,** **M. Surowka**, P. Bruenker, D. Darowski, S. Endres, M. von Bergwelt-Baildon, M. Subklewe, C. Klein, and S. Kobold. *Adaptor Anti-P329G CAR T Cells for Modular Targeting of AML*

1.2. List of conference posters and oral presentations

Posters, first author (5 conferences)

- **M. Surowka**, D. Darowski, I. Hutter-Karakoc, C. Claus, C. Ferrara-Koller, A. Freimoser-Grundschober, T. Hofer, A. Sobieniecki, D. Assisi, R. Gianotti, C. Spick, J. Sam, S. Leclair, M. Amann, E. Moessner, P. Umana, and C. Klein. *P329G-Engager: A Novel Universal Antibody-based Adaptor Platform For Cancer Immunotherapy*
  - American Association for Cancer Research Annual Meeting 2024
  - PEGS Boston 2023
  - Swiss Young Immunologists Society Symposium 2022
  - Festival of Biologics Basel 2022
  - European Network of Immunology Institutes Summer School 2021

Posters, co-author (5 conferences)

- I. Hutter-Karakoc, **M. Surowka**, D. Darowski, C. Claus, C. Ferrara-Koller, T. Hofer, A. Freimoser-Grunschober, E. Moessner, S. Leclair, P. Umana, C. Munz, M. Amann, and C. Klein. *Recruiting Innate Immune Cells Universally: Development of a Novel Universal Innate Cell Engager For Cancer Immunotherapy*
  - AACR: Tumor Immunology and Immunotherapy 2024

- C. Schmidt, G. Leclercq, B. Gaillard, **M. Surowka**, S. Herter, C. Klein, and M. Bacac*. Understanding And Mitigating The Cytokine Release Syndrome (CRS) Mediated By T Cell Bispecific Antibody (TCB) Treatment*
  - The Society for Immunotherapy of Cancer (SITC) Annual Meeting 2024.

- S. Stock, T. Strzalkowski, A. Gottschlich, L. Rohrbacher, L. Fertig, V. Menkhoff, **M. Surowka,** P. Bruenker, D. Darowski, S. Endres, M. von Bergwelt-Baildon, M. Subklewe, C. Klein, and S. Kobold. *Adaptor Anti-P329G CAR T Cells for Modular Targeting of AML*
  - The 65th ASH Annual Meeting 2023
  - 10th Immunotherapy of Cancer Conference 2023

- Z. Riester, **M. Surowka**, A. Schirbel, A.K. Buck, C. Klein, M. Hudecek, and S. Danhof. *Antibody adapter-based P329G CAR T cells enable modular targeting of hematologic tumors*
  - MSNZ Würzburg Symposium 2023

Oral Presentations (1 conference)

- **M. Surowka**. *'Biotechnology in service of patients – T cell bispecific antibody development for cancer immunotherapy'*.
  - Chemistry & Biotechnology International Conference 2021
  - Winner of The Best Oral Presentation Award

1.3. List of patents

- **Patent 5: Undisclosed title, filed in 2024**
  - *Topic: drug concepts in cancer immunotherapy*

- **Patent 4: Undisclosed title, filed in 2023**
  - *Topic: drug concepts in cancer immunotherapy*

- **Patent 3: Undisclosed title, filed in 2023**
  - *Topic: drug concepts in cancer immunotherapy*

- **Patent 2:** A. Bransi, A. Bujotzek, L. J. Hanisch, C. Klein, S. Klostermann, A.K. Kreymborg, C. A. Mueller, and **M. Surowka**. *WO/2024/100170 ANTIBODIES BINDING TO HLA-A*02/FOXP3.* Filed in 2022.

- **Patent 1:** M. Amann, A. Carpy, C. Claus, L. Codarri Deak, D. Darowski, T. Fauti, C. Ferrara-Koller, A. Freimoser-Grunsdschober, S. Herter, T. Hofer, C. Klein, L. Lauener, S. Leclair, E. Moessner, C. Neumann, P. Umana, A. Bransi, and **M. Surowka**. *WO/2021/255138 IMMUNE ACTIVATING FC DOMAIN BINDING MOLECULES*. Filed in 2021

1.4. List of awards

- **Finalist of the Rising Researchers Scientific Innovation Award, 2024**
  - Issued by: Promega Switzerland
  - Finalist in the category of PhD Students in Switzerland for the work titled: P329G-Engager: *A Novel Universal Antibody-based Adaptor Platform For Cancer Immunotherapy*

- **Winner of the Antibody Society's Research Competition, 2024**
  - Issued by: The Antibody Society
  - Winner in the category of PhD Students for the work (poster) titled: P329G-Engager: *A Novel Universal Antibody-based Adaptor Platform For Cancer Immunotherapy*

- **Roche Inventor's Recognition Medal, 2024**
  - Issued by: Roche. Award for two inventions patented in 2023

- **Roche Inventor's Recognition Medal, 2023**
  - Issued by: Roche. Award for an invention patented in 2022

- **Award for the Best Oral Presentation, 2021**
  - Issued by: Chemistry and Biotechnology International Conference (ChemBiotIC)
  - Award for the presentation titled: *Biotechnology in service of patients – T cell bispecific antibody development for cancer immunotherapy*

2. Acronyms

Abs	antibodies
ACT	adoptive cell transfer
ADAs	anti-drug antibodies
ADCC	antibody-dependent cell-mediated cytotoxicity
ADCP	antibody-dependent cellular phagocytosis
ADCs	antibody-drug conjugates
AMSG	avidity-mediated selectivity gain
APCs	antigen-presenting cells
ARMs	antibody-recruiting molecules
AZA / AAZ	Acetazolamide
B-BiTE	bridging BiTE
BCP-ALL	B-cell precursor acute lymphoblastic leukemia
BiTE	bispecific T cell engager
bsAbs	bispecific antibodies
CAIX	carbonic anhydrase IX
CAR	chimeric antigen receptor
CD19	cluster of differentiation 19
CD20	cluster of differentiation 20
CD8a	cluster of differentiation 8a
CDC	complement-dependent cytotoxicity
CDRs	complementarity determining regions
CEACAM5	carcinoembryonic antigen-related cell adhesion molecule 5
CLL	chronic lymphocytic leukemia
CRC	colorectal cancer
CRS	cytokine release syndrome
CTLA-4	cytotoxic T-lymphocyte protein 4
DCs	dendritic cells
DLBCL	diffuse large B-cell lymphoma
DNP	2,4-dinitrophenyl group
DUPA	2-[3-(1, 3-dicarboxy propyl)-ureido] pentanedioic acid
EpCAM	epithelial cell adhesion molecule
ESI	electrospray ionization
E:T	effector-to-target cell ratio
FcRn	neonatal Fc receptor
FDA	U.S. Food and Drug Administration
FITC	fluorescein isothiocyanate
FOLR1	folate receptor alpha
GPCRs	G-protein coupled receptors
HER2	human epidermal growth factor receptor 2
HSA	human serum albumin
huIgG1	human immunoglobulin G 1
ICB	immune checkpoint blockade
ICE	innate cell engager

ICI	immune checkpoint inhibitor/inhibition
Ig	Immunoglobulin
IL2	interleukin 2
KiH	knobs-into-holes
LALA	L234A L235A mutations
LBCL	large B-cell lymphoma
mAbs	monoclonal antibodies
MAC	membrane attack complex
mCRPC	metastatic castration-resistant prostate cancer
MM	multiple myeloma
MSLN	Mesothelin
MW	molecular weight
NHL	non-Hodgkin lymphoma
NK	natural killer
NKCE	NK cell engagers
NLR	NucLightRed
OTOT	on-target off-tumor
pARMs	polymeric ARMs
PD1	programmed cell death protein 1
PD-L1	programmed cell death 1 ligand 1
PET	positron emission tomography
PRIT	pretargeted radioimmunotherapy
pro-TCB / prot-TCB	protease-activated T cell bispecific antibody
PSMA	prostate-specific membrane antigen
R/R	relapsed/refractory
SEC-MS	size-exclusion chromatography-mass spectrometry
scFv	single chain Fv
SMDCs	small molecule-drug conjugates
SPR	surface plasmon resonance
STEAP1	six-transmembrane epithelial antigen of prostate member 1
TAA	tumor associated antigen
TAMs	tumor-associated macrophages
TCB	T cell bispecific antibody
TCE	T cell engager
TCR	T cell receptor
TIL	tumor infiltrating lymphocytes
TME	tumor microenvironment
TSA	tumor specific antigen
WT	wild-type

3. Thesis summary

Bispecific immune cell engaging antibodies are highly promising agents for cancer immunotherapy. However, one major obstacle to achieving efficacy across patient populations remains inter- and intra-patient tumor heterogeneity. This heterogeneity has been observed in terms of both tumor antigen profiles and immune cell compartments and immune fitness. As such, one-size-fits-all drug approaches, targeting specific antigens and specific immune cells within an indication, are bound to show limited therapeutic effects across patients. A proposed solution gaining interest in the scientific community is treatment personalization. While displaying high potential, personalization of drugs to each patient has been proven to substantially increase therapy costs, and pose risks of delayed treatment due to production timelines. An attractive approach, albeit not fully explored in previous studies, would be a combination of personalization potential with off-the-shelf drug availability. In this thesis, three universal and modular therapeutic antibody platforms are presented, aiming to address these issues.

Firstly, a novel universal P329G-Engager antibody platform is developed. The modular platform is based on two libraries enabling mix-and-match drug assembly. The first is a library of tumor antigen-binding adaptor IgG antibodies, each of which bears P329G mutations in its Fc portion. Upon identifying a tumor target of choice, the specific adaptor is selected. The second library consists of bispecific immune engaging antibodies, recognizing both the P329G mutation and an immune receptor of choice, resulting in P329G-T cell bispecifics (P329G-TCB), ADCC-competent P329G innate cell engagers (P329G-ICE), P329G costimulatory molecules (P329G-CD28/4-1BBL) or P329G immunocytokines (P329G-IL2v). A selection of a desired antigen-targeting adaptor, and a desired immune engager, enables assembly into a functional immunotherapeutic drug with a mode of action of choice. The antigen binders, the P329G mutation, the P329G binder and immune receptor binders are all based on clinically-tested and validated immunotherapeutics. *In vitro* assays presented here show all P329G-Engager modalities induce anti-tumoral and/or immunomodulatory cell activity. Anti-tumoral efficacy of secondary antibodies is observed only in the presence of tumor-targeted P329G adaptors both *in vitro* and *in vivo*, while no effect is observed in their absence. Altogether, experimental evidence is provided for the double universal character of the P329G-Engager antibody platform, whereby tumor binding components and immune engaging components enable assembly of functional drugs from modules of choice.

Secondly, in order to tackle on-target off-tumor toxicity linked to classical TCBs, a protease-activated pro-P329G-TCB is developed. To ensure drug activation only in the tumor microenvironment, a tumor-activated switch component is engineered and added to the P329G-TCB structure – a tumor-associated protease-cleavable binder mask. Upon encountering the protease-rich tumor microenvironment, the mask can be released, resulting in activation of the drug. To retain P329G-binder universality a P329G-mutated CH2 fragments engineered as a mask. While the inactivating mask has the same structure as the epitope on the P329G-mutated adaptors, protease-dependent release of the mask enables adaptor-engager assembly and functional T cell engagement against tumor cells. Pro-P329G-TCB is

shown to release the mask upon cleavage by matriptase only when a specific cleavage site is utilized. Moreover, due to being based on the P329G-Engager, pro-P329G-TCB is able to assemble with different tumor-binding P329G-mutated IgG adaptors and exert protease-dependent antitumoral efficacy *in vitro* on different cancer cells. Therefore, pro-P329G-TCB enables next-generation tumor activation of a target-agnostic P329G-directed TCB. Additionally, due to the potential of the P329G-masking being transferrable to other P329G-Engagers such as P329G-ICE, a triple universality is enabled – in terms of protease masking, antigen choice, and immune engager choice.

Thirdly, to capitalize on differences in pharmacological properties of small molecules and antibodies, as well as high affinity hapten binding, an adaptor-based universal DOTAM-TCB platform is developed. The tumor-binding adaptor library consists of a set of small molecules. Their structure is derived from published small molecule ligands to surface tumor targets, and designed to be covalently linked to the Ca^{2+}-loaded chelator DOTAM serving as a hapten. This results in new design of molecules such as Ca-DOTAM-DUPA and Ca-DOTAM-AAZ for targeting PSMA and CAIX expressing tumors, respectively. The immune engager of choice is a bispecific antibody with a hapten binder recognizing Ca-DOTAM and a binder to CD3ε. X-Ray crystallography reveals a deep binding pocket between VH and VL domains of the anti-DOTAM antibody binder. The Ca-DOTAM interaction with the DOTAM antibody binder reaches double-digit femtomolar affinity, enabling stable assembly of the adaptor with the adaptor-specific DOTAM-TCB. This high affinity characteristic was utilized for the development of a novel protocol of non-covalent small molecule-antibody complex formation. Native mass spectrometry method is utilized and optimized to enable verification of the complexing protocol. In functional *in vitro* assays, DOTAM-TCB combined with the haptenated small molecule adaptors is shown to exert antitumoral efficacy on two tumor-associated targets, in both complexed and separate formulations. Administration of adaptors only or DOTAM-TCB only does not lead to tumor killing, highlighting the adaptor-TCB assembly as a requirement for functionality. *In vitro* and *ex vivo* assessments show a lack of nonspecific binding. While Ca-DOTAM-AAZ is based on published *in vivo*-tested AAZ ligands, here, Ca-DOTAM-AAZ with DOTAM-TCB leads to rapid-onset toxicity in a HT-29 (CAIX+)-bearing humanized CD47-BRGS mouse model. With no toxicity observed for Ca-DOTAM-AAZ only, DOTAM-TCB only, and low toxicity observed in the CAIX-TCB group, the hypothesis is raised that both CAIX expression and Ca-DOTAM-AAZ off-tumor activity may contribute to the observed toxicity. Further directions are proposed for the development of small molecule-based adaptors for use in cancer immunotherapy, and specifically, T cell engagement. Despite the aforementioned *in vivo* results, all in all, *in vitro* proof of concept for haptenated small molecule adaptors and universal DOTAM-TCB is achieved, providing in depth biochemical characterization and preliminary data on functionality. Moreover, the Ca-DOTAM high affinity interaction with DOTAM opens avenues to repurposing this interaction for other immunotherapy modalities beyond TCBs.

In summary, this thesis describes three universal, target-agnostic, and modular platforms for use with bispecific immune engagers in cancer immunotherapy. All platforms exploit different avenues of antibody engineering, such as precise paratope use against a P329G Fc mutation, conditional activation of prodrugs in the tumor microenvironment, and high affinity hapten

binding with stable non-covalent complex formation. Importantly, all three platforms described here enable current or future implementation of double universality in terms of targeting an antigen of choice and engaging an immune cell or pathway of choice. Additionally, the platforms utilize antibody structures and binders based on clinical molecules for the majority of their components. As such, the developments presented in this thesis may ultimately be utilized for mix-and-match cancer immunotherapeutics, targeting heterogeneous tumors with off-the-shelf drugs.

4. Thesis introduction

4.1. Cancer burden and cancer immunotherapy

Cancer remains one of the leading causes of death worldwide [1]. Several types of treatments exist as standard of care, such as surgery, chemotherapy, and radiotherapy [2], [3], [4], [5], [6]. Despite the existence of these options, and constant developments of new therapeutic approaches, survival rates in many cancer indications remain low [7]. Aside from potential low efficacy, limitations of these treatments include, for instance, severe side effects, systemic toxicity and lack of specific tumor targeting [8]. However, recent decades have brought new successful modalities into the therapeutic landscape, such as targeted therapies, or targeted radiotherapy [9], [10]. Another successful invention in oncology in the past years was the development of immune checkpoint blockade, which functions by utilizing antibodies (Abs) that block PD-1-PD-L1 or CTLA-4-CD80/CD86 interactions in the tumor microenvironment responsible for inhibiting antitumoral immune responses [11]. This therapeutic approach has significantly increased survival rates in many cancers [12], [13], [14], [15] and has led to the Nobel Prize in Physiology and Medicine granted to James P. Allison and Tasuku Honjo for its development in 2018 [16]. The success of checkpoint inhibition provided evidence for the potential of the immune system to attack cancer cells. Therefore, the recent decade has seen an increasing interest in dissecting tumor immunology and the development of therapies engaging the patient's own immune system against the tumor [17], [18]. However, heterogeneity of tumors within and between patients has been a major obstacle to effective off-the-shelf treatments, including cancer immunotherapy.

Development of tumors inside the body and the interactions of various tumor types with the immune system has been a subject of multiple investigations. In 2013, Mellman and Chen presented the model of the cancer immunity cycle as a description of the multi-step process of developing and failing antitumoral immunity [19]. This review became an important framework to understand tumor immunity by the scientist community, and was later updated in 2023 to include further discoveries [20]. The cancer immunity cycle, as understood currently, involves a release of neoantigens, their uptake by antigen presenting cells (APCs) such as dendritic cells (DCs) for antigen presentation, T cell priming by the APCs, costimulatory signaling, T cell killing of tumor cells, cytokine and chemokine signaling and more [19]. Besides adaptive immune system, innate cells such as natural killer (NK) cells are also involved in antitumoral immunity [21]. In tandem with antitumoral immunity, protumoral activity of tolerance-inducing cells and metabolic factors are also present [19]. In essence, tumor control by the immune system is based on a complex network of intra- and intercellular interactions, and surveillance malfunction in any of the involved steps is set to lead to uncontrolled tumor growth. The failure of the immune system to reject the tumors can often be multifactorial and dynamic over time, as well as vary between cancer indications and between patients [19], [20].

Due to the continuously expanding knowledge of tumor immunology and tumor microenvironment (TME) heterogeneity, the field of cancer immunotherapy has seen

developments of a plethora of different treatment strategies aiming to tackle different facets of the tumor-immune system interactions. These strategies include, but are not limited to recombinant cytokines [22], novel immune checkpoint inhibitors [23], innate cell engagers [24], T cell engagers [25], costimulators [26] or chimeric antigen receptor (CAR) T cells (CAR-T cells) or CAR-NK cells [27]. The diversity of these modalities offers engagement of different immune cells and antitumoral mechanisms, an important considering the complexity and heterogeneity of protumoral pathways contributing to cancer development.

4.2. Molecular design of T cell bispecific antibodies (TCBs) in cancer immunotherapy

To enable targeting various tumor-intrinsic mechanisms, the field of cancer immunotherapy has been focusing on the development of a wide range of therapeutic modalities, in order to exploit their different properties. To this day, immunooncology treatments span drug forms such as small molecules (SM) [28], [29], [30], (bispecific) antibodies [31], [32], [33], [34], antibody-directed pretargeted radioimmunotherapy [35], [36], cancer vaccines [37], or adoptive cell transfer [38]. While each format offers its own advantages and disadvantages, antibody-based drugs and genetically engineered CAR-T cells are highly potent and constitute a substantial portion of tested agents in clinical trials in the cancer immunotherapy field [39], [40].

Monoclonal antibodies (mAbs), and especially a subcategory of bispecific antibodies (bsAbs), have proven their immense versatility and potency in cancer treatment [34]. While potency may vary across targets and indications, antibodies can be favorably differentiated from CAR-T cells, with advantages such as off-the shelf availability for the patients, controllable batch quality, costs and flexibility in engineering influencing e.g. the molecule's activity and half-life in circulation [41].

The specifics of the mode of action of therapeutic modalities in cancer immunotherapy and beyond can be linked to their structural design and the resulting molecular interactions within the human body. Similarly, their advantages and limitations may be addressed by introducing structural modifications. In order to allow in-depth understanding of the structure-driven technologies used in the field of drug discovery and in this thesis, here, the design features of the common therapeutics are introduced.

Evolution of T cell Bispecific Antibodies in Cancer Treatment

One of the challenges for the established immune checkpoint inhibition strategy is its dependency of the presence of tumor antigen-specific T cells in the tumor [42]. A revolutionary approach, based on the cytotoxicity-inducing engagement of T cells against cells regardless of their specificity, began with a 1985 study by Staerz, Kanagawa and Bevan. The researchers presented a hybrid antibody specific to both Thy-1.1 antigen and a portion of a

murine T cell receptor, which induced T cell cytotoxicity against Thy-1.1+ cells, without restriction to TCR specificity [43], thus believed to become the first T cell engager (TCE) in non-clinical use. This development was followed by many similar ones in the following decades [34], [44]. The category of TCEs [45] are currently also known as BiTEs [46], or TCBs [47], [48], [49], depending on their format and developing entity [50].

The mode of action of the first and the following TCBs have basis on its structure. Namely, simultaneous binding of a singular antibody to both the tumor target of interest and the TCR or CD3ε [45], results in crosslinking of CD3ε in the T cell receptor complex, and induction of TCR downstream signaling activating T cell cytotoxicity in the physical direction of the target-expressing cell [45], [51], [52]. Due to the TCR or CD3ε crosslinking being responsible for the cellular signaling, as opposed to TCR and peptide-loaded MHC interaction, T cell's antigen specificity is not required for T cell killing [45].

After the first TCB discoveries, research in the 1990s led to the development of the oncology-focused CD3- and CD19-bispecific antibodies for the T cell-mediated lysis of CD19+ leukemic cells [53], [54] and CD3- and EpCAM-bispecific antibody-based molecules for the lysis of EpCAM+ solid tumor cells [55], [56]. The CD3 x EpCAM antibody concept was developed into the first clinical T cell bispecific catumaxomab, approved in 2009 for use in patients with malignant ascites [57]. It was later withdrawn from the market [58], but continues being evaluated in oncology [58], [59].

In 2000, a notable CD19 x CD3 bispecific single-chain-based antibody was published [60], which later ultimately changed the landscape of clinical cancer immunotherapy. The drug, termed blinatumomab was the second clinical T cell engager, referred to as BiTE [46], and displayed high efficacy in leukemia trials [46]. This led to its FDA approval for treatment of Philadelphia chromosome-negative relapsed/refractory B-cell precursor acute lymphoblastic leukemia (BCP-ALL) in 2014 [61]. The success of this T cell engager was succeeded by 8 further regulatory approvals of this modality in the following decade [34], [62].

With these developments, and their high antitumoral efficacy, T cell engagers have become one of the major classes of cancer immunotherapeutics. Importantly, they overcome the aforementioned reliance of checkpoint inhibitors on preexisting infiltration of tumor antigen-specific T cells.

Glofitamab is an example of a human IgG1-based CD20 x CD3ε T cell bispecific antibody (CD20-TCB) originally developed at the Roche Innovation Center Zurich, approved by the U.S. Food and Drug Administration (FDA) for 3rd line relapsed/refractory diffuse large B-cell lymphoma (DLBCL) in 2023 [63]. Some of the most common features of antibody engineering can be seen in the structure of this drug. As such, its features serve as an appropriate example of antibody design and engineering, the principles of which are used in the work discussed in the subsequent sections of this thesis.

The structure of CD20-TCB alongside an endogenous human IgG1 is presented in **Figure 4.2.1** and described in more detail in the paragraphs below, as well as in [64].

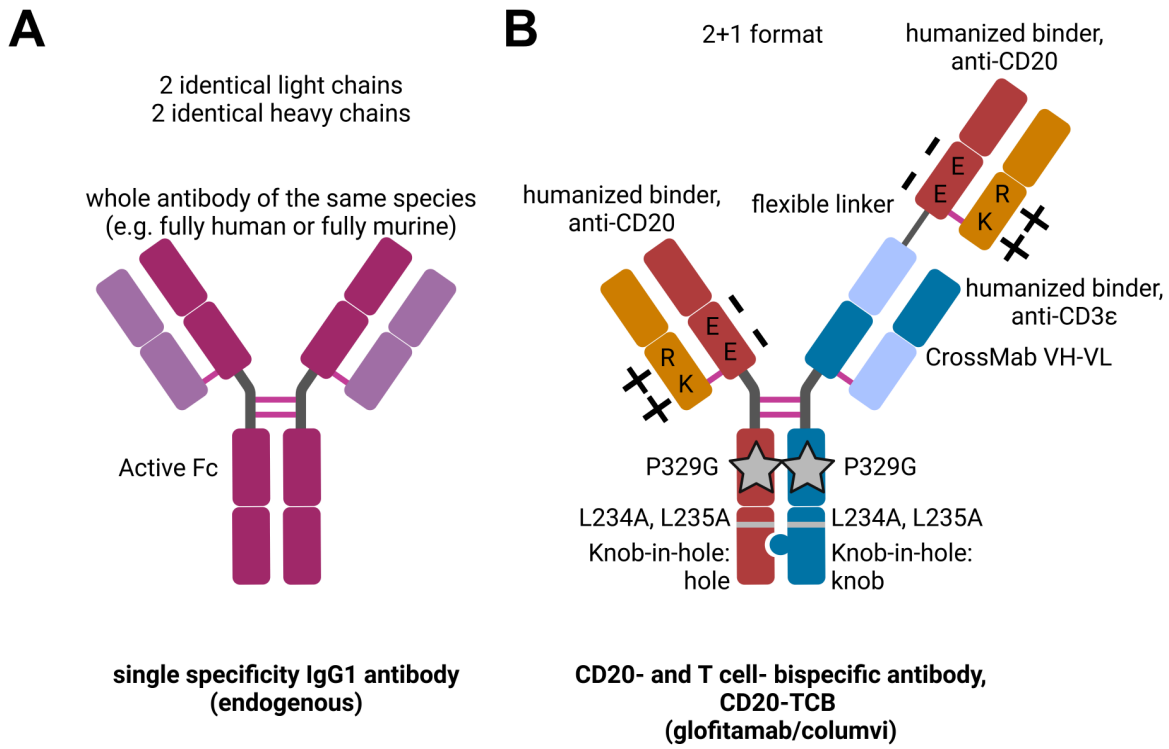

Figure 4.2.1. Structures of selected endogenous and engineered IgG antibodies. A) Structure of endogenous human IgG1. B) Structure and utilized antibody engineering technologies in the clinical cancer immunotherapeutic antibody, glofitamab (CD20-TCB).

Antibody Class

One of the first considerations during antibody drug discovery is the selection of the desired drug format. For antibody-based therapeutics, natural human or animal-derived antibodies serve as a template, modified to achieve the desired characteristics [50]. Human endogenous antibodies can be divided into immunoglobulin (Ig) classes: IgA, IgE, IgD, IgM and IgG [65]. IgG is the main neutralizing antibody of secondary responses [65], and thus an overwhelming majority of therapeutic Abs are based on the IgG format [34], [66], [67]. Within the IgG class, 4 subclasses exist: IgG1, IgG2, IgG3 and IgG4 [68]. Their differing properties include structure, mass, half-life, stability, affinity to activating and inhibitory FcγRs, and potential for complement activation [68]. IgG1 subclass displays high stability and strong effector functions, whereas IgG4 possesses lower stability and minimal effector functions [68]. Therefore, IgG4 has been used previously for antibodies where Fc-functions are not desired as the main mode of action, such as anti-PD1 IgG4 pembrolizumab [69]. On the other hand, IgG1 isotypes continue to be used in Fc-competent antibodies, such as anti-CTLA4 IgG1 ipilimumab or anti-CD20 IgG1 obinutuzumab [68], where antibody-dependent cell-mediated cytotoxicity (ADCC), antibody-dependent cellular phagocytosis (ADCP) and complement-dependent cytotoxicity (CDC), mediated by the Fc part, are desired. Notably, due to its generally favorable characteristics, flexibility in engineering, as well as availability of in-depth biochemical and clinical data in the field, the IgG1 format remains the most common subclass used also in antibodies not reliant on Fc function, by introduction of Fc silencing mutations [34]. In line with this, glofitamab has also been based on human IgG1 (huIgG1) [70].

Antibody Format and Binding Properties

One of the crucial concepts in antibody design is avidity towards the antigen, which can be defined as synergistic binding of a bivalent monospecific molecule to its target, leading to increased apparent affinity compared to monovalent binding [71]. Strong binding to the tumor target is usually a desirable characteristic, since it often correlates with increased efficacy of T cell engagers [72]. On the other hand, lowering affinity may offer avidity-mediated selectivity gain (AMSG) while using bivalent molecules, meaning selective binding to high target expressing cells over cells with low target expression [73], [74], [75]. To introduce avidity-based effects to bispecific antibodies, the 2+1 format can be used, i.e. consisting of 2 binders to the tumor target, and 1 binder to CD3ε (part of the T cell receptor complex), such as is the case in CD20-TCB. The peptide linker between the second Fab domains of the CD20 binder and the CD3ε retains flexibility, allowing both domains to bind to their respective targets simultaneously [73].

Antibody Species and Humanization

Another important aspect are the amino acid sequences of binders themselves. In the past, antibody binders were derived largely from *in vivo* immunizations of animals, such as rabbits or mice, with the target antigen, leading to non-human sequences of the binders. Alternatively, today, many antibodies are derived from *in vitro* libraries *via* phage, yeast, eukaryotic or ribosome display [76]. In case of antibodies derived from non-human species, the use of original binders as drugs in patients can lead to the patient's immune system recognizing the non-self protein structures, and production of undesirable anti-drug antibodies (ADAs), which limit the efficacy and safety of the drug [77], [78], [79]. Therefore, non-human binders in development undergo a so-called humanization process. This process involves grafting the complementarity-determining regions (CDRs) - protein fragments within the antibody responsible for binding of the target – of the original non-human antibody, onto the framework regions – the non-binding regions - of an unrelated human immunoglobulin, such as human IgG1 [79]. In CD20-TCB, both tumor and CD3ε binders are humanized [64].

Antibody Chain Assembly

Endogenously produced IgG1 antibodies consist of 4 chains: two identical heavy chains, and two identical light chains [80] (**Figure 4.2.1A**). Within the antibody-producing cell, be it endogenous plasma cell or an engineered cell of another origin, assembly of constant domains of heavy and light chains is required for proper antibody folding into its quaternary structure, and therefore, antibody secretion [81], [82]. In nature, since each separate clone of an endogenous IgG is produced by a single dedicated plasma cell, only one combination of heavy-light chain pairing exists, and secretion of properly paired chains occurs [83]. However, in a complex 2+1 format like the one of glofitamab, 4 distinct chains exist: two different heavy chains (short and long arm), and two different light chains (**Figure 4.2.1B**). Clinical production of glofitamab-like antibodies involves establishing a CHO producer cell line, by which all chains are produced simultaneously, and are expected to assemble in the correct manner forming a therapeutic antibody [84]. It has been observed that uncontrolled expression of multiple antibody chains leads to multiple incorrectly assembled products, with low yield of the final product [85]. To ensure correct self-assembly of the therapeutic antibody, three technologies are employed in glofitamab-like antibodies. The correct association of two heavy chains is ensured by the steric interactions *via* the knobs-into-holes (KiH) technology [86]. Heavy and light chain assembly in a 2+1 TCB requires two distinct approaches, due to the presence of two distinct binder types (anti-CD20 and anti-CD3ε). One strategy is the introduction of oppositely charged amino acids (charge pair, EE and RK) in heavy and light chains of the binder [87]. Another is the use of CrossMab technology, developed by Schaefer, Klein and colleagues, entailing heavy-light domain crossover of the variable or constant domains or entire Fabs [88], [89], [90]. In 2+1 TCBs, the aforementioned modifications are implemented to ensure high yield of properly assembled glofitamab [90] and others.

Antibody Half-Life *in Vivo*

A crucial feature influencing therapeutic IgG activity is its long serum half-life of up to 21 days in humans [91].This is opposed to several hours for Fc-free single chain Fv (scFv)-based molecules such as bispecific T cell engagers (BiTEs) [92] and 5 min – 6h for small molecules [93]. The long half-life of IgG1-based Abs is due mainly due to FcRn-dependent antibody recycling, although minimized clearance by kidneys due to the large size of IgGs also plays a role [94], [95]. The IgG recycling is a process whereby antibodies endocytosed by cells bind to the neonatal Fc receptor (FcRn) via their Fc portion, which triggers a shift towards a recycling endosome pathway, culminating in a release of the antibody back to the extracellular space [96], [97]. In absence of Fc – FcRn binding, the internalized protein is marked for degradation in the lysosome [97]. Hence, antibody-based therapeutics which lack Fc, such as blinatumomab, display shorter serum half-life (1.25 ± 0.63h) [98] than their Fc-containing counterparts (2-11 days) [99], [100]. Aside from the Fc, FcRn binds human serum albumin (HSA), resulting in the same recycling pathway [101]. Long serum persistence of therapeutic antibodies has been linked to not only lower number or duration of administrations per treatment, providing logistical benefits to patients and hospitals [99], [102], but also to higher efficacy [46], [103]. Therefore, while certain approved drugs, such as glofitamab, contained an Fc from its conception [64], other molecules underwent half-life optimization during their next generation development more recently. Both Fc [99], [100], [104] and HSA/HSA binding tags [105], [106], [107] are being used as half-life extending moieties, including the new generation of BiTEs [108].

Abrogation of Fc Function: P329G LALA

The Fc portion of an IgG1 mediates not only antibody recycling, but is the inducer of effector functions in endogenous antibodies. ADCC, ADCP and CDC functions are all induced by an IgG1 via the Fc binding to: FcγRIIIa on NK cells, FcRIIa on macrophages or C1q of the complement system, respectively [109]. While a necessary function for classical antibodies of the IgG1 isotype and innate cell engagers [110], Fc effector functions are not always desirable [68]. T cell bispecific antibodies, specifically, exert their function by binding both tumor cells and T cells via their Fab fragments [25]. Presence of an active Fc, therefore, could lead to ADCC, ADCP and CDC directed against both tumor cells and T cells, the latter being an unwanted effect. Therefore, certain T cell engagers such as blinatumomab were designed without an Fc [111]. However, as mentioned above, Fc bears a crucial function in the pharmacokinetics of antibodies, and designing an antibody without it, such as was the case in the first generation BiTEs, is not always a viable option. Due to this challenge, strategies of silencing Fc effector functions while retaining FcRn binding have been explored [112]. Initially, the IgG4 format was used for this purpose, due to its weak Fc effector functions, seen for instance in pembrolizumab [69], [113]. However, the IgG4 subclass does not offer full abrogation of Fc functions, and has been observed to induce target cell depletion [114]. Due to this and in parallel to IgG4 developments, in 1990s, Fc-FcγR interaction interface was investigated, leading to identification of amino acids crucial for binding, and resulting in identification of L234A L235A (LALA) double mutation inhibiting Fc function [115], [116]. LALA-

Fc has been later shown, however, to offer only partial abrogation of Fc binding to FcγRs [117]. Consequently, further analysis of Fc-FcγR interface by Sondermann *et al.*resulted in identification of the proline at the position 329 (P329) as a residue involved in IgG1 Fc binding to FcγRIII [118]. Taking this into account, Schlothauer *et al*. devised a P329G Fc-silencing mutation, with substitution of proline to glycine at the 329 position. Combination of P329G and LALA mutations led to full abrogation of Fc effector functions in a human IgG1 [117]. Consequently, P329G LALA-mutated Fc was introduced to the design of the novel 2+1 CD20-TCB, currently known as the clinical molecule glofitamab [64], enabling its design to contain half-life extending Fc.

4.3. Selected types of cancer immunotherapeutics: beyond TCBs

As described before, developments in cancer immunotherapy include molecules targeting various cells, receptors and pathways. The overview of selected major modalities that have contributed to the field, aside from classical TCBs, are described below.

Innate Cell Engagers (ICE)

Alongside T cells, NK cells have a well-established potential for cytotoxicity against cancer [119]. Therapeutically, mimicking endogenous mechanisms, they can be activated with the use of tumor antigen-binding antibodies containing a functional Fc or FcγRIIIa (CD16)-binding domain [119]. These bind to the FcγRIIIa on the surface of NK cells, and trigger antigen-directed release of cytotoxic granules, an aforementioned process termed ADCC. Additionally, both endogenous and therapeutic Fc-competent antibodies are capable of binding to FcγRIIa (CD32a) on macrophages, inducing ADCP, engulfing and eliminating target cells [119]. A third mechanism driven by Fc function in antibodies is CDC, whereby antibodies opsonizing the target cells recruit C1q, triggering the formation of the membrane attack complex (MAC), resulting in target cell death [119]. Due to the multifaceted mode of action of Fc-competent antibodies involving NK cells and macrophages, they are often termed simply mAbs, or more specifically, NK cell engagers (NKCE) [120], [121] or innate cell engagers (ICE) [122], [123]. As early as 1997, a CD20-targeted ICE rituximab has been approved for treatment of non-Hodgkin lymphoma (NHL) [124], [125], and is now included in standard of care alongside chemotherapy [126]. The approval was followed by other developments, including another CD20-ICE obinutuzumab [127], and HER2-targeted trastuzumab [128] and pertuzumab [129]. Additionally, in 2013, Simpson *et al.* showed in mice that the efficacy of the anti-CTLA4 checkpoint blockade is also reliant on the Fc-mediated functions, resulting in Treg depletion [130], which was later confirmed by other groups [131], [132], [133]. The advantages of ICE therapies, besides efficacy, is for example a low risk of cytokine release syndrome initiated by the treatment [134], [135]. An obstacle may be low activity and infiltration of NK cells in solid

tumors [136], [137]. However, multiple ICE approaches, including improved therapeutic strategies, are being currently developed [138].

Interleukin 2 and PD1-IL2v

One of the first described cancer immunotherapies was scientifically based on then newly discovered biology of a T cell growth factor, known as interleukin 2, and its role in boosting the expansion of T cells [139], [140]. Therapeutic IL-2 was developed in a form of a recombinant protein aldesleukin, and was approved by the FDA for high-dose use in metastatic renal cell carcinoma and melanoma in 1992 and 1998, respectively [141], [142]. Since then, hundreds of clinical trials have been initiated to test various IL2-based therapies for cancer patients (ClinicalTrials.gov). Despite continuous interest of scientific community in the activity of IL-2, several challenges hinder its use in the original format – mainly its preferential activation of immunosuppressive regulatory T cells (Tregs) [143] and systemic delivery leading to toxicities such as vascular leak syndrome [144], [145]. Due to this, multiple developments are being pursued to mitigate these obstacles [146], some of them mentioned below.

IL2 receptor consists of three subunits: IL2Rα with high affinity to IL2, and IL2Rβ and IL2Rγ, forming a heterodimer, with intermediate affinity [147], [148], [149]. IL2Rα is constitutively expressed on Tregs and only transiently on other T cells upon activation, but is dispensable for IL2R signaling [147]. Due to the expression and affinity characteristics of IL2Rα, wild-type IL2 therapy generally leads to sequestration of IL2 by Treg cells, as well as their activation, inhibiting IL2 activation of antitumoral T cells [150], [151], [152]. To combat the preferential IL2 delivery to regulatory T cells, in 2013, Klein and others devised a mutated version of this cytokine, termed IL2v, with abrogated binding to IL2Rα, and fused it to an antibody against tumor associated antigen (CEA) [153], [154]. Indeed, IL2v was shown to not activate Tregs preferentially over other T cells [155]. This approach resulted in both improvement of IL2 delivery to non-regulatory T cells, and accumulation of the molecule in the tumor site [155]. However, since IL2 and muteins can initiate signaling without antibody-led crosslinking, IL2R activation was also observed outside the tumor, and delivered to non-tumor-specific cells [156].

To further improve IL2-based treatments and increase the drug delivery to the tumor specific T cells, Codarri Deak and colleagues developed PD1-IL2v with a novel mode of action, a *cis*-targeted IL2v conjugated to an anti-PD1 blocking antibody [157]. Since PD1, alongside being a checkpoint molecule, is often regarded as a bona fide marker for antigen specificity [158], [159], [160], this molecular design was devised to deliver IL2v to antigen-experienced T cells. Indeed, besides preferential targeting of tumor infiltrating lymphocytes (TIL), PD1-IL2v offered expansion of better effector T cells from stem-like CD8+ cells, as well as resulted in antitumoral efficacy in mice [157]. The molecule, called eciskafusp alfa, is being currently evaluated in a clinical trial in patients with advanced and/or metastatic solid tumors (NCT04303858).

Protease-activated T Cell Bispecific Antibodies (proTCBs)

During the course of tumor development, cancer cells undergo multiple genetic or epigenetic modifications, leading to the production and presentation of tumor-specific antigens (TSAs)

[161]. However, due to the variability of their structure and expression patterns within tumors and between patients, they are not often suitable as targets for antibody-based therapeutics [162]. Another category of tumor antigens are tumor-associated antigens, which encompass proteins overexpressed in, but not exclusive to the tumors [163], [164], [165]. As proteins often involved in tumor survival [166], TAAs have been targets of multiple modalities within cancer immunotherapy [167], [168], radiotherapy [169] and antibody-drug conjugates [170]. The expression of TAAs in healthy tissues remains an issue of concern due to potential toxicity unrelated to the tumor, as mentioned above and in the literature [171]. Binding and activity of the targeted therapeutics to the desired tumor target in the healthy tissue is called on-target off-tumor toxicity (OTOT) [172]. This phenomenon, observed clinically for numerous TAA-specific antibody binder-based therapeutics, including CAR-T cells constitutes a major barrier for drug development, safety and efficacy [173], [174], [175], [176], [177]. Thus, to improve tumor specificity, a new generation of conditionally active therapeutics has been proposed and explored by many groups. More specifically, the current next generation antibody drugs comprise molecules utilizing the tumor microenvironment characteristics as an on-switch, namely acidic pH [178], [179], [180], increased activity of certain proteases [181], [182], [183] or heightened ATP levels [184]. A notable example of such a molecule in cancer immunotherapy is a protease-activated T cell bispecific antibody (termed pro-TCB or prot-TCB). Geiger and colleagues developed a conditionally active Prot-FOLR1-TCB against FOLR1 as a TAA [181]. A standard FOLR1-TCB directs T cell cytotoxicity against all cells expressing FOLR1, including ovarian and other cancer cells, while also may be expected to bind to FOLR1 that is known to be present in healthy lung or kidney [185]. As an activating condition, the researchers selected the activity of matriptase and matrix metalloproteinase-2,-9 (MMP-2, MMP-9), overexpressed in ovarian carcinoma. Thus, Prot-FOLR1-TCB was shown to be active only upon encountering the protease-rich environments, and binding FOLR1 on target cells and CD3ε on T cells, minimizing on-target off-tumor effects [181]. Generally, the tumor-activated prodrug approach has attracted substantial interest in drug discovery due to the promise of minimizing drug toxicity [186]. A potential disadvantage of this approach is the complexity of the molecular design required to reach efficient blocking of antibody activity.

Costimulatory Agonists

With TCBs populating the clinical space in an increasing pace, the drug discovery space has seen rise in exploration of the molecules enhancing the activity of these drugs and T cells themselves [187], [188]. Endogenously, T cell activation requires two to three signals to elicit a functional response [65]. Signal 1 is provided by TCR binding of peptide-loaded MHC on target cells, signal 2 constitutes costimulatory signaling, directed by receptors such as CD28 and 4-1BB on T cells, and signal 3 entails cytokine binding in the form or IL2 or IL12, among others (reviewed in [189]). In presence of signal 1 but lacking signal 2, T cell may shift to an anergic state [190], [191], whereas lacking signal 3 may lead to tolerance [189], [192]. TCB activity, *via* crosslinking of CD3ε, can be described as an analogous event to signal 1. However, a notable feature of multiple described TCBs is their activity without external costimulatory signals *in vitro* and *in vivo* [64], [193], [194], [195]. Despite this fact, costimulatory strategies are hypothesized to improve TCB activity, particularly its proliferation, differentiation and

long-term survival [196], [197], [198], [199]. For this reason, Claus *et al*. engineered a tumor stroma- or tumor-targeted 4-1BBL fusion molecules, FAP-4-1BBL and CD19-4-1BBL respectively, to combine with clinical CEA-TCB or CD20-TCB [200]. In preclinical settings, the costimulators led to increased T cell functionality in human tumor samples, and tumor remission with CD8+ T cell accumulation in mouse models. Alternatively, Sam and colleagues developed a B cell-directed CD19-CD28 costimulatory bispecific antibody with agonistic function towards CD28, for use with FDA-approved B cell-directed CD20-TCB (glofitamab) used in NHL [201]. The first CD28-directed clinical antibody, TGN1412, has been developed around two decades ago [202]. However, its superagonistic nature, i.e. ability to activate T cells without signal 1, lead to severe systemic toxicity in a human trial [203]. The preclinical safety assessment did not predict this toxicity [202], [204], and changed the landscape of regulatory requirements for preclinical prediction of adverse events [202]. Importantly, the CD19-CD28 molecule developed by Sam *et al.* in 2024 was shown to be not superagonistic and to rely on both signal 1, and binding to CD19, rendering it a suitable candidate for combination with a TCB [201]. Addition of CD19-CD28 to the CD20-TCB treatment of tumor-bearing mice enhanced tumor T cell infiltration and cytotoxic T cell signature. A triple combination of CD20-TCB with two costimulators: CD19-CD28 and CD19-4-1BBL, a CD19-directed a 4-1BBL protein fusion, further improved antitumoral efficacy [201]. Combination of CD20-TCB with CD19-CD28 costimulation has reached clinical stage and is currently undergoing assessment in phase I (NCT05219513). CD20-TCB with CD19-4-1BBL is also being evaluated clinically, currently in phase I/II (NCT04077723). Both combinations are being tested in patients with Relapsed or Refractory B-Cell Non-Hodgkin Lymphoma. Altogether, promising data is emerging on the safe and effective use of costimulators for combinations with TCBs.

CAR-T Cells

CAR-T cells are T cells genetically engineered to express a chimeric receptor consisting of an antibody-based binder against the TAA, connected to the intracellular T cell activating signaling domains [205]. Therefore, their engagement with the TAA leads to direct activation of the CAR-T cell cytotoxicity, regardless of the TCR specificity [205]. CAR-T cell treatments belong to the category of adoptive cell transfer (ACT) therapies encompassing cell-based, 'living' drugs [206]. As with other drugs, its design requires careful consideration of its continuous biological activity and the advantages and limitations for this modality [207], [208]. While many novel concepts are being explored within the field, such as allogeneic T cells, modified binders or other immune cells expressing CARs, here, the design principles of CAR-T cell products approved to date are introduced. A typical production of CAR-T cells involves harvesting patient's own T cells, their activation, genetically engineering them to express the CAR, cell expansion, and infusing them back to the patient after quality control processes [209]. Standard CARs are synthetic receptors, consisting of an extracellular domain binding a TAA, transmembrane domain, and intracellular signaling domain [208] (**Figure 4.3.1**). The antigen-specific domains in the classical CAR-T cells form an antibody-based scFv [210], [211], [212]. The transmembrane portion acts as an anchor, and a linker between the tumor-binding and signaling domains. The intracellular domain design depends on the generation of the product. Approved products until 2023 utilize 2nd generation CARs: two intracellular signaling

domains: CD3ζ, providing endogenous function of TCR signaling as signal 1, and CD28 or 4-1BB costimulatory domains, providing signal 2 [213]. New, 3rd generations of CAR-T incorporate three intracellular parts, with CD3ζ and two costimulatory domains, and more generations are being developed [213]. Upon binding of the extracellular scFvs to the targets of interest, the CARs form clusters at the immunological synapse, which commences signal transduction of the intracellular domains. Consequently, a CAR-T cell is activated and initiates a cytotoxic program against a TAA-expressing cell [208].

CAR-T therapies have provided remarkable antitumoral efficacy in patients suffering from hematological malignancies [214]. Several limitations, as stated above, have been observed for this modality, limiting its response rates, patient access and safety. The profile of tumor associated antigen expression often changes upon therapeutic pressure, leading to antigen loss, and limiting CAR-T cell efficacy [215]. Expansion of CAR-T cell use to other cancer types, such as solid tumors, necessitates development of separate CAR constructs and production protocols, increasing the required investment of resources eliminates the possibility of off-the-shelf use [216], [217], [218]. As a consequence, manufacturing needs to be performed separately for each patient, resulting in delayed therapy initiation and high costs per therapy, reaching above $350 000, as opposed to circa $72 000 for antibody treatments [41]. Delayed treatment initiation may lead to lowered antitumoral efficacy [219] and high costs entail limited therapy accessibility. Moreover, CAR-T cell persistence after finishing the treatment may pose the risk of secondary T cell cancers [220], [221], [222], [223], although the risk-benefit ratio is being debated in the scientific community, as the occurrence appears to be low [223]. All this prompted research to shift into developments of universal CAR-T cells with a unified construct and an on-off-switch system, as discussed below.

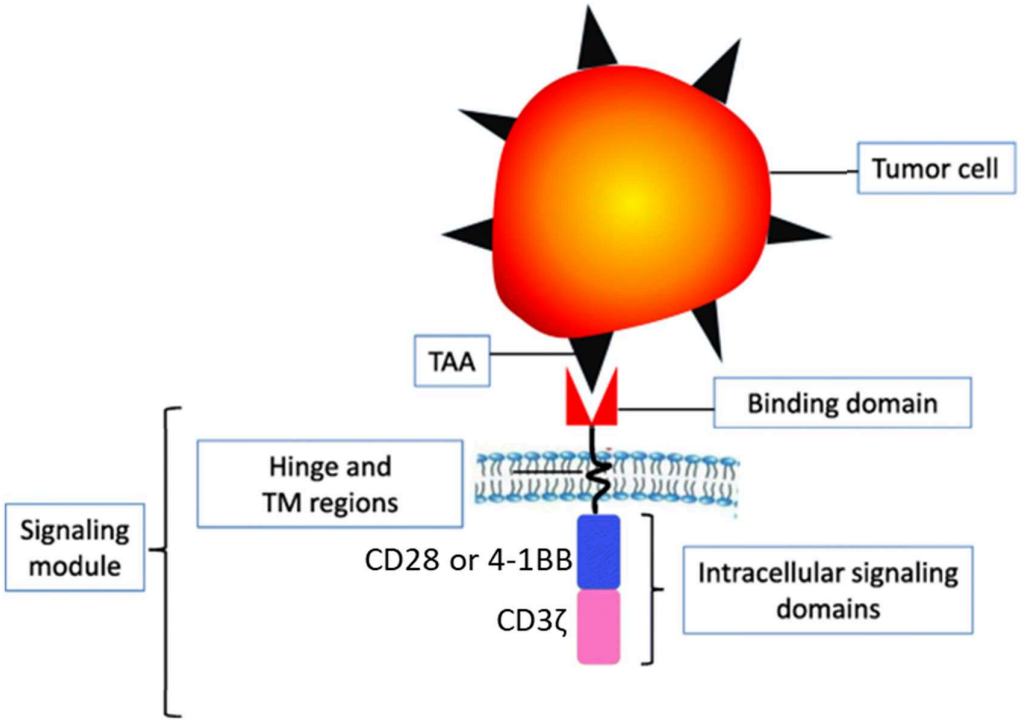

Figure 4.3.1. Design of a classical CAR-T cell (based on FDA approvals until 2023). Tumor associated antigens are by bound the scFv-based CAR binding moiety. This binding leads to receptor crosslinking and downstream signaling in the CAR-T cell, triggering costimulatory and CD3ζ pathways, ultimately leading to T cell-mediated tumor cell killing. Figure adapted from Liu *et al*. [224].

Adaptor-based Universal CAR-T Cells

As a recent development, universal, also called modular or adaptor-based CAR-T cell systems have been developed. There, interchangeable TAA-binding adaptors are used, comprising a tag recognized by the universal CAR-T cell [225]. The concept of universal CAR-T cells is depicted in **Figure 4.3.2**. By this design, only a single CAR construct needs to undergo the development process, regardless of the TAA of interest. Additionally, TAA-binding adaptor molecules can be exchanged and adjusted to the antigen profile within and across indications [225], [226]. Notably, due to the inactivity of tag-specific CAR-T cells in the absence of the adaptors, as well as limited half-life of the adaptor molecules, adaptors can act as on-switches, potentially increasing the therapy safety profile [224], [227], [228].

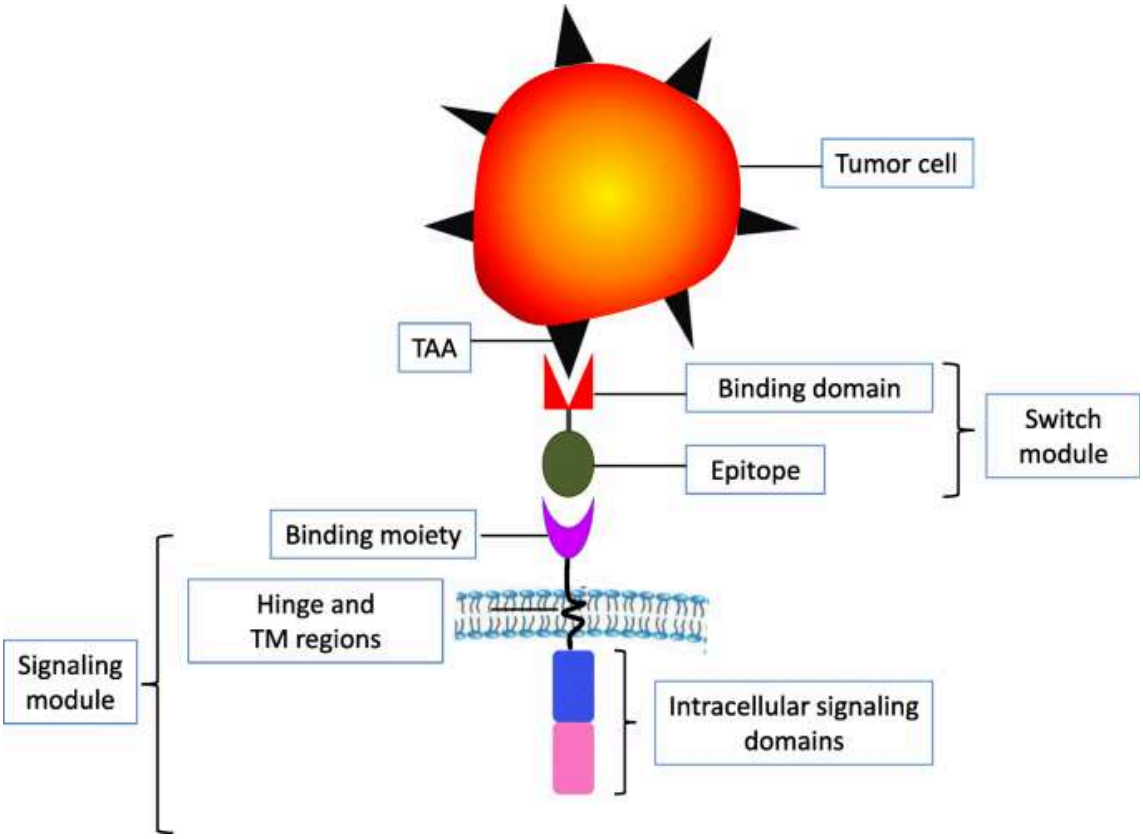

Figure 4.3.2. Design of a universal, adaptor-based CAR-T cell. Tumor cells are targeted with interchangeable adaptors, consisting of a tumor associated-antigen binding domain and a tag (epitope) for recognition by the CAR binding moiety. Simultaneous binding of the tumor cell and the universal CAR-T cell by the adaptor molecule leads to receptor crosslinking and downstream signaling in the CAR-T cell. While in all adaptors the tag remains the same, the TAA-binding domains in the adaptors can be selected to bind to the desired target or targets on a specific cancer cell of choice. Figure from Liu *et al*. [224].

The design of the adaptor molecule format, as any molecule, can influence its antigen specificity, biodistribution and PK/PD characteristics, immunogenicity, administration route, as well as production complexity and costs [229] . In 2012, Urbanska and colleagues introduced their proof-of-concept data for anti-biotin adaptor-based CAR-T cells combined with biotinylated antitumoral adaptors, which included full-length antibodies or scFvs [230]. To date, the published TAA-binding adaptors for universal CAR-T cell systems have fallen into the categories of: Fc-competent IgGs [231], [232], [233], bispecific antibodies [234], [235], [236], FITC-labelled antibodies [237], [238], FITC-conjugated small molecules [238], [239], [240], [241], leucine zipper-conjugated scFvs [242], diketone-conjugated small molecules forming covalent bonds [243], and P329G-mutated IgGs developed by Darowski, Stock, Klein and colleagues [226], [244], [245], among others.

IgG Adaptor-based Anti-P329G CAR-T Cells

The aforementioned universal CAR-T cell using P329G-mutated IgGs entails the utilization of full-length IgG adaptors. They bear modified Fc regions for CAR recognition, diverging from the conventional attachment of attached tags. The concept of this system is shown in Figure **4.3.3**. Considering that the obstacles for CAR-T cell treatments are both resource requirements during discovery, and CAR restriction to one TAA of interest, Darowski, Stock and colleagues group developed universal CAR-T cells specific to adaptors with structure based on clinical binders [226], [245], [246]. Since multiple antibody-based clinical-stage therapeutics bear Fc silencing P329G LALA mutations (for instance, glofitamab in NCT03075696 or IgG adaptors in NCT05199519), utilization of P329G-mutated IgGs as adaptors was opted for, with tumor-binding moieties based on clinical antibodies. Darowski *et al.* developed a novel antibody binder recognizing P329G-mutated CH2 domain of the IgG1 Fc specifically, and engineered CAR-T cells with P329G-specific CAR (P329G-CAR), for use with a library of P329G-mutated human IgG1s as adaptors [246]. Initially, anti-P329G CAR-T was used for a unique screening system employing anti-P329G CAR-Jurkat (P329G-CAR-J) reporter cells, for use with P329G-mutated adaptors, to enable binder evaluation on target cells [246]. The P329G-CAR-J system continues being utilized in drug discovery Roche. To develop the system further, investigating the utility of anti-P329G CAR-T was started for use in a therapeutic context. Two clinical trials have been initiated, utilizing patient-derived anti-P329G CAR-T cells. The trials utilized anti-P329G CAR-T cells combined with either Claudin18.2-targeted P329G adaptor IgG for Claudin18.2-expressing cancers (NCT05199519) or with BCMA-targeted P329G adaptor IgG for relapsed/refractory (R/R) multiple myeloma (MM) (NCT05270928, NCT05266768) [247].

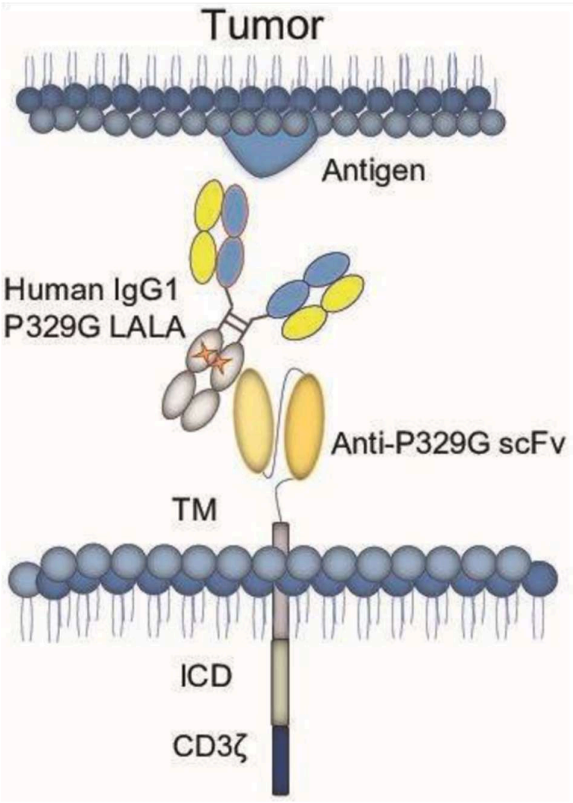

Figure 4.3.3. Concept of a universal anti-P329G CAR-T cell. Tumor antigen is bound by an antigen-specific full length IgG adaptors, which bear P329G mutations in their Fc. The P329G mutation is then recognized by an anti-P329G scFV CAR. Simultaneous binding of the adaptors to the tumor antigen and the CAR, triggers CAR crosslinking, leading to initiation of intracellular CAR signaling, and T cell mediated tumor cell killing. Figure from Stock *et al.* [248].

Aside from clinical use, this adaptor system can be utilized for preclinical and academic assessments of tumor biology and adaptor CAR-T biology. Recent work by Stock and colleagues demonstrated the efficacy of P329G CAR-T cells only when paired with P329G-mutated adaptor IgGs, thereby providing proof-of-concept data for non-tag adaptor recognition within a therapeutic CAR-T cell system. Importantly, this study investigated evidence of modularity *in vivo with* adaptor exchange. In a continuous *in vivo* study of mice bearing HER2+ tumor cells, mice treated with HER2-targeted P329G-mutated adaptor and anti-P329G CAR-T cells showed significant tumor control. The remaining mice from the study were then re-challenged with mesothelin (MSLN)+ cancer cells, and administered MSLN-targeted P329G-mutated adaptors, resulting in inhibited tumor growth. Thus, the adaptor-based anti-P329G CAR-T cell system has been shown to provide effective tumor control *in vivo* and universality in relation to the targeted antigen within the same, demonstrating the potential of this approach for tackling antigen heterogeneity and potentially antigen escape.

While adaptor-based CAR-T cell systems offer numerous advantages such as tunable activity, the development of a single construct for multiple targets and the potential for target combination therapies, these systems are not without their disadvantages. CAR-T cell therapies, despite promising results in both preclinical and clinical studies, still encounter

challenges inherent to T cell-based adoptive cell transfer. These include: preclinical and clinical development costs, therapy costs, treatment delays, batch variability, lack of off-the-shelf availability for the majority of products, and more [41].

Furthermore, due to the design principles, CAR-T cell preclinical development requires consideration of multitude of aspects. The presence of antibody-based TAA binders in these engineered cells necessitates processes similar to that of antibody therapeutics – including binder discovery [210], humanization [249], affinity/avidity modifications [250], immunogenicity assessments [251], among others. The preclinical processes used in T cell bispecific antibody development, but not applicable to CAR-T cells, are Fc- or HSA-based half-life modifications [95], chain assembly [50], and Fc silencing technologies [252]. CAR-T specific evaluations include selection of genetic engineering technology [253], [254], optimization of transduction efficiency [254], assessment of CAR expression levels [255], CAR signaling strength [256], batch variability [257], and localization of the manufacturing facility [216], [258]. Altogether, CAR-T cell preclinical development necessitates substantial resource investments in optimization processes, relating to both antibody and cellular aspects. This issue, together with complex and personalized production protocols, contributes to the high costs of CAR-T cell treatments even for adaptor-based concepts.

Universal Antibody-Based Immune Cell Engagers

In contrast, antibodies require lower preclinical and production costs [41], and enable off-the-shelf use [200], [201], [259]. Direct, non-modular antibodies require extensive characterization and development of production protocols; a process which needs to be performed for each new TAA and immune cell receptor of interest.

Modular antibodies, on the other hand, could utilize a set of interchangeable adaptor molecules and a single universal immune cell engager, enabling focus of resources on the development of a single immunomodulatory antibody can be of value, especially in case of structurally complex engagers. On the other hand, adaptors might be also used for recruitment of endogenous antibodies, redirecting them against tumors [260], [261]. Additionally, tackling antigen heterogeneity or cost-effectiveness may be brought by adaptor approaches.

While few studies have explored this topic, platforms published to date include several categories of adaptor-based antibody immune cell engagers. One of the approaches are called antibody recruiting molecules (ARMs). In 2009, Spiegel group published the concept of ARMs, small molecules consisting of a ligand to PSMA, a TAA overexpressed in prostate cancer, covalently linked to a 2,4-dinitrophenyl (DNP) group [261]. These small molecule adaptors were designed to be bound by endogenous DNP-specific antibodies, resulting in cytotoxicity against PSMA-expressing cancer cells. The general principle of ARM technology is depicted in **Figure 4.3.4.**

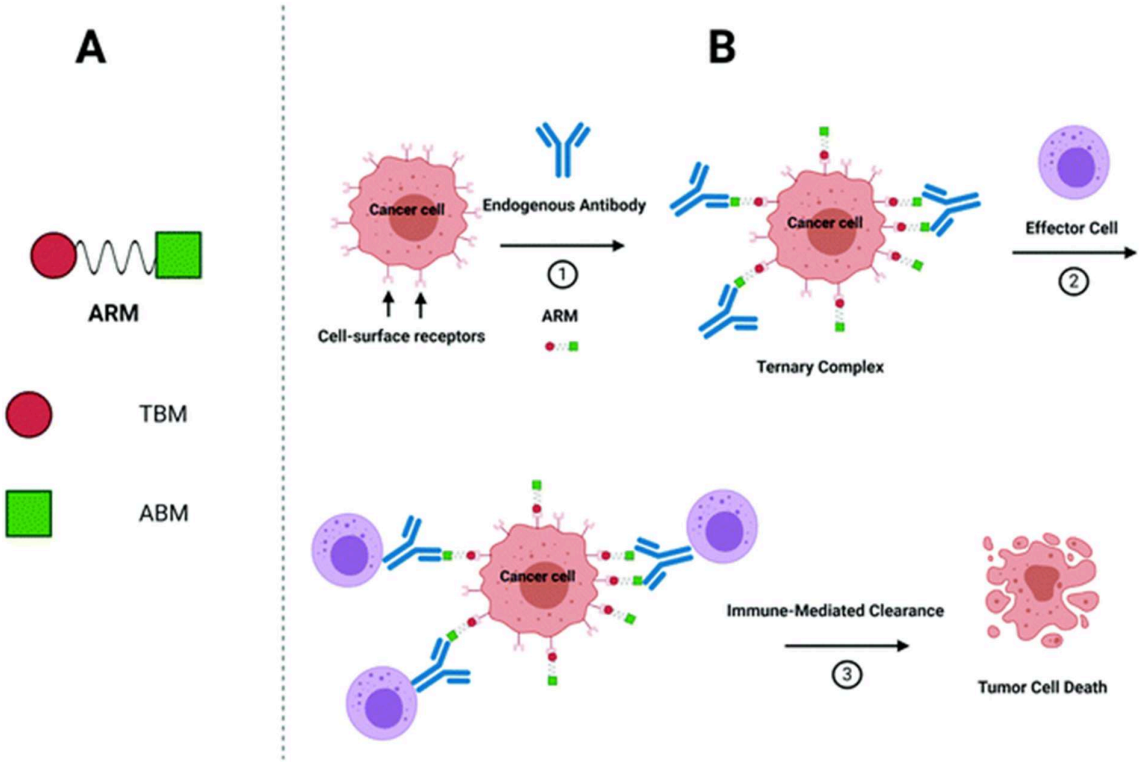

Figure 4.3.4. Design and mode of action of antibody recruiting molecules. A) Structure of ARM adaptors: tumor binding module (TMB) is connected to an antibody binding module (ABM) via a linker. B) Mode of action of ARMs. ARMs bind cell surface receptors on cancer cells via their TBM portion, and recruit endogenous antibodies via their ABM portion to the surface of cancer cells. This, in turn, initiates immune-mediated attack of ARM-decorated cancer cells. Figure from a publication by Achilli *et al*. [262].

As a further expansion of the ARM modality, Lake and colleagues introduced small molecule polymeric ARMs (pARMs) enabling efficient targeting of cells with low antigen expression [263]. pARMs were based on a backbone linking multiple PSMA ligands with multiple DNP groups, for use with anti-DNP antibodies as effector moieties. These pARMs were demonstrated to induce ADCP of PSMA+ cancer cells in vitro [263]. Generally, in the published studies, SM adaptors have been used for redirection of ADCC and ADCP-competent endogenous antibodies, limiting the type of immune engagement to be used against tumors. While SM adaptors have been used as adaptors for CAR-T cells, exploiting T cell cytotoxicity, their use with adaptor-specific immune cell engaging antibodies in a modular fashion had not been done to the best of current knowledge.

Small molecule-protein fusions have also been explored as ARM adaptors. In 2020, Sasaki *et al.* further expanded the ARM recruitment of endogenous effector antibody repertoire by devising an Fc- and TAA-bispecific ARM, termed Fc-ARM [264]. This adaptor consisted of a small molecule ligand to folate receptor alpha (FOLR1), based on its natural ligand folic acid, covalently linked to a peptide specific to an Fc portion of antibodies. Fc-ARM was able to recruit human antibodies to the FOLR1+ tumor cells regardless of their specificity in *in vivo* mouse models [264].

Another, distinct adaptor system published by Martinko *et al.* in 2022 used antibodies binding tumor targets, combined with separate antibodies binding CD3ε. These molecules formed an active TCB only upon antibody heterodimerization, induced by an addition of specific FDA-approved small molecules repurposed for this platform [265]. The concept is depicted in **Figure 4.3.5**.

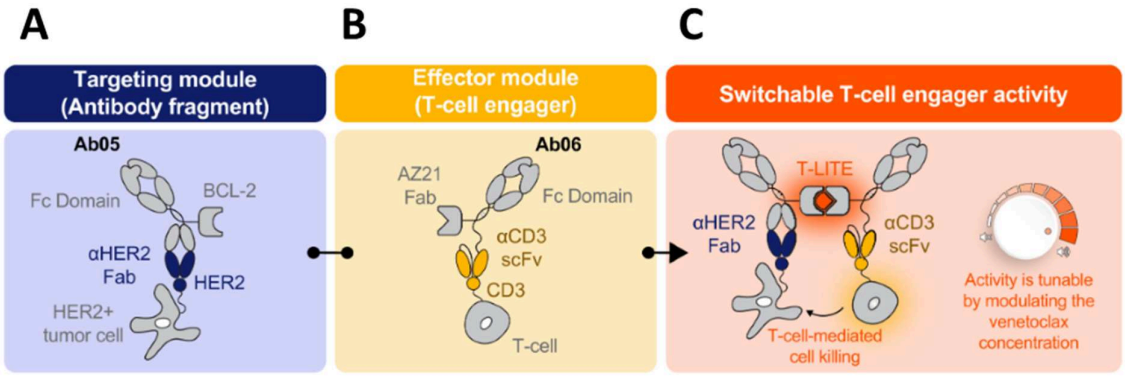

Figure 4.3.5. Design and mode of action of switchable T cell engagers. A) Design of the tumor-targeting adaptor antibody fragment, based on IgG structures, bispecific to HER2 and the small molecule venetoclax. B) Design of the T cell engager effector molecule, based on IgG structures, bispecific to CD3ε and venetoclax. C) Mode of action of the switchable assembly of the triple complex. Venetoclax acts as an on-switch to assemble the tumor-binding adaptor and the T cell-binding molecule into a functional T cell engager, which initiates T cell cytotoxicity against adaptor-bound cancer cells. Figure taken from Martinko *et al*. [265].

The final category includes so-called bridging BiTE (B-BiTE) published by Konishi *et al.* in 2023 [266]. This concept uses a CD3ε- and IgG Fc-bispecific molecule, designed for complex formation with FDA-approved Fc-competent mAbs in multiple myeloma model. Assembly of these molecules enable formation a functional TCB and redirect T cells against the mAb targets. Importantly, the Fc binder enables repurposing of multiple clinical Fc-containing antibodies. B-BiTE mode of action is depicted in **Figure 4.3.6**.

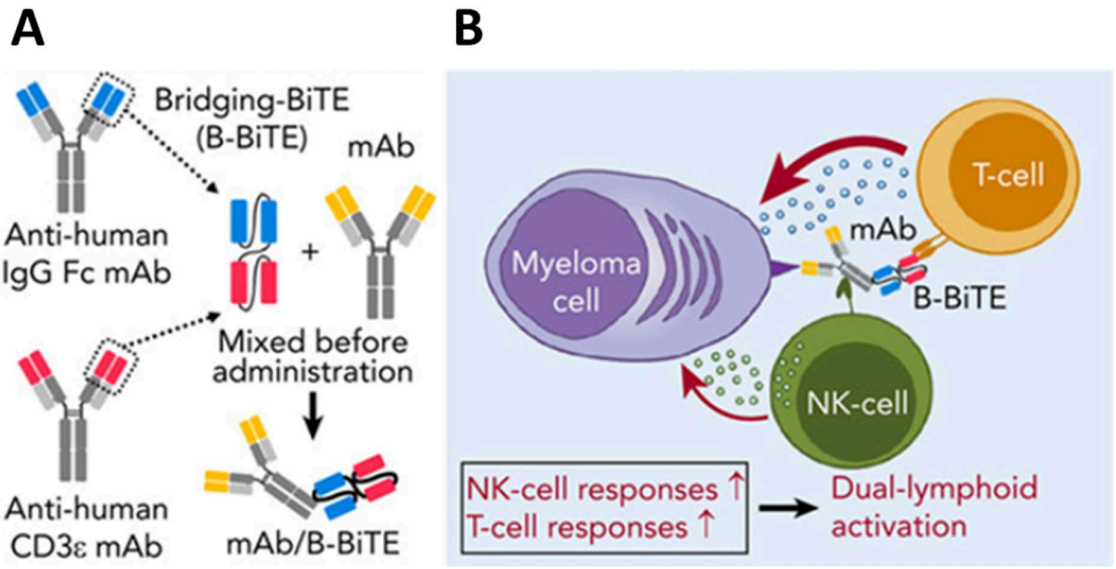

Figure 4.3.6. Design and mode of action of bridging BiTEs. A) Modular design of B-BiTE, whereby a clinical mAb targeted to the cancer cell is premixed with bispecific antibody- and CD3ε-bispecific BiTE. B) Mode of action of the B-BiTE concept. mAb binds target melanoma cells and recruits NK cells *via* their active Fc. In case of using the B-BiTE, B-BiTE molecules recruit T cells to the mAb-decorated target cells and initiate T cell-mediated cytotoxicity against them. Figure taken from Konishi *et al*. [267].

4.4. Introduction to Chapter 1 – P329G-Engager: A novel universal antibody-based adaptor platform for cancer immunotherapy

Altogether, multiple tumor-targeted adaptor-based systems have been developed to date, with the ARM concept prevailing in the field. The molecules used as effector entities are mostly endogenous antibodies [261], [263], [264], T cell engagers [265], [267], or a radioligand fusion [265]. Despite these advances, current concepts describe systems of interchangeable tumor-binding adaptors, while utilizing only a single or double universal effector entity, limiting antitumoral activity to a certain type, such as ADCC or T cell cytotoxicity [260], [261], [263], [266], without the flexibility to include cytokine or costimulatory signaling. Alternatively, other published work shows various effector entities for use with custom small molecule adaptors [265].To fully exploit off-the-shelf advantages of universal antibodies in cancer immunotherapy, and tackle tumor heterogeneity, one ought to enable the use of interchangeable components in terms of both tumor and immune cell targeting. Namely, devising a doubly universal platform would be of value, where an array of tumor-targeted adaptors can be used with an array of immune cell engagers, utilizing the same adaptor recognition system. As such, decades of developments of various cancer immunotherapeutics, such as these mentioned above, could be combined into one system.

Therefore, conceptualization and devising of an antibody-based adaptor platform was done in this work, with interchangeable components enabling binding across tumor antigens and immune cell receptors, to tackle antigen and immune heterogeneity (**Figure 4.4.1A**).

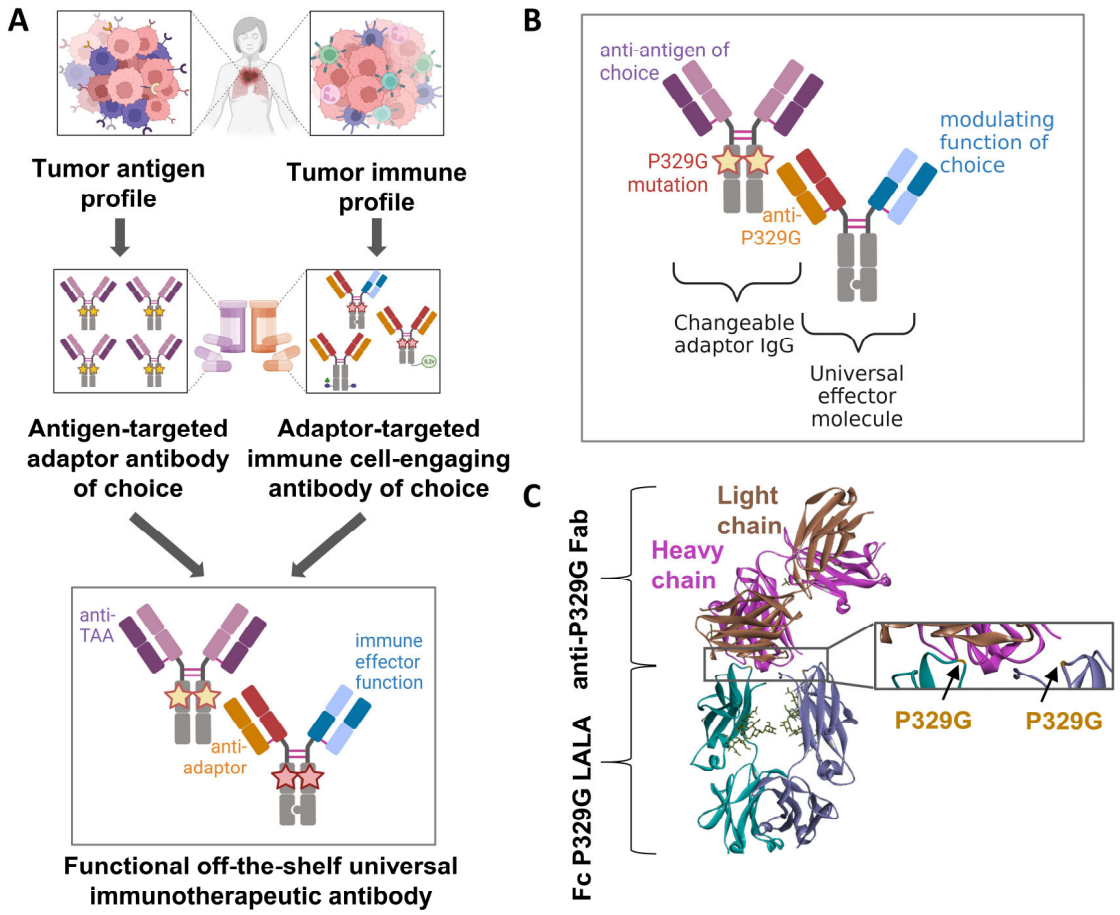

Figure 4.4.1. Universal adaptor-based P329G antibody platform and its mechanism. A) Aim and the suggested workflow of the off-the-shelf patient personalization, as enabled by the P329G platform development. B) Details of the adaptor recognition via P329G mutations, and C) the crystal structure of the P329G-mutated Fc with a bound anti-P329G Fab. Crystal structure adapted from PDB 6S5A.

Darowski and colleagues have previously repurposed clinically-based binders and IgG formats as adaptors for the universal anti-P329G CAR-T cell system [226], [245], [246]. Also in the currently described platform, universality was achieved in terms of binding to the TAA of choice, but immune cell engagement was limited to the engineered T cells. Stock *et al.* showed previously that the CAR-T cell-mediated cytotoxicity was indeed dependent on the binding of the P329G-specific CAR to the P329G-mutated adaptors [226]. Therefore, for the doubly universal engager platform in this work, the array of P329G-mutated adaptor IgGs as the moieties targeting a TAA of choice was opted for. For universal immune cell engagement, it was hypothesized that the P329G binder from the clinical CAR-T cell may be grafted on bispecific antibodies (**Figure 4.3.1B**) with various immune engagement functions, and lead to adaptor-dependent antibody function, such as TCB activity (mode of action depicted in **Figure 4.3.2**). Since the clinical P329G CAR was based on an antibody-derived scFv, the available binder sequence was utilized to create an array of P329G-specific effector antibodies. Up to

this point in the design process, all the components of the novel system were based on clinically applied components – tumor binders, adaptor IgG1 format, P329G binder and the P329G mutations. To retain the advantages of basing new molecules on the clinical therapeutics, such availability of in-depth characterization data and resource effectiveness, immune engagement moieties were also utilized based on clinical or advanced and published preclinical candidates. The immune engagement molecule fragments, as well as their antibody formats, were based on molecules either undergoing clinical assessment or having been approved for cancer treatment.

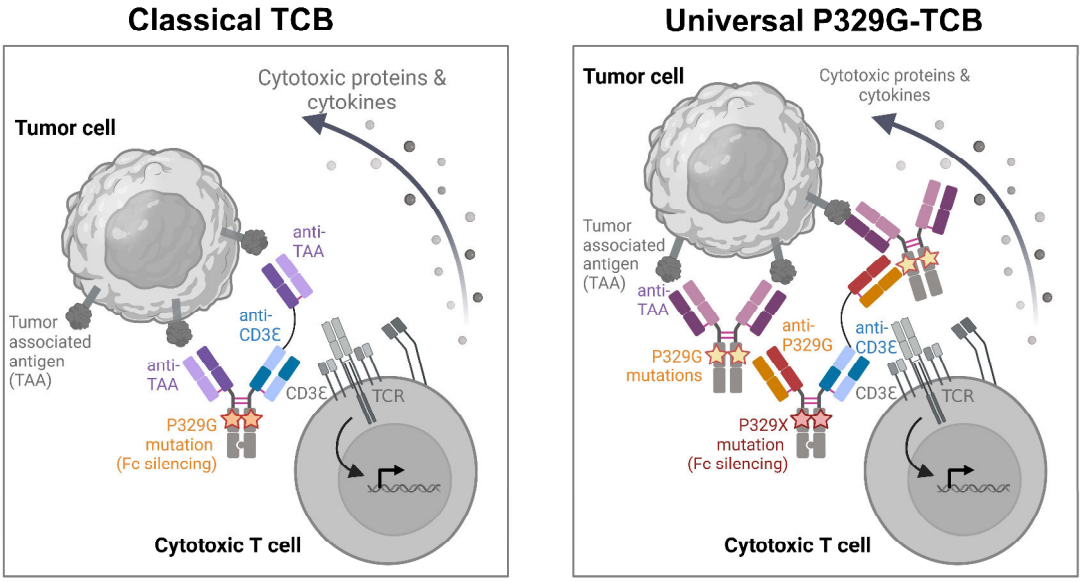

Figure 4.3.2. Comparison of the modes of action of the classical TCB and the universal P329G-TCB. A classical TCB binds its target antigen directly, and upon simultaneous CD3ε binding initiates T cell activation and cytotoxicity. A universal P329G-TCB, on the other hand, utilizes TAA-binding adaptors to target antigen of choice, and the P329G-TCB itself binds P329G mutations on adaptor IgG and CD3ε on T cells, initiating adaptor-dependent T cell activation and cytotoxicity.

Consequently, an array of P329G-specific immune cell engagers (P329G-Engagers) was designed, utilizing antibody engineering technologies and sequences of well characterized molecules. These P329G-Engagers included: anti-P32G x anti-CD3 T cell bispecific (P329G-TCB), a glycoengineered, ADCC-competent anti-P329G ADCC-competent antibody/innate cell engager (P329G-ICE) (based on [268]), anti-P329G-4-1BBL T cell costimulatory fusion protein (P329G-4-1BBL) (based on [269]), anti-P329G x anti-CD28 bispecific T cell costimulator (P329G-CD28) (based on [270]) and anti-P329G IL2v antibody fusion protein/immunocytokine (P329G-IL2v) (based on [157]). This array of immune cell engagers was designed for use with an array of various TAA-binding P329G-mutated adaptor IgGs. The overview of the platform, with adaptors and engagers, is presented in **Figure 4.4.3**.

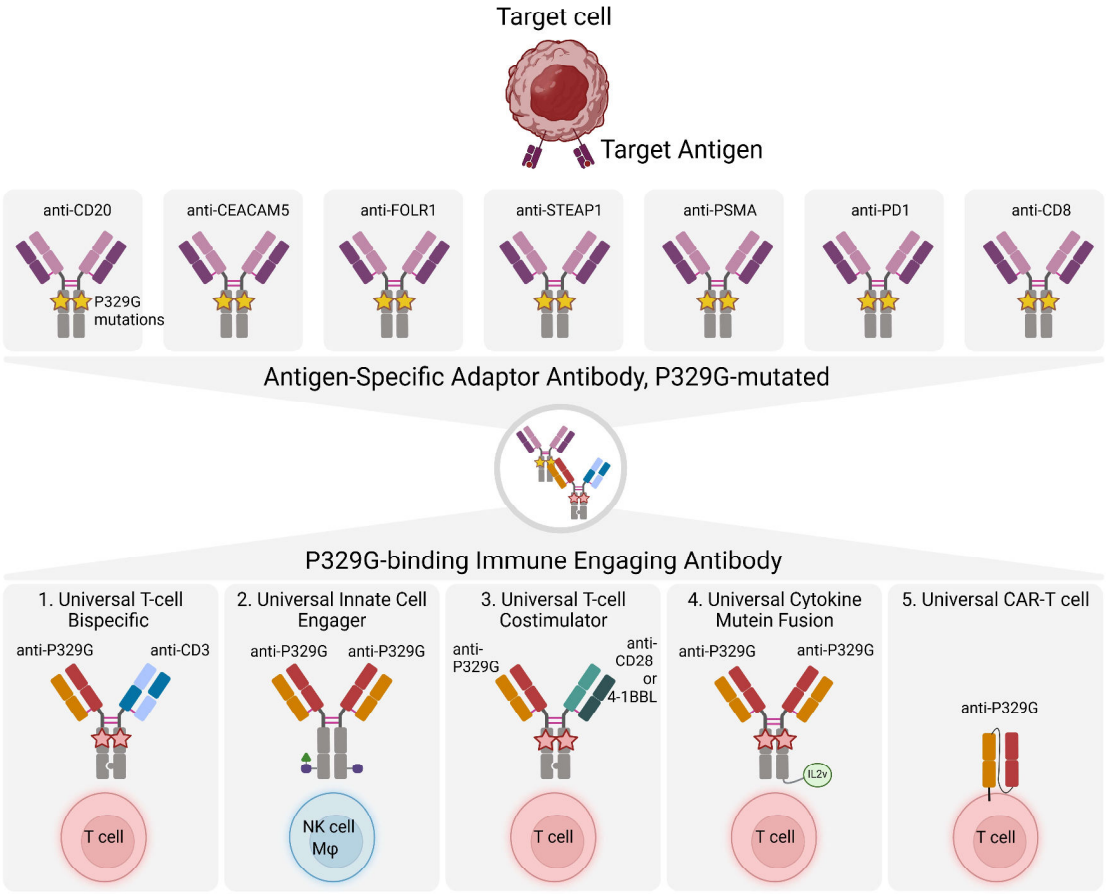

Figure 4.4.3. Summary of the universal P329G-Engager antibody platform. On the top, a library of antigen-specific adaptors is presented, each bearing P329G mutations in the Fc portion. On the bottom, a library of bispecific P329G-binding immune engagers is shown. The two libraries enable selection of one or multiple molecules from each of them, to fit the desired antigen and immune engagement of choice.

In this work, *in vitro* characterization of this novel platform is shown, and evidence that each engager can be functionally directed against multiple antigens is provided. Additionally, it is demonstrated that tumor antigens can be targeted by various engagers. The platform is shown to provide a wide therapeutic window in various adaptor and engager formats, and can be used *in vitro* for both hematological and solid tumor antigens. Moreover, evidence is provided of *in vivo* antitumoral efficacy of the adaptor CEACAM5 IgG with P329G-TCB in humanized mice, utilizing a pretargeting approach. As such, a functional, doubly universal P329G-Engager platform was devised, where tumor-targeted moieties of choice can be combined with immune effector moieties of choice, forming a functional therapeutic entity for use in cancer immunotherapy preclinically.

4.5. Introduction to Chapter 2 – Universal protease-activated cancer immunotherapy using target-agnostic antibodies

Antibody-based tumor targeting and the scarcity of tumor specific antigens

Conventional antibody-based therapies offer substantial target specificity [271]. However, when it comes to tumor associated antigens themselves, their expression is generally not exclusive to the tumor [162]. Aside from notable B cell targets in hematological tumors, such as CD20 in DLBCL, which selectively deplete mature B cells on cancer cells while sparing precursor cells capable of replenishing a the B cell population, there has been a scarcity of such selective and druggable targets [162]. Most target antigens in oncology for antibody-based or adoptive cell therapies involve proteins that are overexpressed in the cancerous tissue, but still present in lower numbers in non-targeted healthy organs [162]. One such target antigen is FOLR1 of high interest in oncology, which demonstrates heightened expression in tumors involving female-specific tissues, such as ovarian, endometrial and breast cancer, and other cancers such as lung cancer or mesothelioma [272]. However, studies have shown that while the majority of ovarian cancers display constitutive expression of FOLR1, it is also present in lower levels in healthy ovaries [185], [273], [274]. Additionally, FOLR1 expression is also observable in healthy kidneys and lungs [185]. This kind of expression pattern is common also for other tumor associated antigens, with similar patterns being observed for EGFR [275], CEACAM5 [276], HER2 [277], ROR1 [278] and others. Despite risks of targeting healthy tissues to some extent, lack of druggable and entirely tumor-specific cell surface proteins rendered these tumor-overexpressing proteins viable targets for antibody-based cancer therapy [162]. However, as drugs targeting these antigens entered the clinics, non-specific expression of these targets, along with the off-target binding, has emerged as a substantial concern due to the potential for causing severe on-target and off-target off-tumor toxicities [176], [279], [280], [281], [282].

Current solutions to tackle on-target off-tumor toxicity

To tackle the problem of on-target off-tumor cytotoxicity, certain research groups pivoted to developing antibodies exerting efficacy only against high target-expressing tumor cells, remaining inactive in healthy low-expressing tissues [283]. Others focused their strategy on *in vivo* assembly of functional therapeutics only upon binding two targets simultaneously, increasing molecule selectivity [284], [285]. Another strategy for overcoming lack of tumor-specific targeting is the use of local injections of the therapeutics into the tumor [286], [287], [288]. While both antibodies and CAR-T cells offer the potential to leverage aforementioned strategies, CAR-T cells also enable the use of more complex logic gating, such as activating signaling cascades dependent on both the presence of one target antigen and the absence of another, among others [289], [290], [291]. Logic gating in antibodies necessitates different technologies, but has also been investigated, and is a subject of a growing field [292], [293], [294].

One of the next-generation strategies for overcoming on-target off-tumor activity that surfaced in the recent years is exploitation of preexisting tumor microenvironment as a prodrug-activating condition. More specifically, identification of tumor-specific non-protein microenvironment characteristics lead to the discovery of low pH, increased protease activity, and elevated ATP levels as tumor-specific characteristics [295], [296], [297], [298], [299]. Combining targeting of the tumor-overexpressed antigens that have low expression in healthy tissue with molecule activation only in the tumor microenvironment, could offer enhanced tumor specificity and potentially reduced toxicity, due to sparing healthy tissue from the prodrug attack [300].

Protease-rich tumor microenvironment activated antibody prodrugs

One of the proteases of interest in tumor microenvironment studies is matriptase. Matriptase is a type II transmembrane serine protease which performs crucial enzymatic functions in multiple physiological processes, such as degradation of the extracellular matrix of activation of growth factors (reviewed in [296]). In cancer, such as ovarian and breast malignancies, matriptase and other proteases are often overexpressed [301], [302], [303], [304]. Their high levels and activity are also often correlated with poor prognosis [305], [306]. Importantly, protein levels of matriptase do not directly correlate with its activity, since its regulated by protease inhibitors [303]. For instance, in breast cancer, the increased activity of matriptase has not been linked to an increase in protein or mRNA levels directly, but to an altered matriptase:inhibitor ratio within the tumor, favoring protease activity [303]. This suggests that while matriptase is present in both tumor and normal breast tissue, its presence and activity may be key factors in tumorigenesis.

Due to these characteristics, matriptase activity has been explored as the activator of immunotherapeutic prodrugs designed to be activated upon entering tumor microenvironment [181], [307], [308], [309]. Protease-activated antibodies represent a novel class of therapeutic agents that exploit this unique proteolytic environment of tumors. Many of the protease-dependent approaches involve antibodies targeting a tumor or immune target of interest, with a masking moiety obstructing the binding site while in the prodrug state. The mask can be cleaved off and released when encountering a protease-rich tumor microenvironment, releasing the antigen binder and thereby activating the antibody [300]. This strategy can enhance the specificity of the therapeutic agent, reducing the risk of on-target off-tumor effects in healthy tissues which express tumor-associated antigens but lack matriptase activity.

An example of a protease-activated immunotherapeutic is Prot-FOLR1-TCB, a protease-activated antibody targeting FOLR1 on ovarian cancer cells, and CD3ε on T cells [181]. This drug utilizes matriptase activity as an additional condition for activation of the TCB, ensuring that the prodrug TCB is converted to its active form preferentially within the tumor microenvironment where matriptase is active, as opposed to benign tissues where its activity is minimal. The design of Prot-FOLR1-TCB is based on a standard FOLR1-TCB, with added scFv-based mask bearing affinity against the CD3ε binder, connected to the rest of the antibody via a linker containing a matriptase cleavage site. In absence of matriptase, Prot-FOLR1-TCB can

bind FOLR1 but not T cells, therefore preventing unwanted T cell-mediated toxicity. Upon encountering active matriptase, the linker is cleaved, releasing the mask and unlocking the CD3ε binder, activating the TCB [181].

Several other groups reported development of protease-activated immunotherapeutics. In 2012 Metz *et al*. presented a HER3- and cMET-bispecific antibody with the cMET binder released sterically only upon proteolytic cleavage [310]. Within the innate cell engager category, tumor-targeted protease activated Abs include anti-EGFR mAbs with masked tumor binders [307], [311] and an anti-HER2 mAb with masked Fc [312]. Anti-CTLA4 antibody has also been developed in a protease-activated format via binder masking [308]. Within the TCB space, several approaches have been devised for condition activation. DuBridge group developed EGFR-binding T cell engagers, which undergo domain exchange and assemble a functional CD3ε binder only upon protease cleavage [313], [314]. Cattaruzza *et al.* engineered HER2- and EGFR- binding T cell engagers, with both TAA and T cell binders masked via steric hindrance masks until occurrence of proteolytic cleavage [315]. Similarly, Liu *et al.* designed double-masked PD-L1-binding T cell engager, where both binders are inactivated by steric hindrance domain, released upon protease activity [316]. In general, this conditional activity has been shown to be an attractive approach to improve the therapeutic index of cancer treatments across many modalities, potentially leading to more effective and safer therapies within the field of TAA-targeting therapies.

Resource-consuming development of TME-activated versions of antibody-based drugs

While certainly a promising approach to cancer immunotherapy, an undeniable fact remains that the development of TME-activated drugs, and especially antibodies, such as protease-activated TCBs (pro-TCBs), requires additional investment in resources regarding time, expertise, and development tools, on top of already complex and costly process of standard antibody development. Considering anti-idiotypic masks (bearing affinity to the target-binding part of an antibody, i.e. an idiotype), which can offer strong masking capacity [317], each new developed lead binder must undergo a new phage/ribosome display campaign to identify an efficient mask. Additional work package includes a breadth of functional assays determining masking capacity, protease linker cleavage and eventual mask release. Moreover, a new domain added to an antibody-based therapeutic introduces risks of additional protein sites capable of inducing anti-drug-antibody production and necessitating evaluation of this risk. The protease cleavage site also needs in-depth characterization in terms of survival of the FcRn-based endosomal recycling, the resulting molecule half-life and exit of the active, cleaved prodrug away from the tumor microenvironment, which can lead to toxicity. The prolongation and complication of the TME-activated drug discovery process associated with TME-activated drugs pose significant challenges, particularly in terms of resource consumption for each newly developed binder or antibody. Balancing the potential benefits of enhanced tumor specificity and reduced off-tumor effects with the resource-intensive drug development remains a critical consideration in the pursuit of effective cancer immunotherapies.

Introduction of double universality in TME-activated drugs: Pro-P329G-TCB

Taking this into account, it was hypothesized that a target-agnostic protease-cleavable mask would be of high value, where development resources can be focused one universal protease-activated antibody, regardless of targeted protein of interest, therefore saving the resources and costs of TME-activated antibody. To tackle this, the decision was made to utilize the existing P329G-TCB universal antibody platform (**Chapter 1**), which by itself offers a target-agnostic universal T cell engaging antibody, and add a universal protease-dependent element to this TCB, eliminating the need for the binder selection campaign done for anti-idiotypic antibodies. The goal of this project was to introduce a protease-cleavable mask that is universal and can be used with multiple target binders, while also exploiting the advantages of affinity-based masking.

While the P329G-TCB contains two different binders – anti-P329G and anti-CD3ε, the efforts were focused on masking the P329G binder. This decision was made, since the P329G binder specifically was conferring target universality of the entire platform, as well as was usable in modalities beyond TCBs. Masking the CD3ε binder, while possible, would not allow further studies with other modalities such as anti-P329G costimulators, anti-P329G CAR-T cells or anti-P329G innate cell engagers. Therefore, by masking the P329G binders, the aim was to offer protease-induced activity regardless of both the tumor target and the immune cell target, maximizing the platform's potential for broad application, and retaining its double universality. With this goal in mind, the task to develop a universal mask for the P329G binder arose. The aim was to design a suitable mask while omitting the need for new anti-idiotypic binder discovery campaign or fully new steric hindrance technology development.

In 2009, Donaldson and colleagues omitted the need for development of a fully new mask by utilizing target antigen fragments as masks for the protease-cleavable antibodies [318]. There, anti-EGFR antibodies were fused to the mutated EGFRvIII epitope fragments via protease-cleavable linkers. The fragment mutations were introduced to reduce affinity to the antibody binders, in order to facilitate the cell-bound EGFRvIII to outcompete the mask after linker cleavage.

A 2023 study by Goudy *et al*. showed a similar design of masking for protease activation [319]. The researchers developed a PD-1 mimetic and opted to utilize a masking moiety in form of its endogenous ligand and a competitor of its target, PD-L1, connected to the antibody *via* a protease-sensitive linker. Interestingly, intact linker stabilized the masking and prevented binding to cellular PD-L1, while protease cleavage enabled competition between the cell surface ligand and the mask, allowing for effective binding of the protease-activated PD-1 mimetic [319]. This study introduced to a concept of the target competing with the target-resembling mask linked the therapeutic molecule. Based on the aforementioned promising results in the PD-L1 mask study, the decision was made to design a concept that similarly utilizes a mask that is competing with the target. In this case, it would constitute the target being an adaptor P329G-mutated IgG. Considering that the P329G-binders recognize specific

P329G-mutated CH2 Fc domains of the adaptors as targets, it was hypothesized that a CH2 domain containing P329G mutation, separated from an Fc and the rest of the adaptor IgG, may serve as a blocking mask. Such a mask would offer previously undescribed advantageous system - mimicking anti-idiotypic masks in terms of affinity present between the binder and the mask, while simultaneously offering a universal masking design agnostic to the tumor and immune target. To evaluate this idea, the structure of a standard P329G-TCB (itself mutated with P329R LALA as Fc silencing mutations) was utilized as a structural basis, and conceptualized a masked pro-P329G-TCB, where anti-P329G paratopes of the antibody are masked by P329G-mutated CH2 domains, connected to the TCB via G4S-based linkers with protease-cleavage sites. The structural details of the pro-P329G-TCB platform antibodies are depicted in **Figure 4.5.1**.

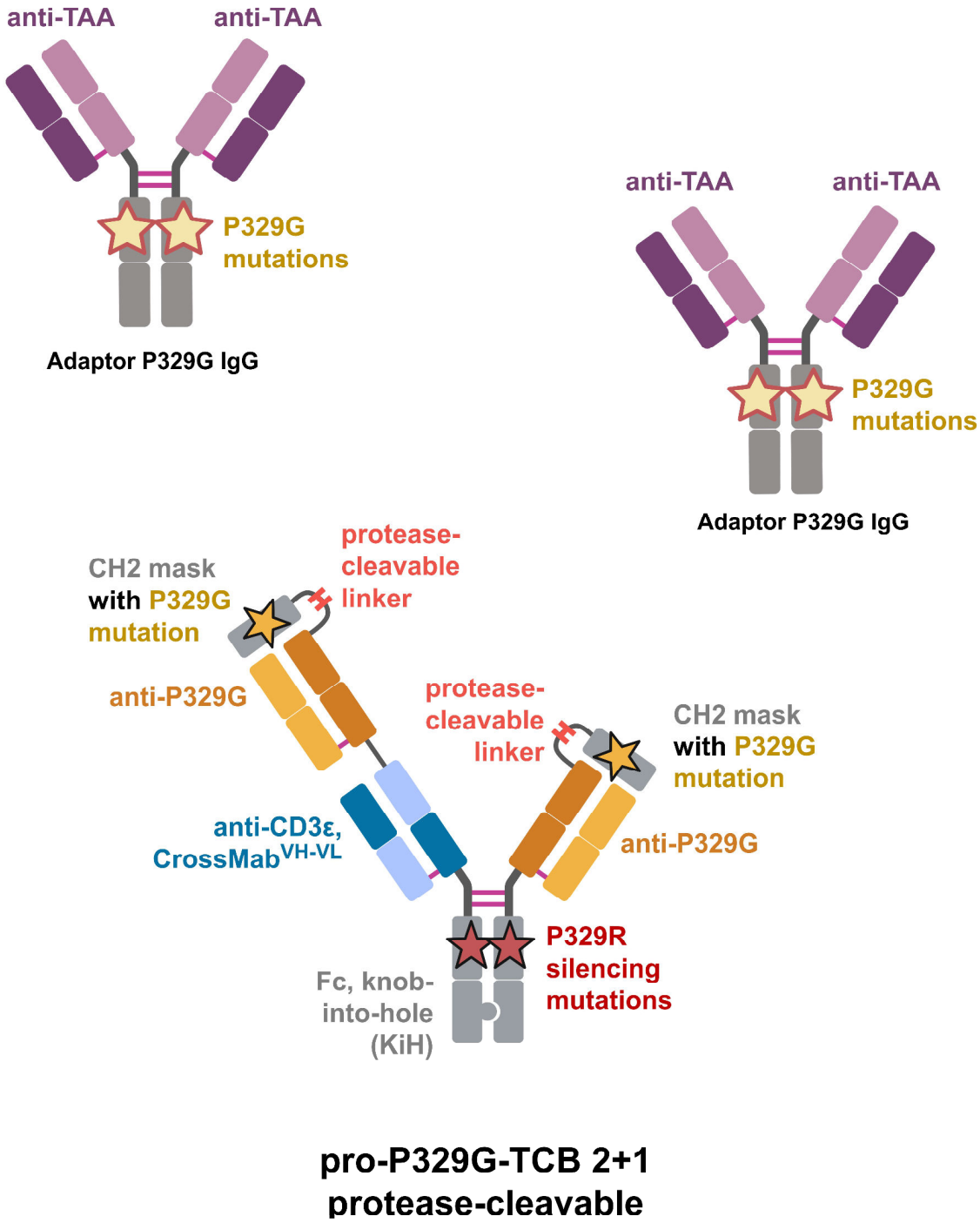

Figure 4.5.1. Structure of the pro-P329G-TCB with its adaptors. The tumor associated antigens (TAA) of choice are targeted by adaptor P329G-mutated IgGs. In absence of proteases, pro-P329G-TCB retains its CH2 P329G-mutated masks, which block binding by the anti-P329G Fabs, and therefore prevent binding to the adaptors.

The linker details are shown in **Figure 4.5.2,** where two different matriptase cleavage sites are inserted into the G4S linkers. By this design, in absence of proteases, the linkers remain intact, stabilizing the mask attachment to the P329G binders. Upon protease encounter, the linkers are intended to be cleaved at the specific protease cleavage site, enabling the detachment of the mask in the covalent terms, and facilitating the adaptor P329G IgG binding to the pro-P329G-TCB to outcompete the mask binding.

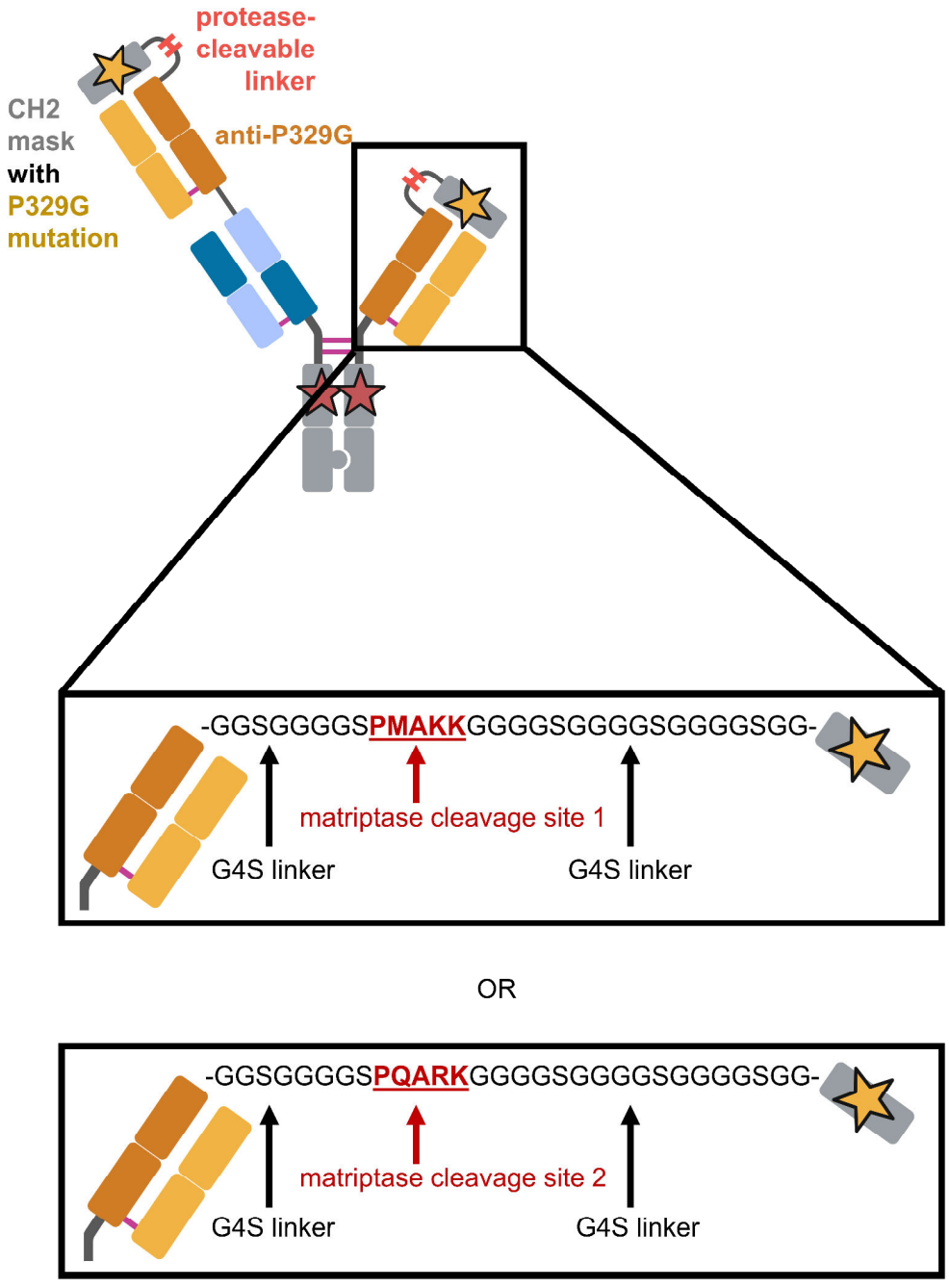

Figure 4.5.2. Details of the protease-cleavable linkers, connecting the CH2 P329G-mutated masks and the anti-P329G Fabs. Amino acid sequences of the linkers are depicted. Matriptase cleavage sites are shown in red.

The mode of action of the pro-P329G-TCB concept is presented in **Figure 4.5.3**. As shown in the **Figure 4.5.3A,** in healthy tissues expressing the target antigen but lacking enhanced protease activity, adaptor P329G IgGs bind the antigen but remain inactive immunologically. At the same time, the pro-P329G-TCB binds CD3ε on T cells, with its P329G binders remaining masked, therefore preventing binding of the TCB to the adaptors, and therefore to the antigen. This blocked interaction prevents crosslinking of the CD3ε on T cells, subsequent TCR signaling and T cell cytotoxic activity. The pro-P329G-TCB, therefore, remains inactive in absence of proteases. Presented in the **Figure 4.5.3B**, in case of protease-rich and antigen-expressing tumor microenvironment, the linkers connecting the P329G-mutated CH2 masks to the pro-P329G-TCB are cleaved, leading to the release of the masks and unblocking the P329G binders on the pro-P329G-TCB. The antigen-targeted adaptor P329G IgGs bound to the tumor associated antigens are then bound by the unmasked pro-P329G-TCB. The pro-P329G-TCB, binding both CD3ε on T cells and the P329G on the adaptors, induces antigen-dependent crosslinking of the CD3ε within the TCR complex. This leads to TCR signaling, initiating a tumor cell-directed release of cytotoxic proteins and cytokines, and T cell-mediated tumor cell killing.

To enable better control of target binding, confirmations of antibodies within the synapse and avidity, multiple antibody formats ought to be produced. Considering the influence of TCB formats on their activity, three formats were designed – 2+1, 1+1 and 1+1 one-armed TCBs in the protease-cleavable format. As controls of masking and cleavage, unmasked P329G-TCBs, as well as masked non-cleavable pro-P329G-TCBs were designed and produced (**Figure 4.5.4**).

Such a system, if successfully developed and validated, would provide a universal pro-P329G-TCB as an inactive prodrug, active only in a microenvironment fulfilling two conditions – presence of any tumor associated antigen of choice, and presence of active proteases. As such, firstly, pro-P329G-TCB could minimize TCB on-target off-tumor activity, thereby potentially increasing safety of the TCB treatment by reducing the risk of adverse effects in healthy tissues. Secondly, this approach could broaden the target repertoire to include those that may not exhibit highly tumor-specific expression patterns. Thirdly, the adaptor-based approach, which to date has not been integrated with protease-activation, could offer an additional potential feature enhancing safety. Namely, tumor pretargeting and enrichment of the adaptors in the tissues is possible prior to pro-P329G-TCB administration, preventing the accumulation of active TCBs in circulation. Fourthly, a P329G-mutated CH2 mask added to a P329G-TCB is a truly universal mask, agnostic to both the tumor target and the immune cell engager of choice. This universal mask can also be seamlessly integrated with various effector cell-engaging modalities, including innate cell engagers, CAR-T cells or costimulators, further expanding the scope of potential applications for the pro-P329G system. Overall, the pro-P329G-TCB system holds potential to be a promising advancement in the field, offering a novel strategy for selective and effective targeting of tumor cells while minimizing on-target off-tumor and on-target off-tumor effects, while expanding the range of potential target antigens.

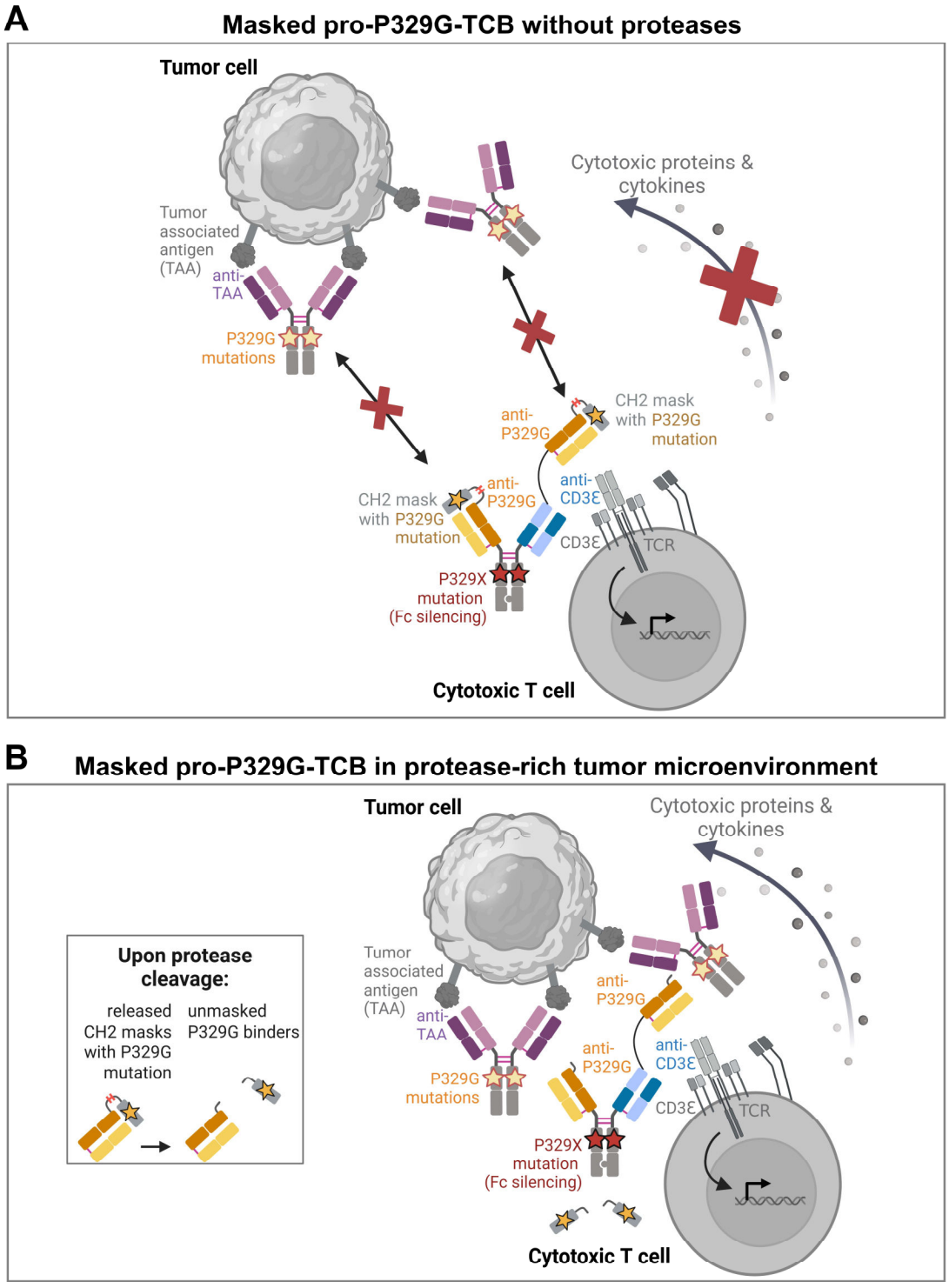

Figure 4.5.3. Mode of action of masked pro-P329G-TCB without proteases and in protease-rich tumor microenvironment. A) Inactivity of the platform components in absence of proteases. B) Activation of the pro-P329G-TCBs upon proteolytic cleavage of the linkers.

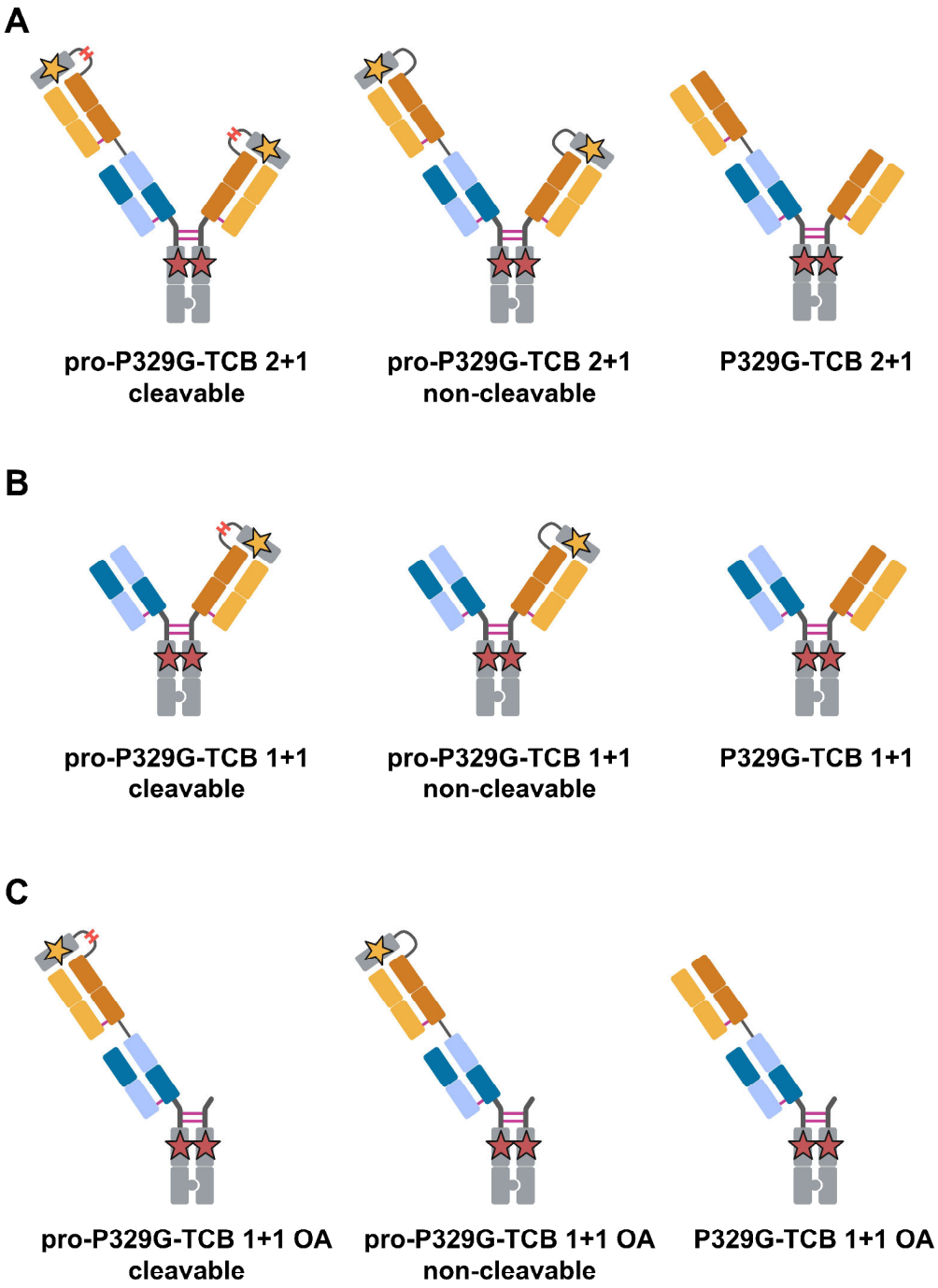

Figure 4.5.4. Designed antibody formats of the pro-P329G-TCB platform. The tested antibodies include: A) 2+1 TCB formats, B) 1+1 TCB formats, and C) 1+1 OA TCB formats. Within the produced antibody groups A-C, the following were produced and tested: masked TCBs with cleavable linkers (left), masked TCBs with non-cleavable linkers (middle), unmasked (WT) TCBs (right).

4.6. Introduction to Chapter 3 – DOTAM-TCB: universal small molecule-guided hapten- and T cell-bispecific antibodies for cancer immunotherapy

Small molecule adaptor molecules

Despite the evident enhancements introduced by the adaptor-based systems in cancer therapies, one must consider the distinct logistical, pharmacological and safety attributes of the adaptors themselves. Antibody-based adaptors, while potentially mitigating the overall high therapy costs, require their own characterization of developability, immunogenicity, along with the establishment of their own production cell lines for clinical trials and beyond. Additionally, a notable challenge associated with adaptors in form of IgG1 antibodies is the relatively long half-life of around 21 days [91]. This may prove advantageous for efficacy, but is undesirable in contexts of efficacy-related toxicities, such as such as cytokine release syndrome (CRS) or on-target off-tumor activity, where prolonged exposure to an active drug bears safety risks [320]. Another hurdle encountered with antibody-based adaptors, similar to all antibody-based therapies, relates to the inherent difficulty in developing binders to certain proteins, such as G protein-coupled receptors (GPCRs). Such targets have posed difficulties in protein isolation for phage display, due to loss of original 3D structure during the process, until recent advancements [321], [322]. Moreover, when contemplating the computational design of molecules targeting defined antigens, *in silico* screening or antibody design against a protein target with an empirically determined structure remains challenging, although it a subject of continuous developments [323].

In contrast to antibodies, small molecules as target-binding agents offer a distinct set of favorable characteristics. For instance, devoid of carrier proteins, small molecules are usually not immunogenic and do not trigger anti-drug antibody (ADA) production by themselves [324]. The production process of therapeutic small molecules does not require cell line development, and is more cost-effective [325]. Moreover, short half-life of most small molecules – between several minutes to several hours [93] may offer better control of the duration of drug exposure. Additionally, *in vitro* and *silico* screening of small molecule ligands to protein targets is well developed, and may facilitate the design of ligands to difficult-to-express target proteins, provided their crystal structure is known [326], [327], [328], [329].

Small molecules as ligands to cell surface tumor antigens

Protein-specific small molecules have traditionally been utilized in cancer therapy primarily for modulating the activity of intracellular targets, such as receptor tyrosine kinases [330], due to their ability to permeate cell membranes, a characteristic not available for antibodies without applying additional technologies [331]. However, recent years have witnessed a growing interest in utilizing small molecules as ligands for cell surface antigens on tumor cells. Examples of such approaches are the small molecule-drug conjugates [332], [333], [334],

diagnostic or intraoperative imaging agents [335], [336], and delivery ligands for radiotherapy [337].

The most known small molecule ligands of tumor-associated surface proteins are: folate, targeting FOLR1 [338], 2-[3-(1,3-fdicarboxypropyl)ureido]pentanedioic acid (DUPA), targeting prostate-specific membrane antigen (PSMA) [339], and acetazolamide (AAZ), targeting carbonic anhydrase IX (CAIX) [340]. These proteins are cell-surface localized antigens associated with several cancer types, including: ovarian and uterine (FOLR1) [273], [341], prostate (PSMA) [342], [343] or renal cancers (CAIX) [344], [345].

Small molecules are generally known to exhibit lower target specificity and affinity than their antibody counterparts [346], [347], [348]. However, notable reason for their development as surface-binding agents is their potential not only to bind to transmembrane receptors, but also to inhibit receptor enzymatic activity [349], [350]. Another role small molecules play in drug development is in their use as haptens, which are small molecules that, combined with a protein carrier, are capable of eliciting antibody production against them [65]. This phenomenon enables the development of recombinant anti-hapten antibodies with several potential applications. One notable use of this approach is pretargeted radioimmunotherapy (PRIT), where bispecific anti-tumoral anti-hapten antibodies are administered to patients, followed by the administration of a radioactive hapten; a process resulting in pretargeted radiotherapy delivery [351], [352], [353].

Adaptors, small molecules and haptens in CAR-T cell context

With the developments in CAR-T cells and small molecule ligands as separate research domains, an interesting new field has emerged combining both. Namely, tumor-targeting capabilities of small molecule ligands are being explored for combination with immune effector functions of T cells, in order to form one antitumoral therapeutic entity. Such advancements involved the development of recombinant anti-hapten antibody binders in CAR-T cells, paired with haptenated small molecule adaptors. In 2015, Kim et al. introduced anti-FITC CAR-T cells for use with folate-FITC small molecule adaptors [239], with similar approaches being explored by others [240], [354]. Next to FOLR1 antigen, CIAX and PSMA have also been targeted in an adaptor-based CAR-T cell system [240]. Using a related approach, Stepanov and colleagues pioneered the development of covalent CAR-T cells, recognizing adaptors targeting folate and PSMA and forming a covalent bond with the CAR [355].

Adaptors, small molecules and haptens in antibody context

Given the inherent challenges and costs associated with personalization of CAR-T cell therapies, an alternative approach that attracted interest was the redirection of patient's endogenous immune cells toward cancer cells using antibodies and small molecules. In 2002, Lu and Low published a concept of a haptenated small molecule, folate-FITC, for recruitment of endogenous hapten-specific antibodies to FOLR1-overexpressing cancer cells [356]. In 2013, the group developed a different approach involving this adaptor, where metastatic renal

cell carcinoma patients underwent vaccination against a FITC-based hapten, and subsequently were treated with folate-FITC, to elicit an immune response against FOLR1+ cells bound by folate [357], [358]. The study reached a clinical trial phase II, but was eventually terminated (NCT00485563).

In 2009, Spiegel group pioneered a small molecule-based antibody redirection system, with a PSMA ligand conjugated to a hapten tag DNP (2,4-dinitrophenyl), for use with anti-DNP antibodies to induce antibody-dependent cell-mediated cytotoxicity (ADCC) [261]. Such haptenated small molecules, termed antibody-recruiting molecules (ARMs), exhibited the additional capability to inhibit the enzymatic activity of PSMA [261]. Since then, there have been further reports of ARMs development, targeting tumor-associated antigens such as PSMA with DUPA molecule [260] or FOLR1 with folate molecule [359]. When it comes to endogenous T cell recruitment via antibody-based molecules, in 2013, Lee *et al*. introduced an approach in which omitted the use of haptens, instead employing an anti-CD3ε antigen-binding fragment (Fab) covalently linked to a PSMA-targeting small molecule ligand DUPA [360]. Remarkably, the molecule progressed to clinical trials in patients with metastatic castration-resistant prostate cancer (mCRPC) [361], albeit it eventually underwent termination (NCT04077021).

The development and characterization of small molecule tumor ligands, whether through covalent attachment or hapten binding, have significantly expanded the landscape of treatment modalities for cancer and beyond. Despite many advancements, the utilization of haptenated small molecule tumor ligands as adaptors has been limited to tumor redirection of CAR-T cells or endogenous antibodies. As such, the potential of engineered antibodies as effector molecules has not been utilized within this space. For instance, redirection of universal adaptor-binding TCBs, by a set or interchangeable haptenated small molecule adaptors, remained unexplored. This presents an exciting area for further research, potentially combining advantages of small molecules with desirable off-the-shelf features and biological flexibility of the antibodies. Importantly, adaptor-based character of such a platform could enable universality in terms of targeting a tumor antigen of choice, without the need for separate production of an immune cell engager for each target. As part of this thesis, a novel small molecule-hapten-T cell engaging bispecific antibody platform was developed.

DOTAM-TCB design

Considering the above, an aim arose to design a platform enabling the use of an array of interchangeable small molecule-based tumor ligands, each conjugated to the same hapten, redirecting a universal hapten-specific T cell engaging antibody. Despite the non-covalent binding between such a hypothesized immune cell engager antibody and the adaptor small molecule, it was postulated that a hapten – anti-hapten antibody interaction could provide sufficiently high affinity. Consequently, the tumor-targeting adaptor small molecule, bearing a hapten-based tag, would be recognized by an anti-tag T cell bispecific antibody (TCB), and form a functional TCB. Such a small molecule adaptor-based TCB, in contrast to IgG-based adaptor-based TCBs, could potentially offer a reduced size of the immunological synapse owing to the smaller size of the small molecule adaptor.

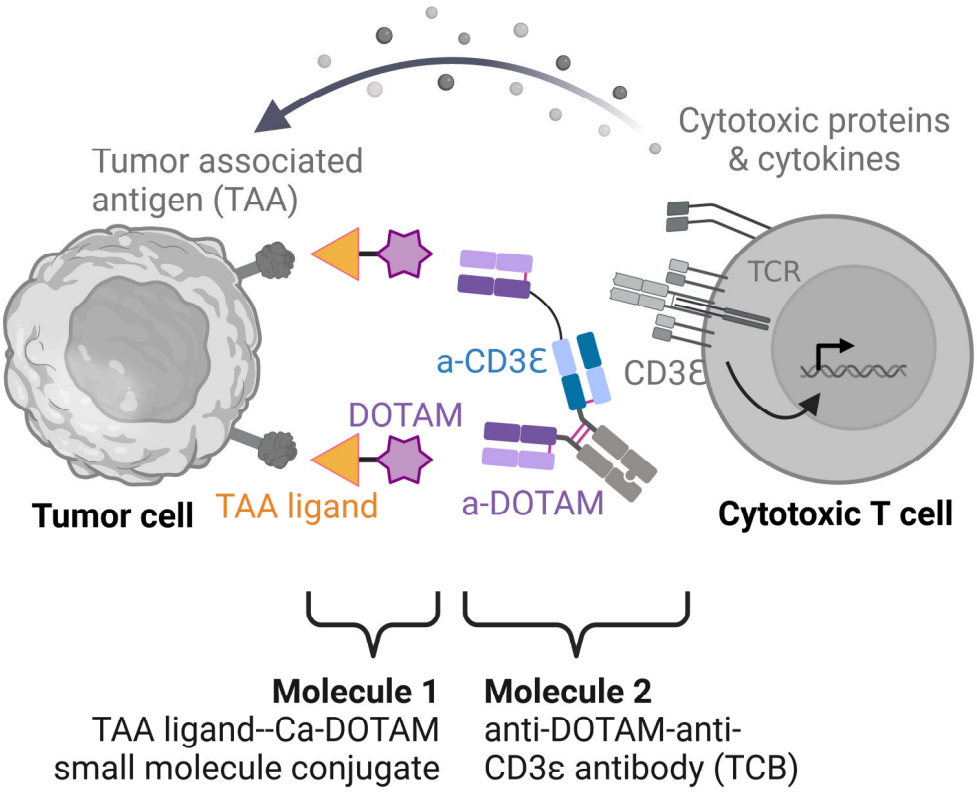

Figure 4.6.1. Mode of action of the universal DOTAM TCB 2+1 with haptenated small molecule adaptors. Various tumor-associated antigens are targeted by interchangeable small molecule ligands (TAA ligands), which are covalently bound to a Ca 2+-loaded DOTAM hapten, regardless of the targeted TAA. The adaptors are then bound by DOTAM- and T cell- bispecific antibody (DOTAM-TCB) in the 2+1 format. This triggers CD3ε crosslinking, leading to activation of T cells, cytokine release and tumor-directed cytotoxicity. The same DOTAM-TCB can be used with various adaptors, rendering it universal in terms of antigen targeting.

Given the considerations outlined above, a small molecule adaptor-based TCB platform was designed, with its mode of action depicted in **Figure 4.6.1**.

For the proof of concept experiments, the small molecule adaptors were designed based on small molecule ligands available in the literature, and use Ca^{2+}-loaded DOTAM as the hapten of choice, with anti-DOTAM anti-CD3ε T cell engaging antibody as an effector molecule (**Figure 4.6.2**).

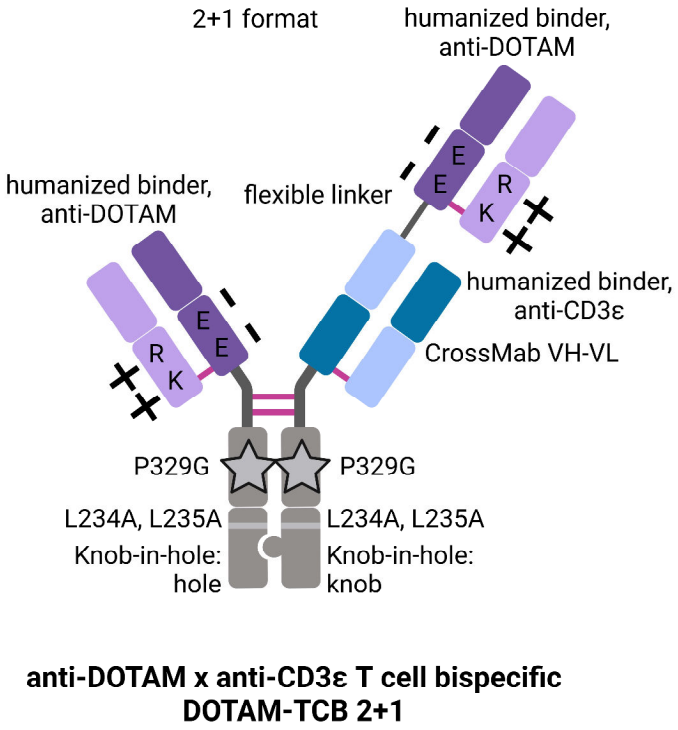

Figure 4.6.2. Antibody engineering principles incorporated in the design of the DOTAM-TCB.

DOTAM is a known chelator of bivalent cations, and is used in radiotherapy applications [362], [363]. Ca^{2+}-loaded DOTAM with DOTAM antibody binder was selected as the hapten anti-hapten binding pair, due to the host group's previous work on DOTAM-specific high affinity antibodies [363]. In detail, the design of the small molecule adaptor consisted of: 1) the hapten, Ca^{2+}-loaded DOTAM, where Ca^{2+} was added to stably load DOTAM, 2) a linker, and 3) a small molecule ligand to a tumor associated cell surface antigen. Three antigens were selected for targeting the tumor: PSMA, CAIX and FOLR1, due to their tumor association, and the availability of the structure of the surface-bound small molecule ligands in the literature: DUPA, AAZ and folate binding to PSMA, CAIX and FOLR1, respectively [238], [240], [360], [364], [365]. As a result, three adaptors were designed: Ca-DOTAM-DUPA, Ca-DOTAM-AAZ, and Ca-DOTAM-Folate, with their chemical structure depicted in **Figure 4.6.3**. The ligands and their linkers were derived from FITC-conjugated adaptors published by Low group [240]. Given the widespread expression of these antigens across various cancer types, it was concluded that targeting them can provide universality of the platform not only across antigens, but also indications. As an immune engaging moiety, anti-DOTAM anti-CD3ε T cell bispecific antibody was used, referred to here as DOTAM-TCB. The TCB structure was derived from an FDA-approved CD20-TCB antibody, glofitamab [63], [70]. The binding between the haptenated small molecule ligand and the DOTAM-TCB antibody, was designed to form a functional T cell engager. With this approach, the aim was to combine the benefits of small molecules, hapten binding and antibody-mediated T cell engagement, while retaining target-agnostic character of the effector antibody.

In this study, *in vitro* proof-of-concept data for the DOTAM-TCB antibody with literature-based small molecule ligands is shown, whereby antitumoral T cell-mediated efficacy is dependent on the presence of both components. It is demonstrated that a single universal hapten- and T cell-bispecific DOTAM-TCB can be used to induce T cell activation against different tumor antigens. Moreover, Ca^{2+}-DOTAM and anti-DOTAM binding is demonstrated to be highly stable and reach femtomolar affinity range, enabling the formation of stable non-covalent complexes of adaptors and TCBs with slow off-rates, and offering the use of the system as either modular or single molecule modality. After characterization *in vitro*, preliminary results from an *in vivo* study of DOTAM-TCB with CAIX-targeting acetazolamide-based adaptor were shown. Anti-tumor efficacy is reported, limited by ligand-driven on-target off-tumor toxicity, offering preliminary insights into risks associated with small molecule tumor targeting.

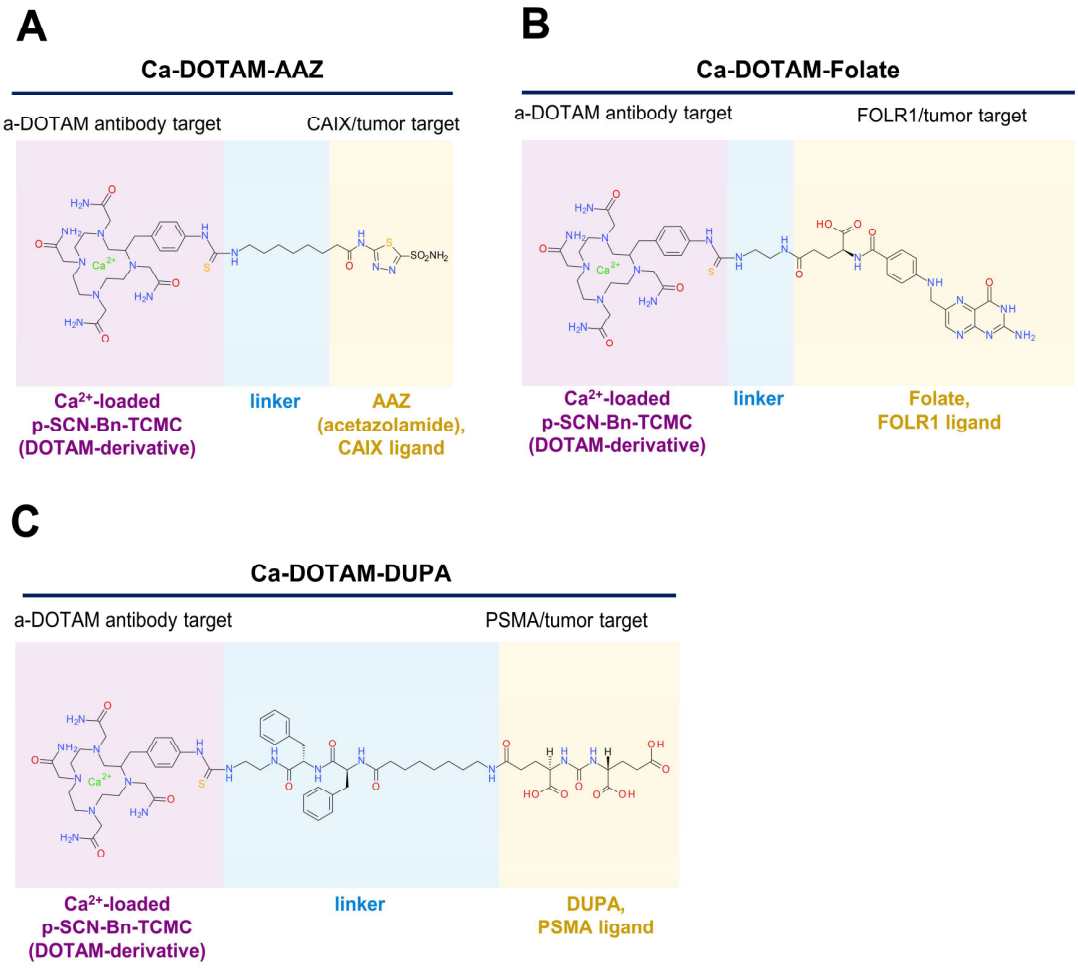

Figure 4.6.3. Structures of the small molecule adaptors for use with DOTAM-TCB. A) Ca-DOTAM-AAZ for CAIX targeting, B) Ca-DOTAM-Folate for FOLR1 targeting, and C) Ca-DOTAM-DUPA for PSMA targeting.

5. Objectives and scope of the thesis

This doctoral thesis deals with and explores antibody and small molecule adaptor-based platforms for cancer immunotherapy. More specifically, it presents the development and characterization of the libraries of tumor antigen-specific adaptors and the libraries or singular adaptor- and immune receptor-bispecifIc antibodies engaging immune cells against cancer. Furthermore, this work investigates the assembly of the immune-inactive adaptors and immune-inactive immune cell engagers into functional immunotherapeutics. This is based on mix-and-match principles, potentially enabling future off-the-shelf selection of the components based on tumor antigen and tumor immune profile.

In **Chapter 1** of the thesis (P329G-Engager: A Novel Universal Antibody-based Adaptor Platform for Cancer Immunotherapy), the goal was preclinical development and investigation of the library of P329G-mutated tumor-binding adaptor IgGs with the library of P329G- and immune cell receptor-bispecific immune cell engaging antibodies. This research aimed to provide the first preliminary evidence of the proof of concept of the platform. The scope was planned as the initial step, enabling future exploration in more advanced settings, such as incorporating tumor and immune profiling on tumor samples to enable personalization.

In **Chapter 2** of the thesis (Universal Protease-Activated Cancer Immunotherapy Using Target-Agnostic Antibodies), the aim was to expand the double universal P329G-Engager platform, P329G-TCB specifically, to include next-generation technology of conditional activation of the molecules by proteases in the tumor microenvironment. The project's goal was to develop molecules which do not show on-target off-tumor activity, and enable increased safety profile when targeting antigens which are not fully tumor-specific. On a technical level, the goal was identify a protease-activated system, which would not only retain universal character of the P329G-TCB, but also similarly utilize clinical stage components. The scope of the chapter included design, production and preliminary *in vitro* proof of concept characterization.

In **Chapter 3** of the thesis (DOTAM-TCB: Universal Small Molecule-Guided Hapten- and T Cell-Bispecific Antibodies for Cancer Immunotherapy), the goal was preclinical exploration of small molecules as potential tumor-binding adaptor molecules, and combination with an appropriate hapten-specific T cell bispecific antibody. Specifically, the aim included design of haptenated small molecule adaptors, based on separately published structures of its components – tumor ligands, linkers, and the Ca^{2+}-loaded DOTAM acting as a hapten, as well as design of a DOTAM- and T cell- bispecific antibody. Moreover, functionality and affinity of the assembly of such a system was analyzed. The scope of the chapter included multiple biochemical, structural and *in vitro* functional characteristics of the DOTAM-TCB platform, with several tumor-targeted adaptors. Additionally, preliminary *in vivo* test was conducted, and indicated potential toxicity liabilities. These results laid the groundwork for potential future directions of research into specificity of small molecule ligands, and their suitability for TCB redirection.

6. Materials and methods

6.1. Molecule synthesis methods

Synthesis of Ca-DOTAM-DUPA

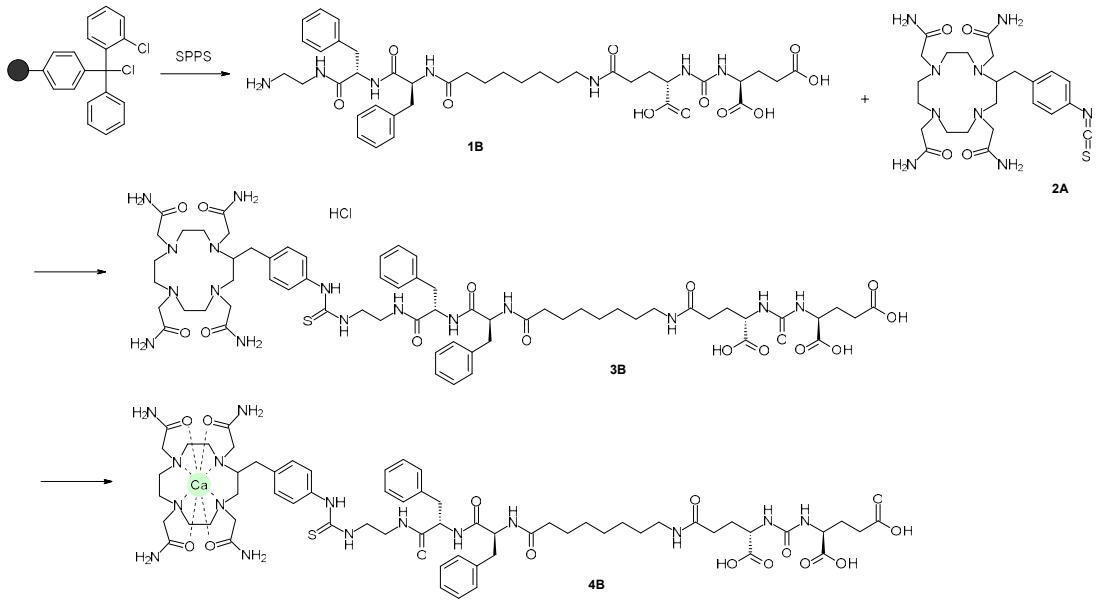

Figure 6.1. Synthesis steps of Ca-DOTAM-DUPA.

The synthesis of Ca-DOTAM-DUPA was planned by Dr. Dario Venetz (Roche Innovation Center Zurich), Antonio Ricci and Dr. Moreno Wichert (Roche Innovation Center Basel), and performed at a CRO. The steps are summarized in **Figure 6.1**.

The peptide was synthesized using standard Fmoc chemistry. Resin preparation: To the 2-CTC Resin (1.00 mmol, 1.00 eq, Sub 1.00 mmol/g) was added ethane-1,2-diamine (3.00 eq) and DIPEA (4.00 eq) in DCM (10.0 mL) was agitated with N_2 for 2h at 20°C. Then added MeOH (1.00 mL) for another 30 min. The resin was washed with DMF (10.0 mL * 3) and filtered to get the resin. 20% Piperidine in DMF (10.0 mL) was added and agitated the resin with N_2 for another 30 min. The resin was washed with DMF (10.0 mL * 5) and filtered to get the resin. Coupling: A solution of Fmoc-Phe-OH (2.00 eq), DIEA (4.00 eq) and HBTU (1.90 eq) in DMF (5.00 mL) was added to the resin and agitated with N_2 for 30 min at 20 °C. The resin was then washed with DMF (10.0 mL * 3). Deprotection: 20% piperidine in DMF (10.0 mL) was added to the resin and the mixture was agitated with N_2 for 30 min at 20 °C. The resin was then washed with DMF (10.0 mL * 5). Coupling steps were repeated for the following amino acids (**Table 6.1**):

Table 6.1. Coupling reagents used in the synthesis of Ca-DOTAM-DUPA.

#	Materials	Coupling reagents
1	1 ethane-1,2-diamine (3.00 eq)	DIEA (4.00 eq)
2	FMOC-Phe-OH (2.00 eq)	HBTU (1.9 eq) and DIEA (4.00 eq)
3	FMOC-Phe-OH (2.00 eq)	HBTU (1.9 eq) and DIEA (4.00 eq)
4	8-((((9H-fluoren-9-yl)methoxy)carbonyl)amino)octanoic acid (2.00 eq)	HBTU (1.9 eq) and DIEA (4.00 eq)
5	(S)-4-((((9H-fluoren-9-yl)methoxy)carbonyl)amino)-5- (tert-butoxy)-5-oxopentanoic acid (2.00 eq)	HBTU (1.9 eq) and DIEA (4.00 eq)
6	CDI (3.00 eq)	DMAP (3.00 eq)
7	(S)-di-tert-butyl 2-aminopentanedioate (5.00 eq)	DMAP (1.00 eq)

20% piperidine in DMF was used for Fmoc deprotection for 30 min. The coupling reaction was monitored by ninhydrin test, and the resin was washed with DMF for 5 times. After Fmoc deprotection, the resin was washed with DMF (10 mL *3), THF (10 mL *3). Then CDI (486.4 mg, 3.0 eq) and DMAP (366.5 mg, 3.0 eq) was added to the resin and agitated with N_2 for 2 hours at 20 °C in THF (5 mL). The resin was then washed with DMF (10 mL * 3) THF (10 mL * 2). (S)-Di-tert-butyl 2-aminopentanedioate (1.30 g, 5.00 eq) and DMAP (122.1 mg, 1.0 eq) in THF (5mL) was added to the resin and agitated with N_2 for 1 h at 20°C. Cleavage buffer (90% TFA / 2.5% EDT / 2.5% TIS / 2.5% H_2O / 2.5% methylsulfanylbenzene) was added to the flask containing the side chain protected peptide at room temperature and stir for 2.5 hours. The peptide was precipitated with cold tert-butyl methyl ether, filteres, and the filter cake was collected. The filter cake was washed with tert-butyl methyl ether washes two times. The crude peptide was dried under vacuum 2 hours. The crude peptide (0.90 g) was purified by prep-HPLC (A: 0.075% TFA in H_2O, B: ACN) to give the product **Compound 1B** (380 mg) as a white solid.

To a solution of **compound 1B** (118 mg, 1.5 eq) in DMF (5 mL) / H_2O (1 mL), then DIEA was added to adjust pH=9, to get **solution 1**. To a solution of 2-[4,7,10-tris(2-amino-2-oxo-ethyl)-6-[(4-isothiocyanatophenyl)methyl]-1,4,7,10-tetrazacyclododec-1-yl]acetamide- **compound 2A** (60 mg) in DMF (5 mL) and H_2O (1 mL), to get **solution 2**. Then **solution 2** was added into the **solution 1** dropwise. The mixture was stirred at 20 °C for 30 min. The reaction solution was purified by prep-HPLC (A: 0.075% TFA in H_2O, B: ACN) and lyophlized by 0.05% HCl/H_2O again to give the product **compound 3B** (51.8 mg, 36.2 umol, 41.9% yield, 96.6% purity, HCl) as a white solid; m/z: $[M+1]^+$ = 1345.9. To a clear solution of **compound 3B** (20.0 mg, 0.013 mmol, 1.0 eq) in water (0.2 mL) was added calcium acetate hydrate (6.0 mg, 0.034 mmol, 2.5 eq). The reaction mixture was stirred at 25 °C for 5 min. The reaction mixture was dried by lyophilization directly to afford **compound 4A** (16 mg, 99% yield) was obtained as a white solid; m/z: $[M+1]^+$ = 1345.7.

Synthesis of Ca-DOTAM-AAZ

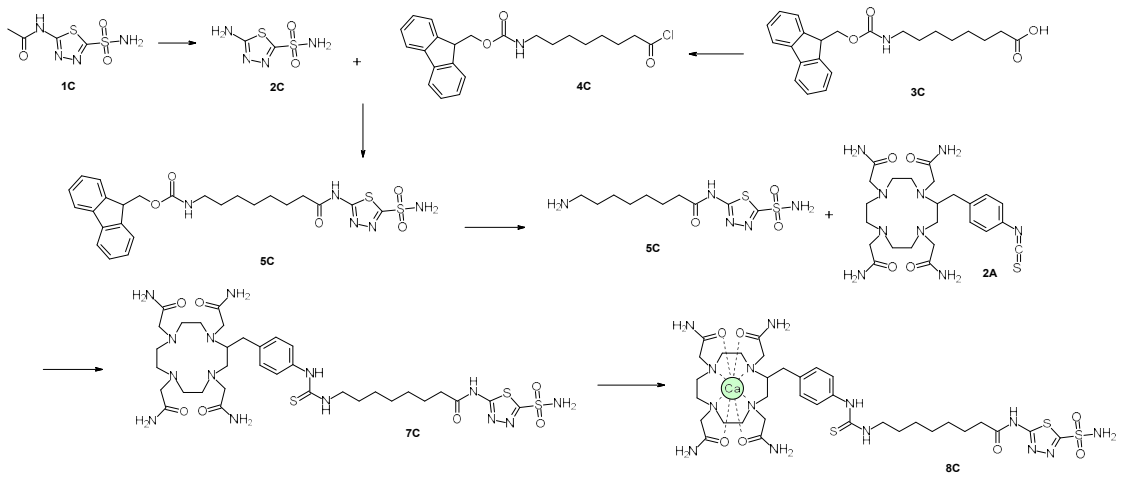

Figure 6.2. Synthesis steps of Ca-DOTAM-AAZ.

The synthesis of Ca-DOTAM-AAZ was planned by Antonio Ricci, and performed at a CRO. The steps are summarized in **Figure 6.2.**

A mixture of **compound 1C** (25 g, 112.49 mmol, 1.00 eq), HCl (12 M, 37.5 mL, 4.00 eq) in ethanol (250 mL) was heated to reflux for 16 hours at 78 °C. The reaction solution was cooled to 30 °C, then concentrated under reduced pressure to remove ethanol. The residue was diluted with H_2O 60 mL, and the mixture was adjusted pH = 7 with saturated $NaHCO_3$ solution. The mixture was filtered and the filtered cake was dried over vacuum to afford **compound 2C** (13 g, 72.14 mmol, 64.1% yield) as white solid. To a solution of **compound 3C** (1.50 g, 3.93 mmol, 1.00 eq) in DCM (10.0 mL) thionyl chloride (523.95 mg, 4.40 mmol, 319.4 uL, 1.12 eq) was added. The solution was cooled to 0 °C. The DMF (114.96 mg, 1.57 mmol, 121.0 uL, 0.40 eq) was added dropwise to mixture. The mixture was stirred at 20 °C for 3 hours. The reaction mixture was concentrated under reduced pressure to remove DCM to get residue. The crude (1.90 g) was used to the next step without further purification. A solution of **compound 2C** (675.94 mg, 3.75 mmol, 1 eq) and pyridine (593.38 mg, 7.50 mmol, 605.5 uL, 2.00 eq) in DMF (5.00 mL) was cooled to 0 °C, then a solution of **compound 4C** (1.50 g, crude) in DCM (10 mL) was added dropwise into the resulting mixture at 0 °C, the mixture was stirred at 25 °C for 12 hours. Water (20.0 mL) was added into reaction solution, and precipitation was formed. The suspension was filtered and the filtered cake was washed with water (5.0 mL *2), then the filtered cake was dry under reduced pressure to afford **compound 5C** (1.60 g, 2.71 mmol, 72.1% yield, 92% purity) as white solid; m/z: $[M+1]^+$ = 544.3. To a solution of **compound 5C** (1.30 g, 2.20 mmol, 92% purity, 1.00 eq) in DMF (8.00 mL) piperidine (1.59 g, 18.62 mmol, 1.84

mL, 8.5 eq) was added. The mixture was stirred at 20 °C for 2 hours. The reaction mixture was concentrated under reduced pressure to remove DMF, the residue was purified by prep-HPLC (NH_4CO_3) to afford **compound 6C** (376 mg, 1.17 mmol, 48.8% yield) as a white solid; m/z: $[M+1]^+$ = 321.9. To a mixture of **compound 6C** (140.85 mg, 0.44 mmol, 1.2 eq) and triethylamine (0.08 mL, 0.55 mmol, 1.5 eq) in anhydrous DMA (5 mL) (dried over 4A MS) **compound 2A** was added (200.0 mg, 0.37 mmol, 1.0 eq) in portions at 25 °C, after addition the reaction mixture was stirred at 25 °C for 16 hours. The reaction mixture was diluted with MTBE (35 ml) and separated by centrifugation. The residual was dissolved in water (3.5 ml) and filtered. The filtrate was purified by prep-HPLC column: Unisil 3-100 C18 Ultra 150*50mm*3 um; mobile phase: [water (FA)-ACN]; B%: 1%-27%, 7min and dried by lyophilization to afford **compound 7C** (150.0 mg, 0.17 mmol, 47.3% yield) as a light yellow solid; m/z: $[M+1]^+$ = 869.9. To a clear solution of **compound 7C** (150.0 mg, 0.17 mmol, 1.0 eq) in water (8 mL) diacetoxycalcium (81.9 mg, 0.52 mmol, 3.0 eq) was added in portions. The reaction mixture was stirred at 25 °C for 2 hours. The reaction mixture was dried by lyophilization directly to afford **compound 8C** (200.0 mg, 0.19 mmol, 99.4% yield) was obtained as a white solid; m/z: $[M+1]^+$ = 907.2.

Synthesis of Ca-DOTAM-Folate

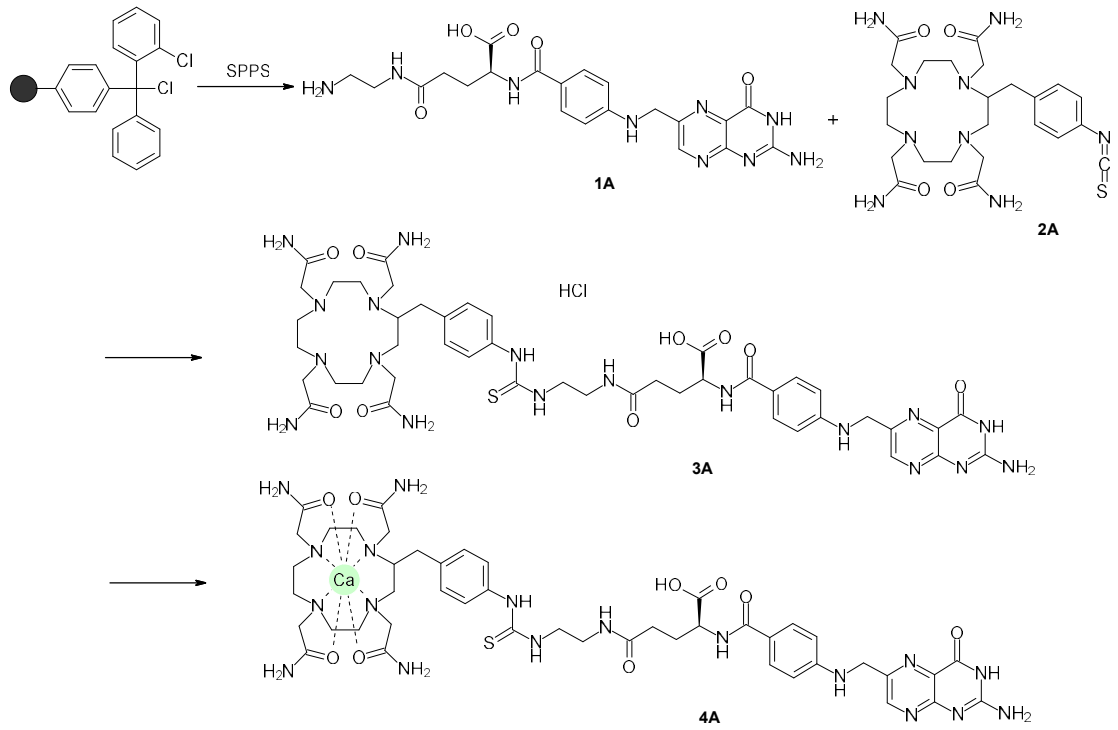

Figure 6.3.Synthesis steps of Ca-DOTAM-Folate.

The synthesis of Ca-DOTAM-Folate was planned by Dr. Dario Venetz (Roche Innovation Center Zurich), Antonio Ricci and Dr. Moreno Wichert (Roche Innovation Center Basel), and performed at a CRO. The steps are summarized in **Figure 6.3**.

The peptide was synthesized using standard Fmoc chemistry. Resin preparation: To the 2-CTC Resin (1.00 mmol, 1.00 eq, Sub 1.00 mmol/g) was added ethane-1,2-diamine (3.00 eq) and DIPEA (4.00 eq) in DCM (10.0 mL) was agitated with N2 for 2 hours at 20 °C. Then added MeOH (1.00 mL) for another 30 min. The resin was washed with DMF (10.0 mL * 3) and filtered to get the resin. Coupling: A solution of Fmoc-Glu-OtBu (2.00 eq), DIEA (4.00 eq) and HBTU (1.90 eq) in DMF (5.00 mL) was added to the resin and agitated with N2 for 30 min at 20 °C. The resin was then washed with DMF (10.0 mL * 3). Deprotection: 20% piperidine in DMF (10.0 mL) was added to the resin and the mixture was agitated with N2 for 30 min at 20 °C. The resin was then washed with DMF (10.0 mL * 5). Coupling: A solution of Pteroic acid (CAS# 119-24-4) (2.00 eq), DIEA (4.00 eq) and HBTU (1.90 eq) in DMSO (10.00 mL) was added to the resin and agitated with N2 for 30 min at 20 °C. The resin was then washed with DMF (10.0 mL * 3) and MeOH (10.0 mL * 3). The peptide resin was dried under vacuum and get 1.6 g.

Cleavage buffer (90% TFA / 2.5% EDT / 2.5% TIS / 2.5% H2O / 2.5% methylsulfanylbenzene) 16 mL was added to the flask containing the peptide resin (1.6 g) at room temperature and stir for 2.5 hours. The molecule was precipitated with cold tert-butyl methyl ether, filtered, and filter cake was collected. The cake was washed wit tert-butyl methyl ether two more times. The crude peptide was dried under vacuum for 2h. The crude peptide (0.50 g) was purified by prep-HPLC (A: 0.075% TFA in H2O, B: ACN) to give the compound 1A (180 mg, TFA salt) as a white solid. To a solution of compound 1A (105 mg, 1.5 eq) in DMSO (5 mL) and H2O (1 mL), then DIEA was added to adjust pH=9, to get solution 1. To a solution of 2-[4,7,10-tris(2-amino-2-oxo-ethyl)-6-[(4-isothiocyanatophenyl)methyl]-1,4,7,10-tetrazacyclododec-1-yl]acetamide-compound 2A (100 mg, , 1.0 eq) in DMSO (5 mL) and H2O (1 mL), to get solution 2. Then solution 2 was added into the solution 1 dropwise. The mixture was stirred at 20 °C for 30 min. The reaction was monitored by LCMS, and purified directly after the main peak was observed to be the desired m/z. The reaction solution was purified by prep-HPLC (A: 0.05% HCl in H2O, B: ACN) and lyophilized to give the product compound 3A (50.5 mg, 48.9 µmol, 33.9% yield, 94% purity, HCl salt) as a yellow solid; m/z: [M+1] + = 1031.7. To a clear solution of compound 3A (20.0 mg, 0.016 mmol, 1.0 eq) in water (0.2 mL) was added calcium acetate hydrate (7.0 mg, 0.04 mmol, 2.5 eq). The reaction mixture was stirred at 25 °C for 5 min. The reaction mixture was dried by lyophilization directly to afford compound 4A (16.2 mg, 99% yield) was obtained as a white solid; m/z: [M+1] + = 1069.4.

Antibody synthesis

The antibody production was performed by teams at Roche Innovation Center Zurich, by a CRO, or by the thesis author.

Antibodies were synthesized with Roche internal or CRO external technology *via* transient transfection in HEK-293T cells, followed by triple purification process and sterilization. Quality control process included liquid chromatography-mass spectrometry protein identification, purity control, endotoxin quantification and concentration determination. The antibodies were stored in sterile 20 mM Histidine, 140 mM NaCl, pH 6.0 buffer.

SM-TCB complexing

Ca-DOTAM-Ligands (SM) and DOTAM-TCBs were mixed in in protein buffer (20mM Histidine, 140mM Sodium chloride, pH 6.0) at the molar ratio of SM:TCB of 4:1 or 100:1. Then the mix was incubated for 1h at RT at a laboratory tube carousel. Subsequently, the preparations were purified by Amicon Ultra Centrifugal Filter, 30 kDa MWCO (Milipore # UFC5030) according to manufacturer's protocol. The protein concentration was measured by a Dropsense spectrophotometer (Trinean #100382).

6.2. Analytical and biochemical methods

KinExA binding measurement

Polymethylmethacrylate (PMMA) beads (Sapidyne Instruments #440176) were absorption coated according to the KinExA Handbook protocol for biotinylated molecules (Sapidyne Instruments). Briefly, 10 µg of Biotin-BSA (Sigma #A8549) in 1 ml PBS pH7.4 (Roche #11666789001) was added per vial (200 mg) of beads. After rotating for 2 h at RT, the supernatant was removed and beads were washed 5x with 1 ml of PBS. Then, 1 ml of 100 µg of NeutrAvidin Biotin-Binding Protein (Thermo Scientific #31000) in PBS containing 10 mg/ml BSA (Sigma-Aldrich # A2153) was added to the beads and incubated at RT for additional 2 h. The NeutrAvidin-coated-beads were then rinsed 5x with 1 ml PBS. Finally, the beads were coated with 200 ng/ml biotinylated Pb-DOTAM-Isomer Mix (50 ng for each Isomer) (Roche-in house) in PBS and incubated for further 2h at RT. Beads were then resuspended in PBS and used immediately.
All KinExA experiments were performed at RT using PBS pH 7.4 as running buffer. Samples were prepared in running buffer supplemented with 1 mg/ml BSA as sample buffer. A flow rate of 0.25 ml/min was used. For Ca-DOTAM, Ca-DOTAM-folate and Ca-DOTAM-DUPA, a constant amount of anti-DOTAM antibodies - DOTAM-TCBs (200 pM and 1 pM) was titrated with antigen by twofold serial dilution starting at 2 nM for 200 pM anti-DOTAM antibody (concentration range 0.97 – 2000 pM) and 100pM for 1 pM anti-DOTAM antibodies - DOTAM-TCBs (0.048 -100 pM). One sample of antibody without antigen served as 100% signal (i.e. without inhibition). Antigen–antibody complexes were incubated at RT for 24 - 72h to allow equilibrium to be reached. Equilibrated mixtures were then drawn through a column of Pb-

DOTAM-coupled beads in the KinExA system permitting unbound antibody to be captured by the beads without perturbing the equilibrium state of the solution. Captured antibody was detected using 250 ng/ml AF647-conjugated anti-human Fc antibody (Jackson #109-605-097) in sample buffer. Each sample was measured in duplicates for all equilibrium experiments. KinExA data were analyzed with the KinExA software (Version 4.2.14) using the "standard analysis" method. The software calculated the K_D and determined the 95% confidence interval by fitting the data points to a theoretical K_D curve. The 95% confidence interval was given as K_D low and K_D high. For the final K_D determination, an n-curve analysis of at least 2 measurements using different constant anti-DOTAM antibody concentrations was performed. This global analysis is used to analyze multiple standard K_D experiments on the same axis to obtain a more accurate determination of the K_D.

SPR: TCB-SM complexes binding to their respective receptors

SPR experiments were performed on a Biacore T200 at 25 °C with HBS-EP as running buffer (Cytiva #BR100669). An anti-P329G antibody (Roche, in house) was directly coupled on a CM3 sensor chip (Cytiva #BR100536) at pH 5.0 using the standard amine coupling kit (Cytiva #BR100050). The immobilization level was approximately 300 RU.
The complexes of Ca-DOTAM-AAZ with DOTAM-TCB 1+1 were captured for 60 seconds at 15 nM. The recombinant human CAIX homodimer, Fc Tag (Sino Biologicals #10107-h02h) was passed at a concentration range from 0.41 to 33 nM with a flow rate of 30 µL/min through the flow cells over 240 seconds. The other molecules tested were: FOLR1-TCB 2+1 or a complex of Ca-DOTAM-Folate with DOTAM-TCB 1+1 for FOLR1 binding, or PSMA-TCB 2+1 or a complex of Ca-DOTAM-DUPA with DOTAM-TCB 1+1 for PSMA binding, and empty DOTAM-TCB 1+1 as negative control. The molecules were captured for variable contact times at 15 nM. The recombinant human PSMA homodimer Avi-Biot Fc tag (Roche, in house) or the recombinant human FOLR1 monomer Avi-Biot Fc tag (Roche, in house) were passed at the concentration of 300 nM with a flow rate of 30 µL/min through the flow cells over 240 seconds.
The dissociation was monitored for 600-1500 s. The chip surface was regenerated after every cycle using two injections of 10 mM Glycine pH 2.0 for 60 s each. Bulk refractive index differences were corrected by subtracting the response obtained on a reference flow cell. The affinity constant was not calculated due to the dimeric form of the analyte.

SPR: FcγRIIIa binding to P329X IgG variants

SPR experiments were performed on a Biacore T200 at 25 °C with HBS-EP as running buffer (Cytiva #BR100669). An anti-His IgG antibody (Qiagen #34650) was directly coupled on a CM3 sensor chip (Cytiva #BR100536) at pH 5.0 using the standard amine coupling kit (Cytiva #BR100050). The immobilization level was approximately 6500 RU. Subsequently, 1 M ethanolamine was injected to block unreacted groups. The His-FcγRIIIa (Roche, in-house) was captured at 10 nM with a flow rate of 30 µL/min through the flow cells for 60 s. The P329X IgG variants or controls were captured sequentially at 150 nM, 300 nM and 600 nM with a flow

rate of 30 µL/min through the flow cells 90 s each. The dissociation was monitored for 65 s. The chip surface was regenerated after every cycle using two injections of 10 mM Glycine pH 1.5 for 65 s each. Bulk refractive index differences were corrected by subtracting the response obtained on a reference flow cell.

SPR: anti-P329G binding to P329X IgG variants

SPR experiments were performed on a Biacore T200 at 25 °C with HBS-EP as running buffer (Cytiva #BR100669). An anti-P329G antibody (Roche, in house) was directly coupled on a CM3 sensor chip (Cytiva #BR100536) at pH 5.0 using the standard amine coupling kit (Cytiva #BR100050). The immobilization level was approximately 1200 RU. The P329X IgG variants or controls were captured at 500 nM with a flow rate of 10 µL/min through the flow cells over 240 seconds. The dissociation was monitored for 800 s. The chip surface was regenerated after every cycle using two injections of 10 mM Glycine pH 2.1 for 60 s each. Bulk refractive index differences were corrected by subtracting the response obtained on a reference flow cell.

ELISA with SM spike

For ELISA, streptavidin-coated plates (Roche #604192) were coated with either biotinylated recombinant human PSMA (R&D Systems #AVI4234-025) at 12 nM or biotinylated recombinant human CAIX (MedChemExpress #HY-P72348-20uG) at 12 nM, diluted in 15% SuperBlock Blocking Buffer (Thermo #37515), by incubation for 1h at RT. The plates were then washed 3x with PBST buffer (Roche, in-house). Serial dilutions of the analytes (empty TCB or SM-TCB complexes, starting from 10 nM) were prepared in 15% Superblock. In case of SM spike, the analytes were mixed with constant concentration of SM (144 nM) to provide excess SM. The molecule dilutions were mixed, added to the plates, and incubated for 2h at RT. The plates were washed 3x with PBST buffer. Digoxin-fusion anti-huFc (Roche, in-house) was diluted 1:50 000 in 15% Superblock and added to the plate, followed by 1h incubation at RT. After 3 washes with PBST buffer, POD anti-Dig antibody (Roche #11633716001) was diluted in 15% Superblock (1:2000 dilution) and added to the wells. The plates were incubated for 1h at RT. After 3 washes with PBST buffer, the POD substrate (Roche #55198300) was added to the wells. The plates were shaken to achieve substrate distribution and were incubated for 20 min at RT. The readout consisted of calculated OD_{405} – OD_{490} measurements at the TECAN EVO machine (Tecan, custom).

Native Size Exclusion Chromatography-Mass Spectrometry (native SEC-MS)

Protein samples were prepared in a native buffer containing 100 mM Sodium phosphate, pH 7.1, at 1 mg/mL and were deglycosylated for 16h with PNGase F (Promega #V4831) at 37°C in a thermocycler at 400 rpm. Native size exclusion chromatography was performed on a Vanquish Horizon UPHLC system (Thermo Scientific #IQLAAAGABHFAPUMZZZ) and a high-

resolution SEC column (Acquity Premier Protein SEC, 250 Å, 1.7 µm, 4.6 x 300 mm (Waters #PN186009964) equilibrated with the native mobile phase (200 mM ammonium acetate, pH 5.4). The column was maintained at a constant temperature of 25°C. A flow rate of 0.25 ml/min was used, and the injection volume was 5 µL. The chromatography system was coupled to a mass spectrometer through a nano electrospray ionization (ESI) source. To obtain the required low flow rate for nano-ESI the eluting flow from the UHPLC system is splitted at ratio 1:100. The MS instrument used was a Q Exactive UHMR Mass Spectrometer (Thermo Scientific #0726090). The mass spectrometer was operated in positive ion mode with a capillary voltage of 2.1 kV. The source temperature was set to 250°C. The mass range was set to m/z 350-15000 to capture the intact mass of the protein complexes. The standard method involved desolvation/fragmentation step with the in-source CID of 30.0 eV and IST desolvation of -175. The soft method involved desolvation/fragmentation step with the in-source CID of 20.0 eV and IST desolvation of -25.

SDS-PAGE and Western blot

The molecules were mixed with either PBS (Gibco #10010023) or 5.3 nM recombinant matriptase thawed on ice (Enzo #50-200-7957) in pH 9.0 matriptase buffer (Roche, internal) and incubated overnight at RT. Subsequently, the samples were reduced and analyzed via SDS-PAGE followed by Coomassie staining or by Western blot according to Invitrogen NuPAGE Technical guide (Invitrogen #IM-1001). The Western blot staining was done by either directly by an anti-huFc HRP (Sigma #A0170) or by a murine anti-PG antibody (Roche, internal) followed by anti-murine IgG HRP (Jackson # 515-035-062). The image acquisition was performed with BioRad ChemiDoc MP machine.

6.3. Structural analysis

X-Ray crystallography

For crystallization, the anti-DOTAM Fab fragment, with the sequence derived from the DOTAM-TCB, was concentrated to 28.7 mg/mL. The Ca-DOTAM-AAZ compound was dissolved in DMSO and added to the Fab fragment solution in a molar excess of 1.5:1. The mix was incubated for 3h on ice. Crystallization trials were performed in sitting drop vapor diffusion setups at 21 °C using a JCSG+ screen (Qiagen). Spherulites appeared within 1 day out of various screening conditions. Plate type clusters grew within 20 days out of 0.1 M Tris pH 8.5, 20 %w/v PEG 1000 and 0.2 M $MgCl_2$. These clusters were crushed into micro crystals and used in fresh crystallization setups as nucleation seeds. With seeding three dimensional crystals could be obtained out of 0.1 M KSCN and 30% w/v PEG MME 2000.
For data collection, the crystals were flash-cooled at 100K with 20 % ethylene glycol (VWR #BDH1125-4LG) added as a cryo-protectant. X-ray diffraction data were collected at a wavelength of 1.0005 Å using an Eiger2X 16M detector (Dectris) at the beamline X10SA of the

Swiss Light Source (Villigen, Switzerland). Data were processed with XDS (MPI for Medical Research) and scaled with SADABS software (Bruker). The crystals belong to space group $P2_12_12_1$ with cell axes of a= 56.18 Å, b= 66.64 Å, c= 105.56 Å and diffract to a resolution of 1.45 Å. The structure was determined by molecular replacement with Phaser software (University of Cambridge) using the coordinates of an in-house Fab fragment structure as a search model. Difference electron density was used to place the compound Ca-DOTAM-AAZ. The Ca-DOTAM moiety of the compound was well defined, whereas no electron density could be observed for the remaining part of the compound. The structure was refined with programs from the CCP4 suite (Rutherford Appleton Laboratory). Manual rebuilding was done with Coot software (University of Oxford).

6.4. Cell-based biological assays

Cell lines and cell culture

Cell lines were ordered from an internal Roche cell biorepository (previously derived from ATCC, DSMZ, Promega or academic/industrial collaborators), and cultured according to ATCC or DSMZ protocols, without antibiotics.

Assay medium

Assay media used in all functional *in vitro* and *ex vivo* experiments consisted of sterile RPMI 1640 with GlutaMAX (Gibco #61870036), 10% FBS (Sigma-Aldrich #F2442), 1x NEAA (Gibco #11140050) and 1mM NaPyr (Gibco # 11360070).

Binding assay

Tumor cells from selected cell lines were harvested with TrypLE Express Enzyme (Gibco #12605010), and washed 2x with assay media. Subsequently, the cells were plated at 0.100 x 10^6 cells/well in a U-bottom clear 96-well plate (TPP #92097). Next, the molecules (premixed small molecule adaptors and effector molecules) were added to the plate at 100 nM each. The assay components were incubated for 1h at 37°C and 5% CO_2. After the incubation time, the cells were washed 1x with assay media and 2x with FACS buffer (Roche, in-house). Then, the cells were stained with the secondary PE- or £AF647-conjugated anti-P329G antibody (Roche, in house) diluted in FACS buffer (Roche, in house), and incubated for 20 min at RT. The cells were washed 3x with FACS buffer, resuspended in FACS buffer, and acquired at BD FACSymphony A5 (BD, custom) or BD LSRFortessa (BD, custom). The flow cytometry data was analyzed using Flowjo software.

Human PBMC and pan T Cell isolation

Healthy human donor buffy coats were sourced from Blutspende Zürich SRK. PBMCs were isolated via a standard protocol by Lymphoprep (STEMCELL #07851). Pan T cells were isolated

either from PBMCs with the Pan T Cell Isolation Kit, human (Miltenyi #130-096-535) or directly from buffy coats by RosetteSep Human T Cell Enrichment Cocktail (STEMCELL #15061).

Jurkat reporter assays

Tumor cells from selected cell lines were plated at 0.002 x 10^6 cells/well in a flat-bottom, white-walled clear bottom 384-well-plate (Corning #3826) in assay medium one day before the assay. In case of P329G-pro-TCB and control antibodies, the molecules were mixed with either PBS (Gibco #10010023) or 5.3 nM recombinant matriptase thawed on ice (Enzo #50-200-7957) in protein buffer (20mM Histidine, 140mM Sodium chloride, pH 6.0) and incubated overnight at RT. On the assay day, Jurkat reporter cells - Jurkat CD3/NFAT (Promega #CS176501), Jurkat FcγRIII (Promega, custom cell line), or Jurkat NFκB (Promega, custom cell line) were plated in assay medium to obtain a final effector-to-target cell ratio (E:T) of 5:1. Subsequently, diluted molecules were added to the assay plate to obtain a final volume of 40 µl. The adaptors and effector molecules were premixed before addition, with the exception of cross-titration assays with separate administration to the assay plates. The assay components were incubated for 5-6h at 37°C and 5% CO_2. After the incubation time, 40 µl of a luciferase substrate, ONE-Glo Luciferase Assay reagent (Promega #E6120) was used, allowing for a measurement of relative luminescence units (RLU). Readout was performed using a Tecan Spark 10M reader. The luminescent signal was acquired for 300 ms/well, and calculated to reflect RLU/s per well.

Jurkat CD3/NFAT reporter assay with SM/TCB spike

HT-29 cells were plated at 0.002 x 10^6 cells/well in a flat-bottom, white-walled clear bottom 384-well-plate (Corning #3826) in assay medium one day before the assay. On the assay day, Jurkat CD3/NFAT (Promega #CS176501) reporter cells were plated in assay medium to obtain a final effector-to-target cell ratio (E:T) of 5:1. The molecules were prepared in a serial dilution. For SM or TCB spiking, the serial dilutions were mixed with a constant concentrations of either Ca-DOTAM-AAZ or DOTAM-TCB 2+1 to achieve a final assay concentration of 100 nM and 1 nM, respectively. The diluted molecules were added to the 384 well plate to obtain a final volume of 40 µl. The assay components were incubated for 5-6h at 37°C and 5% CO_2. After the incubation time, a luciferase substrate, ONE-Glo™ Luciferase Assay reagent (Promega #E6120) was used according to the manufactures protocol, allowing for a measurement of relative luminescence units (RLU). Readout was performed using a Tecan Spark 10M reader. The luminescent signal was acquired for 300 ms/well, and calculated to reflect RLU/s per well.

pSTAT5 assay

For T cell preactivation to induce PD1 expression, 6-well plates were coated with 1 µg/ml of anti-human CD3 antibody (Biolegend #317325) diluted in PBS (Gibco #10010023) overnight at 4°C. Next, PBS solution was carefully removed, 4 ml/well of healthy donor PBMCs were added

to the wells in assay media at 2.5 x 106 cells/ml and 1 µg/ml of soluble anti-human CD28 antibody (Biolegend #302933). The cells were incubated for 4-5 days at 37°C and 5% CO2. Cells were pooled and washed 2x with assay media. Next, the cells were resuspended in fresh assay media and rested for 3-4h in 37°C and 5% CO2, to remove residual IL2 signaling. Then, the cells were washed 2x with assay media and and plated in a V-bottom 96-well plate (#NUMBER) at the final number of 0.350 x 106 cells/well in assay media. Subsequently, the adaptor IgGs were added into all wells, and the assay components were incubated for 30 min at room temperature. The cells were then washed 2x with assay media. Assay media containing IL2v fusion molecules and Human TruStain Fc Receptor Blocking Solution (Biolegend #422302) was added to all wells simultaneously. The assay components were incubated for 12 min at 37°C and 5% CO2. The IL2 signaling was stopped by the addition of 37°C-prewarmed BD Cytofix Fixation buffer (BD #554655) simultaneously to all wells, followed by a 30 min incubation at 37°C and 5% CO2. The cells were subsequently washed 2x with FACS buffer (Roche, in-house), and resuspended in 4°C-precooled BD Phosflow Perm Buffer III (BD #558050). The cells were incubated overnight at -20°C. The cells were washed 2x with FACS buffer, and were stained with surface and intracellular markers simultaneously. The staining panel consisted of Phosflow protocol-compatible antibodies a-CD3 in FITC (Biolegend #300406), a-CD4 in APC (Biolegend #300537), a-CD8a in PerCP/Cy-5.5 (Biolegend #344710) not competing with internal anti-CD8 binder, and anti-pSTAT5 in PE (BD #562077), diluted in FACs buffer, and incubated with cells for 30 min at 4°C. The cells were washed 2x with FACS buffer, resuspended in FACS buffer, and acquired at BD FACSymphony A5 (BD, custom) or BD LSRFortessa (BD, custom). The flow cytometry data was analyzed using Flowjo software.

Incucyte imaging

NLR-expressing tumor cells from selected cell lines were plated at 0.005 x 10^6 cells/well in a flat-bottom, transparent 96-well plate (TPP #92696) or 384-well-plate (Corning #3701) in assay medium one day before the assay. On the assay day, human pan T cells from healthy donors were plated in assay medium to obtain a final effector-to-target cell ratio (E:T) of 5:1. Subsequently, diluted antibodies were added to the plate. The assay components were places into an incubator containing Sartorius Incucyte S3 system (Sartorius, custom), and incubated for 5-7 days at 37°C and 5% CO_2. Bright-field and red fluorescence imaging of all wells were obtained at 4h intervals. Readout and data analysis, including quantification of NLR-containing cells was performed in Sartorius Incucyte software.

Killing assay: cytotoxicity, cytokine release and T Cell activation

Tumor cells from selected cell lines were plated at 0.012 x 10^6 cells/well in a flat-bottom, white-walled clear bottom 384-well-plate (Corning #3826) in assay medium one day before the assay. In case of P329G-pro-TCB and control antibodies, the molecules were mixed with either PBS (Gibco #10010023) or 5.3 nM recombinant matriptase thawed on ice (Enzo #50-200-7957) in protein buffer (20mM Histidine, 140mM Sodium chloride, pH 6.0) and incubated overnight at RT. On the assay day, either PBMCs or pan T cells from healthy donors were used.

The cells were plated in assay medium to obtain a final effector-to-target cell ratio (E:T) of 10:1 for human PBMCs or 5:1 for human pan T cells. Subsequently, diluted small molecules or antibodies (adaptors and effector molecules premixed, except for cross-titration experiments) were added to the assay well plate. The assay components were incubated for 48h-72h at 37°C and 5% CO2. After the incubation time, supernatant was collected for cytotoxicity readout and cytokine readout, and the cells were harvested for flow cytometry staining.

Cytotoxicity representing dead cell proteases was measured with a Cytotox-Glo kit (Promega #G9291), according to manufacturer's protocol, and read with a Tecan Spark 10M reader. The luminescent signal was acquired for 300 ms/well, and calculated to reflect RLU/s per well. Cytokine release was assessed by Bio-Plex Pro Human Cytokine 8-plex Assay (Bio-Rad #M50000007A), and read with Bio-Plex 200 System (Bio-Rad #171000205). T cell activation was assessed by harvesting and washing the cells with PBS (Gibco #10010023), followed by a Live/Dead staining with Zombie Aqua (Biolegend #423102) for 20 min at RT. The cells were washed 2x with PBS and, in case of using PBMCs, resuspended in FACS buffer containing Human TruStain Fc Receptor Blocking Solution (Biolegend #422302) followed by a 15 min incubation at RT. Subsequently, the cells were stained for 20 min at RT in FACs buffer containing the following antibodies: a-CD4 in PerCP/Cy5.5 (Biolegend #317428), a-CD8a in BV711 (Biolegend #301044), a-CD25 in PE (Biolegend #302606) and a-CD69 in FITC (Biolegend #310904). The cells were washed 3x with FACS buffer, resuspended in FACS buffer, and acquired at BD FACSymphony A5 (BD, custom) or BD LSRFortessa (BD, custom). The flow cytometry data was analyzed using Flowjo software.

6.5. *In vivo* and *ex vivo* experimental methods

Histology staining of tumor samples from mouse studies

The tumors were collected from mice after sacrifice, and fixed in 4% paraformaldehyde (Thermo # J60401.AK) overnight. Then, the tumors were embedded in paraffin with a Sakura VIP6 AI tissue processor (Sakura # 6040). Paraffin sections (3 µm) were prepared using a microtome (Leica #RM2235). Immunohistochemistry was performed on paraffin sections with either a standard H&E protocol, using Mayer's hematoxylin solution (Biosystems #3870.2500) and eosin 2% (Biosystems #84-0023-00), or with an anti-human CD3 antibody (Diagnostic Biosystems @RMAB005), or with an anti-human CAIX antibody (Cell Signaling #5649) in the Leica Autostainer platform (Leica #ST5010) following the manufacturer's instructions. Images were captured with the slide scanner (Olympus #VS200).

In vivo efficacy study – P329G-TCB

Humanized NSG mice were purchased from the Jackson Laboratory. The study protocol was approved by The Institutional Animal Care and Use Committee of Roche Innovation Center

Zurich as well as the Cantonal Veterinary Office of Zurich under the Veterinary License ZH 180/2020 in agreement with The Swiss Animal Welfare Act. The MKN-45 cell line was ordered from a Roche internal cell bank, and expanded according to DSMZ culture protocol (DSMZ #ACC 409). The cells were authenticated and tested (negative) for pathogens and mycoplasma. On the inoculation day, the cells were harvested with TrypLE Express Enzyme (Gibco #12605036), and mixed with Matrigel (Corning #354230) on ice, in the volume ratio 1:1 to achieve the concentration of 1 x 10^6 cells in 100 µl. The cells were injected subcutaneously into the shaved left flank in the volume of 100 µl per mouse. Body weight was measured 3 times per week, and tumor growth was measured 3 times per week by calipers. Upon reaching a median tumor volume of 110 mm^3, the mice were randomized into treatment groups. The next day, the treatments were initiated. In each treatment cycle, groups with 5mg/kg of adaptor CEACAM5 IgG in protein buffer (20mM Histidine, 140mM Sodium chloride, pH 6.0) were injected intravenously, followed by a 24h window, and intravenous injection of other treatments (protein buffer as vehicle or 0.5 mg/kg of effector molecules). At scout time point, representative mice were anesthetized, and blood was collected by retro-orbital bleeding into heparin tubes (Sarstedt #41.1503.015). The scout mice were sacrificed, and tumors and spleens were collected in PBS (Gibco #10010023) and stored at 4 °C.

In vivo efficacy study – DOTAM-TCB

Humanized BRGS-CD47 mice were purchased from the Jackson Laboratory. The study protocol was approved by The Institutional Animal Care and Use Committee of Roche Innovation Center Zurich as well as the Cantonal Veterinary Office of Zurich under the Veterinary License ZH 180/2020 in agreement with
The Swiss Animal Welfare Act. The HT-29 cell line was ordered from an internal cell bank, and expanded according to ATCC culture protocol (ATCC #HTB-38). The cells were authenticated and tested (negative) for pathogens and mycoplasma. On the inoculation day, the cells were harvested with TrypLE Express Enzyme (Gibco #12605036), and mixed with Matrigel (Corning #354230) on ice, in the volume ratio 1:1 to achieve the concentration of 2 x 10^6 cells in 100 µl. The cells were injected subcutaneously into the shaved left flank in the volume of 100 µl per mouse. Body weight was measured 3 times per week, and tumor growth was measured 3 times per week by calipers. Upon reaching a median tumor volume of 125 mm^3, the mice were randomized into treatment groups and the treatments were initiated. In a treatment cycle, groups with 0.45 mg/kg of adaptor Ca-DOTAM-AAZ in protein buffer (20mM Histidine, 140mM Sodium chloride, pH 6.0) were injected intraperitoneally, followed by a 2h time window, followed by intravenous injection of other treatments (protein buffer as vehicle or 5.0 mg/kg of effector molecules).

Ex vivo co-culture assay

Humanized BRGD-CD47 mice were purchased from the Jackson Laboratory. The study protocol was approved by The Institutional Animal Care and Use Committee of Roche Innovation Center Zurich as well as the Cantonal Veterinary Office of Zurich under the

Veterinary License ZH 177/2020 and in accordance with the Swiss Animal Welfare Act. The HT-29 cell line was ordered from an internal cell bank, and expanded according to ATCC culture protocol (ATCC #HTB-38). The cells were authenticated and tested (negative) for pathogens and mycoplasma. On the inoculation day, the cells were harvested with TrypLE Express Enzyme (Gibco #12605036), and mixed with Matrigel (Corning #354230) on ice, in the volume ratio 1:1 to achieve the concentration of 2 x 10^6 cells in 100 µl. The cells were injected subcutaneously into the shaved left flank in the volume of 100 µl. Body weight was measured 2-3 times per week, and tumor growth was measured 2-3 times per week by calipers. Upon reaching a tumor volume of ~400 mm^3, the scout mouse was sacrificed, and tumor was collected in PBS (Gibco #10010023).

The tumor was cut into small pieces and placed in the RPMI 1640 (Gibco # 11875093) containing 50x diluted collagenase D (Roche #11088882001) and 200x diluted DNAse I (Sigma Aldrich #10104159001). The suspension was placed inside gentleMAC C Tubes (Miltenyi #130-093-237), followed by dissociation in the gentleMAC Octo Dissociator with Heaters (Miltenyi #130-096-427). Next, the cells were strained through MACS SmartStrainers 100 µm (Miltenyi #130-098-463), and washed 3x with assay media.

Subsequently, the single cell suspension of the tumor cells was prepared in assay media + 1x Penicillin-Streptomycin (Gibco # 15140122), and was plated at 0.030 x 10^6 cells/well in a U-bottom clear 96-well plate (TPP #92097). As effector cells, PBMCs from two healthy human donors were plated to obtain a final effector-to-target cell ratio (E:T) of 10:1. Subsequently, molecules (premixed adaptors and effector molecules or direct molecules) were added to the plate to obtain a final volume of 200 µl. The assay components were incubated for 48h at 37°C and 5% CO_2.

T cell activation was assessed by harvesting and washing the cells with PBS (Gibco #10010023), followed by a Live/Dead staining with Zombie Aqua (Biolegend #423102) for 20 min at RT. The cells were washed 2x with PBS and, in case of using PBMCs, resuspended in FACS buffer containing Human TruStain Fc Receptor Blocking Solution (Biolegend #422302) followed by a 15 min incubation at RT. Subsequently, the cells were stained for 20 min at RT in FACs buffer containing the following antibodies: a-CD4 in PerCP/Cy5.5 (Biolegend #317428), a-CD8a in BV711 (Biolegend #301044), a-CD25 in PE (Biolegend #302606) and a-CD69 in FITC (Biolegend #310904). The cells were washed 3x with FACS buffer, resuspended in FACS buffer, and acquired at BD FACSymphony A5 (BD, custom) or BD LSRFortessa (BD, custom). The flow cytometry data was analyzed using Flowjo software.

Scout *ex vivo* digestion and staining of blood, tumor and spleen samples

The tumors were cut into small pieces and placed in the RPMI 1640 (Gibco # 11875093) containing 50x diluted collagenase D (Roche #11088882001) and 200x diluted DNAse I (Sigma Aldrich #10104159001). The suspension was placed inside gentleMACS C Tubes (Miltenyi

#130-093-237), followed by dissociation in the gentleMAC Octo Dissociator with Heaters (Miltenyi #130-096-427). Next, the cells were strained through MACS SmartStrainers 100 µm (Miltenyi #130-098-463), and washed 3x with assay media. The spleens were placed on MACS SmartStrainers 100 µm (Miltenyi #130-098-463) and smashed with syringe pistons (BD #309658), followed by flushing the strainer with 20 ml of FACS buffer (Roche, in-house). The cell suspension was washed 1x, and each pellet was resuspended in 3 ml of 1x BD Pharm Lyse (BD #555899) lysis buffer, and incubated for 3 min at RT. The cells were then washed 1x with FACS buffer. Blood samples were mixed with 3 ml of 1x BD Pharm Lyse (BD #555899) lysis buffer, and incubated for 3 min at RT, and washed 3x with FACS buffer. Cells from all organs were placed in a U-bottom 96-well plate (TPP #92097), and were washed with PBS (Gibco #10010023), followed by a Live/Dead staining with Fixable Blue Dad Cell Stain Kit (Invitrogen #L23105) for 20 min at RT. The cells were washed 2x with PBS and, in case of using PBMCs, resuspended in FACS buffer containing Human TruStain Fc Receptor Blocking Solution (Biolegend #422302) followed by a 15 min incubation at RT. Subsequently, the cells were stained for 30 min at 4°C in FACS buffer containing the following antibodies: AF700 anti-human CD45 (Biolegend #368514), BV605 anti-human CD3 (Biolegend #317322), BV737 anti-human CD8 (BD Horizon #612754), APC-Cy7 anti-human CD4 (Biolegend #317418), BV421 anti-human CD69 (Biolegend #310930), PE-Dazzle 594 anti-human CD25 (Biolegend #356126), BV510 anti-human PD-1 (Biolegend #367424), BV711 anti-human TIM3 (Biolegend #345024), PE-Cy5 anti-human CD127 (Biolegend #351324). Next, the cells were washed 3x with FACS buffer, followed by permeabilization and intracellular staining procedure using eBioscience Foxp3 / Transcription Factor Staining Buffer Set (Invitrogen #00-5523-00). The cells were stained with AF647 anti-human FOXP3 (Biolegend #320014), PE anti-human GrB (BD Pharmigen #561142), PE-Cy7 anti-human Ki67 (Biolegend #350526) according to manufacturer's protocol. After the final wash, the cells were resuspended in FACS buffer and acquired at BD FACSymphony A5 (BD, custom) or BD LSRFortessa (BD, custom). The flow cytometry data was analyzed using Flowjo software.

6.6. Data analysis methods

Data visualization

Raw data from all experiments were plotted using Tibco Spotfire for Roche pRED 13&14 coupled with Microsoft Excel 2016, or using GraphPad Prism 10.2.3. Non-linear regression curves were calculated and drawn either in Tibco Spotfire or GraphPad Prism. Molecule and cell pictograms were created in Biorender.com.

Statistical analysis

Statistical analysis was performed with GraphPad Prism 10.2.3. For dose response curves, area under the curve values were calculated from two to three technical triplicates and one to three biological replicates (PBMC/T cell donors or separate experiments). For protease-activated molecules, area under the curve values were calculated to obtain fold-change to area under the curve values of non-binding, non-protease-activated controls. The values were statistically analyzed by paired one-way ANOVA with either Dunnett's multiple comparison test for comparison to one control group, or Tukey's multiple comparison test for comparison between all groups. Experiments with time and dose variables with multiple groups were analyzed with unpaired two-way ANOVA with Tukey's multiple comparison test. P values in the figures were represented by the following: *$p<0.05$, **$p<0.01$, ***$p<0.001$ and ****$p<0.0001$.

7. Results

7.1. Chapter 1 – P329G-Engager: A novel universal antibody-based adaptor platform for cancer immunotherapy

Universal P329G immune cell engagers show proof of concept activity across tumor and immune targets

In the first step, a P329G-targeting T cell bispecific antibody (P329G-TCB) was generated, comprising two humanized anti-P329G Fabs and one humanized anti-CD3ε Fab (format termed TCB 2+1) in a huIgG1 subclass. The detailed design of this T cell engager is based on the design of the recently approved CD20-TCB glofitamab [64], [366]. The silencing mutations introduced to the Fc consisted of L234A and L235A (termed LALA). The P329G binder sequence was derived from previously published work describing a P329G CAR-T cell [246]. For ensuring correct chain assembly, CrossMab format [90], as well as knobs-into-holes [86] technology were utilized.

To test the universality of the P329G-Engager platform, several antibody-based anti-P329G immune cell engagers with alternative MoAs were generated. Among those were: a glycoengineered, ADCC-competent anti-P329G ADCC-competent antibody/innate cell engager (P329G-ICE), anti-P329G-4-1BBL T cell costimulatory fusion protein (P329G-4-1BBL), anti-P329G x anti-CD28 bispecific T cell costimulator (P329G-CD28), and anti-P329G IL2v antibody fusion protein/immunocytokine (P329G-IL2v). The engagers are depicted in **Section 4.4, Figure 4.4.3**.

In order to evaluate the activity of the P329G platform antibodies, *in vitro* assays were performed with readouts corresponding to the mode of action of the specific immune cell engager. The selected method for majority of these initial proof of concept experiments were custom Jurkat reporter assays, which generate a luminescent signal correlating with receptor crosslinking and signaling capacity, which occurs upon simultaneous binding of the molecules to the target antigen and the effector Jurkat cells.

TCB modality was tested with Jurkat CD3/NFAT reporter cells on target-expressing cell lines for its potential for target-dependent CD3 crosslinking. The reporter cells were successfully activated in a dose-dependent manner when induced by adaptor FOLR1 IgG with P329G-TCB 2+1 on FOLR1+ cells HeLa (**Figure 7.1.1A**) or same molecules on FOLR1+ SKOV-3 huCEA cells (**Figure 7.1.1B**). Innate cell engaging molecules were tested for target-dependent FcγRIII crosslinking, by Jurkat FcγRIII reporter cell activation upon co-culture with tumor cells **(Figure 7.1.1C,D**). The reporter cells were strongly activated by adaptor CD20 IgG with P329G-ICE on CD20+ OCI-LY18 cells (**Figure 7.1.1C**) or adaptor HER2 IgG with P329G-ICE on HER2+ NCI-N87 cells (**Figure 7.1.1D**), indicating successful target-mediated FcγRIII-crosslinking. Costimulatory molecules were tested with Jurkat NFκB reporter cells, due to the impact of both CD28 and 4-1BBL on NFκB signaling pathway. The reporter cells were co-cultured with SKOV-3 huCEA (huCEA-overexpressing SKOV-3) tumor cells, a constant and suboptimal concentration of the

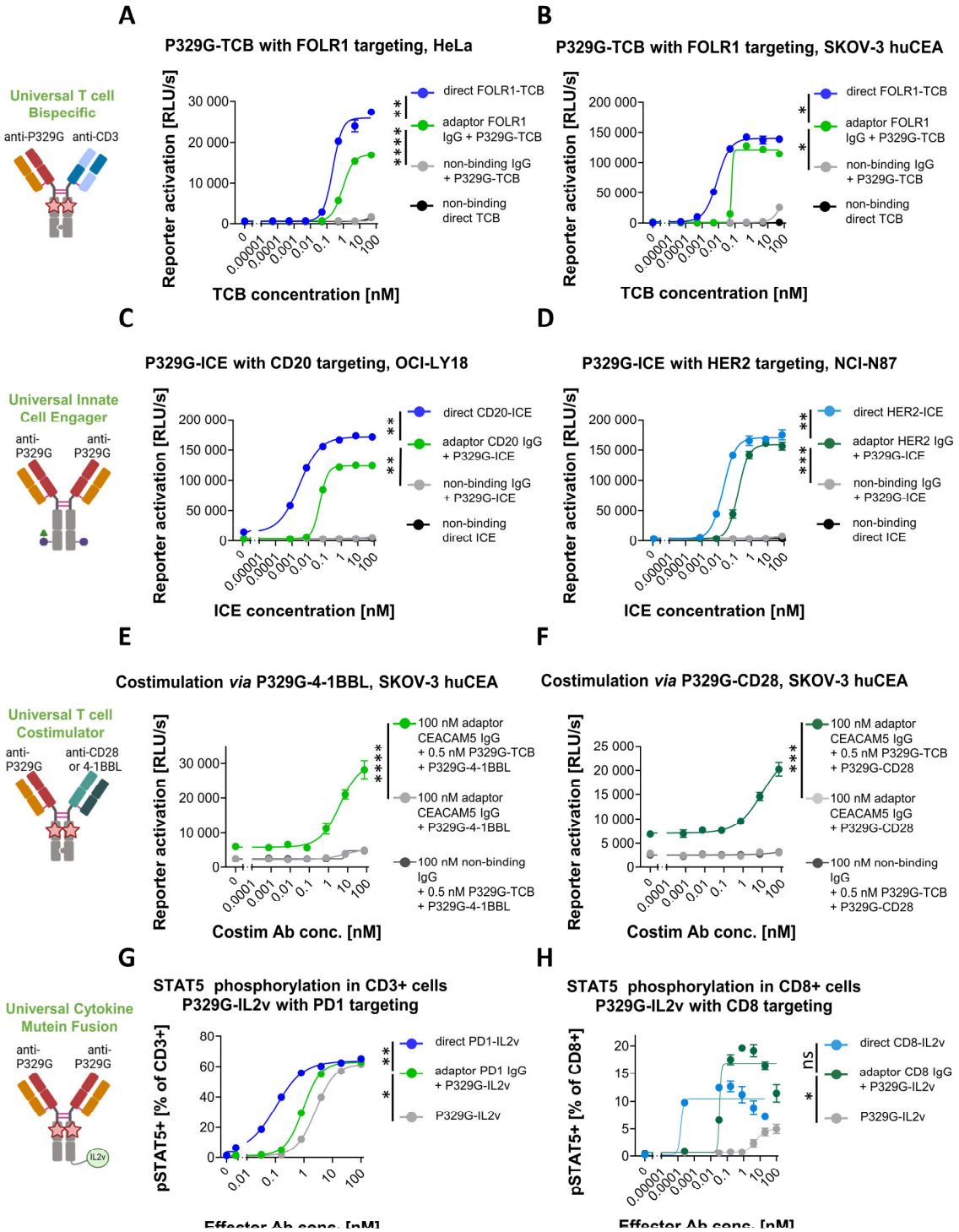

Figure 7.1.1. *In vitro* efficacy of a range of P329G-mutated adaptor IgGs and a range of anti-P329G universal immune cell engagers. A-B) CD3/NFAT reporter cell activation capacity of the universal P329G-TCB against FOLR1+ cells HeLa (A) or FOLR1+ cells SKOV-3 huCEA (B). C-D) FcγRIII reporter cell activation capacity of the universal P329G-ICE against CD20+ cells (C) or HER2+ cells (D). E-F) NFκB reporter cell activation capacity of the universal P329G-4-1BBL (E) or the universal P329G-CD28 (F) against CEACAM5+ cells. G-H) STAT5 phosphorylation capacity of the universal P329G-IL2v upon binding to PD1+ cells (G) or to CD8+ cells (H). The graphs show representative data of 1 to 3 independent experiments or separate T cell donors. Data collected in technical triplicates. Error bars indicate standard error.

molecules (**Figure 7.1.1E,F)**. The reporter cells were activated in a dose-dependent manner when treated with adaptor CEACAM5 IgG with P329G-TCB and with P329G-4-1BBL (**Figure 7.1.1E**) or for adaptor CEACAM5 IgG with P329G-TCB and with P329G-CD28 (**Figure 7.1.1F**), showing successful triggering of NFκB signaling. Finally, IL2v constructs were tested for their potential for induction of phosphorylated STAT5 (pSTAT5) levels, which indicate IL2R signaling. Treatment of preactivated CD3+ cells with PD1 IgG with P329G-IL2v resulted in a dose response in terms of a percentage of primary human pre-activated CD3+ T cells with phosphorylated STAT5 (**Figure 7.1.1G**), with a potency observed in-between the effects of direct PD1-IL2v and untargeted P329G-IL2v. Treatment with CD8 IgG with P329G-IL2v resulted in a strong pSTAT5 dose response in the CD8+ cell population, exceeding the signaling strength of both direct CD8-IL2v and P329G-IL2v (**Figure 7.1.1H**). Based on previous reports on *cis*-targeted activity of direct PD1-IL2v [157] and presented here untargeted P329G-IL2v response curves, it may be concluded that adaptor IgGs with P329G-IL2v initiated IL2R downstream signaling also in a *cis*-targeted manner upon binding to PD1 or CD8 on specific T cells.

As demonstrated in this set of experiments, a set of P329G-mutated adaptor IgGs, directed to either tumor or immune cell targets, could recruit various P329G-directed immune cell engagers to exert an immune function of choice in a dose-dependent manner.

Universal P329G-TCB induces reporter T cell activation against a range of tumor targets *in vitro*

Next, T cell activation capacity of the combination of adaptor P329G-mutated adaptor IgGs with P329G-TCB 2+1 was evaluated, across many tumor targets. The universal P329G-TCB was tested in CD3/NFAT Jurkat reporter assay across a range of 8 tumor targets on several cancer cell lines: liquid tumor antigens CD19 and CD20 (**Figure 7.1.2A and B**, respectively), and solid tumor antigens PSMA, HER2, EpCAM, CEACAM5, and STEAP1 (**Figure 7.1.2C-G**, respectively). The target-binding adaptor IgGs and P329G-TCB 2+1 were co-titrated in a molar ratio 2:1. The target-binding adaptor IgGs with P329G-TCB 2+1 activated Jurkat cells in a dose-dependent manner across all tested targets, while P329G-TCB with non-binding P329G-mutated IgGs or non-binding direct TCB did not (Figure 2 A-H). The adaptor IgGs with P329G-TCB, as compared to the target-binding direct TCBs used as positive controls, displayed lower (**Figure 7.1.2 A-H**) or higher (**Figure 7.1.2 F,G**) Jurkat T cell activation capacity.

Overall, various adaptor IgGs combined with the same P329G-TCB 2+1 elicited a response in all tested cell lines and targeted tumor-associated antigens, providing evidence for universality of the P329G-TCB.

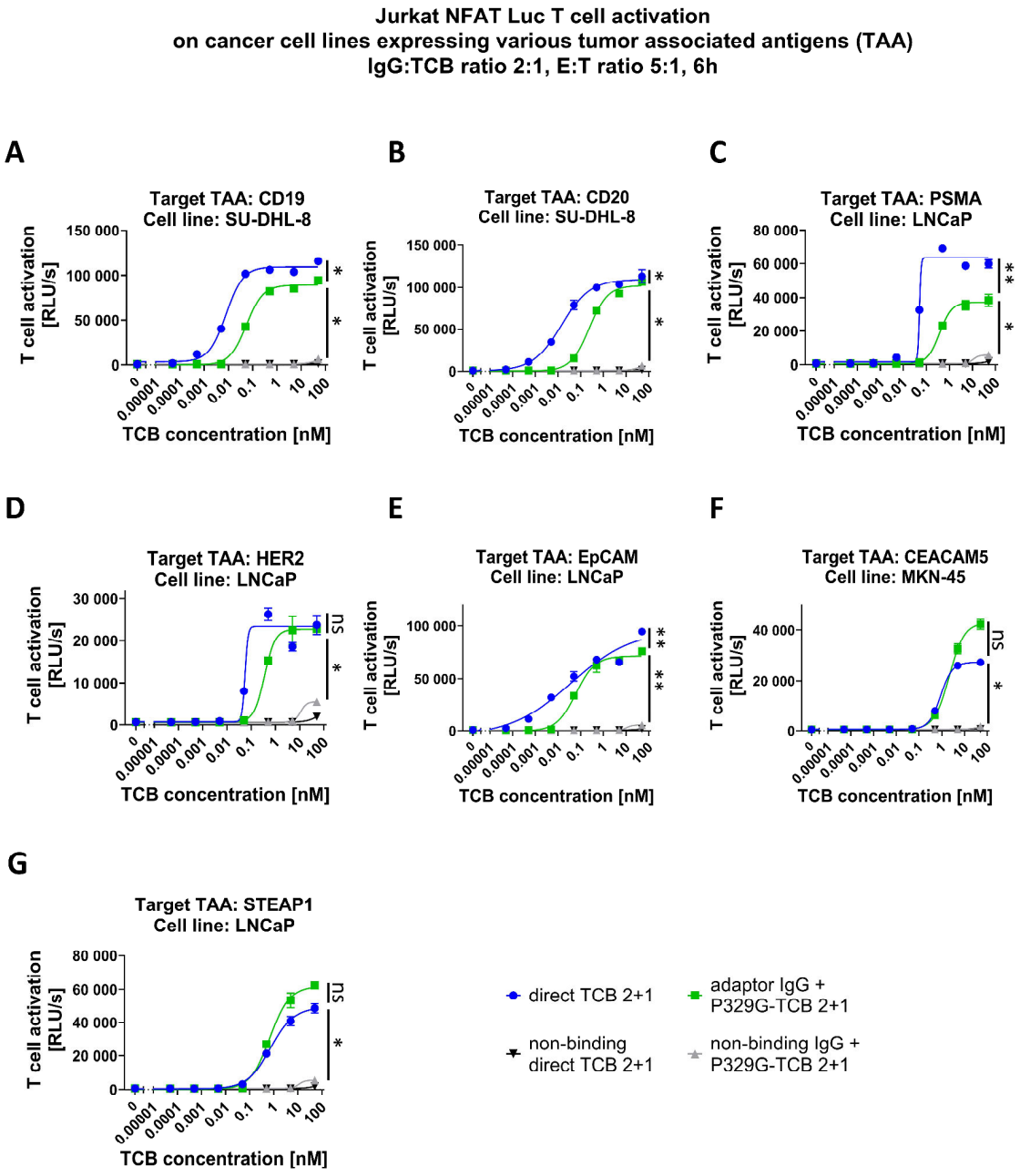

Figure 7.1.2. *In vitro* efficacy of a range of P329G-mutated adaptor IgGs and corresponding targets with one universal P329G-TCB. CD3/NFAT Jurkat reporter cell activation capacity of the universal P329G-TCB against multiple targets on several cancer cell lines. A) CD19 targeting on SU-DHL-8 cells. B) CD20 targeting on SU-DHL-8 cells. C) PSMA targeting on LNCaP cells. D) HER2 targeting on LNCaP cells. E) EpCAM targeting on LNCaP cells. F) CEACAM5 targeting on MKN-45 cells. G) STEAP1 targeting on LNCaP cells. The graphs show representative data of 1-5 independent experiments on at least 2 cell lines for each target. Data collected in technical triplicates. Error bars indicate standard error. Statistics show comparison between adaptor IgG + P329G-TCB 2+1 vs. either direct TCB or vs. non-binding IgG + P329G-TCB 2+1.

A novel P329R LALA-mutated Fc enables improved silencing of Fc effector functions in anti-P329G antibodies

With the objective of further development of P329G-TCB for therapeutic purposes, additional modifications in the antibody sequence were necessary, specifically an improved Fc silencing. Since the development of P329G mutation for its combination with LALA mutations [367], While suitable for direct tumor-targeted TCBs, P329G-directed TCB is incompatible with the incorporation of P329G mutation, due to TCB-TCB binding. For this reason, the initial proof of concept design of the P329G-TCB included solely LALA mutations. However, it has been demonstrated that LALA mutations alone do not adequately attenuate the Fc effector functions of IgG1s [367].

In line with this, P329G-TCB bearing LALA mutations only, regardless of combined adaptor IgG, lead to non-specific CD8+ T cell activation in absence of target cells, as measured by CD25 expression (**Figure 7.1.3A**). P329G-TCB did not induce T cell activation when cultured with pan T cells only (left panel), but lead to non-specific T cell activation when cultured with PBMCs only (middle panel) or with target tumor cells and PBMCs (right panel). This indicates TCB cross-linking of effector CD8+ T cells with targets that are present in PBMCs but not in T cells, such as FcγRs.

Such a non-specificity is undesirable *in vivo*, due to ubiquitous presence of FcγR-expressing cells. Therefore, for the P329G-TCB and the general platform development, efforts were undertaken to identify a novel Fc-silencing mutation that remains unrecognized by anti-P329G antibodies while improving Fc silencing beyond LALA alone. To achieve this aim, four amino acid substitutions at the position 329 were proposed: P329L, P329I, P329A, and P329R (termed P329X, developed by Diana Darowski and Ekkehard Moessner, Roche Innovation Center Zurich). Correspondingly, four P329X huIgG1 antibodies incorporating each of these mutations, as well as LALA mutations, in the Fc were produced for experimental assessment.

The initial step involved assessing the interaction of the P329X IgGs to FcγRs via surface plasmon resonance (SPR, performed by Reto Gianotti, Roche Innovation Center Zurich, and Christian Spick, Roche Innovation Center Munich). **Figure 7.1.3B** illustrates the configuration of the SPR assay (left panel) and a sensorgram depicting the binding profile of the P329X IgGs to FcγRIIIa (right panel). All four variants of P329X LALA huIgG1s demonstrated robust and comparable capacity to abrogate the binding of the Fc region to FcγRs. Subsequently, the binding of the anti-P329G antibody to P329X IgGs was evaluated via SPR. **Figure 7.1.3C** illustrates the configuration of the SPR assay (left panel) and a sensorgram depicting the binding profile of the P329X IgGs to an anti-P329G antibody (right panel). All four variants of P329X LALA huIgG1s showed extremely low binding akin to that of the negative control.

While all P329X variants possessed desirable characteristics, P329R amino acid substitution was selected as the lead mutation to be utilized. This was done in conjunction with the LALA mutations, for the subsequent designs and synthesis of P329G-TCBs and other P329G-based immune cell engagers where Fc effector function is undesirable, such as P329G-IL2v, among others.

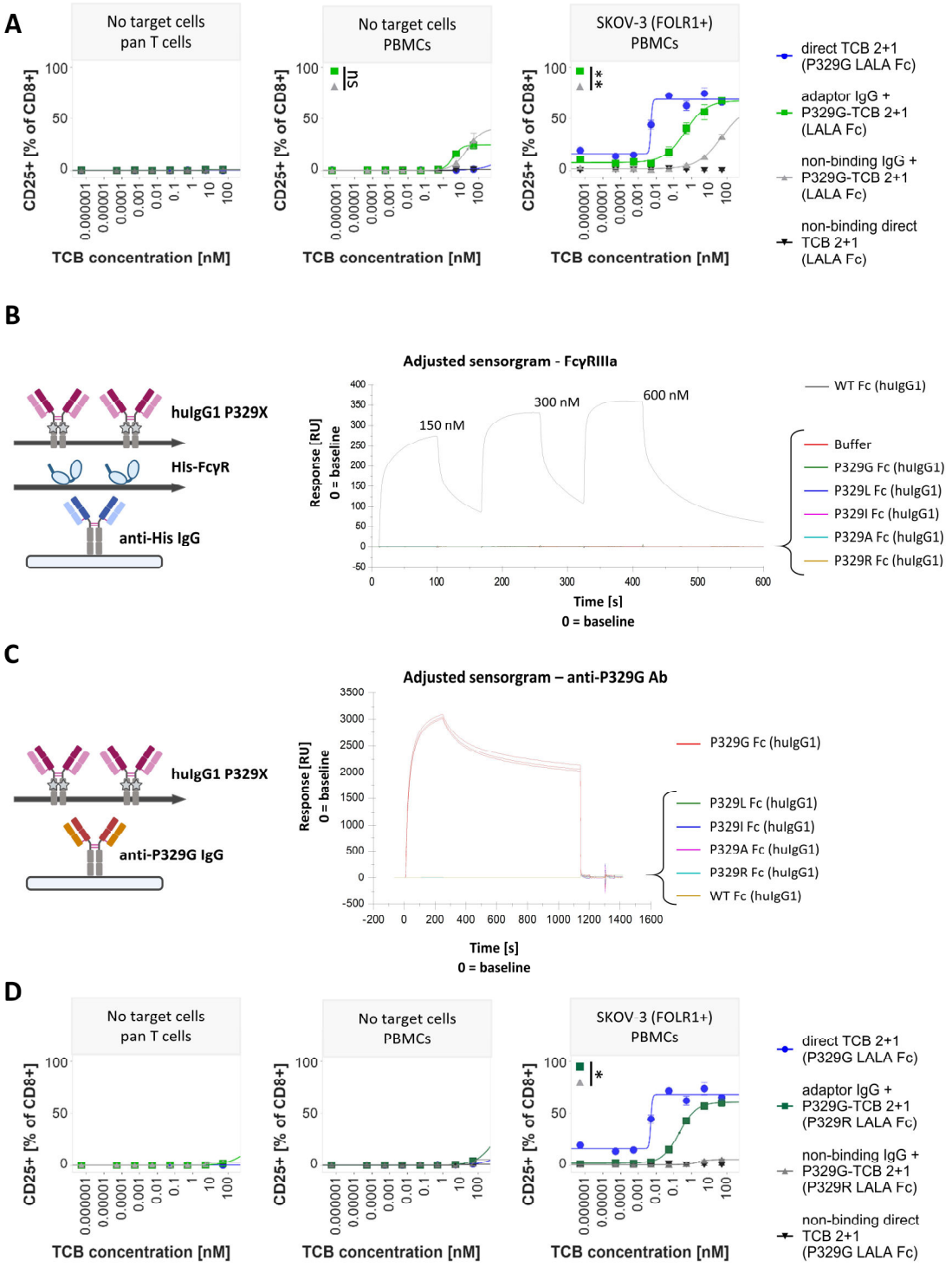

Figure 7.1.3. Impact of Fc-silencing mutations on antibody specificity, and development of new Fc-silencing mutations P329X: P329L, P329I, P329A, and P329R. A) CD8+ T cell activation, as measured by CD25 expression, induced by adaptor IgG and P329G-TCB with incompletely silenced Fc bearing LALA mutations only. B) SPR binding results of P329X LALA-mutated huIgG1 antibodies to the FcγRIIIa. C) SPR binding results of P329X LALA-mutated huIgG1 antibodies to anti-P329G huIgG1. D) CD8+ T cell activation, as measured by CD25 expression, induced by adaptor IgG and P329G-TCB with improved silenced Fc bearing P329R LALA mutations. The graphs show representative data from 2 experiments/PBMC donors on 2 different cell lines. Data collected in technical duplicates or triplicates. Error bars indicate standard error.

To test whether the P329R LALA Fc indeed results in improved Fc silencing, and consequently reduced non-specific T cell activation, an *in vitro* functional assay was performed, analogous to the assay depicted in **Figure 7.1.3A**. However, instead of P329G-TCB with LALA Fc, P329G-TCB with the novel P329R LALA Fc was assessed and compared to previous results. As shown in **Figure 7.1.3D**, P329G-TCB, regardless of combined adaptor IgG, did not induce CD8+ T cell activation in absence of target cells, as measured by CD25 expression. This effect was irrespective of being cultured with pan T cells only (left panel) or with PBMCs only (middle panel). Similarly, in the assay with target cells and PBMCs, there was no non-specificity observed for non-binding adaptor IgG combined with P329G-TCB P329R LALA.

Together, these data provide evidence of the impact of Fc silencing mutations on the TCB tumor non-specific activity. Additionally, the results introduce P329L, P329I, P329A, P329R as potential substitutes of the well-established P329G mutation, with P329R being the most promising candidate. In subsequent phases of the project, P329G-TCB variants with the P329R LALA mutation were utilized.

Universal P329G-TCB induces activation and anti-tumoral activity of human primary T cells *in vitro*

Following the optimization of the Fc silencing of the P329G-TCB, the molecule was suitable for more in-depth evaluation regarding its effects on primary human T cells, as well as its consequent primary T cell-mediated antitumoral efficacy. For this purpose, a series of killing assays were performed using co-culture of human cancer cell lines and human primary pan T cells.

An imaging-based Incucyte assay was conducted to assess both the tumor killing capacity of the P329G-TCB when combined with suitable adaptors, as well as kinetics of the P329G-TCB activity as compared to direct TCBs (**Figure 7.1.4A**). As target cells, human cancer cells expressing red fluorescent protein were used. As visible in **Figure 7.1.4A** on the left panel, P329G-TCB 2+1 led to tumor cell death as measured at 180 h when combined with adaptor CEACAM5 IgG, but not when used with non-binding IgG, in the assay using CEACAM5+ cells. Analogously, on the right panel with FOLR1+ cells, P329G-TCB 2+1 led to tumor cell death at 180 h when combined with adaptor FOLR1 IgG, but not when combined with non-binding IgG. The kinetics of the assay are presented in **Figure 7.1.4B**. At a concentration of 0.5 nM TCB (and IgG:TCB ratio 2:1), tumor cell lysis for adaptor IgG with P329G-TCB 2+1 occurred with comparable kinetics to the direct TCB 2+1, for both CEACAM5 and FOLR1 targeting. In terms of maximal tumoricidal activity, adaptor CEACAM5 IgG with P329G-TCB 2+1 displayed comparable effects to the direct CEACAM5-TCB 2+1, while adaptor FOLR1 IgG with P329G-TCB 2+1 displayed weaker antitumoral effects when compared to the direct FOLR1-TCB 2+1.

Additional characterization of P329G-TCB activity included quantification of cytokines released into the supernatant during the killing assay. The quantified levels of IL-2, IFN-γ AND TNF-α released by pan T cells upon co-culture with MKN-45 (CEACAM5+) cells are depicted in **Figure 7.1.4C**. For all tested cytokines, the combination of the adaptor CEACAM5 IgG with

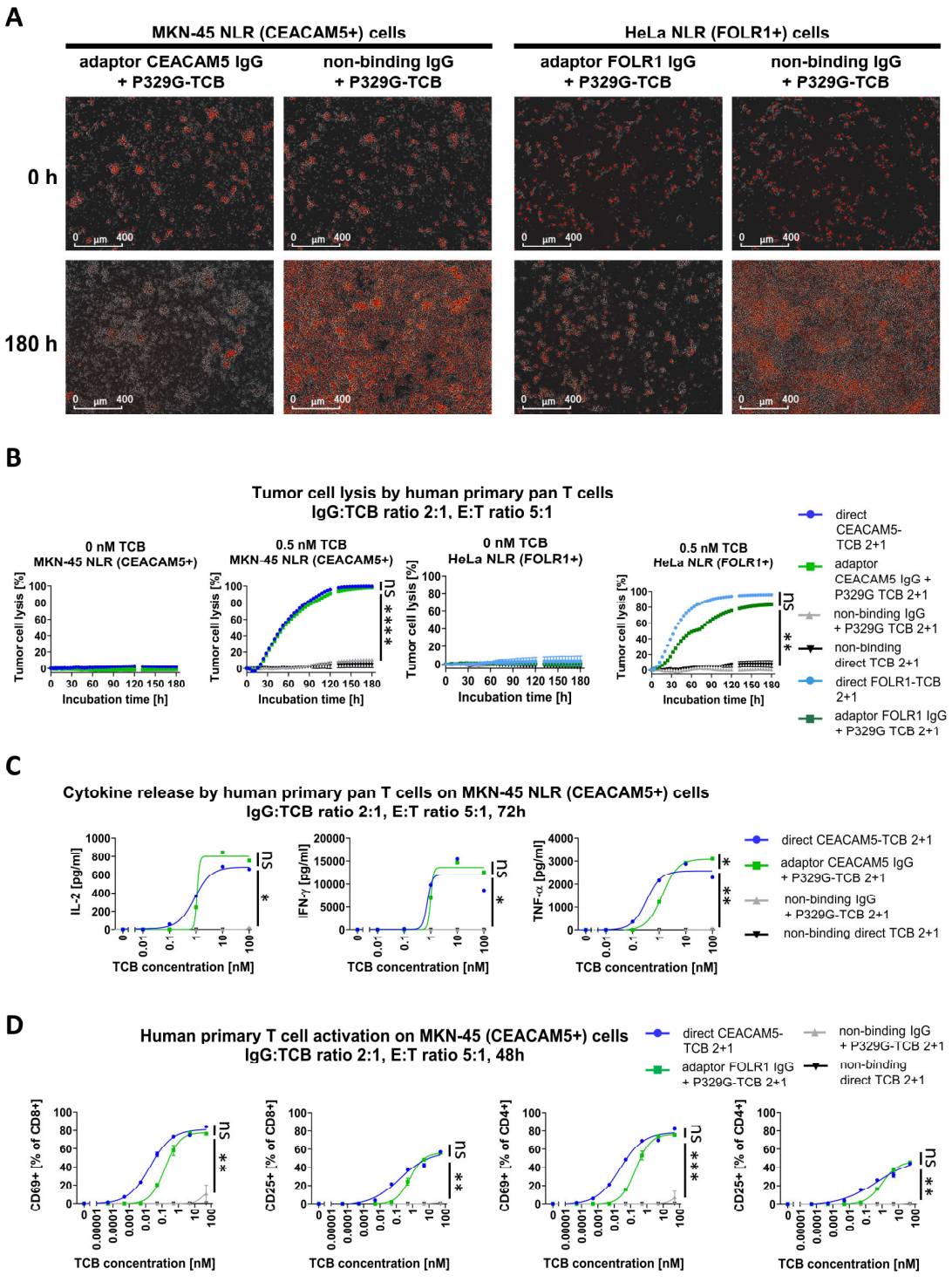

Figure 7.1.4. Capacity of human primary T cell killing, cytokine release and T cell activation induced by P329G-TCB against two targets *in vitro*. A) Incucyte imaging readout of red fluorescent tumor cell killing capacity by primary pan T cells activated by adaptor IgG and P329G-TCB against CEACAM5+ or FOLR1+ cells. B) Incucyte quantification of tumor cell killing capacity over time by T cells, as induced by adaptor + P329G-TCB. C) Cytokine release into the supernatant upon tumor cell killing mediated by T cells, as induced by adaptor CEACAM5 IgG with P329G-TCB. D) T cell activation upon co-culture with MKN-45 tumor cells, induced by adaptor CEACAM5 IgG with P329G-TCB. Statistical annotations show comparison between adaptor IgG + P329G-TCB 2+1 with either direct TCB or non-binding IgG + P329G-TCB 2+1. Data collected in technical triplicates. Cytokines measured on pooled triplicates. Error bars indicate standard error.

P329G-TCB 2+1 resulted in a dose-dependent release, in a similar range to the release induced by direct CEACAM5-TCB 2+1.

To verify if the pan T cell used in the killing assay are displaying signs of activation, the cells from a FOLR1 targeting assay were assessed by flow cytometry for the expression for activation markers CD69 and CD25. **Figure 7.1.4D** depicts dose-dependent upregulation of CD69 and CD25 on CD8+ and CD4+ T cells, as induced by adaptor FOLR1 IgG with P329G-TCB 2+1, and the comparison to the direct FOLR1-TCB 2+1. The upregulation by the adaptor with the P329G-TCB was detectable and dose-dependent, although reached a lower extent than the direct TCB. This is in line with the tumor cell lysis comparison depicted in **Figure 7.1.4B**.

Collectively, these data demonstrate that the P329G-TCB is capable of activating primary T cells, prompting the release pro-inflammatory cytokines and eliciting tumor cell killing in a human cell setting i*n vitro*. Additionally, owing to comparable results of P329G-TCB to those of a direct TCB, CEACAM5 targeting emerged as a viable option for forthcoming *in vivo* efficacy studies.

P329G-mutated adaptor IgGs and P329G-TCB display wide efficacious windows in terms of optimal concentration ratios

To ensure thorough preparation for the forthcoming *in vivo* efficacy study, it was deemed necessary to explore the influence of concentration levels and of ratios of adaptor:TCB on therapeutic efficacy. The intent was to evaluate whether precise concentrations of both the adaptor and the TCB are required to remain within the therapeutic window.

One of the factors contributing to the narrowing of the therapeutic window at higher concentrations is so-called bell-shaped curve. In the context of bispecific antibody therapy, low concentrations lead can lead to low efficacy, but excessively high concentrations can result in oversaturation and complete antibody occupancy of the binding sites on both the target and effector cells. This leads to the bispecific antibodies saturating these cells separately, thereby preventing simultaneous engagement of the antibody with both target and effector cells. This simultaneous engagement is required for activity of many bispecifics, including TCBs.

While a known phenomenon, a bell-shaped curve needs to be investigated for each antibody. Splitting a TCB into adaptor and an anti-adaptor TCB, such as is the case of P329G-TCB, introduces additional complexity and warrants additional caution. **Figure 7.1.5A** exemplifies the mechanism of antibody activity in the case of optimal concentration of both adaptor IgG and P329G-TCB (left panel) and oversaturation of both adaptor IgG and P329G-TCB (right panel), hypothetically leading to drop in efficacy described in bell-shaped-curve scenarios.

To investigate the optimal adaptor IgG:TCB ratios, optimal concentrations and determining the width of the therapeutic window in various targets *in vitro*, a set of cross-titration Jurkat CD3/NFAT reporter assays was performed. **Figure 7.1.5B** depicts a heat map of the reporter cell activation level upon co-culture of the reporter cells with human cancer cells SU-DHL-8 and the molecules. The molecules were cross-titrated, such that a 4-fold serial dilution of

bivalent adaptor CD20 IgG, starting from 800 nM, was mixed with a 4-fold serial dilution of P329G-TCB 2+1, starting from 100 nM. The resulting concentration combinations lead to an array of IgG:TCB ratios (of which selected several are depicted on the heat map), where a wide

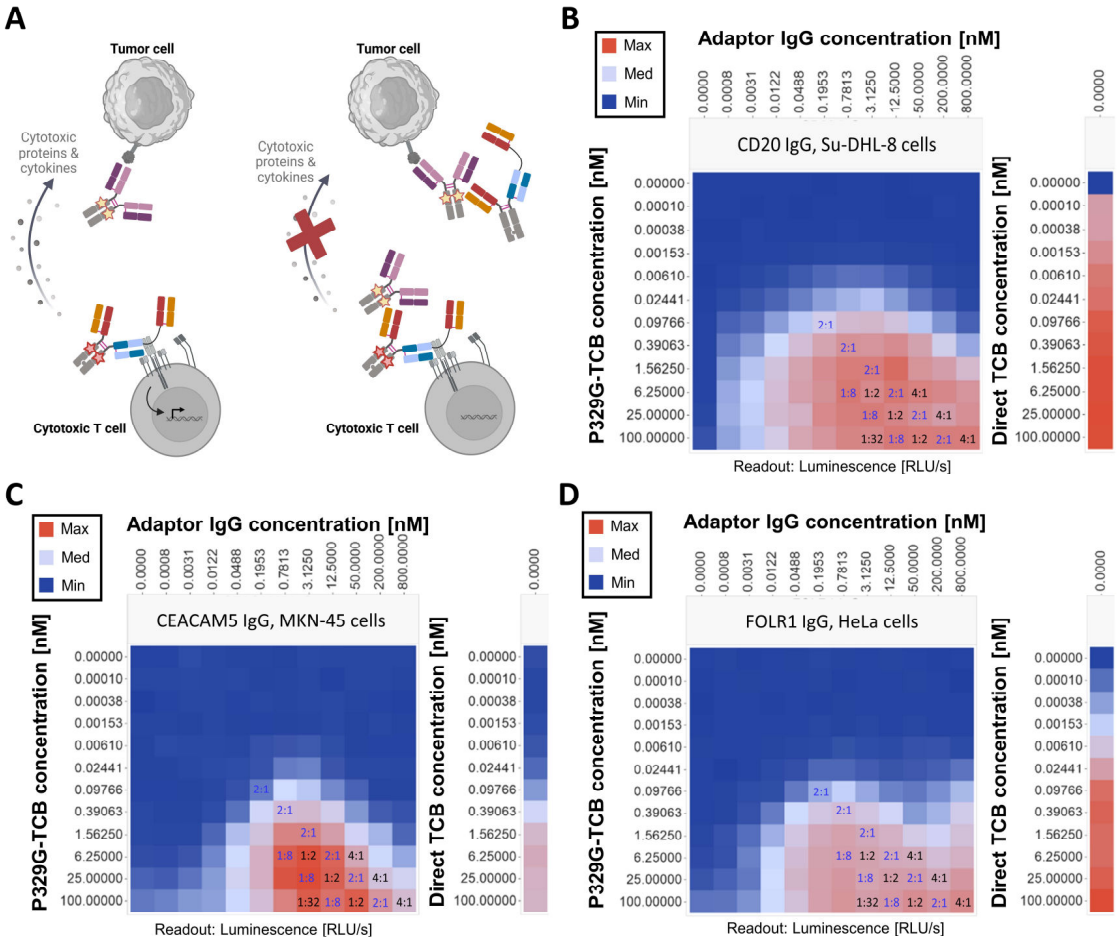

Figure 7.1.5. Characterization of the optimal adaptor IgG : P329G-TCB 2+1 concentration ratios and elucidation of the therapeutic window in a CD3/NFAT Jurkat T cell reporter assay. A) Mechanism of P329G-TCB-mediated killing with optimal concentrations (left) and an expected mechanism of the drop in efficacy upon high concentration (bell-shaped curve) of the adaptor and/or P329G-TCB (right). B) Cross-titration of the adaptor CD20 IgG and the P329G-TCB 2+1, and comparison to a direct CD20 TCB, on CD20+ SU-DHL-8 cancer cells and CD3/NFAT Jurkat reporter cells. Selected IgG:TCB molar ratios are indicated on the heat map. C) Cross-titration of the adaptor CECAM5 IgG and the P329G-TCB 2+1, and comparison to a direct CEACAM5-TCB, on CEACAM5+ MKN-45 cancer cells and CD3/NFAT Jurkat reporter cells. Selected IgG:TCB molar ratios are indicated on the heat map. D) Cross-titration of the adaptor FOLR1 IgG and the P329G-TCB 2+1, and comparison to a direct FOLR1-TCB, on FOLR1+ HeLa cancer cells and CD3/NFAT Jurkat reporter cells. Selected IgG:TCB molar ratios are indicated on the heat map. The graphs show representative data from 2 independent experiments. Data collected in technical triplicates.

range of both adaptor concentrations and of TCB concentrations induced reporter cell activation. Despite this fact, the signal was lower as compared to direct CD20 TCB 2+1. **Figure 7.1.5C** depicts results from an analogous assay, with CEACAM5 targeting on MKN-45 cells. Here, the resulting combinations led to a narrower, yet still relatively broad range of concentrations resulting in reporter cell activation. However, in CEACAM5 targeting, several tested conditions outperformed the positive control direct CEACAM5-TCB 2+1. **Figure 7.1.5D** depicts results from an analogous cross-titration assay, with FOLR1 targeting on HeLa cells. The resulting combinations led to a relatively broad range of concentrations inducing reporter cell activation, with direct FOLR1-TCB 2+1, however, leading to the highest signal overall. The result from CD20-, CEACAM5- and FOLR1-targeted cross-titrations indicate that a very specific concentration or IgG:TCB ratio is not a prerequisite for achieving efficacy and remaining within the therapeutic window. One must note that these results are specific to the tested cell lines and their target expression levels. However, overall, the adaptor IgG with P329G-TCB seemed to be efficacious across a range of IgG:TCB ratios and IgG and TCB concentrations. Given the difficulty in ensuring specific concentrations at the tumor site *in vivo*, the data showing a wide therapeutic window was favorable with regards to dosing complexity levels in planned mouse efficacy studies.

Antibody format and valence of both adaptor IgGs and P329G-TCBs influence efficacy

An additional parameter to consider in therapeutic antibody development, particularly for TCBs, is antibody valence and its influence on antibody potency. This aspect is significant for the direct TCBs; however, it has even more importance in an adaptor-based system. This is because the binding of adaptor and effector antibodies to each other can lead to a multiplication of the valence of the assembled molecule. Such binding can influence the ratio of the number of bound tumor targets per single CD3 beyond the capability of a standard TCB. This, in turn, can affect avidity or, potentially, a number of T cells engaged against the tumor cell.

To test the influence of both the adaptor and P329G-TCB valence and their various combinations, a set of P329G platform and control molecules was produced, consisting of: bivalent adaptor IgG, monovalent adaptor IgG, TCB 1+1, TCB 1+1 one-armed (OA), TCB 2+1 (**Figure 7.1.6A**). An example of valence influencing target:CD3 engagement ratio for the adaptor-based system is depicted in **Figure 7.1.6B**. The produced molecules in various formats were evaluated in a CD3/NFAT Jurkat reporter assay co-cultured with human cancer cells expressing CEACAM5 (**Figure 7.1.6C**). For a more comprehensive assessment of the influence of the antibody format, valence, and their combination on target engagement and T cell activation capacity, an additional variable was introduced in form of various target expression levels. Figure 7C depicts a heat map of reporter cell activation across adaptor format, TCB format and target expression level.

The adaptor CEACAM5 IgGs were cross-titrated with P329G-TCBs in the available formats, as well as matched with corresponding direct CEACAM5-TCBs. Both direct and P329G-TCB

combined with adaptor IgG showed low signal on low-expressing target cells HT-29, with very low dependence on format visible. On medium- and high-expressing cells, the strongest signal was observed for P329G-TCB 2+1 regardless of adaptor valence. Additionally, on these cells, regardless of TCB format, the use of monovalent adaptor IgG led to a stronger signal than the bivalent adaptor IgG. Of all conditions, the strongest signal was provided by P329G-TCB 2+1 combined with monovalent adaptor IgG, followed by P329G-TCB 2+1 combined with bivalent adaptor IgG. These data showed that TCB format had apparent stronger influence on TCB potency than adaptor format. This demonstrated that the hypothesis of target:CD3 engagement ratio alone is insufficient to account for the experimental observations, highlighting the complexity of the molecular interactions in an adaptor-based system.

In light of these findings, P329G-TCB in a 2+1 format was selected as the lead T cell engaging molecule. With regards to the adaptor IgG, the bivalent format was selected as the lead adaptor format, due to the anticipated impact of avidity on potency to a greater extent *in vivo* beyond what can be observed and concluded *in vitro*.

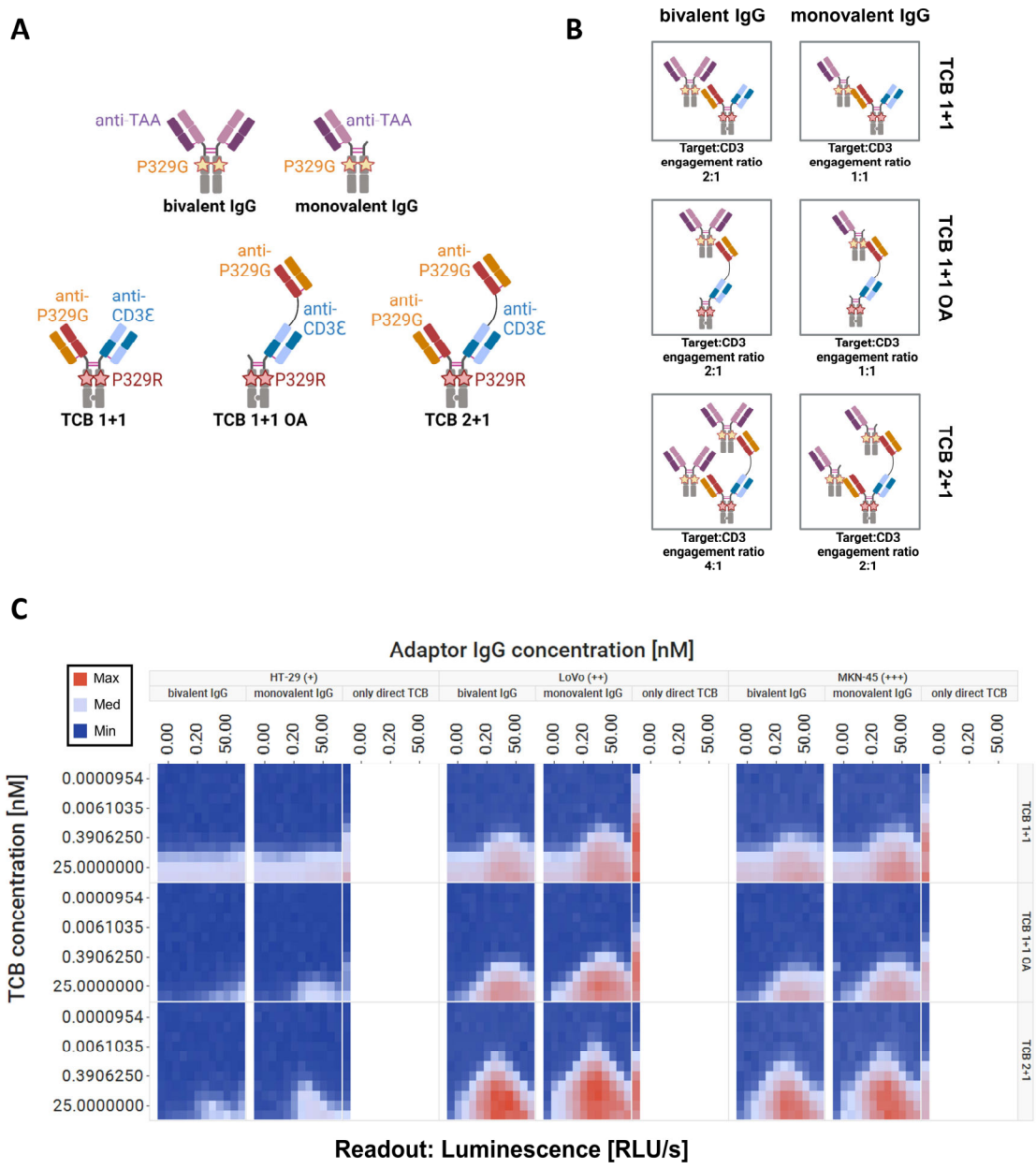

Figure 7.1.6. Characterization of the P329G-TCB activity across the following variables: mono- vs. bivalent adaptor IgG formats, 2+1 vs. 1+1 vs. 1+1 one-armed TCB formats, and low vs. medium vs. high antigen expression on target cells. A) Pictograms of tested antibody formats: bivalent IgG, monovalent IgG, TCB 1+1, TCB 1+1 OA (one-armed) and TCB 2+1. B) Example theoretical target:CD3 engagement ratios dependent on the specific combination of used adaptor IgG and TCB formats. C) CD3/NFAT Jurkat T cell reporter assay upon cross-titration of bivalent CEACAM5 adaptor IgG or monovalent CEACAM5 adaptor IgG, with P329G-TCB 1+1 or P329G-TCB 1+1 OA or P329G-TCB 2+1, on CEACAM5-low-expressing HT-29 cells or CEACAM5-medium-expressing LoVo cells or CEACAM5-high-expressing MKN-45 cells. The graphs show data from one experiment, collected in technical triplicates.

Universal P329G-TCB induces antitumoral activity in humanized NSG mice

To test P329G-TCB efficacy in a more biologically complex and relevant system, an *in vivo* proof of concept study was designed in human xenograft tumor bearing fully cord-blood stem cell-humanized NSG mice. Following a comprehensive characterization and development of adaptor IgGs and P329G-TCBs, selected lead target was CEACAM5 on MKN-45 cell line, the lead adaptor was bivalent adaptor CEACAM5 IgG, and lead TCB was P329G-TCB 2+1 P329R LALA. The adaptor was injected 24h prior to the P329G-TCB 2+1. As a positive control, direct CEACAM5-TCB 2+1 was used, an as negative controls, protein buffer (vehicle), adaptor alone and P329G-TCB 2+1 alone were used. Study design details are depicted in **Figure 7.1.7A,B**. The model consisted of tumor cells injected subcutaneously into humanized NSG mice, and initiation of therapy injections after the tumors had reached 110 mm^3. In the treatment group of adaptor CEACAM5 IgG combined with P329G-TCB 2+1, the adaptor was injected 24h prior to TCB treatment to allow for enrichment of the antibody in the tumor (**Figure 7.1.7B**). As shown in Figure 8C, adaptor CEACAM5 IgG combined with P329G-TCB 2+1 provided partial tumor growth control, in contrast to the adaptor alone or the P329G-TCB 2+1 alone, effects of which were comparable to the vehicle control. The direct CEACAM5-TCB 2+1 displayed the highest efficacy of all groups tested. The treatment did not lead to substantial reductions of body weight in any of the groups, as illustrated in **Figure 7.1.7D**. On day 14 of the study, blood, spleen and tumor tissue samples were harvested from a subset of mice, and analyzed via flow cytometry for immune cell count, followed by normalization to tissue weight. **Figure 7.1.7E** shows CD45+ CD3+ cell count in blood, spleen and tumor for all the groups. Particularly evident in tumor samples, mice treated with direct CEACAM5-TCB 2+1 demonstrated the most pronounced T cell infiltration/expansion. Mice treated with adaptor CEACAM5 IgG with P329G-TCB 2+1 had a T cell count in blood and spleen higher than the control groups and comparable to positive control direct TCB, while in tumor the T cell count was significantly lower than the positive control. This difference in T cell infiltration to the tumor is in line with the observed results in the differences in tumor growth inhibition extent between adaptor with P329G-TCB and direct TCB.

Figure 7.1.8F shows a summary of quantified infiltration of various T cell types per group in tumor tissue. For majority of evaluated cell populations, including CD4+ cells, CD8+ cells, CD8+ CD25+ cells, CD8+ GrB+ cells, cell infiltration was higher in mice treated with direct CEACAM5-TCB 2+1, as compared to mice treated with adaptor IgG with P329G-TCB 2+1. This finding is consistent with the results observed in the tumor growth inhibition.

Overall, in the tested model, adaptor CEACAM5 IgG combined with P329G-TCB 2+1 showed tumor growth inhibition and therefore provided the first proof of concept data for *in vivo* efficacy for the P329G-TCB approach. The combination of the adaptor with P329G-TCB resulted in lower number of T cells and activated T cells in the tumor tissue relative to the direct TCB treatment. The diminished T cell presence in the tumor microenvironment is in line with, and may account for lower efficacy of the adaptor combined with P329G-TCB treatment as compared to the direct TCB.

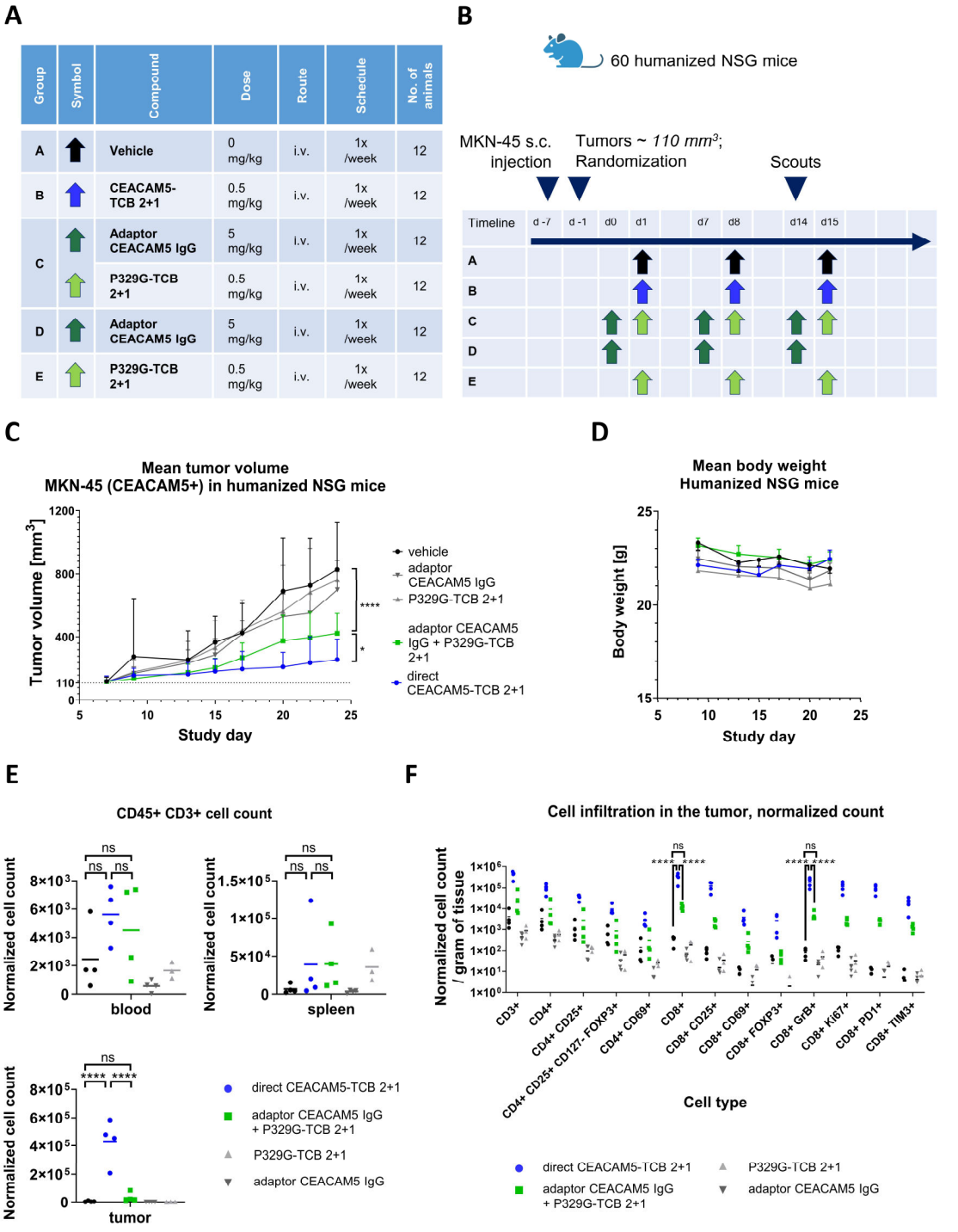

Figure 7.1.7. *In vivo* anti-tumoral efficacy of adaptor CEACAM5 IgG with P329G-TCB against MKN-45 subcutaneous tumors in humanized NSG mice. A) Details of the groups in the efficacy *in vivo* study. B) Scheduling details of the efficacy *in vivo* study. C) Mean tumor volume upon treatment over time. Error bars indicate SEM. D). Mean body weight upon treatment over time. Error bars indicate SEM. E) CD45+ CD3+ T cell count, normalized per tissue weight, measured at the scout time point from individual mice (n = 3-4). From the top: T cell count in plasma per treatment group, T cell count in spleen per treatment group, T cell count in tumor per treatment group. (Number of mice n = 3-4). F) Various cell type counts in the tumor, normalized per tissue weight, measured at the scout time point from individual mice (n = 3-4). The graphs show data from one experiment.

7.2. Chapter 2 – Universal protease-activated cancer immunotherapy using target-agnostic antibodies

Matriptase cleaves the protease-cleavable linker and enables detachment the P329G binder-blocking mask from the universal pro-P329G-TCB *in vitro*

To test whether matriptase can successfully cleave the designed linkers, the molecules depicted in **Section 4.6, Figure 4.6.3** were tested. As the first step, analytic assays of pro-P329G-TCBs were performed. Freshly thawed recombinant matriptase was incubated with pro-P329G-TCBs containing PMAKK linkers in 1+1 format and 1+1 OA format, including a positive control based on the sequence of the pro-FOLR1-TCB described previously [181]. As further controls, masked TCBs with non-cleavable linkers (G4S linkers without the cleavage site) and non-masked TCBs were included. As an analytic method, Western blot was used, with molecules prepared under reducing conditions and analyze bands for resulting antibody chains. To exemplify the detection method, **Figure 7.2.1** depicts an example huIgG1 antibody with its chains, domains and their respective molecular weight predicted by amino acid sequence, before and after reducing conditions. Reducing conditions break disulfide bridges, and produce several separate proteins (chains) with different molecular weights detectable in SDS-PAGE or Western blot.

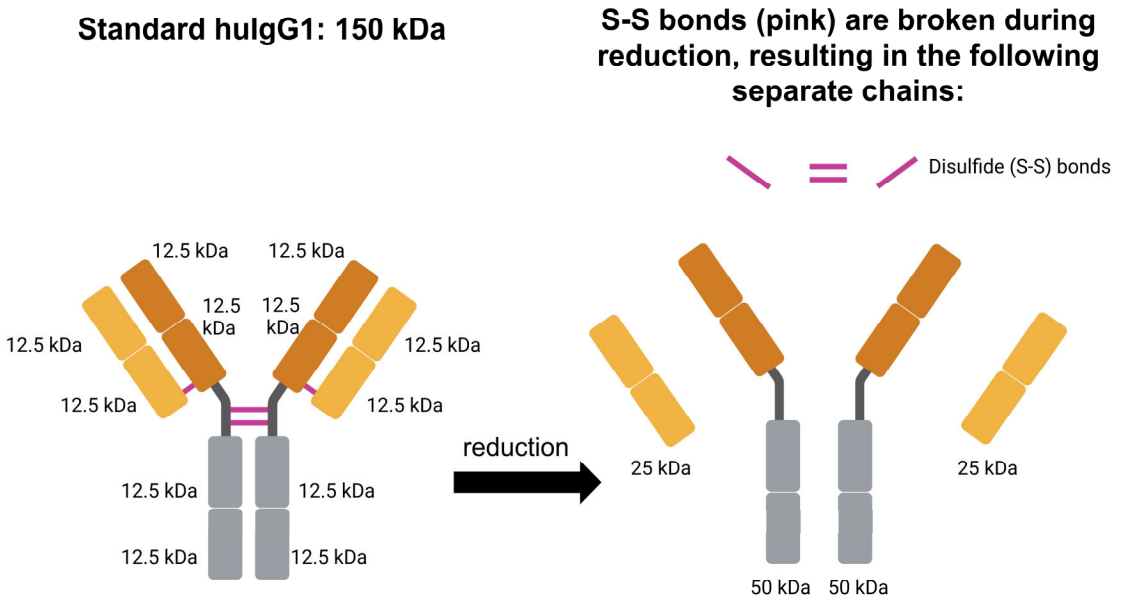

Figure 7.2.1. Structure and molecular weight of a standard huIgG1 and its chains before and after reduction process performed for SDS-PAGE and Western blot assays.

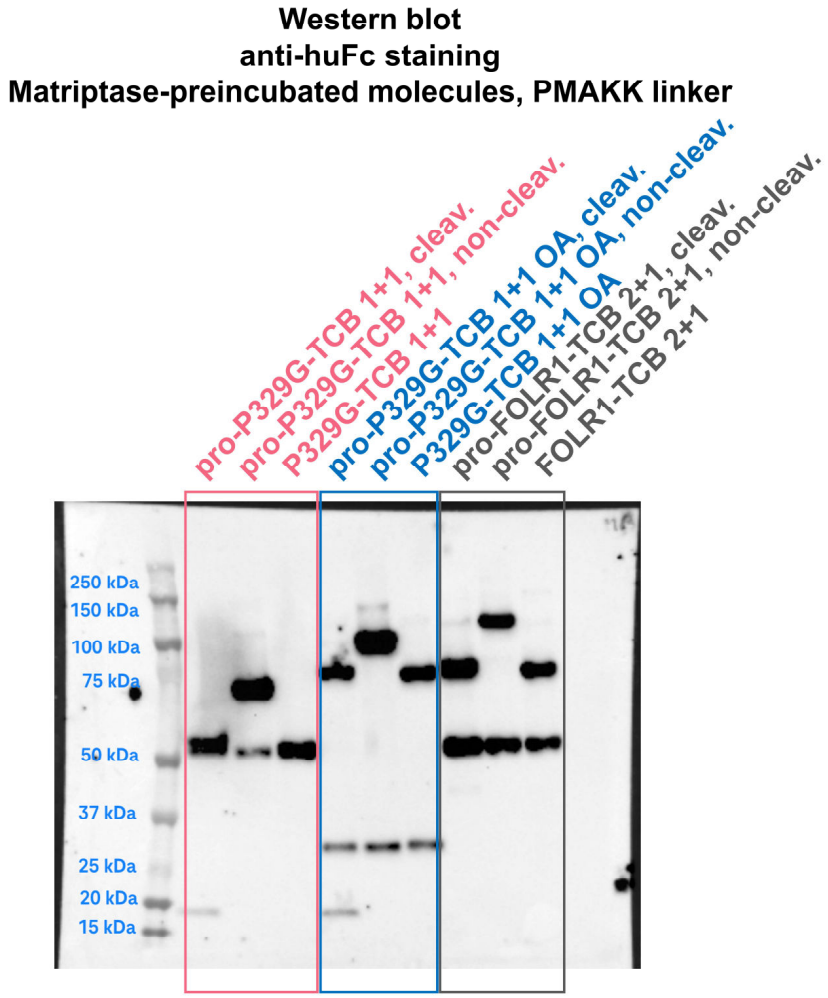

Figure 7.2.2. Western blot results with anti-huFc staining of matriptase-preincubated test antibodies. The pro-P329G-TCB and control antibodies with PMAKK matriptase-cleavable linker, pre-treated with matriptase overnight, assessed via Western blot. Data from one experiment.

Figure 7.2.2 shows a summary of Western blot results of the matriptase-preincubated molecules analyzes after reducing conditions and stained with an anti-human Fc antibody. **Figures 12.3-5** offer a detailed view of tested molecules of the same Western blot, and the interpretation of the bands. **Figure 7.2.3A** shows three tested 1+1 P329G-TCB variants: cleavable, non-cleavable and unmasked/wild-type (WT), as well as the chains resulting from reducing conditions. Interpretation of the Western blot is shown in **Figure 7.2.3B**. For cleavable masked pro-P329G-TCB 1+1, the visible bands represent predicted molecular weight of unmasked or WT chains (~50 kDa) and the detached P32G-mutated mask (~12.5 kDa). The mask was detected by anti-Fc antibody due to being based on CH2 part of the Fc. As shown, the chains predicted molecular weight (MW) and the observable, protein-ladder matched MW differ, showing e.g. a band at ca. 18 kDa instead of 12.5 kDa. This is a known phenomenon in SDS-PAGE-based assays, with displayed MW being larger than the one predicted by amino acid sequence. This is likely due to e.g. protein charges influencing migration or post-translational modifications, such as protein glycosylation, not being incorporated in the

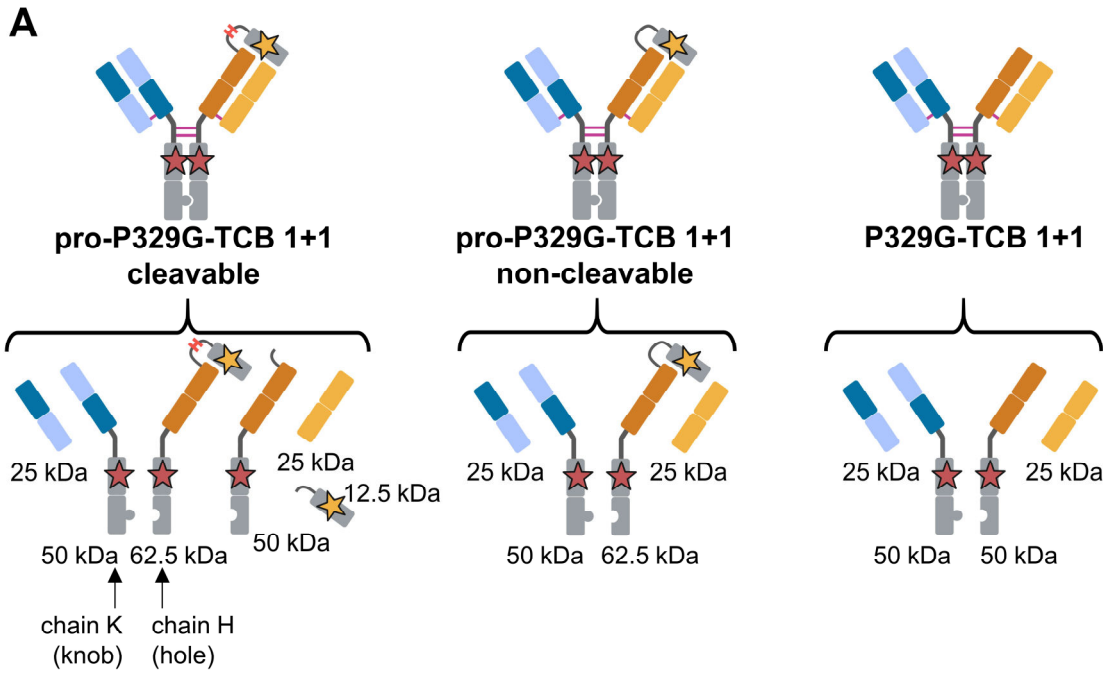

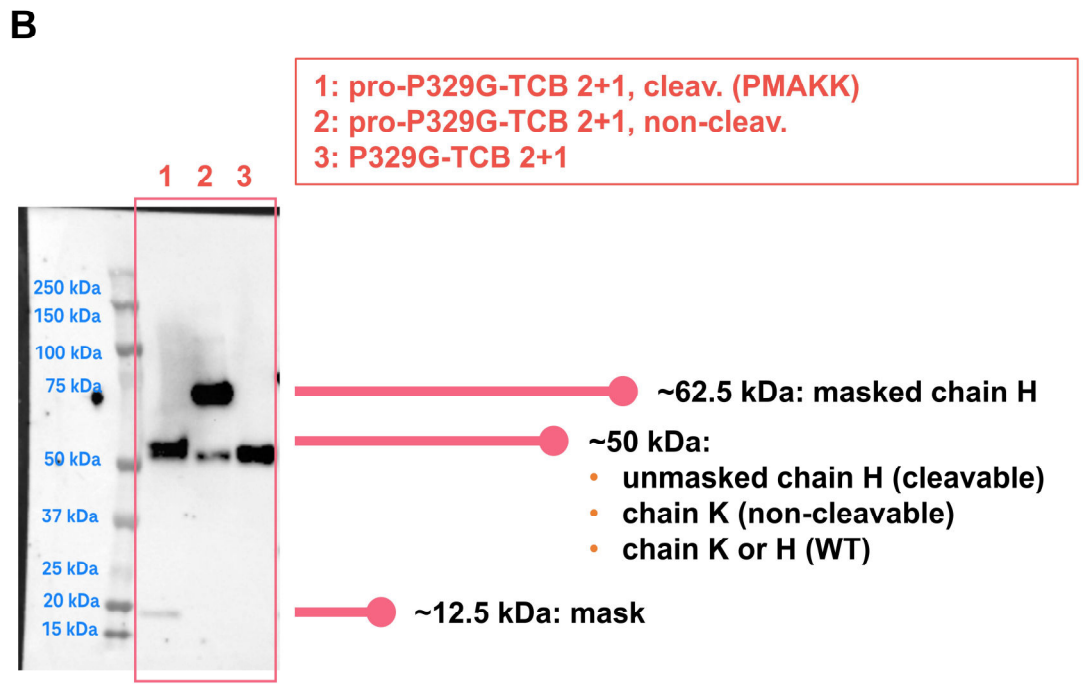

Figure 7.2.3. Chains resulting from a reduction process of pro-P329G-TCB 1+1, and anti-huFc Western blot analysis. A) Possible chains resulting from reduction of pro-P329G-TCB 1+1 and control TCBs. B) Bands representing chains of matriptase-pretreated pro-P329G-TCB 1+1 and the control TCBs. Data from one experiment.

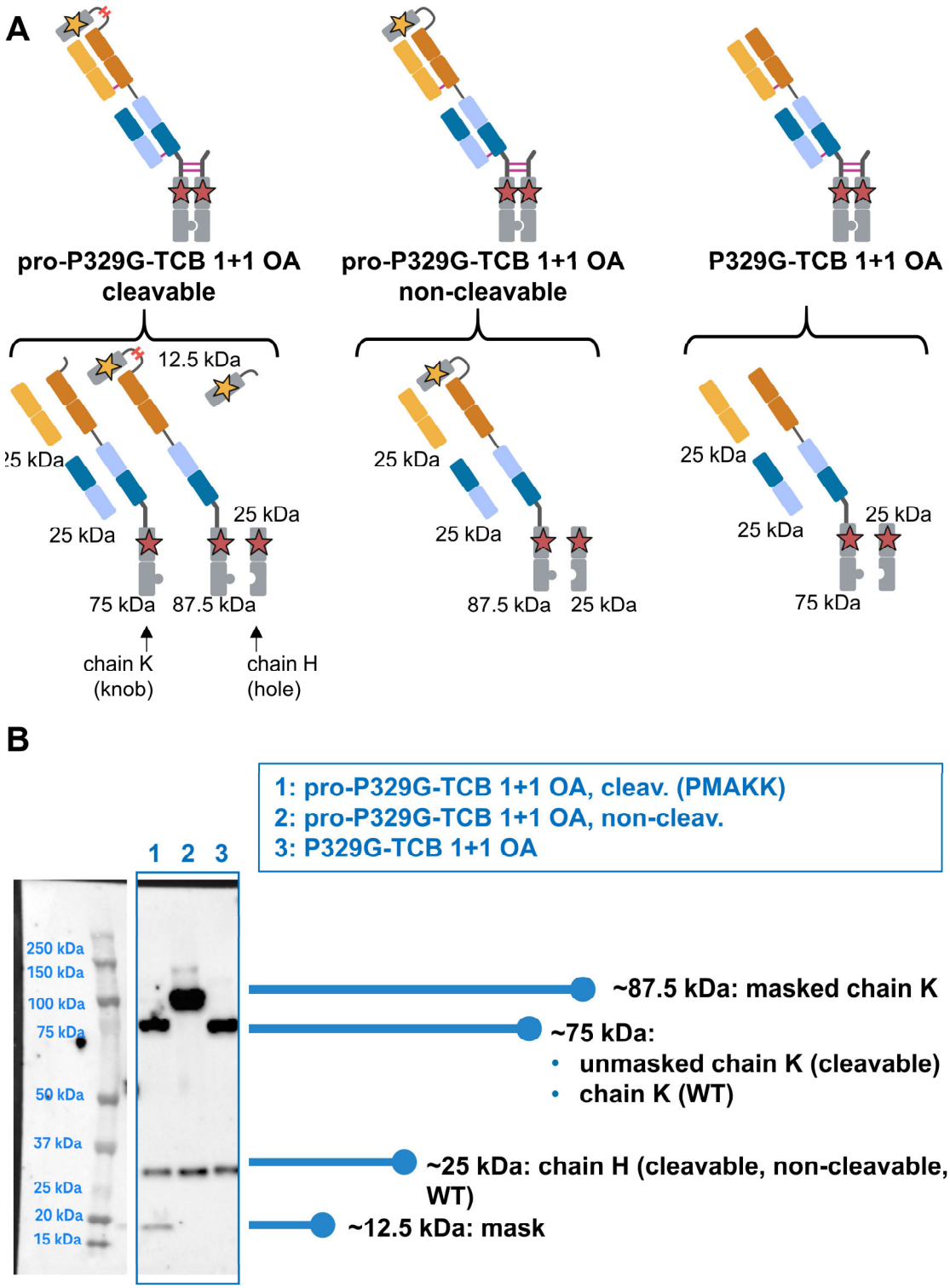

Figure 7.2.4. Chains resulting from a reduction process of pro-P329G-TCB 1+1 OA, and anti-huFc Western blot analysis. A) Possible chains resulting from reduction of pro-P329G-TCB 1+1 OA and control TCBs. B) Bands representing chains of matriptase-pretreated pro-P329G-TCB 1+1 OA and the control TCBs. Data from one experiment.

sequence-based MW prediction [368], [369][. For non-cleavable pro-P329G-TCB 1+1, a band representing masked (non-cleaved) chains is visible (~62.5 kDa), as well as WT chains K not bearing the mask (~50 kDa). The band representing the cleaved masks (~12.5 kDa) is not detectable. For non-masked WT P329G-TCB 1+1, only bands representing WT chains (~50 kDa) are present, with no detectable masked chains or cleaved masks. None of the molecules had detected levels of light chains (~25 kDa), which is due to the staining for Fc containing chains only. This data shows that the pro-P329G-TCB 1+1 underwent full cleavage and detachment of the mask, which was dependent on presence of the PMAKK protease-cleavable site in the linker joining the mask and P329G binder.

Figure 7.2.4 show analogous details of the assay performed on pro-P329G-TCB 1+1 OA formats. **Figure 7.2.4A** shows amino acid sequence-predicted MW of the chains resulting from reduction process, and **Figure 7.2.4B** shows band interpretation of the Western blot experiment. Cleavable pro-P329G-TCB 1+1 OA analysis showed no presence of masked chain, with detectable levels of unmasked chain (~75 kDa), Fc-only H chain (~25 kDa), and detached mask (~12.5 kDa). Non-cleavable pro-P329G-TCB 1+1 OA analysis showed only masked chain (~87.5 kDa), Fc-only H chain, no unmasked chain (~75 kDa) and no mask (~12.5 kDa). Non-masked WT pro-P329G-TCB 1+1 OA analysis showed WT chain K (~75 kDa) and Fc-only chain H (~25 kDa). Similarly to pro-P329G-TCB 1+1, these results for pro-P329G-TCB 1+1 OA show that the mask is successfully cleaved and detached, in a manner dependent on the presence of PMAKK cleavage site.

Figure 7.2.5 shows details of the Western blot performed on positive control pro-FOLR1-TCB 2+1 formats. The mask in pro-FOLR1-TCB 2+1 was based on an scFv format, resulting in a different MW of the mask than the P329G-mutated CH2 mask, as well as no predicted detection by anti-Fc staining. The linker between the mask and the CD3 binder in pro-FOLR1-TCB was the same as in the pro-P329G-TCBs (**Figure 7.2.5A**). As shown in **Figure 7.2.5B**, Cleavable pro-FOLR1-TCB 2+1 analyzed by Western blot showed bands representing fully unmasked chains (~75 kDa) or WT H chains (~50 kDa), with no detectable levels of non-cleaved chains (~104 kDa). Non-cleavable pro-FOLR1-TCB 2+1 analysis showed presence of masked chains (~104 kDa) and WT H chains (~50 kDa), with no detectable levels of unmasked chains (~75 kDa). This dataset also shows successful cleavage of the mask dependent on the PMAKK cleavage site. For the sake of completion, the pictograms of chains resulting from reduction of pro-P329G-TCBs 2+1 are included in **Figure 7.2.6**, which were analyzed at a later time point.

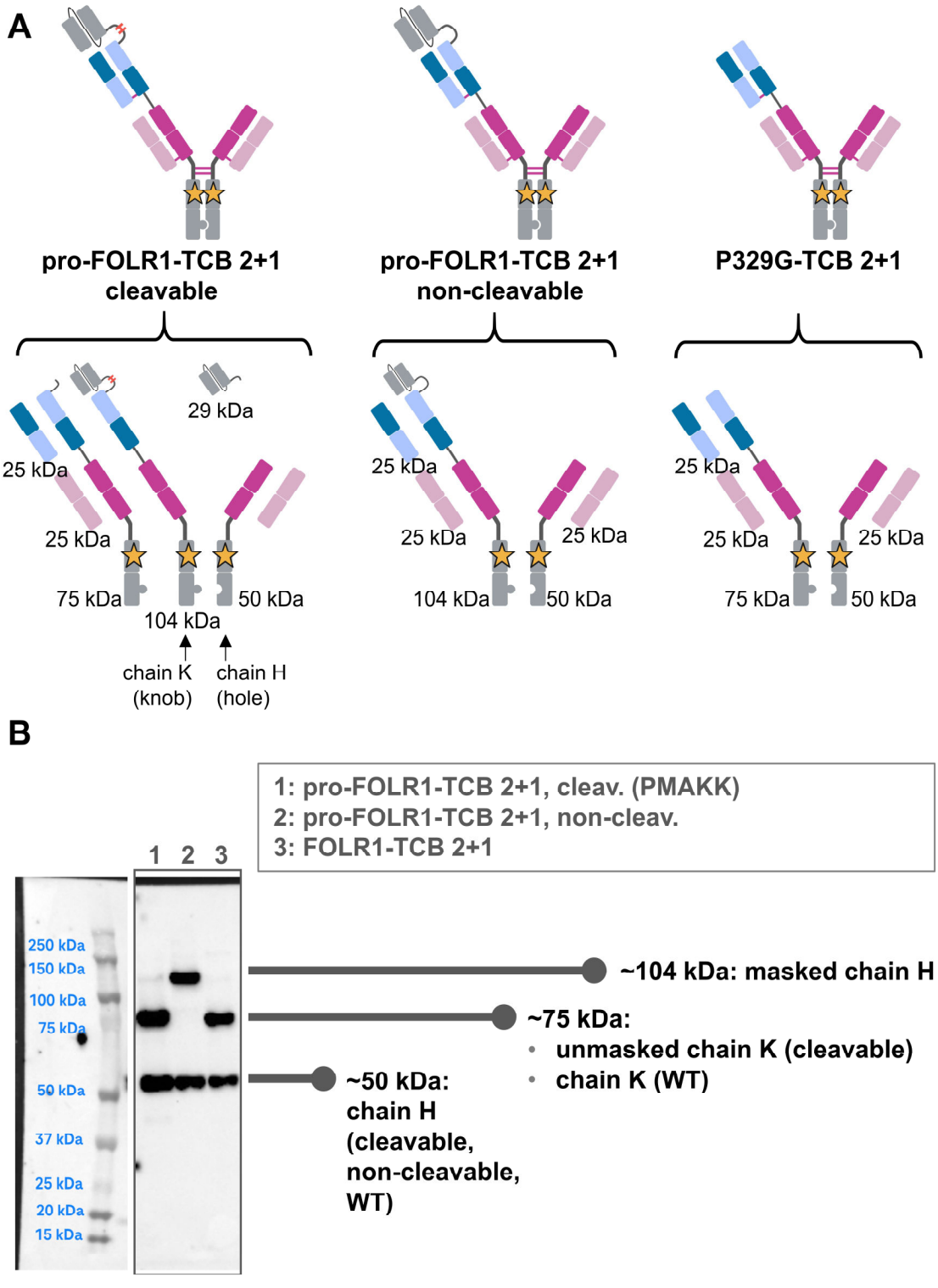

Figure 7.2.5. Chains resulting from a reduction process of the pro-FOLR1-TCB 2+1, and anti-huFc Western blot analysis. A) Possible chains resulting from reduction of pro-FOLR1-TCB 2+1 and control TCBs. B) Bands representing chains of matriptase-pretreated pro-FOLR1-TCB 2+1 and the control TCBs. Data from one experiment.

Additionally to the anti-Fc staining for the samples, anti-P329G staining was included for the matriptase-preincubated antibodies for more specific details on the detected chains (**Figure 7.2.7**). Pro-P329G-TCBs do not contain P329G mutation in the Fc part, but rather a P329R mutation, which was verified in this thesis to not be bound by anti-P329G antibodies (**Figure 7.1.3 in Chapter 1**). The only P329G-containing part of the molecule, being potentially detected by anti-P329G staining, was the P329G-mutated CH2 mask. Therefore, anti-P329G staining would allow verification of presence of any masked, pro-P329G-TCB chains and identify any cleaved P329G masks. As shown in **Figure 7.2.7**, Western blot with anti-P329G staining resulted in detection of 2 bands, representing masked chain H of the non-cleavable pro-P329G-TCB 1+1 (~62.5 kDa), and masked chain K of the non-cleavable pro-P329G-TCB 1+1 OA (~87.5 kDa). In contrast, cleavable pro-P329G-TCBs were not detected, suggesting a lack

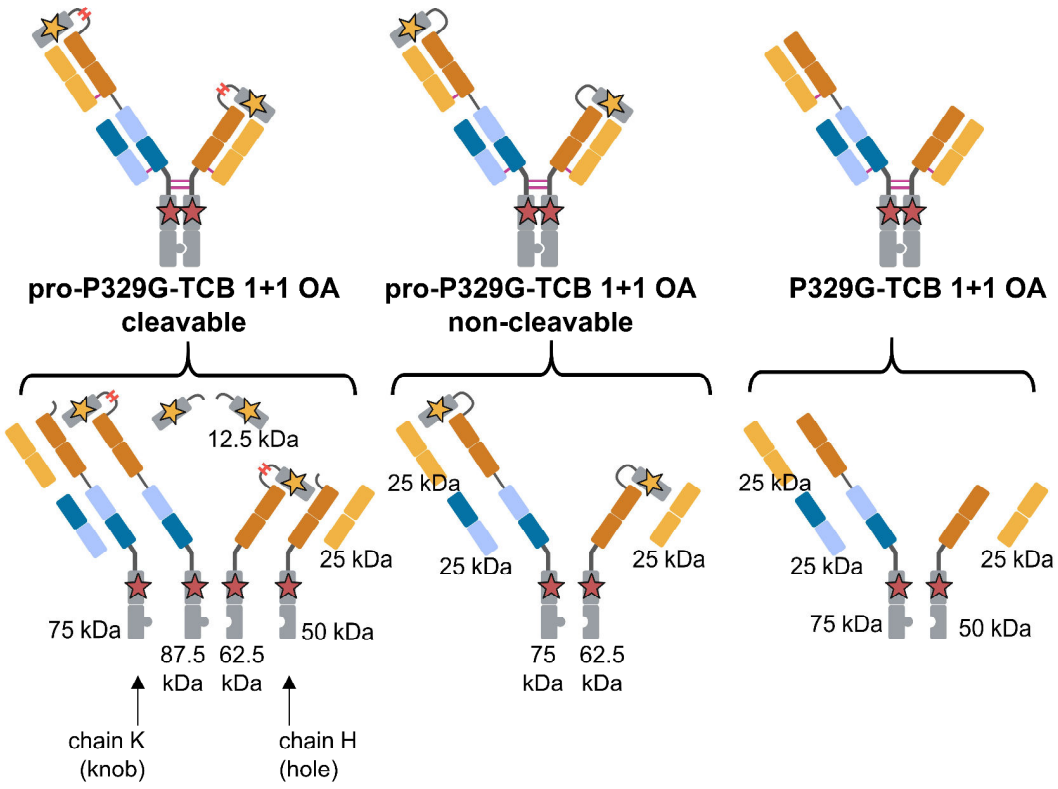

Figure 7.2.6. Chains resulting from a reduction process of the pro-P329G-TCB 2+1. Possible chains resulting from reduction of pro-P329G-TCB 2+1 and control TCBs.

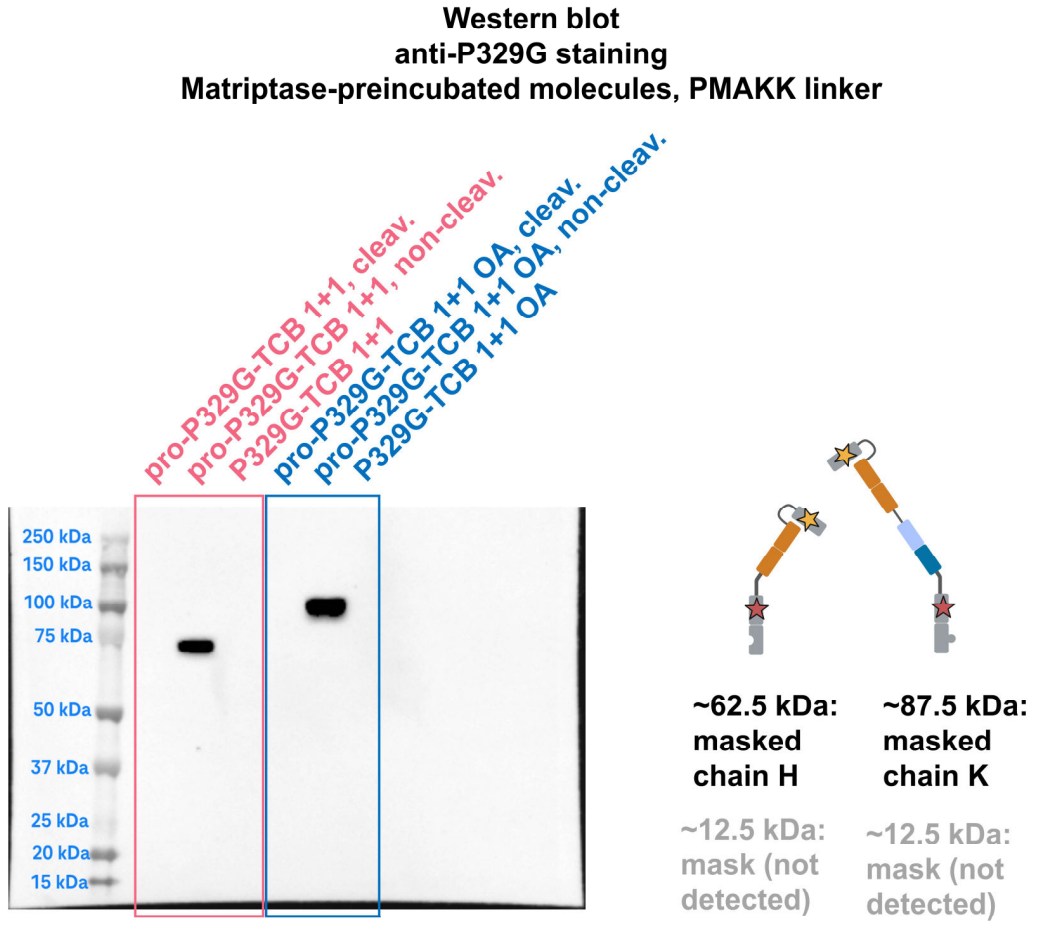

Figure 7.2.7. Chains represented in the anti-P329G Western blot analysis of reduced pro-P329G-TCBs. A) Bands representing chains of matriptase-pretreated pro-P329G-TCBs and the control TCBs. B) Pictograms of chains represented by the visible bands. Data from one experiment.

of the P329G mask. Interestingly, ~12.5 kDa bands representing the P329G masks were not observed. This may be due to lower sensitivity of anti-P329G staining as opposed to anti-Fc staining, low mass of the mask in the gel, or some denaturation of the mask upon cleavage. As expected, WT TCBs were not detected due to the absence of P329G. This data shows that the ~62.5 kDa and ~87.5 kDa bands seen in the anti-Fc blot were indeed P329G masked antibodies. Additionally, full cleavage of the cleavable pro-P329G-TCBs was confirmed.

Next, pro-P329G-TCBs with another matriptase cleavage site in the linker, namely PQARK, were designed and produced. Analogously to the Western blot assay for PMAKK linker, the aim was to test the cleavage capacity of the matriptase on the tested linker. To this end, a methodologic shift to SDS-PAGE was done, to increase assay throughput (as compared to Western blot throughput). This was possible due to the samples containing pure identified protein solutions and no need for distinguishing a mix of different proteins within a sample. Additionally, to show matriptase dependency, pro-P329G-TCBs with PQARK linker and their controls were preincubated with either matriptase or PBS. SDS-PAGE results of the samples

run under reducing conditions, as well as band description based on MW are shown in **Figure 7.2.8**. The upper panel shows a gel with the data from pro-P329G-TCBs in 1+1 and 1+1 OA formats, and the lower panel shows a gel with the data from pro-P329G-TCBs in 2+1 formats and the positive control pro-FOLR1-TCB 2+1. All tested cleavable TCBs showed different band profile with and without matriptase, retaining the mask without preincubation, and having completely cleaved off masks when preincubated with the tested protease. Non-cleavable TCBs had the same chain profile with or without matriptase, with the mask retained. The WT TCBs remained unchanged with or without matriptase. Together, these data shows that the masked pro-P329G-TCB molecules have successfully cleaved off masks only when preincubated with matriptase and only with cleavage site present in the linker.

Masked cleavable pro-P329G-TCBs induce reporter cell activation only in the presence of matriptase and the adaptor P329G IgG

After having established matriptase dependency in analytical assay, functional activity of the TCBs was tested. To do this, a CD3/NFAT Jurkat reporter assay was utilized, which is an assay that produces luminescence relative to the strength/level of CD3ε crosslinking-induced NFAT signaling. The molecules were preincubated with matriptase or PBS overnight, and then co-cultured human cancer cells expressing target of interest (HeLa for FOLR1-targeting in **Figure 7.2.9A** or MKN-45 for CEACAM- targeting in **Figure 7.2.9B**) with the PMAKK cleavable, non-cleavable or unmasked (WT) pro-P329G-TCBs 2+1 bearing P035-093 CD3ε binder, and with the CD3/NFAT Jurkat cells. As shown in **Figure 7.2.9A,B**, the positive control pro-FOLR1-TCBs 2+1 or CEACAM5-TCBs 2+1 (in blue) showed a dose-dependent activity with and without matriptase, and were active also as an unmasked version for both targets. This suggested incomplete masking of the binder, removing the activity dependence on matriptase. In contrast, for both targets, pro-P329G-TCBs 2+1 combined with the adaptor FOLR1 IgG or adaptor CEACAM5 IgG mutated with P329G (in red) resulted in minimal activation without matriptase and in unmasked format, and relatively stronger dose-dependent activity when preincubated with matriptase. Of note, pro-P329G-TCB without an adaptor was mostly inactive at lower concentrations, but showed some non-specific activity in both cleavable and non-cleavable format at high concentrations. Despite this phenomenon, adaptor+pro-P329G-TCB offered a sizeable therapeutic window of activity. The adaptor IgGs alone did not induce activity in any of the tested conditions. Despite lower activity than the positive control, pro-P329G-TCB showed better masking and higher matriptase dependent activity. Additionally, pro-P329G-TCB 2+1 was active against both targets, highlighting its target-agnostic universal potential of the molecule.

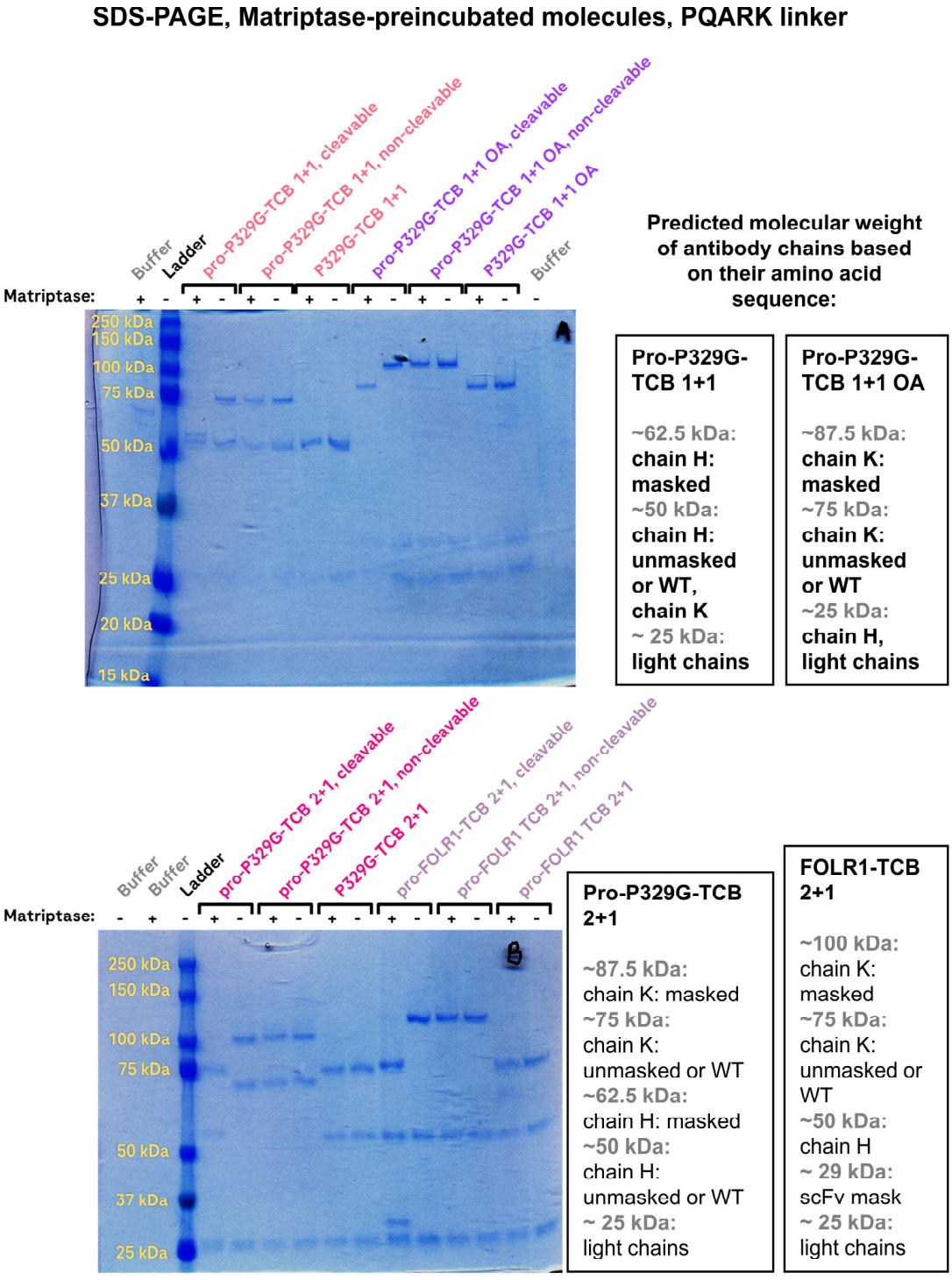

Figure 7.2.8. SDS-PAGE analysis of matriptase- or buffer-pretreated pro-P329G-TCBs and control molecules. A) SDS-PAGE results of pro-P329G-TCBs in 1+1 and 1+1 OA formats. B) SDS-PAGE results of pro-P329G-TCBs in 2+1 format, and of pro-FOLR1-TCB in 2+1 format. Data from one experiment.

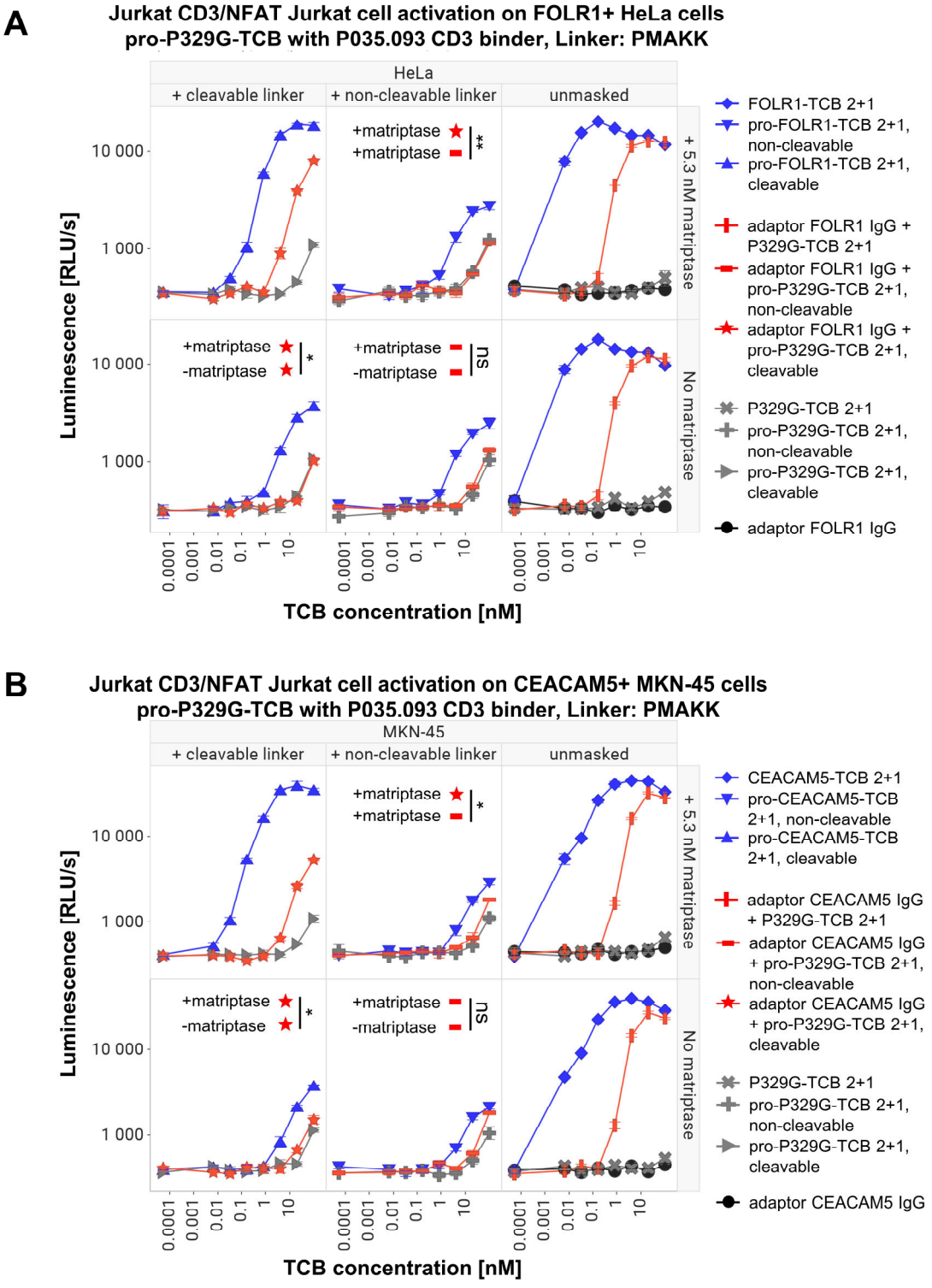

Figure 7.2.9. Matriptase-dependent Jurkat CD3/NFAT reporter cell activation of universal pro-P329G-TCBs containing PMAKK linker and P035.093 CD3ε binder on FOLR1+ and CEACAM5+ cancer cells. A) Matriptase-dependent Jurkat activation on FOLR1+ HeLa cells. B) Matriptase-dependent Jurkat activation on CEACAM5+ MKN-45 cells. Graphs show representative data from 2 or 3 independent experiments. Data collected in technical triplicates. Error bars indicate standard error.

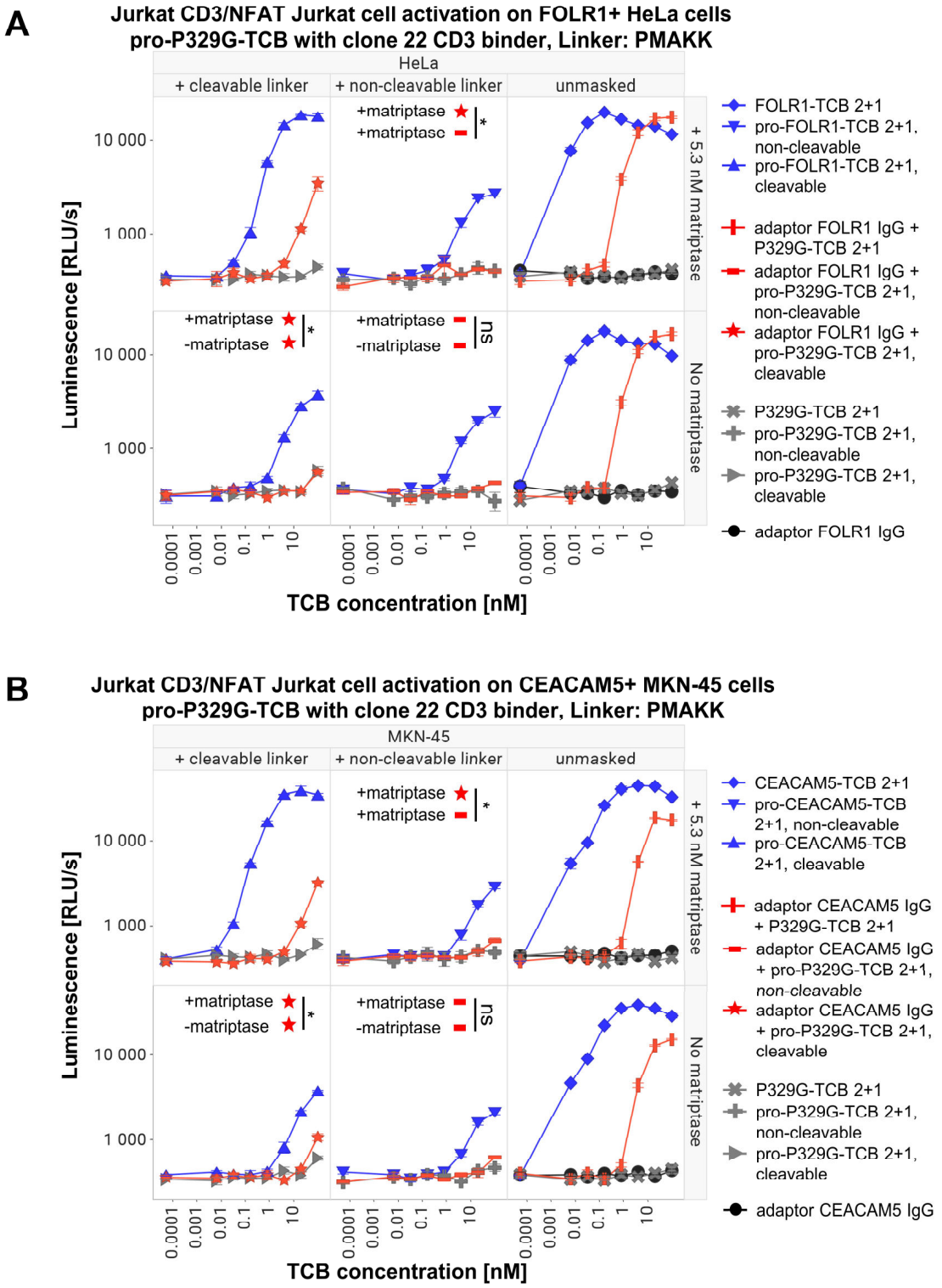

Figure 7.2.10. Matriptase-dependent Jurkat CD3/NFAT reporter cell activation of universal pro-P329G-TCBs containing PMAKK linker and clone 22 CD3ε binder on FOLR1+ and CEACAM5+ cancer cells. A) Matriptase-dependent Jurkat activation on FOLR1+ HeLa cells. B) Matriptase-dependent Jurkat activation on CEACAM5+ MKN-45 cells. Data of one (A) or representative of two (B) independent experiments. Data collected in technical triplicates. Error bars indicate standard error.

CD3ε binder influences specificity of the pro-P329G-TCB activity

With an aim to reduce the non-specific Jurkat cell activation induced by P035.093/PMAKK pro-P329G-TCB 2+1, the same set of antibodies were produced with changed CD3ε binder clone 22 that has circa 10-fold lower affinity for CD3e, and decided to test its influence in an analogous CD3-NFAT Jurkat assay. The positive control molecules tested had the P035.093 CD3ε binders and PMAKK linkers as tested previously. As shown in **Figure 7.2.10A,B**, clone 22/PMAKK-containing pro-P329G-TCBs, combined with adaptor FOLR1 IgG (**Figure 7.2.10A**, in red) or CEACAM5 IgG (**Figure 7.2.10B**, in red), displayed dose-dependent activity only in WT format or cleavable format only when preincubated with matriptase. Non-cleavable pro-P329G-TCBs showed no activity, with or without adaptor molecules, achieving reduced non-specificity. While the pro-FOLR1-TCB and pro-CEACAM5-TCBs showed the highest activity of all tested molecules, both showed high level of non-specificity. The data from **Figure 7.2.9** (P035.093 binder) and **Figure 7.2.10** (clone 22 CD3 binder) are summarized in **Figure 7.2.11** as area under the curve (AUC) and AUC fold change of matriptase-preincubated antibodies over no matriptase-preincubated antibodies. Both P035.093 and clone 22 pro-P329G-TCBs displayed matriptase-dependent activity in cleavable variants and complete masking in both matriptase-untreated cleavable and non-cleavable variants. The data showed that P035.093 CD3ε binder was contributing to a low level of non-specific activation, and clone 22 CD3ε binder offered improved specificity profile for the pro-P329G-TCBs. While lowering activity of the pro-P329G-TCB 2+1, clone 22 binder's improved specificity resulted in the selection of this clone as the lead CD3ε binder in further experiments.

Proteolysis of both PMAKK and PQARK matriptase cleavage sites result in comparable efficacy profile of the pro-P329G-TCBs

Having established matriptase-induced cleavage of pro-P329G-TCBs with either PMAKK or PQARK cleavable linkers using SDS-PAGE/Western blot, evaluation and comparison of their activity was proceeded with in functional assays. A CD3/NFAT Jurkat reporter assay was used as described above, with MKN-45 cells (CEACAM5+) as target cells. As shown in **Figure 7.2.12**, cleavable pro-P329G-TCB (clone 22 variants, PMAKK or PQARK linkers) combined with adaptor CEACAM5 IgG resulted in the same activity profile with both linkers when preincubated with or without matriptase. Both molecules combined with the adaptors showed a strong dose response with matriptase and a sizeable therapeutic window in terms of matriptase dependence.

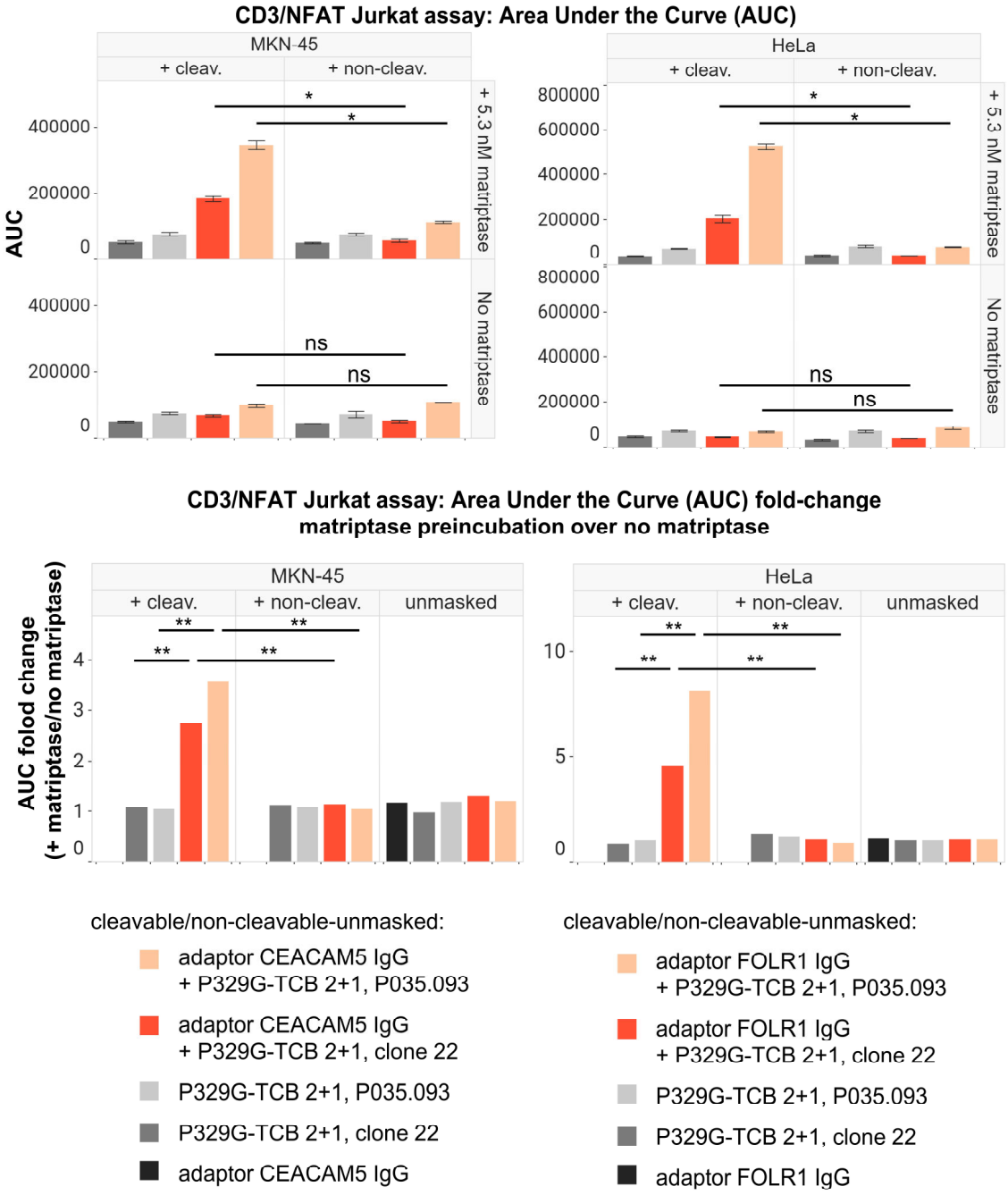

Figure 7.2.11. Area under the curve values from Jurkat CD3/NFAT reporter cell assays representing matriptase dependency and masking efficiency of pro-P329G-TCBs with PMAKK linkers and two different CD3ε binders, against two tumor targets. A) Area under the curve results across matriptase conditions and molecule formats for CEACAM5 targeting and FOLR1 targeting. B) Fold change of areas under the curves (from average values) over conditions of no matriptase pretreatment (average values), across molecule formats, for CEACAM5 and FOLR1 targeting. Data from 1 or 2 independent experiments, collected in technical triplicates. Error bars indicate standard error.

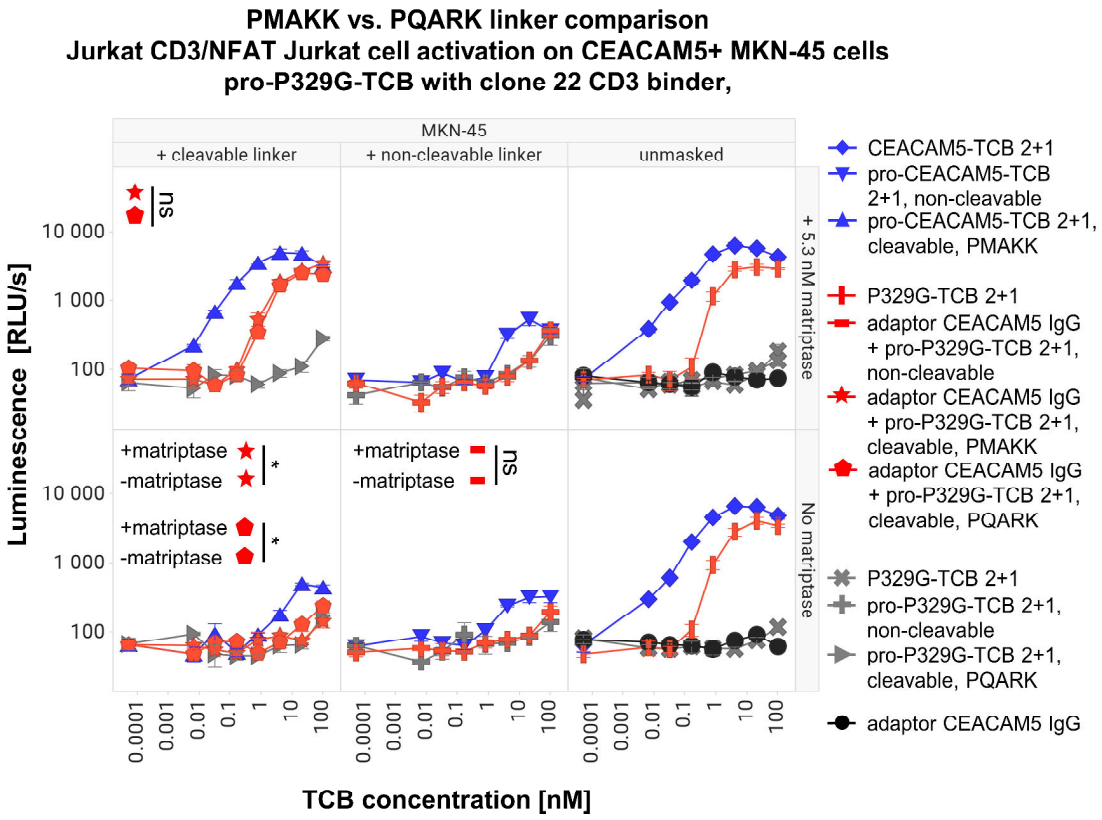

Figure 7.2.12. Comparison of PMAKK and PQARK linkers in matriptase-dependent Jurkat CD3/NFAT reporter cell activation of universal pro-P329G-TCBs containing clone 22 CD3ε binder on CEACAM5+ cancer cells. Data from 1 to 3 independent experiments, collected in technical triplicates. Error bars indicate standard error.

Pro-P329G-TCB shows matriptase- and adaptor-dependent activity in three antibody formats: 2+1, 1+1 and 1+1 OA

In order to evaluate activity of all the produced TCB formats, a further CD3/NFAT Jurkat assay was performed, on the same target MKN-45 with the same adaptor CEACAM5 P329G-mutated IgGs but different TCB formats: 2+1, 1+1 and 1+1 OA. As shown in **Figure 7.2.13**, all tested formats showed dose-dependent and matriptase dependent activity when combined with the adaptor IgG: pro-P329G-TCB 2+1 (**Figure 7.2.13A**), pro-P329G-TCB 1+1 (**Figure 7.2.13B**), and pro-P329G-TCB 1+1 OA (**Figure 7.2.13C**). 1+1 format showed non-specificity at high concentrations (without an adaptor) (**Figure 7.2.13B**), nevertheless providing a therapeutic window when compared to the adaptor-combined pro-P329G-TCB. An overlay of the dose response curves from all the cleavable formats in the matriptase-preincubated conditions are shown in **Figure 7.2.14**. All formats show similar activity profile. This data shows that all TCB formats can be utilized for the universal pro-P329G-TCB platform.

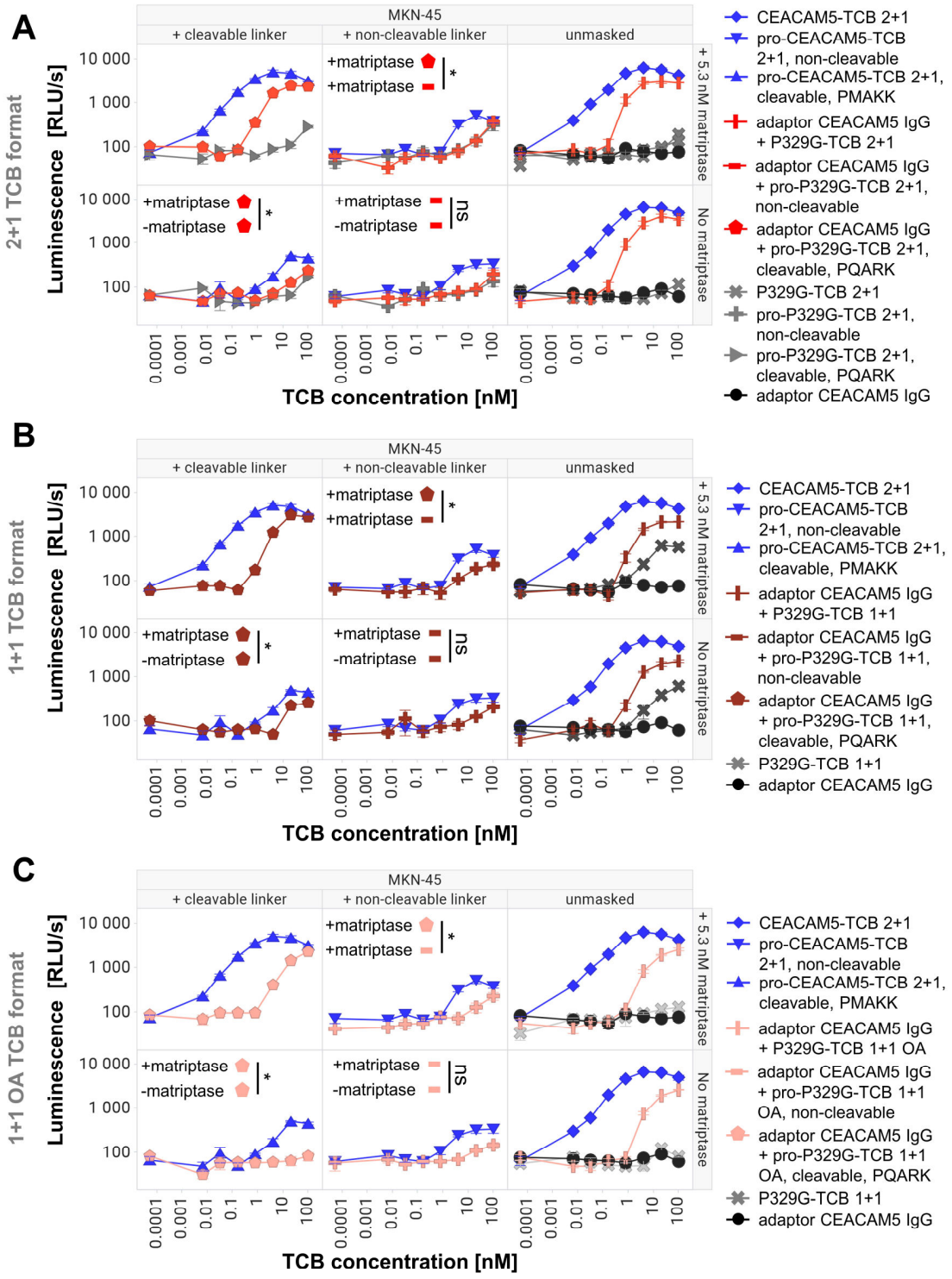

Figure 7.2.13. Antibody format comparison in matriptase-dependent Jurkat CD3/NFAT reporter cell activation of universal pro-P329G-TCBs (clone 22) on CEACAM5+ cancer cells. A) Matriptase-dependent Jurkat activation of pro-P329G-TCB format. B) Matriptase-dependent Jurkat activation of 1+1 pro-P329G-TCB format C) Matriptase-dependent Jurkat activation of 1+1 OA pro-P329G-TCB format. Data from one experiment, collected in technical triplicates. Error bars indicate standard error.

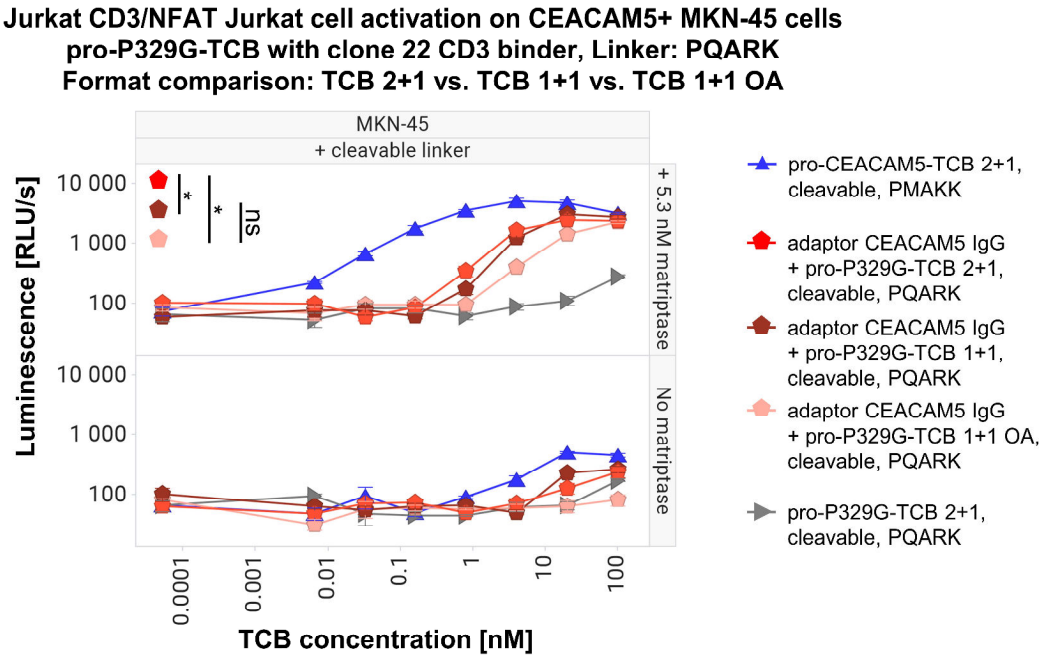

Figure 7.2.14. Summary of antibody format comparison (2+1, 1+1 and 11+1 OA) in matriptase-dependent Jurkat CD3/NFAT reporter cell activation of universal pro-P329G-TCBs with PQARK linkers on CEACAM5+ cancer cells. Data from one experiment, collected in technical triplicates. Error bars indicate standard error.

Pro-P329G-TCB induces T cell activation and T cell-mediated tumor cell killing *in vitro* in presence of matriptase and adaptor IgG

To further explore functional activity of matriptase-dependency of the pro-P329G-TCB, the molecule's potential for inducing primary T cell activation and tumor cell killing was investigated. To accomplish this, a killing assay was performed, where the pro-TCBs with adaptors were preincubated with recombinant matriptase or PBS overnight, and then co-cultured with FOLR1- expressing HeLa cells and human primary PBMCs from a healthy donor. After 48h, cytotoxicity was measured via relative quantification of dead cell proteases released into the supernatant. Additionally, cells were collected and stained for viability, CD4 and CD8 T cell markers, CD69 and CD25 T cell activation markers. As shown in **Figure 7.2.15**, adaptor FOLR1 IgG combined with pro-P329G-TCB 2+1 showed no cytotoxicity induction in the non-cleavable format. Cleavable pro-P329G-TCB 2+1 combined with the adaptor FOLR1 IgG (in red) induced a dose-dependent cytotoxicity in presence if matriptase, while no matriptase condition had some residual activity at the highest concentration. Of note, cells in the assay might have expressed an active protease affecting the interpretation of the no matriptase condition. Importantly, matriptase preincubation did not diminish the efficacy of the WT non-cleavable P329G-TCB combined with the adaptor IgG. Effects of the molecules on T cell activation are shown in **Figure 7.2.16**. In all tested T cell populations: CD69+ [% of CD4+], CD25+ [% of CD4+], CD69+ [% of CD8+], CD69+ [% of CD8+], there was observable dose-dependent T cell activation only in the matriptase preincubated pro-P329G-TCBs. The positive

control pro-FOLR1-TCB induced T cell activation regardless of matriptase conditions, as well as presence of the cleavable linker, suggesting the inadequate masking of the specific antibody used. Together, this data provides evidence that adaptors combined with pro-P329G-TCB have the capacity of T cell activation and inducing T cell mediated cancer cell killing in a matriptase-dependent manner.

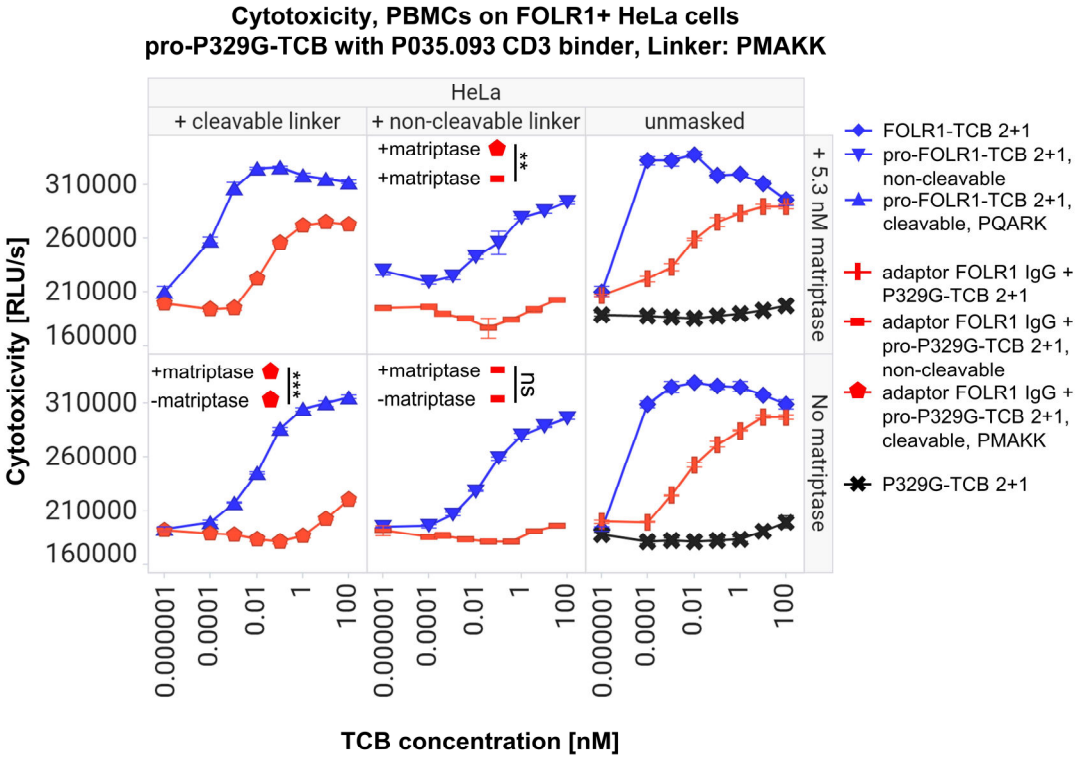

Figure 7.2.15. Matriptase-dependent primary T cell-mediated cytotoxicity induced by universal pro-P329G-TCBs against FOLR1+ HeLa+ cancer cells. Data from one experiment, collected in technical triplicates. Error bars indicate standard error.

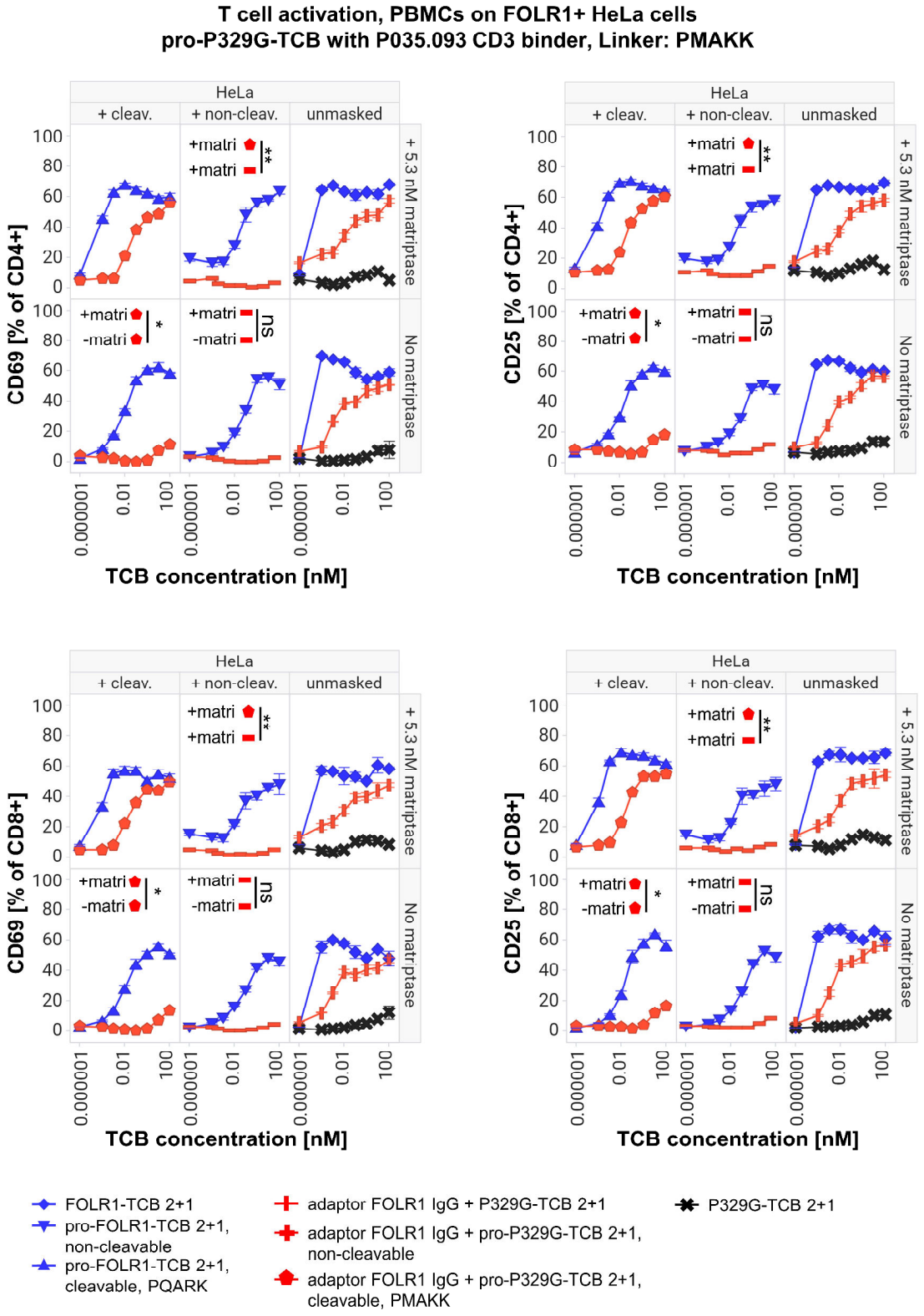

Figure 7.2.16. Matriptase-dependent primary T cell activation induced by universal pro-P329G-TCBs against FOLR1+ HeLa cancer cells. Data from one experiment, collected in technical triplicates. Error bars indicate standard error.

7.3. Chapter 3 – DOTAM-TCB: Universal small molecule-guided hapten- and T cell-bispecific antibodies for cancer immunotherapy

DOTAM-TCB binds Ca-DOTAM-Ligands with femtomolar-range affinity

Two small molecule ligands were designed by Dr. Dario Venetz (Roche Innovation Center Zurich) in collaboration with Antonio Ricci and Moreno Wichert (Roche Innovation Center Basel). Two small molecule ligands, Ca-DOTAM-DUPA and Ca-DOTAM-Folate, were prepared. To validate binding of the DOTAM-TCB to the newly produced Ca-DOTAM-Ligands, KinExA affinity measurement was performed (Daniela Matscheko, Roche Innovation Center Munich). Ca-DOTAM-DUPA and Ca-DOTAM-Folate were tested against two formats of the TCB: DOTAM-TCB 1+1 and DOTAM-TCB 1+1 OA. **Figure 7.3.1A** shows binding curves representing free fraction of constant binding partners. Dose responses were observed for all conditions. Figure 7.3**.1B** depicts a summary of EC_{50} values derived from the curves. The K_D values calculated from the observed interactions were in double-to-triple femtomolar range (51-263 fM), as depicted in **Figure 7.3.2**. The values fell within an expected range, as previous experiments performed for the DOTAM antibody binder to Ca-DOTAM (lacking the tumor ligand part) resulted in similar observed affinity [363] Altogether, binding of Ca-DOTAM-Ligands by DOTAM-TCB was confirmed for both 1+1 and 1+1 OA formats with very high affinity.

Surface Plasmon Resonance (SPR) characterization of binding kinetics

To expand the platform, an additional ligand, Ca-DOTAM-AAZ was designed. Preparation took place in collaboration with Antonio Ricci (Roche Innovation Center Basel). To characterize binding of the adaptors with the DOTAM-TCB to the selected tumor associated antigens, SPR experiments were conducted (performed by Reto Gianotti and Regula Buser, Roche Innovation Center Zurich). In contrast to the cell-based binding assays, by virtue of utilizing a system with strictly defined ligands, SPR allows for a verification of the binding partners, as well as kinetics and affinity. For CAIX binding tests, Ca-DOTAM-AAZ premixed with DOTAM-TCB 1+1 was used as various concentrations against a recombinant CAIX at pH 7.0. As expected from the literature on AAZ, binding was indeed observed. The adjusted SPR sensorgram are depicted in **Figure 7.3.3A**. The equilibrium dissociation constant K_D based on the observed interactions was determined to be 0.378 nM. Analogously to CAIX targeting, DOTAM-TCB 1+1 were mixed with either Ca-DOTAM-DUPA or Ca-DOTAM-Folate and tested for their kinetic binding interaction at pH 7.0 with PSMA or FOLR1, respectively. Direct PSMA-TCB 2+1 and FOLR1-TCB 2+1 were used as positive controls. As expected, for both targets, positive controls displayed rapid association with the respective binding partners (**Figure 7.3.3B,C**). However, the response rate for adaptor-loaded DOTAM-TCBs were low for both PSMA- and CAIX-targeting molecules (**Figure 7.3.3B,C**). This was in contrast to the cell binding assays and the functional assays performed on the same molecule batches at a later time point (data not shown). Therefore, it was hypothesized that the technical conditions of the SPR acquisitions, such as buffer composition, may have influenced the binding results in that system. For this reason, as well as dimeric form of PSMA used, K_D values were not calculated.

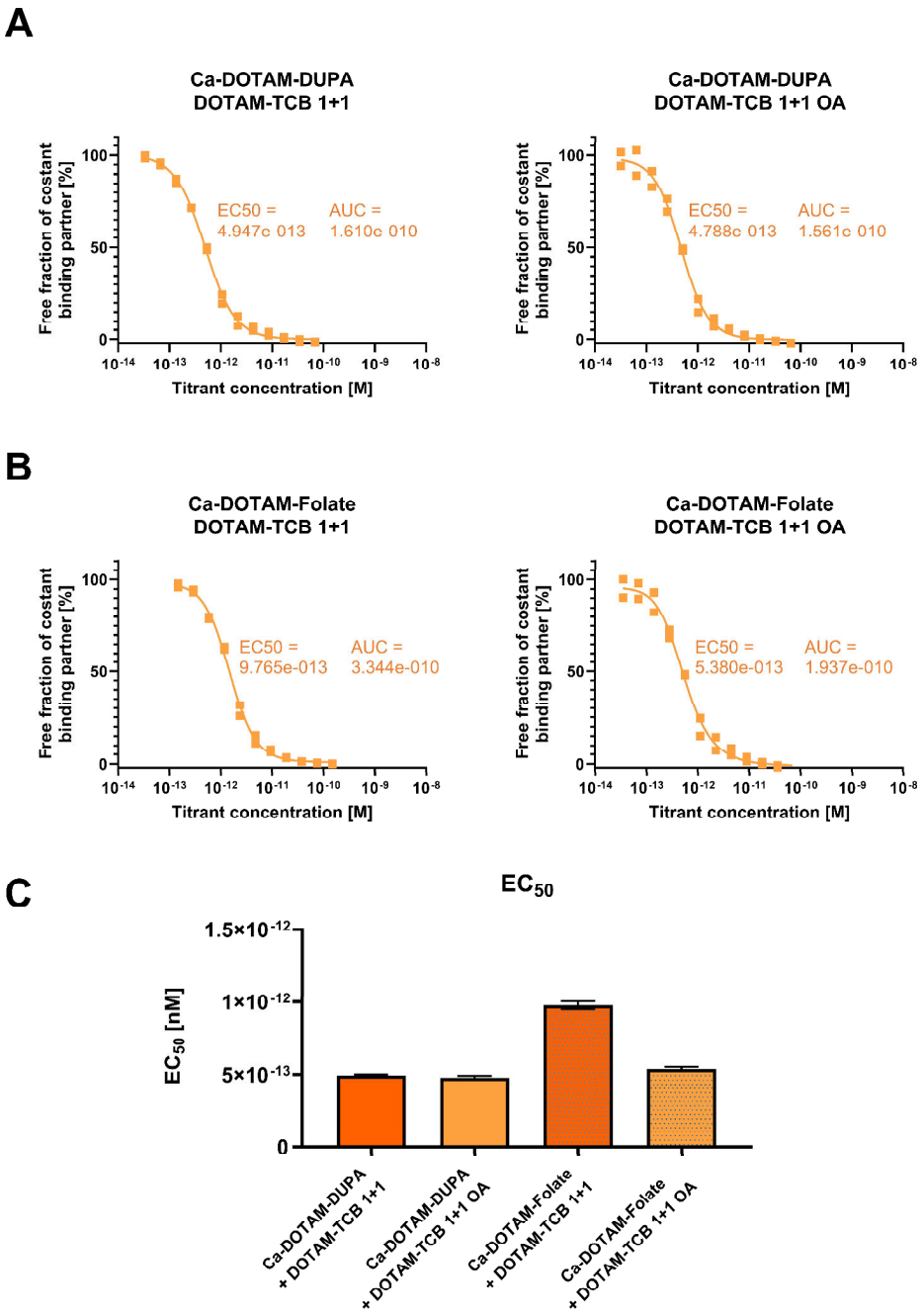

Figure 7.3.1. KinExA measurements of the interactions between DOTAM-TCB formats with Ca-DOTAM-Ligands. Concentration-dependent free fraction of the binding partner, of A) Ca-DOTAM-DUPA with DOTAM-TCB 1+1 and 1+1 OA, and B) Ca-DOTAM-Folate with DOTAM-TCB 1+1 and 1+1 OA. C) Summary of EC_{50} values including standard error from all conditions. Data from one experiment with technical duplicates. Error bars indicate standard error.

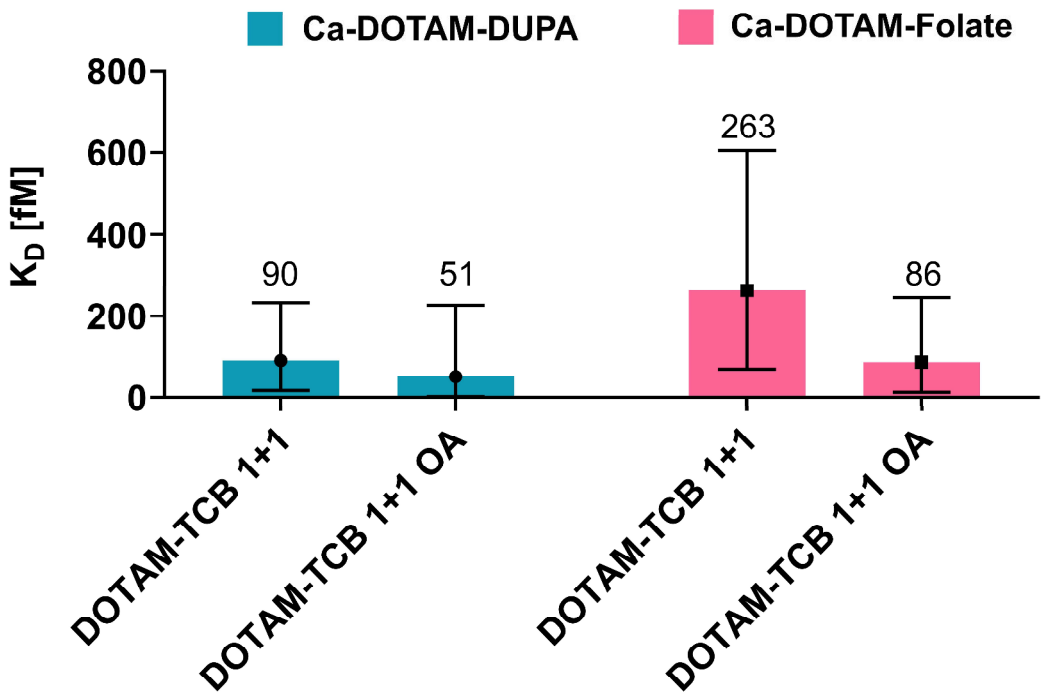

Figure 7.3.2. K_D values derived from KinExA measurements of the interactions between DOTAM-TCB and Ca-DOTAM-Ligands. Data from one experiment with technical duplicates. Error bars indicate 95% confidence

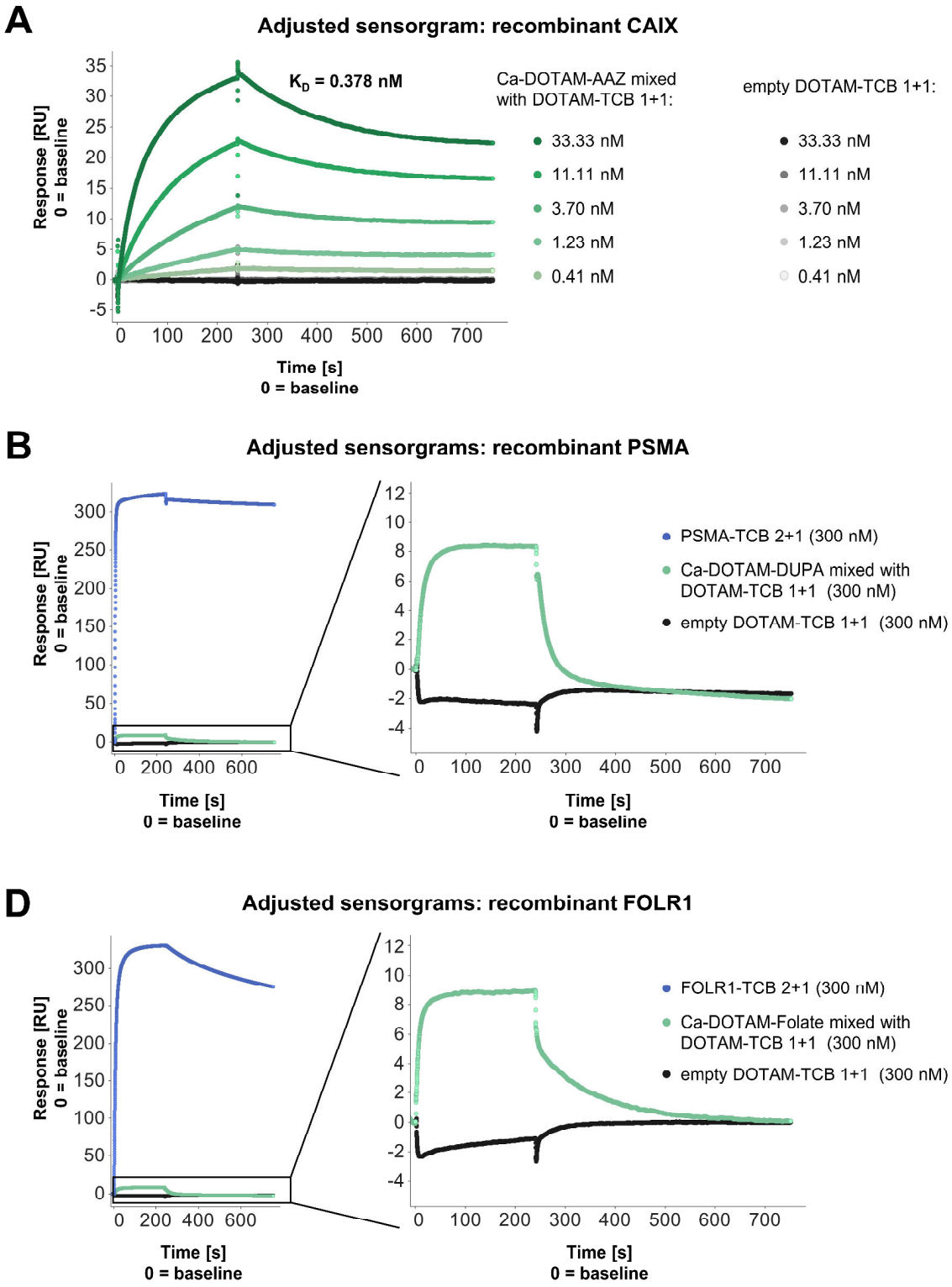

Figure 7.3.3. SPR sensorgrams of the binding kinetics between recombinant CAIX, PSMA and FOLR1 receptors and the Ca-DOTAM-Ligands mixed with DOTAM-TCB 1+1. A) Sensorgram of binding kinetics between CAIX and Ca-DOTAM-AAZ mixed with DOTAM-TCB 1+1 or empty DOTAM-TCB 1+1 at different concentrations. B) Sensorgram of binding kinetics between PSMA and Ca-DOTAM-DUPA mixed with DOTAM-TCB 1+1 or empty DOTAM-TCB 1+1. C) Sensorgram of binding kinetics between FOLR1 and Ca-DOTAM-Folate mixed with DOTAM-TCB 1+1 or empty DOTAM-TCB 1+1. Data from one experiment is shown.

In line with this, determination of K_D values for DOTAM-TCB 1+1 mixed with Ca-DOTAM-DUPA and Ca-DOTAM-Folate were not feasible, and further SPR set up optimization is warranted. Moreover, K_D value of the interaction between CAIX and Ca-DOTAM-AAZ with DOTAM-TCB 1+1 may need further verification. Due to the fact that the structures of the receptor-binding ligands within the adaptors were based on the literature, the K_D values of the original small molecule ligands provide additional information even in absence of SPR data. The data on the literature-derived K_D values is depicted in **Table 7.3.1**, including both small molecules and control antibodies against CAIX, PSMA and FOLR1. Importantly, the antibody binders depicted in **Table 7.3.1** were added to the TCB frame, and used in the TCB format as positive controls throughout this chapter. Nevertheless, it is important to note these values cannot be translated to the novel adaptors. This is due to the fact that addition of linkers and Ca-DOTAM-haptens to the original ligand structures might have changed the capability of the adaptors to access binding pockets in the target receptors. Moreover, Ca-DOTAM positioning in the binding pocket of the anti-DOTAM antibody may have also affected accessibility of the tumor ligand to reach its target. Therefore, further characterization of the adaptor themselves requires optimization.

Table 7.3.1. K_D values of interactions between human CAIX, PSMA and FOLR1 and selected published small molecule ligands and antibody binders.

Target receptor	Ligand	K_D
CAIX	AAZ / AAZ conjugates	3.4 nM [370], 10-50 nM [371]
	Antibody binder G250	4 nM [372]
PSMA	DUPA / DUPA conjugates	8 nM [373] / 14 nM [374]
	Antibody binder J591	1.83 nM [375]
FOLR1	Folate / folate conjugates	1.5 nM [376]
	Antibody binder 16D5	39.5 nM [377]

Due to the potential technical artifacts in SPR, cell-based assays were deemed as more reliable readouts. As mentioned above, Ca-DOTAM-Folate with DOTAM-TCB did not show binding on FOLR1-overexpressing cells. These negative results prompted consideration of deprioritizing Ca-DOTAM-Folate for further experiments. However, since flow cytometry binding assay might be impacted by a cell harvesting protocol, for example shedding the antigen from the target cell, it might not be fully indicative of a binding potential. Therefore, further validation of the functionality of Ca-DOTAM-Folate with DOTAM-TCB was planned for other cell-based assays.

DOTAM binder crystal structure reveals Ca-DOTAM-ligand binding pocket

To gain deeper insights into the interaction between anti-DOTAM and Ca-DOTAM-Ligands, X-ray crystallography was employed to elucidate the spatial organization of the bound molecules (performed and analyzed by Dr. Jörg Benz and Andreas Ehler, Roche Innovation Center Basel). Ca-DOTAM-AAZ was selected for testing. Imaging of the obtained crystals of Ca-DOTAM-AAZ with anti-DOTAM Fab revealed Fab-bound small molecules (**Figure 7.3.4A**) with multiple van der Waals and hydrogen bonds contributing to the interaction (**Figure 7.3.4B**). An electron density map of the Ca^{2+} in the DOTAM cage is depicted in **Figure 7.3.4C**. Importantly, small molecules were observed with incomplete structures, wherein only Ca^{2+}-loaded DOTAM with an exit vector was visibly discernible from the electron density map (**Figure 7.3.4D**) Electron density was observed for the adaptor up to the linker and first phenyl group. The part of the DOTAM with the exit vector for the linker and functional moiety pointed towards the solvent region. The remaining part of the molecule had no defined localization based on the observed electron density in the crystals. This observation likely stemmed from the flexibility of the free/unbound part of the adaptor molecule and lack of a single defined space occupied by it.

The Ca-DOTAM portion was observed bound within a pocket situated between the VH and VL of the anti-DOTAM Fab. The binding pocket was formed by amino acid residues from CDR1 and CDR3 of light and CDR2 and CDR3 of heavy chain. Van der Waals interactions of the DOTAM cage were observed for side chains of TYR29L, TYR100L PHE49H and TYR57H. The amid groups of the DOTAM moiety coordinated the binding of the central calcium atom with three of the amid groups also being involved in hydrogen bonding with residues ASP55H, GLU97H and APS33L of the antibody (**Figure 7.3.4B** and **Table 7.3.2**). The Ca-DOTAM portion observed bound within a pocket situated between the complementary determining regions (CDRs) of the VH and VL domains of the anti-DOTAM Fab illustrates the high shape complementarity as basis for the high affinity binding.

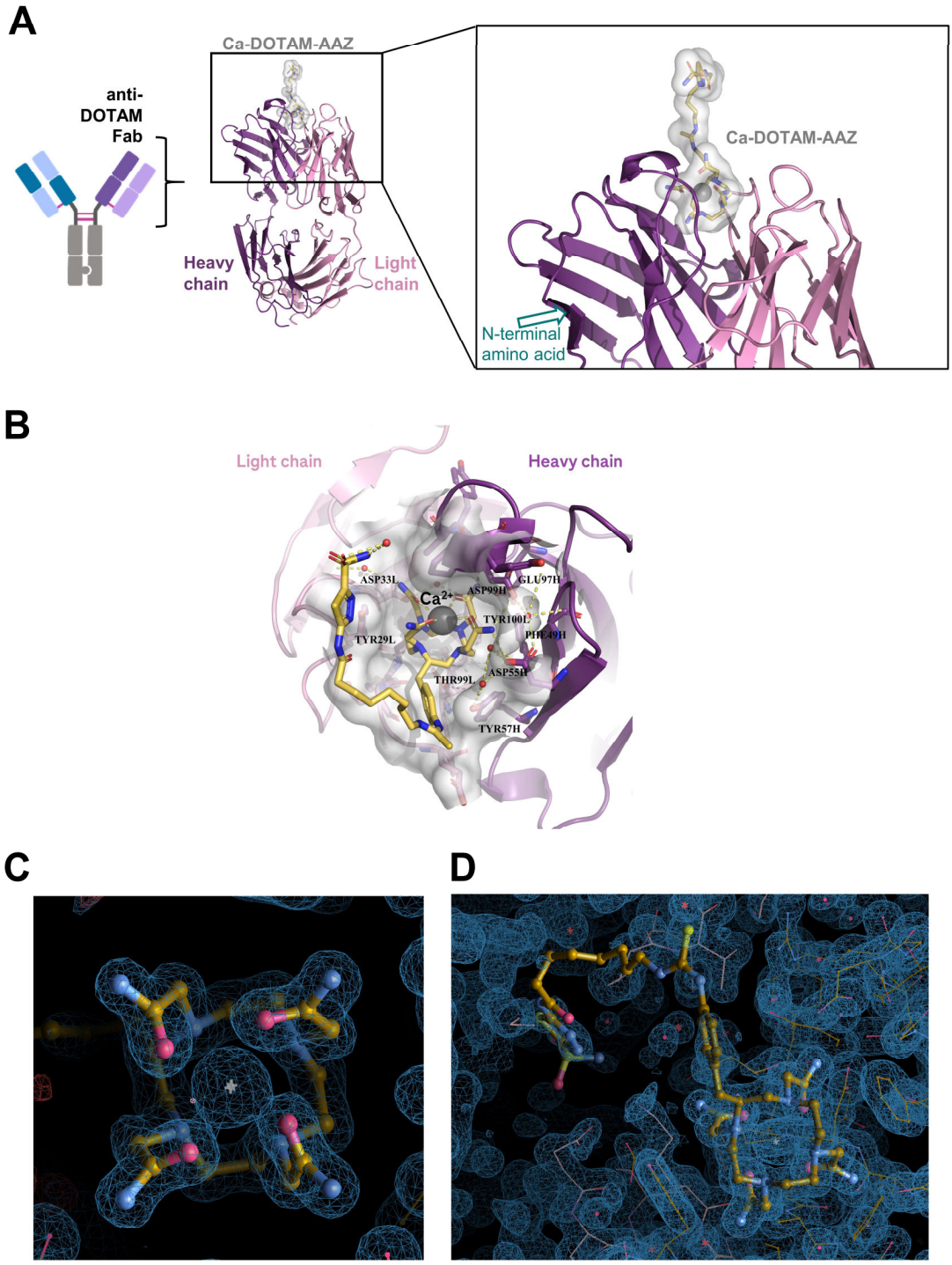

Figure 7.3.4. Crystal structure of anti-DOTAM Fab and Ca-DOTAM-AAZ. A) Modelled anti-DOTAM Fab with Ca-DOTAM-AAZ, displaying the antibody pictogram, the crystal structure of the Fab with the bound haptenated small molecule adaptor. B) Localization of the Ca2+ ion and Van der Waals and hydrogen bonds observed between the side chains of the amino acids in the anti-DOTAM Fab and the Ca-DOTAM-AAZ. C) 2Fo-Fc electron density map of the bound Ca2+-loaded DOTAM. Ca2+ showed as a grey star. D) Observed 2Fo-Fc electron density map of the Ca-DOTAM-AAZ, with defined Ca2+ in the DOTAM cage and the exit vector. Remaining part of the small molecule structure with no defined localization was overlaid on the observed electron density map.

Table 7.3.2. Ligand interactions report for the crystal obtained for anti-DOTAM Fab and Ca-DOTAM-AAZ.

Ligand	Fab fragment		Interaction type	Interaction role	Distance [Å]
	Atom localization	Amino acid/water and position			
C19	OG1	THR 99	(L)	H-donor	3.74
C21	OD2	ASP 55	(H)	H-donor	3.65
C21	O	HOH 47	(W)	H-donor	3.94
N23	OD2	ASP 55	(H)	H-donor	2.85
N23	OD2	ASP 99	(H)	H-donor	3.01
C26	OG1	THR 99	(L)	H-donor	3.46
C28	OE1	GLU 97	(H)	H-donor	3.63
N30	OE1	GLU 97	(H)	H-donor	2.77
N30	O	ARG 98	(H)	H-donor	2.99
C32	O	HOH 85	(W)	H-donor	3.91
C33	OG1	THR 99	(L)	H-donor	3.77
C35	OD2	ASP 33	(L)	H-donor	3.55
C35	O	HOH 5	(W)	H-donor	3.50
N37	OD1	ASP 3	(L)	H-donor	3.02
C40	O	TYR 3	(L)	H-donor	3.35
O24	CB	ASP 99	(H)	H-acceptor	3.24
O57	O	HOH 57	(W)	H-acceptor	2.97
C25	6-ring	PHE 49	(H)	H-pi	4.18
C28	6-ring	PHE 49	(H)	H-pi	3.86

Ca-DOTAM-Ligands combined with DOTAM-TCB bind to the target-expressing cells or recombinant targets *in vitro*

To assess the binding of the molecules on cancer cells, a binding assay. Having established binding of the DOTAM binder to Ca^{2+}-loaded DOTAM-Ligands and Ca-DOTAM-Ligands to the recombinant target antigens, a binding of the small molecules to the cancer cells was assessed. Examination of the binding capacity of combined Ca-DOTAM-AAZ, Ca-DOTAM-DUPA, or Ca-DOTAM-Folate with DOTAM-TCB towards their respective target-expressing cells was conducted. Antigen positive cancer cells were incubated with DOTAM-TCB and the molecules: HT-29 (CAIX+) cells with Ca-DOTAM-AAZ, LNCaP (PSMA+) cells with Ca-DOTAM-DUPA, and HeLa (FOLR1+) cells with Ca-DOTAM-Folate. To detect bound molecules, flow cytometry readout was employed, utilizing an anti-P329G IgG in PE as a secondary antibody. The P329G mutation served as an Fc silencing mutation, and was present in the DOTAM-TCB but not in the adaptor molecules. Consequently, in this set-up, any observed binding events would imply the presence of cell-bound molecules containing either cell-attached small molecule adaptors subsequently bound by the DOTAM-TCB, or solely DOTAM-TCB. As shown in **Figure 7.3.5**,

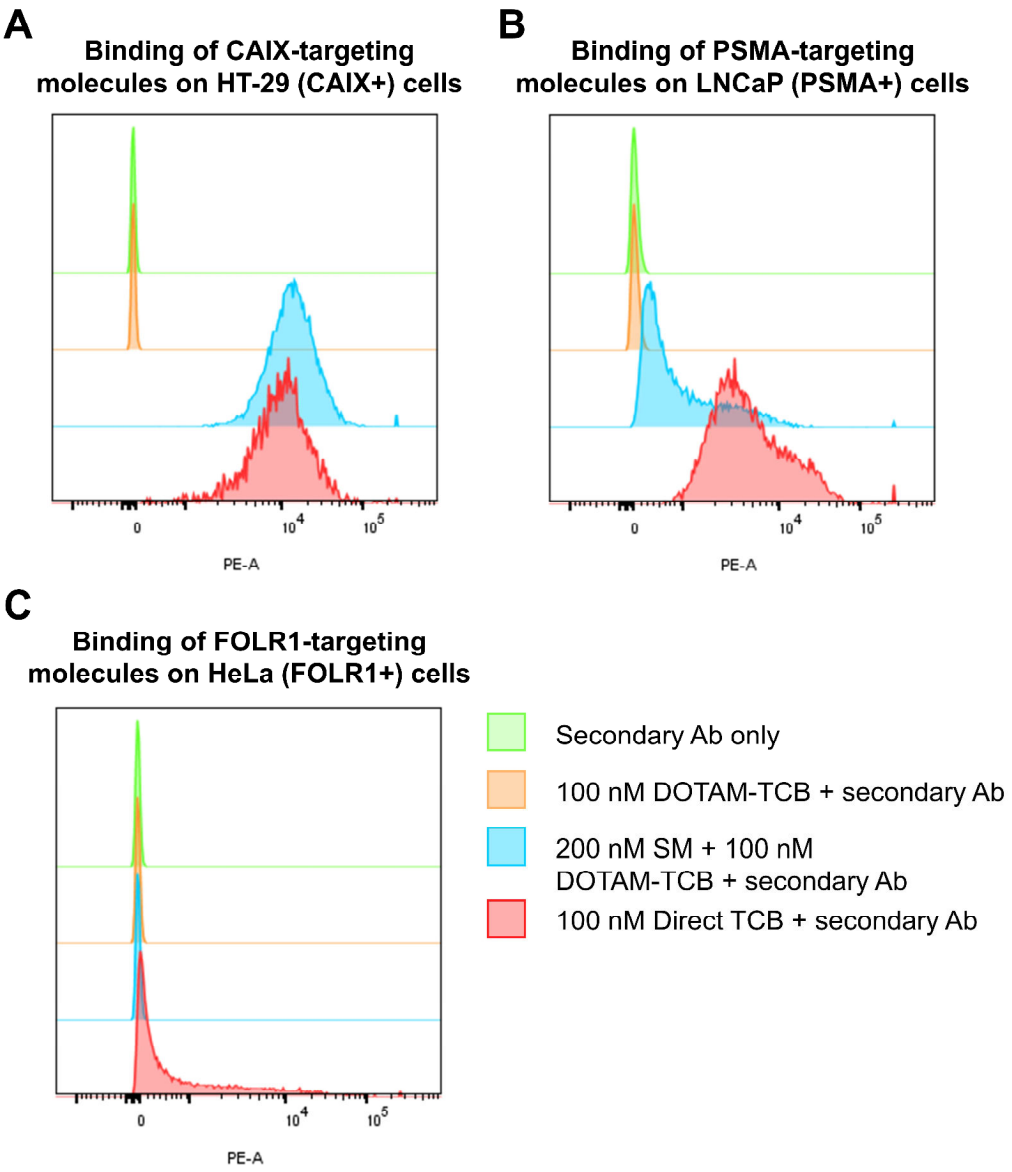

Figure 7.3.5. Binding of the adaptors combined with DOTAM-TCB to different target-expressing cancer cells. Histograms derived from flow cytometry binding assay of DOTAM-TCB combined with: A) Ca-DOTAM-AAZ on CAIX+ HT-29 cells, B) Ca-DOTAM-DUPA on PSMA+ LNCaP cells, and C) Ca-DOTAM-Folate on FOLR1+ HeLa cells. Representative histograms of triplicates from 2 experiments are shown.

across all three tested cell lines, secondary antibody negative control or DOTAM-TCB only with secondary antibody staining resulted in negative populations. Binding of DOTAM-TCB was observed only when combined with cell line-appropriate small molecule adaptor. Specifically, Ca-DOTAM-AAZ with DOTAM-TCB demonstrated stronger binding compared to the positive control direct CAIX-TCB (**Figure 7.3.5A**), while Ca-DOTAM-DUPA with DOTAM-TCB exhibited weaker binding than the positive control direct PSMA-TCB (**Figure 7.3.5B**). In contrast, Ca-DOTAM-Folate with DOTAM-TCB did not yield a positive population, whereas weak binding was observed with the positive control direct FOLR1-TCB (**Figure 7.3.5C**).

Universal DOTAM-TCB shows *in vitro* proof of concept T cell activating activity when combined with Ca-DOTAM-DUPA or Ca-DOTAM-AAZ against PSMA+ cancer cells or CAIX+ cancer cells, respectively

As a next step, functional activity experiments were performed. The potential of universal DOTAM-TCB to crosslink CD3ε when bound to the adaptors targeting cancer cells was assessed. For this purpose, the CD3/NFAT Jurkat reporter assay was used. Target-expressing cells were seeded into plates, and after overnight incubation allowing for renewed expression of surface proteins, co-cultured with CD3/NFAT Jurkat reporter cells and the molecules. As controls, cell lines known not to express the targeted antigen were included. As illustrated in **Figure 7.3.6A**, Ca-DOTAM-DUPA combined with DOTAM-TCB in a 2+1 format (dosed in molar ratio SM:TCB 2:1) resulted in dose-dependent Jurkat cell activation across the three target-expressing cell lines while remaining inactive on target non-expressing cells. Both the adaptor and DOTAM-TCB alone, which served as negative controls, were inactive. Similarly, Ca-DOTAM-AAZ with DOTAM-TCB induced Jurkat cell activation only when combined and solely on target-expressing cells (**Figure 7.3.6B**).

Notably, while exhibiting a higher EC_{50} compared to the positive control CAIX-TCB, the activity plateau for Ca-DOTAM-AAZ with DOTAM-TCB was significantly elevated. In the case of FOLR1 targeting, Ca-DOTAM-Folate with DOTAM-TCB failed to demonstrate efficacy, despite the positive control FOLR1-TCB activating the Jurkat cells in a dose-dependent manner (**Figure 7.3.6C**). This discrepancy of this data with the SPR binding results led to hypothesize that the negative results of Ca-DOTAM-Folate with DOTAM-TCB were unrelated to the target (FOLR1) expression.

An additional hypothesis arose that the assay media, typically containing folate in a molecular form akin to the folate-based adaptor, might have competed with Ca-DOTAM-Folate and interfered with adaptor binding to the cancer cells. To verify this, folate-free and standard folate-containing media were prepared and the molecules were tested on two FOLR1+ cell lines in the CD3/NFAT Jurkat assay. Ca-DOTAM-Folate + DOTAM-TCB were preincubated prior to the assay. **Figure 7.3.6D** depicts impact of the presence of folate in the assay media on the activity of FOLR1-targeting TCB molecules. Activity of the antibody-based positive control FOLR1-TCB was unaffected by folate. For antigen targeting with Ca-DOTAM-Folate and DOTAM-TCB, a significantly increased dose-dependent Jurkat activity was observed in folate-free media, compared to standard media, on Hela cells, but not on SKOV-3 cells. Both

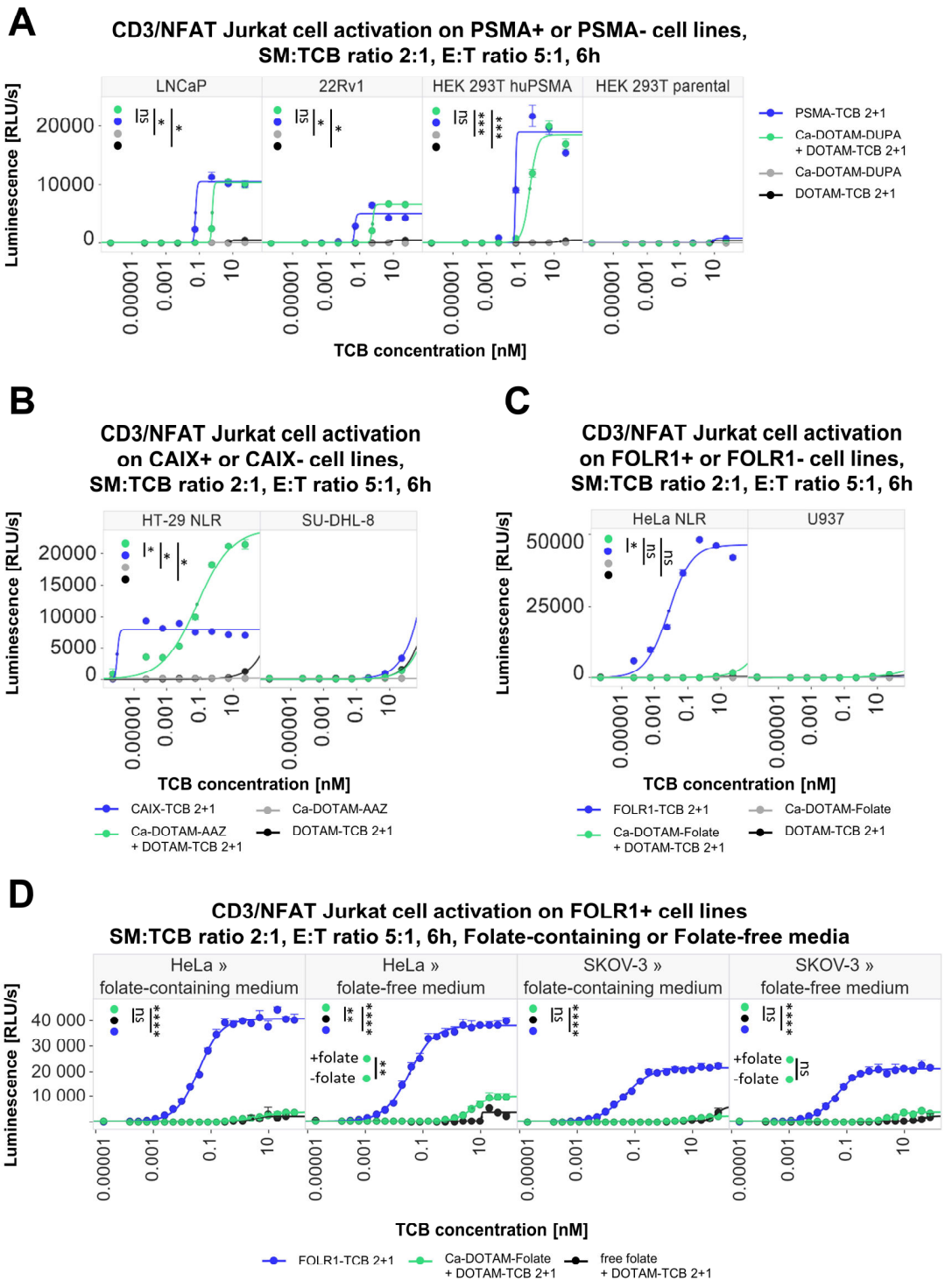

Figure 7.3.6. Reporter cell activation capacity by DOTAM-TCB with various small molecule ligands against cancer cell lines. CD3/NFAT Jurkat cell activation capacity of DOTAM-TCB combined with: A) Ca-DOTAM-DUPA against PSMA+ (LNCaP, 22Rv1, HEK 239T huPSMA) or PSMA- (HEK 293T parental) cell lines, B) Ca-DOTAM-AAZ against CAIX+ (HT-29 NLR) or CAIX- (SU-DHL-8) cell lines, C) Ca-DOTAM-Folate against FOLR1+ (HeLa NLR) or FOLR1- (U937) cell lines, D) Ca-DOTAM-Folate against FOLR1+ cell lines (HeLa and SKOV-3), in folate-containing or folate-free media. Graph show representative data of 2-3 experiments, collected in technical triplicates. Error bars indicate standard error.

conditions on both cell lines exhibited very low Jurkat activating capacity. Due to the low efficacy, coupled with the presence of folate in circulation in humans, it was elected to discontinue Ca-DOTAM-Folate from further proof-of-concept experiments. In summary, these findings demonstrate that Ca-DOTAM-DUPA and Ca-DOTAM-AAZ, but not Ca-DOTAM-Folate, when combined with DOTAM-TCB, possess the capability to induce CD3ε crosslinking when bound to target-expressing cells. Importantly, as intended, the small molecule adaptors alone and DOTAM-TCB alone were inactive in terms of inducing CD3ε downstream signaling.

Universal DOTAM-TCB shows *in vitro* proof of concept T cell-mediated tumor cell killing activity with comparable kinetics to direct TCBs.

To further explore the functionality of the molecules, tests were conducted to evaluate the cancer cell killing capacity *via* target-directed activation of human primary T cells. Additionally, it was sought to investigate potential differences in the kinetics of killing *in vitro*. This was of particular interest, due to the adaptor and TCB molecules being separate entities, as opposed to classical direct TCBs, therefore enforcing the necessity of binding to each other to form a functional molecule, aside from binding to T cells and target cells. For this purpose, the Incucyte imaging platform was utilized and co-cultured NucLightRed (NLR) (red fluorescent protein)-expressing target-expressing cancer cells with the molecules and human primary T cells isolated from healthy donors (NLR-negative). Cell growth and T cell-mediated killing kinetics were monitored by imaging every 4 hours for 5+ days, with the red fluorescent area quantified for each image. As shown in **Figure 7.3.7A**, Ca-DOTAM-AAZ with DOTAM-TCB (molar ratio SM:TCB 2:1) led to cancer cell growth inhibition in a kinetic manner similar to that of the direct CAIX-TCB. The dose responses of both were comparable, with strong tumor killing efficacy observed at the dose of ≥0.05 nM TCB. Representative images from the assay depicting tumor cells with and without treatment by Ca-DOTAM-AAZ with DOTAM TCB at 0h and 132h are presented in **Figure 7.3.7B**.

Figure 7.3.7C shows the assay results for Ca-DOTAM-DUPA with DOTAM-TCB and the controls. The direct PSMA-TCB displayed stronger efficacy, partially visible at a dose of 0.005 nM TCB and complete tumor cell killing at ≥0.05 nM. Ca-DOTAM-DUPA with DOTAM-TCB demonstrated efficacy starting from 0.5 nM, reaching levels comparable to direct TCB at a concentration of 50 nM TCB. In terms of kinetics, Ca-DOTAM-DUPA with DOTAM-TCB exhibited a similar profile to the direct TCB, with the exception of conditions at suboptimal concentrations of 0.5 nM TCB, where Ca-DOTAM-DUPA with DOTAM-TCB exhibited antitumoral activity more rapidly than PSMA-TCB. Representative images from the assay illustrating tumor cells with and without treatment by Ca-DOTAM-DUPA with DOTAM TCB at 0h and 132h are provided in **Figure 7.3.7D**.

As part of the *in vitro* assessment of molecule functionality, non-image-based killing assays were conducted, allowing evaluation of target cell killing alongside T cell activation and cytokine release. To this end, target-expressing cancer cells were co-cultured with human primary PBMCs isolated from healthy donors and the molecules. After a 48h incubation period, several readouts were collected. From the supernatant, dead cell proteases were

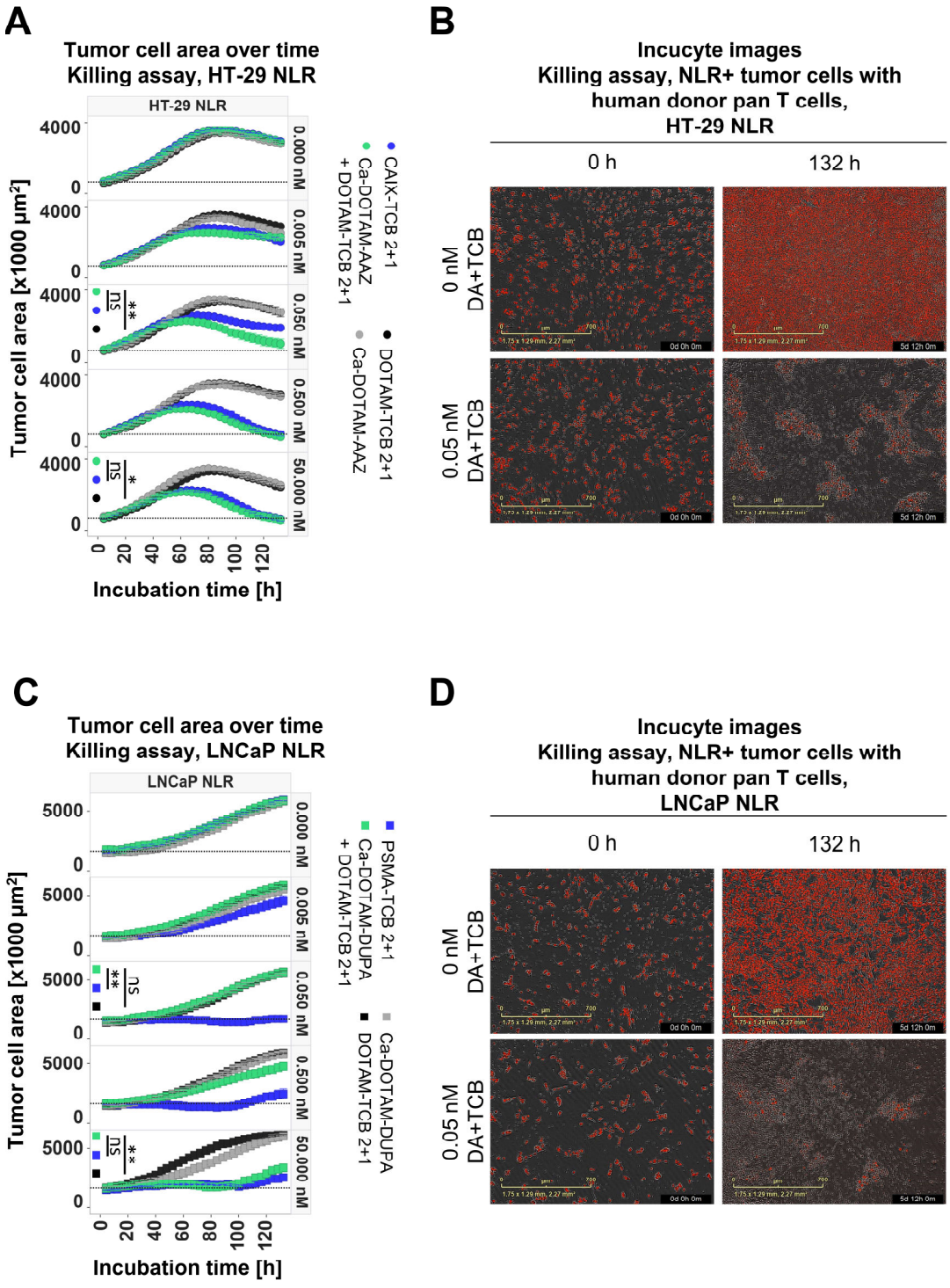

Figure 7.3.7. Kinetics and efficacy of T cell-mediated tumor killing induced by Ca-DOTAM-Ligands with DOTAM-TCB 2+1. Treatment with Ca-DOTAM-AAZ and DOTAM-TCB 2+1 against CAIX+ NLR+ tumor cells: A) Kinetics of tumor growth over time, B) Representative images at 0h and 132h. Treatment with Ca-DOTAM-DUPA and DOTAM-TCB 2+1 against PSMA+ NLR+ tumor cells: C) Kinetics of tumor growth over time, D) Representative images at 0h and 132h. Graph show representative data of 3 healthy pan T cell donors. Data collected in technical triplicates. Error bars indicate standard error.

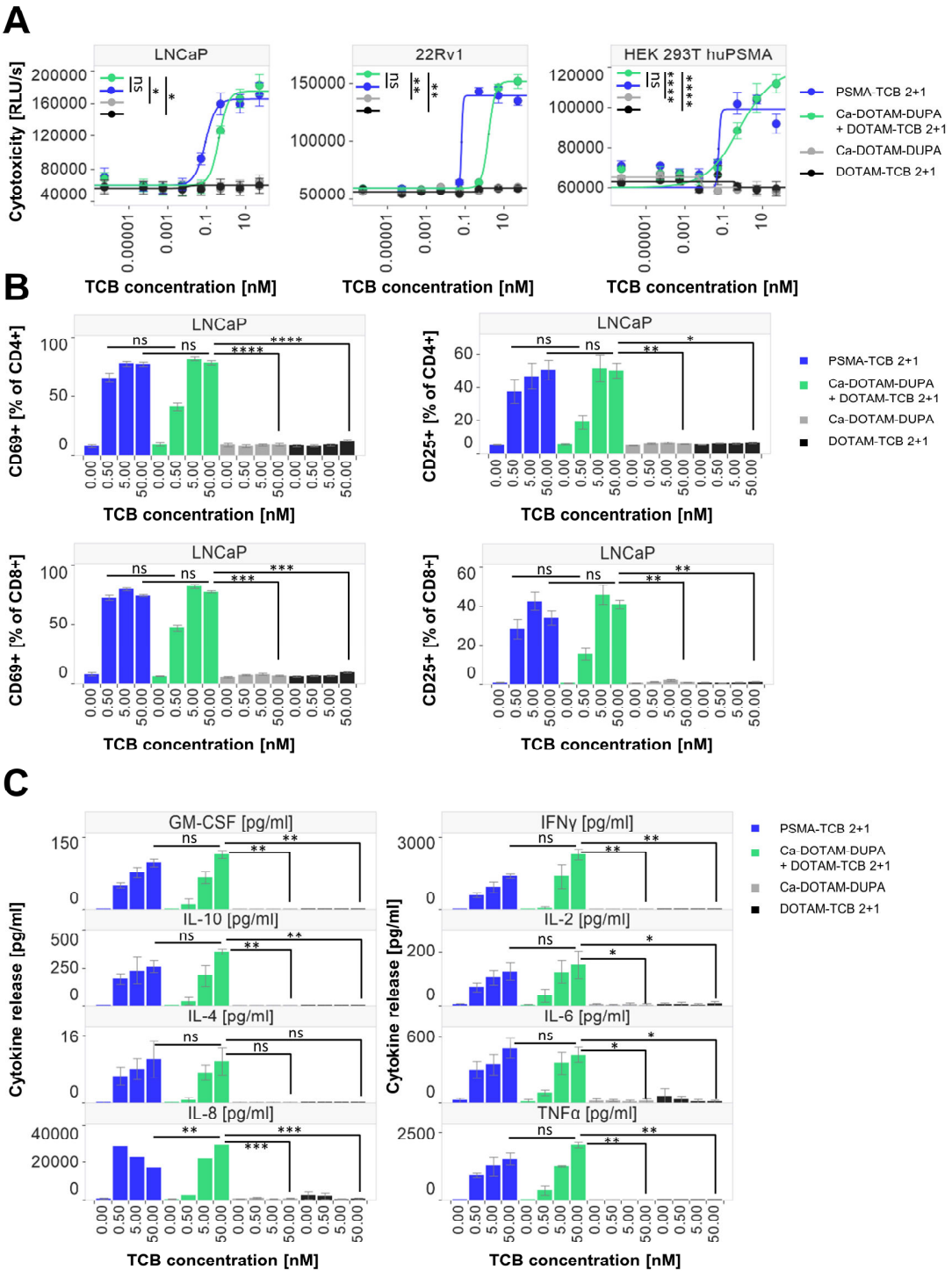

Figure 7.3.8. Ca-DOTAM-DUPA and universal DOTAM-TCB 2+1 induction of primary T cell activation, cytokine release and cytotoxicity against different PSMA+ tumor cells: LNCaP, 22Rv1 and HEK 293T huPSMA. A) T cell-mediated cytotoxicity against PSMA+ cells upon treatment. B) T cell activation marker expression upon treatment. C) T cell-mediated cytokine release upon treatment. Graph show representative data of 3 healthy PBMC donors. Data collected in technical triplicates. Error bars indicate standard error.

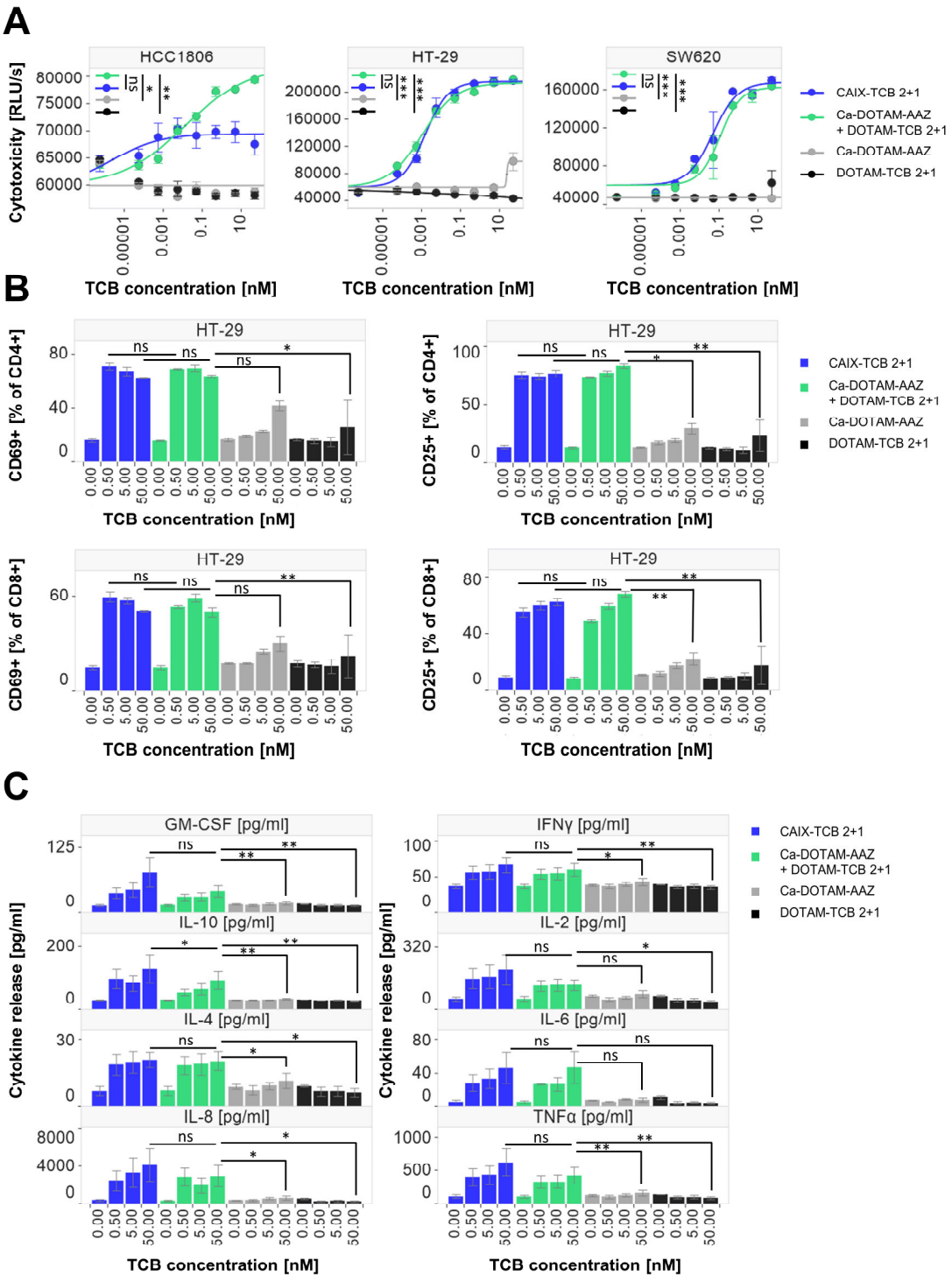

Figure 7.3.9. Ca-DOTAM-AAZ and universal DOTAM-TCB 2+1 induction of primary T cell activation, cytokine release and cytotoxicity against different CAIX+ tumor cells: HCC1806, HT-29 and SW620. A) T cell-mediated cytotoxicity against PSMA+ cells upon treatment. B) T cell activation marker expression upon treatment. C) T cell-mediated cytokine release upon treatment. Graph show representative data of 3 healthy PBMC donors. Data collected in technical triplicates. Error bars indicate standard error.

quantified in a relative manner, reflecting cytotoxicity, as shown in **Figure 7.3.8A** for PSMA-targeting, and **Figure 7.3.9A** for CAIX-targeting. The adaptors combined with DOTAM-TCB induced cytotoxicity in a dose dependent manner in all tested cell lines, while remaining inactive when tested separately. Additionally, T cells were stained for viability, CD4 and CD8 markers, as well as T cell activation markers CD69 and CD25, and assessed via flow cytometry (**Figure 7.3.8B** for PSMA targeting, **Figure 7.3.9B** for CAIX targeting). The data was analyzed to show percentages of activated cells within CD4 and CD8 T cells, using CD69 as early activation marker and CD25 as late activation marker, representing the state of molecule-treated T cells. Either adaptor, combined with DOTAM-TCB, induced dose-dependent activation of T cells, reflected by an increase in the activated population of CD4+ CD69+, CD4+ CD25+, CD8+ CD69+, and CD8+ CD25+ T cells. Furthermore, the remaining assay supernatant was analyzed for the presence of human cytokines, including GM-CSF, IFNγ, TNFα, IL-2, IL-4, IL-6, IL-8, and IL-10 (**Figure 7.3.8B** for PSMA targeting, **Figure 7.3.9B** for CAIX targeting). Both adaptors combined with DOTAM-TCB resulted in release of cytokines into the supernatant in a dose-dependent manner. Together, these data show capacity of tested molecules in terms of inducing cancer cell killing in a dose-dependent manner, linking efficacy to T cell activation and cytokine release.

DOTAM-TCB displays antitumoral activity *in vitro* in various antibody formats

The valence and format of antibodies are some of the most important features in antibody design, dictating avidity and thus impacting efficacy. To explore the influence of antibody valence and format on the efficacy of the molecules, DOTAM-TCBs in the following formats were produced and tested: 2+1 (two binders against DOTAM, one binder against CD3ε), 1+1 (one binder against DOTAM, one binder against CD3ε), and 1+1 one-armed (OA) (one binder against DOTAM, one binder against CD3ε on the same arm) (**Figure 7.3.10A**). The cytotoxic and T cell activation potential of these DOTAM-TCB antibodies combined with Ca-DOTAM-DUPA (all dosed in molar ratio SM:TCB 2:1) were directly assessed. All formats exhibited dose-dependent cytotoxic efficacy and CD8+ T cell activation capacity against PSMA+ LNCaP cells (**Figure 7.3.10B**) and PSMA+ 22Rv1 cells (**Figure 7.3.10C**). The 2+1 TCB format demonstrated the lowest EC_{50}, while the 1+1 OA format achieved the highest efficacy plateau at saturating concentrations, likely due to higher occupancy. Of note, the 1+1 and 1+1 OA formats, despite having the same valence for both DOTAM binder and CD3ε binder, displayed different activity profiles. This observation aligns with previous experiments showing superiority of TCBs in the 1+1 OA format over the 1+1 format (**Chapter 1, Figure 7.1.6**), likely due to a formation of a stronger T cell synapse, and highlights the fact that valence alone is not the sole determinant influencing antibody activity. In general, the high concentrations at which the 1+1 OA format exhibits superior activity are not relevant for *in vivo* experiments. Consequently, considering its low EC_{50}, and the fact that *in vivo* bivalency and avidity may stabilize the binding the optimal TCB format for DOTAM-TCB for further experiments was determined to be a 2+1 TCB.

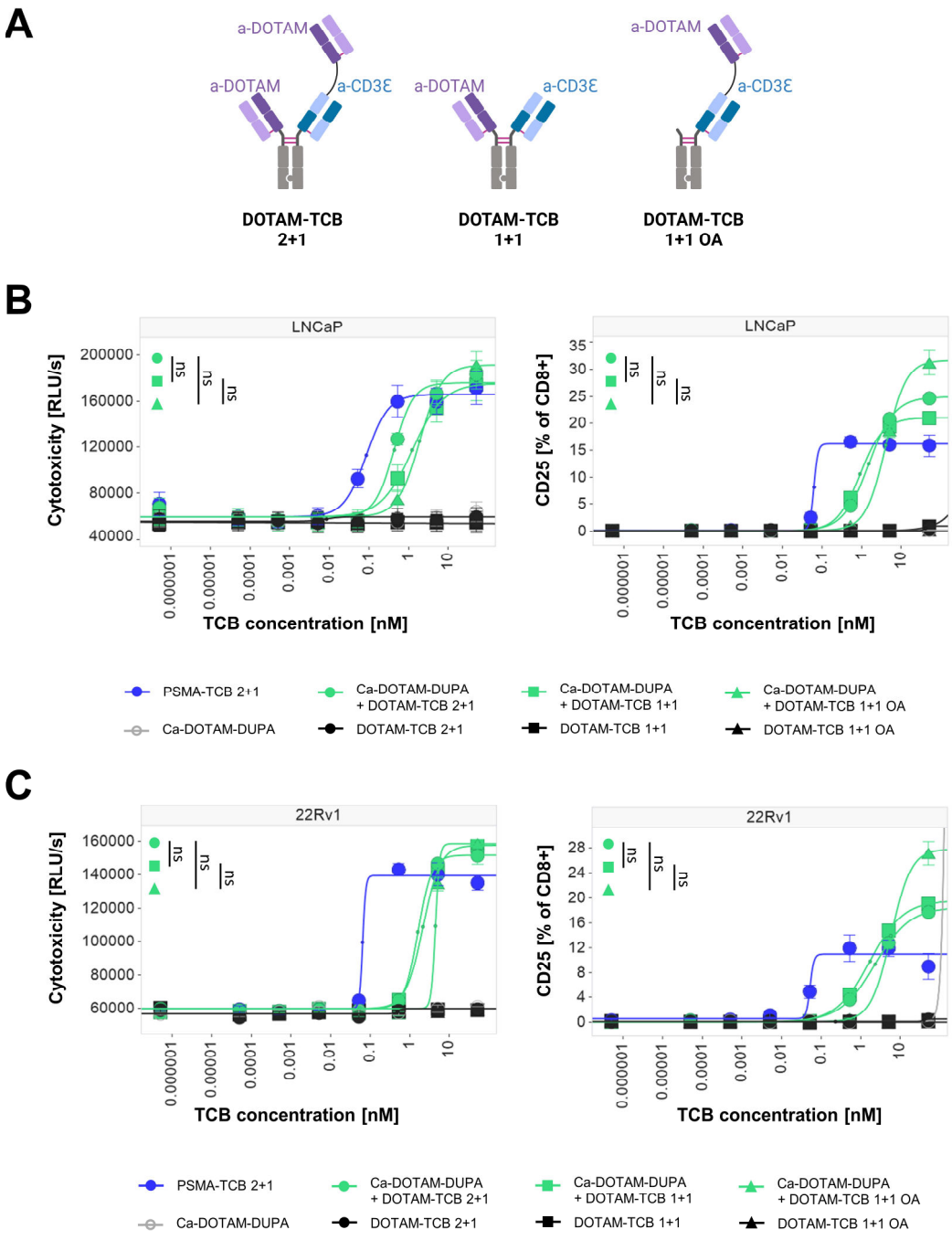

Figure 7.3.10. DOTAM TCB antibody format comparison upon combination with Ca-DOTAM-DUPA, on two different PSMA+ cell lines: LNCaP and 22Rv1. A) LNCaP-directed cytotoxicity and T cell activation marker expression upon treatment by 2+1, 1+1 and 1+1 OA TCB formats. B) 22Rv1-directed cytotoxicity and T cell activation marker expression upon treatment by 2+1, 1+1 and 1+1 OA TCB formats. Representative experiment of 3 healthy PBMC donors. Data collected in technical triplicates. Error bars indicate standard error.

DOTAM-TCB lacking 1st N-terminal amino acid in anti-DOTAM VH displays different activity to full-sequence DOTAM-TCB / Single amino acid change in the DOTAM binder impacts activity

Due to antibody production issues, DOTAM-TCB 1+1 and DOTAM-TCB 1+1 OA antibodies were delivered, lacking the first N-terminal amino acid in the VH framework part of the DOTAM binders. Since this amino acid position falls within the framework region, it is not expected to impact binding via CDRs, unless it affects protein folding or 3D conformation. Therefore, further functional *in vitro* tests were proceeded with using these molecules, hypothesizing comparable activity to full-sequence antibodies. However, the first step was to verify this assumption. A co-culture assay of cancer cells, primary PBMCs and molecules showed that the TCBs missing the 1st amino acid achieved lower efficacy in terms of T cell activation capacity, when compared to full sequence antibodies (**Figure 7.3.11A,B**).

In light of these intriguing findings, the molecules' binding capacity was validated, combining DOTAM-TCBs with different adaptors. KinExA measurement was conducted (performed in by Daniela Matscheko, Roche Innovation Center Munich) for 1+1 and 1+1 OA TCB formats combined with the following adaptors: Ca-DOTAM-DUPA, Ca-DOTAM-Folate, and Ca-DOTAM. **Figure 7.3.12** displays binding curve overlays from KinExA results of TCBs with different sequences, together with EC_{50} and AUC values. The dose response curves of the free fraction of the constant binding partner showed similar patterns. However, overall, as visible in **Figure 7.3.13** depicting K_D values of the tested interactions, DOTAM-TCBs in both 1+1 and 1+1 OA formats displayed loss of affinity to Ca-DOTAM-DUPA upon the loss of the N-terminal framework amino acid. Similar observations of weakened binding were made for Ca-DOTAM-Folate with DOTAM-TCB 1+1 OA, while DOTAM-TCB 1+1 results were inconclusive.

Collectively, these data indicate that despite adaptors being bound by the CDR region, the first N-terminal amino acid in the VH framework of the DOTAM binder is essential for retained binding properties of the TCB-adaptor complexes. Therefore, after these assessments were completed, full sequence antibodies were used for all further testing.

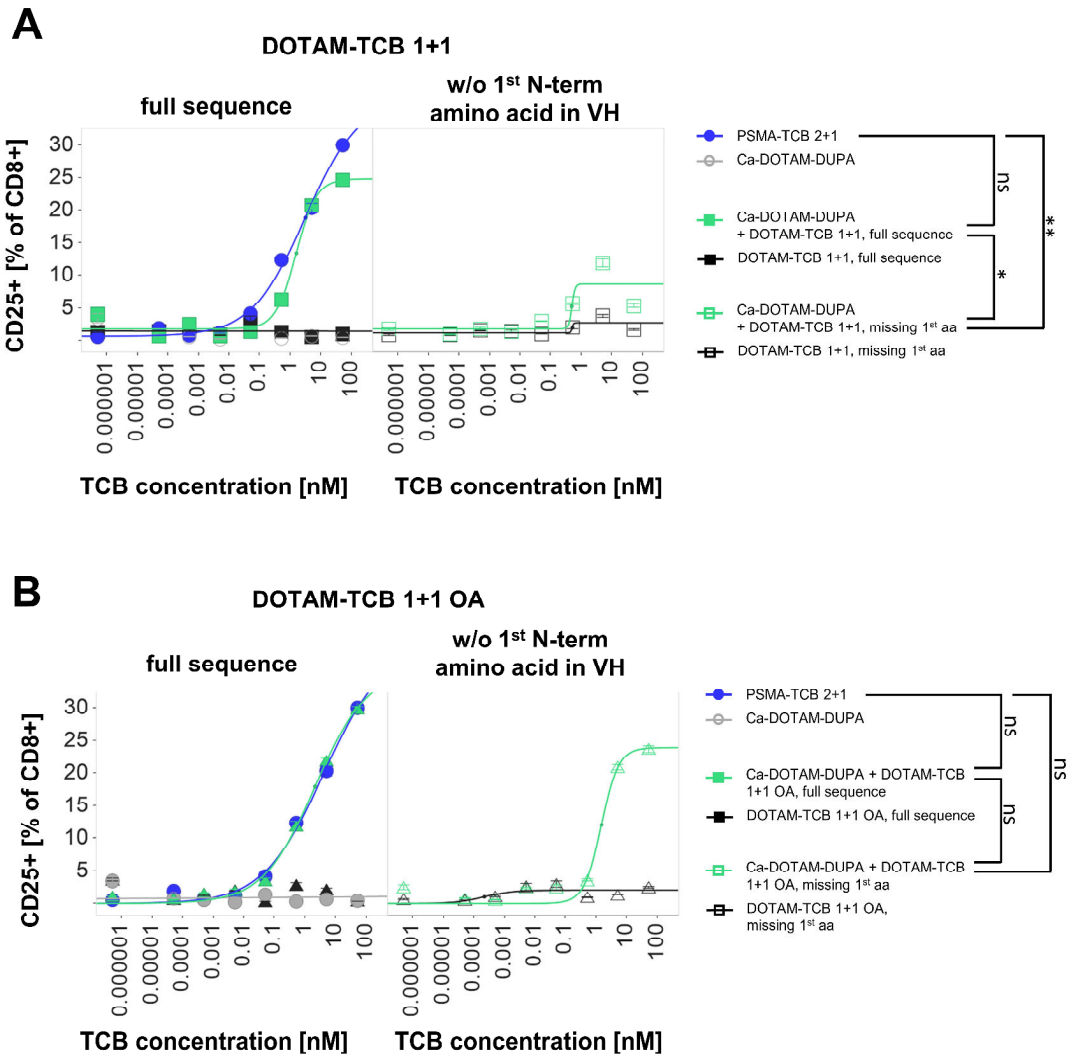

Figure 7.3.11. Functionality comparison of two DOTAM-TCB variants: with full and truncated sequences lacking 1st N-terminal amino acid in DOTAM binder VH. A) T cell activation induced by both TCB 1+1 sequence variants against 22Rv1 PSMA+ cells. B) T cell activation induced by both TCB 1+1 OA sequence variants against 22Rv1 PSMA+ cells. Graph show data of one healthy PBMC donor, with data collected in technical triplicates. Error bars indicate standard error.

Ca-DOTAM-Ligands with DOTAM-TCB can be complexed into a functional TCB in a non-covalent manner due to affinity of Ca-DOTAM-anti-Ca-DOTAM interaction

With a determined double-digit femtomolar affinity between the DOTAM binder and Ca-DOTAM-Ligands, it was hypothesized that the small molecule adaptors might form a non-covalent stable complex with the DOTAM-TCBs through a simple process of co-incubation. It has been reported that an antibody-hapten binding may result in the complex gaining the pharmacokinetic/pharmacodynamic (PK/PD) properties of the antibody [378]. Obtaining such

a complex for the molecules was of special interest for future *in vivo* proof of concept studies, where a single molecule (SM-TCB complex) with antibody-like PK/PD properties could serve as a positive control of a small molecule-directed TCB, providing maximal efficacy without separate optimizations of dosing for SM and TCB. The separately injected small molecule adaptor and DOTAM-TCB would be used in an experimental test group to verify complex formation *in vivo*.

To assess the hypothesis of the potential complex formation in a simple preincubation process, a complexing protocol was developed as part of this thesis (**Figure 7.3.14A**). In this newly developed procedure, the SM adaptor was incubated with DOTAM-TCB 2+1 at a molar ratio of SM:TCB 4:1 (with SM in excess) for 1 hour at room temperature, followed by removal of unbound SM using centrifugal filters with a molecular weight cut-off (30 or 50 kDa). The retained molecules in the protein solution after this procedure theoretically include molecules above 30-50 kDa including, fully complexed SM-TCB (TCB + 2 SM), half-complexed SM-TCB (TCB + 1 SM), or empty TCB (TCB + 0 SM). The relative amounts of these forms in the protein solution would depend on the complexing efficiency.

To verify and quantify this complexing efficiency, native size-exclusion chromatography-mass spectrometry (native SEC-MS) was performed (by Theresa Kober and Dr. José Bonfiglio, Roche Innovation Center Munich). The results of DOTAM-TCB 2+1 complexed with Ca-DOTAM-AAZ are presented in **Figure 7.3.14B**. Peaks corresponding to all predicted theoretical forms were observed, with empty TCB comprising 28.6% of the protein in the sample, half-complexed SM-TCB constituting 43.9%, and fully complexed SM-TCB accounting for 27.5%. Since both half-complexed and fully complexed SM-TCBs could theoretically exhibit TCB activity, the percentage of functional complexes for Ca-DOTAM-AAZ—DOTAM TCB 2+1 was determined to be their sum, resulting in the value of 71.4%. As a concept from the field of antibody drug conjugates, the drug antibody ratio (DAR), where the small molecule adaptor takes place of the 'drug', was calculated to summarize the results, yielding a value of 0.99. As a reference, the desired full complexing would result in a DAR of 2 (2 SM per 1 TCB). The results of DOTAM-TCB 2+1 complexed with Ca-DOTAM-DUPA are shown in **Figure 7.3.14C**. Empty TCB constituted 8.5%, half-complexed SM-TCB was 44.6%, and fully complexed SM-TCB was 47% of the yield. The DAR for DOTAM-DUPA—DOTAM TCB 2+1 was 1.39. These data demonstrate that the established complexing protocol did result in complexed SM-TCB, albeit with relatively low to medium efficiency according to the Native SEC-MS standard method. Interestingly, the complexing efficiencies appeared to be different for the two tested adaptors. Importantly since the SM-TCB complexes are non-covalent, one cannot exclude impact of the native SEC-MS method on its observed integrity. Due to these limitations, the decision was made to expand the complex evaluation to functional and binding assays which do not require harsh processing of the sample. Nevertheless, the obtained mass spectrometry results did confirm that a sufficient level of complexing efficiency is achieved by the developed protocol.

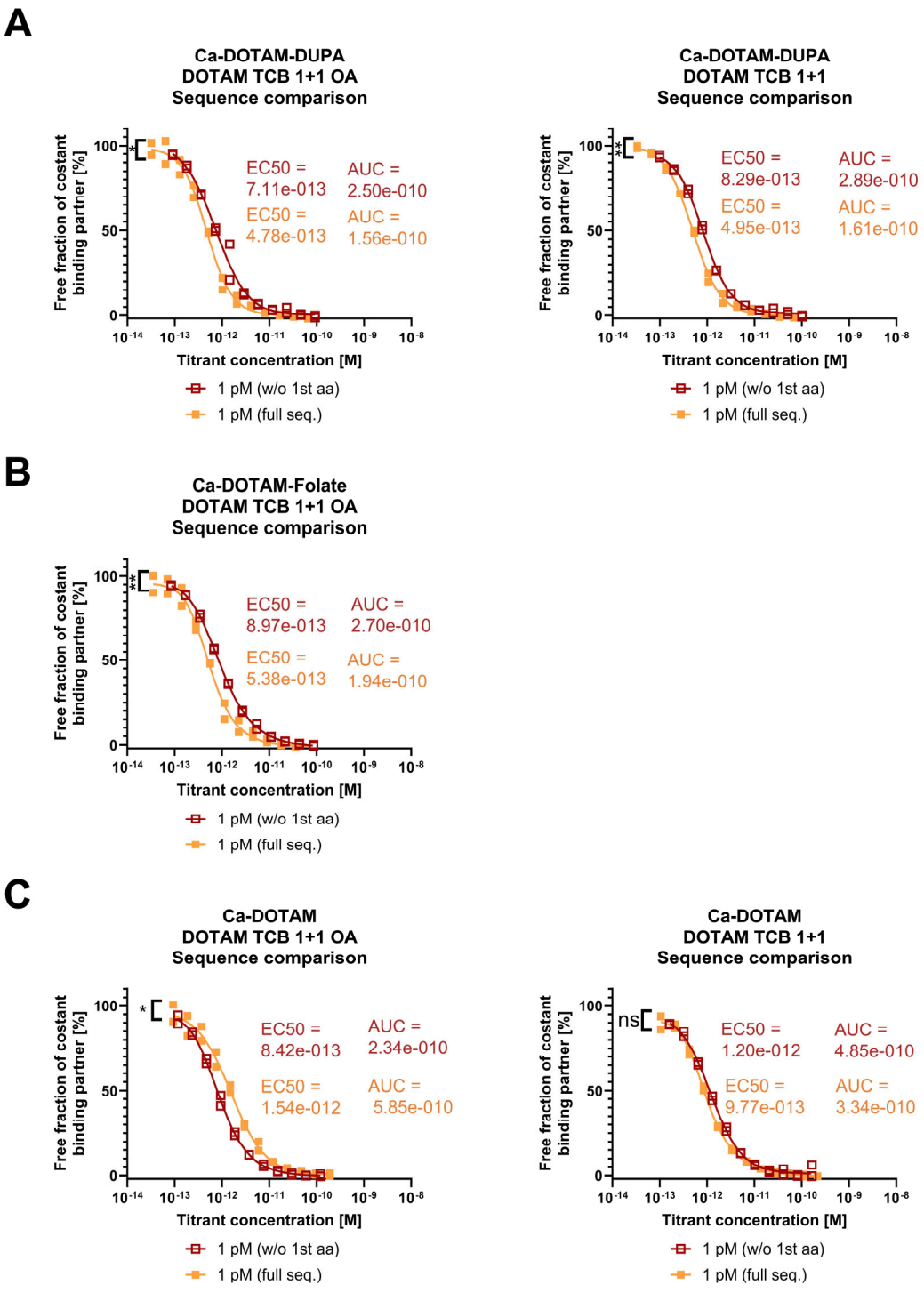

Figure 7.3.12. KinExA measurements of the interactions between DOTAM-TCB variants and formats with Ca-DOTAM-Ligands. Concentration-dependent free fraction of the binding partner, of A) Ca-DOTAM-DUPA with DOTAM-TCB 1+1 and 1+1 OA sequence variants, B) Ca-DOTAM-Folate with DOTAM-TCB 1+1 OA sequence variants, and C) Ca-DOTAM with DOTAM-TCB 1+1 and 1+1 OA sequence variants. Data from one experiment with technical duplicates.

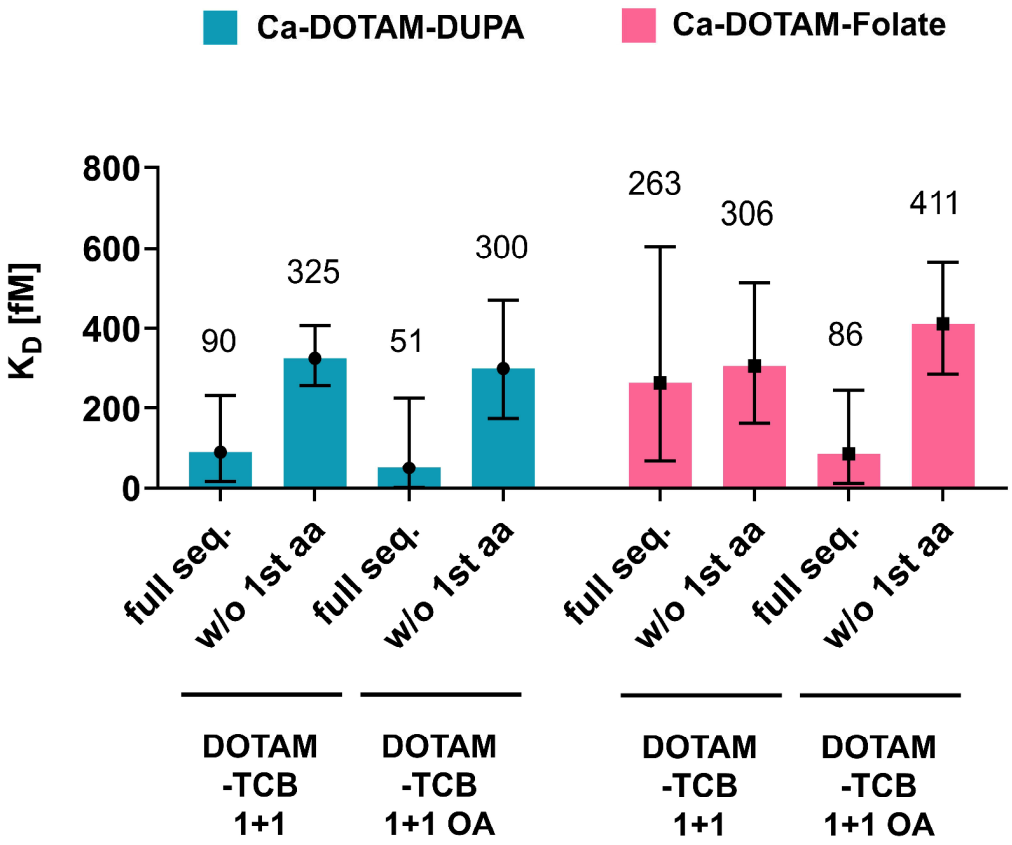

Figure 7.3.13. KD values derived from KinExA measurements of the interactions between DOTAM-TCB sequence variants and formats with Ca-DOTAM-Ligands. Data from one experiment with technical duplicates. Error bars indicate 95% confidence interval.

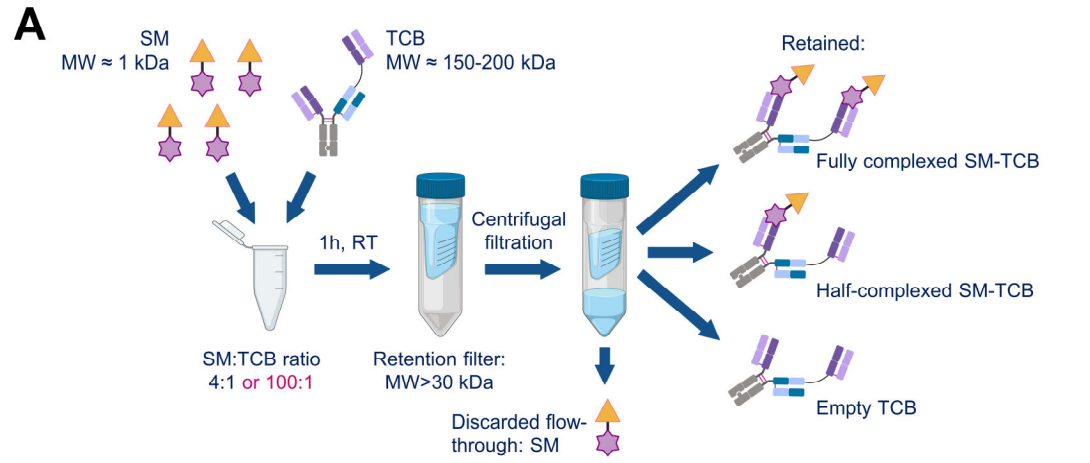

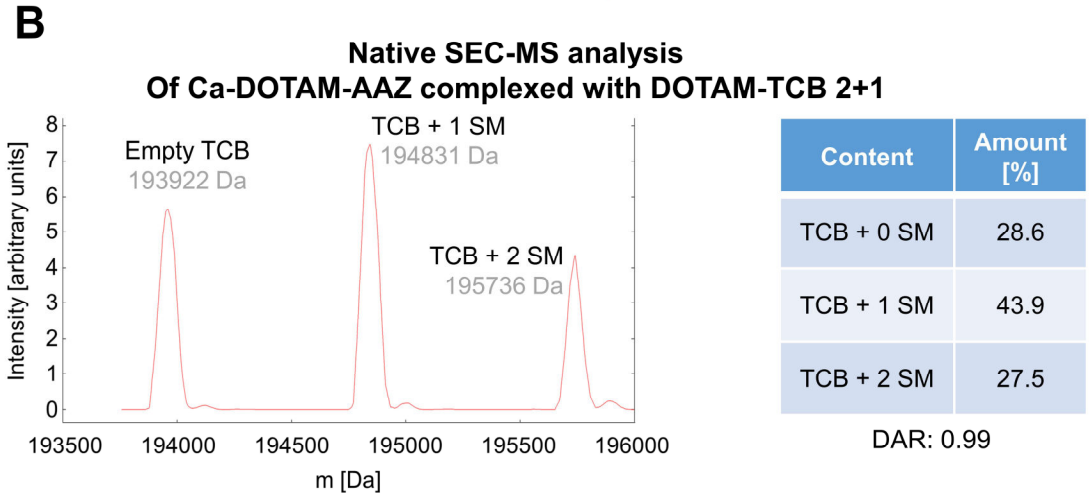

Content	Amount [%]
TCB + 0 SM	28.6
TCB + 1 SM	43.9
TCB + 2 SM	27.5

DAR: 0.99

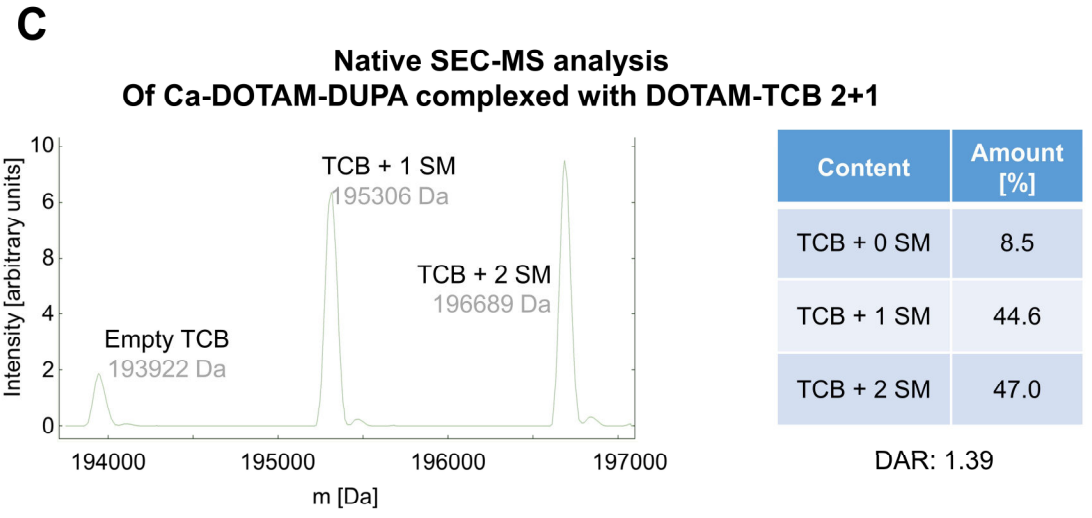

Content	Amount [%]
TCB + 0 SM	8.5
TCB + 1 SM	44.6
TCB + 2 SM	47.0

DAR: 1.39

Figure 7.3.14. Complexing protocol of Ca-DOTAM-Ligands with DOTAM-TCBs and its efficiency. A) Complexing protocol and possible hypothetical products. B) Native SEC-MS analysis of the complexing product of Ca-DOTAM-AAZ with DOTAM-TCB 2+1. C) Native SEC-MS analysis of the complexing product of Ca-DOTAM-DUPA with DOTAM-TCB 2+1. Data from one experiment.

Complexed Ca-DOTAM-Ligand-DOTAM TCBs display comparable *in vitro* activity to separate Ca-DOTAM-Ligand combined with DOTAM-TCBs

With encouraging the verification of complex formation in the established protocol, functional assays were conducted to compare the activity of complexed versus separately added SM adaptors and DOTAM-TCBs. Ca-DOTAM-DUPA was complexed with either DOTAM-TCB 2+1, DOTAM-TCB 1+1, or DOTAM-TCB 1+1 OA. Killing assays were performed, involving co-culture of PSMA-expressing LNCaP cells, human primary PBMCs from healthy donors, and the molecules. Complexed and separately added Ca-DOTAM-DUPA and DOTAM-TCBs were utilized as test molecules.

The cytotoxicity results are presented for TCB format 2+1 (**Figure 7.3.15A**), TCB format 1+1 (**Figure 7.3.15B**), and format 1+1 OA (**Figure 7.3.15C**), while T cell activation is shown for TCB format 2+1 (**Figure 7.3.16A**), TCB format 1+1 (**Figure 7.3.16B**), and format 1+1 OA (**Figure 7.3.16C**). In all tested conditions, complexed and separate molecules exhibited comparable activity profiles with largely overlapping dose-response curves. As an additional readout, the cytokines released into the supernatant were quantified. The results are displayed for TCB format 2+1 (**Figure 7.3.17A**), TCB format 1+1 (**Figure 7.3.17B**), and format 1+1 OA (**Figure 7.3.17C**). Analogously to cytotoxicity results, the cytokine release profiles were similar between the complexed and separate groups. This was with the exception of the 1+1 OA TCB format, where the complexed Ca-DOTAM-DUPA—DOTAM TCB complex showed a lower EC_{50} than the separately added molecules.

Together, these data suggests that both complexed SM-TCB and separately added SM and TCB have comparable efficacy profiles, including dose-dependency. Since such results were in conflict with the obtained native SEC-MS data, two hypotheses were developed to provide an explanation for this phenomenon. Firstly, full complexing may not be necessary to reach comparable efficacy of complexed and separately added molecules. Secondly, the native SEC-MS process used might have partially disassembled the complexes during the acquisition process, providing inaccurately low numbers on complexing efficiency.

ELISA-based assessment of SM-TCB complexing efficiency

In preparation for *in vivo* testing, it was deemed necessary to determine the complexing efficiency with DOTAM TCB 2+1 in a reliable manner, to appropriately match the dosing to the control groups. Therefore, another method was sought for that does not involve harsh sample processing to avoid potential disassembly of the complexes. An ELISA with a coated target protein was decided on as a tool, since it had been previously developed for the planned mouse pharmacokinetic study. The hypothesis posited that empty TCB or half-complexed SM-TCB could exhibit increased target binding if additional SM is spiked into the protein solution after complex purification, effectively occupying residual empty DOTAM binders.

To test this, samples were collected from the Ca-DOTAM-AAZ—DOTAM TCB 2+1 complexing procedure and were divided into unmodified samples and samples spiked with SM (with Ca-DOTAM-AAZ). As a control, an empty non-complexed (non-processed) DOTAM-TCB 2+1 were

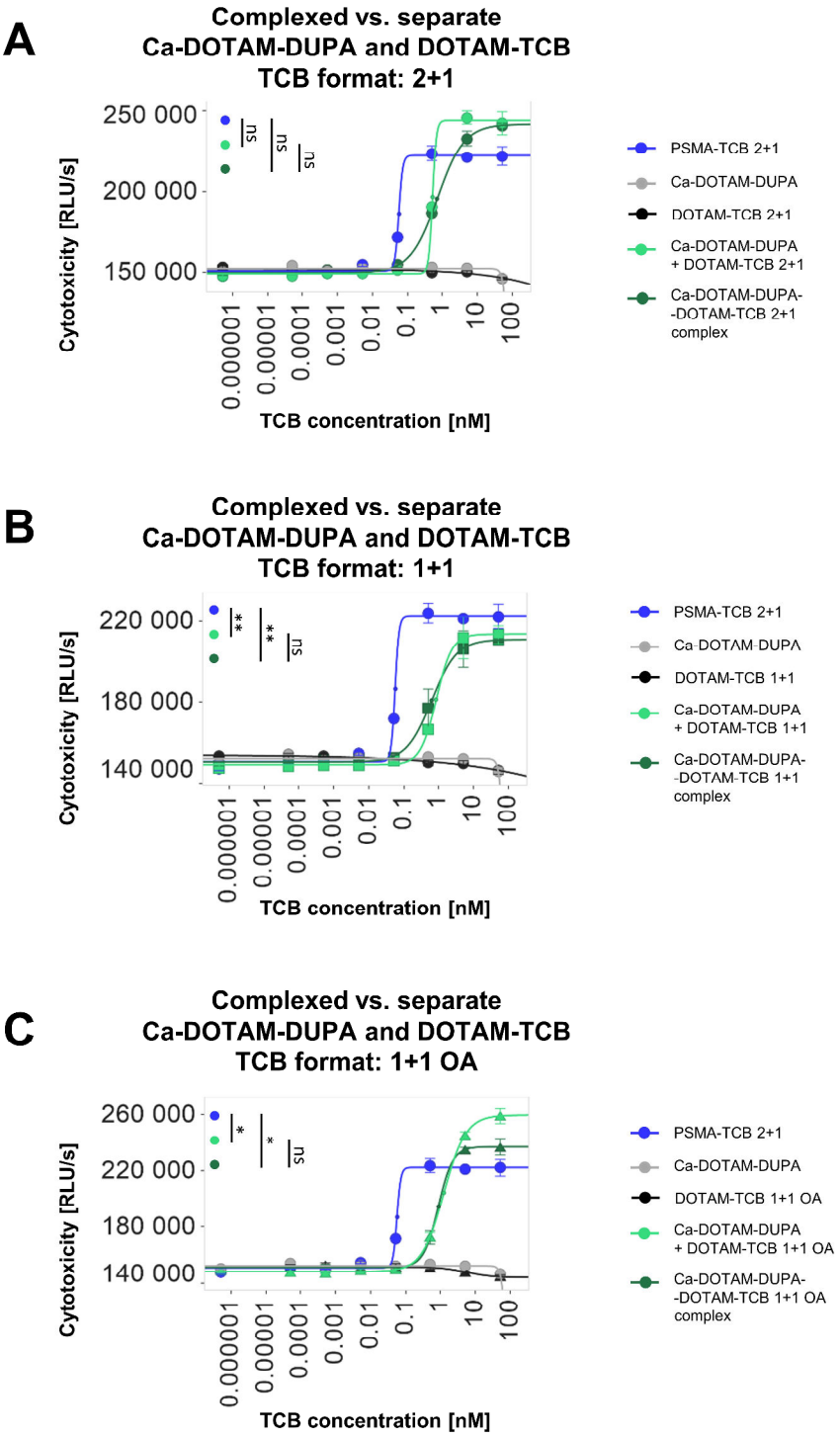

Figure 7.3.15. Cytotoxicity comparison of complexed and separately used Ca-DOTAM-DUPA and DOTAM-TCBs on PSMA+ LNCaP cells, across different TCB formats. T cell activation induced by complexed or separately used Ca-DOTAM-DUPA with: A) DOTAM-TCB 2+1, B) DOTAM-TCB 1+1, C) DOTAM TCB 1+1 OA. Graph show representative data of 3 healthy PBMC donors. Data collected in technical triplicates. Error bars indicate standard error.

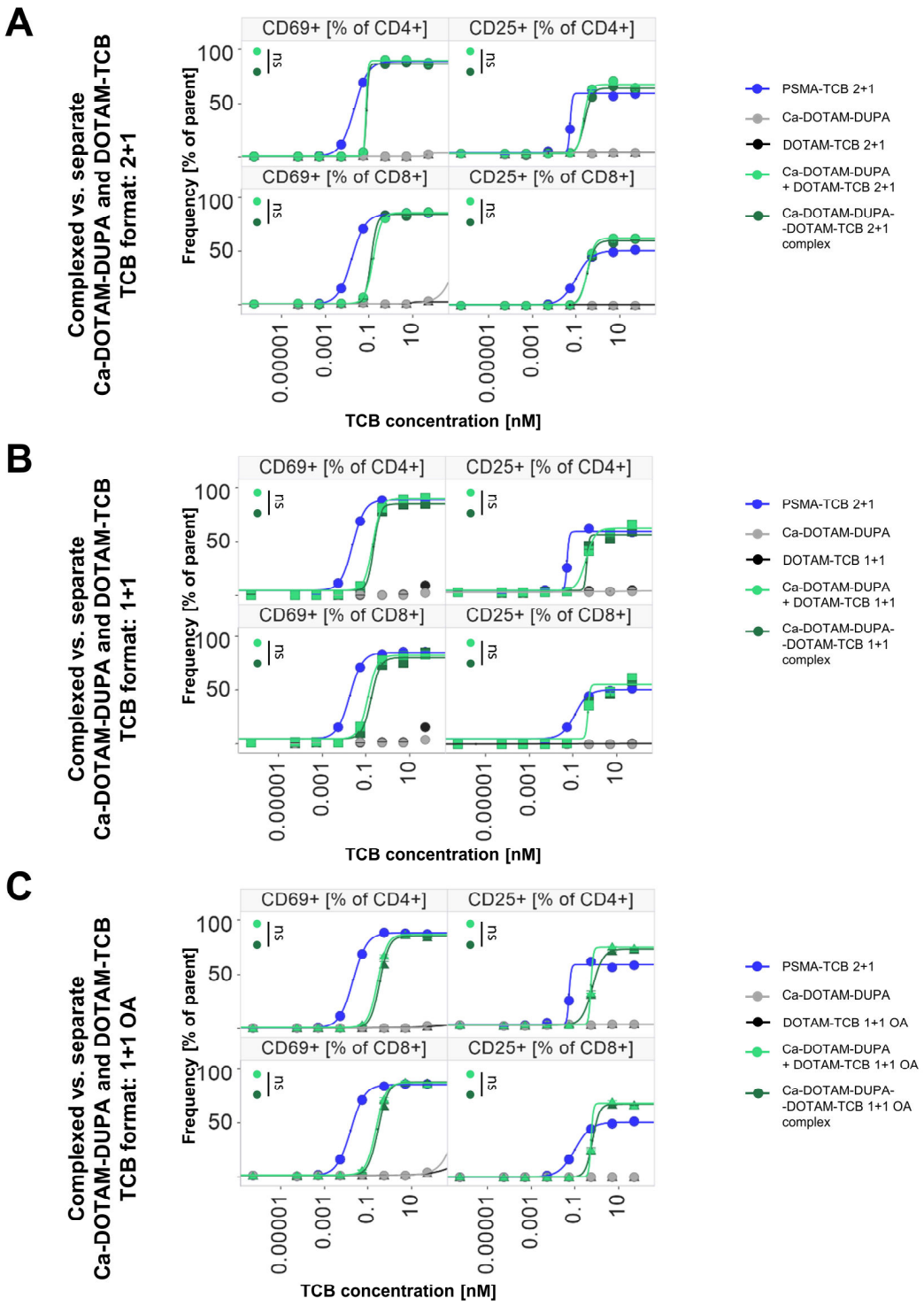

Figure 7.3.16. T cell activation comparison of complexed and separately used Ca-DOTAM-DUPA and DOTAM-TCBs on PSMA+ LNCaP cells, across different TCB formats. T cell activation induced by complexed or separately used Ca-DOTAM-DUPA with: A) DOTAM-TCB 2+1, B) DOTAM-TCB 1+1, C) DOTAM TCB 1+1 OA. Graph show representative data of 3 healthy PBMC donors. Data collected in technical triplicates. Error bars indicate standard error.

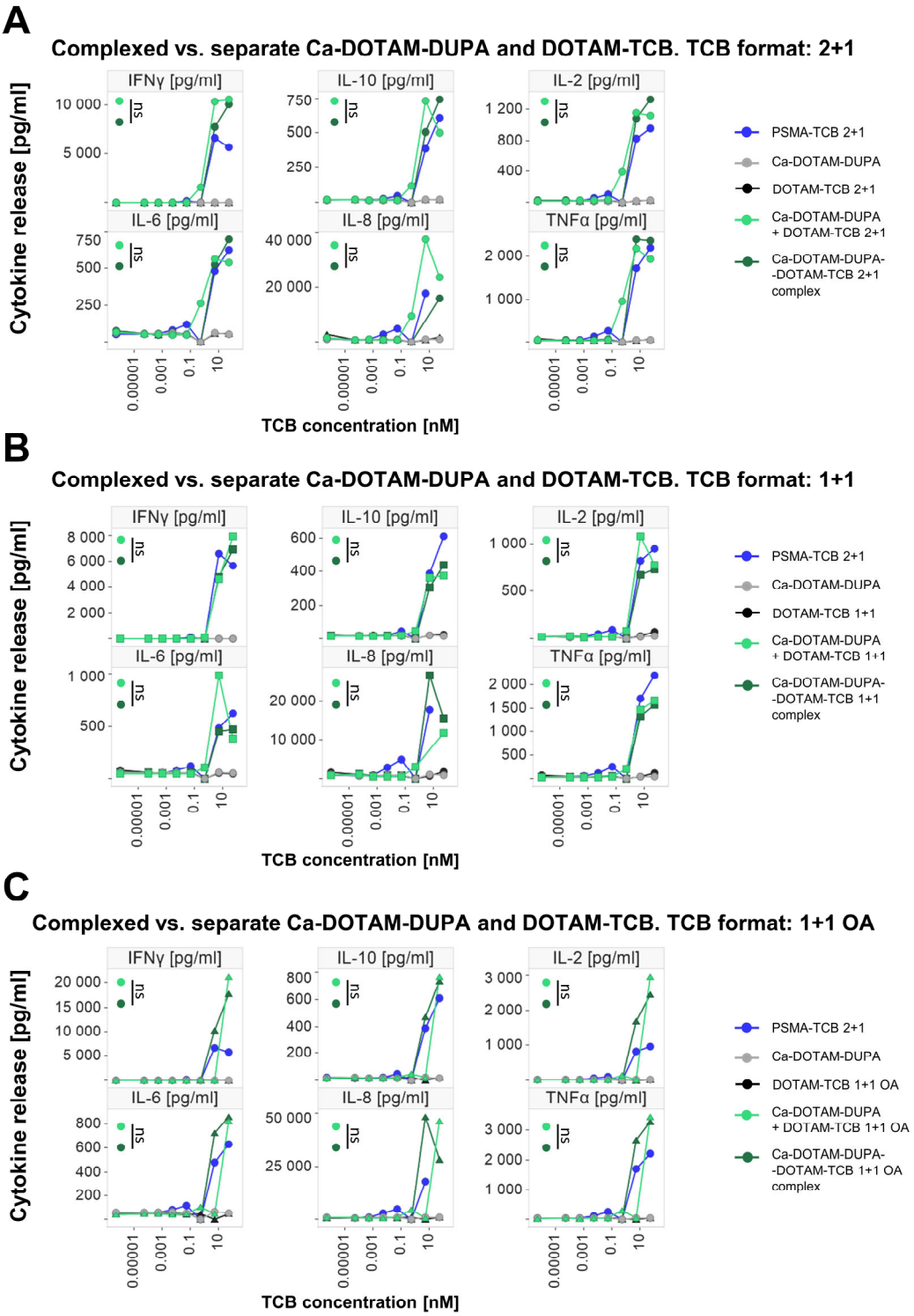

Figure 7.3.17. Cytokine release comparison of complexed and separately used Ca-DOTAM-DUPA and DOTAM-TCBs on PSMA+ LNCaP cells, across different TCB formats. T cell activation induced by complexed or separately used Ca-DOTAM-DUPA with: A) DOTAM-TCB 2+1, B) DOTAM-TCB 1+1, C) DOTAM TCB 1+1 OA. Graph show representative data of 3 healthy PBMC donors. Supernatants pooled from technical triplicates. Error bars indicate standard error.

used, and spiked with the SM as well to verify if occupying empty DOTAM binders during spiking occurs (**Figure 7.3.18A**). After the SM spike, the samples were tested with ELISA for binding to plate-coated CAIX, where only SM adaptors bound to the DOTAM-TCBs were expected to be detected, and SM alone or TCBs alone were not (**Figure 7.3.18B**). As illustrated in **Figure 7.3.18C**, empty DOTAM TCB 2+1 exhibited no binding, while SM spiking of the empty TCB resulted in a similar binding curve to Ca-DOTAM-AAZ—DOTAM-TCB 2+1 complex, confirming the efficacy of SM spiking. The Ca-DOTAM-AAZ—DOTAM-TCB 2+1 complex displayed overlapping binding curves with and without SM spike. This data suggests that the Ca-DOTAM-AAZ—DOTAM-TCB 2+1 complex possibly had too few available empty DOTAM binders for the SM to increase the binding via spiking, indicating high efficiency of the complexing protocol.

Analogous experiments were performed for the Ca-DOTAM-DUPA—DOTAM-TCB 2+1 complex, with spiking with Ca-DOTAM-DUPA as SM (**Figure 7.3.19A**). The samples were tested by to ELISA for binding to plate-coated PSMA (**Figure 7.3.19B**). As depicted in **Figure 7.3.19C**, the empty TCB remained unbound, while the SM spike resulted in dose-dependent binding, confirming spiking functionality. However, the curve for the SM-spiked empty TCB displayed weaker binding compared to the non-spiked Ca-DOTAM-DUPA—DOTAM-TCB 2+1 complex, indicating incomplete occupation of empty DOTAM binders during spiking. The Ca-DOTAM-DUPA—DOTAM-TCB 2+1 complex showed overlapping binding curves with and without the SM spike, with the exception of the plateau, which showed a stronger signal from the spiked sample. This data suggests that the Ca-DOTAM-DUPA—DOTAM-TCB 2+1 complex was produced with high efficiency, although some uncomplexed or half-complexed TCBs may have been present in the final sample.

In addition to the ELISA, the SM spiking was tested with a functional assay. The CD3/NFAT Jurkat reporter assay and Ca-DOTAM-AAZ—DOTAM TCB 2+1 were chosen for this purpose. For this functional experiment, the sample preparation involved spiking both the complexed sample and the previously discarded MW filtering flow-through by either the SM or the TCB (**Figure 7.3.20A**). The TCB spike was introduced to detect any residual SM after molecular weight-based purification. As expected, the empty TCB induced Jurkat activation only when spiked with SM, validating the efficacy of SM spiking in the assay (**Figure 7.3.20B**). TCB spiking yielded a negative signal across the tested doses, indicating the absence of free SM in the spiked solution. The Ca-DOTAM-AAZ—DOTAM-TCB 2+1 complex elicited the same dose-response curves without spiking, with SM spike, and with TCB spike, indicating the absence of SM in solution and empty DTOAM binders (**Figure 7.3.20B**). These results provide additional evidence that the Ca-DOTAM-AAZ—DOTAM-TCB 2+1 complex preparation primarily results in fully complexed SM-TCB. These conclusions are supported by the Jurkat results, ELISA, cancer killing, and T cell activation data, in contrast to conclusions derived from native SEC-MS results.

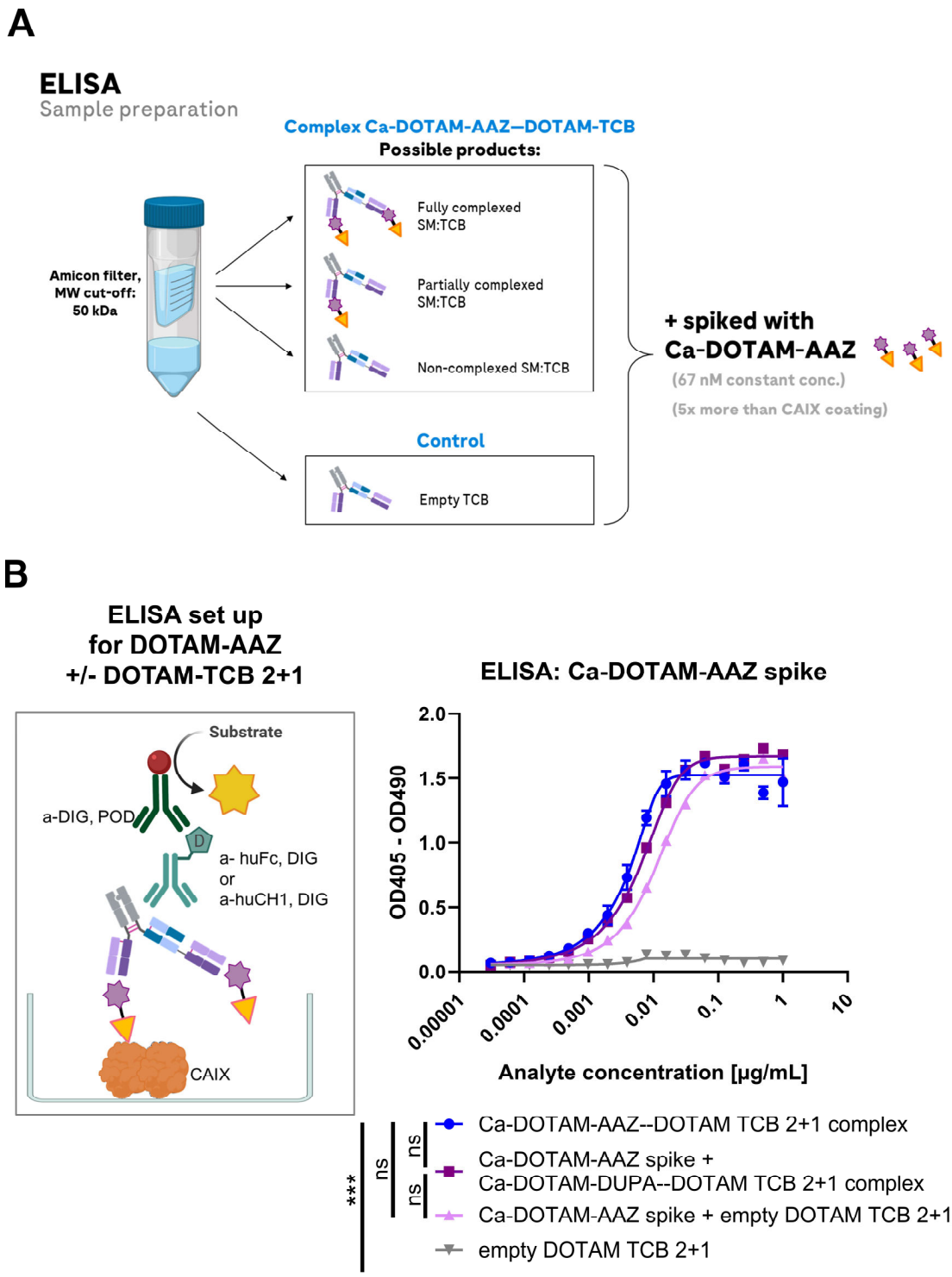

Figure 7.3.18. SM spike ELISA-based assessment of the complexing protocol of Ca-DOTAM-AAZ with DOTAM-TCB. A) Possible products from the complexing procedure and their SM spike pretreatment prior to ELISA. B) CAIX ELISA set-up and binding results after Ca-DOTAM-AAZ spiking. Data from one experiment, collected in technical duplicates. Error bars indicate standard error.

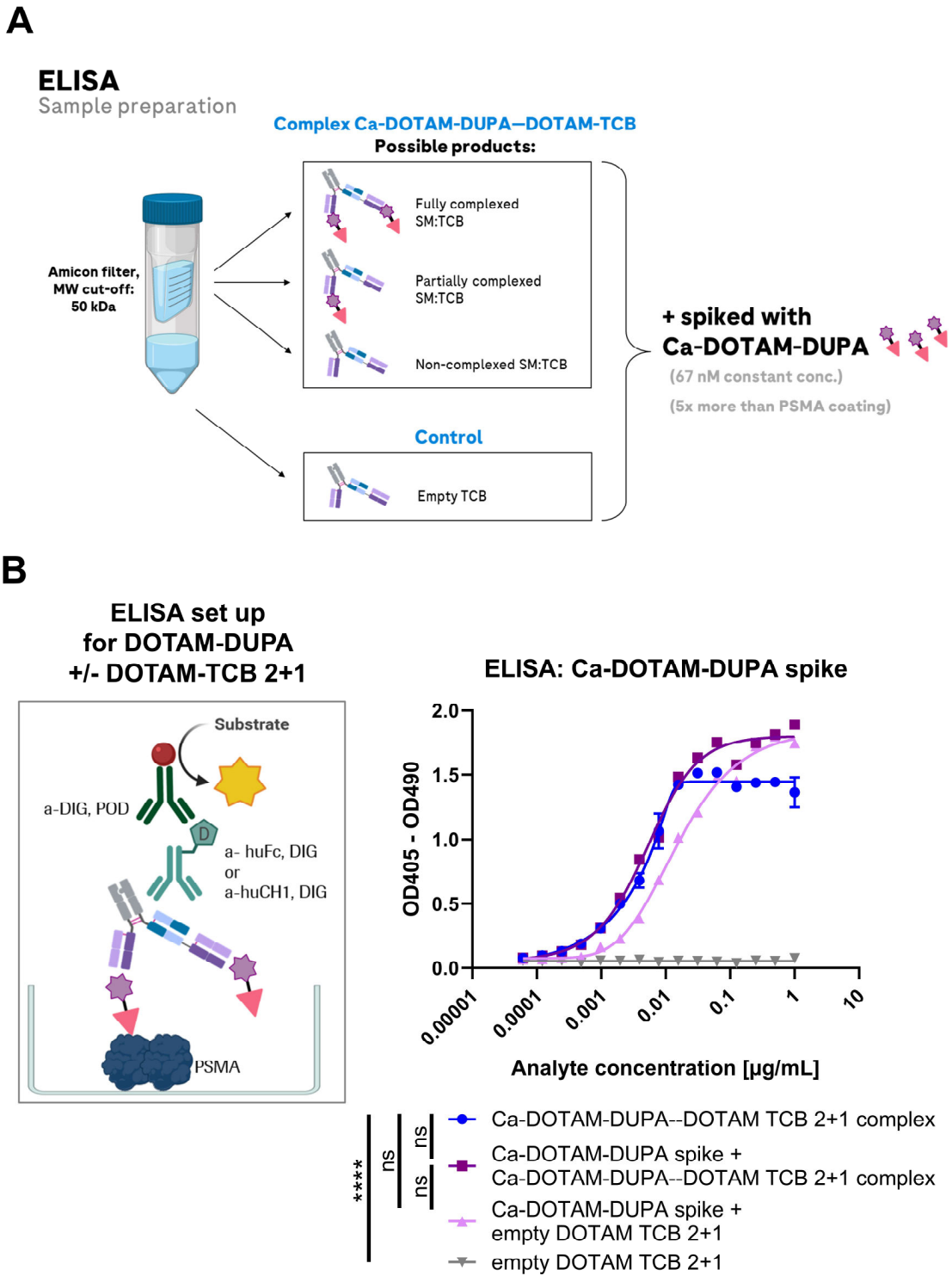

Figure 7.3.19. SM spike ELISA-based assessment of the complexing protocol of Ca-DOTAM-DUPA with DOTAM-TCB. A) Possible products from the complexing procedure and their SM spike pretreatment prior to ELISA. B) PSMA ELISA set-up and binding results after Ca-DOTAM-DUPA spiking. Data from one experiment, collected in technical duplicates. Error bars indicate standard error.

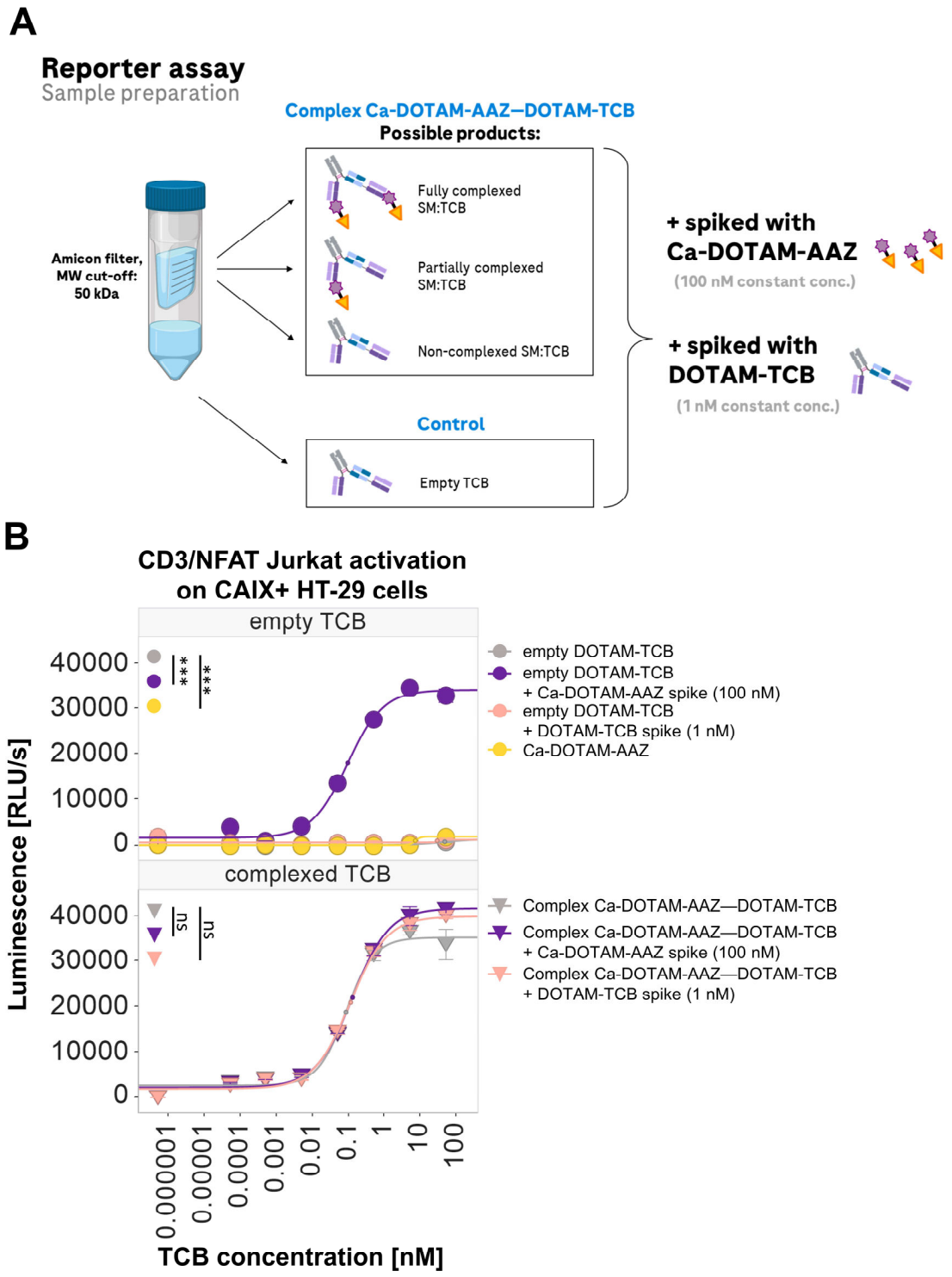

Figure 7.3.20. SM and TCB spike functional reporter-based assessment of the complexing protocol of Ca-DOTAM-AAZ with DOTAM-TCB. A) Possible products from the complexing procedure and their TCB spike or SM spike pretreatments prior to the CD3/NFAT Jurkat reporter assay. B) CD3/NFAT Jurkat cell activation upon co-culture with CAIX+ HT-29 cells and the pretreated molecules. Representative data from 2 experiments, collected in technical triplicates. Error bars indicate standard error.

The experimental details of size-exclusion chromatography-mass spectrometry determine quality control results of the non-covalent complex of Ca-DOTAM-Ligand-DOTAM-TCB

Due to a substantial body of evidence showing that the complexing protocol yields mostly fully complexed SM-TCBs, it was concluded that the results from the past native SEC-MS tests likely did not produce accurate results. In collaboration with Theresa Kober and Dr. José Bonfiglio (Roche Innovation Center Munich), the hypothesis was revisited that the sample acquisition process during native SEC-MS might have disrupted some complexes in the sample. Despite this, native SEC-MS was assessed to be the most direct and promising method for relative complex quantification, and decided to attempt to improve the protocol.

It was hypothesized that a 'softer' sample preparation and acquisition may prevent dissociation of the SM-TCB complex during measurement, and produce different results with higher measured amounts of complexed SM-TCB. Additionally, the possibility was considered that the complexing protocol might need to undergo improvements. Therefore, for the following native SEC-MS tests, samples were prepared using both the previously performed pre-purification incubation of SM:TCB ratio 4:1, as well as the new protocol with a SM:TCB ratio of 100:1. The new ratio was tested to increase SM excess substantially, and therefore potentially minimizing the occurrence of unoccupied DOTAM binders. These samples were tested (Theresa Kober and Dr. José Bonfiglio, Roche Innovation Center Munich) using both the previously used standard method and a new 'soft' method involving lowered energy parameters in the desolvation/fragmentation step, resulting in milder conditions applied to the sample.. Analysis of the 100:1 SM:TCB sample using the standard method for the Ca-DOTAM-AAZ—DOTAM-TCB 2+1 complex revealed three peaks representing empty TCB, half-complexed SM-TCB, and fully complexed SM-TCB (**Figure 7.3.21A**). In contrast, the same sample analyzed with the soft method showed no presence of empty TCB, with a smaller peak for half-complexed SM-TCB and a larger peak for fully complexed SM-TCB. Similar results were obtained for the analysis of the Ca-DOTAM-DUPA—DOTAM-TCB 2+1 as a SM-TCB complex prepared in a 100:1 ratio (**Figure 7.3.21B**). The standard method analysis resulted in three peaks depicting all possible complexing states, whereas the soft method showed no presence of empty TCB peaks, with smaller peaks for half-complexed SM-TCB and larger peaks for fully complexed SM-TCB (**Figure 7.3.21B**). These results clearly depict the influence of the native SEC-MS experimental conditions chosen for the SM-TCB complex analysis, where the method of sample processing and acquisition can disassemble complexes in parts of the sample, resulting in inaccurate data.

After confirmation of the improved conditions in the soft method, the preincubation protocol conditions were compared to identify potential points for improved complexing efficiency. A comparison was done of the SM:TCB preincubation molar ratio of 4:1 (as used in previous assays) to the 100:1 ratio using the soft method of sample processing in native SEC-MS. As depicted in **Figure 7.3.22**, the peaks representing SM-TCB complex 4:1 ratio and SM-TCB complex 100:1 ratio were comparable in readouts representing total main peaks (**Figure 7.3.22A**), combined main peaks with mass to charge ratio (**Figure 7.3.22B**), as well at detailed view of mass to charge ratio of a single selected charge state (**Figure 7.3.22C**). Peaks

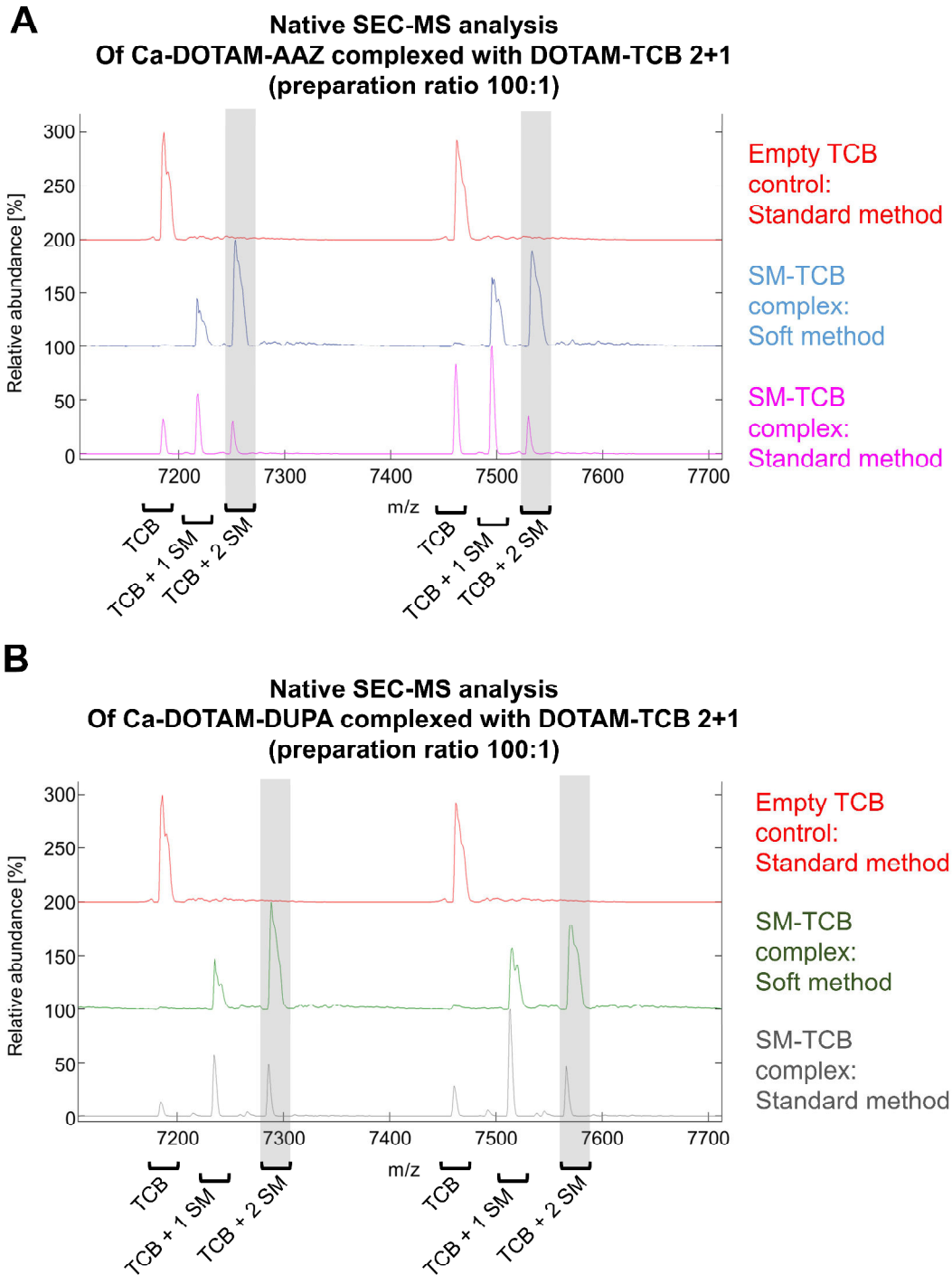

Figure 7.3.21. Comparison of the native SEC-MS results of the standard and soft method of sample processing and acquisition, for the preincubation SM:TCB molar ratio of 100:1. A) Relative abundance of possible complexing products of DOTAM-TCB 2+1 with Ca-DOTAM-AAZ. B) Relative abundance of possible complexing products of DOTAM-TCB 2+1 with Ca-DOTAM-DUPA. Data from one experiment.

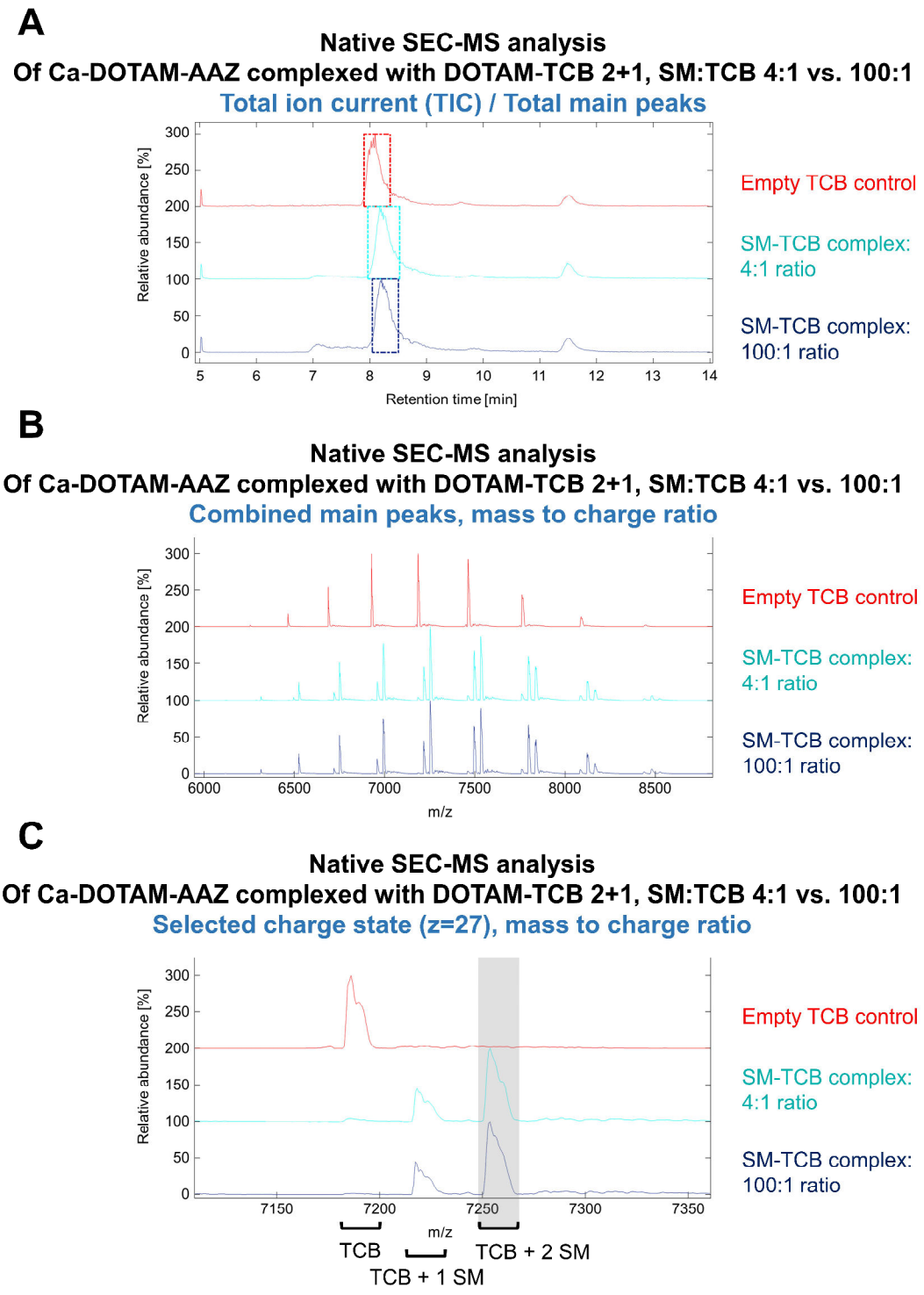

Figure 7.3.22. Comparison of the preincubation SM:TCB molar ratios of 100:1 and 4:1 by native SEC-MS (soft method), after the complexing protocol of Ca-DOTAM-AAZ with DOTAM-TCB 2+1. Peaks from: A) Total ion current results. B) Combined mass peaks. C) z=27 charge state. Data from one experiment.

representing both half-complexed and fully complexed SM-TCB were observed, and were comparable across the SM:TCB ratio samples. Therefore, it was concluded that since increasing the SM:TCB ratio to 100:1 did not improve the complexing efficiency results, the SM:TCB ratio of 4:1 was likely sufficient to saturate the complexing conditions in out protocol. Moreover, TCB-saturating conditions still resulted in the presence of partially complexed SM-TCBs in the native SEC-MS measurements (**Figure 7.3.22C**), highlighting the potential impact of the analysis method rather than the complexing dynamics. Therefore, this indicated that the soft method likely still disrupted the complexes during the sample processing step.

The use of the soft method of sample processing lead to the measured presence of only half-complexed and fully complexed SM-TCBs, absent of uncomplexed TCBs. This is more in line with previous ELISA, Jurkat, and killing assay results of the SM-TCB complexes. This data supports a conclusion that empty TCB is indeed not present in the complex preparation, regardless of used SM:TCB ratio in the preincubation step. However, the accuracy of the other peaks cannot be definitively concluded, since the soft method may still disrupt full complexes, albeit to a lesser extent than the standard method. Nonetheless, the functional data indicated that the prepared complex exhibited comparable activity to separately added SM + TCB, leading to the conclusion that the complexing protocol was ready to use in further functional studies.

Ca-DOTAM-Ligands with DOTAM-TCB display *in vitro* activity across a wide range of molarity and concentration ratios, resulting in wide therapeutic windows.

The *in vivo* efficacy study was planned to include both the SM-TCB complex and separately injected SM and TCB, to support the hypothesis of possible *in vivo* assembly and off-the-shelf mix-and-match character of the platform. Since molecule concentrations in solid tumors are not controllable factors, but optimal local levels of both SM and TCB are needed for efficacy, exploration of the therapeutic window across a range of SM:TCB ratios was initiated. The results from such a study would allow assessment if a specific tumor infiltration range needs to be reached by both molecules to show efficacy. To this end, efficacy of a range of SM adaptors across a range of TCB adaptors *in vitro* was evaluated. A CD3/NFAT Jurkat assay was performed, cross-titrating SM and TCBs from saturating concentrations to 0 nM using serial dilutions. **Figure 7.3.23A** depicts a resulting heatmap of Jurkat cell activation (as reflected by emitted luminescence) across a range of Ca-DOTAM-AAZ and DOTAM-TCB 2+1 concentrations, against HT-29 cells. As comparative controls, SM-TCB complex and direct CAIX-TCB 2+1 were used. **Figure 7.3.23B** shows a heatmap of Jurkat cell activation across a range of Ca-DOTAM-DUPA and DOTAM-TCB 2+1 concentrations, against LNCaP cells, and compared to SM-TB complex and to direct PSMA-TCB 2+1. For both targets, CAIX and PSMA, the therapeutic window was wide across SM and TCB concentrations. The heatmaps revealed bell-shaped curve tendencies across both variables, with the extent of the diminished signal dependent on the molecule concentration (**Figure 7.3.23A,B**). In general, these data provided evidence that efficacy can be achieved with a wide range of SM and TCB concentrations and SM:TCB ratios. With these encouraging results, the decision was made to proceed with

planning efficacy tests *in vivo*, including a group with separate injections of SM and TCB, alongside pre-assembles SM-TCB complex.

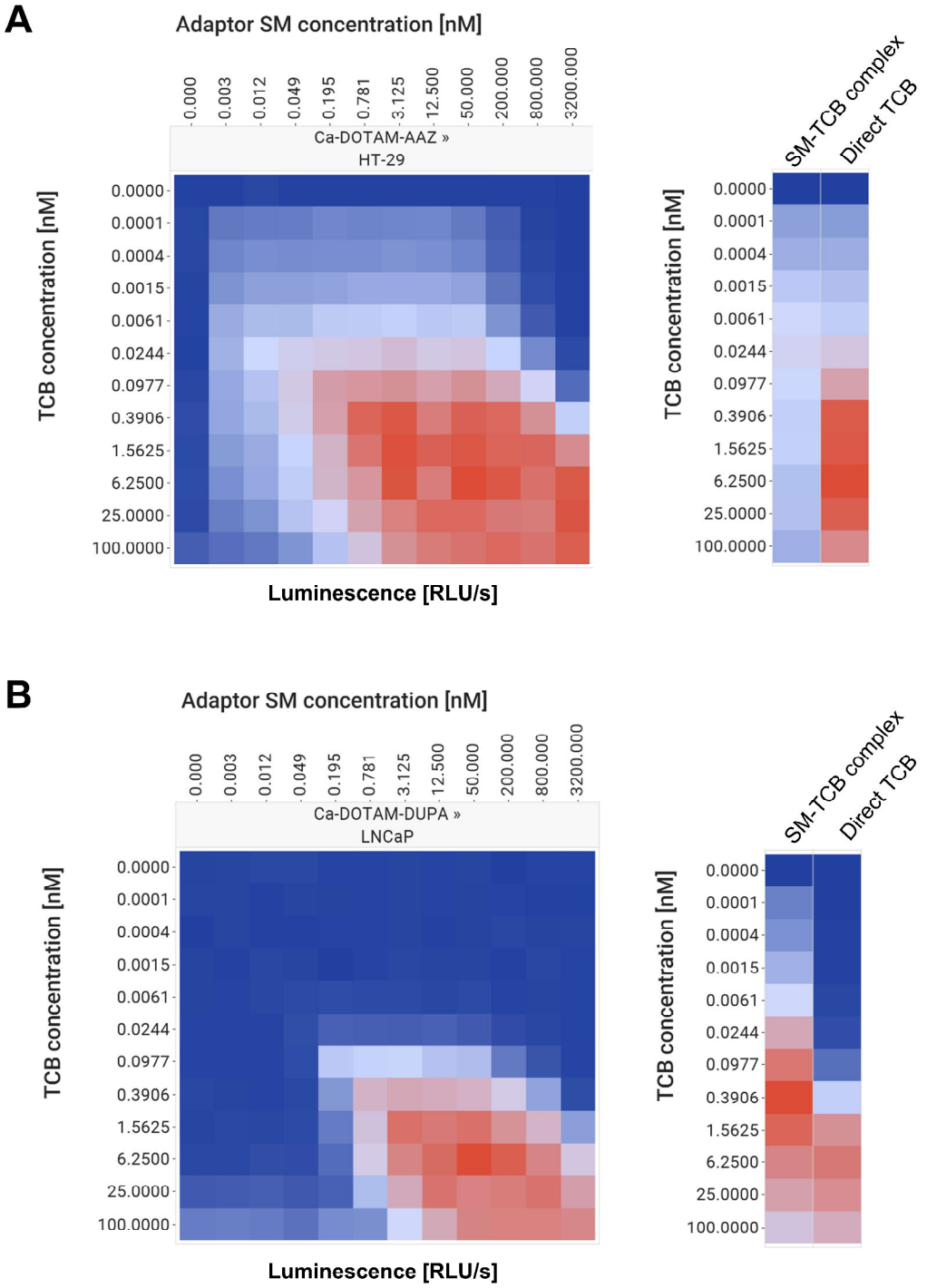

Figure 7.3.23. Therapeutic window assessment by a cross-titration of Ca-DOTAM-AAZ or Ca-DOTAM-DUPA with DOTAM-TCB 2+1 in a functional CD3/NFAT Jurkat reporter assay. CD3/NFAT Jurkat T cell activation upon co-culture with: A) CAIX+ HT-29 cells and Ca-DOTAM-AAZ, and B) PSMA+ LNCaP cells and Ca-DOTAM-DUPA. Data from one experiment.

Decision making process for the model for *in vivo* efficacy study, informed by public databases, in-house assays and an in-house database of established TCB models

In order to select the right model for *in vivo* efficacy studies, a strategy was devised, depicted in **Figure 7.3.24**. Firstly, it was decided that a humanized NSG or humanized BNRGD-CD47 mice with subcutaneously injected human tumor cells model would be suitable model for DOTAM-TCB activity evaluation, based on in-house data (data not shown). Secondly, since Ca-DOTAM-AAZ and Ca-DOTAM-DUPA were both selected as lead candidates for DOTAM-TCB project, publicly available databases were searched for human cancer cell lines with protein expression or mRNA presence for either CAIX or PSMA (**Figure 7.3.24**). Data was extracted from three databases for target-positive cell lines, mentioned below. Target-positive cell lines were selected using an arbitrary threshold of minimum expression, chosen by evaluating expression scored of in-house experimentally validated target-positive cell lines (For CAIX: HT-29, COR-L105 cell lines, for PSMA: LNCaP, 22Rv1, VCaP, MDA-PCa-2b), and expanding the list of cell lines several scores below their expression level. The first database was Gonçalves *et al*. proteomic database [379]. For CAIX, the arbitrary threshold was >4.0 of average protein expression score, which resulted in 57 CAIX+ cell line hits. For PSMA, with the same threshold, the search resulted in 8 PSMA+ cell line hits. The second database was Broad Institute's DepMap Proteomics 23Q2 database [380], resulting in 47 CAIX+ cell lines with >1.0 threshold of relative protein expression, and 6 PSMA+ cell lines with >1.0 threshold. The third database was mRNA-based Broad Institute's DepMap Expression Public 23Q2 database [380], resulting in 153 CAIX+ cell lines with >4.5 threshold of log2(Transcript per million (TPM)+1), and 9 PSMA+ cell lines with >6.0 threshold.

In terms of cell line selection, the aim was to utilize previously established in-house *in vivo* models, in order to expand on preexisting knowledge of T cell infiltration and potential availability of histological slides to assess tumor expression of CAIX or PSMA. Therefore, after compiling a list of potentially target-expressing cancer cell lines from these hits, it was compared with a list of internally established subcutaneous models in humanized mice (data not shown) which consisted of 58 cell lines or PDX models, and identified an overlap between these two subsets. This overlap experiment resulted in 5 cell lines having been both evaluated for target expression in public databases (CAIX or PSMA) and having been established internally as a model for TCB efficacy (**Figure 7.3.24**). Additionally, the past TCB *in vivo* efficacy data of these cell lines was screened, and evaluated for any potential risks of resistance to TCB killing, irrespective of the tumor target tested (data not shown). Out of the 5 leading cell lines, 2 have shown TCB resistance in past *in vivo* TCB efficacy studies, leading to selection of 3 cell line candidates. These candidate cell lines were all CAIX-positive, and included: HT-29 (colorectal adenocarcinoma), HCC1806 (breast squamous cell carcinoma) and SW620 (Dukes' type C colorectal adenocarcinoma) (**Figure 7.3.24**).

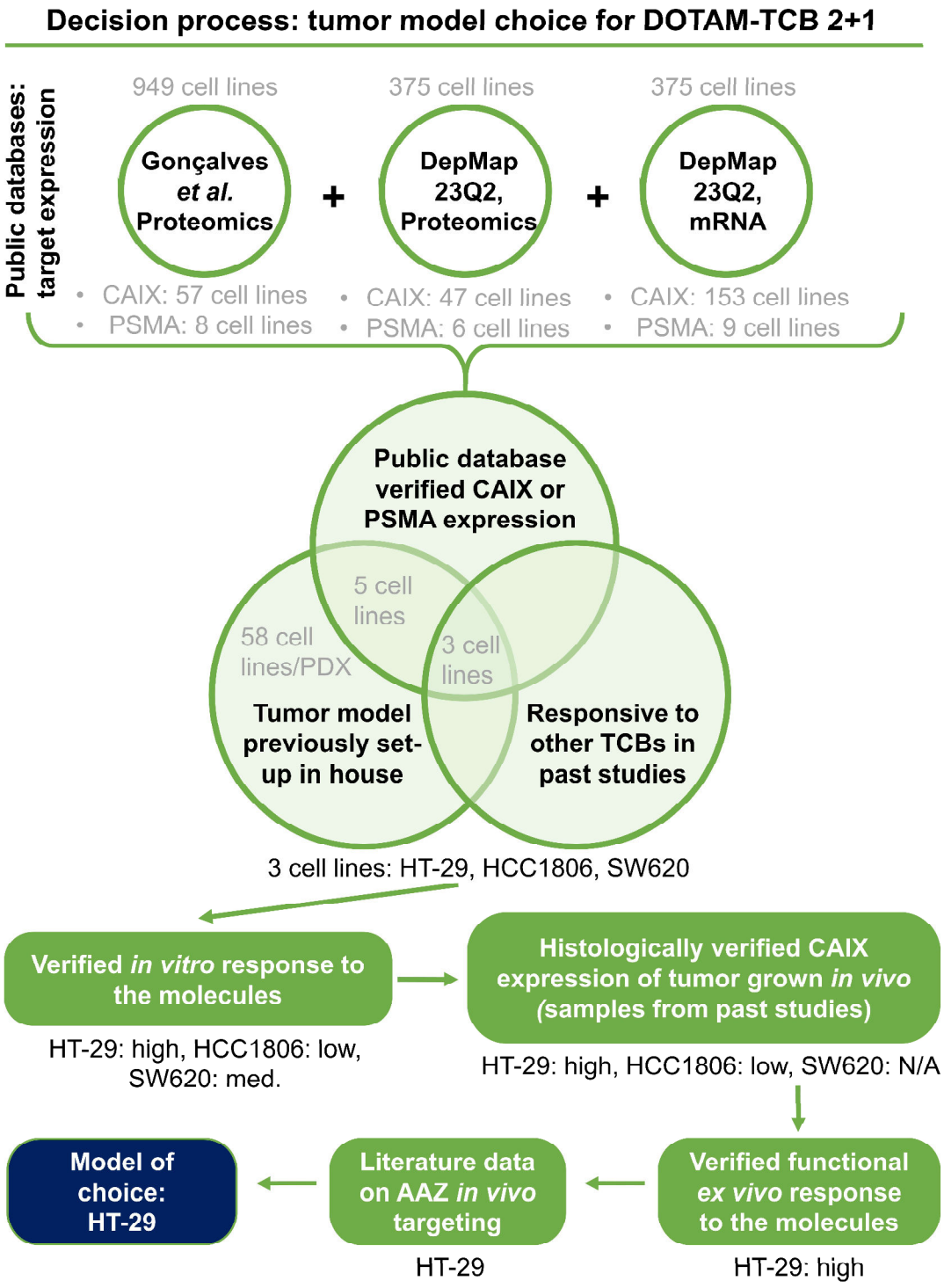

Figure 7.3.24. Workflow for the decision making process for the *in vivo* tumor model.

A comparative evaluation of these cell lines and their response to the molecules *in vitro* was conducted (**Figure 7.3.9**). HT-29, SW620 and HCC1806 were all effectively targeted by the T cell engaging Ca-DOTAM-AAZ with DOTAM-TCB 2+1. HT-29 exhibited the highest plateau of cytotoxic activity, followed by SW620 with a moderate signal, and HCC1806 with the weakest, but still present signal (**Figure 7.3.9A**). Therefore, all three cell lines progressed to the next evaluation step. As the next step, the aim was to verify if these cell lines, when grown *in vivo,* retain their target expression and to which extent. Given that all these cell lines had been previously tested internally in past studies, the goal was to obtain any available unused paraffin-embedded tumor samples for CAIX histology staining. SW620 samples were not available, while HT-29 and HCC1806 tumor samples were successfully obtained and histologically stained for CAIX expression. The histology results for both tumors are discussed below.

The results for hematoxylin and eosin (H&E), huCD3 and huCAIX staining for HT-29 tumors (performed by Marine Richard and Dr. Valeria Nicolini, Roche Innovation Center Zurich) are shown in **Figure 7.3.25**. Based on H&E staining (**Figure 7.3.25A**), well-developed tumors were observed with some necrotic areas in all the mice. No major differences were observed between groups. In terms of huCD3 staining, very low to low-moderate CD3+ cell number was observed, mostly in stroma areas in all tumors analyzed (**Figure 7.3.25B**). In terms of huCAIX staining, most of the tumor cells showed positive CAIX expression from very low to very high with only a few negative tumor cells in all the samples analyzed (**Figure 7.3.25C**). The histology results for H&E, and huCAIX staining for HCC1806 tumors (performed by Javier Torres Barajas and Dr. Valeria Nicolini, Roche Innovation Center Zurich) are depicted in **Figure 7.3.26**. Based on H&E staining, well developed tumors were observed, with large necrotic areas throughout the HCC1806 tumor mass (**Figure 7.3.26A**). HuCAIX staining revealed negative to low-moderate patchy CAIX expression throughout the HCC1806 tumors, mostly at the border between healthy tumor and necrotic areas (**Figure 7.3.26B**).In summary, HT-29 gown subcutaneously *in vivo* in humanized mice showed high CAIX expression, while HCC1806 tumors had low or patchy expression of CAIX.

Due to these results, HCC1806 was deemed unsuitable for the Ca-DOTAM-AAZ with DOTAM-TCB *in vivo* studies. SW620 cell line was similarly removed from a list of potential cell lines due to unavailable data on *in vivo* CAIX expression. Therefore, HT-29 remained as the only suitable model at this stage of verification. Nevertheless, the verification process was continued and the decision was made to perform an *ex vivo* testing of the molecules on the mouse-grown HT-29 tumor cells. One tumor was collected at a termination time point from an *in vivo* set up study of HT-29 tumors in BRGS-CD47 mice (courtesy of Ahmet Varol, Roche Innovation Center Zurich). A co-culture experiment was performed, including a dissociated HT-29 tumor, human primary PBMCs from healthy donors, and Ca-DOTAM-AAZ with DOTAM-TCB 2+1 or control molecules. The molecule-driven response was evaluated by flow cytometry and quantification of the T cell activation markers. The results of the *ex vivo* assay are shown in **Figure 7.3.27**. **Figure 7.3.27A** shows data from one representative PBMC donor, **Figure 7.3.27B** shows area under the curve values from two healthy PBMC donors. For both donors, Ca-DOTAM-AAZ with DOTAM-TCB 2+1 displayed strong dose dependent T cell activating capacity. Interestingly, in the case of both donors and all tested activated T cell populations but CD25+ [% of CD8+],,

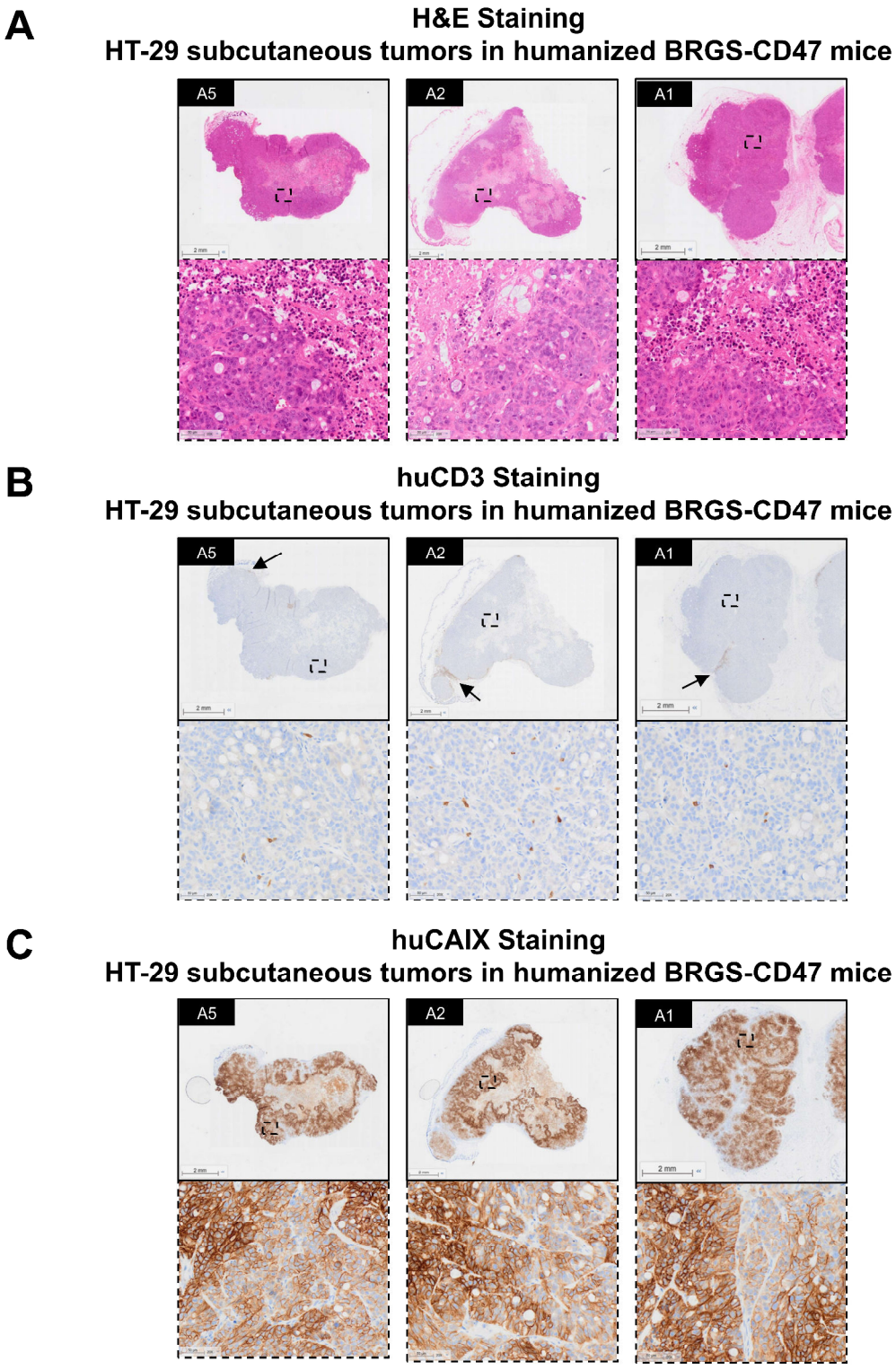

Figure 7.3.25. Histology staining of HT-29 tumors grown in humanized BRGS-CD47 mice. A) H&E staining. B) huCD3 staining. C) huCAIX staining.

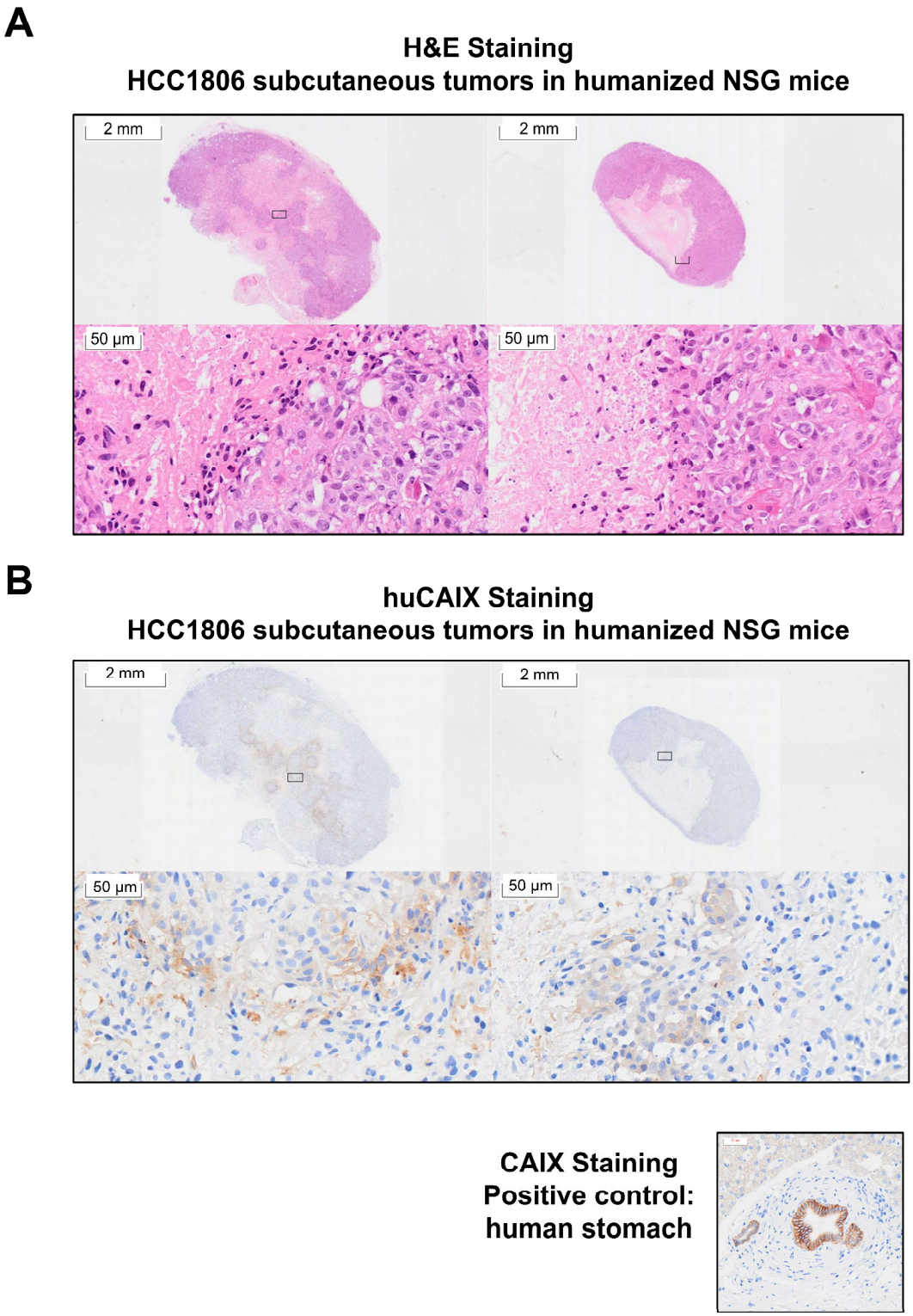

Figure 7.3.26. Histology staining of HCC1806 tumors grown in humanized NSG mice. A) H&E staining. B) huCAIX staining.

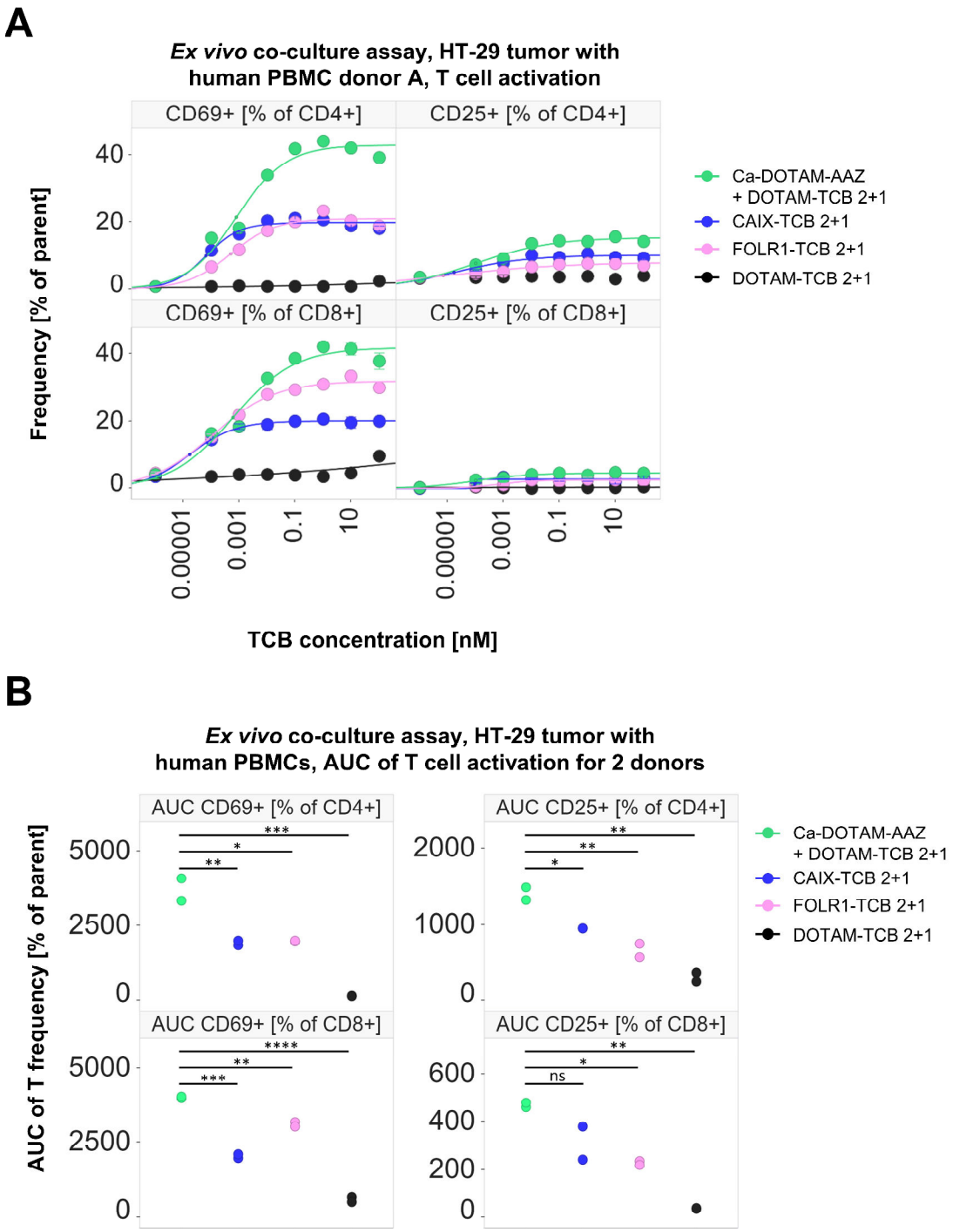

Figure 7.3.27. Ex vivo functional assay results of mouse-grown HT-29 tumors, human healthy donor PBMCs and Ca-DOTAM-AAZ with DOTAM-TCB 2+1. T cell activation marker expression on CD4+ and CD8+ cell subsets from assay results performed with A) individual dose response values from a healthy PBMCs donor. B) AUC values from two healthy donors. Data from a single *ex vivo* experiment.

Ca-DOTAM-AAZ with DOTAM-TCB 2+1 showed significantly higher response than two positive controls – direct CAIX-TCB 21 and direct FOLR1-TCB 2+1. Importantly, empty DOTAM-TCB 2+1 did not elicit any T cell response. These data provided evidence that the level of CAIX expression in mouse-grown HT-29 tumor was sufficient for a potent efficacy of Ca-DOTAM-AAZ with DOTAM-TCB 2+1. The results provided additional verification of the molecule potency and its suitability for the HT-29 model.

As the last step in determining the *in vivo* model, the findings were verified in the literature. Special focus was placed on studies utilizing AAZ as a targeting molecule, since the specificity of CAIX-targeting antibodies and small molecules might differ, and studies utilizing CAIX-specific antibodies are not directly translatable.

Two studies that were consulted used imaging of AAZ-based molecules in mice. One group developed their own AAZ-linked fluorophore and evaluated it in BALB/c nu/nu mice bearing CAIX+ SKRC52 tumors [371]. Their findings indicated preferential accumulation of the molecule in the tumor 4h post-injection. The group also tested small molecule-drug conjugates (SMDCs) in the same model, substituting the fluorophore with a therapeutic payload, and observed antitumoral efficacy without accompanying body weight loss [371]. Similarly, another research group developed AAZ linked to a fluorescent dye (referred to as AZA) [364]. This exact AZA with its linker, which served as the structural basis for the adaptor, was used for visualizing CAIX+ regions in human HT-29 and MDA-MB-231 tumor-bearing mice (athymic nu/nu mice). The group demonstrated that 4h post-injection, there was significant molecule accumulation in HT-29-derived tissue expressing high levels of CAIX, while minimally expressing MDA-MB-231 cells remained negative [364]. Subsequently, in another study, the group generated anti-FITC CAR-T cells for use with haptenated small molecule adaptors, including AAZ-FITC (also termed FITC-AZA). They tested their constructs in NSG mice bearing MDA-MB-231 cells engineered to express CAIX and administered increasing doses of adaptor-loaded CAR-T cells into the mice [240]. The constructs exhibited a robust inhibition of tumor volume over time, with complete tumor rejection achieved by the end of the study, approximately 25 days post first injection. Importantly, no adverse events were reported [240]. Taking all these data, literature and decision steps into consideration, it was concluded that the CAIX-expressing HT-29 model was suitable for in-house efficacy study for Ca-DOTAM-AAZ with DOTAM-TCB 2+1.

In vivo study of Ca-DOTAM-AAZ combined with DOTAM-TCB shows rapid induction of drug-related toxicity

As mentioned above, to test the efficacy, humanized BRGS-CD47 mice and subcutaneous injection of HT-29 cells were selected. The groups of the study design are shown in **Figure 7.3.28A**, and the injection schedule is depicted in **Figure 7.3.28B**. A group with complexed Ca-DOTAM-AAZ—DOTAM-TCB 2+1 was included, to ensure the presence of a fully loaded DOTAM-TCB. Additionally, a test group was planned with separate injections of Ca-DOTAM-AAZ (intraperitoneal) and, 2 hours after, DOTAM-TCB 2+1 (intravenous). This was to evaluate if the SM adaptor and the DOTAM-TCB can be used separately and assemble *in vivo*.

HT-29 cells were injected into the humanized mice subcutaneously. The tumor growth curves are depicted in **Figure 7.3.28C**. Upon reaching an average tumor size of ~125 mm3, the mice were injected with the therapeutic molecules. Three days after the first injections, SM-TCB treatment groups displayed signs of severe drug toxicity, as seen by a drastic drop in body weight (**Figure 7.3.28D,E**). Due to these adverse events and no improvements in mouse condition, the study was terminated the following day (4 day after therapy injections). The vehicle group was kept in order to monitor potential effects of HT-29 injections. As seen in the mean body weight measurement, HT-29 injections or protein buffer injections alone did not lead to toxicity, as shown by stable weight of the mice of the vehicle group (**Figure 7.3.28D**) and 100% survival at 3 weeks (data not shown). Neither Ca-DOTAM-AAZ alone nor DOTAM-TCB 2+1 alone exhibited strong level of toxicity (**Figure 7.3.28E**), indicating that sole binding of either molecule (to CAIX or CD3ε respectively) was not sufficient to trigger adverse reactions. However, both separately injected SM + TCB and SM-TCB complex groups displayed similar body weight-related and survival-related toxicity, suggesting similar activity. As such, the toxicity was linked to the formation of a functional TCB by Ca-DOTAM-AAZ + DOTAM-TCB 2+1. The question arose whether T cell mediated killing of the CAIX-expressing cells was the main culprit of the observed drug reaction. However, the direct CAIX-TCB body weight and survival, albeit to a much lower extent (**Figure 7.3.28D,E**). These data suggests that both small molecule and antibody CAIX-targeted TCBs induced toxicity, with the antibody CAIX-targeted TCB (CAIX-TCB) displaying smaller effects in terms of body weight loss and survival, highlighting the differences between the binders and possibly their specificity.

As mentioned before, small molecules offer lower target specificity than small molecules, and are typically species cross-reactive, binding both mouse and human targets [346], [347], [348]. AAZ has been described to bind to other carbonic anhydrases besides CAIX, and the aforementioned imaging studies indeed indicated non-tumor organs where AAZ-based molecules were accumulated [364]. CAIX antibody binder G250, on the other hand, is not cross-reactive with murine CAIX [381], limiting its activity to injected human tumor cells, and potential off-target proteins in mouse healthy tissues. Due to this and the observed differential activity of antibody and small molecule-based TCB, it was hypothesized that the T cell redirection towards the cells bound by Ca-DOTAM-AAZ was the main aspect leading to the observed toxicity, depending on assembly of the adaptor and the TCB into a functional T cell engager. However, dose escalation of AAZ-FITC adaptors used with FITC-specific CAR-T cell injection were effectively used in an *in vivo* study by Lee et al. In this work, adverse events were not reported, but the mice survived more than 30 days on treatment [241]. Therefore, the fact of T cell-mediated cytotoxicity against AAZ-bound cells does not provide sufficient explanation for these observations. Further studies to establish the cause of the adverse events of Ca-DOTAM-AAZ with DOTAM-TCB are ongoing. .

Overall, a small molecule adaptor-based universal DOTAM-TCB for use with interchangeable tumor-binding adaptors was developed in this work, The universal DOTAM-TCB was able to effectively target adaptor-bound cells *in vitro*. The preliminary *in vivo* study highlighted potential specificity limitations of the Ca-DOTAM-AAZ combined with DOTAM-TCB. Additional studies are needed to evaluate if haptenated small molecule binders and universal hapten-binding TCBs are a suitable modality for safe cancer immunotherapy in human context.

A

Group	Symbol	Compound	Dose	Route	Schedule	No. of animals
A		Vehicle	0 mg/kg	i.v.	1x /week	14
B		CAIX-TCB 2+1	5.0 mg/kg	i.v.	1x /week	14
C		Ca-DOTAM-AAZ	0.45 mg/kg	i.p.	1x /week	14
		DOTAM-TCB 2+1	5.0 mg/kg	i.v.	1x /week	14
D		Ca-DOTAM-AAZ – DOTAM-TCB 2+1 complex	5.0 mg/kg	i.v.	1x /week	14
E		Ca-DOTAM-AAZ	0.45 mg/kg	i.p.	1x /week	14
F		DOTAM-TCB 2+1	5.0 mg/kg	i.v.	1x /week	14

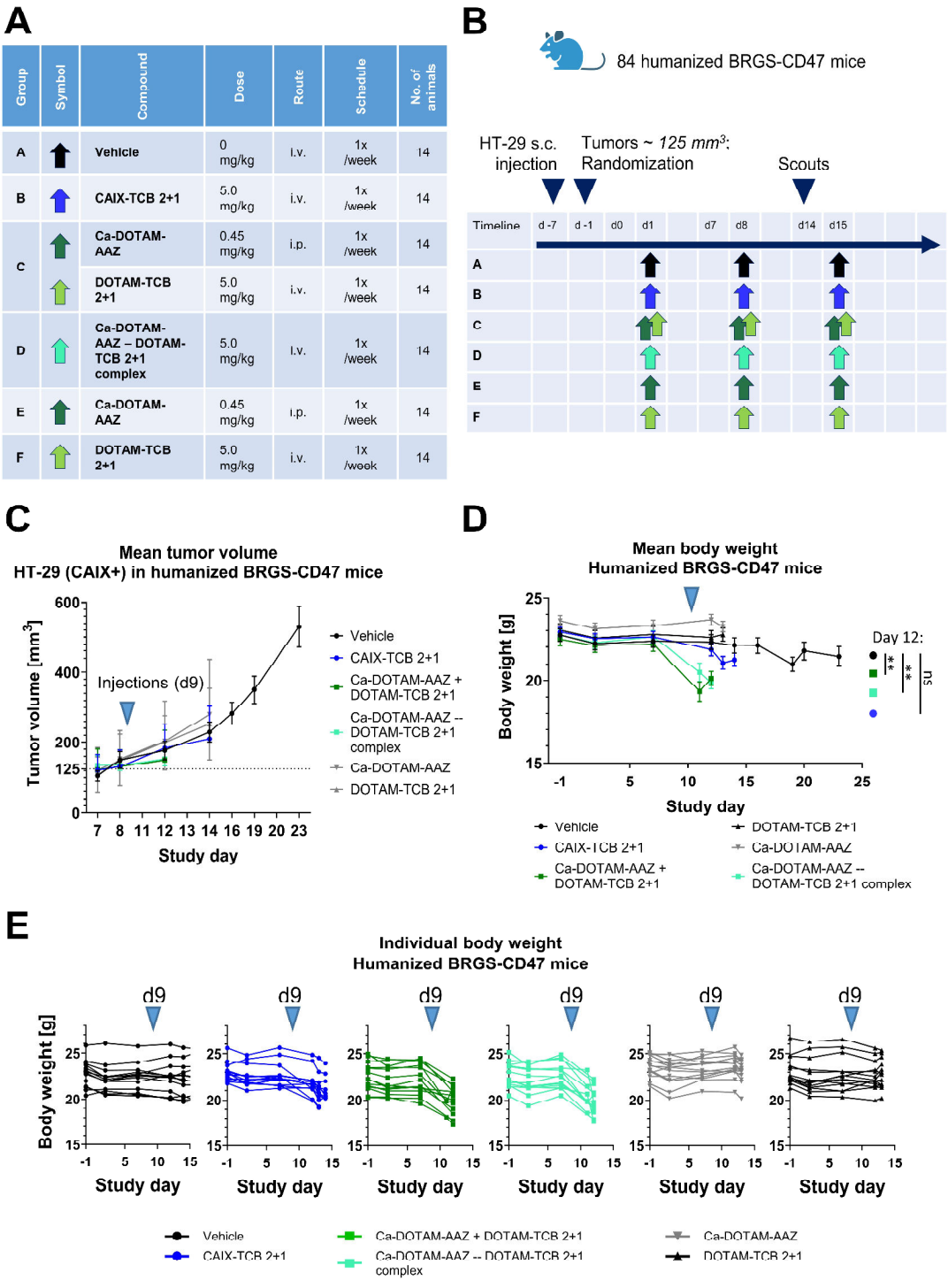

Figure 7.3.28. Design and results of the efficacy in vivo study of HT-29 tumor-bearing mice and Ca-DOTAM-AAZ with DOTAM-TCB 2+1. A) Description of the study groups, molecule doses, and dosing schedules. B) Schedule of the planned in vivo study. C) Mean tumor volume over time, including terminated groups. D) Mean body weight over time. E) Individual mouse body weight across groups. Reversed blue triangle indicates first therapy injection time point. Data from a single *in vivo* experiment.

8. Discussion and Future Outlook

In this thesis, three universal adaptor based antibody platforms for cancer immunotherapy were presented. Firstly, a P329G-Engager antibody-based platform was developed and characterized, offering a mix-and-match assembly of a functional immunotherapeutic from two inactive components, selected based on cancer and immune targets of interest. Secondly, the platform was expanded and a universal protease-dependent pro-P329G-TCB system was engineered, with interchangeable cancer-targeted adaptors, for minimizing on-target off-tumor activity. Thirdly, a DOTAM-TCB platform was developed and explored, utilizing tumor-binding haptenated small molecules and hapten-binding T cell engaging antibody, exploiting small molecule and antibody pharmacological properties. Altogether, this work aimed to offer several target-agnostic universal cancer immunotherapy systems, exploring the recent innovative strategies in protein engineering, and with potential implications for both preclinical drug discovery and clinical applications. Below, the results of this work are discussed in the context of past and current research.

8.1. Tumor heterogeneity in context of cancer immunotherapy

Currently, bispecific antibodies hold immense promise and interest in cancer immunotherapy [34]. Upon gathering clinical data on these molecules, certain challenges were identified in the field. Some of the most common obstacle in reaching efficacy is, for instance, intra- and inter-patient tumor heterogeneity [382], including changing tumor landscape over the course of treatment or cancer progression, pertaining to both tumor antigens and immune compartment characteristics [383], [384], [385], [386], [387], [388], [389], [390]. Thus, one-size-fits-all strategies in immunotherapy treatments are bound to offer limited antitumoral efficacy. Another limitation is on-target off-tumor activity of the therapeutic molecule, with immune cell activation being directed against both tumors and healthy tissues, potentially leading to dose-limiting toxicities, and therefore lowering tumor control potential overall [177], [391], [392].

The current scientific consensus states that redirecting drug development efforts towards patient personalization is an inevitable step to improve therapeutic efficacy for cancer immunotherapy [393]. At present, personalization within the field is applied in a narrow spectrum of modalities, focusing mostly cancer vaccines, but also on cell therapies like TIL or CAR-T treatments [393]. These currently require preparation of the treatment for each patient separately, introducing batch variability, costs and prolonged time before therapy can be initiated [37]. Here, an off-the-shelf availability of antibodies would seem to offer solutions to these challenges. However, currently, off-the-shelf solutions and personalization seem to be mutually exclusive. In terms of antibody-based therapeutics, combining these two aspects would involve development of an array of molecules targeting various tumor antigens and different immune cell receptors. While theoretically possible, a substantial consideration needs to be given to the economic aspects of such an approach. Production and

characterization of such a plethora of antibodies would inflict high costs of both preclinical and clinical stages of drug discovery, and ultimately, for patients and healthcare systems.

8.2. Adaptor-based universal immunotherapeutics – CAR-T cells and beyond

To address this gap, it was hypothesized that a cancer immunotherapy platform which offers a separate array of tumor-targeting adaptors, and an array of adaptor-binding immune cell engagers could offer solutions to the aforementioned obstacles. Separating tumor targeting molecular entities from the ones engaging immune receptors and cells, the resources could be focused on developing universal, target-agnostic immune engagers –for instance one universal TCB - as opposed to separate production and characterization of new engagers for each tumor antigen.

Considering a plethora of P329G-mutated therapeutics which have entered the clinics, with characterized pharmacological properties, as well as long half-life of huIgG1 antibodies thanks to intact FcRn binding, an anti-P329G CAR-T cell for use with antitumoral P329G-mutated tumor-binding huIgG1 adaptors was developed [244]. Due to the versatility of this novel concept of utilizing the mutation as an in-built adaptor tag, and the specificity of the P329G binder to its target, the anti-P329G CAR-T cells were utilized in several directions. Firstly, as a preclinical drug screening tool [244]; secondly, as a clinical CAR-T cell therapy for cancer patients (NCT05199519, NCT05270928, NCT05266768); and thirdly, for academic CAR-T-focused research [226], [245]. Such a unique versatility of the P329G platform highlighted the potential for advantages of carefully designed adaptor platforms beyond initial indications.

In light of this previously undescribed encouragingly wide scope of applications, the question arose if the P329G platform can be expanded even further. CAR-T cells, despite their promise in the clinics, entail several disadvantages for drug development and the clinics, such as – currently – no off-the-shelf availability, delayed initiation of treatment, high costs and more [41]. On the other hand, antibodies as modalities offer improvements over these aspects, as well as additional benefits such as predictable pharmacokinetics and engagement of various different immune cell receptors. Hence, the aim of this work to design, produce and characterize a P329G-binding antibody platform, to compliment and expand the universal immunotherapeutic landscape of the P329G-CAR. Consequently, the P329G-Engager platform was conceptualized and developed.

8.3. Discussion of Chapter 1 – P329G-Engager: A novel universal antibody-based adaptor platform for cancer immunotherapy

Due to the rapidly developing knowledge on tumor immunology, an opportunity for the P329G-Engager platform was identified to include novel immune cell engagers with various modes of action.

T cells are widely known as crucial helper or cytotoxic cells able to attack target cells [19], [20]. In line with this, T cell bispecific antibodies have been shown to offer potent antitumoral activity *via* engaging CD3+ T cells to launch cytotoxicity directed to antigen-expressing cells, and initiating infiltration and proliferation of T cells [394]. Therefore, a P329G-T cell bispecific was developed. CD28 costimulation is described as a necessary signal for initiating T cell response [395], and while its externally introduced agonism is not needed for TCB activity [64], it improves TCB responses [201]. Another costimulatory signal, via 4-1BB, is also considered crucial for improved proliferation, toxicity, and resistance to exhaustion (reviewed in [396]). Therefore, to create the possibility for costimulatory agonism for potential combination with TCBs and beyond, P329G-CD28 antibody and P329G-4-1BBL antibody-protein fusion were developed as part of this work. These approaches offer engagement towards an antigen of interest by activating immune cells regardless of their specificity. While an advantage, an expansion of this research was sought into another crucial aspect of immunotherapy - boosting antigen-specific CD8+ tumor-infiltrating T cells against the cancer cells. Generally, this is achieved by immune checkpoint blockade such as anti-PD-1 or anti-PD-L1 antibodies, by removing the inhibitory signals from the tumor-specific T cells [397]. To improve response rates, combination therapies have been explored, such as PD1 blockade with recombinant IL2 [398], [399]. However, treatment with IL2 is associated with toxicities like vascular-leak syndrome [145], [400]. Recently, novel research by Codarri Deak *et al.* showed that eciskafusp alfa, a clinical stage anti-PD1 antibody fused with IL2Rβγ-biased IL2v (termed PD1-IL2v), not only delivered IL2R signaling to PD1-expressing antigen-specific cells in *cis*, but also differentiated stem-like CD8+ T cells into better effector cells while inhibiting exhaustion potential [157]. The potential of this novel, and formerly unreported crucial functionality of a cancer immunotherapeutic was recognized, and the decision was reached to develop P329G-binding IL2v, incorporating this mode of action into the platform. Aside from T cells, other immune cells are also of interest for immunotherapy. As one of the earliest modalities, Fc-active IgG antibodies have been used to induce antibody-dependent cellular cytotoxicity, antibody-dependent phagocytosis or complement-dependent cytotoxicity against tumor antigens [68], [401]. Notable examples include rituximab and obinutuzumab, both anti-CD20 antibodies for hematological malignancies or trastuzumab and pertuzumab, both anti-HER-2 antibodies for breast cancer [68]. Additionally, the mode of action of anti-CTLA-4 checkpoint blockade has been also highlighted to rely at least in part on Fc functions [130]. Currently, FcγR-engaging therapeutics, and especially NK cell engagers are undergoing a revival (reviewed by Vivier *et al.* in [402]). This is, among other reasons, due to T cell-evading properties of certain tumors [403] and the risk of cytokine release syndrome of T cell engagers and CAR-T cells [404], [405], [406], both of which can be potentially overcome by shifting to or combining with NK cell engagement [407], [408], [409]. Moreover, there exist other Fc-

mediated functions of IgG antibodies, such as ability to induce phagocytosis of the cell bound by the antibody's antigen-binding sites, and activation of the complement system against it [65]. Therefore, Fc-functional antitumoral IgG1 antibodies can exert multifunctional antitumoral activity by activating both NK cells and macrophages [24], potentially leading to potential efficacy in various tumor microenvironments. Due to this potential, P329G-Innate cell engager (P329G-ICE) was also included in this platform.

In summary, a variety of immune cell engagers were designed, including P329G-TCB, P329G-CD28, P329G-4-1BBL, P329G-IL2v and P329G-ICE to introduce a wide range of modes of action to the platform. Importantly, the choice was made to use the P329G-binder from the clinical anti-P329G CAR-T cells. The other effector binders or protein fusions were selected based on clinical molecules, such as FDA-approved CD20-TCB (glofitamab), clinical CD19-CD28, CD19-4-1BBL, PD1-IL2V and FDA-approved CD20-ICE (obinutuzumab). Moreover, both the P329G mutation has been used in the clinics (e.g. in glofitamab, among others), and the tested tumor or immune cell-targeted adaptors such as these against CEACAM5 or PD1.

Altogether, in order to expand on the universal anti-P329G CAR-T system, a commitment was done to follow the newest research in tumor immunology and immunotherapy to translate it into a versatile platform for use beyond a single modality. The aim was to provide an antibody platform which can address not only the heterogeneity in tumor antigen expression – which can be achieved by CAR-T cell adaptor systems – but also tackle heterogeneity in the immune part of the tumor microenvironment. By following the recent literature, as well as preclinical and clinical data, it was possible to identify several immunotherapeutic modalities of interest, which can be used to address specific immune pathways, whose engagement may lead to increased antitumoral efficacy. By basing this project's molecules, binders, and the P329G tag on clinically tested candidates, it was possible to create cost-effective and clinically characterized cancer immunotherapy platform. The P329G-Engager platform offers previously undescribed double universality towards cancer and immune cell targets.

While clinical basis offered access to in-depth characterized structures for use within the platform, it was nevertheless required to partially modify the original structures when designing the platform's engagers. With the exception of CD20-ICE, Fc silencing strategy utilized in the clinical engagers was the P329G mutation, coupled with LALA mutation. Since the P29G-Engagers, by definition, contain a binder to the P329G mutation, it was not feasible to introduce P329G Fc silencing in their Fc, in order to prevent self-binding and aggregation. Removal of the Fc, such as was done in blinatumomab [46], was not of interest. Due to the half-life prolongation conferred by FcRn-mediated recycling [410], the Fc-containing antibodies possess desirable characteristic of prolonged persistence in the body, potentially enhancing efficacy, and limiting logistical hurdles of multiple hospital visits for patients. Thus, the goal was to retain the Fc, while abolishing its functions related to ADCC, ADCP and CDC, to prevent attack on the effector immune cells.

LALA mutations themselves are not recognized by the P329G binder [411]. Despite offering incomplete abrogation of Fc functions, as shown in a publication by Schlothauer *et al.*, LALA mutations do partially inhibit Fc binding to FcγRs [367]. Thus, for the initial designs of the P329G-Engagers which require inactive Fc, LALA-based silencing was opted for. After

gathering primary evidence of the functionality of the concept in assays lacking FcγR-expressing cells, P329G-TCB was tested on healthy human PBMCs. As expected, and in line with the work of Schlothauer and colleagues [367], crosslinking was observed between FcγR+ and CD3ε+ immune cells, even in absence of target cells, likely leading to fratricide amongst different immune cell subsets. For proof of concept experiments, this level of Fc silencing might be considered satisfactory. However, it was considered that the numerous applications of the previously developed anti-P329G CAR-T cells – spanning preclinical, clinical, and academic research endeavors, were enabled because of complete and diligent pharmaceutical development. Therefore, the goal was to develop the P329G-Engagers with clinically focused design.

To this end, the research efforts needed to be directed into developing a novel Fc-silencing mutation, different from P329G, to be introduced with new P329G-Engagers. Importantly, the novel mutation should be additionally unbound by the P329G-binder. Basing on structural knowledge gained while developing P329G silencing, as well as the crystal structure that was solved previously, detailing the interaction of the P329G-binder with P329G-mutated Fc, four novel mutations at the position P329 were proposed, aiming to disrupt the proline-sandwich forming capacity between the Fc and FcγRs. Fc-containing molecules were produced with either of the mutations: P329L, P329I, P329A, P329R, along with LALA mutations. All new constructs displayed the two defined requirements: firstly, inhibiting binding of the Fc to the FcγRs, and consequently abrogating Fc functions, and secondly, remaining unbound by the P329G-binder. The P329R mutation was selected as the lead candidate due to the most favorable profile. The new generation of the P329G-TCBs were designed with the P329R LALA Fc, and confirmed in co-culture assays that the cross-linking events between FcγR+ and CD3ε+ cells were prevented. Thus, the P329G-Engagers gained a crucial characteristic needed for potential use with mouse or human applications. In summary, aside from creating the P329G-Engager platform, a previously unpublished novel Fc-silencing strategy was developed herein, P329R, for use with any Fc-containing IgG1-based therapeutic antibodies, with utility well beyond the described project.

Via the development of the novel P329R LALA Fc silencing strategy for use with any P329G-Engager (except from Fc-competent ICE), evaluation of P329G-Engagers in *in vivo* contexts was enabled. Given the growing recognition of TCBs as potent therapeutics [25], [34], as well as availability of suitable mouse models in-house, the focus evolved onto the *in vivo* proof-of-concept experiments on the P329R LALA-mutated P329G-TCB. Aside from evaluating general antitumoral activity of this molecule, the importance of testing *in vivo* assembly of the adaptor with P329G-TCB was acknowledged. To this end, the efficacy study of MKN-45 tumor-bearing humanized NSG mice was designed, utilizing a pretargeting approach, with CEACAM5 P329G-mutated adaptor IgG being administered 24h prior to P329G-TCB injection. With this approach, the aim was to ensure partial enrichment of the adaptor in the tumor, compared to circulation, upon the administration of the T cell engager. Given the findings from *in vitro* assays, it was expected for T cell mediated killing to occur only upon binding of the P329G-TCB to the adaptor (together with binding to the tumor and T cells), enabling formation of a stable immunological synapse. Hence, any antitumoral T cell cytotoxicity reflected *in vivo* assembly at the site of target and T cell localization. Indeed, what was observed was not only

antitumoral effect of the adaptor with the P329G-TCB, but also inactivity of either compound administered as single agents. The efficacy of the adaptor with P329G-TCB was present, albeit to a weaker extent than the positive control, direct CEACAM5-TCB. The *ex vivo* analysis of the tumor tissue revealed that infiltration of certain T cell subsets, such as CD8+ GrB+, was increased for adaptor with P329G-TCB group. However, the positive control group displayed a higher rise of T cell numbers inside the tumor. This is consistent with the stronger tumor control for this group. In line with this, weaker infiltration or proliferation in the tumors of mice treated with adaptor with P329G-TCB may be causally linked with the weaker antitumoral efficacy. Importantly, the dose selected for this study was suboptimal to ensure comparison of the study group to the positive control. Higher T cell infiltration increase rate in the direct TCB group, therefore, indicates that there is potential for enhancement of the adaptor with P329G-TCB activity, likely via dose optimization. Crucially, despite the lower impact on tumor-infiltrating T cell numbers, the adaptor with P329G-TCB achieved statistically significant tumor control. As such, this mouse efficacy data provided the *in vivo* proof-of-concept for the first P329G-Engager, P329G-TCB. Additionally, the results from this study offered learnings for future evaluation of further P329G-Engagers.

8.4. Discussion of Chapter 2 – Universal protease-activated cancer immunotherapy using target-agnostic antibodies

Aside from addressing the heterogeneity in tumor antigens and immune cell compositions, a need to tackle on-target off-tumor toxicities present in clinical antibody therapeutics was identified. While offering high target specificity, immunotherapeutic antibodies, such as TCBs, can lead to T cell-mediated cytotoxicity in healthy tissues. This is due to the scarcity of currently identified antigens specific only to the tumor site (tumor-specific antigens) that are also express across patients. Within commonly targeted cancer proteins (tumor associated antigens), low expression is observed also in non-cancerous tissues [412], [413]. These clinical observations prompted the drug discovery research to shift focus towards development of conditionally active TCBs. Such antibodies are designed to remain inactive, with masked binders, in healthy tissues even in presence of the target antigen. In contrast, upon entering the protease-rich tumor microenvironment, the masks are released, activating the antibody to exert its activity upon binding the target antigen in the tumor [181], [414], [415]. It was hypothesized that addition of protease-dependency to the P323G-Engager platform could further widen its applicability, and increase its safety.

In previously published reports, the protease-cleavable linkers, connecting binder masks were added to the antibody tumor antigen binding sites [414] or immune cell binding sites, such as CD3ε binders [181] or FcγR binders [415]. With aforementioned double universality of the antibody system, an obstacle was encountered that is not applicable to direct antibody approaches. Introducing masks to the tumor binders of the adaptors, or to the immune effector binders of P329G-Engagers, would involve extensive investments for designing separate masks, thereby being contrary to the objectives of resourcefulness and universality. Thus, it was concluded that the optimal site for protease-conditionality in the platform is the P329G-binder. Considering that thus far, the need to conduct new binder generation campaigns was successfully circumvented, it was questioned whether this can be the case for the protease-cleavable masks. Such a goal would entail utilizing a universal, binder-independent type of mask. Generally, currently developed protease-activated therapeutics utilize two main types of masks. First type are affinity based anti-idiotypic [181], [416] or anti-Fc masks [415] which necessitate new development for each binder [417]. Second type is based on steric hindrance of the idiotype [310], [416], [418], conferring advantageous universality in terms of the masked paratope. For the project's purposes, universality was a priority. However, affinity-based masks offer high tunability of binder blockade via K_D control, and retained structural integrity of the original tumor binder [300]. Thus, the aim was to find a mask that allows utilization affinity-based masking, while avoiding the necessity for new mask development.

The sole affinity-based interaction described for the P329G-binder was the P329G mutation in the CH2 domain of the Fc portion of the huIgG1 adaptors. A question occurred if the P329G-mutated CH2 domain, which itself is a part of clinically used molecules such as glofitamab [64], may act as both a mask and a target of the P329G binder. Thus, the affinity of the P329G-binder would be equal to the mask and to the adaptor. Generally, a hypothesis could be made

that unmasking may not be possible even after protease cleavage of the linker, and the adaptor might not outcompete the mask to achieve adaptor-engager binding. However, it is widely known that binding interactions exist in an equilibrium, consisting of a dynamic process of association and dissociation events between the binding partners [419]. Therefore, it was hypothesized that the inherent off-rate of the P329G binder with its P329G-mutated CH2 mask might still allow the P329G-mutated adaptors to access the P329G binder in the P329G-Engager. Hence, for the proof of concept, a protease-dependent pro-P329G-TCB was designed, produced and characterized. The molecule consists of the P329G-TCB with P329G-mutated CH2 domains acting as masks for the P329G binders, connected to the P329G binder via protease-cleavable linkers. The linker sequences were derived from literature describing matriptase-cleavage sites [181]. In line with the binding equilibrium hypothesis, and upon matriptase cleavage, the masks were released and allowed the pro-P329G-TCB to bind the P329G-mutated adaptors. The P329G-mutated CH2 masks were robustly inactivating the P329G binder in absence of matriptase. The pro-P329G-TCB was not only matriptase-dependent and adequately masked, but also enabled targeting of various tumor antigens via interchangeable P329G-mutated adaptors. Hence, the tumor antigen universality of the pro-P329G-TCB was confirmed. After successful proof-of-concept data on the TCB format, the aim was to provide evidence that the P329G-mutated CH2 mask can confer universality to other P329G-Engager modalities. To this end, pro-P329G-ICE molecules were designed and tested, and achieved robust masking, protease dependency and activity with various tumor-targeted adaptors. Hence, the gathered data supports the conclusion that the P329G-mutated CH2 mask can offer conditional protease-dependent activity of the pro-P329G-Engagers, while retaining the double universal character pertaining to both tumor and immune cell antigens. Thus, the P329G platform underwent development from antigen-agnostic CAR-T cell focus, through addition of various immunomodulatory modalities, and finally, with protease conditional activity, for potential minimization of on-target off-tumor effects. Importantly, these unique advantages of this platform are addressing current challenges in drug discovery for cancer immunotherapy, while utilizing solely clinically tested components – adaptors, P329G-binder, immune engaging structures and binder masks. Thus, the platform exhibited cost-effectiveness not only during the course of its development, but also offers resource-saving processes in drug discovery and academic research, via mix-and-match assembly of desired cancer immunotherapeutic.

8.5. Discussion of Chapter 3 – DOTAM-TCB: Universal small molecule-guided hapten- and T cell-bispecific antibodies for cancer immunotherapy

To further explore adaptor-based possibilities explored in this work, beyond P329G-Engagers, it was questioned if different adaptor structures and engager-adaptor binding characteristics can be utilized. A major class of targeted cancer therapeutics, alongside antibodies, are small molecules [330]. These chemical entities are generally used to target intracellular targets, due to their capability of penetrating the cell membrane [330], which is not possible with the use of antibodies that are designed to engage immune cells [420]. Examples of targeted small molecule therapeutics are gefitinib, a tyrosine kinase inhibitor (TKI), inhibiting phosphorylation of the EGFR intracellular domains [421], or lapatinib, a TKI targeting both EGFR and HER2 on the cytoplasmic side [422], [423]. Despite the main focus of small molecules in oncology remains on targeting intracellular pathways, several research groups explored SM ligands to proteins located on the cell membrane, often as a delivery modality for imaging agents or cytotoxic compounds [424], [425], [426], [427], [428]. SM binding generally relies on the presence of the inherent specific three-dimensional structure of its target, namely the existence of a so-called binding pocket, a cavity structure within the protein [429]. The concave shape, as well as the proper size of the binding pocket, enable entry of the SM to the binding site, followed by the formation of multiple bonds between the SM atoms and the receptor amino acids, stabilizing the binding interaction. Due to these requirements for small molecule-protein binding, the range of cell surface targets available for targeting may be narrower than that of antibodies. However, the fact that the epitope requirements for SM ligands and antibodies differ, even when found on the same protein, may be of interest for drug development and its mode of action. For instance, SM occupying the binding pocket of a receptor may inherently block the endogenous ligand or protein partner from activating its receptor (an orthosteric or competitive inhibition) [430], which may be beneficial therapeutically. Moreover, until recently, certain transmembrane receptors, such as GPCRs, often of interest for drug discovery [431], [432], [433], were proving to be difficult to produce in a recombinant, soluble form with a native conformation [434]. Since this is a general requirement for antibody discovery campaigns, like phage display [435], developing many GPCR-targeted antibodies proved challenging in the recent past [434]. On the other hand, many endogenous and synthetic GPCR small molecule ligands have been described [436]. Furthermore, computational design and virtual screening of small molecule ligands, including modified versions of endogenous ligands, exhibits greater reliability than the methods based on antibody-protein computational simulations [437]. The implication of this fact is that both synthetic and endogenous small molecule ligands of many cell surface receptors, including GPCRs, can be repurposed for developing drugs that bind the proteins of interest. Importantly, epitopes and protein conformations unavailable to or with limited binding by antibodies [438], [439], [440] may be targeted with SM, while potentially inhibiting receptor activity in a therapeutically favorable manner [441], [442], [443], [444], [445].

In light of the above, cell surface-binding SM ligands have been gaining interest across several fields of drug development. FOLR1 is a transmembrane receptor with a cell surface-located binding pocket for its endogenous ligand, folate [446], and is overexpressed, among others, in ovarian [447] or breast [448] cancers. FOLR2 is another receptor with folate as the endogenous ligand, and it is expressed in tumor-associated macrophages (TAMs) [449] and other macrophages [450]. Low and colleagues explored targeting FOLR1 or FOLR2 with folate as the delivery moiety for multiple cargos - imaging agents for positron emission tomography (PET) [451], intraoperative imaging [365], [452], [453], and radiotherapy [454]. Sasaki *et al.* utilized folate as a so-called antibody-recruiting molecule (ARM), consisting of folate covalently linked to an Fc-binding peptide for recruitment of antibodies [264]. The ARM modality with other ligands has been explored in-depth by Spiegel group [455], [456], [457], as well as others [356]. Another interesting concept explores for small molecule-guided delivery is the concept of small molecule-drug conjugates, a counterpart to antibody-drug conjugates, which have also been produced with folate as a targeting moiety [458].

Aside from the direct functions of the aforementioned compounds, SM ligands have been also explored as adaptors for effector molecules or cells. Researchers from the Low laboratory developed ligand-FITC adaptors, such as folate-FITC and others, for use with FITC-immunization in mice [459] and humans [357] or anti-FITC CAR-T cells preclinically [240], [460], [461]. Such concept is being also evaluated clinically for osteosarcoma patients (NCT05312411) [462]. Neri and colleagues developed an extensive platform based on anti-FITC CAR-T cells, for use with various FITC-labelled adaptors: antibodies, diabodies, or small molecule ligands to a CAIX transmembrane protein [238]. Furthermore, Stepanov *et al.* expanded the use of such small molecule ligand-FITC conjugates to create adaptors binding covalently to their universal adaptor-dependent CAR-T cell, termed covCAR [243].

While certainly multiple modalities and modes of action have been researched with the context of small molecule-guided delivery, the cancer immunotherapy aspects explored to date have been limited to CAR-T cells. Taking into account the limitations of CAR-T cells mentioned before in this work, a research gap was identified, with small molecule adaptors having potential for use as adaptors antibody-based immune cell engagers. Considering this context, it was decided to explore such SM ligands as adaptors for adaptor-binding universal TCB. Such a system could facilitate higher control of the TCB activity. Since SM have quicker distribution into tissues than antibodies [463], as well as a shorter half-life, administration of an inactive adaptor-binding TCB can be followed by a SM acting as a rapid on-switch. Moreover, SM often have oral bioavailability [463], which is currently not possible for antibodies [464], rendering the on-switch a potential orally administered molecule. Aside from these properties, SM adaptors bound to their universal TCB would create a smaller functional entity, compared to IgG adaptors with adaptor-binding TCB. This could potentially lead to a smaller synaptic distance between a T cell and a target cell, which has been linked to a more efficient synapse formation [465]. Relating to previously discussed properties of SM ligands, SM-based adaptors may also confer enzymatic inhibition of their receptor, alongside mediating T cell-based cytotoxicity against a target cell. Additionally, new ligands for use in the SM-based adaptors can be screened computationally or designed based on endogenous ligands, limiting the resource investment needed for expanding the universal TCB platform.

To use a SM ligand as an adaptor for antibody, the need arose to devise a tag for antibody recognition. In order to retain SM properties of the adaptors, the focus evolved onto conceptualizing small molecule tags, as opposed to protein or peptide ones, to be bound by a tag-specific TCB. Since no CD3 or TCR-engaging small molecules have been described, likely due to the lack of suitable binding pockets in the TCR complex, it was decided to keep and antibody as an effector, T cell-engaging molecule. Small molecule-antibody interactions are known to have exceptional binding properties. Small molecules by themselves, in general, do not produce an immune response [65]. Antibody production against such targets necessitates preparation of the SM combined with a carrier protein, resulting in a formation of a hapten, enabling anti-hapten binder discovery [324]. Interestingly, several hapten-binding antibodies have been developed with highly affine binders [466], [467], [468], [469], [470].

A hypothesis was formed that a hapten would constitute a suitable tag for the adaptors, for use with hapten-specific antibody binding. In line with the previous goals for the P329G platform, the aim was to find a suitable hapten-specific binder that can be repurposed for the hapten-binding TCB. Highly affine hapten-specific antibodies against chelators were developed previously in our laboratory; more specifically DOTAM, loaded with radionuclides [363]. Since for T cell engager-based therapy radiation is undesired due to predicted toxicity towards T cells, the project described here necessitated the use of a non-toxic tag. The described DOTAM-specific antibody has been also confirmed to bind a Ca^{2+}-loaded DOTAM with similar affinity profile. Therefore, the Ca^{2+}-loaded DOTAM was opted for utilization as a tag, covalently linked to the small molecule ligand to the tumor-associated antigen. Additionally, the aforementioned DOTAM binder was repurposed for use in DOTAM- T cell-bispecific antibody, DOTAM-TCB. The clinical antibody glofitamab [64] was used as the basis for the TCB sequence and structure, by swapping the CD20 binders for the DOTAM binders. For the haptenated adaptors, the structures of published SM ligands were opted for, together with covalently linking them to the Ca^{2+}-loaded DOTAM, resulting in novel SM adaptors – Ca-DOTAM-DUPA, Ca-DOTAM-AAZ and Ca-DOTAM-folate.

In this work, it was shown that Ca-DOTAM in the adaptor format was effectively bound with femto- to picomolar affinity by the DOTAM-TCB. Ca-DOTAM-DUPA binding PSMA and Ca-DOTAM-AAZ binding CAIX, combined with universal DOTAM-TCB, initiated T cell-mediated antitumoral cytotoxicity *in vitro*.

The learnings from the P329G-TCB study *in vivo* highlighted a necessity for optimization of both adaptor and the universal TCB dosing in the adaptor systems. Thus, for DOTAM-TCB project, the goal was to broaden the use of the Ca-DOTAM-X adaptors with DOTAM-TCB to include both separate and premixed molecule complex as two therapeutic modalities. Therefore, in addition to enabling separate addition of the haptenated SM adaptor and the hapten-specific DOTAM-TCB with confirmed assembly in the assays *in vitro*, a straightforward protocol was developed for creation of non-covalent complexes of the aforementioned molecules. Formation of the complexes was evaluated *via* native SEC-MS, and determined that non-covalent complexes of a hapten with an antibody likely do not withstand the standard experimental procedure used in native SEC-MS commonly used for therapeutic antibody analysis. Here, it was discovered that the processing parameters - specifically in the

desolvation - fragmentation step, can be modified to improve the recovery of the complex and more robust results reflecting the efficiency of complex formation.

For the *in vivo* proof of concept study, CAIX as the tumor target was elected, and Ca-DOTAM-AAZ with DOTAM-TCB as effector molecules. The Ca-DOTAM-AAZ ligand was based on the structure of FITC-AZA, a CAIX-targeted adaptor for use with FITC-specific CAR-T cells, published by Gu Lee *et al.* from the Low group [240]. In this study, NSG mice bearing subcutaneous MDA-MB-231 tumor cells engineered to express CAIX, underwent tumor shrinkage upon treatment with FITC-AZA and anti-FITC CAR-T cells. The administration regimen was based on a single injection of CAR-T cells, and a dose escalation of the haptenated small molecule adaptor, from 5 nmol/kg to 500 nmol/kg. In this project's study, the dose of 495 nmol/kg (0.45 mg/kg) without dose escalation was selected, which would correspond to 20x the DOTAM-TCB molar concentration. The decision was made based on the plan of injecting the SM adaptor 2h before the TCB injection, allowing for excretion of the adaptor and decreased concentration. Moreover, the target cells used were HT-29, not engineered to overexpress the antigen, but with confirmed intermediate levels of endogenously expressed CAIX. Furthermore, HT-29 cells were used in AZA-guided imaging study in mice [364], which highlighted specificity of the ligand to the CAIX+ HT-29 tumors. A residual signal was present also in the stomach, as well as in the kidneys, which is in line with the renal excretion expected for small molecules and acetazolamide [471]. Due to the fact that full-size antibodies often display limited renal excretion [472], the assumption was made that TCB cytotoxicity in kidneys may be minimal. However, certain toxicity was to be expected from stomach binding of the Ca-DOTAM-AAZ when combined with DOTAM-TCB.

As described in **Chapter 3**, in this project's *in vivo* study, HT-29 tumor-bearing humanized BRGS-CD47 mice treated with either complexed or separately injected Ca-DOTAM-AAZ and DOTAM-TCB (test groups) displayed signs of severe toxicity 3 to 4 days after therapy initiation. Moreover, CAIX-TCB treated mice (positive control groups) showed adverse events, albeit to a smaller extent. This led to a decision to terminate the study immediately. Due to the toxicity observed in both test and positive control groups, but not in DOTAM-TCB group or Ca-DOTAM-AAZ group, it was hypothesized that the toxicity was driven by T cell-mediated killing. It was likely related to non-tumor specific CAIX expression, as evident by mild adverse events in CAIX-TCB group. In mice, CAIX itself has been observed in different levels in healthy tissues such as stomach, colon, and pancreas [473], [474], and other carbonic anhydrases in the murine heart [475] or kidney [476], [477].

Additionally, heightened toxicity upon use of Ca-DOTAM-AAZ-guided TCB, compared to the antibody-based CAIX-TCB, indicated general non-specificity of AAZ, likely binding other targets beyond CAIX. AAZ has been described to bind other human carbonic anhydrases , including CAI [478], CAII [479], [480], CAIV [481], CAVA [482], CAVII [482], CAXII [483], CAXIII [484] or CAXIV [482]. Due to this, acetazolamide is described as a pan-CA inhibitor [482], and cannot be regarded as CAIX-specific. However, in humans, only CAIV, CAIX, CAXII, CAXIV and CAXV are expressed on the cellular membranes, while the other isoforms are located in cytosol , mitochondria or are soluble proteins [485]. Importantly, membrane-bound localization of the CA is required for activity of a TCB like Ca-DOTAM-AAZ combined with DOTAM-TCB.

Additionally, its activity necessitates co-localization of four components: CA expression, T cell infiltration, presence of SM adaptor and presence of IgG-based TCB.

Nonspecificity issues similar to the ones observed with CAIX targeting by AAZ have been described recently for PSMA small molecule ligands structurally related to DUPA, despite being used in the clinics for different modalities [486], [487], [488]. The aforementioned imaging study performed with AAZ-guided fluorophore indeed highlighted AAZ binding in certain tissue areas of concern [364], but the technology used was likely not sufficiently detailed to inform the studies using potent modalities such as TCBs. The study by Gu Lee *et al.* which used FITC-AZA and CAR-T cells, did not report adverse event rates [240]. However, an assumption can be held that the systemic toxicity was likely not strong to the levels of dose-limiting toxicity, since the study continued for more than 30 days. This led to a hypothesis that perhaps dose escalation of FITC-AZA, bearing the same CAIX ligand as us, used by Gu Lee *et al.* [240] was a necessary step to minimize adverse events, and may assist in evaluating binders with nonspecificity issues *in vivo*. Additionally, the results in this work, compared with the aforementioned published study, highlighted the need for caution for translation of CAR-T cell protocols to TCB-based protocols. Retrospectively, even in presence of supporting literature for the specific ligand, the necessity for conducting a smaller toxicity-focused study before initiating efficacy evaluation is acknowledged herein. Another major conclusion drawn from this data, especially when put in context of P329G-TCB and other in-house TCB *in vivo* experiments, is that small molecule-guided TCBs may not be suitable for testing in murine models. Importantly, expression of CAIX outside the tumor, as well as off-target antigens of AAZ may be different between NSG mice and humans. Therefore, human toxicity prediction based on the model used in this study is not suitable, and the grade of adverse events observed may not be similar in humans. Nevertheless, one cannot exclude that haptenated small molecule tumor ligands may generally not be suitable as adaptors for TCBs, unless explicitly shown to be highly specific to their target.

8.6. Limitations

The universal immune cell engager platforms presented in this thesis offer several advantages to the drug discovery and research communities. For instance, simplified mix-and-match characteristics confer possibility to achieve the desired mode of action against a desired target, and cost-effectiveness in terms of off-the-shelf availability and the use of clinically characterized binders. However, the use of universal immunotherapeutic platforms, like the ones described here, is not without obstacles. It was observed that for P329G-Engagers, pro-P329G-TCBs and DOTAM-TCBs, adaptor-based modalities often display less potent antitumoral activity. With notable exceptions of certain targets and adaptors, such as adaptor CEACAM5 IgG with P329G-TCB or Ca-DOTAM-AAZ with DOTAM-TCB used *in vitro*, the use of adaptor-based systems resulted in a loss of potency against a direct antibody control. Therefore, during drug discovery use of herein presented adaptor platforms, one needs to remain cognizant of the fact that the tested efficacy does not accurately reflect the maximal possible efficacy achievable with direct antibodies. Moreover, the level of observed antitumoral activity of the adaptor-based engagers depends on the used molar ratio of the adaptor to the immune cell engager. The optimal ratio, while explored in this work and evident to provide a wide therapeutic window, may need to be determined for specific application, based on the level of antigen expression and immune cell infiltration. One cannot exclude that the mode of action may also influence the optimum of the relative concentrations of the adaptor and immune cell engagers, especially when comparing *trans* and *cis* targeting. In terms of small molecule-based adaptors, aside from above obstacles, reaching sufficient target specificity may prove to be difficult, as described above.

Another challenge necessitating careful consideration for the adaptor-based platforms is the potential use in the clinics. As described before, the adaptor-based anti-P329G CAR-T cell platform that was developed previously found its use in drug screening [244], academic research [248], and as clinical therapeutic modality [489], [490] (NCT05199519, NCT05270928, NCT05266768).

While preclinical and biological research may leverage the available array of P329G-mutated adaptor IgGs to target various antigens in all assays, clinical regulations at present would necessitate conducting separate trials or arms for each adaptor of interest. Consequently, the clinical application of the anti-P329G CAR-T cells was tested in separate trials to assess its activity with two adaptors (NCT05199519, NCT05270928, NCT05266768). This is expected to be the case for antibody-based adaptor platforms, such as P329G-Engager one. Therefore, clinically, mix-and-match principle would not be feasible without the molecules undergoing separate assessment in all desired combinations. Therefore, clinical use of off-the-shelf use and personalization would necessitate substantial investments. However, the continued evaluation of universal anti-P329G CAR-T cells [489], [490] and other adaptor-based cell therapies in clinical trials [225] brings forth evidence of the value these systems can provide. The regulatory requirement of separate evaluations for specific adaptor-engager combinations does not negate value and cost-efficiency of universal immune cell engagers or CAR-T cells. This is due to the fact that the preclinical resources can be focused on in-depth

characterization of one specific CAR construct of immune cell engager format, which are both very complex, while at the same time developing and producing simply-structured adaptors. In the case of the molecules presented here, especially, the clinical basis of the P329G mutation and the binders to the tumor, immune cells and the P329G-mutated Fc itself, could enable resource-effectiveness regardless of the desired application of the universal immune cell engager platform.

8.7. Future perspectives

Altogether, in this thesis, three major platforms were developed and characterized: the universal P329G-Engager platform, the protease-dependent pro-P329G-TCB, and the universal DOTAM-TCB for use with haptenated small molecule adaptors. Future work involving these universal immune cell engagement platforms should focus on evaluating personalization feasibility *ex vivo*. Namely, analysis of patient tumor samples in terms of antigen profile, immune cell vulnerabilities, and protease activity, followed by selection of specific adaptors and engagers, would be of extreme value for the future personalization goals. In CAR-T cell field, it has been shown that combining different tumor-targeting moieties may provide benefits for tumors where antigen loss occurs. For example, dual targeted CAR-T cells binding CD19 with CD22 [491], [492], or CD19 with CD70 have been explored in B cell malignancies [493], where CD19 loss widely occurs upon therapeutic pressure [494]. For multiple myeloma, BCMA- and GPRC5D- dual targeted CAR-T cells have been proposed to tackle BCMA antigen escape and antigen-related relapse [495]. Therefore, in term of *in vivo* studies, concomitant combination of various adaptors with single engager may be of value. Alternatively, using one P329G-Engager with sequential administration of two different adaptors may provide data on the feasibility of tackling the dynamics antigen escape with universal platforms. On the opposite spectrum of dual targeting, clinical studies in DLBCL have shown cases of patient populations resistant to an innate cell engager rituximab, exhibiting high response rates to a TCB glofitamab, targeting the same CD20 antigen [496]. Thus, in context of the universal platforms presented in this work, evaluating various immune cell engagers with a single antigen-binding adaptor, could further expand the applications of adaptor-based platforms and tackle more complex tumor microenvironments. Additionally, solid tumor targeting, coupled with evaluation of protease activity in the tumor microenvironments, ought to be tackled by the use of pro-P329G-TCB. In terms of small molecule-guided Ca-DOTAM-X adaptors, the research should be prioritized on the development of novel, target-specific small molecules, before expanding the adaptor platforms to include other engagers beyond DOTAM-TCB, to reach the universality level similar to the P329G-Engager platform.

8.8. Discussion summary

In this doctoral dissertation, research work is presented, comprising of design and characterization of modular, universal adaptor-based antibody platforms for cancer immunotherapy. Here, the P329G-Engager adaptor platform was developed for use with interchangeable antibody adaptors and antibody immune cell engagers, to create a double universality with respect to the choice of the tumor antigen, as well as the specific immune pathway to be engaged. To the best of available knowledge, this is the first doubly universal platform for cancer immunotherapy, utilizing clinically evaluated components. Moreover, to tackle on-target off-tumor activity, conditionally active universal pro-P329G-TCB was created, containing a universal P329G-based mask. The pro-P329G-TCB remained inactive until undergoing cleavage by matriptase, which is expected in protease-rich tumor microenvironment. Moreover, DOTAM-TCB platform was developed, a hapten- and T cell-bispecific antibody with femto-to-picomolar affinity to exchangeable haptenated small molecule ligands to cell surface-located tumor antigens. For these platforms, the antibody and small molecule structures were designed, the platform components were produced and characterized biochemically. Moreover, various preclinical models were evaluated and provided *in vitro* and *in vivo* preclinical proofs of concept, while uncovering the details of the molecules' modes of action, their opportunities for future use and their potential liabilities. Altogether, the work presented in this thesis provided an in-depth characterization of multiple approaches to universal cancer immunotherapy, spanning a substantial portion of the drug discovery process. The developments described here enable ready-to-use universal platforms for drug discovery or target and biology assessments with omittance of additional costs for creating new direct modalities. Consequently, this work may contribute not only to scientific community evaluating various cancer immunotherapeutics biologically, but also to the research groups involved in designing new cancer drugs and committed to bringing these to cancer patients.

9. References

[1] World Health Organization, "World health statistics 2024: monitoring health for the SDGs, Sustainable Development Goals," 2024. [Online]. Available: https://iris.who.int/bitstream/handle/10665/376869/9789240094703-eng.pdf?

[2] M. Arruebo *et al.*, "Assessment of the evolution of cancer treatment therapies," 2011. doi: 10.3390/cancers3033279.

[3] L. A. Korde *et al.*, "Neoadjuvant Chemotherapy, Endocrine Therapy, and Targeted Therapy for Breast Cancer: ASCO Guideline," *J. Clin. Oncol.*, vol. 39, no. 13, 2021, doi: 10.1200/JCO.20.03399.

[4] M. E. Daly *et al.*, "Management of Stage III Non-Small-Cell Lung Cancer: ASCO Guideline," *J. Clin. Oncol.*, vol. 40, no. 12, 2022, doi: 10.1200/JCO.21.02528.

[5] V. K. Morris *et al.*, "Treatment of Metastatic Colorectal Cancer: ASCO Guideline," *J. Clin. Oncol.*, vol. 41, no. 3, 2023, doi: 10.1200/JCO.22.01690.

[6] K. S. Virgo, R. B. Rumble, and J. Talcott, "Initial Management of Noncastrate Advanced, Recurrent, or Metastatic Prostate Cancer: ASCO Guideline Update," *J. Clin. Oncol.*, vol. 41, no. 20, 2023, doi: 10.1200/JCO.23.00155.

[7] F. Bray *et al.*, "Global cancer statistics 2022: GLOBOCAN estimates of incidence and mortality worldwide for 36 cancers in 185 countries," *CA. Cancer J. Clin.*, vol. 74, no. 3, pp. 229–263, 2024, doi: 10.3322/caac.21834.

[8] M. B. Lustberg, N. M. Kuderer, A. Desai, C. Bergerot, and G. H. Lyman, "Mitigating long-term and delayed adverse events associated with cancer treatment: implications for survivorship," 2023. doi: 10.1038/s41571-023-00776-9.

[9] A. M. Tsimberidou, "Targeted therapy in cancer," *Cancer Chemother. Pharmacol.*, vol. 76, no. 6, pp. 1113–1132, Dec. 2015, doi: 10.1007/S00280-015-2861-1/TABLES/1.

[10] A. C. Begg, F. A. Stewart, and C. Vens, "Strategies to improve radiotherapy with targeted drugs," 2011. doi: 10.1038/nrc3007.

[11] B. Li, H. L. Chan, and P. Chen, "Immune Checkpoint Inhibitors: Basics and Challenges," *Curr. Med. Chem.*, vol. 26, no. 17, 2017, doi: 10.2174/0929867324666170804143706.

[12] P. Darvin, S. M. Toor, V. Sasidharan Nair, and E. Elkord, "Immune checkpoint inhibitors: recent progress and potential biomarkers," 2018. doi: 10.1038/s12276-018-0191-1.

[13] L. Barrueto, F. Caminero, L. Cash, C. Makris, P. Lamichhane, and R. R. Deshmukh, "Resistance to Checkpoint Inhibition in Cancer Immunotherapy," 2020. doi: 10.1016/j.tranon.2019.12.010.

[14] B. Melosky *et al.*, "Prolonging Survival: The Role of Immune Checkpoint Inhibitors in the Treatment of Extensive-Stage Small Cell Lung Cancer," *Oncologist*, vol. 25, no. 11, 2020, doi: 10.1634/theoncologist.2020-0193.

[15] F. Petrelli *et al.*, "Immune-related Adverse Events and Survival in Solid Tumors Treated with Immune Checkpoint Inhibitors: A Systematic Review and Meta-Analysis," 2020. doi: 10.1097/CJI.0000000000000300.

[16] The Nobel Assembly at Karolinska Institutet, "The Nobel Prize in Physiology or Medicine 2018 - Press Release." Accessed: Aug. 15, 2024. [Online]. Available: https://www.nobelprize.org/prizes/medicine/2018/press-release/

[17] A. D. Waldman, J. M. Fritz, and M. J. Lenardo, "A guide to cancer immunotherapy: from T cell basic science to clinical practice," Nov. 01, 2020, *Nature Research*. doi: 10.1038/s41577-020-0306-5.

[18] Y. Wang, M. Wang, H. X. Wu, and R. H. Xu, "Advancing to the era of cancer immunotherapy," 2021. doi: 10.1002/cac2.12178.

[19] D. S. Chen and I. Mellman, "Oncology meets immunology: The cancer-immunity cycle," 2013. doi: 10.1016/j.immuni.2013.07.012.

[20] I. Mellman, D. S. Chen, T. Powles, and S. J. Turley, "The cancer-immunity cycle: Indication, genotype, and immunotype," Oct. 10, 2023, *Cell Press*. doi: 10.1016/j.immuni.2023.09.011.

[21] B. Cózar, M. Greppi, S. Carpentier, E. Narni-Mancinelli, L. Chiossone, and E. Vivier, "Tumor-infiltrating natural killer cells," 2021. doi: 10.1158/2159-8290.CD-20-0655.

[22] P. Berraondo *et al.*, "Cytokines in clinical cancer immunotherapy," 2019. doi: 10.1038/s41416-018-0328-y.

[23] P. Sharma *et al.*, "Immune checkpoint therapy—current perspectives and future directions," Apr. 13, 2023, *Elsevier B.V.* doi: 10.1016/j.cell.2023.03.006.

[24] A. Fenis, O. Demaria, L. Gauthier, E. Vivier, and E. Narni-Mancinelli, "New immune cell engagers for cancer immunotherapy," 2024, *Nature Research*. doi: 10.1038/s41577-023-00982-7.

[25] M. E. Goebeler and R. C. Bargou, "T cell-engaging therapies — BiTEs and beyond," Jul. 01, 2020, *Nature Research*. doi: 10.1038/s41571-020-0347-5.

[26] D. Nandi *et al.*, "T cell costimulation, checkpoint inhibitors and anti-tumor therapy," 2020. doi: 10.1007/s12038-020-0020-2.

[27] O. K. Dagher and A. D. Posey, "Forks in the road for CAR T and CAR NK cell cancer therapies," Dec. 01, 2023, *Nature Research*. doi: 10.1038/s41590-023-01659-y.

[28] S. Y. van der Zanden, J. J. Luimstra, J. Neefjes, J. Borst, and H. Ovaa, "Opportunities for Small Molecules in Cancer Immunotherapy," 2020. doi: 10.1016/j.it.2020.04.004.

[29] M. Zhang, X. Dai, Y. Xiang, L. Xie, M. Sun, and J. Shi, "Advances in CD73 inhibitors for immunotherapy:

Antibodies, synthetic small molecule compounds, and natural compounds," 2023. doi: 10.1016/j.ejmech.2023.115546.

[30] C. Zwergel, R. Fioravanti, and A. Mai, "PD-L1 small-molecule modulators: A new hope in epigenetic-based multidrug cancer therapy?," 2023. doi: 10.1016/j.drudis.2022.103435.

[31] A. Tapia-Galisteo, M. Compte, L. Álvarez-Vallina, and L. Sanz, "When three is not a crowd: trispecific antibodies for enhanced cancer immunotherapy," 2023, *Ivyspring International Publisher*. doi: 10.7150/thno.81494.

[32] L. Liu and J. Chen, "Therapeutic antibodies for precise cancer immunotherapy: Current and future perspectives," Dec. 01, 2022, *Walter de Gruyter GmbH*. doi: 10.1515/mr-2022-0033.

[33] X. Guo, Y. Wu, Y. Xue, N. Xie, and G. Shen, "Revolutionizing cancer immunotherapy: unleashing the potential of bispecific antibodies for targeted treatment," 2023, *Frontiers Media SA*. doi: 10.3389/fimmu.2023.1291836.

[34] M. Surowka and C. Klein, "A pivotal decade for bispecific antibodies?," *MAbs*, vol. 16, no. 1, 2024, doi: 10.1080/19420862.2024.2321635.

[35] S. M. Cheal, S. K. Chung, B. A. Vaughn, N. K. V. Cheung, and S. M. Larson, "Pretargeting: A Path Forward for Radioimmunotherapy," 2022. doi: 10.2967/jnumed.121.262186.

[36] H. Goto, Y. Shiraishi, and S. Okada, "Recent preclinical and clinical advances in radioimmunotherapy for non-Hodgkin's lymphoma," 2024. doi: 10.37349/etat.2024.00213.

[37] M. J. Lin *et al.*, "Cancer vaccines: the next immunotherapy frontier," Aug. 01, 2022, *Nature Research*. doi: 10.1038/s43018-022-00418-6.

[38] K. Kirtane, H. Elmariah, C. H. Chung, and D. Abate-Daga, "Adoptive cellular therapy in solid tumor malignancies: Review of the literature and challenges ahead," 2021. doi: 10.1136/jitc-2021-002723.

[39] C. Liu, M. Yang, D. Zhang, M. Chen, and D. Zhu, "Clinical cancer immunotherapy: Current progress and prospects," 2022. doi: 10.3389/fimmu.2022.961805.

[40] S. Zhou, M. Liu, F. Ren, X. Meng, and J. Yu, "The landscape of bispecific T cell engager in cancer treatment," Dec. 01, 2021, *BioMed Central Ltd*. doi: 10.1186/s40364-021-00294-9.

[41] M. Subklewe, "BiTEs better than CAR T cells," *Blood Adv.*, vol. 5, no. 2, pp. 607–612, Jan. 2021, doi: 10.1182/bloodadvances.2020001792.

[42] S. C. Wei, C. R. Duffy, and J. P. Allison, "Fundamental mechanisms of immune checkpoint blockade therapy," 2018. doi: 10.1158/2159-8290.CD-18-0367.

[43] U. D. Staerz, O. Kanagawa, and M. J. Bevan, "Hybrid antibodies can target sites for attack by T cells," *Nature*, vol. 314, no. 6012, 1985, doi: 10.1038/314628a0.

[44] M. E. Goebeler and R. C. Bargou, "T cell-engaging therapies — BiTEs and beyond," 2020. doi: 10.1038/s41571-020-0347-5.

[45] T. Arvedson, J. M. Bailis, T. Urbig, and J. L. Stevens, "Considerations for design, manufacture, and delivery for effective and safe T-cell engager therapies," 2022. doi: 10.1016/j.copbio.2022.102799.

[46] D. Nagorsen, P. Kufer, P. A. Baeuerle, and R. Bargou, "Blinatumomab: A historical perspective," Dec. 2012. doi: 10.1016/j.pharmthera.2012.07.013.

[47] M. Bacac *et al.*, "A novel carcinoembryonic antigen T-cell bispecific antibody (CEA TCB) for the treatment of solid tumors," *Clin. Cancer Res.*, vol. 22, no. 13, pp. 3286–3297, 2016, doi: 10.1158/1078-0432.CCR-15-1696.

[48] I. R. Ruiz *et al.*, "P95HER2–T cell bispecific antibody for breast cancer treatment," *Sci. Transl. Med.*, vol. 10, no. 461, Oct. 2018, doi: 10.1126/SCITRANSLMED.AAT1445.

[49] A. Minson and M. Dickinson, "Glofitamab CD20-TCB bispecific antibody," *Leuk. Lymphoma*, vol. 62, no. 13, pp. 3098–3108, 2021, doi: 10.1080/10428194.2021.1953016.

[50] U. Brinkmann and R. E. Kontermann, "The making of bispecific antibodies," Feb. 17, 2017, *Taylor and Francis Inc.* doi: 10.1080/19420862.2016.1268307.

[51] J. F. P. Dixon, J. L. Law, and J. J. Favero, "Activation of human T lymphocytes by crosslinking of anti-CD3 monoclonal antibodies," *J. Leukoc. Biol.*, vol. 46, no. 3, 1989, doi: 10.1002/jlb.46.3.214.

[52] S. Ferrini *et al.*, "Targeting of T lymphocytes against egf-receptor+ tumor cells by bispecific monoclonal antibodies: Requirement of CD3 molecule cross-linking for t-cell activation," *Int. J. Cancer*, vol. 55, no. 6, 1993, doi: 10.1002/ijc.2910550610.

[53] P. M. Anderson, W. Crist, D. Hasz, A. J. Carroll, D. E. Myers, and F. M. Uckun, "G19.4(αCD3) × B43(αCD19) monoclonal antibody heteroconjugate triggers CD19 antigen-specific lysis of t(4;11) acute lymphoblastic leukemia cells by activated CD3 antigen-positive cytotoxic T cells," *Blood*, vol. 80, no. 11, 1992, doi: 10.1182/blood.v80.11.2826.bloodjournal80112826.

[54] H. Bohlen *et al.*, "Lysis of malignant B cells from patients with B-chronic lymphocytic leukemia by autologous T cells activated with CD3 X CD19 bispecific antibodies in combination with bivalent CD28 antibodies," *Blood*, vol. 82, no. 6, 1993, doi: 10.1182/blood.v82.6.1803.bloodjournal8261803.

[55] M. Mack, G. Riethmüller, and P. Kufer, "A small bispecific antibody construct expressed as a functional single-chain molecule with high tumor cell cytotoxicity," *Proc. Natl. Acad. Sci. U. S. A.*, vol. 92, no. 15, 1995, doi: 10.1073/pnas.92.15.7021.

[56] R. Zeidler *et al.*, "Simultaneous Activation of T Cells and Accessory Cells by a New Class of Intact Bispecific Antibody Results in Efficient Tumor Cell Killing," *J. Immunol.*, vol. 163, no. 3, 1999, doi: 10.4049/jimmunol.163.3.1246.

[57] D. Seimetz, H. Lindhofer, and C. Bokemeyer, "Development and approval of the trifunctional antibody catumaxomab (anti-EpCAM×anti-CD3) as a targeted cancer immunotherapy," 2010. doi: 10.1016/j.ctrv.2010.03.001.

[58] P. Ruf, H. W. Bauer, A. Schoberth, C. Kellermann, and H. Lindhofer, "First time intravesically administered

trifunctional antibody catumaxomab in patients with recurrent non-muscle invasive bladder cancer indicates high tolerability and local immunological activity," *Cancer Immunol. Immunother.*, vol. 70, no. 9, pp. 2727–2735, Sep. 2021, doi: 10.1007/s00262-021-02930-7.

[59] C. QI *et al.*, "Global multi-center phase I trial of the intraperitoneal infusion of anti-EpCAM x anti-CD3 bispecific antibody catumaxomab for advanced gastric carcinoma with peritoneal metastasis.," *J. Clin. Oncol.*, vol. 40, no. 16_suppl, 2022, doi: 10.1200/jco.2022.40.16_suppl.e16102.

[60] A. Löffler *et al.*, "A recombinant bispecific single-chain antibody, CD19 x CD3, induces rapid and high lymphoma-directed cytotoxicity by unstimulated T lymphocytes," *Blood*, vol. 95, no. 6, 2000, doi: 10.1182/blood.v95.6.2098.

[61] M. Sanford, "Blinatumomab: First global approval," *Drugs*, vol. 75, no. 3, 2015, doi: 10.1007/s40265-015-0356-3.

[62] U.S. Food and Drug Administration, "BLA 761344 Accelerated Approval Letter," May 2024. Accessed: Aug. 15, 2024. [Online]. Available: https://www.accessdata.fda.gov/drugsatfda_docs/appletter/2024/761344Orig1s000ltr.pdf

[63] M. Shirley, "Glofitamab: First Approval," *Drugs*, vol. 83, no. 10, pp. 935–941, Jul. 2023, doi: 10.1007/s40265-023-01894-5.

[64] M. Bacac *et al.*, "CD20-TCB with obinutuzumab pretreatment as next-generation treatment of hematologic malignancies," *Clin. Cancer Res.*, 2018, doi: 10.1158/1078-0432.CCR-18-0455.

[65] K. Murphy and C. Weaver, *Immunobiology 9th edition*. 2017.

[66] C. Klein, U. Brinkmann, J. M. Reichert, and R. E. Kontermann, "The present and future of bispecific antibodies for cancer therapy," 2024. doi: 10.1038/s41573-024-00896-6.

[67] S. Crescioli, H. Kaplon, A. Chenoweth, L. Wang, J. Visweswaraiah, and J. M. Reichert, "Antibodies to watch in 2024," *MAbs*, vol. 16, no. 1, 2024, doi: 10.1080/19420862.2023.2297450.

[68] J. Yu, Y. Song, and W. Tian, "How to select IgG subclasses in developing anti-tumor therapeutic antibodies," 2020. doi: 10.1186/s13045-020-00876-4.

[69] G. Scapin *et al.*, "Structure of full-length human anti-PD1 therapeutic IgG4 antibody pembrolizumab," *Nat. Struct. Mol. Biol.*, 2015, doi: 10.1038/nsmb.3129.

[70] M. Bacac *et al.*, "CD20-TCB with obinutuzumab pretreatment as next-generation treatment of hematologic malignancies," *Clin. Cancer Res.*, vol. 24, no. 19, pp. 4785–4797, Oct. 2018, doi: 10.1158/1078-0432.CCR-18-0455.

[71] G. Vauquelin and S. J. Charlton, "Exploring avidity: Understanding the potential gains in functional affinity and target residence time of bivalent and heterobivalent ligands," *Br. J. Pharmacol.*, 2013, doi: 10.1111/bph.12106.

[72] D. Ellerman, "Bispecific T-cell engagers: Towards understanding variables influencing the in vitro potency and tumor selectivity and their modulation to enhance their efficacy and safety," *Methods*, vol. 154, pp. 102–117, Feb. 2019, doi: 10.1016/j.ymeth.2018.10.026.

[73] M. Bacac *et al.*, "A novel carcinoembryonic antigen T-cell bispecific antibody (CEA TCB) for the treatment of solid tumors," *Clin. Cancer Res.*, vol. 22, no. 13, pp. 3286–3297, Jul. 2016, doi: 10.1158/1078-0432.CCR-15-1696.

[74] Y. Mazor *et al.*, "Insights into the molecular basis of a bispecific antibody's target selectivity," *MAbs*, vol. 7, no. 3, 2015, doi: 10.1080/19420862.2015.1022695.

[75] S. J. Kerns *et al.*, "Human immunocompetent organ-on-chip platforms allow safety profiling of tumor-targeted t-cell bispecific antibodies," *Elife*, vol. 10, Aug. 2021, doi: 10.7554/eLife.67106.

[76] A. H. Laustsen, V. Greiff, A. Karatt-Vellatt, S. Muyldermans, and T. P. Jenkins, "Animal Immunization, in Vitro Display Technologies, and Machine Learning for Antibody Discovery," 2021. doi: 10.1016/j.tibtech.2021.03.003.

[77] R. W. Schroff, K. A. Foon, S. M. Beatty, R. K. Oldham, and A. C. Morgan, "Human Anti-Murine Immunoglobulin Responses in Patients Receiving Monoclonal Antibody Therapy," *Cancer Res.*, vol. 45, no. 2, 1985.

[78] P. Tan, D. A. Mitchell, T. N. Buss, M. A. Holmes, C. Anasetti, and J. Foote, "'Superhumanized' Antibodies: Reduction of Immunogenic Potential by Complementarity-Determining Region Grafting with Human Germline Sequences: Application to an Anti-CD28," *J. Immunol.*, vol. 169, no. 2, 2002, doi: 10.4049/jimmunol.169.2.1119.

[79] H. Waldmann, "Human monoclonal antibodies: The benefits of humanization," in *Methods in Molecular Biology*, vol. 1904, 2019. doi: 10.1007/978-1-4939-8958-4_1.

[80] R. Huber, J. Deisenhofer, P. M. Colman, M. Matsushima, and W. Palm, "Crystallographic structure studies of an IgG molecule and an Fc fragment," *Nature*, vol. 264, no. 5585, 1976, doi: 10.1038/264415a0.

[81] M. J. Feige *et al.*, "An Unfolded CH1 Domain Controls the Assembly and Secretion of IgG Antibodies," *Mol. Cell*, vol. 34, no. 5, 2009, doi: 10.1016/j.molcel.2009.04.028.

[82] C. R. Kaloff and I. G. Haas, "Coordination of immunoglobulin chain folding and immunoglobulin chain assembly is essential for the formation of functional IgG," *Immunity*, vol. 2, no. 6, 1995, doi: 10.1016/1074-7613(95)90007-1.

[83] R. Sitia, "Assembly and Function of Immunoglobulins During B Cell Development. From Basic Immunology to Immune-Mediated Demyelination," G. Martino and L. Adorini, Eds., Milano: Springer Milan, 1999, pp. 16–25. doi: 10.1007/978-88-470-2143-3_3.

[84] B. Tihanyi and L. Nyitray, "Recent advances in CHO cell line development for recombinant protein production," 2020. doi: 10.1016/j.ddtec.2021.02.003.

[85] M. R. Suresh, A. C. Cuello, and C. Milstein, "Bispecific monoclonal antibodies from hybrid hybridomas,"

Methods Enzymol., vol. 121, no. C, 1986, doi: 10.1016/0076-6879(86)21019-8.

[86] A. M. Merchant *et al.*, "An efficient route to human bispecific IgG," *Nat. Biotechnol.*, 1998, doi: 10.1038/nbt0798-677.

[87] J. T. Regula *et al.*, "Variable heavy-variable light domain and Fab-arm CrossMabs with charged residue exchanges to enforce correct light chain assembly," *Protein Eng. Des. Sel.*, vol. 31, no. 7–8, pp. 289–299, Jul. 2018, doi: 10.1093/protein/gzy021.

[88] M. Grote, A. K. Haas, C. Klein, W. Schaefer, and U. Brinkmann, "Bispecific antibody derivatives based on full-length IgG formats," *Methods Mol. Biol.*, 2012, doi: 10.1007/978-1-61779-931-0_16.

[89] W. Schaefer *et al.*, "Immunoglobulin domain crossover as a generic approach for the production of bispecific IgG antibodies," *Proc. Natl. Acad. Sci. U. S. A.*, vol. 108, no. 27, pp. 11187–11192, Jul. 2011, doi: 10.1073/pnas.1019002108.

[90] M. Surowka, W. Schaefer, and C. Klein, "Ten years in the making: application of CrossMab technology for the development of therapeutic bispecific antibodies and antibody fusion proteins," 2021. doi: 10.1080/19420862.2021.1967714.

[91] A. Morell, W. D. Terry, and T. A. Waldmann, "Metabolic properties of IgG subclasses in man.," *J. Clin. Invest.*, 1970, doi: 10.1172/JCI106279.

[92] A. Trivedi *et al.*, "Clinical Pharmacology and Translational Aspects of Bispecific Antibodies," 2017. doi: 10.1111/cts.12459.

[93] J. Fan *et al.*, "Predicting Elimination of Small-Molecule Drug Half-Life in Pharmacokinetics Using Ensemble and Consensus Machine Learning Methods," *J. Chem. Inf. Model.*, vol. 64, no. 8, pp. 3080–3092, Apr. 2024, doi: 10.1021/ACS.JCIM.3C02030.

[94] U. H. Weidle, R. E. Kontermann, and U. Brinkmann, "Tumor-antigen-binding bispecific antibodies for cancer treatment," *Semin. Oncol.*, 2014, doi: 10.1053/j.seminoncol.2014.08.004.

[95] R. E. Kontermann, "Strategies to extend plasma half-lives of recombinant antibodies," 2009. doi: 10.2165/00063030-200923020-00003.

[96] D. K. Challa, R. Velmurugan, R. J. Ober, and E. S. Ward, "FcRn: From molecular interactions to regulation of IgG pharmacokinetics and functions," 2014. doi: 10.1007/978-3-319-07911-0_12.

[97] E. S. Ward, S. C. Devanaboyina, and R. J. Ober, "Targeting FcRn for the modulation of antibody dynamics," 2015. doi: 10.1016/j.molimm.2015.02.007.

[98] C. A. Portell, C. M. Wenzell, and A. S. Advani, "Clinical and pharmacologic aspects of blinatumomab in the treatment of B-cell acute lymphoblastic leukemia," 2013. doi: 10.2147/CPAA.S42689.

[99] G. Lorenczewski *et al.*, "Generation of a Half-Life Extended Anti-CD19 BiTE® Antibody Construct Compatible with Once-Weekly Dosing for Treatment of CD19-Positive Malignancies," *Blood*, vol. 130, no. Supplement 1, 2017.

[100] T. L. Arvedson *et al.*, "Abstract 55: Generation of half-life extended anti-CD33 BiTE® antibody constructs compatible with once-weekly dosing," *Cancer Res.*, vol. 77, no. 13_Supplement, 2017, doi: 10.1158/1538-7445.am2017-55.

[101] K. M. Knudsen Sand, M. Bern, J. Nilsen, H. T. Noordzij, I. Sandlie, and J. T. Andersen, "Unraveling the interaction between FcRn and albumin: Opportunities for design of albumin-based therapeutics," 2015. doi: 10.3389/fimmu.2014.00682.

[102] J. Tabernero, P. Pfeiffer, and A. Cervantes, "Administration of Cetuximab Every 2 Weeks in the Treatment of Metastatic Colorectal Cancer: An Effective, More Convenient Alternative to Weekly Administration?," *Oncologist*, vol. 13, no. 2, 2008, doi: 10.1634/theoncologist.2007-0201.

[103] J. Zalevsky *et al.*, "Enhanced antibody half-life improves in vivo activity," *Nat. Biotechnol.*, vol. 28, no. 2, pp. 157–159, Feb. 2010, doi: 10.1038/nbt.1601.

[104] P. Deegen *et al.*, "The PSMA-targeting half-life extended BiTE therapy AMG 160 has potent antitumor activity in preclinical models of metastatic castration-resistant prostate cancer," *Clin. Cancer Res.*, vol. 27, no. 10, pp. 2928–2937, May 2021, doi: 10.1158/1078-0432.CCR-20-3725.

[105] O. A. Mandrup *et al.*, "Programmable half-life and anti-tumour effects of bispecific T-cell engager-albumin fusions with tuned FcRn affinity," *Commun. Biol.*, vol. 4, no. 1, p. 310, Mar. 2021, doi: 10.1038/s42003-021-01790-2.

[106] K. A. Meetze *et al.*, "1024 CLN-978, a novel CD19/CD3/HSA T cell engager with extended serum half-life, is effective against lymphoma cells expressing very low levels of CD19," 2023. doi: 10.1136/jitc-2023-sitc2023.1024.

[107] D. Snell *et al.*, "Abstract 2276: Preclinical development and mechanism of action studies of NM21-1480, a PD-L1/4-1BB/HSA trispecific MATCH3 therapeutic clinical candidate," *Cancer Res.*, vol. 80, no. 16_Supplement, 2020, doi: 10.1158/1538-7445.am2020-2276.

[108] H. Einsele *et al.*, "The BiTE (bispecific T-cell engager) platform: Development and future potential of a targeted immuno-oncology therapy across tumor types," Jul. 15, 2020, *John Wiley and Sons Inc.* doi: 10.1002/cncr.32909.

[109] G. Vidarsson, G. Dekkers, and T. Rispens, "IgG subclasses and allotypes: From structure to effector functions," *Front. Immunol.*, vol. 5, no. OCT, 2014, doi: 10.3389/fimmu.2014.00520.

[110] A. Awasthi *et al.*, "Obinutuzumab (GA101) compared to rituximab significantly enhances cell death and antibody-dependent cytotoxicity and improves overall survival against CD20+ rituximab-sensitive/-resistant Burkitt lymphoma (BL) and precursor B-acute lymphoblastic leukaemia (pre-B-ALL): Potential targeted therapy in patients with poor risk CD20+ BL and pre-B-ALL," *Br. J. Haematol.*, vol. 171, no. 5, 2015, doi: 10.1111/bjh.13764.

[111] D. Nagorsen, R. Bargou, D. Rüttinger, P. Kufer, P. A. Baeuerle, and G. Zugmaier, "Immunotherapy of lymphoma and leukemia with T-cell engaging BiTE antibody blinatumomab," 2009. doi: 10.1080/10428190902943077.

[112] W. R. Strohl, "Optimization of Fc-mediated effector

functions of monoclonal antibodies," 2009. doi: 10.1016/j.copbio.2009.10.011.

[113] S. D. Gillies, V. Lan, K. M. Lo, M. Super, and J. Wesolowski, "Improving the efficacy of antibody-interleukin 2 fusion proteins by reducing their interaction with Fc receptors," *Cancer Res.*, 1999.

[114] J. D. Isaacs, M. G. Wing, J. D. Greenwood, B. L. Hazleman, G. Hale, and H. Waldmann, "A therapeutic human IgG4 monoclonal antibody that depletes target cells in humans," *Clin. Exp. Immunol.*, 1996, doi: 10.1046/j.1365-2249.1996.d01-876.x.

[115] A. Tamm and R. E. Schmidt, "IgG binding sites on human Fcγ receptors," *Int. Rev. Immunol.*, vol. 16, no. 1–2, pp. 57–85, 1997, doi: 10.3109/08830189709045703.

[116] J. Lund *et al.*, "Multiple binding sites on the CH2 domain of IgG for mouse FcγR11," *Mol. Immunol.*, vol. 29, no. 1, pp. 53–59, 1992, doi: 10.1016/0161-5890(92)90156-R.

[117] T. Schlothauer *et al.*, "Novel human IgG1 and IgG4 Fc-engineered antibodies with completely abolished immune effector functions," *Protein Eng. Des. Sel.*, vol. 29, no. 10, pp. 457–466, Oct. 2016, doi: 10.1093/protein/gzw040.

[118] P. Sondermann, R. Huber, V. Oosthulzen, and U. Jacob, "The 3.2-A crystal structure of the human IgG1 Fc fragment-Fc gammaRIII complex," *Nature*, vol. 406, no. 6793, pp. 267–273, Jul. 2000, doi: 10.1038/35018508.

[119] N. Shimasaki, A. Jain, and D. Campana, "NK cells for cancer immunotherapy," Mar. 01, 2020, *Nature Research*. doi: 10.1038/s41573-019-0052-1.

[120] O. Demaria, L. Gauthier, G. Debroas, and E. Vivier, "Natural killer cell engagers in cancer immunotherapy: Next generation of immuno-oncology treatments," Aug. 01, 2021, *John Wiley and Sons Inc*. doi: 10.1002/eji.202048953.

[121] M. Zhang, K. P. Lam, and S. Xu, "Natural Killer Cell Engagers (NKCEs): a new frontier in cancer immunotherapy," 2023, *Frontiers Media SA*. doi: 10.3389/fimmu.2023.1207276.

[122] S. Wingert *et al.*, "Preclinical evaluation of AFM24, a novel CD16A-specific innate immune cell engager targeting EGFR-positive tumors," *MAbs*, vol. 13, no. 1, 2021, doi: 10.1080/19420862.2021.1950264.

[123] S. Kakiuchi-Kiyota *et al.*, "A BCMA/CD16A bispecific innate cell engager for the treatment of multiple myeloma," *Leukemia*, vol. 36, no. 4, pp. 1006–1014, Apr. 2022, doi: 10.1038/s41375-021-01478-w.

[124] P. McLaughlin *et al.*, "Rituximab chimeric anti-CD20 monoclonal antibody therapy for relapsed indolent lymphoma: Half of patients respond to a four-dose treatment program," *J. Clin. Oncol.*, 1998, doi: 10.1200/JCO.1998.16.8.2825.

[125] U. Storz, "Rituximab: How approval history is reflected by a corresponding patent filing strategy," 2014. doi: 10.4161/mabs.29105.

[126] H. Tilly *et al.*, "Diffuse large B-cell lymphoma (DLBCL): ESMO Clinical Practice Guidelines for diagnosis, treatment and follow-up," *Ann. Oncol.*, vol. 26, 2015, doi: 10.1093/annonc/mdv304.

[127] K. Tobinai, C. Klein, N. Oya, and G. Fingerle-Rowson, "A Review of Obinutuzumab (GA101), a Novel Type II Anti-CD20 Monoclonal Antibody, for the Treatment of Patients with B-Cell Malignancies," 2017. doi: 10.1007/s12325-016-0451-1.

[128] J. Baselga, "Clinical trials of Herceptin® (trastuzumab)," *Eur. J. Cancer*, vol. 37, no. SUPPL. 1, 2001, doi: 10.1016/s0959-8049(00)00404-4.

[129] O. Metzger-Filho, E. P. Winer, and I. Krop, "Pertuzumab: Optimizing HER2 blockade," *Clin. Cancer Res.*, vol. 19, no. 20, 2013, doi: 10.1158/1078-0432.CCR-13-0518.

[130] T. R. Simpson *et al.*, "Fc-dependent depletion of tumor-infiltrating regulatory T cells co-defines the efficacy of anti–CTLA-4 therapy against melanoma," *J. Exp. Med.*, 2013, doi: 10.1084/jem.20130579.

[131] B. M. Lax *et al.*, "Both intratumoral regulatory T cell depletion and CTLA-4 antagonism are required for maximum efficacy of anti-CTLA-4 antibodies," *Proc. Natl. Acad. Sci. U. S. A.*, vol. 120, no. 31, 2023, doi: 10.1073/pnas.2300895120.

[132] J. R. Ingram *et al.*, "Anti-CTLA-4 therapy requires an Fc domain for efficacy," *Proc. Natl. Acad. Sci. U. S. A.*, vol. 115, no. 15, 2018, doi: 10.1073/pnas.1801524115.

[133] F. A. Vargas *et al.*, "Fc Effector Function Contributes to the Activity of Human Anti-CTLA-4 Antibodies," *Cancer Cell*, vol. 33, no. 4, 2018, doi: 10.1016/j.ccell.2018.02.010.

[134] G. M. Konjević, A. M. Vuletić, K. M. Mirjačić Martinović, A. K. Larsen, and V. B. Jurišić, "The role of cytokines in the regulation of NK cells in the tumor environment," 2019. doi: 10.1016/j.cyto.2019.02.001.

[135] N. Lamers-Kok *et al.*, "Natural killer cells in clinical development as non-engineered, engineered, and combination therapies," 2022. doi: 10.1186/s13045-022-01382-5.

[136] N. Tumino *et al.*, "The tumor microenvironment drives NK cell metabolic dysfunction leading to impaired antitumor activity," *Int. J. Cancer*, vol. 152, no. 8, 2023, doi: 10.1002/ijc.34389.

[137] L. Riggan, S. Shah, and T. E. O'Sullivan, "Arrested development: suppression of NK cell function in the tumor microenvironment," 2021. doi: 10.1002/cti2.1238.

[138] E. Vivier, L. Rebuffet, E. Narni-Mancinelli, S. Cornen, R. Y. Igarashi, and V. R. Fantin, "Natural killer cell therapies," 2024. doi: 10.1038/s41586-023-06945-1.

[139] J. W. Mier and R. C. Gallo, "Purification and some characteristics of human T-cell growth factor from phytohemagglutinin-stimulated lymphocyte-conditioned media," *Proc. Natl. Acad. Sci. U. S. A.*, 1980, doi: 10.1073/pnas.77.10.6134.

[140] D. A. Morgan, F. W. Ruscetti, and R. Gallo, "Selective in vitro growth of T lymphocytes from normal human bone marrows," *Science (80-.).*, 1976, doi: 10.1126/science.181845.

[141] G. Fyfe, R. I. Fisher, S. A. Rosenberg, M. Sznol, D. R. Parkinson, and A. C. Louie, "Results of treatment of 255 patients with metastatic renal cell carcinoma who received high-dose recombinant interleukin-2

therapy," *J. Clin. Oncol.*, 1995, doi: 10.1200/JCO.1995.13.3.688.

[142] M. B. Atkins *et al.*, "High-dose recombinant interleukin 2 therapy for patients with metastatic melanoma: Analysis of 270 patients treated between 1985 and 1993," *J. Clin. Oncol.*, 1999, doi: 10.1200/jco.1999.17.7.2105.

[143] M. Ahmadzadeh and S. A. Rosenberg, "IL-2 administration increases CD4+CD25hi Foxp3 + regulatory T cells in cancer patients," *Blood*, vol. 107, no. 6, 2006, doi: 10.1182/blood-2005-06-2399.

[144] R. Baluna and E. S. Vitetta, "Vascular leak syndrome: A side effect of immunotherapy," 1997. doi: 10.1016/S0162-3109(97)00041-6.

[145] G. H. Jeong *et al.*, "Incidence of capillary leak syndrome as an adverse effect of drugs in cancer patients: A systematic review and meta-analysis," 2019. doi: 10.3390/jcm8020143.

[146] R. Hernandez, J. Põder, K. M. LaPorte, and T. R. Malek, "Engineering IL-2 for immunotherapy of autoimmunity and cancer," Oct. 01, 2022, *Nature Research*. doi: 10.1038/s41577-022-00680-w.

[147] T. A. Waldmann, "The biology of interleukin-2 and interleukin-15: Implications for cancer therapy and vaccine design," 2006. doi: 10.1038/nri1901.

[148] O. Boyman and J. Sprent, "The role of interleukin-2 during homeostasis and activation of the immune system," Mar. 2012. doi: 10.1038/nri3156.

[149] O. Boyman, C. Krieg, D. Homann, and J. Sprent, "Homeostatic maintenance of T cells and natural killer cells," 2012. doi: 10.1007/s00018-012-0968-7.

[150] T. Barthlott *et al.*, "CD25+CD4+ T cells compete with naive CD4+ T cells for IL-2 and exploit it for the induction of IL-10 production," *Int. Immunol.*, vol. 17, no. 3, 2005, doi: 10.1093/intimm/dxh207.

[151] A. Sharabi, M. G. Tsokos, Y. Ding, T. R. Malek, D. Klatzmann, and G. C. Tsokos, "Regulatory T cells in the treatment of disease," 2018. doi: 10.1038/nrd.2018.148.

[152] R. Roychoudhuri, R. L. Eil, and N. P. Restifo, "The interplay of effector and regulatory T cells in cancer," 2015. doi: 10.1016/j.coi.2015.02.003.

[153] C. Klein *et al.*, "Abstract 486: Tumor-targeted, engineered IL-2 variant (IL-2v)-based immunocytokines for the immunotherapy of cancer.," *Cancer Res.*, vol. 73, no. 8_Supplement, 2013, doi: 10.1158/1538-7445.am2013-486.

[154] C. Klein *et al.*, "Novel Tumor-Targeted, Engineered IL-2 Variant (IL2v)-Based Immunocytokines For Immunotherapy Of Cancer," *Blood*, vol. 122, no. 21, 2013, doi: 10.1182/blood.v122.21.2278.2278.

[155] C. Klein *et al.*, "Cergutuzumab amunaleukin (CEA-IL2v), a CEA-targeted IL-2 variant-based immunocytokine for combination cancer immunotherapy: Overcoming limitations of aldesleukin and conventional IL-2-based immunocytokines," *Oncoimmunology*, vol. 6, no. 3, Mar. 2017, doi: 10.1080/2162402X.2016.1277306.

[156] A. Tang and F. Harding, "The challenges and molecular approaches surrounding interleukin-2-based therapeutics in cancer," 2019. doi: 10.1016/j.cytox.2018.100001.

[157] L. Codarri Deak *et al.*, "PD-1-cis IL-2R agonism yields better effectors from stem-like CD8+ T cells," *Nature*, 2022, doi: 10.1038/s41586-022-05192-0.

[158] T. Inozume *et al.*, "Selection of CD8++PD-1+ lymphocytes in fresh human melanomas enriches for tumor-reactive T cells," *J. Immunother.*, 2010, doi: 10.1097/CJI.0b013e3181fad2b0.

[159] A. Gros *et al.*, "PD-1 identifies the patient-specific CD8+ tumor-reactive repertoire infiltrating human tumors," *J. Clin. Invest.*, 2014, doi: 10.1172/JCI73639.

[160] S. J. Im *et al.*, "Defining CD8+ T cells that provide the proliferative burst after PD-1 therapy," *Nature*, 2016, doi: 10.1038/nature19330.

[161] A. Apavaloaei, M. P. Hardy, P. Thibault, and C. Perreault, "The origin and immune recognition of tumor-specific antigens," 2020. doi: 10.3390/cancers12092607.

[162] S. Feola, J. Chiaro, B. Martins, and V. Cerullo, "Uncovering the tumor antigen landscape: What to know about the discovery process," 2020. doi: 10.3390/cancers12061660.

[163] C. Criscitiello, "Tumor-associated antigens in breast cancer," 2012. doi: 10.1159/000342164.

[164] H. Westdorp *et al.*, "Immunotherapy for prostate cancer: Lessons from responses to tumor-associated antigens," 2014. doi: 10.3389/fimmu.2014.00191.

[165] J. D. Lewis, B. D. Reilly, and R. K. Bright, "Tumor-associated antigens: From discovery to immunity," 2003. doi: 10.1080/08830180305221.

[166] C. C. Liu, H. Yang, R. Zhang, J. J. Zhao, and D. J. Hao, "Tumour-associated antigens and their anti-cancer applications," 2017. doi: 10.1111/ecc.12446.

[167] T. Yan, L. Zhu, and J. Chen, "Current advances and challenges in CAR T-Cell therapy for solid tumors: tumor-associated antigens and the tumor microenvironment," 2023. doi: 10.1186/s40164-023-00373-7.

[168] M. Shanshal, P. F. Caimi, A. A. Adjei, and W. W. Ma, "T-Cell Engagers in Solid Cancers—Current Landscape and Future Directions," May 01, 2023, *MDPI*. doi: 10.3390/cancers15102824.

[169] P. L. Weiden and H. B. Breitz, "Pretargeted radioimmunotherapy (PRIT™) for treatment of non-Hodgkin's lymphoma (NHL)," 2001. doi: 10.1016/S1040-8428(01)00133-0.

[170] B. Yao *et al.*, "Selection of Payloads for Antibody–Drug Conjugates Targeting Ubiquitously Expressed Tumor-Associated Antigens: a Case Study," *AAPS J.*, vol. 24, no. 4, 2022, doi: 10.1208/s12248-022-00720-2.

[171] S. Ilyas and J. C. Yang, "Landscape of Tumor Antigens in T Cell Immunotherapy," *J. Immunol.*, vol. 195, no. 11, 2015, doi: 10.4049/jimmunol.1501657.

[172] Y. Jin, Y. Dong, J. Zhang, J. Sun, Y. Liu, and Y. Chen, "The toxicity of cell therapy: Mechanism, manifestations, and challenges," 2021. doi: 10.1002/jat.4100.

[173] K. A. Autio, V. Boni, R. W. Humphrey, and A. Naing, "Probody therapeutics: An emerging class of therapies

designed to enhance on-target effects with reduced off-tumor toxicity for use in immuno-oncology," Mar. 01, 2020, *American Association for Cancer Research Inc.* doi: 10.1158/1078-0432.CCR-19-1457.

[174] Y. Zhang *et al.*, "Single-Cell Analysis of Target Antigens of CAR-T Reveals a Potential Landscape of 'On-Target, Off-Tumor Toxicity,'" *Front. Immunol.*, vol. 12, 2021, doi: 10.3389/fimmu.2021.799206.

[175] R. A. Morgan, J. C. Yang, M. Kitano, M. E. Dudley, C. M. Laurencot, and S. A. Rosenberg, "Case report of a serious adverse event following the administration of t cells transduced with a chimeric antigen receptor recognizing ERBB2," *Mol. Ther.*, vol. 18, no. 4, 2010, doi: 10.1038/mt.2010.24.

[176] C. H. J. Lamers *et al.*, "Treatment of metastatic renal cell carcinoma with CAIX CAR-engineered T cells: Clinical evaluation and management of on-target toxicity," *Mol. Ther.*, 2013, doi: 10.1038/mt.2013.17.

[177] C. L. Flugel *et al.*, "Overcoming on-target, off-tumour toxicity of CAR T cell therapy for solid tumours," Jan. 01, 2023, *Springer Nature*. doi: 10.1038/s41571-022-00704-3.

[178] P. S. Lee *et al.*, "Improved therapeutic index of an acidic pH-selective antibody," *MAbs*, vol. 14, no. 1, 2022, doi: 10.1080/19420862.2021.2024642.

[179] Y. Liu, A. G. Lee, A. W. Nguyen, and J. A. Maynard, "An antibody Fc engineered for conditional antibody-dependent cellular cytotoxicity at the low tumor microenvironment pH," *J. Biol. Chem.*, vol. 298, no. 4, Apr. 2022, doi: 10.1016/j.jbc.2022.101798.

[180] T. Sulea *et al.*, "Structure-based engineering of pH-dependent antibody binding for selective targeting of solid-tumor microenvironment," *MAbs*, 2020, doi: 10.1080/19420862.2019.1682866.

[181] M. Geiger *et al.*, "Protease-activation using anti-idiotypic masks enables tumor specificity of a folate receptor 1-T cell bispecific antibody," *Nat. Commun.*, vol. 11, no. 1, Dec. 2020, doi: 10.1038/s41467-020-16838-w.

[182] L. Sandersjöö, A. Jonsson, and J. Löfblom, "A new prodrug form of Affibody molecules (pro-Affibody) is selectively activated by cancer-associated proteases," *Cell. Mol. Life Sci.*, vol. 72, no. 7, 2015, doi: 10.1007/s00018-014-1751-8.

[183] A. I. Spira *et al.*, "PROCLAIM-001: A first-in-human trial to assess tolerability of the protease-activatable anti-PD-L1 Probody CX-072 in solid tumors and lymphomas.," *J. Clin. Oncol.*, vol. 35, no. 15_suppl, 2017, doi: 10.1200/jco.2017.35.15_suppl.tps3107.

[184] M. Kamata-Sakurai *et al.*, "Antibody to cd137 activated by extracellular adenosine triphosphate is tumor selective and broadly effective in vivo without systemic immune activation," *Cancer Discov.*, vol. 11, no. 1, pp. 158–175, Jan. 2021, doi: 10.1158/2159-8290.CD-20-0328.

[185] N. Parker, M. J. Turk, E. Westrick, J. D. Lewis, P. S. Low, and C. P. Leamon, "Folate receptor expression in carcinomas and normal tissues determined by a quantitative radioligand binding assay," *Anal. Biochem.*, 2005, doi: 10.1016/j.ab.2004.12.026.

[186] W. M. Kavanaugh, "Antibody prodrugs for cancer," Feb. 01, 2020, *Taylor and Francis Ltd.* doi: 10.1080/14712598.2020.1699053.

[187] W. M. Zhu and M. R. Middleton, "Combination therapies for the optimisation of Bispecific T-cell Engagers in cancer treatment," 2023. doi: 10.1093/immadv/ltad013.

[188] S. Mortaheb, P. S. Pezeshki, and N. Rezaei, "Bispecific therapeutics: a state-of-the-art review on the combination of immune checkpoint inhibition with costimulatory and non-checkpoint targeted therapy," *Expert Opin. Biol. Ther.*, Nov. 2024, doi: 10.1080/14712598.2024.2426636.

[189] J. M. Curtsinger and M. F. Mescher, "Inflammatory cytokines as a third signal for T cell activation," 2010. doi: 10.1016/j.coi.2010.02.013.

[190] G. R. Otten and R. N. Germain, " Split Anergy in a CD8 + T Cell: Receptor-dependent Cytolysis in the Absence of Interleukin-2 Production ," *Science (80-.).*, vol. 251, no. 4998, 1991, doi: 10.1126/science.1900952.

[191] S. Goral, "The three-signal hypothesis of lymphocyte activation/targets for immunosuppression," *Dial. Transplant.*, vol. 40, no. 1, 2011, doi: 10.1002/dat.20527.

[192] J. M. Curtsinger, D. C. Lins, and M. F. Mescher, "Signal 3 Determines Tolerance versus Full Activation of Naive CD8 T Cells," *J. Exp. Med.*, vol. 197, no. 9, 2003, doi: 10.1084/jem.20021910.

[193] T. Dreier *et al.*, "T Cell Costimulus-Independent and Very Efficacious Inhibition of Tumor Growth in Mice Bearing Subcutaneous or Leukemic Human B Cell Lymphoma Xenografts by a CD19-/CD3- Bispecific Single-Chain Antibody Construct," *J. Immunol.*, vol. 170, no. 8, pp. 4397–4402, Apr. 2003, doi: 10.4049/jimmunol.170.8.4397.

[194] T. Dreier *et al.*, "Extremely potent, rapid and costimulation-independent cytotoxic T-cell response against lymphoma cells catalyzed by a single-chain bispecific antibody," *Int. J. Cancer*, vol. 100, no. 6, pp. 690–697, Aug. 2002, doi: 10.1002/ijc.10557.

[195] B. Schlereth *et al.*, "Eradication of tumors from a human colon cancer cell line and from ovarian cancer metastases in immunodeficient mice by a single-chain Ep-CAM-/CD3- bispecific antibody construct," *Cancer Res.*, vol. 65, no. 7, 2005, doi: 10.1158/0008-5472.CAN-04-2637.

[196] A. Marcinek *et al.*, "The Ratio of Costimulatory Vs Coinhibitory Molecules on AML Cells Determines the CD33-BiTE® Mediated T-Cell Response," *Blood*, vol. 132, no. Supplement 1, 2018, doi: 10.1182/blood-2018-99-116297.

[197] C. E. Correnti *et al.*, "Simultaneous multiple interaction T-cell engaging (SMITE) bispecific antibodies overcome bispecific T-cell engager (BiTE) resistance via CD28 co-stimulation," *Leukemia*, vol. 32, no. 5, pp. 1239–1243, May 2018, doi: 10.1038/s41375-018-0014-3.

[198] H. Mikami *et al.*, "Engineering CD3/CD137 Dual Specificity into a DLL3-Targeted T-Cell Engager Enhances T-Cell Infiltration and Efficacy against Small-Cell Lung Cancer," *Cancer Immunol. Res.*, vol. 12, no. 6, pp. 719–730, 2024, doi: 10.1158/2326-6066.CIR-23-0638.

[199] P. Repenning *et al.*, "Abstract 6716: DLL3 TriTCE Co-Stim: A next generation trispecific T cell engager with integrated CD28 costimulation for the treatment of DLL3-expressing cancers," *Cancer Res.*, vol. 84, no. 6_Supplement, pp. 6716–6716, Mar. 2024, doi: 10.1158/1538-7445.AM2024-6716.

[200] C. Claus *et al.*, "Tumor-Targeted 4-1BB agonists for combination with T cell bispecific antibodies as off-The-shelf therapy," *Sci. Transl. Med.*, 2019, doi: 10.1126/scitranslmed.aav5989.

[201] J. Sam *et al.*, "CD19-CD28: an affinity-optimized CD28 agonist for combination with glofitamab (CD20-TCB) as off-the-shelf immunotherapy," *Blood*, vol. 143, no. 21, 2024, doi: 10.1182/blood.2023023381.

[202] T. Hünig, "The rise and fall of the CD28 superagonist TGN1412 and its return as TAB08: a personal account," *FEBS J.*, pp. 3325–3334, Sep. 2016, doi: 10.1111/febs.13754.

[203] Z. Waibler *et al.*, "Signaling signatures and functional properties of anti-human CD28 superagonistic antibodies," *PLoS One*, vol. 3, no. 3, 2008, doi: 10.1371/journal.pone.0001708.

[204] C. Horvath *et al.*, "Storm forecasting: additional lessons from the CD28 superagonist TGN1412 trial," *Nat. Rev. Immunol.*, vol. 12, no. 10, 2012, doi: 10.1038/nri3192-c1.

[205] R. C. Larson and M. V. Maus, "Recent advances and discoveries in the mechanisms and functions of CAR T cells," Mar. 01, 2021, *Nature Research*. doi: 10.1038/s41568-020-00323-z.

[206] P. Zhang, G. Zhang, and X. Wan, "Challenges and new technologies in adoptive cell therapy," 2023. doi: 10.1186/s13045-023-01492-8.

[207] S. Rafiq, C. S. Hackett, and R. J. Brentjens, "Engineering strategies to overcome the current roadblocks in CAR T cell therapy," Mar. 01, 2020, *Nature Research*. doi: 10.1038/s41571-019-0297-y.

[208] J. Jayaraman *et al.*, "CAR-T design: Elements and their synergistic function," Aug. 01, 2020, *Elsevier B.V.* doi: 10.1016/j.ebiom.2020.102931.

[209] P. Vormittag, R. Gunn, S. Ghorashian, and F. S. Veraitch, "A guide to manufacturing CAR T cell therapies," 2018. doi: 10.1016/j.copbio.2018.01.025.

[210] N. F. Leyton-Castro, M. M. Brigido, and A. Q. Maranhão, "Selection of Antibody Fragments for CAR-T Cell Therapy from Phage Display Libraries," in *Methods in Molecular Biology*, vol. 2086, 2020. doi: 10.1007/978-1-0716-0146-4_2.

[211] C. R. J. Pameijer *et al.*, "Conversion of a tumor-binding peptide identified by phage display to a functional chimeric T cell antigen receptor," *Cancer Gene Ther.*, vol. 14, no. 1, 2007, doi: 10.1038/sj.cgt.7700993.

[212] L. Yu *et al.*, "Development of a Tetravalent T-Cell Engaging Bispecific Antibody Against Glypican-3 for Hepatocellular Carcinoma MATERIALS AND METHODS Cell Lines and Culture The suspension cultured cells (HEK-293F cells) and serum-free medium were purchased from OPM Biosciences," 2020. [Online]. Available: www.immunotherapy-journal.com%7C1

[213] J. Tomasik, M. Jasiński, and G. W. Basak, "Next generations of CAR-T cells - new therapeutic opportunities in hematology?," 2022. doi: 10.3389/fimmu.2022.1034707.

[214] D. Han, Z. Xu, Y. Zhuang, Z. Ye, and Q. Qian, "Current progress in CAR-T cell therapy for hematological malignancies," 2021. doi: 10.7150/JCA.48976.

[215] A. Mishra, R. Maiti, P. Mohan, and P. Gupta, "Antigen loss following CAR-T cell therapy: Mechanisms, implications, and potential solutions," 2024. doi: 10.1111/ejh.14101.

[216] M. Elsallab and M. V. Maus, "Expanding access to CAR T cell therapies through local manufacturing," *Nat. Biotechnol.*, vol. 41, no. 12, 2023, doi: 10.1038/s41587-023-01981-8.

[217] R. M. T. ten Ham *et al.*, "Estimation of manufacturing development costs of cell-based therapies: a feasibility study," *Cytotherapy*, vol. 23, no. 8, 2021, doi: 10.1016/j.jcyt.2020.12.014.

[218] A. K. Arunachalam, C. Grégoire, B. Coutinho de Oliveira, and J. J. Melenhorst, "Advancing CAR T-cell therapies: Preclinical insights and clinical translation for hematological malignancies," *Blood Rev.*, no. September, 2024, doi: 10.1016/j.blre.2024.101241.

[219] J. T. Snider *et al.*, "The potential impact of CAR T-cell treatment delays on society," *Am. J. Manag. Care*, vol. 25, no. 8, 2019.

[220] Z. Zhou *et al.*, "The underlying mechanism of chimeric antigen receptor (CAR)-T cell therapy triggering secondary T-cell cancers: Mystery of the Sphinx?," *Cancer Lett.*, vol. 597, p. 217083, Aug. 2024, doi: 10.1016/J.CANLET.2024.217083.

[221] G. Ghilardi *et al.*, "T cell lymphoma and secondary primary malignancy risk after commercial CAR T cell therapy," *Nat. Med.*, vol. 30, no. 4, 2024, doi: 10.1038/s41591-024-02826-w.

[222] N. Verdun and P. Marks, "Secondary Cancers after Chimeric Antigen Receptor T-Cell Therapy," *N. Engl. J. Med.*, vol. 390, no. 7, 2024, doi: 10.1056/nejmp2400209.

[223] T. Tix *et al.*, "Second Primary Malignancies after CAR T-Cell Therapy: A Systematic Review and Meta-analysis of 5,517 Lymphoma and Myeloma Patients," *Clin. Cancer Res.*, pp. OF1–OF11, Sep. 2024, doi: 10.1158/1078-0432.CCR-24-1798.

[224] D. Liu, J. Zhao, and Y. Song, "Engineering switchable and programmable universal CARs for CAR T therapy," Jul. 04, 2019, *BioMed Central Ltd.* doi: 10.1186/s13045-019-0763-0.

[225] L. S. Schlegel, C. Werbrouck, M. Boettcher, and P. Schlegel, "Universal CAR 2.0 to overcome current limitations in CAR therapy," *Front. Immunol.*, vol. 15, p. 1383894, Jun. 2024, doi: 10.3389/FIMMU.2024.1383894/BIBTEX.

[226] S. Stock *et al.*, "Chimeric antigen receptor T cells engineered to recognize the P329G-mutated Fc part of effector-silenced tumor antigen-targeting human IgG1 antibodies enable modular targeting of solid tumors," *J. Immunother. Cancer*, 2022, doi: 10.1136/jitc-2022-005054.

[227] L. Nikolaenko *et al.*, "First in Human Study of an on/Off

Switchable CAR-T Cell Platform Targeting CD19 for B Cell Malignancies (CLBR001 + SWI019)," *Blood*, vol. 138, no. Supplement 1, 2021, doi: 10.1182/blood-2021-151727.

[228] M. Wermke *et al.*, "Updated Results from a Phase I Dose Escalation Study of the Rapidly-Switchable Universal CAR-T Therapy UniCAR-T-CD123 in Relapsed/Refractory AML," *Blood*, vol. 142, no. Supplement 1, 2023, doi: 10.1182/blood-2023-177867.

[229] P. Głowacki and P. Rieske, "Application and Design of Switches Used in CAR," 2022. doi: 10.3390/cells11121910.

[230] K. Urbanska *et al.*, "A universal strategy for adoptive immunotherapy of cancer through use of a novel T-cell antigen receptor," *Cancer Res.*, vol. 72, no. 7, pp. 1844–1852, Apr. 2012, doi: 10.1158/0008-5472.CAN-11-3890/650231/AM/A-UNIVERSAL-STRATEGY-FOR-ADOPTIVE-IMMUNOTHERAPY-OF.

[231] B. Atrice Clé Menceau *et al.*, "Antibody-dependent cellular cytotoxicity (ADCC) is mediated by genetically modified antigen-specific human T lymphocytes," vol. 107, pp. 4669–4677, 2006, doi: 10.1182/blood-2005.

[232] H. Tanaka *et al.*, "Development of engineered t cells expressing a chimeric CD16-CD3ζ Receptor to improve the clinical efficacy of mogamulizumab therapy against adult T-Cell leukemia," *Clin. Cancer Res.*, vol. 22, no. 17, pp. 4405–4416, Sep. 2016, doi: 10.1158/1078-0432.CCR-15-2714.

[233] F. Rataj *et al.*, "High-affinity CD16-polymorphism and Fc-engineered antibodies enable activity of CD16-chimeric antigen receptor-modified T cells for cancer therapy," *Br. J. Cancer*, vol. 120, no. 1, pp. 79–87, Jan. 2019, doi: 10.1038/s41416-018-0341-1.

[234] K. Urbanska, R. C. Lynn, C. Stashwick, A. Thakur, L. G. Lum, and D. J. Powell, "Targeted cancer immunotherapy via combination of designer bispecific antibody and novel gene-engineered T cells," *J. Transl. Med.*, 2014, doi: 10.1186/s12967-014-0347-2.

[235] C. H. Karches *et al.*, "Bispecific antibodies enable synthetic agonisti receptor-transduced T cells for tumor immunotherapy," *Clin. Cancer Res.*, vol. 25, no. 19, pp. 5890–5900, Oct. 2019, doi: 10.1158/1078-0432.CCR-18-3927.

[236] S. Stamova *et al.*, "Cancer immunotherapy by retargeting of immune effector cells via recombinant bispecific antibody constructs," 2012. doi: 10.3390/antib1020172.

[237] K. Tamada *et al.*, "Redirecting gene-modified T cells toward various cancer types using tagged antibodies," *Clin. Cancer Res.*, 2012, doi: 10.1158/1078-0432.CCR-12-1449.

[238] C. Pellegrino *et al.*, "Impact of Ligand Size and Conjugation Chemistry on the Performance of Universal Chimeric Antigen Receptor T-Cells for Tumor Killing," *Bioconjug. Chem.*, vol. 31, no. 7, pp. 1775–1783, Jul. 2020, doi: 10.1021/acs.bioconjchem.0c00258.

[239] M. S. Kim *et al.*, "Redirection of genetically engineered CAR-T cells using bifunctional small molecules," *J. Am. Chem. Soc.*, 2015, doi: 10.1021/jacs.5b00106.

[240] Y. G. Lee *et al.*, "Use of a single CAR T cell and several bispecific adapters facilitates eradication of multiple antigenically different solid tumors," *Cancer Res.*, vol. 79, no. 2, pp. 387–396, Jan. 2019, doi: 10.1158/0008-5472.CAN-18-1834.

[241] Y. G. Lee *et al.*, "Use of a single CAR T cell and several bispecific adapters facilitates eradication of multiple antigenically different solid tumors," *Cancer Res.*, 2019, doi: 10.1158/0008-5472.CAN-18-1834.

[242] J. H. Cho, J. J. Collins, and W. W. Wong, "Universal Chimeric Antigen Receptors for Multiplexed and Logical Control of T Cell Responses," *Cell*, vol. 173, no. 6, pp. 1426-1438.e11, May 2018, doi: 10.1016/j.cell.2018.03.038.

[243] A. V. Stepanov *et al.*, "Control of the antitumour activity and specificity of CAR T cells via organic adapters covalently tethering the CAR to tumour cells," *Nat. Biomed. Eng.*, 2024, doi: 10.1038/s41551-023-01102-5.

[244] D. Darowski *et al.*, "P329G-CAR-J: A novel Jurkat-NFAT-based CAR-T reporter system recognizing the P329G Fc mutation," *Protein Eng. Des. Sel.*, vol. 32, no. 5, pp. 207–218, May 2019, doi: 10.1093/protein/gzz027.

[245] S. Stock *et al.*, "Adaptor Anti-P329G CAR T Cells for Modular Targeting of AML," *Blood*, vol. 142, no. Supplement 1, p. 4805, Nov. 2023, doi: 10.1182/BLOOD-2023-182864.

[246] D. Darowski *et al.*, "P329G-CAR-J: A novel Jurkat-NFAT-based CAR-T reporter system recognizing the P329G Fc mutation," *Protein Eng. Des. Sel.*, 2019, doi: 10.1093/protein/gzz027.

[247] C. Fu *et al.*, "P1406: SAFETY AND EFFICACY OF IBI346, A FIRST-IN-CLASS BCMA-TARGETING MODULAR CAR-T CELL THERAPY, FOR PATIENTS WITH RELAPSED/REFRACTORY MULTIPLE MYELOMA (RRMM): PRELIMINARY RESULTS FROM TWO PHASE I STUDIES," *HemaSphere*, 2023, doi: 10.1097/01.hs9.0000972512.53497.1f.

[248] S. Stock *et al.*, "Chimeric antigen receptor T cells engineered to recognize the P329G-mutated Fc part of effector-silenced tumor antigen-targeting human IgG1 antibodies enable modular targeting of solid tumors," *J. Immunother. Cancer*, vol. 10, no. 7, Jul. 2022, doi: 10.1136/jitc-2022-005054.

[249] "Humanized Chimeric Antigen Receptor (CAR) T cells," *J. Cancer Immunol.*, vol. 3, no. 4, 2021, doi: 10.33696/cancerimmunol.3.055.

[250] R. Greenman *et al.*, "Shaping functional avidity of CAR T Cells: Affinity, avidity, and antigen density that regulate response," *Mol. Cancer Ther.*, vol. 20, no. 5, pp. 872–884, May 2021, doi: 10.1158/1535-7163.MCT-19-1109.

[251] A. N. Khan *et al.*, "Immunogenicity of CAR-T Cell Therapeutics: Evidence, Mechanism and Mitigation," 2022. doi: 10.3389/fimmu.2022.886546.

[252] K. O. Saunders, "Conceptual approaches to modulating antibody effector functions and circulation half-life," 2019, *Frontiers Media S.A.* doi: 10.3389/fimmu.2019.01296.

[253] V. Lukjanov, I. Koutná, and P. Šimara, "CAR T-cell production using nonviral approaches," 2021. doi:

10.1155/2021/6644685.

[254] E. Noaks, C. Peticone, E. Kotsopoulou, and D. G. Bracewell, "Enriching leukapheresis improves T cell activation and transduction efficiency during CAR T processing," *Mol. Ther. Methods Clin. Dev.*, vol. 20, 2021, doi: 10.1016/j.omtm.2021.02.002.

[255] S. Kailayangiri, B. Altvater, M. Wiebel, S. Jamitzky, and C. Rossig, "Overcoming heterogeneity of antigen expression for effective car t cell targeting of cancers," 2020. doi: 10.3390/cancers12051075.

[256] E. Roselli, J. S. Frieling, K. Thorner, M. C. Ramello, C. C. Lynch, and D. Abate-Daga, "CAR-T Engineering: Optimizing Signal Transduction and Effector Mechanisms," 2019. doi: 10.1007/s40259-019-00384-z.

[257] S. Tyagarajan, T. Spencer, and J. Smith, "Optimizing CAR-T Cell Manufacturing Processes during Pivotal Clinical Trials," 2020. doi: 10.1016/j.omtm.2019.11.018.

[258] B. L. Levine, J. Miskin, K. Wonnacott, and C. Keir, "Global Manufacturing of CAR T Cell Therapy," 2017. doi: 10.1016/j.omtm.2016.12.006.

[259] G. Barilà, R. Rizzi, R. Zambello, and P. Musto, "Drug conjugated and bispecific antibodies for multiple myeloma: Improving immunotherapies off the shelf," 2021. doi: 10.3390/ph14010040.

[260] K. Sasaki *et al.*, "Fc-Binding Antibody-Recruiting Molecules Targeting Prostate-Specific Membrane Antigen: Defucosylation of Antibody for Efficacy Improvement**," *ChemBioChem*, 2021, doi: 10.1002/cbic.202000577.

[261] R. P. Murelli, A. X. Zhang, J. Michel, W. L. Jorgensen, and D. A. Spiegel, "Chemical control over immune recognition: A class of antibody-recruiting small molecules that target prostate cancer," *J. Am. Chem. Soc.*, 2009, doi: 10.1021/ja906844e.

[262] S. Achilli, N. Berthet, and O. Renaudet, "Antibody recruiting molecules (ARMs): Synthetic immunotherapeutics to fight cancer," 2021. doi: 10.1039/d1cb00007a.

[263] B. P. M. Lake, R. G. Wylie, C. Bařinka, and A. F. Rullo, "Tunable Multivalent Platform for Immune Recruitment to Lower Antigen Expressing Cancers," *Angew. Chemie - Int. Ed.*, 2023, doi: 10.1002/anie.202214659.

[264] K. Sasaki *et al.*, "Fc-binding antibody-recruiting molecules exploit endogenous antibodies for anti-tumor immune responses," *Chem. Sci.*, vol. 11, no. 12, 2020, doi: 10.1039/d0sc00017e.

[265] A. J. Martinko *et al.*, "Switchable assembly and function of antibody complexes in vivo using a small molecule," *Proc. Natl. Acad. Sci. U. S. A.*, 2022, doi: 10.1073/pnas.2117402119.

[266] T. Konishi *et al.*, "Reinforced antimyeloma therapy via dual-lymphoid activation mediated by a panel of antibodies armed with bridging-BiTE," *Blood*, 2023, doi: 10.1182/blood.2022019082.

[267] T. Konishi, "Reinforced anti-myeloma therapy via dual-lymphoid activation mediated by a panel of antibodies armed with Bridging-BiTE."

[268] E. Mössner *et al.*, "Increasing the efficacy of CD20 antibody therapy through the engineering of a new type II anti-CD20 antibody with enhanced direct and immune effector cell - mediated B-cell cytotoxicity," *Blood*, 2010, doi: 10.1182/blood-2009-06-225979.

[269] C. Claus *et al.*, "Tumor-targeted 4-1BB agonists for combination with T cell bispecific antibodies as off-the-shelf therapy," *Sci. Transl. Med.*, vol. 11, no. 496, p. eaav5989, Jun. 2019, doi: 10.1126/scitranslmed.aav5989.

[270] J. Sam *et al.*, "RG6333 (CD19-CD28), a CD19-Targeted Affinity-Optimized CD28 Bispecific Antibody, Enhances and Prolongs the Anti-Tumor Activity of Glofitamab (CD20-TCB) in Preclinical Models," *Blood*, 2022, doi: 10.1182/blood-2022-159941.

[271] T. Jain *et al.*, "Biophysical properties of the clinical-stage antibody landscape," *Proc. Natl. Acad. Sci. U. S. A.*, 2017, doi: 10.1073/pnas.1616408114.

[272] Y. G. Assaraf, C. P. Leamon, and J. A. Reddy, "The folate receptor as a rational therapeutic target for personalized cancer treatment," 2014. doi: 10.1016/j.drup.2014.10.002.

[273] G. Toffoli, C. Cernigoi, A. Russo, A. Gallo, M. Bagnoli, and M. Boiocchi, "Overexpression of folate binding protein in ovarian cancers," *Int. J. Cancer*, 1997, doi: 10.1002/(SICI)1097-0215(19970422)74:2<193::AID-IJC10>3.0.CO;2-F.

[274] S. Markert *et al.*, "Alpha-folate receptor expression in epithelial ovarian carcinoma and non-neoplastic ovarian tissue," *Anticancer Res.*, 2008.

[275] J. Chen, F. Zeng, S. J. Forrester, S. Eguchi, M. Z. Zhang, and R. C. Harris, "Expression and function of the epidermal growth factor receptor in physiology and disease," *Physiol. Rev.*, 2016, doi: 10.1152/physrev.00030.2015.

[276] J. Zhou *et al.*, "Identification of CEACAM5 as a Biomarker for Prewarning and Prognosis in Gastric Cancer," *J. Histochem. Cytochem.*, 2015, doi: 10.1369/0022155415609098.

[277] C. Gutierrez and R. Schiff, "HER2: Biology, detection, and clinical implications," *Arch. Pathol. Lab. Med.*, 2011, doi: 10.5858/2010-0454-rar.1.

[278] A. Balakrishnan *et al.*, "Analysis of ROR1 protein expression in human cancer and normal tissues," *Clin. Cancer Res.*, 2017, doi: 10.1158/1078-0432.CCR-16-2083.

[279] O. Cunningham, M. Scott, Z. S. Zhou, and W. J. J. Finlay, "Polyreactivity and polyspecificity in therapeutic antibody development: risk factors for failure in preclinical and clinical development campaigns," 2021, *Taylor and Francis Ltd.* doi: 10.1080/19420862.2021.1999195.

[280] H. Ausserwöger *et al.*, "Non-specificity as the sticky problem in therapeutic antibody development," Dec. 01, 2022, *Nature Research*. doi: 10.1038/s41570-022-00438-x.

[281] M. R. Parkhurst *et al.*, "T cells targeting carcinoembryonic antigen can mediate regression of metastatic colorectal cancer but induce severe transient colitis," *Mol. Ther.*, vol. 19, no. 3, pp. 620–626, 2011, doi: 10.1038/MT.2010.272.

[282] R. A. Morgan *et al.*, "Cancer regression and neurological toxicity following anti-MAGE-A3 TCR gene therapy," *J. Immunother.*, 2013, doi: 10.1097/CJI.0b013e3182829903.

[283] M. Bacac, C. Klein, and P. Umana, "CEA TCB: A novel head-to-tail 2:1 T cell bispecific antibody for treatment of CEA-positive solid tumors," *Oncoimmunology*, 2016, doi: 10.1080/2162402X.2016.1203498.

[284] S. Dickopf *et al.*, "Prodrug-Activating Chain Exchange (PACE) converts targeted prodrug derivatives to functional bi- or multispecific antibodies," *Biol. Chem.*, vol. 403, no. 5, pp. 495–508, Apr. 2022, doi: 10.1515/hsz-2021-0401.

[285] A. Banaszek *et al.*, "On-target restoration of a split T cell-engaging antibody for precision immunotherapy," *Nat. Commun.*, vol. 10, no. 1, Dec. 2019, doi: 10.1038/s41467-019-13196-0.

[286] N. Momin *et al.*, "Anchoring of intratumorally administered cytokines to collagen safely potentiates systemic cancer immunotherapy," *Sci. Transl. Med.*, 2019, doi: 10.1126/scitranslmed.aaw2614.

[287] C. C. Baniel *et al.*, "Intratumoral injection reduces toxicity and antibody-mediated neutralization of immunocytokine in a mouse melanoma model," *J. Immunother. Cancer*, 2020, doi: 10.1136/jitc-2020-001262.

[288] M. Gilardi *et al.*, "Microneedle-mediated Intratumoral Delivery of Anti-CTLA-4 Promotes cDC1-dependent Eradication of Oral Squamous Cell Carcinoma with Limited irAEs," *Mol. Cancer Ther.*, 2022, doi: 10.1158/1535-7163.MCT-21-0234.

[289] N. J. Bangayan *et al.*, "Dual-inhibitory domain iCARs improve the efficiency of the AND-NOT gate CAR T strategy," *Proc. Natl. Acad. Sci. U. S. A.*, 2023, doi: 10.1073/pnas.2312374120.

[290] J. Kwon *et al.*, "Single-cell mapping of combinatorial target antigens for CAR switches using logic gates," *Nat. Biotechnol.*, vol. 41, no. 11, pp. 1593–1605, Nov. 2023, doi: 10.1038/s41587-023-01686-y.

[291] A. M. Tousley *et al.*, "Co-opting signalling molecules enables logic-gated control of CAR T cells," *Nature*, vol. 615, no. 7952, pp. 507–516, Mar. 2023, doi: 10.1038/s41586-023-05778-2.

[292] S. C. Oostindie *et al.*, "Logic-gated antibody pairs that selectively act on cells co-expressing two antigens," *Nat. Biotechnol.*, vol. 40, no. 10, pp. 1509–1519, Oct. 2022, doi: 10.1038/s41587-022-01384-1.

[293] S. B. Gunnoo, H. M. Finney, T. S. Baker, A. D. Lawson, D. C. Anthony, and B. G. Davis, "Creation of a gated antibody as a conditionally functional synthetic protein," *Nat. Commun.*, 2014, doi: 10.1038/ncomms5388.

[294] S. Dickopf *et al.*, "Prodrug-Activating Chain Exchange (PACE) converts targeted prodrug derivatives to functional bi- or multispecific antibodies," *Biol. Chem.*, 2022, doi: 10.1515/hsz-2021-0401.

[295] P. Pellegatti, L. Raffaghello, G. Bianchi, F. Piccardi, V. Pistoia, and F. Di Virgilio, "Increased level of extracellular ATP at tumor sites: In vivo imaging with plasma membrane luciferase," *PLoS One*, 2008, doi: 10.1371/journal.pone.0002599.

[296] K. Uhland, "Matriptase and its putative role in cancer," 2006. doi: 10.1007/s00018-006-6298-x.

[297] K. U. Sales, S. Friis, L. Abusleme, N. M. Moutsopoulos, and T. H. Bugge, "Matriptase promotes inflammatory cell accumulation and progression of established epidermal tumors," *Oncogene*, vol. 34, no. 35, 2015, doi: 10.1038/onc.2014.391.

[298] E. Boedtkjer and S. F. Pedersen, "The Acidic Tumor Microenvironment as a Driver of Cancer," 2020. doi: 10.1146/annurev-physiol-021119-034627.

[299] M. M. Audero, N. Prevarskaya, and A. F. Pla, "Ca2+Signalling and Hypoxia/Acidic Tumour Microenvironment Interplay in Tumour Progression," 2022. doi: 10.3390/ijms23137377.

[300] R. Lucchi, J. Bentanachs, and B. Oller-Salvia, "The Masking Game: Design of Activatable Antibodies and Mimetics for Selective Therapeutics and Cell Control," *ACS Cent. Sci.*, vol. 7, no. 5, pp. 724–738, May 2021, doi: 10.1021/acscentsci.0c01448.

[301] H. Tanimoto, L. J. Underwood, Y. Wang, K. Shigemasa, T. H. Parmley, and T. J. O'Brien, "Ovarian tumor cells express a transmembrane serine protease: A potential candidate for early diagnosis and therapeutic intervention," *Tumor Biol.*, 2001, doi: 10.1159/000050604.

[302] H. Tanimoto *et al.*, "Transmembrane serine protease TADG-15 (ST14/Matriptase/MT-SP1): Expression and prognostic value in ovarian cancer," *Br. J. Cancer*, 2005, doi: 10.1038/sj.bjc.6602320.

[303] M. Oberst *et al.*, "Matriptase and HAI-1 are expressed by normal and malignant epithelial cells in vitro and in vivo," *Am. J. Pathol.*, 2001, doi: 10.1016/S0002-9440(10)64081-3.

[304] B. Schmalfeldt *et al.*, "Increased expression of matrix metalloproteinases (MMP)-2, MMP-9, and the urokinase-type plasminogen activator is associated with progression from benign to advanced ovarian cancer," *Clin. Cancer Res.*, 2001.

[305] M. D. Oberst *et al.*, "Expression of the serine protease matriptase and its inhibitor HAI-1 in epithelial ovarian cancer: Correlation with clinical outcome and tumor clinicopathological parameters," *Clin. Cancer Res.*, 2002.

[306] J. Y. Kang *et al.*, "Tissue microarray analysis of hepatocyte growth factor/Met pathway components reveals a role for Met, matriptase, and hepatocyte growth factor activator inhibitor 1 in the progression of node-negative breast cancer," *Cancer Res.*, 2003.

[307] L. R. Desnoyers *et al.*, "Tumor-specific activation of an EGFR-targeting probody enhances therapeutic index," *Sci. Transl. Med.*, vol. 5, no. 207, Oct. 2013, doi: 10.1126/SCITRANSLMED.3006682/SUPPL_FILE/5-207RA144_SM.PDF.

[308] C. C. S. Pai *et al.*, "Tumor-conditional anti-CTLA4 uncouples antitumor efficacy from immunotherapy-related toxicity," *J. Clin. Invest.*, vol. 129, no. 1, Jan. 2019, doi: 10.1172/JCI123391.

[309] I. Etxeberria *et al.*, "Antitumor efficacy and reduced toxicity using an anti-CD137 Probody therapeutic", doi: 10.1073/pnas.2025930118/-/DCSupplemental.

[310] S. Metz *et al.*, "Bispecific antibody derivatives with restricted binding functionalities that are activated by proteolytic processing," *Protein Eng. Des. Sel.*, 2012, doi: 10.1093/protein/gzs064.

[311] I. J. Chen *et al.*, "Selective antibody activation through protease-activated pro-antibodies that mask binding sites with inhibitory domains," *Sci. Reports 2017 71*, vol. 7, no. 1, pp. 1–12, Sep. 2017, doi: 10.1038/s41598-017-11886-7.

[312] A. Elter *et al.*, "Protease-Activation of Fc-Masked Therapeutic Antibodies to Alleviate Off-Tumor Cytotoxicity," *Front. Immunol.*, vol. 12, Aug. 2021, doi: 10.3389/fimmu.2021.715719.

[313] A. Panchal *et al.*, "COBRA™: a highly potent conditionally active T cell engager engineered for the treatment of solid tumors," *MAbs*, vol. 12, no. 1, Jan. 2020, doi: 10.1080/19420862.2020.1792130.

[314] D. E. Dettling *et al.*, "Regression of EGFR positive established solid tumors in mice with the conditionally active T cell engager TAK-186," *J. Immunother. Cancer*, vol. 10, no. 6, Jun. 2022, doi: 10.1136/jitc-2021-004336.

[315] F. Cattaruzza *et al.*, "Precision-activated T-cell engagers targeting HER2 or EGFR and CD3 mitigate on-target, off-tumor toxicity for immunotherapy in solid tumors," *Nat. Cancer*, vol. 4, no. 4, pp. 485–501, Apr. 2023, doi: 10.1038/s43018-023-00536-9.

[316] D. Liu *et al.*, "Microenvironment-responsive anti-PD-L1 × CD3 bispecific T-cell engager for solid tumor immunotherapy," *J. Control. Release*, 2023, doi: 10.1016/j.jconrel.2023.01.041.

[317] C. T. Orozco *et al.*, "Mechanistic insights into the rational design of masked antibodies," *MAbs*, vol. 14, no. 1, 2022, doi: 10.1080/19420862.2022.2095701.

[318] J. M. Donaldson, C. Kari, R. C. Fragoso, U. Rodeck, and J. C. Williams, "Design and development of masked therapeutic antibodies to limit off-target effects: Application to anti-EGFR antibodies," *Cancer Biol. Ther.*, vol. 8, no. 22, 2009, doi: 10.4161/cbt.8.22.9765.

[319] O. J. Goudy, A. Peng, A. Tripathy, and B. Kuhlman, "Design of a protease-activated PD-L1 inhibitor," *Protein Sci.*, 2023, doi: 10.1002/pro.4578.

[320] K. A. Hay *et al.*, "Kinetics and biomarkers of severe cytokine release syndrome after CD19 chimeric antigen receptor–modified T-cell therapy," *Blood*, 2017, doi: 10.1182/blood-2017-06-793141.

[321] M. S. Ju and S. T. Jung, "Antigen Design for Successful Isolation of Highly Challenging Therapeutic Anti-GPCR Antibodies," 2020. doi: 10.3390/ijms21218240.

[322] M. A. Ayoub *et al.*, "Antibodies targeting G protein-coupled receptors: Recent advances and therapeutic challenges," in *mAbs*, 2017. doi: 10.1080/19420862.2017.1325052.

[323] W. Wilman *et al.*, "Machine-designed biotherapeutics: Opportunities, feasibility and advantages of deep learning in computational antibody discovery," *Brief. Bioinform.*, 2022, doi: 10.1093/bib/bbac267.

[324] C. Sheedy, C. Roger MacKenzie, and J. C. Hall, "Isolation and affinity maturation of hapten-specific antibodies," 2007. doi: 10.1016/j.biotechadv.2007.02.003.

[325] F. D. Makurvet, "Biologics vs. small molecules: Drug costs and patient access," *Med. Drug Discov.*, vol. 9, p. 100075, Mar. 2021, doi: 10.1016/j.medidd.2020.100075.

[326] J. Vázquez, M. López, E. Gibert, E. Herrero, and F. Javier Luque, "Merging ligand-based and structure-based methods in drug discovery: an overview of combined virtual screening approaches," 2020. doi: 10.3390/molecules25204723.

[327] H. Zhu, Y. Zhang, W. Li, and N. Huang, "A Comprehensive Survey of Prospective Structure-Based Virtual Screening for Early Drug Discovery in the Past Fifteen Years," 2022. doi: 10.3390/ijms232415961.

[328] X. C. Yan *et al.*, "Augmenting hit identification by virtual screening techniques in small molecule drug discovery," 2020. doi: 10.1021/acs.jcim.0c00113.

[329] A. V. Sadybekov and V. Katritch, "Computational approaches streamlining drug discovery," 2023. doi: 10.1038/s41586-023-05905-z.

[330] P. L. Bedard, D. M. Hyman, M. S. Davids, and L. L. Siu, "Small molecules, big impact: 20 years of targeted therapy in oncology," 2020. doi: 10.1016/S0140-6736(20)30164-1.

[331] I. Trenevska, D. Li, and A. H. Banham, "Therapeutic antibodies against intracellular tumor antigens," 2017. doi: 10.3389/fimmu.2017.01001.

[332] M. Chen, L. Cai, Y. Xiang, L. Zhong, and J. Shi, "Advances in non-radioactive PSMA-targeted small molecule-drug conjugates in the treatment of prostate cancer," 2023. doi: 10.1016/j.bioorg.2023.106889.

[333] A. Zana *et al.*, "A Comparative Analysis of Fibroblast Activation Protein-Targeted Small Molecule-Drug, Antibody-Drug, and Peptide-Drug Conjugates," *Bioconjug. Chem.*, 2023, doi: 10.1021/acs.bioconjchem.3c00244.

[334] J. Millul *et al.*, "Immunotherapy with immunocytokines and PD-1 blockade enhances the anticancer activity of small molecule-drug conjugates targeting carbonic anhydrase IX," *Mol. Cancer Ther.*, 2021, doi: 10.1158/1535-7163.MCT-20-0361.

[335] E. Eppard *et al.*, "Clinical translation and first in-human use of [44Sc]Sc-PSMA-617 for pet imaging of metastasized castrate-resistant prostate cancer," *Theranostics*, 2017, doi: 10.7150/thno.20586.

[336] J. L. Tanyi *et al.*, "A Phase III Study of Pafolacianine Injection (OTL38) for Intraoperative Imaging of Folate Receptor-Positive Ovarian Cancer (Study 006)," *J. Clin. Oncol.*, 2023, doi: 10.1200/JCO.22.00291.

[337] O. Sartor *et al.*, "Lutetium-177–PSMA-617 for Metastatic Castration-Resistant Prostate Cancer," *N. Engl. J. Med.*, 2021, doi: 10.1056/nejmoa2107322.

[338] Y. Zheng and L. C. Cantley, "Toward a better understanding of folate metabolism in health and disease," 2019. doi: 10.1084/jem.20181965.

[339] A. E. Machulkin *et al.*, "Small-molecule PSMA ligands. Current state, SAR and perspectives," 2016. doi: 10.3109/1061186X.2016.1154564.

[340] M. Wichert and N. Krall, "Targeting carbonic anhydrase IX with small organic ligands," Jun. 01, 2015, *Elsevier Ltd*. doi: 10.1016/j.cbpa.2015.02.005.

[341] L. A. Dainty *et al.*, "Overexpression of folate binding protein and mesothelin are associated with uterine serous carcinoma," *Gynecol. Oncol.*, 2007, doi: 10.1016/j.ygyno.2006.10.063.

[342] M. C. Hupe *et al.*, "Expression of prostate-specific membrane antigen (PSMA) on biopsies is an independent risk stratifier of prostate cancer patients at time of initial diagnosis," *Front. Oncol.*, 2018, doi: 10.3389/fonc.2018.00623.

[343] G. L. Wright *et al.*, "Upregulation of prostate-specific membrane antigen after androgen- deprivation therapy," *Urology*, vol. 48, no. 2, pp. 326–334, 1996, doi: 10.1016/S0090-4295(96)00184-7.

[344] E. Oosterwdk *et al.*, "Monoclonal antibody G 250 recognizes a determinant present in renal-cell carcinoma and absent from normal kidney," *Int. J. Cancer*, 1986, doi: 10.1002/ijc.2910380406.

[345] T. Dorai, I. Sawczuk, J. Pastorek, P. H. Wiernik, and J. P. Dutcher, "Role of carbonic anhydrases in the progression of renal cell carcinoma subtypes: Proposal of a unified hypothesis," 2006. doi: 10.1080/07357900601062321.

[346] A. Peón, S. Naulaerts, and P. J. Ballester, "Predicting the Reliability of Drug-target Interaction Predictions with Maximum Coverage of Target Space," *Sci. Rep.*, 2017, doi: 10.1038/s41598-017-04264-w.

[347] M. S. Rao *et al.*, "Novel Computational Approach to Predict Off-Target Interactions for Small Molecules," *Front. Big Data*, 2019, doi: 10.3389/fdata.2019.00025.

[348] J. T. Metz and P. J. Hajduk, "Rational approaches to targeted polypharmacology: Creating and navigating protein-ligand interaction networks," 2010. doi: 10.1016/j.cbpa.2010.06.166.

[349] H. Tang *et al.*, "Prostate targeting ligands based on N-acetylated α-linked acidic dipeptidase," *Biochem. Biophys. Res. Commun.*, 2003, doi: 10.1016/S0006-291X(03)01119-7.

[350] M. Y. Mboge *et al.*, "Inhibition of Carbonic Anhydrase Using SLC-149: Support for a Noncatalytic Function of CAIX in Breast Cancer," *J. Med. Chem.*, 2021, doi: 10.1021/acs.jmedchem.0c02077.

[351] P. J. Yazaki *et al.*, "A series of anti-CEA/anti-DOTA bispecific antibody formats evaluated for pre-targeting: comparison of tumor uptake and blood clearance," *Protein Eng. Des. Sel.*, 2013, doi: 10.1093/protein/gzs096.

[352] K. D. Orcutt, K. A. Nasr, D. G. Whitehead, J. V. Frangioni, and K. D. Wittrup, "Biodistribution and clearance of small molecule hapten chelates for pretargeted radioimmunotherapy," *Mol. Imaging Biol.*, 2011, doi: 10.1007/s11307-010-0353-6.

[353] S. M. Cheal *et al.*, "Alpha radioimmunotherapy using 225Ac-proteus-DOTA for solid tumors – Safety at curative doses," *Theranostics*, 2020, doi: 10.7150/thno.48810.

[354] Y. J. Lu *et al.*, "Preclinical evaluation of bispecific adaptor molecule controlled folate receptor CAR-T cell therapy with special focus on pediatric malignancies," *Front. Oncol.*, vol. 9, no. MAR, 2019, doi: 10.3389/fonc.2019.00151.

[355] A. V. Stepanov *et al.*, "Control of the antitumour activity and specificity of CAR T cells via organic adapters covalently tethering the CAR to tumour cells," *Nat. Biomed. Eng.*, 2023, doi: 10.1038/s41551-023-01102-5.

[356] Y. Lu and P. S. Low, "Folate targeting of haptens to cancer cell surfaces mediates immunotherapy of syngeneic murine tumors," *Cancer Immunol. Immunother.*, 2002, doi: 10.1007/s00262-002-0266-6.

[357] R. J. Amato, A. Shetty, Y. Lu, R. Ellis, and P. S. Low, "A phase i study of Folate immune therapy (EC90 vaccine administered with GPI-0100 adjuvant followed by EC17) in patients with renal cell carcinoma," *J. Immunother.*, 2013, doi: 10.1097/CJI.0b013e3182917f59.

[358] R. J. Amato *et al.*, "A phase I/Ib study of folate immune (EC90 vaccine administered with gpi-0100 adjuvant followed by EC17) with interferon-α and interleukin-2 in patients with renal cell carcinoma," *J. Immunother.*, vol. 37, no. 4, pp. 237–244, 2014, doi: 10.1097/CJI.0000000000000029.

[359] K. Sasaki *et al.*, "Fc-binding antibody-recruiting molecules exploit endogenous antibodies for anti-tumor immune responses," *Chem. Sci.*, 2020, doi: 10.1039/d0sc00017e.

[360] S. Chang Lee *et al.*, "A PSMA-targeted bispecific antibody for prostate cancer driven by a small-molecule targeting ligand," 2021. [Online]. Available: http://advances.sciencemag.org/

[361] M. C. Markowski *et al.*, "Phase I study of CCW702, a bispecific small molecule-antibody conjugate targeting PSMA and CD3 in patients with metastatic castration-resistant prostate cancer (mCRPC).," *J. Clin. Oncol.*, 2021, doi: 10.1200/jco.2021.39.15_suppl.tps5094.

[362] E. S. Delpassand *et al.*, "Targeted α-Emitter Therapy with 212Pb-DOTAMTATE for the Treatment of Metastatic SSTR-Expressing Neuroendocrine Tumors: First-in-Humans Dose-Escalation Clinical Trial," *J. Nucl. Med.*, vol. 63, no. 9, 2022, doi: 10.2967/jnumed.121.263230.

[363] C. Klein *et al.*, "Antibodies For Chelated Radionuclides," WO/2019/201959, 2019 [Online]. Available: https://patentscope.wipo.int/search/en/detail.jsf?docId=WO2019201959

[364] S. M. Mahalingam, H. Chu, X. Liu, C. P. Leamon, and P. S. Low, "Carbonic Anhydrase IX-Targeted Near-Infrared Dye for Fluorescence Imaging of Hypoxic Tumors," *Bioconjug. Chem.*, vol. 29, no. 10, 2018, doi: 10.1021/acs.bioconjchem.8b00509.

[365] J. E. Sulek *et al.*, "Folate-targeted intraoperative fluorescence, OTL38, in robotic-assisted laparoscopic partial nephrectomy," *Scand. J. Urol.*, 2021, doi: 10.1080/21681805.2021.1933168.

[366] M. Shirley, "Glofitamab: First Approval," *Drugs*, 2023, doi: 10.1007/s40265-023-01894-5.

[367] T. Schlothauer *et al.*, "Novel human IgG1 and IgG4 Fc-engineered antibodies with completely abolished immune effector functions," *Protein Eng. Des. Sel.*, 2016, doi: 10.1093/protein/gzw040.

[368] Y. Guan, Q. Zhu, D. Huang, S. Zhao, L. Jan Lo, and J. Peng, "An equation to estimate the difference

between theoretically predicted and SDS PAGE-displayed molecular weights for an acidic peptide," *Sci. Rep.*, vol. 5, 2015, doi: 10.1038/srep13370.

[369] C. Scheller, F. Krebs, R. Wiesner, H. Wätzig, and I. Oltmann-Norden, "A comparative study of CE-SDS, SDS-PAGE, and Simple Western—Precision, repeatability, and apparent molecular mass shifts by glycosylation," *Electrophoresis*, vol. 42, no. 14–15, 2021, doi: 10.1002/elps.202100068.

[370] S. Cazzamalli *et al.*, "In Vivo Antitumor Activity of a Novel Acetazolamide-Cryptophycin Conjugate for the Treatment of Renal Cell Carcinomas," *ACS Omega*, 2018, doi: 10.1021/acsomega.8b02350.

[371] N. Krall, F. Pretto, W. Decurtins, G. J. L. Bernardes, C. T. Supuran, and D. Neri, "A small-molecule drug conjugate for the treatment of carbonic anhydrase IX expressing tumors," *Angew. Chemie - Int. Ed.*, 2014, doi: 10.1002/anie.201310709.

[372] J. C. Oosterwijk-Wakka, O. C. Boerman, P. F. A. M. Mulders, and E. Oosterwijk, "Application of monoclonal antibody G250 recognizing carbonic anhydrase IX in renal cell carcinoma," 2013. doi: 10.3390/ijms140611402.

[373] J. Roy *et al.*, "DUPA Conjugation of a Cytotoxic Indenoisoquinoline Topoisomerase i Inhibitor for Selective Prostate Cancer Cell Targeting," *J. Med. Chem.*, 2015, doi: 10.1021/jm5018384.

[374] S. A. Kularatne, K. Wang, H. K. R. Santhapuram, and P. S. Low, "Prostate-specific membrane antigen targeted imaging and therapy of prostate cancer using a PSMA inhibitor as a homing ligand," *Mol. Pharm.*, 2009, doi: 10.1021/mp900069d.

[375] P. M. Smith-Jones *et al.*, "In vitro characterization of radiolabeled monoclonal antibodies specific for the extracellular domain of prostate-specific membrane antigen," *Cancer Res.*, 2000.

[376] W. Xin, S. Feng, J. H. Freisheim, L. E. Gentry, and M. Ratnam, "Differential stereospecificities and affinities of folate receptor isoforms for folate compounds and antifolates," *Biochem. Pharmacol.*, vol. 44, no. 9, 1992, doi: 10.1016/0006-2952(92)90089-2.

[377] M. BACAC *et al.*, "WO2016079076 - T CELL ACTIVATING BISPECIFIC ANTIGEN BINDING MOLECULES AGIANT FOLR1 AND CD3," WO/2016/079076, 2016 [Online]. Available: https://patentscope.wipo.int/search/en/detail.jsf?docId=WO2016079076

[378] S. Dengl, C. Sustmann, and U. Brinkmann, "Engineered hapten-binding antibody derivatives for modulation of pharmacokinetic properties of small molecules and targeted payload delivery," 2016. doi: 10.1111/imr.12386.

[379] E. Gonçalves *et al.*, "Pan-cancer proteomic map of 949 human cell lines," *Cancer Cell*, 2022, doi: 10.1016/j.ccell.2022.06.010.

[380] Broad Institute, "DepMap Portal."

[381] M. Zatovicova *et al.*, "Monoclonal antibody G250 targeting CA IX: Binding specificity, internalization and therapeutic effects in a non-renal cancer model," *Int. J. Oncol.*, 2014, doi: 10.3892/ijo.2014.2658.

[382] P. H. Lizotte *et al.*, "Multiparametric profiling of non–small-cell lung cancers reveals distinct immunophenotypes," *JCI Insight*, 2016, doi: 10.1172/jci.insight.89014.

[383] D. A. Landau *et al.*, "Evolution and impact of subclonal mutations in chronic lymphocytic leukemia," *Cell*, 2013, doi: 10.1016/j.cell.2013.01.019.

[384] L. Ding *et al.*, "Clonal evolution in relapsed acute myeloid leukaemia revealed by whole-genome sequencing," *Nature*, 2012, doi: 10.1038/nature10738.

[385] J. J. Keats *et al.*, "Clonal competition with alternating dominance in multiple myeloma," *Blood*, 2012, doi: 10.1182/blood-2012-01-405985.

[386] S. Misale *et al.*, "Emergence of KRAS mutations and acquired resistance to anti-EGFR therapy in colorectal cancer," *Nature*, 2012, doi: 10.1038/nature11156.

[387] R. Liu *et al.*, "Co-evolution of tumor and immune cells during progression of multiple myeloma," *Nat. Commun.*, 2021, doi: 10.1038/s41467-021-22804-x.

[388] M. Binnewies *et al.*, "Understanding the tumor immune microenvironment (TIME) for effective therapy," *Nat. Med.*, 2018, doi: 10.1038/s41591-018-0014-x.

[389] Y. Zhang and L. Chen, "Classification of advanced human cancers based on tumor immunity in the MicroEnvironment (TIME) for cancer immunotherapy," 2016. doi: 10.1001/jamaoncol.2016.2450.

[390] M. del M. Valenzuela-Membrives *et al.*, "Progressive changes in composition of lymphocytes in lung tissues from patients with non-small-cell lung cancer," *Oncotarget*, 2016, doi: 10.18632/oncotarget.12264.

[391] M. Kebenko *et al.*, "A multicenter phase 1 study of solitomab (MT110, AMG 110), a bispecific EpCAM/CD3 T-cell engager (BiTE®) antibody construct, in patients with refractory solid tumors," *Oncoimmunology*, vol. 7, no. 8, 2018, doi: 10.1080/2162402X.2018.1450710.

[392] C. H. J. Lamers, Y. Klaver, J. W. Gratama, S. Sleijfer, and R. Debets, "Treatment of metastatic renal cell carcinoma (mRCC) with CAIX CAR-engineered T-cells - A completed study overview," *Biochem. Soc. Trans.*, vol. 44, no. 3, 2016, doi: 10.1042/BST20160037.

[393] H. Nakajima and T. Nakatsura, "Towards the era of immune checkpoint inhibitors and personalized cancer immunotherapy," 2020. doi: 10.1080/25785826.2020.1785654.

[394] F. Cremasco *et al.*, "Cross-linking of T cell to B cell lymphoma by the T cell bispecific antibody CD20-TCB induces IFNγ/CXCL10-dependent peripheral T cell recruitment in humanized murine model," *PLoS One*, vol. 16, no. 1 January, Jan. 2021, doi: 10.1371/journal.pone.0241091.

[395] J. H. Esensten, Y. A. Helou, G. Chopra, A. Weiss, and J. A. Bluestone, "CD28 Costimulation: From Mechanism to Therapy," 2016. doi: 10.1016/j.immuni.2016.04.020.

[396] C. Claus, C. Ferrara-Koller, and C. Klein, "The emerging landscape of novel 4-1BB (CD137) agonistic drugs for cancer immunotherapy," 2023, *Taylor and Francis Ltd.* doi: 10.1080/19420862.2023.2167189.

[397] H. Luo, W. Wang, J. Mai, R. Yin, X. Cai, and Q. Li, "The nexus of dynamic T cell states and immune checkpoint blockade therapy in the periphery and tumor microenvironment," 2023. doi: 10.3389/fimmu.2023.1267918.

[398] J. G. Pol, P. Caudana, J. Paillet, E. Piaggio, and G. Kroemer, "Effects of interleukin-2 in immunostimulation and immunosuppression," 2020. doi: 10.1084/jem.20191247.

[399] W. W. Overwijk, M. A. Tagliaferri, and J. Zalevsky, "Engineering IL-2 to Give New Life to T Cell Immunotherapy," *Annu. Rev. Med. 2021*, vol. 72, pp. 281–311, 2021, doi: 10.1146/annurev-med-073118.

[400] A. L. Esptein, M. M. Mizokami, J. Li, P. Hu, and L. A. Khawli, "Identification of a protein fragment of interleukin 2 responsible for vasopermeability," *J. Natl. Cancer Inst.*, vol. 95, no. 10, 2003, doi: 10.1093/jnci/95.10.741.

[401] C. Kellner, A. Otte, E. Cappuzzello, K. Klausz, and M. Peipp, "Modulating Cytotoxic Effector Functions by Fc Engineering to Improve Cancer Therapy," 2017. doi: 10.1159/000479980.

[402] E. Vivier, L. Rebuffet, E. Narni-Mancinelli, S. Cornen, R. Y. Igarashi, and V. R. Fantin, "Natural killer cell therapies," Feb. 22, 2024, *Nature Research*. doi: 10.1038/s41586-023-06945-1.

[403] S. K. Kim and S. W. Cho, "The Evasion Mechanisms of Cancer Immunity and Drug Intervention in the Tumor Microenvironment," 2022. doi: 10.3389/fphar.2022.868695.

[404] G. Leclercq, N. Steinhoff, H. Haegel, D. De Marco, M. Bacac, and C. Klein, "Novel strategies for the mitigation of cytokine release syndrome induced by T cell engaging therapies with a focus on the use of kinase inhibitors," 2022, *Taylor and Francis Ltd.* doi: 10.1080/2162402X.2022.2083479.

[405] C. W. Freyer and D. L. Porter, "Cytokine release syndrome and neurotoxicity following CAR T-cell therapy for hematologic malignancies," *J. Allergy Clin. Immunol.*, 2020, doi: 10.1016/j.jaci.2020.07.025.

[406] M. Cosenza, S. Sacchi, and S. Pozzi, "Cytokine release syndrome associated with T-cell-based therapies for hematological malignancies: Pathophysiology, clinical presentation, and treatment," Jul. 02, 2021, *MDPI*. doi: 10.3390/ijms22147652.

[407] S. Pinto, J. Pahl, A. Schottelius, P. J. Carter, and J. Koch, "Reimagining antibody-dependent cellular cytotoxicity in cancer: the potential of natural killer cell engagers," Nov. 01, 2022, *Elsevier Ltd*. doi: 10.1016/j.it.2022.09.007.

[408] P. Minetto *et al.*, "Harnessing NK Cells for Cancer Treatment," 2019. doi: 10.3389/fimmu.2019.02836.

[409] F. Cichocki *et al.*, "iPSC-derived NK cells maintain high cytotoxicity and enhance in vivo tumor control in concert with T cells and anti–PD-1 therapy," *Sci. Transl. Med.*, 2020, doi: 10.1126/scitranslmed.aaz5618.

[410] A. Saxena and D. Wu, "Advances in therapeutic Fc engineering - modulation of IgG-associated effector functions and serum half-life," 2016. doi: 10.3389/fimmu.2016.00580.

[411] M. Amann *et al.*, "WO2021255138 - IMMUNE ACTIVATING FC DOMAIN BINDING MOLECULES," WO/2021/255138, 2021 [Online]. Available: https://patentscope.wipo.int/search/en/detail.jsf?docId=WO2021255138

[412] C. Chong, G. Coukos, and M. Bassani-Sternberg, "Identification of tumor antigens with immunopeptidomics," Feb. 01, 2022, *Nature Research*. doi: 10.1038/s41587-021-01038-8.

[413] V. Leko and S. A. Rosenberg, "Identifying and Targeting Human Tumor Antigens for T Cell-Based Immunotherapy of Solid Tumors," 2020. doi: 10.1016/j.ccell.2020.07.013.

[414] I. J. Chen *et al.*, "Selective antibody activation through protease-activated pro-antibodies that mask binding sites with inhibitory domains," *Sci. Rep.*, 2017, doi: 10.1038/s41598-017-11886-7.

[415] A. Elter *et al.*, "Protease-Activation of Fc-Masked Therapeutic Antibodies to Alleviate Off-Tumor Cytotoxicity," *Front. Immunol.*, 2021, doi: 10.3389/fimmu.2021.715719.

[416] W. W. Lin, Y. C. Lu, C. H. Chuang, and T. L. Cheng, "Ab locks for improving the selectivity and safety of antibody drugs," Jun. 25, 2020, *NLM (Medline)*. doi: 10.1186/s12929-020-00652-z.

[417] Y. Liu, A. W. Nguyen, and J. A. Maynard, "Engineering antibodies for conditional activity in the solid tumor microenvironment," 2022. doi: 10.1016/j.copbio.2022.102809.

[418] V. H. Trang *et al.*, "A coiled-coil masking domain for selective activation of therapeutic antibodies," *Nat. Biotechnol.*, vol. 37, no. 7, pp. 761–765, Jul. 2019, doi: 10.1038/s41587-019-0135-x.

[419] G. A. Weiland and P. B. Molinoff, "Quantitative analysis of drug-receptor interactions: I. Determination of kinetic and equilibrium properties," *Life Sci.*, 1981, doi: 10.1016/0024-3205(81)90324-6.

[420] G. Fucà, A. Spagnoletti, M. Ambrosini, F. de Braud, and M. Di Nicola, "Immune cell engagers in solid tumors: promises and challenges of the next generation immunotherapy," Feb. 01, 2021, *Elsevier B.V.* doi: 10.1016/j.esmoop.2020.100046.

[421] M. Ranson and S. Wardell, "Gefitinib, a novel, orally administered agent for the treatment of cancer," 2004. doi: 10.1111/j.1365-2710.2004.00543.x.

[422] D. W. Rusnak *et al.*, "The effects of the novel, reversible epidermal growth factor receptor/ErbB-2 tyrosine kinase inhibitor, GW2016, on the growth of human normal and tumor-derived cell lines in vitro and in vivo," *Mol. Cancer Ther.*, vol. 1, no. 2, 2001.

[423] D. W. Rusnak *et al.*, "The characterization of novel, dual ErbB-2/EGFR, tyrosine kinase inhibitors: Potential therapy for cancer," *Cancer Res.*, 2001.

[424] H. Wang *et al.*, "Advances in Prostate-Specific Membrane Antigen (PSMA)-Targeted Phototheranostics of Prostate Cancer," 2022. doi: 10.1002/sstr.202200036.

[425] K. T. Chen and Y. Seimbille, "New Developments in Carbonic Anhydrase IX-Targeted Fluorescence and Nuclear Imaging Agents," 2022. doi:

10.3390/ijms23116125.

[426] T. Lindner, F. L. Giesel, C. Kratochwil, and S. E. Serfling, "Radioligands targeting fibroblast activation protein (FAP)," 2021. doi: 10.3390/cancers13225744.

[427] P. S. Low and S. A. Kularatne, "Folate-targeted therapeutic and imaging agents for cancer," 2009. doi: 10.1016/j.cbpa.2009.03.022.

[428] G. Casi and D. Neri, "Antibody-Drug Conjugates and Small Molecule-Drug Conjugates: Opportunities and Challenges for the Development of Selective Anticancer Cytotoxic Agents," 2015. doi: 10.1021/acs.jmedchem.5b00457.

[429] A. Stank, D. B. Kokh, J. C. Fuller, and R. C. Wade, "Protein Binding Pocket Dynamics," *Acc. Chem. Res.*, 2016, doi: 10.1021/acs.accounts.5b00516.

[430] R. Nussinov and C.-J. Tsai, "The Different Ways through Which Specificity Works in Orthosteric and Allosteric Drugs," *Curr. Drug Metab.*, vol. 18, no. 9, 2012, doi: 10.2174/138920012799362855.

[431] S. Usman, M. Khawer, S. Rafique, Z. Naz, and K. Saleem, "The current status of anti-GPCR drugs against different cancers," 2020. doi: 10.1016/j.jpha.2020.01.001.

[432] J. Duan, X. H. He, S. J. Li, and H. E. Xu, "Cryo-electron microscopy for GPCR research and drug discovery in endocrinology and metabolism," 2024. doi: 10.1038/s41574-024-00957-1.

[433] J. Park, C. J. Langmead, and D. M. Riddy, "New Advances in Targeting the Resolution of Inflammation: Implications for Specialized Pro-Resolving Mediator GPCR Drug Discovery," 2020. doi: 10.1021/acsptsci.9b00075.

[434] C. J. Hutchings, M. Koglin, and F. H. Marshall, "Therapeutic antibodies directed at G protein-coupled receptors," 2010. doi: 10.4161/mabs.2.6.13420.

[435] L. Ledsgaard, M. Kilstrup, A. Karatt-Vellatt, J. McCafferty, and A. H. Laustsen, "Basics of antibody phage display technology," 2018. doi: 10.3390/toxins10060236.

[436] D. Wacker, R. C. Stevens, and B. L. Roth, "How Ligands Illuminate GPCR Molecular Pharmacology," 2017. doi: 10.1016/j.cell.2017.07.009.

[437] A. M. Hummer, B. Abanades, and C. M. Deane, "Advances in computational structure-based antibody design," 2022. doi: 10.1016/j.sbi.2022.102379.

[438] R. Cowan and P. A. Underwood, "Steric effects in antibody reactions with polyvalent antigen," *J. Theor. Biol.*, vol. 132, no. 3, 1988, doi: 10.1016/S0022-5193(88)80218-2.

[439] G. M. Mortimer and R. F. Minchin, "Cryptic epitopes and functional diversity in extracellular proteins," 2016. doi: 10.1016/j.biocel.2016.10.020.

[440] M. C. Panelli *et al.*, "A Tumor-Infiltrating Lymphocyte from a Melanoma Metastasis with Decreased Expression of Melanoma Differentiation Antigens Recognizes MAGE-12," *J. Immunol.*, vol. 164, no. 8, 2000, doi: 10.4049/jimmunol.164.8.4382.

[441] R. C. Panicker, S. Chattopadhaya, A. G. Coyne, and R. Srinivasan, "Allosteric small-molecule serine/threonine kinase inhibitors," in *Advances in Experimental Medicine and Biology*, vol. 1163, 2019. doi: 10.1007/978-981-13-8719-7_11.

[442] A. Shen, "Allosteric regulation of protease activity by small molecules," 2010. doi: 10.1039/c003913f.

[443] K. Zuo *et al.*, "Specifically targeting cancer proliferation and metastasis processes: the development of matriptase inhibitors," 2019. doi: 10.1007/s10555-019-09802-8.

[444] M. R. A. Pillai, R. Nanabala, A. Joy, A. Sasikumar, and F. F. Russ Knapp, "Radiolabeled enzyme inhibitors and binding agents targeting PSMA: Effective theranostic tools for imaging and therapy of prostate cancer," 2016. doi: 10.1016/j.nucmedbio.2016.08.006.

[445] C. T. Supuran, "Development of small molecule carbonic anhydrase IX inhibitors," 2008. doi: 10.1111/j.1464-410x.2008.07648.x.

[446] A. S. Wibowo *et al.*, "Structures of human folate receptors reveal biological trafficking states and diversity in folate and antifolate recognition," *Proc. Natl. Acad. Sci. U. S. A.*, 2013, doi: 10.1073/pnas.1308827110.

[447] S. Notaro *et al.*, "Evaluation of folate receptor 1 (FOLR1) mRNA expression, its specific promoter methylation and global DNA hypomethylation in type I and type II ovarian cancers," *BMC Cancer*, vol. 16, no. 1, 2016, doi: 10.1186/s12885-016-2637-y.

[448] L. C. Hartmann *et al.*, "Folate receptor overexpression is associated with poor outcome in breast cancer," *Int. J. Cancer*, 2007, doi: 10.1002/ijc.22811.

[449] A. Puig-Kröger *et al.*, "Folate receptor β is expressed by tumor-associated macrophages and constitutes a marker for M2 anti-inflammatory/regulatory Macrophages," *Cancer Res.*, 2009, doi: 10.1158/0008-5472.CAN-09-2050.

[450] W. Xia, A. R. Hilgenbrink, E. L. Matteson, M. B. Lockwood, J. X. Cheng, and P. S. Low, "A functional folate receptor is induced during macrophage activation and can be used to target drugs to activated macrophages," *Blood*, 2009, doi: 10.1182/blood-2008-04-150789.

[451] M. W. G. Miner *et al.*, "High folate receptor expression in gliomas can be detected in vivo using folate-based positron emission tomography with high tumor-to-brain uptake ratio divulging potential future targeting possibilities," *Front. Immunol.*, vol. 14, 2023, doi: 10.3389/fimmu.2023.1145473.

[452] A. D. Newton, J. D. Predina, L. G. Frenzel-Sulyok, P. S. Low, S. Singhal, and R. E. Roses, "Intraoperative Molecular Imaging Utilizing a Folate Receptor-Targeted Near-Infrared Probe Can Identify Macroscopic Gastric Adenocarcinomas," *Mol. Imaging Biol.*, 2021, doi: 10.1007/s11307-020-01549-x.

[453] L. M. Randall, R. M. Wenham, P. S. Low, S. C. Dowdy, and J. L. Tanyi, "A phase II, multicenter, open-label trial of OTL38 injection for the intra-operative imaging of folate receptor-alpha positive ovarian cancer," *Gynecol. Oncol.*, 2019, doi: 10.1016/j.ygyno.2019.07.010.

[454] C. J. Mathias, S. Wang, R. J. Lee, D. J. Waters, P. S. Low, and M. A. Green, "Tumor-Selective

Radiopharmaceutical Targeting via Receptor-Mediated Endocytosis of Gallium-67-Deferoxamine-Folate," *J. Nucl. Med.*, vol. 37, no. 6, 1996.

[455] A. X. Zhang *et al.*, "A Remote arene-binding site on prostate specific membrane antigen revealed by antibody-recruiting small molecules," *J. Am. Chem. Soc.*, vol. 132, no. 36, 2010, doi: 10.1021/ja104591m.

[456] C. G. Parker, R. A. Domaoal, K. S. Anderson, and D. A. Spiegel, "An antibody-recruiting small molecule that targets HIV gp120," *J. Am. Chem. Soc.*, vol. 131, no. 45, 2009, doi: 10.1021/ja9057647.

[457] C. E. Jakobsche, P. J. McEnaney, A. X. Zhang, and D. A. Spiegel, "Reprogramming urokinase into an antibody-recruiting anticancer agent," *ACS Chem. Biol.*, vol. 7, no. 2, 2012, doi: 10.1021/cb200374e.

[458] R. I. Pinhassi *et al.*, "Arabinogalactan-folic acid-drug conjugate for targeted delivery and target-activated release of anticancer drugs to folate receptor-overexpressing cells," *Biomacromolecules*, vol. 11, no. 1, 2010, doi: 10.1021/bm900853z.

[459] Y. Lu *et al.*, "Preclinical pharmacokinetics, tissue distribution, and antitumor activity of a folate-hapten conjugate-targeted immunotherapy in hapten-immunized mice," *Mol. Cancer Ther.*, vol. 5, no. 12, 2006, doi: 10.1158/1535-7163.MCT-06-0439.

[460] Y. G. Lee *et al.*, "Regulation of CAR T cell-mediated cytokine release syndrome-like toxicity using low molecular weight adapters," *Nat. Commun.*, vol. 10, no. 1, Dec. 2019, doi: 10.1038/s41467-019-10565-7.

[461] Y. J. Lu *et al.*, "Preclinical evaluation of bispecific adaptor molecule controlled folate receptor CAR-T cell therapy with special focus on pediatric malignancies," *Front. Oncol.*, 2019, doi: 10.3389/fonc.2019.00151.

[462] C. M. Albert *et al.*, "ENLIGHten-01: A phase 1 study of fluorescein-specific (FITC-E2)-CAR T cells in combination with folate-fluorescein (UB-TT170) for osteosarcoma.," *J. Clin. Oncol.*, vol. 41, no. 16_suppl, 2023, doi: 10.1200/jco.2023.41.16_suppl.tps11581.

[463] G. Z. Ferl, F. P. Theil, and H. Wong, "Physiologically based pharmacokinetic models of small molecules and therapeutic antibodies: A mini-review on fundamental concepts and applications," *Biopharm. Drug Dispos.*, 2016, doi: 10.1002/bdd.1994.

[464] R. G. Strickley and W. J. Lambert, "A review of Formulations of Commercially Available Antibodies," 2021. doi: 10.1016/j.xphs.2021.03.017.

[465] J. Li *et al.*, "Membrane-Proximal Epitope Facilitates Efficient T Cell Synapse Formation by Anti-FcRH5/CD3 and Is a Requirement for Myeloma Cell Killing," *Cancer Cell*, 2017, doi: 10.1016/j.ccell.2017.02.001.

[466] K. D. Orcutt *et al.*, "Engineering an antibody with picomolar affinity to DOTA chelates of multiple radionuclides for pretargeted radioimmunotherapy and imaging," *Nucl. Med. Biol.*, vol. 38, no. 2, 2011, doi: 10.1016/j.nucmedbio.2010.08.013.

[467] A. Piatesi and D. Hilvert, "Immunological optimization of a generic hydrophobic pocket for high affinity hapten binding and Diels-Alder activity," *ChemBioChem*, 2004, doi: 10.1002/cbic.200300806.

[468] N. Kobayashi, T. Karibe, and J. Goto, "Dissociation-independent selection of high-affinity anti-hapten phage antibodies using cleavable biotin-conjugated haptens," *Anal. Biochem.*, 2005, doi: 10.1016/j.ab.2005.09.016.

[469] E. T. Boder, K. S. Midelfort, and K. D. Wittrup, "Directed evolution of antibody fragments with monovalent femtomolar antigen-binding affinity," *Proc. Natl. Acad. Sci. U. S. A.*, 2000, doi: 10.1073/pnas.170297297.

[470] M. M. Al Qaraghuli, S. Palliyil, G. Broadbent, D. C. Cullen, K. A. Charlton, and A. J. Porter, "Defining the complementarities between antibodies and haptens to refine our understanding and aid the prediction of a successful binding interaction," *BMC Biotechnol.*, 2015, doi: 10.1186/s12896-015-0217-x.

[471] D. Tsikas, "Acetazolamide and human carbonic anhydrases: retrospect, review and discussion of an intimate relationship," 2024. doi: 10.1080/14756366.2023.2291336.

[472] J. W. Lee, "ADME of monoclonal antibody biotherapeutics: Knowledge gaps and emerging tools," 2013. doi: 10.4155/bio.13.144.

[473] M. Hilvo, M. Rafajová, S. Pastoreková, J. Pastorek, and S. Parkkila, "Expression of Carbonic Anhydrase IX in Mouse Tissues," *J. Histochem. Cytochem.*, 2004, doi: 10.1177/002215540405201007.

[474] M. Takacova *et al.*, "Carbonic anhydrase IX—mouse versus human," *Int. J. Mol. Sci.*, 2020, doi: 10.3390/ijms21010246.

[475] R. J. Scheibe *et al.*, "Expression of membrane-bound carbonic anhydrases IV, IX, and XIV in the mouse heart," *J. Histochem. Cytochem.*, 2006, doi: 10.1369/jhc.6A7003.2006.

[476] K. Kaunisto, S. Parkkila, H. Rajaniemi, A. Waheed, J. Grubb, and W. S. Sly, "Carbonic anhydrase XIV: Luminal expression suggests key role in renal acidification," *Kidney Int.*, 2002, doi: 10.1046/j.1523-1755.2002.00371.x.

[477] P. Halmi, J. Lehtonen, A. Waheed, W. S. Sly, and S. Parkkila, "Expression of Hypoxia-Inducible, Membrane-Bound Carbonic Anhydrase Isozyme XII in Mouse Tissues," *Anat. Rec. - Part A Discov. Mol. Cell. Evol. Biol.*, 2004, doi: 10.1002/ar.a.20001.

[478] S. Chakravarty and K. K. Kannan, "Drug-protein interactions. Refined structures of three sulfonamide drug complexes of human carbonic anhydrase I enzyme," *J. Mol. Biol.*, 1994, doi: 10.1006/jmbi.1994.1655.

[479] M. T. B. Clabbers, S. Z. Fisher, M. Coinçon, X. Zou, and H. Xu, "Visualizing drug binding interactions using microcrystal electron diffraction," *Commun. Biol.*, 2020, doi: 10.1038/s42003-020-01155-1.

[480] K. H. Sippel, A. H. Robbins, J. Domsic, C. Genis, M. Agbandje-Mckenna, and R. McKenna, "High-resolution structure of human carbonic anhydrase II complexed with acetazolamide reveals insights into inhibitor drug design," *Acta Crystallogr. Sect. F Struct. Biol. Cryst. Commun.*, 2009, doi: 10.1107/S1744309109036665.

[481] V. Alterio *et al.*, "The structural comparison between membrane-associated human carbonic anhydrases provides insights into drug design of selective inhibitors," *Biopolymers*, 2014, doi:

10.1002/bip.22456.

[482] J. Y. Winum *et al.*, "Carbonic anhydrase inhibitors. Inhibition of isoforms I, II, IV, VA, VII, IX, and XIV with sulfonamides incorporating fructopyranose-thioureido tails," *Bioorganic Med. Chem. Lett.*, 2007, doi: 10.1016/j.bmcl.2007.03.008.

[483] D. A. Whittington *et al.*, "Crystal structure of the dimeric extracellular domain of human carbonic anhydrase XII, a bitopic membrane protein overexpressed in certain cancer tumor cells," *Proc. Natl. Acad. Sci. U. S. A.*, 2001, doi: 10.1073/pnas.161301298.

[484] A. Di Fiore *et al.*, "Crystal structure of human carbonic anhydrase XIII and its complex with the inhibitor acetazolamide," *Proteins Struct. Funct. Bioinforma.*, 2009, doi: 10.1002/prot.22144.

[485] C. T. Supuran, "Carbonic anhydrases: Novel therapeutic applications for inhibitors and activators," 2008. doi: 10.1038/nrd2467.

[486] L. Lucaroni *et al.*, "Cross-reactivity to glutamate carboxypeptidase III causes undesired salivary gland and kidney uptake of PSMA-targeted small-molecule radionuclide therapeutics," *Eur. J. Nucl. Med. Mol. Imaging*, vol. 50, no. 3, 2023, doi: 10.1007/s00259-022-05982-8.

[487] Z. Lee, W. D. Heston, X. Wang, and J. P. Basilion, "GCP III is not the 'off-target' for urea-based PSMA ligands," 2023. doi: 10.1007/s00259-023-06265-6.

[488] G. Bassi *et al.*, "Response to: GCP III is not the 'off-target' for urea-based PSMA-ligands," 2023. doi: 10.1007/s00259-023-06302-4.

[489] C. Fu *et al.*, "P1406: SAFETY AND EFFICACY OF IBI346, A FIRST-IN-CLASS BCMA-TARGETING MODULAR CAR-T CELL THERAPY, FOR PATIENTS WITH RELAPSED/REFRACTORY MULTIPLE MYELOMA (RRMM): PRELIMINARY RESULTS FROM TWO PHASE I STUDIES," *HemaSphere*, vol. 7, no. Suppl, p. e534971f, Aug. 2023, doi: 10.1097/01.HS9.0000972512.53497.1F.

[490] S. Qin *et al.*, "1054P A phase Ia study to evaluate the safety, tolerability, pharmacokinetics and preliminary efficacy of a modular CLDN18.2-targeting PG CAR-T therapy (IBI345) in patients with CLDN18.2+ solid tumors," *Ann. Oncol.*, 2023, doi: 10.1016/j.annonc.2023.09.2193.

[491] J. Y. Spiegel *et al.*, "CAR T cells with dual targeting of CD19 and CD22 in adult patients with recurrent or refractory B cell malignancies: a phase 1 trial," *Nat. Med.*, vol. 27, no. 8, 2021, doi: 10.1038/s41591-021-01436-0.

[492] G. Wei *et al.*, "CD19/CD22 dual-targeted car t-cell therapy for relapsed/refractory aggressive b-cell lymphoma: A safety and efficacy study," *Cancer Immunol. Res.*, vol. 9, no. 9, 2021, doi: 10.1158/2326-6066.CIR-20-0675.

[493] S. Tu *et al.*, "CD19 and CD70 Dual-Target Chimeric Antigen Receptor T-Cell Therapy for the Treatment of Relapsed and Refractory Primary Central Nervous System Diffuse Large B-Cell Lymphoma," *Front. Oncol.*, vol. 9, 2019, doi: 10.3389/fonc.2019.01350.

[494] M. Ruella and M. V. Maus, "Catch me if you can: Leukemia Escape after CD19-Directed T Cell Immunotherapies," 2016. doi: 10.1016/j.csbj.2016.09.003.

[495] C. F. de Larrea *et al.*, "Defining an Optimal Dual-Targeted CAR T-cell Therapy Approach Simultaneously Targeting BCMA and GPRC5D to Prevent BCMA Escape–Driven Relapse in Multiple Myeloma," *Blood Cancer Discov.*, vol. 1, no. 2, 2020, doi: 10.1158/2643-3230.BCD-20-0020.

[496] M. Hutchings *et al.*, "Glofitamab, a Novel, Bivalent CD20-Targeting T-Cell-Engaging Bispecific Antibody, Induces Durable Complete Remissions in Relapsed or Refractory B-Cell Lymphoma: A Phase I Trial," *Commun. J Clin Oncol*, vol. 39, pp. 1959–1970, 2021, doi: 10.1200/JCO.20.

10. Acknowledgements

Christian Klein

Dear Christian, it was during my internship in your department in 2016-17 when I saw cancer immunotherapy that I fell in love with. I observed the discussions between you and all the scientists, the motivation and critical thinking, and promised to myself that I will do everything in my power to one day be a part of that. After a lot of work, a Master's degree, and strategizing, I was ready to ask you to take me on as a PhD student, and you happily agreed. So firstly, thank you for letting me in, because I got my dream job that day. Secondly, I want to express so much gratitude that I cannot put into words - for being so kind, respectful and understanding in this PhD endeavor. You did all that while retaining high expectations, with which you motivated me further. Thank you for sharing your knowledge with me. Thank you for your trust when presenting in front of small and big audiences, when writing patents, when doing short- and long-term experimental plans. Thank you for giving me responsibilities, as if I was ready even at the beginning - because of that I became ready. Thank you for your down-to-earth approach to scientific and work problems. So many of these moments seemed to be enormous storms for my young mind, but every time your response was so calm. I saw that these situations were mere bumps in the road for you, and it gave me courage to treat them as bumps in the road too - growing my resilience and preparing me for the future roads. I also appreciate, and always have, you going out of your own way to treat people with great respect and appreciation, regardless of their standing in hierarchy. I am also in awe of your scientific brilliance combined with so much humility. It will remain a big inspiration for my further development. I consider myself extremely lucky for an opportunity to work with such a scientist and such a person – so, thank you.

Roche Innovation Center Zurich

I would like to express my utmost gratitude to Roche Innovation Center Zurich / Roche Glycart for funding this research and providing me with so many opportunities for growth and learnings from brilliant scientists around me.

Joerg Benz, Andres Ehler, Antonio Ricci, Moreno Wichert, Daniela Matscheko, Theresa Kober, Jose Bonfiglio, Andrzej Sobieniecki

I would like to share my gratitude for Joerg Benz, Andres Ehler, Antonio Ricci, Moreno Wichert, Daniela Matscheko, Theresa Kober, Jose Bonfiglio and Andrzej Sobieniecki for so enthusiastically agreeing to collaborate together, always offering their time, expertise, interesting questions, and above all, always being ready to help. As a young student, I was hesitant to bother my busy colleagues with my requests for collaboration. But you all have been so welcoming and excited about the science and working together. I had then no choice but to drop my hesitation, find confidence in asking for help and being able to focus on our common scientific goals. It was very enjoyable and fulfilling to work together – a huge thank you.

Pablo Umaña

My deepest gratitude is also sent to Pablo Umaña, for being such an exceptional leader and a scientific inspiration. Pablo, you created this place from ground up, and made it to such an exceptional site, full of patient-caring scientists with brilliant minds and – above all – with care for each other beyond office and laboratory walls. Before coming here, I did not know such a workplace was possible. I planned to come only for 6 months as an intern, and here we are 8.5 years later. I spent most of my 20s at Roche Glycart, working in different positions, and was grateful every day for the opportunity to be here. My formative years as a as a scientist, and as a human, took place at this site. Without you crafting the teams and work this way, it would not have been possible. Thank you for building and caring for this site, creating the exceptional atmosphere and showing us how a leader can be mission-driven, unstoppable, business-savvy, scientifically brilliant, and empathetic at the same time. Roche Glycart, with you leading it, will always have a special place in my heart.

PTE unit

Dear Sylvia, Marina, Gabrielle and team, I am beyond grateful that you took me in as a fresh scientist to work in your group, while finishing up my PhD at the same time. The past months have been so busy, but also very motivating, extremely intellectually stimulating, and also simply fun. I could not have asked for a better finishing line.

Maria Amann and Sylvia Herter

Dear Maria and Sylvia, in the last stressful weeks of my PhD, you took me under your wings and fought for my ability to continue my research. I cannot stress it enough – to know I am in such good hands gave me a lot of peace in this hectic time. It is wonderful seeing how unstoppable you are, together with the care you have for people. The people under your leadership are lucky to have you. Thank you so much.

Dario Venetz

Dear Dario, thank you for guiding me in my scientific endeavors, and sharing your knowledge and creativity. It was a pleasure to work together and share the commitment to science.

Diana Darowski

Dear Diana, thank you for passing me the torch while you were closing the PhD chapter for yourself. Thank you for establishing the PhD community, your mental support through this journey, your encouragement. I would be happy if our work paths cross together again.

Johannes Sam

Dear Johannes, while our collaborations happened only a few times, I always sensed your strong enthusiasm and curiosity in our discussions. This, in turn had an impact on my own motivation rising, and gave me confidence that I might be doing things right. More than that - during times of stress, you have been nothing but a rock in the middle of a stormy sea. You went out of your way to be present, give guidance, give rational feedback and help me. You did not have to, but you were there – and I am so deeply grateful for that.

RICZ, RICB, RICM colleagues and the PhD community

Dear colleagues from past and present, you made this journey an exceptionally precious time in my life. I learned so much from you, so thank you for sharing your scientific expertise, mentoring advice and giving me an example of wonderful teamwork and caring leadership. Special thank you to my RICZ colleagues, from 2016 until now, thanks to whom I managed to have the best months-long times of my life (three times!) during my internships and PhD. I also want to thank the PhD community, who has been an infinite source of fun, intellectually stimulating discussions, and support. I am grateful to have worked alongside you. I would also like to thank Brenda Gaillard, Florian Limani and Roberto Adelfio for always making work and after work such an amazingly enjoyable time.

Denis Assisi

Dear Denis, I will always miss our cell culture parties, our library support sessions, and your mentoring. My deepest thank you for being my supervisor, then my colleague, then my close friend. You were a very big part of why I never wanted to leave Roche once I joined. Your drive and mission, expertise, curiosity, readiness to help and empathy are so unique. Thank you for your patience, for teaching me and accompanying me in my growth from a young intern to a scientist I am today. Thank you for making the work so special, and for so selflessly giving your unwavering support over the years. I am stronger thanks to you.

Ali Bransi

Dear Ali, let me start by thanking you for taking me on as an intern back in 2016, and teaching me all these scientific topics over the years. I had a fantastic time working with you, Denis and Nina, which undoubtedly led me to commit to cancer immunotherapy field. Thank you for your trust and taking me on again as a Master thesis student back in 2019. And thank you for encouraging me to do the PhD and welcoming me to the lab – once again. I always felt so safe and welcome in the team, it has felt really like home and being surrounded by friends who have nothing but good intentions for each other and for patients.

Maria Karagianni

Dear Maria, you first had an impact on me during my first month as a PhD student, when you advised me to surf the wave of my imposter syndrome. I have been surfing with joy ever since. Your well-intentioned heart, resilience and drive to help others have paved the way for me, and lightened the dark roads I had to pass through before getting to this moment. Our shared PhD struggles brought us together – what a valuable silver lining. Huge thank you for being you and helping me in my journey.

Gabrielle Leclercq, Camilla Trevor, Floriana Cremasco, Lucia Campos Carrascosa

Dear ladies, I will always remember the gentle beginnings of our friendship, bonding over mutual support and together raising the standards for the quality of science we all do. Thank you for the memories of the time spent together, either enjoying aperos or bumping to each other by the FACS or the nanodrop machine on the weekend. I appreciate you for your insights into human connections, creating opportunities for each other, your absolute commitment to

science, combined with finding time to truly enjoy life after hours. It was truly special to me to have the chance to spend so much time together with people like you.

Idil Karakoc-Hutter

Dear Idil, you showed up in my life when I was longing to have some impact, and you allowed me to feel that when I got to help you start your project. More than that, you immediately became my discussion partner for science as if we were tailor-made for these moments. Our minds synergize like a well-designed drug combination. Thank you, I cherish you not only for your mind, but for deep care for friends, empathy, and readiness to be the rock they need.

John Challier

Dear John, you have always been the adventure and flavor in my daily life, breaking all stereotypes and giving me the strongest laughs and the loudest tired sighs. You helped me grow from a little intern to a scientist I am today. And I hope I never have to stop bothering you with lab questions, just to keep the sight of your eyes rolling while you happily stand up to help me (while pretending to be reluctant). Your helping ear, our hours in the lab together, and your creative solutions to all life's problems have eased my path tremendously. Thank you.

Marta Requesens Rueda

Dear Marta, from our time as young Master students, to now as almost-PhDs, I have been lucky to have you as my friend. I deeply appreciate your strong goal-setting attitude and strong stances on the quality of science for yourself and those around you. Also, your understanding and empathy of others is so exceptional. So many times, the strength I got was thanks to your support. I cannot express it in words how grateful I am for your friendship. I am looking forward to both of us growing a lot in life and science, side by side.

Agata Geisseler (Kubiak)

Dear Agata, despite your passions and experience laying in another field, I have always felt supported and understood by you, in this PhD endeavor and outside of it. You have shown me the stability and beauty of a long lasting friendship despite, and maybe because, diverging life paths, and the enrichment to the mind it can bring. I am so deeply grateful to have you as my friend.

Wataha z Wrocławia

Dear Kuba, Struna and Brewa, I am beyond happy that biotechnology, chemistry, and student dorms brought us together. You have been a fundamental – and so joyful – part of my life, and I must credit some of my confidence in your belief in me and my goals. I see this memory as if it happened yesterday – you, my crew, walking me to my bus going from Poland to Switzerland, the place which later became my new home, and from where I never came back. And yet, whenever I come to visit, you make me feel home again. Thank you for being part of my life, and for being proud of me. It means the world to me.

Przyjaciele z Gliwic

Dear Kasia, Dudek and Edek, I am so deeply grateful that our friendship has been continuing and growing for so many years. It is you who has seen me attempt to figure out my life as a teenager, and accomplish my biggest dreams now as an adult. I have always, truly always, felt support from you. Thank you for listening to me sharing my excitement about my work so much, for being so happy for me, for rooting for me along the (long) way. Especially Kasia i Edek, I may have never told you this, but my mission, what I do, is in big part dedicated to you.

11. Appendix

11.1. Appendix I. Review publication I: *Ten years in the making: application of CrossMab technology for the development of therapeutic bispecific antibodies and antibody fusion proteins*

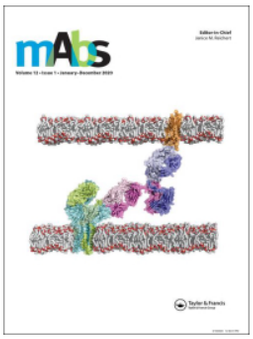

mAbs

ISSN: (Print) (Online) Journal homepage: www.tandfonline.com/journals/kmab20

Ten years in the making: application of CrossMab technology for the development of therapeutic bispecific antibodies and antibody fusion proteins

Marlena Surowka, Wolfgang Schaefer & Christian Klein

To cite this article: Marlena Surowka, Wolfgang Schaefer & Christian Klein (2021) Ten years in the making: application of CrossMab technology for the development of therapeutic bispecific antibodies and antibody fusion proteins, mAbs, 13:1, 1967714, DOI: 10.1080/19420862.2021.1967714

To link to this article: https://doi.org/10.1080/19420862.2021.1967714

Published online: 07 Sep 2021.

MABS
2021, VOL. 13, NO. 1, e1967714 (17 pages)
https://doi.org/10.1080/19420862.2021.1967714

Taylor & Francis
Taylor & Francis Group

REVIEW

OPEN ACCESS Check for updates

Ten years in the making: application of CrossMab technology for the development of therapeutic bispecific antibodies and antibody fusion proteins

Marlena Surowka[a], Wolfgang Schaefer[b], and Christian Klein[a]

[a]Roche Innovation Center Zurich, Schlieren, Switzerland; [b]Roche Innovation Center Munich, Penzberg, Germany

ABSTRACT

Bispecific antibodies have recently attracted intense interest. CrossMab technology was described in 2011 as novel approach enabling correct antibody light-chain association with their respective heavy chain in bispecific antibodies, together with methods enabling correct heavy-chain association using existing pairs of antibodies. Since the original description, CrossMab technology has evolved in the past decade into one of the most mature, versatile, and broadly applied technologies in the field, and nearly 20 bispecific antibodies based on CrossMab technology developed by Roche and others have entered clinical trials. The most advanced of these are the Ang-2/VEGF bispecific antibody faricimab, currently undergoing regulatory review, and the CD20/CD3 T cell bispecific antibody glofitamab, currently in pivotal Phase 3 trials. In this review, we introduce the principles of CrossMab technology, including its application for the generation of bi-/multispecific antibodies with different geometries and mechanisms of action, and provide an overview of CrossMab-based therapeutics in clinical trials.

ARTICLE HISTORY
Received 15 July 2021
Revised 3 August 2021
Accepted 10 August 2021

KEYWORDS
Bispecific; CrossMab; Immunotherapy; Oncology; Ophthalmology; TCB; T cell engager

Introduction into bispecific antibodies

Antibodies, or so-called immunoglobulins, are Y-shaped proteins of ca. 150 kDa generated by B and plasma cells of the immune system as response to infection. They consist of two identical heavy and two identical light chains forming: 1) two variable antigen-binding sites within the antigen-binding fragments (Fabs) that serve for the specific recognition of (foreign) antigens; and 2) a constant Fc domain that serves for the recruitment of the human immune system.

Recombinant antibodies have been used therapeutically for over 30 years, and today more than 120 therapeutic antibodies are approved or under regulatory review by health authorities for use in humans (source: https://www.antibodysociety.org/resources/approved-antibodies/). Since the advent of recombinant antibody technologies, there has been substantial interest in the generation of engineered and bispecific antibodies that are characterized by having two independent specificities in the Fabs, resulting in novel mechanisms of action that typically cannot be achieved with conventional monospecific antibodies. More than 100 bispecific antibodies are currently being tested in clinical trials.[1–6]

While uncountable approaches for the generation of bispecific antibodies have been described, [1–6] some of the most broadly applied technologies for the generation of bispecific antibodies include ART-Ig,[7–10] BEAT,[11] BiTE,[12,13] common light chains,[9,10,14–16] DAF,[17] DART,[18] DuoBody,[19] DutaFab,[20] DVD-Ig,[21] Fab arm exchange,[22] Fcab,[23–25] FORCE,[26] half antibody assembly,[27] Hetero-Ig,[28,29] IgG-scFv,[3031,131] κλ-bodies,[32] Multiclonics,[14] orthogonal Fab interface,[33] Tandab,[34] XmAb,[35] VELOCI-Bi,[15] and WuxiBODY.[36]

As of August 2021, three bispecific antibodies have been approved, the tandem single-chain variable fragment (Fv)-based CD19/CD3 Bispecific T-cell Engager (BiTE) blinatumomab developed by Amgen for the treatment of acute lymphocytic leukemia (ALL),[37] the heterodimeric ART-Ig-based coagulation factor IX/X bispecific IgG antibody emicizumab developed by Chugai and Roche for the treatment of hemophilia A,[7,8,10] and the heterodimeric DuoBody-based EGFR/c-Met bispecific IgG antibody amivantamab developed by Janssen for treatment of non-small cell lung cancer harboring EGFR exon 20 insertion mutations.[38–40]

CrossMab technology for the generation of bispecific antibodies

We have developed an alternative technology, known as CrossMab technology, which together with methods enabling correct heavy-chain association such as the so-called knobs-into-holes technology (KiH),[16] that enables the correct association of the different antibody light chains with their respective counterparts. This is achieved in different antibody formats and geometries by the exchange or crossover of antibody domains.[41–43] Here, we give a brief overview of the basic principles of CrossMab technology and its application for the generation of various CrossMabs with different molecular formats and mechanisms of action.[42,44,45] In fact, back in 2011, this approach was the first technology described allowing the conversion of two pre-existing antibodies into heterodimeric bispecific antibodies of the bivalent

CONTACT Christian Klein christian.klein.ck1@roche.com Roche Innovation Center Zurich, Roche Pharma Research & Early Development, Roche Glycart AG, Wagistrasse 10, 8952, Schlieren, Switzerland

IgG format without the need to rely on so-called common light-chain antibodies that have identical light chains in each Fab.[42]

Since in bispecific antibodies the two heavy chains as well as the two light chains are different and can randomly associate, expression of these four chains leads to the formation of ten different antibody variants.[46] Correct heavy-chain association resulting in a heterodimeric Fc can be enforced using KiH technology by introducing a bulky tryptophan (Trp) residue in one Fc fragment and forming a corresponding cavity on the other Fc fragment that can accommodate the Trp residue.[16,47,48] More recently, multiple alternative approaches to enable correct heavy-chain association have been described, such as relying on charge interactions.[7–11,14,29,49]

Although KiH technology was developed in the late 1990s,[16] enabling correct light-chain association remained a major problem, and the only approach to achieve this at the time relied on the use of common light chains for both specificities.[9,10,14–16] However, the use of a common light chain requires the *de novo* identification of the corresponding antibody pairs, which can be challenging and/or time-consuming depending on the desired target, and restricts the availability and diversity of antibodies that can be used; thus, methods allowing the generation of bispecific antibodies from pre-existing antibody pairs were highly desired.

Figure 1 shows the basic principle of the domain crossover applied in CrossMab technology to enable correct light-chain association in bispecific antibodies.[41] By incorporating the original heavy chain VH-CH1 domains in the Fab of the second specificity of the bispecific antibody as the novel "light chain" and the original light chain VL-CL domains for the novel "heavy chain" by fusing them to the hinge region of the Fc fragment, correct light-chain association can be enforced in the CrossMab^{Fab} format. This format has recently also been described as Fabs-in-Tandem Ig (FIT-Ig).[50,51]

Alternatively, only the VH-VL or only the CH1-CL domains can be exchanged in the CrossMab$^{VH\text{-}VL}$ and CrossMab^{CH1-CL} formats (Figure 1). In the case of the CH1-CL crossover, no theoretical side product due to domain crossover is expected and crystal structure analysis confirmed the structural integrity of the crossed Fab domain in the CrossMab$^{CH11-CL}$ format.[52] In the case of the Fab crossover in the CrossMab^{Fab}, two heavy and light chain-based monovalent side products can be observed. However, the correct preferential formation of the CrossMab^{Fab} can be fostered by relative over-expression of the respective light chains so that the respective undesired monovalent and binding inactive side products do not form in significant amounts. Similarly, in the case of VH-VL crossover, a Bence-Jones-like side product based on VL-VL together with the CH1-CL interaction can be observed. In order to avoid formation of this side product, natural charge pairs in the Fab were identified and the respective orthogonal charge interactions were introduced into the non-exchanged antibody CH1-CL domains.[53] As a consequence, the undesired Bence-Jones-like side product does not form due to repulsive charge interactions, whereas the desired light-chain pairs correctly in the non-crossed Fab due to attractive charge interactions so that the corresponding CrossMab$^{VH\text{-}VL\pm}$ constructs can subsequently be obtained in high yields and purity without major side products.

Notably, these design principles can be applied not only to heterodimeric antibodies where one arm is directed to the first antigen, the other arm to the second antigen (1 + 1 format), but the CrossMab technology also allows generation of so-called MonoMabs, monovalent antibodies with one Fc portion, and DuoMabs, bivalent antibodies with two Fc portions (Figure 1).[54] Furthermore, it can be applied to enable the correct light-chain association in hetero-/homodimeric bi-/multispecific antibody appended or tandem-Fab formats with, for example, 2 + 1, 2 + 2, 3 + 1, 4 + 1 or 4 + 2 valencies and in antibody fusion proteins (Figure 2).[44,45] In line with this, Wu and colleagues from Lilly applied Fab crossover to generate orthogonal Fab-based trispecific antibody formats termed "OrthoTsAbs".[55,56] Interestingly, domain crossover has also been described as a means to prevent mispairing of T-cell receptor (TCR) domains in adoptive T-cell therapy.[57]

Because the CrossMab approach showed advantages in terms of production, stability, developability, and versatility over analogous formats based on either single-chain Fv[58–60] or single-chain Fab[61–67] building blocks, it was ultimately cho-

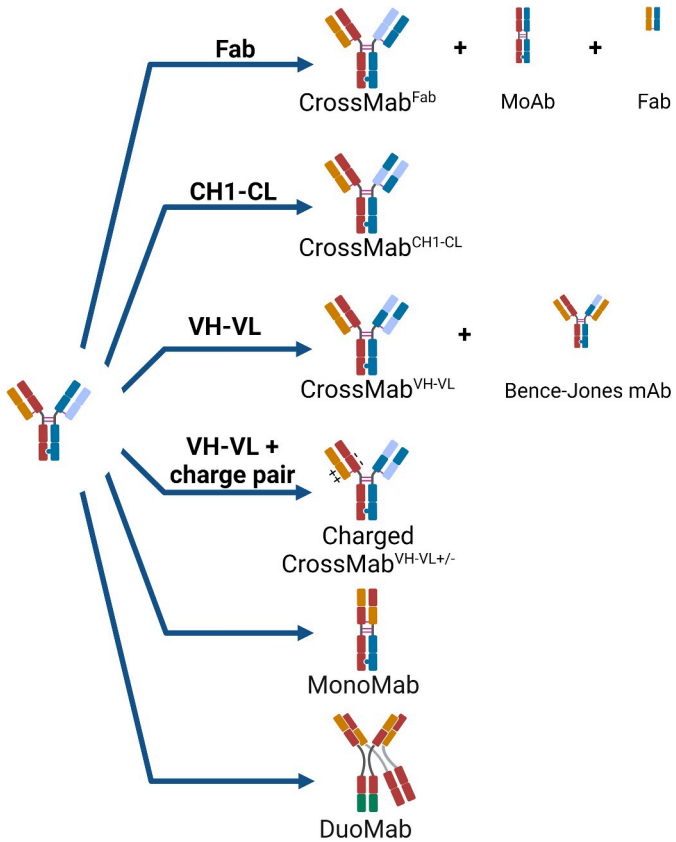

Figure 1. Principles of CrossMab technology: The four major CrossMab formats as applied to 1 + 1 heterodimeric bispecific antibodies are depicted as well as potential side products. On the bottom, the structure of mono- and duomabs is indicated. Heavy-chain domains are depicted in dark colors and respective light-chain domains are depicted with corresponding bright colors. Created with BioRender.com.

sen as the antibody engineering approach of choice for the generation of various clinical development candidates. Obviously, in order to develop CrossMabs for therapeutic use, the establishment of various methods covering CMC (Chemistry, Manufacturing, and Controls) aspects, including upstream and downstream processing (USP, DSP) and the establishment of the respective bioassay and (bio-) analytical methods was and is essential.[68–8081] When considering the formation of (undesired) side products, it has to be taken into account that, independent of CrossMab technology, other unrelated side products can occur, such as half- or ¾-antibodies missing two or one light chains, respectively, or hole-hole/knob-knob heavy-chain homodimers. In order to avoid the formation of these side products, achieving equal expression levels for the four heavy and light chains during transient expression and/or stable cell line generation by selecting suitable clones is advantageous. Based on the general advancement in the field of therapeutic antibody manufacturing, as well as considering these specific learnings, bispecific antibodies of different formats based on CrossMab technology can generally be manufactured in a consistent and reproducible fashion with volumetric yields in the several g/L range and in quality comparable to conventional therapeutic antibodies using established USP and DSP platforms.

Consequently, since the original description of this concept, the technology has evolved in the past decade into one of the most mature, versatile, and broadly applied technologies in the field for the generation of various bispecific antibody formats. As of mid-2021, at least 19 bispecific antibodies and fusion proteins based on CrossMab technology developed by Roche and others have entered clinical trials, of which 16 continue to be evaluated in active clinical trials (Table 1 and Figure 2). In the following sections, an overview of therapeutic bispecific antibodies and fusion proteins based on CrossMab technology is provided, with a focus on those in clinical trials.

Applications in targeted cancer therapy: Angiogenesis, receptor tyrosine kinases, and death receptor signaling

For many years, anti-angiogenesis approaches blocking the vascular endothelial growth factor-A (VEGF-A) have been a major area of targeted cancer therapy.[95–96] One of the first IgG-based antibodies and the first bispecific CrossMab to enter clinical trials, in 2012, was the heterodimeric 1 + 1 VEGF/Ang-2 CrossMab^{CH1-CL} vanucizumab (RG7221) (Figure 2a) targeting the pro-angiogenic ligands VEGF-A and angiopoietin-2 (Ang-2), which are involved in (tumor) angiogenesis.[95,96,97] Vanucizumab, as well as a mouse-specific surrogate bispecific, mediated potent anti-tumoral and anti-angiogenic efficacy in various preclinical models as monotherapy and in combination with chemotherapy,[81,98–101] as well as combined with PD-1 checkpoint inhibition[102–104] and CD40 agonism.[105,106] Vanucizumab was generally well tolerated as a monotherapy in a Phase 1 clinical trial and demonstrated promising anti-tumor efficacy, IgG-like pharmacokinetics and low immunogenicity,[107] as well as the anticipated pharmacodynamic mechanism of action.[108] Based on the negative outcome of the randomized McCAVE Phase 2 study, where it was compared to bevacizumab in combination with FOLFOX-6 chemotherapy in patients with untreated metastatic colorectal carcinoma, clinical development was discontinued.[109] Similarly, in spite of promising preclinical data, Phase 1b studies of vanucizumab in combination with the PD-L1 antibody atezolizumab (NCT01688206) and the CD40 antibody selicrelumab (NCT02665416) were ultimately discontinued. Recently, preclinical data demonstrated that dual inhibition of VEGF and Ang-2 by the vanucizumab mouse-specific surrogate bispecific in murine sepsis models improved the outcomes, making it a potential therapeutic against vascular barrier breakdown.[110] Similarly, Zhou and colleagues reported on an alternative anti-angiogenic approach for cancer therapy using a heterodimeric 1 + 1 VEGF/DLL4 CrossMab^{CH1-CL} called HB-32 that mediated potent anti-angiogenic activity *in vitro*, as well as *in vivo* anti-tumor activity in breast cancer xenograft models.[111]

In addition to anti-angiogenesis, targeting receptor tyrosine kinases (RTKs) like EGFR, HER2 or c-Met has been a major area for cancer therapy during the past decades.[112] Accordingly, various preclinical-stage bispecific CrossMabs targeting RTKs have been developed during the past years, but none of these have advanced to clinical trials so far. Zhang and colleagues created a biparatopic HER2/HER2 1 + 1 CrossMab^{Fab} based on trastuzumab and an avidity-improved variant L56TY derived from pertuzumab called Tras-Permut CrossMab. Tras-Permut CrossMab mediated improved activity against trastuzumab-resistant breast cancer and enhanced calreticulin exposure, which may contribute to the induction of tumor-specific T-cell responses.[113] Lu and colleagues, in turn, generated a bispecific HER2/EGFR 1 + 1 CrossMab^{CH1-CL} based on the trastuzumab and cetuximab.[72] Interestingly, Hu and colleagues went a step further and generated so-called four-in-one antibodies that exhibited four different specificities against EGFR, HER2, HER3, and VEGF by generating a 1 + 1 CrossMAb^{CH1-CL} using dual-acting Fabs (DAF) as building blocks in the FL518 bispecific or by combining CrossMab and DVD-Ig technology in the tetraspecific, tetravalent antibody CRTB6 to enable correct light-chain association in the DVD format.[114] Not surprisingly, these tetraspecific antibodies showed superior efficacy as compared to the respective bispecific antibodies.[114] Finally, different bispecific EGFR/Notch CrossMabs were described to block EGFR signaling together with Notch signaling. The first of these antibodies, termed CT16, combined the EGFR antibody cetuximab and the Notch 2/3 antibody tarextumab using the prototypical heterodimeric 1 + 1 CrossMab$^{CH11-CL}$ format, which served as a radiosensitizer and prevented acquisition of resistance to EGFR inhibitors and radiation in cell line models of non–small cell lung cancer and patient-derived xenograft tumors.[115] In a second publication from the same group, three heterodimeric bispecific 1 + 1 CrossMab^{CH1-CL} antibodies (PTG12, RTB3, MTJ16) were generated from panitumumab/tarextumab, RG7116/tarextumab, and MEHD7945A/tarextumab and were shown to increase the response to PI3K inhibition with GDC-0941 by inhibiting stem cell–like subpopulation, reducing tumor-initiating cell frequency, and downregulating mesenchymal gene expression.[116]

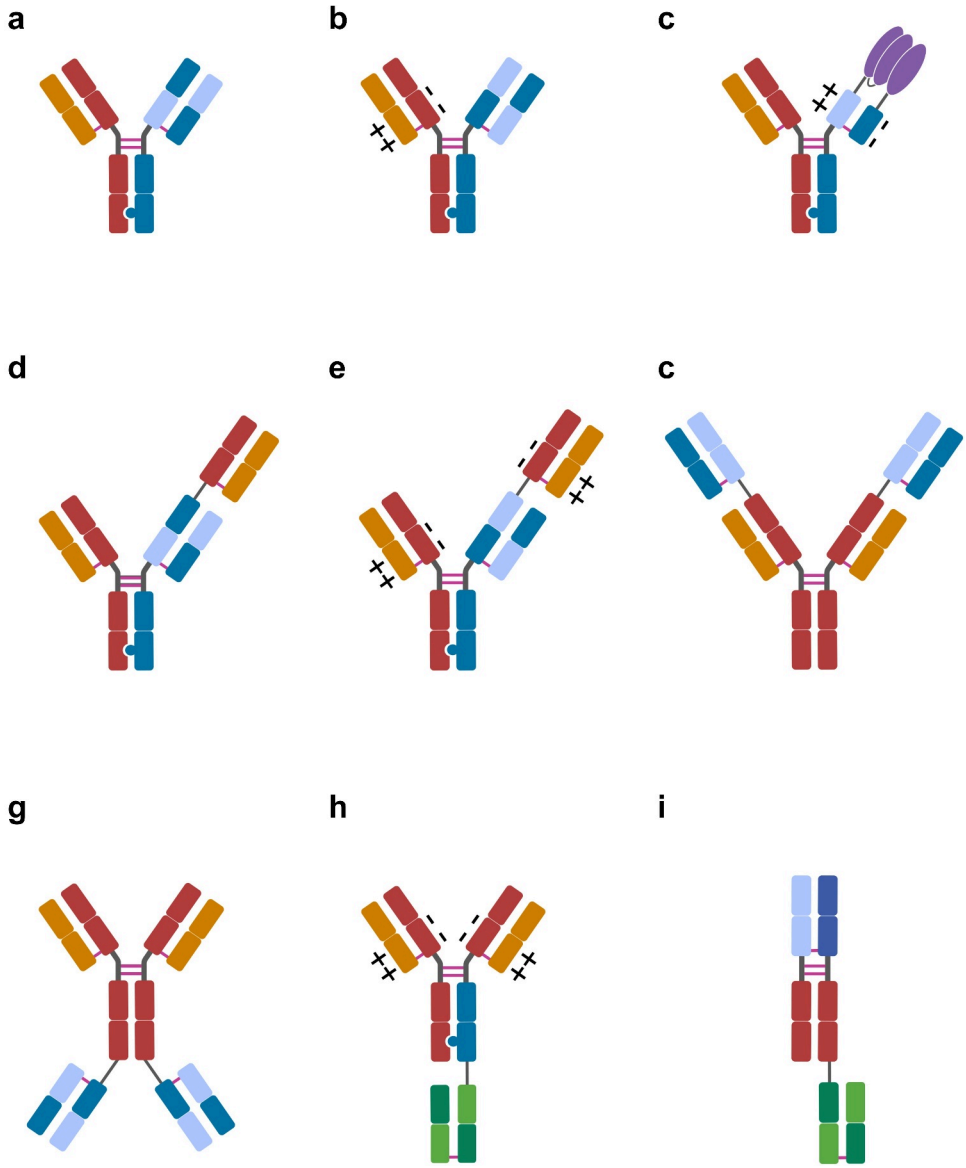

Figure 2. Major CrossMab formats: A) 1 + 1 CrossMab:$^{CH1-CL}$ vanucizumab, faricimab, 10E8.4/iMab 1 + 1; **B)** 1 + 1 CrossMab$^{VH-VL\pm}$: PD1-TIM3, PD1-LAG3; **C)** CrossMab$^{CH1-CL+/-}$based FAP-4-1BBL, CD19-4-1BBL fusion proteins; **D)** 2 + 1 CrossMab:$^{CH1-CL}$ cibisatamab; **E)** 2 + 1 CrossMab$^{VH-VL\pm}$: glofitamab, CC-93269, TYRP1-TCB, WT1-TCB, RG6123; **F)** 2 + 2 CrossMab^{CH1-CL}-based FIT-Ig EMB-01, EMB-02, EMB-06; **G)** 2 + 2 CrossMab:$^{CH1-CL}$ FAP-DR5; **H)** 2 + 1 CrossMab $^{VH-VL\pm}$: BS-GANT, FAP-CD40; **I)** 1 + 1 CrossMab^{CH1-CL}-based Nkp46-based NK cell engager (NKCE). Heavy-chain domains are depicted in dark colors and respective light-chain domains are depicted with corresponding bright colors. Fusion protein depicted in purple. Note: Differences in variable regions and/or isotype and Fc engineering are not depicted. Created with BioRender.com.

Another major field in targeted cancer therapy has been and continues to be apoptosis induction through death receptor (DR) signaling.[117,118] As conventional DR5 antibodies have not been successful in clinical trials, approaches for tumor-targeted DR5 agonism have been pursued. Expression of the fibroblast activation protein (FAP) on tumor fibroblasts is found in the majority of solid tumors, making FAP an attractive antigen for tumor targeting.[119,120] Based on this rationale, FAP-targeted bispecific antibodies and fusion proteins have been created using CrossMab technology that rely on FAP binding with one moiety to induce, with their second moiety, hyper-clustering of tumor necrosis factor (TNF) receptor superfamily members[121] like DR5 for apoptosis induction,[85] 4–1BB/CD137 for T cell activation,[89] or CD40 for activation of antigen-presenting cells,[94,122] as described below. The first of these conditional FAP-targeted TNFR agonistic antibodies entering Phase 1 clinical trials was the symmetric tetravalent C-terminally fused FAP/DR5 targeted 2 + 2 CrossMab^{CH1-CL} RG7386 (Figure 2g). Preclinical data demonstrated that RG7386 effectively triggered FAP-dependent, avidity-driven DR5 hyper-clustering and subsequent tumor cell apoptosis,[85] but ultimately, clinical development of RG7383 was not further continued after the completed Phase 1 study (NCT02558140) due to portfolio reprioritization.

Finally, Tung and colleagues described novel HER2 or CD19 tumor-targeted heterodimeric 1 + 1 CrossMab^{CH1-CL} antibodies that recognize with their second specificity PEGylated proteins, liposomes, and nanoparticles. Using these bispecific antibodies, cytotoxic cargo such as PEGylated liposomal doxorubicin can be delivered to tumor cells.[123]

Table 1. CrossMabs in clinical trials (status July 2021), FP: Fusion protein, FIT-Ig: Fabs-in-tandem Ig, EIH: Entry into human date.

	Name	Target A/B	Format	Indication	Stage	Company	EIH	Clinical trial	Reference
1	Vanucizumab (RG7221)	Ang-2/VEGF-A	1 + 1 CrossMab^{CH1-CL}	Oncology	Terminated Ph 2	Roche	2012	NCT02141295, NCT01688206, NCT02665416	81
2	Faricimab (RG7716)	Ang-2/VEGF-A	1 + 1 CrossMab^{CH1-CL}	DME, wAMD	Ph 3	Roche	2013	NCT03823287, NCT03823300, NCT03622580, NCT03622593	82,83
3	Cibisatamab (RG7802)	CEA/CD3ε	2 + 1 CrossMab$^{CH11-CL}$	Oncology	Ph 1b	Roche	2014	NCT03866239, NCT04826003	84
4	FAP-DR5 (RG7386)	FAP/DR5	2 + 2 CrossMab$^{CH11-CL}$	Oncology	Terminated Ph 1	Roche	2015	NCT02558140	85
5	Glofitamab, RG6026)	CD20/CD3ε	2 + 1 CrossMab$^{VH-VL\pm}$	NHL	Ph 2/3	Roche	2017	NCT04703686, NCT04914741 NCT04077723, NCT04408638	86
6	PD1-TIM3 (RG7769)	PD-1/TIM-3	1 + 1 CrossMab$^{VH-VL\pm}$	Oncology	Ph 1/2	Roche	2018	NCT03708328, NCT04785820	87
7	RG6123	CEACAM5/CD3ε	2 + 1 CrossMab$^{VH-VL\pm}$	Oncology	Terminated Ph 1	Roche	2018	NCT03539484	-
8	BCMA TCE (CC-93269)	BCMA/CD3ε	2 + 1 CrossMab$^{VH-VL\pm}$	Multiple Myeloma	Ph 1	BMS	2018	NCT03486067	88
9	FAP-4-1BBL (RG7827)	FAP/4-1BB	1 + 3 CrossMab$^{CH1-CL\pm}$ 4-1BBL FP	Oncology	Ph 1b	Roche	2018	NCT03869190, NCT04826003	89
10	10E8.4/iMab, TMB-370	HIV-1 Env/CD4	1 + 1 CrossMab^{CH1-CL}	HIV-1	Ph 1	TaiMed	2019	NCT03875209	90
11	EMB-01	EGFR/c-Met	2 + 2 CrossMab^{Fab} /FIT-Ig	Oncology	Ph 1	EpimAb	2019	NCT03797391	50,151
12	BS-GANT (RG6102)	Abeta/TfR	2 + 1 CrossMab$^{VH-VL\pm}$	Alzheimer's	Ph 2	Roche	2019	NCT04639050	
13	CD19-4-1BBL (RG6076)	CD19/4-1BB	1 + 3 CrossMab$^{CH1-CL\pm}$ 4-1BBL FP	NHL	Ph 1b	Roche	2019	NCT04077723	89
14	PD1-LAG3 (RG6139)	PD-1/LAG-3	1 + 1 CrossMab$^{VH-VL\pm}$	Oncology	Ph 1/2	Roche	2019	NCT04140500, NCT04785820	91
15	TYRP1-TCB (RG6232)	TYRP1/CD3ε	2 + 1 CrossMab$^{VH-VL\pm}$	Melanoma	Ph 1	Roche	2020	NCT04551352	92
16	WT1-TCB (RG6007)	WT1/CD3ε	2 + 1 CrossMab$^{VH-VL\pm}$	AML	Ph 1	Roche	2020	NCT04580121	93
17	EMB-02	PD-1/LAG-3	2 + 2 CrossMab^{Fab} /FIT-Ig	Oncology	Ph 1	EpimAb	2020	NCT04618393	-
18	EMB-06	BCMA/CD3ε	2 + 2 CrossMab^{Fab} /FIT-Ig	Multiple Myeloma	Ph 1	EpimAb	2021	NCT04735575	-
19	FAP-CD40	FAP/CD40	2 + 1 CrossMab$^{VH-VL\pm}$	Oncology	Ph 1	Roche	2021	NCT04857138	94

Applications in cancer immunotherapy: Dual checkpoint inhibitors, T and innate cell engaging bispecifics and tumor-targeted co-stimulation

With the advent of cancer immunotherapy and checkpoint inhibitor antibodies during the past decade, the development of bispecific antibodies for immunotherapy has attracted substantial attention in industry and academia, whereas the interest in anti-angiogenic and pro-apoptotic therapies has declined. In this context, bispecific monovalent dual checkpoint inhibitory PD-1 antibodies co-targeting the checkpoint inhibitory receptors TIM-3 or LAG-3 have been designed based on a bispecific 1 + 1 CrossMab$^{VH-VL\pm}$ format (Figure 2b), allowing avidity-mediated selectivity gain and thus enhanced selectivity for PD-1^{+} and PD-1^{+} TIM-3^{+}/LAG-3^{+} double-positive T cells. Both of these bispecific dual checkpoint inhibitory antibodies, PD1-TIM3 (RG7769) [87] and PD1-LAG3 (RG6139),[91] are currently in Phase 1 and 2 clinical trials (NCT03708328, NCT04140500, NCT04785820).[124,125] Preclinically, a heterodimeric 1 + 1 PD-1/RANKL CrossMab^{CH1-CL} was shown to demonstrate potent tumor growth inhibition as a monotherapy and combined with CTLA-4 antibodies, particularly in models showing checkpoint inhibitor resistance to PD-1 antibodies.[126]

Many of bispecific antibodies currently being developed are bispecific T-cell engagers.[22,127–131] One of the first IgG-based, and Roche's first, T-cell bispecific antibody (TCB) to enter clinical trials was the heterodimeric and trivalent CEA/CD3ε 2 + 1 TCB cibisatamab (RG7802). It is a heterodimeric CEA/CD3ε bispecific antibody in the 1 + 1 CrossMab^{CH1-CL} format to which a single additional Fab targeting CEA is fused to the N-terminus of the knob-containing heavy chain (Figure 2d).[84,132] FcγR and C1q binding are abolished by introduction of P329G LALA mutations.[133] This so-called 2 + 1 TCB format provides advantages over conventional heterodimeric 1 + 1 TCB formats through the highly flexible head-to-tail fusion in the tandem Fab arm and by being bivalent for the tumor antigen, allowing a better differentiation between tumor and normal cells due to avidity-mediated affinity tuning.[132] Cibisatamab demonstrated tumor targeting and *in vitro* and *in vivo* anti-tumor efficacy dependent on CEA over-expression due to the bivalent binding mode in models of colorectal and gastric cancer,[84,134–137] which was further enhanced when combined with PD-L1 inhibition.[138] Based on these data and using a MABEL approach due to the lack of cross-reactive toxicology species,[139,140] clinical studies were initiated in relapsed/refractory CEA-positive colorectal cancer patients. Cibisatamab is currently in Phase 1b clinical trials in combination with the PD-L1 antibody atezolizumab (NCT03866239) and with FAP-4-1-BBL (NCT04826003) (see below). Pre-treatment with obinutuzumab is being clinically explored to mitigate the potential development and impact of anti-drug antibodies that could be observed in patients treated with cibisatamab.

The most advanced 2 + 1 T cell bispecific antibody is glofitamab (RG6026), which, in contrast to cibisatamab, is based on a 2 + 1 CrossMab$^{VH\text{-}VL}$ format with charge interactions using variable regions derived from obinutuzumab (Figure 2e). Glofitamab showed potent tumor cell killing and antitumor efficacy in preclinical *in vitro, ex vivo* and *in vivo* lymphoma models, as well as superiority over the respective conventional heterodimeric 1 + 1 TCB formats as a consequence of its head-to-tail orientation and bivalent binding to CD20, allowing pre-treatment with obinutuzumab, in this case as a strategy to reduce the incidence of cytokine-release syndrome by glofitamab.[86,141,142] Based on the clinical efficacy and safety in the Phase 1 clinical trial in relapsed/refractory non-Hodgkin lymphoma (NHL) patients and particularly the high rate of durable complete responses,[143,144] glofitamab is currently being evaluated in multiple clinical trials in lymphoma patients, including trials in patients relapsed after CAR-T cell therapy (NCT04703686) and in Phase 3 clinical trials in relapsed/refractory diffuse large B cell lymphoma patients (NCT04077723, NCT04408638).[145] No anti-drug antibodies recognizing glofitamab were detected in the Phase 1 clinical study.[143]

Additional analogous 2 + 1 T cell bispecific antibodies using this technology have entered early clinical Phase 1 trials, including the BCMA-TCE CC-93269 for the treatment of multiple myeloma (NCT03486067)[88] and the TYRP1-TCB (RG6232) for the treatment of TYRP1-expressing melanoma (NCT04551352).[92] Recently, the WT1-peptide-MHC-specific TCR-like WT1-TCB (RG6007) for the treatment of acute myeloid leukemia (AML) became the first TCR-like bispecific antibody to enter a clinical trial (NCT04580121).[93] While Immunocore pioneered the field of targeting peptide-MHC complexes with recombinant TCR-based bispecific T-cell engagers, the so-called ImmTACs,[146] WT1-TCB is based on a TCR-like antibody fragment recognizing the RMF WT1 peptide-HLA-A*02 complex. WT1-TCB can mediate specific killing of AML cell lines and primary AML cells, and it has antitumor activity in humanized mice bearing SKM-1 tumors.[93]

Additional preclinical stage 2 + 1 TCBs based on this format have been described, including ones that target HER2[147,148] or the p95 HER2 fragment.[149] The p95 HER2 fragment is only found on a portion of ~ 30–40% of HER2^{+++} tumor cells, and as such can be considered a highly tumor-specific neoantigen. Thus, 2 + 1 TCBs targeting specifically p95 HER2 are of particular interest as they do not mediate T cell killing of normal cells that express HER2, such as cardiomyocytes or breast epithelial cells, as opposed to conventional HER2-TCBs.[149] An alternative approach to overcome the on-target off-tumor killing of normal cells is tumor-specific activation of TCBs by protease expressed in the tumor. For this purpose, a protease-activated mesothelin-TCB using CrossMab technology has been described that is blocked by an anti-CD3 anti-idiotypic mask that is cleaved in the tumor-microenvironment.[150] Alternatively, to counteract and manage any undesired T cell activation, it was shown that the Src/lck inhibitor dasatinib is able to reversibly switch off cytokine release and T-cell cytotoxicity following stimulation with different 2 + 1 TCBs targeting CEA, CD19 and WT1.[151] Finally, related to the TCB approach, 2 + 1 bispecific antibodies designed based on CrossMab technology have been developed specifically for the recruitment of synthetic agonistic receptor transduced T-cells (SAR-T) in adoptive T-cell therapy together with Kobold and colleagues.[152–154]

In order to further boost the potency of T-cell bispecific antibodies, the tumor (stroma)-targeted FAP-4-1BBL (RG7827), CD19-4-1BBL (RG6076) and CEA-4-1BBL fusion proteins have been developed for solid tumors and NHL. These molecules are used to provide the co-stimulatory TNF receptor superfamily-mediated signal 2 to T cells in combination with the T-cell bispecific antibodies cibisatamab or glofitamab, which provide the signal 1.[89,155,156] These 4–1BBL fusion proteins contain a split trimeric 4–1BB ligand fused to the CH1 and CL domains, and constant chain mispairing is abolished by CH1-CL domain crossover in conjunction with the respective charge pairs (Figure 2c).[89] FAP-4-1BBL and CD19-4-1BBL have been designed to trigger 4–1BB/CD137 hyper-clustering specifically in the tumor microenvironment, but not in circulation or in the liver, with the goal to overcome typical 4–1BB antibody-mediated toxicities.[89] Tumor-targeted 4–1BBL fusion proteins were shown to mediate improved T-cell activation, superior tumor control in combination with TCBs and checkpoint inhibitors, and strong T-cell infiltration in preclinical models.[89,155,157] Clinical Phase 1b studies combining cibisatamab with FAP-4-1-BBL (NCT04826003) and glofitamab with CD19-4-1BBL (NCT04077723) are currently ongoing.

A similar rationale was applied to trigger the TNF receptor superfamily member CD40 on antigen-presenting cells (APCs) through a trivalent C-terminally fused FAP/CD40 2 + 1 bispecific antibody in a 2 + 1 CrossMab$^{VH\text{-}VL\pm}$ format with charges (Figure 2h). This design was chosen to make FAP-CD40 (RG6189), a FAP-targeted CD40 agonistic bispecific antibody, with the goal of abrogating systemic toxicity and enabling administration of doses sufficiently high to result in highly tumor- and lymph node-specific activation of APCs with subsequent induction of antitumor immunity.[94,122] Phase 1 clinical trials have been initiated to validate this approach in the clinic (NCT04857138).

Notably, the domain crossover/CrossMab technology has also been used by researchers outside of Roche for the development of bispecific antibodies for cancer immunotherapy. This includes the so-called Fabs-in-tandem Ig (FIT-Ig) approach developed by Gong and colleagues from EpimAb, which relies on Fab crossover to enable correct light-chain association for the generation of symmetric tetravalent N-terminally fused bispecific antibodies in the 2 + 2 CrossMab^{Fab} format (Figure 2f).[50,51] Three different bispecific FIT-Igs have reached clinical Phase 1 trials to date co-targeting: 1) EGFR/c-Met for receptor tyrosine kinase inhibition (EMB-01) (NCT03797391), 2) PD-1/LAG-3 for dual checkpoint inhibition (EMB-02) (NCT04618393), and 3) BCMA/CD3ε for T cell engagement in multiple myeloma (EMB-06) (NCT04735575).

In order to recruit innate immune cells for cancer cell killing, Gauthier and colleagues from Innate Pharma recently described an advanced preclinical approach to generate multifunctional natural killer cell engagers (NKCE) targeting a tumor antigen and the NK cell ligand NKp46 in a FcγRIII-binding competent monovalent C-terminally fused 1 + 1 antibody format using CH1-CL crossover to ensure correct light-

chain association (Figure 2i).[158] Trifunctional NKCEs targeting CD19, CD20, or EGFR as tumor antigens triggered tumor killing by human primary NK cells *in vitro* and induced NK cell infiltration and anti-tumor efficacy, as well as protective tumor immunity *in vivo*.[158]

Zhao and colleagues demonstrated that a bispecific heterodimeric CD20/HLA-DR 1 + 1 CrossMab^{CH1-CL} termed CD20–243 CrossMab for the treatment of NHL patients co-expressing CD20 and HLA-DR mediated strong complement-dependent cytotoxicity, antibody-dependent cell-mediated cytotoxicity and anti-proliferative activity.[159] Similarly, Rajendran and colleagues generated a bispecific heterodimeric CD30/CD137 1 + 1 CrossMab^{CH1-CL} to target specifically these two co-expressed antigens on Hodgkin and Reed-Sternberg cells without inducing CD137 signaling.[160]

In an alternative approach to activate innate immunity, Du and colleagues devised a bispecific heterodimeric GPC3/CD47 1 + 1 CrossMab^{CH1-CL} to bind to GPC3 and CD47 on hepatocellular cancer cells, and at the same time inhibit the CD47 interaction with SIRP1α responsible for the "do-not-eat-me signal" to recruit myeloid cells for phagocytosis.[161] The GPC3/CD47 CrossMab induced enhanced Fc-mediated effector functions by both macrophages and neutrophils toward dual antigen-expressing hepatocellular carcinoma (HCC) cells *in vitro*, and strong *in vivo* efficacy against xenograft HCC tumors in a fashion superior to the respective monotherapies and combination thereof.[161]

In order to further boost antigen presentation and foster the generation of a secondary anti-tumor immune response, again Zhao and colleagues created a novel CD20/Flt3 ligand antibody fusion protein, termed CD20-Flex BiFP using CrossMab technology.[162] CD20-Flex BiFP not only eliminated lymphoma temporarily but also potentiated tumor-specific T-cell immunity by expanding and fostering infiltration of antigen-presenting dendritic cells into the tumor tissue.[162]

Most recently, Panina and colleagues described a novel bispecific heterodimeric HER2/IFNα-1 + 1 CrossMab^{CH1-CL} with the ultimate goal to deliver IFNα into HER2 expressing tumors.[163]

Applications in therapy of viral infections and autoimmune diseases

The application of CrossMab technology has become quite popular for the generation of bispecific and multispecific antibodies targeting various viruses. During the past years, multiple highly potent bispecific antibodies targeting HIV-1 have been generated using CrossMab technology for the prevention and treatment of HIV-1.[164,165] Examples of these approaches are: 1) four different 1 + 1 CrossMab^{CH1-CL}-based bispecific antibodies, of which the one based on VRC07 and PG9-16 displayed the most favorable neutralization profile and IgG-like pharmacokinetic properties in monkeys;[166] 2) 1 + 1 CrossMab^{CH1-CL}-based bispecific antibodies that, however, did not allow intra-spike binding;[167] 3) unique bispecific antibodies based on the broadly neutralizing antibodies (bNAbs) 3BNC117 and 10–1074 with a modified hinge region of human IgG3 isotype for increased Fab flexibility and improved neutralization potency based on a 1 + 1 CrossMab^{CH1-CL} format;[168] 4) a 1 + 1 CrossMab^{CH1-CL}-based bispecific antibody targeting two non-competing epitopes on the HIV-1 co-receptor CCR5 based on RoAb13 and PRO 140 to increase avidity;[169] 5) the 1 + 1 CrossMab^{CH1-CL}-based bispecific antibody iMab-CAP256 comprising the highly potent CAP256.VRC26.25 bNAb and the host-directed CD4 antibody, ibalizumab (iMab);[170] and 6) the 1 + 1 CrossMab^{CH1-CL}-based bispecific antibody BICM-1A for simultaneous recognition of two critical V2- and V3-glycan epitopes of the single HIV-1 envelope glycoprotein.[171] Of all these approaches, the heterodimeric bispecific 1 + 1 CrossMab^{CH1-CL} antibody 10E8.4/iMab showed exquisite potency and breadth against various HIV-1 strains, including activity in HIV-1 *in vivo* treatment and prevention models,[90,172] and compared very favorably to conventional antibodies and other bispecific bNAbs.[173] Based on these data, 10E8.4/iMab is currently being evaluated in a Phase 1 clinical trial (NCT03875209).[174]

Wang and colleagues generated a symmetric and tetravalent FIT-Ig-based bispecific antibody against Zika virus that showed high *in vitro* and *in vivo* potency, and prevented viral escape, supporting its potential use for the therapy of Zika virus prevention or infections.[175]

Interestingly, and most recently, De Gasparo and colleagues described the first bispecific antibody targeting SARS-CoV-2 based on a 1 + 1 CrossMab^{CH1-CL} format targeting two non-overlapping sites on the receptor binding domain of SARS-CoV-2 and blocking binding to angiotensin-converting enzyme 2 (ACE2).[176] The respective bispecific antibody CoV-X2 was designed using C121 and C135, two antibodies derived from donors who had recovered from COVID-19. Most notably, CoV-X2 neutralized wild-type SARS-CoV-2 and variants of concern and escape, protected mice from disease and suppressed viral escape.[176] Along these lines, Jette and colleagues described a subset of donor-derived neutralizing bispecific CrossMabs with broad cross-reactivity to sarbecoviruses.[177]

Bispecific CrossMab-based antibodies have also been generated with the goal of treating autoimmune diseases.[178,179] Fischer and colleagues showed that combined inhibition of TNFα and IL-17 was more effective in inhibiting the development of inflammation and bone and cartilage destruction in arthritic mice compared to the respective monotherapies. For this purpose, bispecific TNFα/IL-17 1 + 1 and 2 + 2 CrossMab^{CH1-CL} antibodies were prepared that showed superior efficacy in blocking cytokine and chemokine responses *in vitro*.[180] Similarly, Xu and colleagues showed that a tetravalent bispecific TNFα/IL-17 1 + 1 CrossMab^{VH-VL} together with electrostatic steering for heavy-chain heterodimerization significantly decreased the expression level of neutrophil and Th17 chemokines, and the secretion of IL-6/IL-8 on fibroblast-like synoviocytes. Moreover, combined inhibition of both cytokines by the bispecific antibody was superior to inhibition of either cytokine alone.[181] Based on these data,

dual-targeting bispecific antibodies neutralizing pro-inflammatory cytokines may provide novel treatment options for autoimmune diseases. However, as they are not necessarily differentiated from the combination of the respective monotherapies, the benefit of using a bispecific antibody over a combination therapy needs to be assessed on a case-by-case basis.

Applications in ophthalmology and therapy of central nervous system diseases

The heterodimeric 1 + 1 VEGF/Ang-2 CrossMab^{CH1-CL} vanucizumab (RG7221) was the first anti-angiogenic bispecific antibody to enter clinical trials with the goal of suppressing tumor angiogenesis via simultaneous blockade of the pro-angiogenic ligands VEGF-A and Ang-2. VEGF and Ang-2 have also been shown to play an important role in ocular angiogenesis in diseases like wet age-related macular degeneration (wAMD) and diabetic macular edema (DME).96[182–184] However, until now only the VEGF blocking antibody fragments ranibizumab and brolucizumab and the VEGFR1/2-ECD-Fc fusion protein aflibercept are approved for use in ophthalmology.[185]

Faricimab (RG7716) is a heterodimeric 1 + 1 VEGF/Ang-2 CrossMab^{CH1-CL} specifically optimized for intraocular use and high concentration formulation in ophthalmology indications by use of optimized anti-VEGF and anti-Ang-2 Fabs, as compared to vanucizumab, and by the introduction of P329G LALA and Triple A mutations in the KiH-containing IgG1 Fc portion to abolish FcγR-mediated effector functions and FcRn recycling for low systemic exposure.[82,83,186–189] While faricimab neutralizes two soluble ligands, particularly in the field of ophthalmology the use of such a bispecific antibody provides advantages in terms of intraocular administration via a single injection due to the simultaneous inhibition of two different angiogenic pathways with a single agent. Importantly, as compared to VEGF inhibition alone, faricimab mediated improved anti-angiogenic activity in various preclinical models to limit pathological angiogenesis in the eye.[82,83,190,191] Based on these data, faricimab was the first bispecific antibody worldwide entering Phase 1 clinical trials in ophthalmology, where it was well tolerated and exhibited a favorable safety profile with evidence of improvements in best-corrected visual acuity (BCVA) and anatomic parameters supporting further clinical investigation.[192] Subsequently, faricimab was compared head-to-head to ranibizumab in the BOULEVARD Phase 2 randomized clinical trial in patients with DME, where it met the primary end point and demonstrated statistically superior visual acuity gains versus ranibizumab, suggesting a benefit of simultaneous inhibition of angiopoietin-2 and VEGF-A.[193] In the AVENUE Phase 2 randomized clinical trial in patients with AMD, it did not meet the primary end point of superiority over ranibizumab in BCVA at week 36, but visual and anatomical gains observed with faricimab supported pursuing Phase 3 trials for an alternative to monthly anti-VEGF therapy.[194] This was taken into account together with the data from the STAIRWAY Phase 2 randomized clinical trial in AMD where faricimab dosed every 16 weeks or 12 weeks resulted in maintenance of initial vision and anatomic improvements comparable with monthly ranibizumab.[195,196] Recently, positive outcomes were reported from four independent pivotal Phase 3 trials in wAMD and DME patients where faricimab was compared to aflibercept and met the primary endpoints (NCT03823287, NCT03823300, NCT03622580, NCT03622593). Based on these data, marketing applications for faricimab have been filed with health authorities for approval in DME and wAMD, with FDA granting it a priority review.[197]

The treatment of central nervous system (CNS) diseases with monoclonal antibodies is hampered by the low penetration of antibodies through the blood-brain barrier, and the field still is in its infancy.[198] To overcome this limitation, Niewoehner and colleagues have generated transferrin receptor-targeted bispecific antibodies that allowed delivery of these antibodies through the blood-brain barrier and showed improved brain exposure and prevented plaque formation.[66,67] Using this approach, BS-GANT (RG6102) was generated based on the amyloid-beta antibody gantenerumab[199] as a trivalent C-terminally fused amyloid-beta/TfR 2 + 1 bispecific antibody in a 2 + 1 CrossMab$^{VH-VL\pm}$ format with charges (Figure 2h). BS-GANT (RG6102) recently entered Phase 2 clinical trials in patients with prodromal or mild-to-moderate Alzheimer's disease (NCT04639050).

Conclusions

During the past 20 years, numerous technologies have been developed to generate bispecific antibodies, and these molecules represent a rapidly growing class of biopharmaceuticals in clinical trials and on the market. CrossMab technology was first described in 2011 as a novel approach enabling correct antibody light-chain association with their respective heavy chain in bi-/multispecific antibodies, together with methods enabling correct heavy-chain association.

As briefly mentioned in the introduction, alternative technologies to achieve correct heavy-light-chain pairing are currently being applied for the generation of prototypical (heterodimeric) IgG-like bispecific antibodies. These include *in vitro* assembly approaches, where the two bispecific antibodies are produced separately and subsequently assembled *in vitro* like DuoBody,[19] Fab arm exchange,[22] FORCE[26] or half antibody assembly,[27] as well as approaches allowing the production of bispecific antibodies in one cell line, for example via the use of common light chains or orthogonal Fab interfaces. Recently, several groups have also reported that the specific pairing preferences of selected heavy and light chain pairs can be used to drive the assembly of correct bispecific antibodies.[200,201] In the field of common light chains, much progress has been made in the selection of suitable common light-chain antibodies from common light-chain-bearing animals or use of *in vitro* display technologies.[9,10,14–16,202–205] Based

on this progress, several bispecific common light-chain-based IgG antibodies are currently in clinical trials, including odronextamab, REGN4018, REGN5678, REGN7075, MCLA-145, MCLA-158, and others.[7,8,10,15,206–213] Alternatively, the correct light-chain-heavy-chain association can be enforced using orthogonal Fab interfaces by introduction of (several) mutations in the Fab interface.[28,29,33,55,56,214,215]

CrossMab technology continues to represent a simple, straightforward and clinically validated antibody engineering solution to achieve correct light-chain association with minimal engineering using existing pairs of antibodies. In fact, since its original description, it has evolved into one of the most mature, versatile, and broadly applied technologies in industry and academia, in conjunction with the KiH technology. Until now ~20 bispecific antibodies and fusion proteins based on CrossMab technology developed by Roche and others have entered clinical trials. Based on the available clinical data, CrossMabs show favorable IgG-like properties in terms of pharmacokinetics and immunogenicity similar to conventional therapeutic monoclonal antibodies. The most advanced of these bispecific antibodies are: 1) the 1 + 1 heterodimeric Ang-2/VEGF bispecific antibody faricimab for the treatment of DME and wAMD, which is currently undergoing regulatory review, and 2) the 2 + 1 heterodimeric CD20/CD3 T-cell bispecific antibody glofitamab for the treatment of relapsed/refractory DLBCL or follicular NHL, which is currently in pivotal Phase 3 clinical trials.

Based on the progress in making bi- and multispecific antibodies, we anticipate that this class of therapeutics with novel mechanisms of actions as compared to conventional therapeutic antibodies will have a major impact on the treatment of various diseases, including oncology, infectious diseases, autoimmunity, CNS, and metabolic diseases. Taken together, CrossMab technology has proven to be very useful for the fast and straightforward generation of bispecific antibody formats to tackle novel biological challenges and help to develop novel therapeutic concepts for patients in need.

Acknowledgments

The authors want to thank all contributors and project team members from Roche Innovation Centers Zurich, Munich and Basel, Roche pRED as well as all other collaborators within and outside of Roche contributing to the development of CrossMab technology and individual drug candidates for their support and effort. The authors apologize to those authors whose work could not be cited due to space restrictions.

Disclosure statement

MS declares employment with Roche, WS declares patents/royalties with Roche and CK declares employment, stock ownership, and patents/royalties with Roche. CROSSMAB® is a registered trademark by Genentech/Roche.

Abbreviations

ACE2	Angiotensin-Converting Enzyme 2
ALL	Acute Lymphocytic Leukemia
AML	acute myeloid leukemia
Ang-2	Angiopoietin-2
BCVA	Best-Corrected Visual Acuity
BiTE	Bispecific T cell Engager
bNAbs	broadly Neutralizing Antibodies
CEA	Carcinoembryonic antigen
CMC	Chemistry, Manufacturing, and Controls
CNS	Central Nervous System
DAF	Dual Acting Fab
DME	Diabetic Macular Edema
DSP	Downstream Processing
DVD-Ig	Dual Variable Domain-Ig
FDA	Federal Drug Administration
FAP	Fibroblast Activation Protein
FIT-Ig	Fabs-In-Tandem-Ig
Ig	Immunoglobulin
KiH	Knobs-into-Holes
NKCE	NK Cell Engager
SAR	Synthetic Agonistic Receptor
TCB	T-Cell Bispecific Antibody
TCR	T-Cell Receptor
TfR	Transferrin Receptor
TNFR	TNF Receptor
USP	Upstream Processing
VEGF-A	Vascular Endothelial Growth Factor-A
wAMD	wet Age-Related Macular Degeneration

ORCID

Christian Klein http://orcid.org/0000-0001-7594-7280

References

1. Brinkmann U, Kontermann RE. The making of bispecific antibodies. MAbs. 2017;9(2):182–212. PubMed PMID: 28071970; PubMed Central PMCID: PMCPMC5297537. doi:10.1080/19420862.2016.1268307. Feb/Mar.
2. Labrijn AF, Janmaat ML, Reichert JM, et al. Bispecific antibodies: a mechanistic review of the pipeline. Nat Rev Drug Discov. 2019 Aug;18(8):585–608. 10.1038/s41573-019-0028-1: PubMed PMID: 31175342
3. Carter PJ, Lazar GA. Next generation antibody drugs: pursuit of the 'high-hanging fruit'. Nat Rev Drug Discov. 2018 Mar;17(3):197–223. PubMed PMID: 29192287. doi:10.1038/nrd.2017.227.
4. Sheridan C. Bispecific antibodies poised to deliver wave of cancer therapies. Nat Biotechnol. 2021 Mar;39(3):251–54. PubMed PMID: 33692520. doi:10.1038/s41587-021-00850-6.
5. Suurs FV, Lub-de Hooge MN, De Vries EGE, et al. A review of bispecific antibodies and antibody constructs in oncology and clinical challenges. Pharmacol Ther. 2019 Sep;201:103–19. doi:10.1016/j.pharmthera.2019.04.006. PubMed PMID: 31028837.
6. Zhang J, Yi J, Zhou P. Development of bispecific antibodies in China: overview and prospects. Antib Ther. 2020 Apr;3(2):126–45. doi:10.1093/abt/tbaa011. PubMed PMID: 33928227; PubMed Central PMCID: PMCPMC7990247.
7. Kitazawa T, Igawa T, Sampei Z, et al. A bispecific antibody to factors IXa and X restores factor VIII hemostatic activity in a hemophilia A model. Nat Med. 2012 Oct;18(10):1570–74. 10.1038/nm.2942: PubMed PMID: 23023498

8. Kitazawa T, Esaki K, Tachibana T, et al. Factor VIIIa-mimetic cofactor activity of a bispecific antibody to factors IX/IXa and X/Xa, emicizumab, depends on its ability to bridge the antigens. Thromb Haemost. 2017 Jun 28;117(7):1348–57. PubMed PMID: 28451690; PubMed Central PMCID: PMCPMC6292136. doi:10.1160/TH17-01-0030
9. Igawa T. Next generation antibody therapeutics using bispecific antibody technology. Yakugaku Zasshi. 2017;137(7):831–36. doi:10.1248/yakushi.16-00252-3. PubMed PMID: 28674296
10. Sampei Z, Igawa T, Soeda T, et al. Identification and multidimensional optimization of an asymmetric bispecific IgG antibody mimicking the function of factor VIII cofactor activity. PLoS One. 2013;8(2):e57479. PubMed PMID: 23468998; PubMed Central PMCID: PMCPMC3585358. doi:10.1371/journal.pone.0057479.
11. Skegro D, Stutz C, Ollier R, et al. Immunoglobulin domain interface exchange as a platform technology for the generation of Fc heterodimers and bispecific antibodies. J Biol Chem. 2017 Jun 9;292(23):9745–59. PubMed PMID: 28450393; PubMed Central PMCID: PMCPMC5465497. doi:10.1074/jbc.M117.782433
12. Einsele H, Borghaei H, Orlowski RZ, et al. The BiTE (bispecific T-cell engager) platform: development and future potential of a targeted immuno-oncology therapy across tumor types. Cancer. 2020 Jul 15;126(14):3192–201. PubMed PMID: 32401342. doi:10.1002/cncr.32909
13. Wolf E, Hofmeister R, Kufer P, et al. BiTEs: bispecific antibody constructs with unique anti-tumor activity. Drug Discov Today. 2005 Sep 15;10(18):1237–44. PubMed PMID: 16213416. doi:10.1016/S1359-6446(05)03554-3
14. De Nardis C, Hendriks LJA, Poirier E, et al. A new approach for generating bispecific antibodies based on a common light chain format and the stable architecture of human immunoglobulin G1. J Biol Chem. 2017 Sep 1;292(35):14706–17. PubMed PMID: 28655766; PubMed Central PMCID: PMCPMC5582861. doi:10.1074/jbc.M117.793497
15. Smith EJ, Olson K, Haber LJ, et al. A novel, native-format bispecific antibody triggering T-cell killing of B-cells is robustly active in mouse tumor models and cynomolgus monkeys. Sci Rep. 2015 Dec 11;5(1):17943. PubMed PMID: 26659273; PubMed Central PMCID: PMCPMC4675964. doi:10.1038/srep17943
16. Merchant AM, Zhu Z, Yuan JQ, et al. An efficient route to human bispecific IgG. Nat Biotechnol. 1998 Jul;16(7):677–81. 10.1038/nbt0798-677: PubMed PMID: 9661204
17. Bostrom J, Yu SF, Kan D, et al. Variants of the antibody herceptin that interact with HER2 and VEGF at the antigen binding site. Science. 2009 Mar 20;323(5921):1610–14. PubMed PMID: 19299620. doi:10.1126/science.1165480
18. Johnson S, Burke S, Huang L, et al. Effector cell recruitment with novel Fv-based dual-affinity re-targeting protein leads to potent tumor cytolysis and in vivo B-cell depletion. J Mol Biol. 2010 Jun 11;399(3):436–49. PubMed PMID: 20382161. doi:10.1016/j.jmb.2010.04.001
19. Labrijn AF, Meesters JI, De Goeij BE, et al. Efficient generation of stable bispecific IgG1 by controlled Fab-arm exchange. Proc Natl Acad Sci U S A. 2013 Mar 26;110(13):5145–50. PubMed PMID: 23479652; PubMed Central PMCID: PMCPMC3612680. doi:10.1073/pnas.1220145110
20. Beckmann R, Jensen K, Fenn S, et al. DutaFabs are engineered therapeutic Fab fragments that can bind two targets simultaneously. Nat Commun. 2021 Jan 29;12(1):708. PubMed PMID: 33514724; PubMed Central PMCID: PMCPMC7846786. doi:10.1038/s41467-021-20949-3
21. Wu C, Ying H, Grinnell C, et al. Simultaneous targeting of multiple disease mediators by a dual-variable-domain immunoglobulin. Nat Biotechnol. 2007 Nov;25(11):1290–97. 10.1038/nbt1345: PubMed PMID: 17934452
22. Strop P, Ho WH, Boustany LM, et al. Generating bispecific human IgG1 and IgG2 antibodies from any antibody pair. J Mol Biol. 2012 Jul 13;420(3):204–19. PubMed PMID: 22543237. doi:10.1016/j.jmb.2012.04.020
23. Leung KM, Batey S, Rowlands R, et al. A HER2-specific modified fc fragment (fcab) induces antitumor effects through degradation of HER2 and Apoptosis. Mol Ther. 2015 Nov;23(11):1722–33. 10.1038/mt.2015.127: PubMed PMID: 26234505; PubMed Central PMCID: PMCPMC4817942
24. Woisetschlager M, Antes B, Borrowdale R, et al. In vivo and in vitro activity of an immunoglobulin Fc fragment (Fcab) with engineered Her-2/neu binding sites. Biotechnol J. 2014 Jun;9(6):844–51. 10.1002/biot.201300387: PubMed PMID: 24806546
25. Wozniak-Knopp G, Stadlmayr G, Perthold JW, et al. Designing Fcabs: well-expressed and stable high affinity antigen-binding Fc fragments. Protein Eng Des Sel. 2017 Sep 1;30(9):657–71. PubMed PMID: 28981753. doi:10.1093/protein/gzx042
26. Dengl S, Mayer K, Bormann F, et al. Format chain exchange (FORCE) for high-throughput generation of bispecific antibodies in combinatorial binder-format matrices. Nat Commun. 2020 Oct 2;11(1):4974. PubMed PMID: 33009381; PubMed Central PMCID: PMCPMC7532213. doi:10.1038/s41467-020-18477-7
27. Spiess C, Merchant M, Huang A, et al. Bispecific antibodies with natural architecture produced by co-culture of bacteria expressing two distinct half-antibodies. Nat Biotechnol. 2013 Aug;31(8):753–58. 10.1038/nbt.2621: PubMed PMID: 23831709
28. Liu Z, Leng EC, Gunasekaran K, et al. A novel antibody engineering strategy for making monovalent bispecific heterodimeric IgG antibodies by electrostatic steering mechanism. J Biol Chem. 2015 Mar 20;290(12):7535–62. PubMed PMID: 25583986; PubMed Central PMCID: PMCPMC4367261. doi:10.1074/jbc.M114.620260
29. Gunasekaran K, Pentony M, Shen M, et al. Enhancing antibody Fc heterodimer formation through electrostatic steering effects: applications to bispecific molecules and monovalent IgG. J Biol Chem. 2010 Jun 18;285(25):19637–46. PubMed PMID: 20400508; PubMed Central PMCID: PMCPMC2885242. doi:10.1074/jbc.M110.117382
30. Coloma MJ, Morrison SL. Design and production of novel tetravalent bispecific antibodies. Nat Biotechnol. 1997 Feb;15(2):159–63. PubMed PMID: 9035142. doi:10.1038/nbt0297-159.
31. Dong J, Sereno A, Aivazian D, et al. A stable IgG-like bispecific antibody targeting the epidermal growth factor receptor and the type I insulin-like growth factor receptor demonstrates superior anti-tumor activity. MAbs. 2011 May-Jun;3(3):273–88. 10.4161/mabs.3.3.15188: PubMed PMID: 21393993; PubMed Central PMCID: PMCPMC3149708
32. Fischer N, Elson G, Magistrelli G, et al. Exploiting light chains for the scalable generation and platform purification of native human bispecific IgG. Nat Commun. 2015 Feb 12;6:6113. 10.1038/ncomms7113: PubMed PMID: 25672245; PubMed Central PMCID: PMCPMC4339886
33. Lewis SM, Wu X, Pustilnik A, et al. Generation of bispecific IgG antibodies by structure-based design of an orthogonal Fab interface. Nat Biotechnol. 2014 Feb;32(2):191–98. 10.1038/nbt.2797: PubMed PMID: 24463572
34. Cochlovius B, Kipriyanov SM, Stassar MJ, et al. Cure of Burkitt's lymphoma in severe combined immunodeficiency mice by T cells, tetravalent CD3 x CD19 tandem diabody, and CD28 costimulation. Cancer Res. 2000 Aug 15;60(16):4336–41. PubMed PMID: 10969772.
35. Moore GL, Bernett MJ, Rashid R, et al. A robust heterodimeric Fc platform engineered for efficient development of bispecific antibodies of multiple formats. Methods. 2019 Feb 1;154:38–50. 10.1016/j.ymeth.2018.10.006: PubMed PMID: 30366098
36. Guo G, Han J, Wang Y, et al. A potential downstream platform approach for WuXiBody-based IgG-like bispecific antibodies. Protein Expr Purif. 2020 Sep;173:105647. doi:10.1016/j.pep.2020.105647. PubMed PMID: 32334139.
37. Bargou R, Leo E, Zugmaier G, et al. Tumor regression in cancer patients by very low doses of a T cell-engaging antibody. Science. 2008 Aug 15;321(5891):974–77. PubMed PMID: 18703743. doi:10.1126/science.1158545

38. Neijssen J, Cardoso RMF, Chevalier KM, et al. Discovery of amivantamab (JNJ-61186372), a bispecific antibody targeting EGFR and MET. J Biol Chem. 2021 Apr;8:100641. doi:10.1016/j.jbc.2021.100641. PubMed PMID: 33839159; PubMed Central PMCID: PMCPMC8113745.
39. Vijayaraghavan S, Lipfert L, Chevalier K, et al. Amivantamab (JNJ-61186372), an Fc Enhanced EGFR/cMet Bispecific Antibody, Induces Receptor Downmodulation and Antitumor Activity by Monocyte/Macrophage Trogocytosis. Mol Cancer Ther. 2020 Oct;19(10):2044–56. 10.1158/1535-7163.MCT-20-0071: PubMed PMID: 32747419
40. Yun J, Lee SH, Kim SY, et al. Antitumor Activity of Amivantamab (JNJ-61186372), an EGFR-MET bispecific antibody, in diverse models of EGFR Exon 20 Insertion-Driven NSCLC. Cancer Discov. 2020 Aug;10(8):1194–209. 10.1158/2159-8290.CD-20-0116: PubMed PMID: 32414908
41. Schaefer W, Regula JT, Bahner M, et al. Immunoglobulin domain crossover as a generic approach for the production of bispecific IgG antibodies. Proc Natl Acad Sci U S A. 2011 Jul 5;108(27):11187–92. PubMed PMID: 21690412; PubMed Central PMCID: PMCPMC3131342. doi:10.1073/pnas.1019002108
42. Klein C, Sustmann C, Thomas M, et al. Progress in overcoming the chain association issue in bispecific heterodimeric IgG antibodies. MAbs. 2012 Nov-Dec;4(6):653–63. 10.4161/mabs.21379: PubMed PMID: 22925968; PubMed Central PMCID: PMCPMC3502232
43. Grote M, Haas AK, Klein C, et al. Bispecific antibody derivatives based on full-length IgG formats. Methods Mol Biol. 2012;901:247–63. PubMed PMID: 22723106. doi:10.1007/978-1-61779-931-0_16.
44. Klein C, Schaefer W, Regula JT. The use of CrossMAb technology for the generation of bi- and multispecific antibodies. MAbs. 2016 Aug-Sep;8(6):1010–20. PubMed PMID: 27285945; PubMed Central PMCID: PMCPMC4968094. doi:10.1080/19420862.2016.1197457.
45. Klein C, Schaefer W, Regula JT, et al. Engineering therapeutic bispecific antibodies using CrossMab technology. Methods. 2019 Feb 1;154:21–31. 10.1016/j.ymeth.2018.11.008: PubMed PMID: 30453028
46. Schaefer W, Volger HR, Lorenz S, et al. Heavy and light chain pairing of bivalent quadroma and knobs-into-holes antibodies analyzed by UHR-ESI-QTOF mass spectrometry. MAbs. 2016;8(1):49–55. PubMed PMID: 26496506; PubMed Central PMCID: PMCPMC4966523. doi:10.1080/19420862.2015.1111498.
47. Ridgway JB, Presta LG, Carter P. 'Knobs-into-holes' engineering of antibody CH3 domains for heavy chain heterodimerization. Protein Eng. 1996 Jul;9(7):617–21. doi:10.1093/protein/9.7.617. PubMed PMID: 8844834.
48. Kuglstatter A, Stihle M, Neumann C, et al. Structural differences between glycosylated, disulfide-linked heterodimeric Knob-into-Hole Fc fragment and its homodimeric Knob-Knob and Hole-Hole side products. Protein Eng Des Sel. 2017 Sep 1;30(9):649–56. PubMed PMID: 28985438. doi:10.1093/protein/gzx041
49. Stutz C, Blein S. A single mutation increases heavy-chain heterodimer assembly of bispecific antibodies by inducing structural disorder in one homodimer species. J Biol Chem. 2020 Jul 10;295(28):9392–408. PubMed PMID: 32404368; PubMed Central PMCID: PMCPMC7363136. doi:10.1074/jbc.RA119.012335.
50. Gong S, Ren F, Wu D, et al. Fabs-in-tandem immunoglobulin is a novel and versatile bispecific design for engaging multiple therapeutic targets. MAbs. 2017 Oct 9;7:1118–28. doi:10.1080/19420862.2017.1345401. PubMed PMID: 28692328; PubMed Central PMCID: PMCPMC5627593.
51. Gong S, Wu C. Generation of Fabs-in-tandem immunoglobulin molecules for dual-specific targeting. Methods. 2019 Feb 1;154:87–92. doi:10.1016/j.ymeth.2018.07.014. PubMed PMID: 30081078.
52. Fenn S, Schiller CB, Griese JJ, et al. Crystal structure of an anti-Ang2 CrossFab demonstrates complete structural and functional integrity of the variable domain. PLoS One. 2013;8(4):e61953. PubMed PMID: 23613981; PubMed Central PMCID: PMCPMC3629102. doi:10.1371/journal.pone.0061953.
53. Regula JT, Imhof-Jung S, Molhoj M, et al. Variable heavy-variable light domain and Fab-arm CrossMabs with charged residue exchanges to enforce correct light chain assembly. Protein Eng Des Sel. 2018 Jul 1;31(7–8):289–99. PubMed PMID: 30169707; PubMed Central PMCID: PMCPMC6277175. doi:10.1093/protein/gzy021
54. Sustmann C, Dickopf S, Regula JT, et al. DuoMab: a novel CrossMab-based IgG-derived antibody format for enhanced antibody-dependent cell-mediated cytotoxicity. MAbs. 2019 Nov-Dec;11(8):1402–14. 10.1080/19420862.2019.1661736: PubMed PMID: 31526159; PubMed Central PMCID: PMCPMC6816436
55. Wu X, Yuan R, Bacica M, et al. Generation of orthogonal Fab-based trispecific antibody formats. Protein Eng Des Sel. 2018 Jul 1;31(7–8):249–56. PubMed PMID: 29718394. doi:10.1093/protein/gzy007
56. Wu X, Demarest SJ. Building blocks for bispecific and trispecific antibodies. Methods. 2019 Feb 1;154:3–9. doi:10.1016/j.ymeth.2018.08.010. PubMed PMID: 30172007.
57. Bethune MT, Gee MH, Bunse M, et al. Domain-swapped T cell receptors improve the safety of TCR gene therapy. Elife. 2016 Nov;8:5. doi:10.7554/eLife.19095. PubMed PMID: 27823582; PubMed Central PMCID: PMCPMC5101000.
58. Croasdale R, Wartha K, Schanzer JM, et al. Development of tetravalent IgG1 dual targeting IGF-1R-EGFR antibodies with potent tumor inhibition. Arch Biochem Biophys. 2012 Oct 15;526(2):206–18. PubMed PMID: 22464987. doi:10.1016/j.abb.2012.03.016
59. Scheuer W, Thomas M, Hanke P, et al. Anti-tumoral, anti-angiogenic and anti-metastatic efficacy of a tetravalent bispecific antibody (TAvi6) targeting VEGF-A and angiopoietin-2. MAbs. 2016;8(3):562–73. PubMed PMID: 26864324; PubMed Central PMCID: PMCPMC4966847. doi:10.1080/19420862.2016.1147640.
60. Schanzer J, Jekle A, Nezu J, et al. Development of tetravalent, bispecific CCR5 antibodies with antiviral activity against CCR5 monoclonal antibody-resistant HIV-1 strains. Antimicrob Agents Chemother. 2011 May;55(5):2369–78. 10.1128/AAC.00215-10: PubMed PMID: 21300827; PubMed Central PMCID: PMCPMC3088204
61. Castoldi R, Ecker V, Wiehle L, et al. A novel bispecific EGFR/Met antibody blocks tumor-promoting phenotypic effects induced by resistance to EGFR inhibition and has potent antitumor activity. Oncogene. 2013 Dec 12;32(50):5593–601. PubMed PMID: 23812422; PubMed Central PMCID: PMCPMC3898114. doi:10.1038/onc.2013.245
62. Castoldi R, Jucknischke U, Pradel LP, et al. Molecular characterization of novel trispecific ErbB-cMet-IGF1R antibodies and their antigen-binding properties. Protein Eng Des Sel. 2012 Oct;25(10):551–59. 10.1093/protein/gzs048: PubMed PMID: 22936109; PubMed Central PMCID: PMCPMC3449402
63. Castoldi R, Schanzer J, Panke C, et al. TetraMabs: simultaneous targeting of four oncogenic receptor tyrosine kinases for tumor growth inhibition in heterogeneous tumor cell populations. Protein Eng Des Sel. 2016 Oct;29(10):467–75. 10.1093/protein/gzw037: PubMed PMID: 27578890; PubMed Central PMCID: PMCPMC5036864
64. Schanzer JM, Wartha K, Croasdale R, et al. A novel glycoengineered bispecific antibody format for targeted inhibition of epidermal growth factor receptor (EGFR) and insulin-like growth factor receptor type I (IGF-1R) demonstrating unique molecular properties. J Biol Chem. 2014 Jul 4;289(27):18693–706. PubMed PMID: 24841203; PubMed Central PMCID: PMCPMC4081915. doi:10.1074/jbc.M113.528109

65. Schanzer JM, Wartha K, Moessner E, et al. XGFR*, a novel affinity-matured bispecific antibody targeting IGF-1R and EGFR with combined signaling inhibition and enhanced immune activation for the treatment of pancreatic cancer. MAbs. 2016 May-Jun;8(4):811–27. 10.1080/19420862.2016.1160989: PubMed PMID: 26984378; PubMed Central PMCID: PMCPMC4966845
66. Niewoehner J, Bohrmann B, Collin L, et al. Increased brain penetration and potency of a therapeutic antibody using a monovalent molecular shuttle. Neuron. 2014 Jan 8;81(1):49–60. PubMed PMID: 24411731. doi:10.1016/j.neuron.2013.10.061
67. Weber F, Bohrmann B, Niewoehner J, et al. Brain shuttle antibody for alzheimer's disease with attenuated peripheral effector function due to an inverted binding mode. Cell Rep. 2018 Jan 2;22(1):149–62. PubMed PMID: 29298417. doi:10.1016/j.celrep.2017.12.019
68. Dengl S, Wehmer M, Hesse F, et al. Aggregation and chemical modification of monoclonal antibodies under upstream processing conditions. Pharm Res. 2013 May;30(5):1380–99. 10.1007/s11095-013-0977-8: PubMed PMID: 23322133
69. Haberger M, Leiss M, Heidenreich AK, et al. Rapid characterization of biotherapeutic proteins by size-exclusion chromatography coupled to native mass spectrometry. MAbs. 2016;8(2):331–39. PubMed PMID: 26655595; PubMed Central PMCID: PMCPMC4966600. doi:10.1080/19420862.2015.1122150.
70. Lee YF, Kluters S, Hillmann M, et al. Modeling of bispecific antibody elution in mixed-mode cation-exchange chromatography. J Sep Sci. 2017 Sep;40(18):3632–45. 10.1002/jssc.201700313: PubMed PMID: 28714211
71. Meschendoerfer W, Gassner C, Lipsmeier F, et al. SPR-based assays enable the full functional analysis of bispecific molecules. J Pharm Biomed Anal. 2017 Jan 5;132:141–47. 10.1016/j.jpba.2016.09.028: PubMed PMID: 27721070
72. Lu Y, Zhou Q, Han Q, et al. Inactivation of deubiquitinase CYLD enhances therapeutic antibody production in Chinese hamster ovary cells. Appl Microbiol Biotechnol. 2018 Jul;102(14):6081–93. 10.1007/s00253-018-9070-x: PubMed PMID: 29766242
73. Gstottner C, Nicolardi S, Haberger M, et al. Intact and subunit-specific analysis of bispecific antibodies by sheathless CE-MS. Anal Chim Acta. 2020 Oct 16;1134:18–27. 10.1016/j.aca.2020.07.069: PubMed PMID: 33059862
74. Gstottner C, Reusch D, Haberger M, et al. Monitoring glycation levels of a bispecific monoclonal antibody at subunit level by ultrahigh-resolution MALDI FT-ICR mass spectrometry. MAbs. 2020 Jan-Dec;12(1):1682403. 10.1080/19420862.2019.1682403: PubMed PMID: 31630606; PubMed Central PMCID: PMCPMC6927770
75. Graf T, Heinrich K, Grunert I, et al. Recent advances in LC-MS based characterization of protein-based bio-therapeutics - mastering analytical challenges posed by the increasing format complexity. J Pharm Biomed Anal. 2020 Jul 15;186:113251. 10.1016/j.jpba.2020.113251: PubMed PMID: 32251978
76. Filep C, Szigeti M, Farsang R, et al. Multilevel capillary gel electrophoresis characterization of new antibody modalities. Anal Chim Acta. 2021 Jun 29;1166:338492. 10.1016/j.aca.2021.338492: PubMed PMID: 34023000
77. Chen SW, Zhang W. Current trends and challenges in the downstream purification of bispecific antibodies. Antib Ther. 2021 Apr;4(2):73–88. doi:10.1093/abt/tbab007. PubMed PMID: 34056544; PubMed Central PMCID: PMCPMC8155696.
78. Register AC, Tarighat SS, Lee HY. Bioassay development for bispecific antibodies-challenges and opportunities. Int J Mol Sci. 2021 May 19;22(10). PubMed PMID: 34069573; PubMed Central PMCID: PMCPMC8160952. doi:10.3390/ijms22105350.
79. Haberger M, Heidenreich AK, Hook M, et al. Multiattribute monitoring of antibody charge variants by cation-exchange chromatography coupled to native mass spectrometry. J Am Soc Mass Spectrom. 2021 Mar 9 [PubMed PMID: 33687195]. doi:10.1021/jasms.0c00446.
80. Wan Y, Wang Y, Zhang T, et al. Application of pH-salt dual gradient elution in purifying a WuXiBody-based bispecific antibody by MMC ImpRes mixed-mode chromatography. Protein Expr Purif. 2021 May;181:105822. doi:10.1016/j.pep.2021.105822. PubMed PMID: 33429037.
81. Kienast Y, Klein C, Scheuer W, et al. Ang-2-VEGF-A CrossMab, a novel bispecific human IgG1 antibody blocking VEGF-A and Ang-2 functions simultaneously, mediates potent antitumor, anti-angiogenic, and antimetastatic efficacy. Clin Cancer Res. 2013 Dec 15;19(24):6730–40. PubMed PMID: 24097868. doi:10.1158/1078-0432.CCR-13-0081
82. Regula JT, Lundh von Leithner P, Foxton R, et al. Targeting key angiogenic pathways with a bispecific Cross MAb optimized for neovascular eye diseases. EMBO Mol Med. 2016 Nov 8;8(11):1265–88. PubMed PMID: 27742718; PubMed Central PMCID: PMCPMC5090659. doi:10.15252/emmm.201505889
83. Regula JT, Lundh von Leithner P, Foxton R, et al. Targeting key angiogenic pathways with a bispecific CrossMAb optimized for neovascular eye diseases. EMBO Mol Med. 2019 May;11(5):10.15252/emmm.201910666. PubMed PMID: 31040127; PubMed Central PMCID: PMCPMC6505574.
84. Bacac M, Fauti T, Sam J, et al. A novel carcinoembryonic antigen T-cell bispecific antibody (CEA TCB) for the treatment of solid tumors. Clin Cancer Res. 2016 Jul 1;22(13):3286–97. PubMed PMID: 26861458. doi:10.1158/1078-0432.CCR-15-1696
85. Brunker P, Wartha K, Friess T, et al. RG7386, a novel tetravalent FAP-DR5 antibody, effectively triggers fap-dependent, avidity-driven dr5 hyperclustering and tumor cell apoptosis. Mol Cancer Ther. 2016 May;15(5):946–57. 10.1158/1535-7163.MCT-15-0647: PubMed PMID: 27037412
86. Bacac M, Colombetti S, Herter S, et al. CD20-TCB with obinutuzumab pretreatment as next-generation treatment of hematologic malignancies. Clin Cancer Res. 2018 Oct 1;24(19):4785–97. PubMed PMID: 29716920. doi:10.1158/1078-0432.CCR-18-0455
87. Deak LLC, Seeber S, Perro M, et al. Abstract 2270: RG7769 (PD1-TIM3), a novel heterodimeric avidity-driven T cell specific PD-1/TIM-3 bispecific antibody lacking Fc-mediated effector functions for dual checkpoint inhibition to reactivate dysfunctional T cells. Cancer Research. 2020;80(16 Supplement):2270–2270. doi:10.1158/1538-7445.am2020-2270.
88. Seckinger A, Delgado JA, Moser S, et al. Target expression, generation, preclinical activity, and pharmacokinetics of the BCMA-T cell bispecific antibody EM801 for multiple myeloma treatment. Cancer Cell. 2017 Mar 13;31(3):396–410. PubMed PMID: 28262554. doi:10.1016/j.ccell.2017.02.002
89. Claus C, Ferrara C, Xu W, et al. Tumor-targeted 4-1BB agonists for combination with T cell bispecific antibodies as off-the-shelf therapy. Sci Transl Med. 2019 Jun 12;11(496):eaav5989. PubMed PMID: 31189721; PubMed Central PMCID: PMCPMC7181714. doi:10.1126/scitranslmed.aav5989
90. Huang Y, Yu J, Lanzi A, et al. Engineered Bispecific Antibodies with Exquisite HIV-1-Neutralizing Activity. Cell. 2016 Jun 16;165(7):1621–31. PubMed PMID: 27315479; PubMed Central PMCID: PMCPMC4972332. doi:10.1016/j.cell.2016.05.024
91. Deak LC, Weber P, Seeber S, et al. editors. A novel bispecific checkpoint inhibitor antibody to preferentially block PD-1 and LAG-3 on dysfunctional TILs whilst sparing Treg activation. In: JOURNAL FOR IMMUNOTHERAPY OF CANCER. ENGLAND: BMC CAMPUS, 4 CRINAN ST, LONDON N1 9XW; 2019.
92. Nicolini VG, Waldhauer I, Freimoser-Grundschober A, et al. Abstract LB-389: combination of TYRP1-TCB, a novel T cell bispecific antibody for the treatment of melanoma, with immunomodulatory agents. Cancer Research. 2020;80(16Supplement):LB-389-LB-389. doi:10.1158/1538-7445.am2020-lb-389.
93. Augsberger C, Hanel G, Xu W, et al. Targeting intracellular WT1 in AML with a novel RMF-peptide-MHC specific T-cell bispecific antibody. Blood. 2021 Jul 19 [PubMed PMID: 34280257]. doi:10.1182/blood.2020010477.
94. Sum E, Rapp M, Frobel P, et al. Fibroblast activation protein alpha-targeted CD40 agonism abrogates systemic toxicity and enables administration of high doses to induce effective antitumor immunity. Clin Cancer Res. 2021 Mar 26;27(14):4036–53. PubMed PMID: 33771854. doi:10.1158/1078-0432.CCR-20-4001

95. Chung AS, Lee J, Ferrara N. Targeting the tumour vasculature: insights from physiological angiogenesis. Nat Rev Cancer. 2010 Jul;10(7):505–14. PubMed PMID: 20574450. doi:10.1038/nrc2868.
96. Ferrara N, Adamis AP. Ten years of anti-vascular endothelial growth factor therapy. Nat Rev Drug Discov. 2016 Jun;15 (6):385–403. PubMed PMID: 26775688. doi:10.1038/nrd.2015.17.
97. Parmar D, Apte M. Angiopoietin inhibitors: a review on targeting tumor angiogenesis. Eur J Pharmacol. 2021 May 15;899:174021. doi:10.1016/j.ejphar.2021.174021. PubMed PMID: 33741382.
98. Kloepper J, Riedemann L, Amoozgar Z, et al. Ang-2/VEGF bispecific antibody reprograms macrophages and resident microglia to anti-tumor phenotype and prolongs glioblastoma survival. Proc Natl Acad Sci U S A. 2016 Apr 19;113(16):4476–81. PubMed PMID: 27044098; PubMed Central PMCID: PMCPMC4843473. doi:10.1073/pnas.1525360113
99. Baker LCJ, Boult JKR, Thomas M, et al. Acute tumour response to a bispecific Ang-2-VEGF-A antibody: insights from multiparametric MRI and gene expression profiling. Br J Cancer. 2016 Sep 6;115(6):691–702. PubMed PMID: 27529514; PubMed Central PMCID: PMCPMC5023775. doi:10.1038/bjc.2016.236
100. Solecki G, Osswald M, Weber D, et al. Differential effects of ang-2/VEGF-A inhibiting antibodies in combination with radio- or chemotherapy in glioma. Cancers (Basel). 2019 Mar 6;11(3): 10.3390/cancers11030314. PubMed PMID: 30845704; PubMed Central PMCID: PMCPMC6468722.
101. Mueller T, Freystein J, Lucas H, et al. Efficacy of a bispecific antibody co-targeting VEGFA and Ang-2 in combination with chemotherapy in a chemoresistant colorectal carcinoma xenograft model. Molecules. 2019 Aug 7;24(16): 10.3390/molecules24162865. PubMed PMID: 31394786; PubMed Central PMCID: PMCPMC6719918.
102. Schmittnaegel M, Rigamonti N, Kadioglu E, et al. Dual angiopoietin-2 and VEGFA inhibition elicits antitumor immunity that is enhanced by PD-1 checkpoint blockade. Sci Transl Med. 2017 Apr 12;9(385): 10.1126/scitranslmed.aak9670. PubMed PMID: 28404865.
103. Killock D. Immunotherapy: combine and conquer - antiangiogenic immunotherapy. Nat Rev Clin Oncol. 2017 Jun;14(6):327. PubMed PMID: 28466876. doi:10.1038/nrclinonc.2017.65.
104. Schmittnaegel M, De Palma M. Reprogramming tumor blood vessels for enhancing immunotherapy. Trends Cancer. 2017 Dec;3(12):809–12. doi:10.1016/j.trecan.2017.10.002. PubMed PMID: 29198436.
105. Kashyap AS, Schmittnaegel M, Rigamonti N, et al. Optimized antiangiogenic reprogramming of the tumor microenvironment potentiates CD40 immunotherapy. Proc Natl Acad Sci U S A. 2020 Jan 7;117 (1):541–51. PubMed PMID: 31889004; PubMed Central PMCID: PMCPMC6955310. doi:10.1073/pnas.1902145116
106. Ragusa S, Prat-Luri B, Gonzalez-Loyola A, et al. Antiangiogenic immunotherapy suppresses desmoplastic and chemoresistant intestinal tumors in mice. J Clin Invest. 2020 Mar 2;130 (3):1199–216. PubMed PMID: 32015230; PubMed Central PMCID: PMCPMC7269598. doi:10.1172/JCI129558
107. Hidalgo M, Martinez-Garcia M, Le Tourneau C, et al. First-in-human phase i study of single-agent vanucizumab, a first-in-class bispecific anti-angiopoietin-2/Anti-VEGF-A antibody, in adult patients with advanced solid tumors. Clin Cancer Res. 2018 Apr 1;24(7):1536–45. PubMed PMID: 29217526. doi:10.1158/1078-0432.CCR-17-1588
108. Heil F, Babitzki G, Julien-Laferriere A, et al. Vanucizumab mode of action: serial biomarkers in plasma, tumor, and skin-wound-healing biopsies. Transl Oncol. 2021 Feb;14(2):100984. 10.1016/j.tranon.2020.100984: PubMed PMID: 33338877; PubMed Central PMCID: PMCPMC7749407
109. Bendell JC, Sauri T, Gracian AC, et al. The McCAVE Trial: vanucizumab plus mFOLFOX-6 Versus Bevacizumab plus mFOLFOX-6 in patients with previously untreated metastatic colorectal carcinoma (mCRC). Oncologist. 2020 Mar;25(3):e451–e459. 10.1634/theoncologist.2019-0291: PubMed PMID: 32162804; PubMed Central PMCID: PMCPMC7066709
110. Hauschildt J, Schrimpf C, Thamm K, et al. Dual Pharmacological Inhibition of Angiopoietin-2 and VEGF-A in murine experimental sepsis. J Vasc Res. 2020;57(1):34–45. PubMed PMID: 31726451. doi:10.1159/000503787.
111. Zhou R, Wang S, Wen H, et al. The bispecific antibody HB-32, blockade of both VEGF and DLL4 shows potent anti-angiogenic activity in vitro and anti-tumor activity in breast cancer xenograft models. Exp Cell Res. 2019 Jul 15;380(2):141–48. PubMed PMID: 31034805. doi:10.1016/j.yexcr.2019.04.025
112. Gschwind A, Fischer OM, Ullrich A. The discovery of receptor tyrosine kinases: targets for cancer therapy. Nat Rev Cancer. 2004 May;4(5):361–70. doi:10.1038/nrc1360. PubMed PMID: 15122207.
113. Zhang F, Zhang J, Liu M, et al. Combating HER2-overexpressing breast cancer through induction of calreticulin exposure by Tras-Permut CrossMab. Oncoimmunology. 2015 Mar;4(3):e994391. 10.4161/2162402X.2014.994391: PubMed PMID: 25949918; PubMed Central PMCID: PMCPMC4404837
114. Hu S, Fu W, Xu W, et al. Four-in-one antibodies have superior cancer inhibitory activity against EGFR, HER2, HER3, and VEGF through disruption of HER/MET crosstalk. Cancer Res. 2015 Jan 1;75(1):159–70. PubMed PMID: 25371409. doi:10.1158/0008-5472.CAN-14-1670
115. Hu S, Fu W, Li T, et al. Antagonism of EGFR and Notch limits resistance to EGFR inhibitors and radiation by decreasing tumor-initiating cell frequency. Sci Transl Med. 2017 Mar 8;9 (380):eaag0339. PubMed PMID: 28275151. doi:10.1126/scitranslmed.aag0339
116. Fu W, Lei C, Yu Y, et al. EGFR/notch antagonists enhance the response to inhibitors of the PI3K-Akt pathway by decreasing tumor-initiating cell frequency. Clin Cancer Res. 2019 May 1;25 (9):2835–47. PubMed PMID: 30670492. doi:10.1158/1078-0432.CCR-18-2732
117. Lim B, Greer Y, Lipkowitz S, et al. Novel Apoptosis-Inducing Agents for the Treatment of Cancer, a New Arsenal in the Toolbox. Cancers (Basel). 2019 Jul 31;11(8):1087. PubMed PMID: 31370269; PubMed Central PMCID: PMCPMC6721450. doi:10.3390/cancers11081087
118. Carneiro BA, El-Deiry WS. Targeting apoptosis in cancer therapy. Nat Rev Clin Oncol. 2020 Jul;17(7):395–417. PubMed PMID: 32203277; PubMed Central PMCID: PMCPMC8211386. doi:10.1038/s41571-020-0341-y.
119. Davidson S, Coles M, Thomas T, et al. Fibroblasts as immune regulators in infection, inflammation and cancer. Nat Rev Immunol. 2021 Apr 28 [PubMed PMID: 33911232]. doi:10.1038/s41577-021-00540-z.
120. Kratochwil C, Flechsig P, Lindner T, et al. (68)Ga-FAPIPET/CT: tracer uptake in 28 different kinds of cancer. J Nucl Med. 2019 Jun;60(6):801–05. 10.2967/jnumed.119.227967: PubMed PMID: 30954939; PubMed Central PMCID: PMCPMC6581228
121. Locksley RM, Killeen N, Lenardo MJ. The TNF and TNF receptor superfamilies: integrating mammalian biology. Cell. 2001 Feb 23;104(4):487–501. PubMed PMID: 11239407. doi:10.1016/s0092-8674(01)00237-9.
122. Labiano S, Roh V, Godfroid C, et al. CD40 agonist targeted to fibroblast activation protein alpha synergizes with radiotherapy in murine hpv-positive head and neck tumors. Clin Cancer Res. 2021 Apr 26;27(14):4054–65. PubMed PMID: 33903200. doi:10.1158/1078-0432.CCR-20-4717
123. Tung HY, Su YC, Chen BM, et al. Selective delivery of PEGylated compounds to tumor cells by anti-PEG hybrid antibodies. Mol Cancer Ther. 2015 Jun;14(6):1317–26. 10.1158/1535-7163.MCT-15-0151: PubMed PMID: 25852063
124. Herrera-Camacho I, Anaya-Ruiz M, Perez-Santos M, et al. Cancer immunotherapy using anti-TIM3/PD-1 bispecific antibody: a patent evaluation of EP3356411A1. Expert Opin Ther Pat. 2019 Aug;29(8):587–93. 10.1080/13543776.2019.1637422: PubMed PMID: 31241380

125. Cebada J, Flores A, Bandala C, et al. Bispecific anti-PD-1/LAG-3 antibodies for treatment of advanced or metastatic solid tumors: a patent evaluation of US2018326054. Expert Opin Ther Pat. 2020 Jul;30(7):487–94. 10.1080/13543776.2020.1767071: PubMed PMID: 32397849
126. Dougall WC, Roman Aguilera A, Smyth MJ. Dual targeting of RANKL and PD-1 with a bispecific antibody improves anti-tumor immunity. Clin Transl Immunology. 2019;8(10): e01081. doi:10.1002/cti2.1081. PubMed PMID: 31572609; PubMed Central PMCID: PMCPMC6763724
127. De Miguel M, Umana P, Gomes de Morais AL, et al. T-cell-engaging Therapy for Solid Tumors. Clin Cancer Res. 2021 Mar 15;27(6):1595–603. PubMed PMID: 33082210. doi:10.1158/1078-0432.CCR-20-2448
128. Singh A, Dees S, Grewal IS. Overcoming the challenges associated with CD3+ T-cell redirection in cancer. Br J Cancer. 2021 Mar;124 (6):1037–48. PubMed PMID: 33469153; PubMed Central PMCID: PMCPMC7960983. doi:10.1038/s41416-020-01225-5.
129. Crawford A, Chiu D. Targeting solid tumors using CD3 bispecific antibodies. Mol Cancer Ther. 2021 May 27;20(8):1350–58. PubMed PMID: 34045228. doi:10.1158/1535-7163.MCT-21-0073.
130. Kaiser J. Forced into battle. Science. 2020 May 29;368 (6494):930–33. PubMed PMID: 32467373. doi:10.1126/science.368.6494.930.
131. Wu Z, Cheung NV. T cell engaging bispecific antibody (T-BsAb): from technology to therapeutics. Pharmacol Ther. 2018 Feb;182:161–75 . PubMed PMID: 28834699; PubMed Central PMCID: PMCPMC5785550. doi:10.1016/j.pharmthera.2017.08.005.
132. Bacac M, Klein C, CEA TCB: UP. A novel head-to-tail 2:1 T cell bispecific antibody for treatment of CEA-positive solid tumors. Oncoimmunology. 2016 Aug 5;5(8):e1203498. PubMed PMID: 27622073; PubMed Central PMCID: PMCPMC5007959. doi:10.1080/2162402X.2016.1203498.
133. Schlothauer T, Herter S, Koller CF, et al. Novel human IgG1 and IgG4 Fc-engineered antibodies with completely abolished immune effector functions. Protein Eng Des Sel. 2016 Oct;29(10):457–66. 10.1093/protein/gzw040: PubMed PMID: 27578889
134. Lehmann S, Perera R, Grimm HP, et al. In Vivo Fluorescence Imaging of the Activity of CEA TCB, a novel T-cell bispecific antibody, reveals highly specific tumor targeting and fast induction of T-cell-mediated tumor killing. Clin Cancer Res. 2016 Sep 1;22 (17):4417–27. PubMed PMID: 27117182. doi:10.1158/1078-0432.CCR-15-2622
135. Van De Vyver AJ, Weinzierl T, Eigenmann MJ, et al. Predicting tumor killing and T-cell activation by T-cell bispecific antibodies as a function of target expression: combining in vitro experiments with systems modeling. Mol Cancer Ther. 2021 Feb;20(2):357–66. 10.1158/1535-7163.MCT-20-0269: PubMed PMID: 33298591
136. Gonzalez-Exposito R, Semiannikova M, Griffiths B, et al. CEA expression heterogeneity and plasticity confer resistance to the CEA-targeting bispecific immunotherapy antibody cibisatamab (CEA-TCB) in patient-derived colorectal cancer organoids. J Immunother Cancer. 2019 Apr 15;7(1):101. PubMed PMID: 30982469; PubMed Central PMCID: PMCPMC6463631. doi:10.1186/s40425-019-0575-3
137. Teijeira A, Etxeberria I, Ponz-Sarvise M, et al. Immunotherapy of cancer visualized by live microscopy: seeing is believing. Clin Cancer Res. 2016 Sep 1;22(17):4277–79. PubMed PMID: 27330056. doi:10.1158/1078-0432.CCR-16-1072
138. Sam J, Colombetti S, Fauti T, et al. Combination of T-cell bispecific antibodies With PD-L1 checkpoint inhibition elicits superior anti-tumor activity. Front Oncol. 2020;10:575737. PubMed PMID: 33330050; PubMed Central PMCID: PMCPMC7735156. doi:10.3389/fonc.2020.575737.
139. Dudal S, Hinton H, Giusti AM, et al. Application of a MABEL approach for a T-cell-bispecific monoclonal antibody: CEA TCB. J Immunother. 2016 Sep;39(7):279–89. 10.1097/CJI.0000000000000132: PubMed PMID: 27404941
140. Kamperschroer C, Shenton J, Lebrec H, et al. Summary of a workshop on preclinical and translational safety assessment of CD3 bispecifics. J Immunotoxicol. 2020 Dec;17(1):67–85. 10.1080/1547691X.2020.1729902: PubMed PMID: 32100588
141. Cremasco F, Menietti E, Speziale D, et al. Cross-linking of T cell to B cell lymphoma by the T cell bispecific antibody CD20-TCB induces IFNgamma/CXCL10-dependent peripheral T cell recruitment in humanized murine model. PLoS One. 2021;16(1):e0241091. PubMed PMID: 33406104; PubMed Central PMCID: PMCPMC7787458 and SC declare ownership of Roche stocks. MP, PU, MB, CK, SC, JS are inventors on patent applications related to the CD20-TCB. This affiliation and patent participation do not alter our adherence to PLOS ONE policies on sharing data and materials. doi:10.1371/journal.pone.0241091.
142. Prakash A, Diefenbach CS. Immunity War: a Novel Therapy for Lymphoma Using T-cell Bispecific Antibodies. Clin Cancer Res. 2018 Oct 1;24(19):4631–32. PubMed PMID: 29884742. doi:10.1158/1078-0432.CCR-18-1363.
143. Hutchings M, Morschhauser F, Iacoboni G, et al. Glofitamab, a novel, bivalent CD20-Targeting T-cell-engaging bispecific antibody, induces durable complete remissions in relapsed or refractory B-cell lymphoma: a phase I trial. J Clin Oncol. 2021 Jun 20;39(18):1959–70. PubMed PMID: 33739857; PubMed Central PMCID: PMCPMC8210975. doi:10.1200/JCO.20.03175
144. Killock D. Engaging results with glofitamab. Nat Rev Clin Oncol. 2021 May;18(5):257. PubMed PMID: 33828233. doi:10.1038/s41571-021-00510-3.
145. Minson A, Glofitamab DM. CD20-TCB bispecific antibody. Leuk Lymphoma. 2021 Jul 15. 1–11. PubMed PMID: 34263696. doi:10.1080/10428194.2021.1953016.
146. Liddy N, Bossi G, Adams KJ, et al. Monoclonal TCR-redirected tumor cell killing. Nat Med. 2012 Jun;18(6):980–87. 10.1038/nm.2764: PubMed PMID: 22561687
147. Arenas EJ, Martinez-Sabadell A, Rius Ruiz I, et al. Acquired cancer cell resistance to T cell bispecific antibodies and CAR T targeting HER2 through JAK2 down-modulation. Nat Commun. 2021 Feb 23;12(1):1237. PubMed PMID: 33623012; PubMed Central PMCID: PMCPMC7902842. doi:10.1038/s41467-021-21445-4
148. Loo Yau H, Bell E, Ettayebi I, et al. DNA hypomethylating agents increase activation and cytolytic activity of CD8(+) T cells. Mol Cell. 2021 Apr 1;81(7):1469–1483e8. PubMed PMID: 33609448. doi:10.1016/j.molcel.2021.01.038
149. Rius Ruiz I, Vicario R, Morancho B, et al. p95HER2-T cell bispecific antibody for breast cancer treatment. Sci Transl Med. 2018 Oct 3;10 (461):eaat1445. PubMed PMID: 30282693; PubMed Central PMCID: PMCPMC6498439. doi:10.1126/scitranslmed.aat1445
150. Geiger M, Stubenrauch KG, Sam J, et al. Protease-activation using anti-idiotypic masks enables tumor specificity of a folate receptor 1-T cell bispecific antibody. Nat Commun. 2020 Jun 24;11(1):3196. PubMed PMID: 32581215; PubMed Central PMCID: PMCPMC7314773. doi:10.1038/s41467-020-16838-w
151. Leclercq G, Haegel H, Schneider A, et al. Src/lck inhibitor dasatinib reversibly switches off cytokine release and T cell cytotoxicity following stimulation with T cell bispecific antibodies. J Immunother Cancer. 2021 Jul 9;9(7):e002582. PubMed PMID: 34326166. doi:10.1136/jitc-2021-002582
152. Karches CH, Benmebarek MR, Schmidbauer ML, et al. Bispecific antibodies enable synthetic agonistic receptor-transduced t cells for tumor immunotherapy. Clin Cancer Res. 2019 Oct 1;25 (19):5890–900. PubMed PMID: 31285373. doi:10.1158/1078-0432.CCR-18-3927
153. Darowski D, Kobold S, Jost C, et al. Combining the best of two worlds: highly flexible chimeric antigen receptor adaptor molecules (CAR-adaptors) for the recruitment of chimeric antigen receptor T cells. MAbs. 2019;11(4):621–31. PubMed PMID: 30892136; PubMed Central PMCID: PMCPMC6601549. doi:10.1080/19420862.2019.1596511. May/Jun.

154. Kobold S, Steffen J, Chaloupka M, et al. Selective bispecific T cell recruiting antibody and antitumor activity of adoptive T cell transfer. J Natl Cancer Inst 2015 Jan;107(1):364. 10.1093/jnci/dju364: PubMed PMID: 25424197
155. Griessinger CM, Olafsen T, Mascioni A, et al. The PET-tracer (89) Zr-Df-IAB22M2CEnables monitoring of intratumoral CD8 T-cell infiltrates in tumor-bearing humanized mice after t-cell bispecific antibody treatment. Cancer Res. 2020 Jul 1;80 (13):2903–13. PubMed PMID: 32409308. doi:10.1158/0008-5472.CAN-19-3269
156. Villanueva MT. Building on bispecifics. Nat Rev Drug Discov. 2019 Jul;18(8):582. PubMed PMID: 31367057. doi:10.1038/d41573-019-00117-5.
157. Trub M, Uhlenbrock F, Claus C, et al. Fibroblast activation protein-targeted-4-1BB ligand agonist amplifies effector functions of intratumoral T cells in human cancer. J Immunother Cancer. 2020 Jul;8(2):e000238. 10.1136/jitc-2019-000238: PubMed PMID: 32616554; PubMed Central PMCID: PMCPMC7333869
158. Gauthier L, Morel A, Anceriz N, et al. Multifunctional natural killer cell engagers targeting NKp46 trigger protective tumor immunity. Cell. 2019 Jun 13;177(7):1701–1713e16. PubMed PMID: 31155232. doi:10.1016/j.cell.2019.04.041
159. Zhao L, Xie F, Tong X, et al. Combating non-Hodgkin lymphoma by targeting both CD20 and HLA-DR through CD20-243 CrossMab. MAbs. 2014 May-Jun;6(3):740–48. 10.4161/mabs.28613: PubMed PMID: 24670986; PubMed Central PMCID: PMCPMC4011918
160. Rajendran S, Li Y, Ngoh E, et al. Development of a bispecific antibody targeting CD30 and CD137 on hodgkin and reed-sternberg cells. Front Oncol. 2019;9:945. PubMed PMID: 31616638; PubMed Central PMCID: PMCPMC6768943. doi:10.3389/fonc.2019.00945.
161. Du K, Li Y, Liu J, et al. A bispecific antibody targeting GPC3 and CD47 induced enhanced antitumor efficacy against dual antigen-expressing HCC. Mol Ther. 2021 Apr 7;29(4):1572–84. PubMed PMID: 33429083; PubMed Central PMCID: PMCPMC8058486. doi:10.1016/j.ymthe.2021.01.006
162. Zhao L, Tong Q, Qian W, et al. Eradication of non-Hodgkin lymphoma through the induction of tumor-specific T-cell immunity by CD20-Flex BiFP. Blood. 2013 Dec 19;122 (26):4230–36. PubMed PMID: 24178967. doi:10.1182/blood-2013-04-496554
163. Panina AA, Rybchenko VS, Solopova ON, et al. Recombinant bispecific antibodies to the human erbb2 receptor and interferon-beta. Acta Naturae. 2020 Apr-Jun;12(2):95–104. 10.32607/actanaturae.10903: PubMed PMID: 32742732; PubMed Central PMCID: PMCPMC7385087
164. Montefiori DC. Bispecific Antibodies Against HIV. Cell. 2016 Jun 16;165(7):1563–64. PubMed PMID: 27315470. doi:10.1016/j.cell.2016.06.004.
165. Kingwell K. Infectious diseases: two-pronged attack on HIV. Nat Rev Immunol. 2016 Jul 27;16(8):465. PubMed PMID: 27461148. doi:10.1038/nri.2016.87.
166. Asokan M, Rudicell RS, Louder M, et al. Bispecific Antibodies Targeting Different Epitopes on the HIV-1 Envelope Exhibit Broad and Potent Neutralization. J Virol. 2015 Dec;89 (24):12501–12. 10.1128/JVI.02097-15: PubMed PMID: 26446600; PubMed Central PMCID: PMCPMC4665248
167. Galimidi RP, Klein JS, Politzer MS, et al. Intra-spike crosslinking overcomes antibody evasion by HIV-1. Cell. 2015 Jan 29;160 (3):433–46. PubMed PMID: 25635457; PubMed Central PMCID: PMCPMC4401576. doi:10.1016/j.cell.2015.01.016
168. Bournazos S, Gazumyan A, Seaman MS, et al. Bispecific Anti-HIV-1 antibodies with enhanced breadth and potency. Cell. 2016 Jun 16;165(7):1609–20. PubMed PMID: 27315478; PubMed Central PMCID: PMCPMC4970321. doi:10.1016/j.cell.2016.04.050
169. Khan SN, Sok D, Tran K, et al. Targeting the HIV-1 spike and coreceptor with bi- and trispecific antibodies for single-component broad inhibition of entry. J Virol. 2018 Sep 15;92(18): 10.1128/JVI.00384-18. PubMed PMID: 29976677; PubMed Central PMCID: PMCPMC6146690.
170. Moshoette T, Ali SA, Papathanasopoulos MA, et al. Engineering and characterising a novel, highly potent bispecific antibody iMab-CAP256 that targets HIV-1. Retrovirology. 2019 Nov 8;16(1):31. PubMed PMID: 31703699; PubMed Central PMCID: PMCPMC6842167. doi:10.1186/s12977-019-0493-y
171. Davis-Gardner ME, Alfant B, Weber JA, et al. A Bispecific Antibody That Simultaneously Recognizes the V2- and V3-Glycan Epitopes of the HIV-1 envelope glycoprotein is broader and more potent than its parental antibodies. mBio. 2020 Jan 14;11 (1): 10.1128/mBio.03080-19. PubMed PMID: 31937648; PubMed Central PMCID: PMCPMC6960291.
172. Guttman M, Padte NN, Huang Y, et al. The influence of proline isomerization on potency and stability of anti-HIV antibody 10E8. Sci Rep. 2020 Aug 31;10(1):14313. PubMed PMID: 32868832; PubMed Central PMCID: PMCPMC7458915. doi:10.1038/s41598-020-71184-7
173. Wagh K, Seaman MS, Zingg M, et al. Potential of conventional & bispecific broadly neutralizing antibodies for prevention of HIV-1 subtype A, C & D infections. PLoS Pathog. 2018 Mar;14(3): e1006860. 10.1371/journal.ppat.1006860: PubMed PMID: 29505593; PubMed Central PMCID: PMCPMC5854441
174. Padte NN, Yu J, Huang Y, et al. Engineering multi-specific antibodies against HIV-1. Retrovirology. 2018 Aug 29;15(1):60. PubMed PMID: 30157871; PubMed Central PMCID: PMCPMC6114543. doi:10.1186/s12977-018-0439-9
175. Wang J, Bardelli M, Espinosa DA, et al. A human bi-specific antibody against zika virus with high therapeutic potential. Cell. 2017 Sep 21;171(1):229–241e15. PubMed PMID: 28938115; PubMed Central PMCID: PMCPMC5673489. doi:10.1016/j.cell.2017.09.002
176. De Gasparo R, Pedotti M, Simonelli L, et al. Bispecific IgG neutralizes SARS-CoV-2 variants and prevents escape in mice. Nature. 2021 May;593(7859):424–28. 10.1038/s41586-021-03461-y: PubMed PMID: 33767445
177. Jette CA, Cohen AA, Gnanapragasam PNP, et al. Broad cross-reactivity across sarbecoviruses exhibited by a subset of COVID-19 donor-derived neutralizing antibodies. bioRxiv. 2021 Apr 26 [PubMed PMID: 33948592; PubMed Central PMCID: PMCPMC8095199]. doi:10.1101/2021.04.23.441195.
178. Taylor PC, Williams RO. Combination cytokine blockade: the way forward in therapy for rheumatoid arthritis? Arthritis Rheumatol. 2015 Jan;67(1):14–16. PubMed PMID: 25302944. doi:10.1002/art.38893.
179. Buckland J. Rheumatoid arthritis: anti-TNF and anti-IL-17 antibodies–better together! Nat Rev Rheumatol. 2014 Dec;10(12):699. PubMed PMID: 25348041. doi:10.1038/nrrheum.2014.183.
180. Fischer JA, Hueber AJ, Wilson S, et al. Combined inhibition of tumor necrosis factor alpha and interleukin-17 as a therapeutic opportunity in rheumatoid arthritis: development and characterization of a novel bispecific antibody. Arthritis Rheumatol. 2015 Jan;67(1):51–62. 10.1002/art.38896: PubMed PMID: 25303306
181. Xu T, Ying T, Wang L, et al. A native-like bispecific antibody suppresses the inflammatory cytokine response by simultaneously neutralizing tumor necrosis factor-alpha and interleukin-17A. Oncotarget. 2017 Oct 10;8(47):81860–72. PubMed PMID: 29137228; PubMed Central PMCID: PMCPMC5669854. doi:10.18632/oncotarget.19899
182. Heier JS, Singh RP, Wykoff CC, et al. The angiopoietin/tie pathway in retinal vascular diseases: a Review. Retina. 2021 Jan 1;41 (1):1–19. PubMed PMID: 33136975. doi:10.1097/IAE.0000000000003003

183. Hussain RM, Neiweem AE, Kansara V, et al. Tie-2/Angiopoietin pathway modulation as a therapeutic strategy for retinal disease. Expert Opin Investig Drugs. 2019 Oct;28(10):861–69. 10.1080/13543784.2019.1667333: PubMed PMID: 31513439
184. Fleckenstein M, Keenan TDL, Guymer RH, et al. Age-related macular degeneration. Nat Rev Dis Primers. 2021 May 6;7(1):31. PubMed PMID: 33958600. doi:10.1038/s41572-021-00265-2
185. Hussain RM, Shaukat BA, Ciulla LM, et al. Vascular endothelial growth factor antagonists: promising players in the treatment of neovascular age-related macular degeneration. Drug Des Devel Ther. 2021;15:2653–65. PubMed PMID: 34188445; PubMed Central PMCID: PMCPMC8232378. doi:10.2147/DDDT.S295223.
186. Sharma A, Kumar N, Kuppermann BD, et al. Faricimab: expanding horizon beyond VEGF. Eye (Lond). 2020 May;34(5):802–04. 10.1038/s41433-019-0670-1: PubMed PMID: 31695160; PubMed Central PMCID: PMCPMC7182558
187. Jakubiak P, Alvarez-Sanchez R, Fueth M, et al. Ocular pharmacokinetics of intravitreally injected protein therapeutics: comparison among standard-of-care formats. Mol Pharm. 2021 Jun 7;18(6):2208–17. PubMed PMID: 34014104. doi:10.1021/acs.molpharmaceut.0c01218
188. Joussen AM, Ricci F, Paris LP, et al. Angiopoietin/Tie2 signalling and its role in retinal and choroidal vascular diseases: a review of preclinical data. Eye (Lond). 2021 May;35(5):1305–16. 10.1038/s41433-020-01377-x: PubMed PMID: 33564135; PubMed Central PMCID: PMCPMC8182896
189. Nicolo M, Ferro Desideri L, Vagge A, et al. Faricimab: an investigational agent targeting the Tie-2/angiopoietin pathway and VEGF-A for the treatment of retinal diseases. Expert Opin Investig Drugs. 2021 Mar;30(3):193–200. 10.1080/13543784.2021.1879791: PubMed PMID: 33471572
190. Foxton RH, Uhles S, Gruner S, et al. Efficacy of simultaneous VEGF-A/ANG-2 neutralization in suppressing spontaneous choroidal neovascularization. EMBO Mol Med. 2019 May;11(5):10.15252/emmm.201810204. PubMed PMID: 31040126; PubMed Central PMCID: PMCPMC6505683.
191. Wolf A, Langmann T. Anti-VEGF-A/ANG2 combotherapy limits pathological angiogenesis in the eye: a replication study. EMBO Mol Med. 2019 May;11(5): 10.15252/emmm.201910362. PubMed PMID: 31040129; PubMed Central PMCID: PMCPMC6505573.
192. Chakravarthy U, Bailey C, Brown D, et al. Phase I trial of anti-vascular endothelial growth factor/anti-angiopoietin 2 bispecific antibody rg7716 for neovascular age-related macular degeneration. Ophthalmol Retina. 2017 Nov - Dec;1(6):474–85. 10.1016/j.oret.2017.03.003: PubMed PMID: 31047438
193. Sahni J, Patel SS, Dugel PU, et al. Simultaneous inhibition of angiopoietin-2 and vascular endothelial growth factor-a with faricimab in diabetic macular edema: BOULEVARD phase 2 Randomized Trial. Ophthalmology. 2019 Aug;126(8):1155–70. 10.1016/j.ophtha.2019.03.023: PubMed PMID: 30905643
194. Sahni J, Dugel PU, Patel SS, et al. Safety and efficacy of different doses and regimens of faricimab vs ranibizumab in neovascular age-related macular degeneration: the avenue phase 2 randomized clinical trial. JAMA Ophthalmol. 2020 Sep 1;138(9):955–63. PubMed PMID: 32729888; PubMed Central PMCID: PMCPMC7393587. doi:10.1001/jamaophthalmol.2020.2685
195. Khanani AM, Patel SS, Ferrone PJ, et al. Efficacy of every four monthly and quarterly dosing of faricimab vs ranibizumab in neovascular age-related macular degeneration: the stairway phase 2 randomized clinical trial. JAMA Ophthalmol. 2020 Sep 1;138(9):964–72. PubMed PMID: 32729897; PubMed Central PMCID: PMCPMC7489851. doi:10.1001/jamaophthalmol.2020.2699
196. De La Huerta I, Kim SJ, Sternberg P Jr. Faricimab combination therapy for sustained efficacy in neovascular age-related macular degeneration. JAMA Ophthalmol. 2020 Sep 1;138(9):972–73. PubMed PMID: 32729885. doi:10.1001/jamaophthalmol.2020.2723.
197. Sharma A, Kumar N, Parachuri N, et al. Faricimab: two in the bush is proving better than one in the hand? Ocul Immunol Inflamm. 2021 Jul;9:1–3. doi:10.1080/09273948.2021.1931350. PubMed PMID: 34242102.
198. Terstappen GC, Meyer AH, Bell RD, et al. Strategies for delivering therapeutics across the blood-brain barrier. Nat Rev Drug Discov. 2021 May;20(5):362–83. 10.1038/s41573-021-00139-y: . PubMed PMID: 33649582
199. Bohrmann B, Baumann K, Benz J, et al. Gantenerumab: a novel human anti-Abeta antibody demonstrates sustained cerebral amyloid-beta binding and elicits cell-mediated removal of human amyloid-beta. J Alzheimers Dis. 2012;28(1):49–69. PubMed PMID: 21955818. doi:10.3233/JAD-2011-110977.
200. Joshi KK, Phung W, Han G, et al. Elucidating heavy/light chain pairing preferences to facilitate the assembly of bispecific IgG in single cells. MAbs. 2019 Oct;11(7):1254–65. 10.1080/19420862.2019.1640549: PubMed PMID: 31286843; PubMed Central PMCID: PMCPMC6748609
201. Gong D, Riley TP, Bzymek KP, et al. Rational selection of building blocks for the assembly of bispecific antibodies. MAbs. 2021 Jan-Dec;13(1):1870058. 10.1080/19420862.2020.1870058: PubMed PMID: 33397191; PubMed Central PMCID: PMCPMC7808324
202. Tustian AD, Endicott C, Adams B, et al. Development of purification processes for fully human bispecific antibodies based upon modification of protein A binding avidity. MAbs. 2016 May-Jun;8(4):828–38. 10.1080/19420862.2016.1160192: PubMed PMID: 26963837; PubMed Central PMCID: PMCPMC4966828
203. Bogen JP, Carrara SC, Fiebig D, et al. Expeditious generation of biparatopic common light chain antibodies via chicken immunization and yeast display screening. Front Immunol. 2020;11:606878. PubMed PMID: 33424853; PubMed Central PMCID: PMCPMC7786285. doi:10.3389/fimmu.2020.606878.
204. Bogen JP, Carrara SC, Fiebig D, et al. Design of a Trispecific Checkpoint Inhibitor And Natural Killer Cell Engager Based On A 2 + 1 Common Light Chain Antibody Architecture. Front Immunol. 2021;12:669496. PubMed PMID: 34040611; PubMed Central PMCID: PMCPMC8141644. doi:10.3389/fimmu.2021.669496.
205. Bogen JP, Storka J, Yanakieva D, et al. Isolation of common light chain antibodies from immunized chickens using yeast biopanning and fluorescence-activated cell sorting. Biotechnol J. 2021 Mar;16(3):e2000240. 10.1002/biot.202000240: PubMed PMID: 32914549
206. Chiu D, Tavare R, Haber L, et al. A PSMA-Targeting CD3 Bispecific Antibody Induces Antitumor Responses that Are Enhanced by 4-1BB Costimulation. Cancer Immunol Res. 2020 May;8(5):596–608. 10.1158/2326-6066.CIR-19-0518: PubMed PMID: 32184296
207. Crawford A, Haber L, Kelly MP, et al. A Mucin 16 bispecific T cell-engaging antibody for the treatment of ovarian cancer. Sci Transl Med. 2019 Jun 19;11(497): 10.1126/scitranslmed.aau7534. PubMed PMID: 31217340.
208. Skokos D, Waite JC, Haber L, et al. A class of costimulatory CD28-bispecific antibodies that enhance the antitumor activity of CD3-bispecific antibodies. Sci Transl Med. 2020 Jan 8;12:525. 10.1126/scitranslmed.aaw7888: PubMed PMID: 31915305
209. Waite JC, Wang B, Haber L, et al. Tumor-targeted CD28 bispecific antibodies enhance the antitumor efficacy of PD-1 immunotherapy. Sci Transl Med. 2020 Jun 24;12(549): 10.1126/scitranslmed.aba2325. PubMed PMID: 32581132.
210. Geuijen C, Tacken P, Wang LC, et al. A human CD137xPD-L1 bispecific antibody promotes anti-tumor immunity via context-dependent T cell costimulation and checkpoint blockade. Nat Commun. 2021 Jul 21;12(1):4445. PubMed PMID: 34290245. doi:10.1038/s41467-021-24767-5
211. Geuijen CAW, De Nardis C, Maussang D, et al. Unbiased combinatorial screening identifies a bispecific igg1 that potently inhibits her3 signaling via her2-guided ligand blockade. Cancer Cell. 2018 May 14;33(5):922–936e10. PubMed PMID: 29763625. doi:10.1016/j.ccell.2018.04.003

212. Van Loo PF, Hangalapura BN, Thordardottir S, et al. MCLA-117, a CLEC12AxCD3 bispecific antibody targeting a leukaemic stem cell antigen, induces T cell-mediated AML blast lysis. Expert Opin Biol Ther. 2019 Jul;19(7):721–33. 10.1080/14712598.2019.1623200: PubMed PMID: 31286786
213. Shiraiwa H, Narita A, Kamata-Sakurai M, et al. Engineering a bispecific antibody with a common light chain: identification and optimization of an anti-CD3 epsilon and anti-GPC3 bispecific antibody, ERY974. Methods. 2019 Feb 1;154:10–20. 10.1016/j.ymeth.2018.10.005: PubMed PMID: 30326272
214. Bonisch M, Sellmann C, Maresch D, et al. Novel CH1: cLinterfaces that enhance correct light chain pairing in heterodimeric bispecific antibodies. Protein Eng Des Sel. 2017 Sep 1;30(9):685–96. PubMed PMID: 28981885; PubMed Central PMCID: PMCPMC5914326. doi:10.1093/protein/gzx044
215. Dillon M, Yin Y, Zhou J, et al. Efficient production of bispecific IgG of different isotypes and species of origin in single mammalian cells. MAbs. 2017;9(2):213–30. PubMed PMID: 27929752; PubMed Central PMCID: PMCPMC5297516. doi:10.1080/19420862.2016.1267089. Feb/Mar.

11.2. Appendix II. Review publication II: *A pivotal decade for bispecific antibodies?*

mAbs

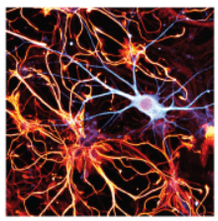

ISSN: (Print) (Online) Journal homepage: www.tandfonline.com/journals/kmab20

A pivotal decade for bispecific antibodies?

Marlena Surowka & Christian Klein

To cite this article: Marlena Surowka & Christian Klein (2024) A pivotal decade for bispecific antibodies?, mAbs, 16:1, 2321635, DOI: 10.1080/19420862.2024.2321635

To link to this article: https://doi.org/10.1080/19420862.2024.2321635

Published online: 11 Mar 2024.

MABS
2024, VOL. 16, NO. 1, 2321635
https://doi.org/10.1080/19420862.2024.2321635

Taylor & Francis
Taylor & Francis Group

A pivotal decade for bispecific antibodies?

Marlena Surowka and Christian Klein

Roche Innovation Center Zurich, Roche Pharma Research & Early Development, Roche Glycart AG, Schlieren, Switzerland

ABSTRACT

Bispecific antibodies (bsAbs) are a class of antibodies that can mediate novel mechanisms of action compared to monospecific monoclonal antibodies (mAbs). Since the discovery of mAbs and their adoption as therapeutic agents in the 1980s and 1990s, the development of bsAbs has held substantial appeal. Nevertheless, only three bsAbs (catumaxomab, blinatumomab, emicizumab) were approved through the end of 2020. However, since then, 11 bsAbs received regulatory agency approvals, of which nine (amivantamab, tebentafusp, mosunetuzumab, cadonilimab, teclistamab, glofitamab, epcoritamab, talquetamab, elranatamab) were approved for the treatment of cancer and two (faricimab, ozoralizumab) in non-oncology indications. Notably, of the 13 currently approved bsAbs, two, emicizumab and faricimab, have achieved blockbuster status, showing the promise of this novel class of therapeutics. In the 2020s, the approval of additional bsAbs can be expected in hematological malignancies, solid tumors and non-oncology indications, establishing bsAbs as essential part of the therapeutic armamentarium.

ARTICLE HISTORY
Received 23 January 2024
Revised 15 February 2024
Accepted 16 February 2024

KEYWORDS
bsAb; bsADC; CD3ε; CPI; IgG; mab; TCE

Introduction

Since the discovery of monoclonal antibodies, bispecific versions that could be used as therapeutics have been of intense interest.[1–5] However, development was slowed due to challenges with the generation and production of bispecific antibodies (bsAbs) for clinical trials and the biological understanding of the more complicated mechanisms of action (MOAs). The first bsAb, the EpCAM/CD3ε T cell engager catumaxomab, was finally approved in 2009 as a treatment of patients with malignant ascites (Figure 1).[6] This bsAb was subsequently withdrawn 2013 from the market, likely related to the fact that it could only be administered intraperitoneally, as patients had severe infusion reactions when administered intravenously, and the high immunogenicity due to its rat-mouse chimeric quadrome design with a fully functional Fc portion.[6] From 2009 to 2020, only two additional bsAbs were approved: (1) in 2014, the Fc-free tandem single-chain variable fragment (scFv)-based CD19/CD3ε bispecific T cell engager (BiTE) blinatumomab (Amgen) for the treatment of acute lymphoblastic leukemia (ALL),[7–9] and (2) in 2017, the humanized hetero-dimeric coagulation factor IXa/X bispecific ART-Ig emicizumab (Roche group), which acts as a Factor VIII mimetic for the treatment of hemophilia A (Figure 1).[10,11]

Due to the intense interest in these molecules and advances in the technologies used to develop them during the past two decades, hundreds of bsAbs have been described, engineered using various different technologies and developed preclinically.[1–5] Of these, over 100 bsAbs have reached clinical trials.[1,3,5] Based on this major effort in developing novel bsAb formats, novel target combinations and bispecific lead molecules, the landscape has substantially changed recently and bsAb approvals are becoming frequent since 2021. In the past three years alone (2021–2023), 11 novel bsAbs were approved by health authorities in the US, Europe, Japan and/or China for use in patients (Figure 1, Table 1). Of these 11 bsAbs, nine were approved for treatment of cancer: (1) the EGFR/c-MET bsAb amivantamab (Johnson & Johnson (J&J)) for the treatment of non-small cell lung cancer (NSCLC) with EGFR exon 20 insertion mutations,[12,13] (2) the gp100-pMHC/CD3ε bsAb tebentafusp (Immunocore) for the treatment of unresectable or metastatic uveal melanoma,[14,15] (3) the CD20/CD3ε T cell engager (TCE) mosunetuzumab (Roche group) for the treatment of relapsed/refractory (R/R) follicular lymphoma,[16,17] (4) the PD-1/CTLA-4 bsAb cadonilimab (Akeso) for treatment of patients with relapsed or metastatic cervical cancer,[18,19] (5) the BCMA/CD3ε TCE teclistamab (J&J) for the treatment of R/R multiple myeloma,[20,21] (6) the CD20/CD3ε TCE glofitamab (Roche group) for the treatment of R/R diffuse large B cell lymphoma (DLBCL),[22,23] (7) the CD20/CD3ε TCE epcoritamab (AbbVie/Genmab) for the treatment of R/R DLBCL,[24,25] (8) the GPRC5D/CD3ε TCE talquetamab (J&J) for the treatment of R/R multiple myeloma[26,27] and (9) the BCMA/CD3ε TCE elranatamab (Pfizer) for the treatment of R/R multiple myeloma.[28,29] Two additional bsAbs were approved for non-oncology indications, the VEGF-A/Ang-2 bsAb faricimab (Roche group) for the treatment of wet age-related macular degeneration, diabetic macular edema, and macular edema following retinal vein occlusion,[30–33] which was the first

CONTACT Christian Klein christian.klein.ck1@roche.com Roche Innovation Center Zurich, Roche Pharma Research & Early Development, Roche Glycart AG, Wagistrasse 10, Schlieren 8952, Switzerland

This article was originally published with errors, which have now been corrected in the online version. Please see Correction (http://dx.doi.org/10.1080/19420862.2024.2335597)

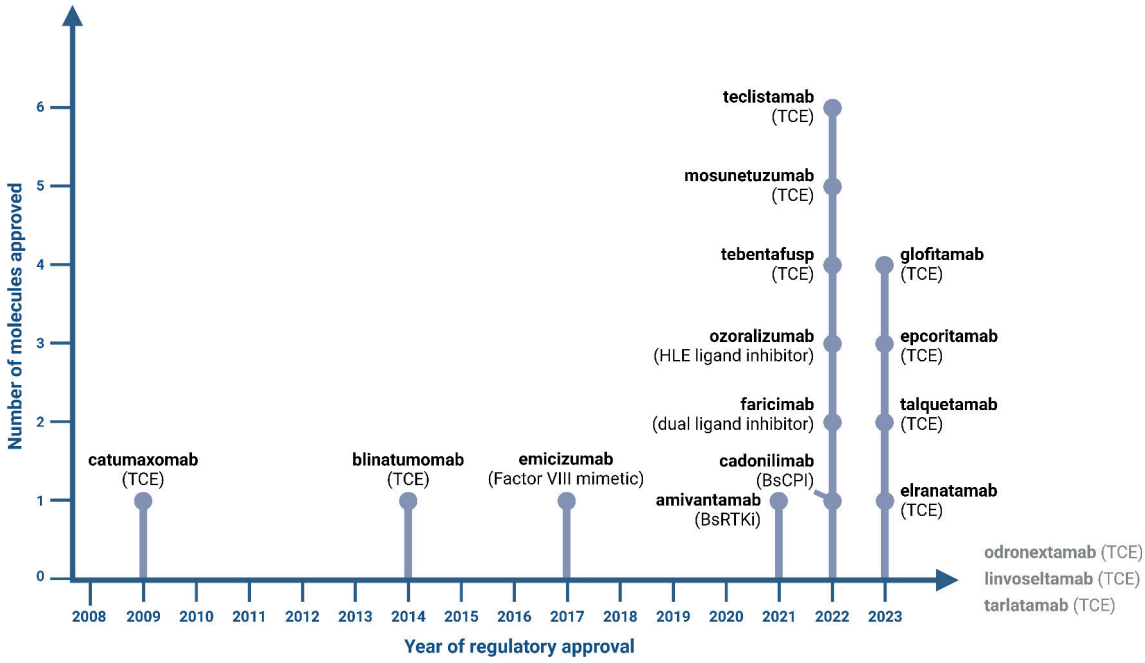

Figure 1. Timeline of regulatory approval of bsAbs with their respective MOA. Linvoseltamab, odronextamab and tarlatamab are currently under regulatory review with a decision anticipated in 2024. Created with Biorender.com.

bsAb approved for use in ophthalmology, and the TNF/human serum albumin (HSA) bsAb ozoralizumab (Taisho) for the treatment of inadequately managed rheumatoid arthritis.[34–36] The Roche group with Chugai is currently leading the field with four approved bsAbs, followed by J&J with three approved bsAbs. Notably, of the 13 currently approved bsAbs, two, emicizumab and faricimab, have already achieved blockbuster status with annual sales exceeding four and two billion dollars, respectively, underlining the commercial promise of this novel class of therapeutics.

Bispecific antibody formats

The variety of bispecific antibody formats developed reflects the diversity of technologies applied in these approved bsAbs (Figure 2). The respective bsAb formats cover non-IgG-like bsAbs, with 1) Amgen's short half-life tandem-scFv-based BiTE format applied in blinatumomab,[37,38] 2) Immunocore's T cell receptor (TCR)-scFv fusion-based ImmTac format applied in tebentafusp[39,40] and 3) Ablynx's trivalent bispecific tandem nanobody format with half-life extension via HSA binding applied in ozoralizumab.[41] Most bsAbs, however, are IgG-like molecules with pharmacokinetics that are similar to antibodies due to the presence of an Fc. Five asymmetric 1 + 1 IgG-like bsAbs are derived from either controlled Fab arm exchange, based on Duobody technology applied in amivantamab,[42] teclistamab,[43] epcoritamab,[44] and talquetamab,[45] or related chain exchange technology by Pfizer[46] applied in elranatamab.[47] Alternatively, correct chain association is enforced via Chugai's ART-Ig technology[48] applied in the asymmetric 1 + 1 IgG-like bsAb emicizumab[49,50] together with common light chains. Correct heavy chain association can also be ensured in asymmetric 1 + 1 IgG-like bsAbs using knobs-into-holes technology applied together with in vitro assembly in mosunetuzumab,[51] or together with CrossMab technology to enforce correct light chain association in the 1 + 1 IgG-like bsAb faricimab[52] or the trivalent 2 + 1 bsAb glofitamab.[53] Finally, Akeso's cadonilimab comprises a symmetric tetravalent 2 + 2 C-terminal IgG-scFv fusion.[54] Among the approved bsAbs, four apply Genmab's Duobody technology,[55,56] three apply Genentech's knobs-into-holes[57,58] and two apply Roche pRED's CrossMab technology.[59–61] The diversity of formats available suggests that "standardized" bsAbs are unlikely to arise, but recent approvals underpin a focus on classical heterodimeric IgG-like bsAb formats. These bsAbs typically show IgG-like pharmacokinetics and low incidence of anti-drug antibodies.

MOAs for approved bsAbs

TCEs are bispecific antibodies that bind with one specificity to a cell surface tumor antigen, and with the second specificity to a subunit of the TCR complex, so that, upon simultaneous binding to the tumor antigen and the TCR, the T cell is subsequently activated to kill the tumor cell, secrete cytokines and start to proliferate.[62] Apparently, T cell engagement strictly relies on bispecificity and cannot be achieved by the combination of two conventional mAbs. For the treatment of cancer, the pre-dominant MOA is T cell engagement, with the largest number of bsAbs approved and in clinical trials being TCEs.[5] Figure 2a shows an overview of the evolution of approved TCE bsAb formats. This class of molecules includes TCEs for the treatment of relapsed/refractory hematological cancers: 1) CD19/CD3ε blinatumomab for the treatment of ALL,[7–9] 2) the CD20/CD3ε TCEs mosunetuzumab for the treatment of R/R non-Hodgkin's lymphoma (NHL),[51] and

Table 1. Approved bsAbs and bsAbs under regulatory review.

	Trade name	INN	Targets	MOA	Format	Indications	Year	1st Approval	Company
Discontinued									
1	Removab	Catumaxomab	EpCAM/CD3ε	T cell engager	1+1 Quadroma	Ovarian ascites (intraperitonael)	2009	Europe	Trion Pharma
Approved									
1	Blincyto	Blinatumomab	CD19/CD3ε	T cell engager	1+1 (scFv)2 BiTE	Acute lymphocytic leukemia	2014	US	Amgen
2	Hemlibra	Emicizumab	factor IXa/factor X	Factor VIII mimetic	1+1 ART-Ig	Haemophilia A	2017	US	Roche group
3	Rybrevant	Amivantamab	EGFR/c-Met	Dual signaling inhibitor + ADCC	1+1 Duobody	Non-Small Cell Lung Cancer, EGFR exon 20 mutated	2021	US	Johnson & Johnson
4	Kimmtrak	Tebentafusp	gp100-HLA-A*02 /CD3ε	T cell engager	1+1 TCR-scFv	Uveal melanoma	2022	US	Immunocore
5	Vabysmo	Faricimab	Ang-2/VEGF	Dual ligand inhibitor	1+1 CrossMab	wAMD, DME, RVO	2022	US	Roche group
6	Lunsumio	Mosunetuzumab	CD20/CD3ε	T cell engager	1+1 IgG-KiH	Relapsed/refractory fNHL	2022	Europe	Roche group
7	Kaitanni	Cadonilimab	PD-1/CTLA-4	Dual checkpoint inhibitor	2+2 IgG-scFv Tetrabody	Cervical cancer	2022	China	Akeso
8	Tecvayli	Teclistamab	BCMA/CD3ε	T cell engager	1+1 Duobody	Relapsed/refractory multiple myeloma	2022	Europe	Johnson & Johnson
9	Nanozora	Ozoralizumab	TNFa/HSA	Ligand inhibitor	2+1 Nanobody	Rheumatoid arthritis	2022	Japan	Taisho Pharmaceutical, Ablynx
10	Columvi	Glofitamab	CD20/CD3ε	T cell engager	2+1 CrossMab	Relapsed/refractory DLBCL	2023	Canada	Roche group
11	(T)Epkinly	Epcoritamab	CD20/CD3ε	T cell engager	1+1 Duobody	Relapsed/refractory DLBCL	2023	US	Genmab, AbbVie
12	Talvey	Talquetamab	GPRC5D/CD3ε	T cell engager	1+1 Duobody	Relapsed/refractory multiple myeloma	2023	US	Johnson & Johnson
13	Elrexfio	Elranatamab	BCMA/CD3ε	T cell engager	1+1 bsAb	Relapsed/refractory multiple myeloma	2023	US	Pfizer
Under regulatory review									
1	n.a.	Linvoseltamab	BCMA/CD3ε	T cell engager	1+1 Veloci-Bi	Relapsed/refractory multiple myeloma	n.a	Pending US	Regeneron
2	n.a.	Odronextamab	CD20/CD3ε	T cell engager	1+1 Veloci-Bi	Relapsed/refractory DLBCL	n.a.	Pending US	Regeneron
3	n.a.	Tarlatamab	DLL3/CD3ε	T cell engager	1+1 Fc-(scFv)2 Fc-BiTE	Relapsed advanced small cell lung cancer	n.a.	Pending US	Amgen
4	n.a.	Zanidatamab	HER2/HER2	Dual signaling inhibitor + ADCC + CDC	1+1 Azymetric	Biliary tract cancer	n.a.	Pending US	Zymeworks/Jazz Pharmaceuticals
5	n.a.	Ivonescimab	PD-1/VEGF	Dual checkpoint/ligand inhibitor	2+2 IgG-scFv Tetrabody	Non-Small Cell Lung Cancer	n.a.	Pending China	Akeso

ADCC, antibody-dependent cellular cytotoxicity; ART-Ig, bispecific antibody manufacturing technology; BiTE, bispecific T cell engager; CDC, complement-dependent cytotoxicity; DLBCL, diffuse large b cell lymphoma; DME, diabetic macular edema; fNHL, follicular non-Hodgkin's lymphoma; KIH, knobs-into-holes; n.a., not applicable; RVO, Retinal vein occlusion; scFv, single-chain Fv fragment; TCR, T cell receptor; wAMD, wet age-related macular degeneration.

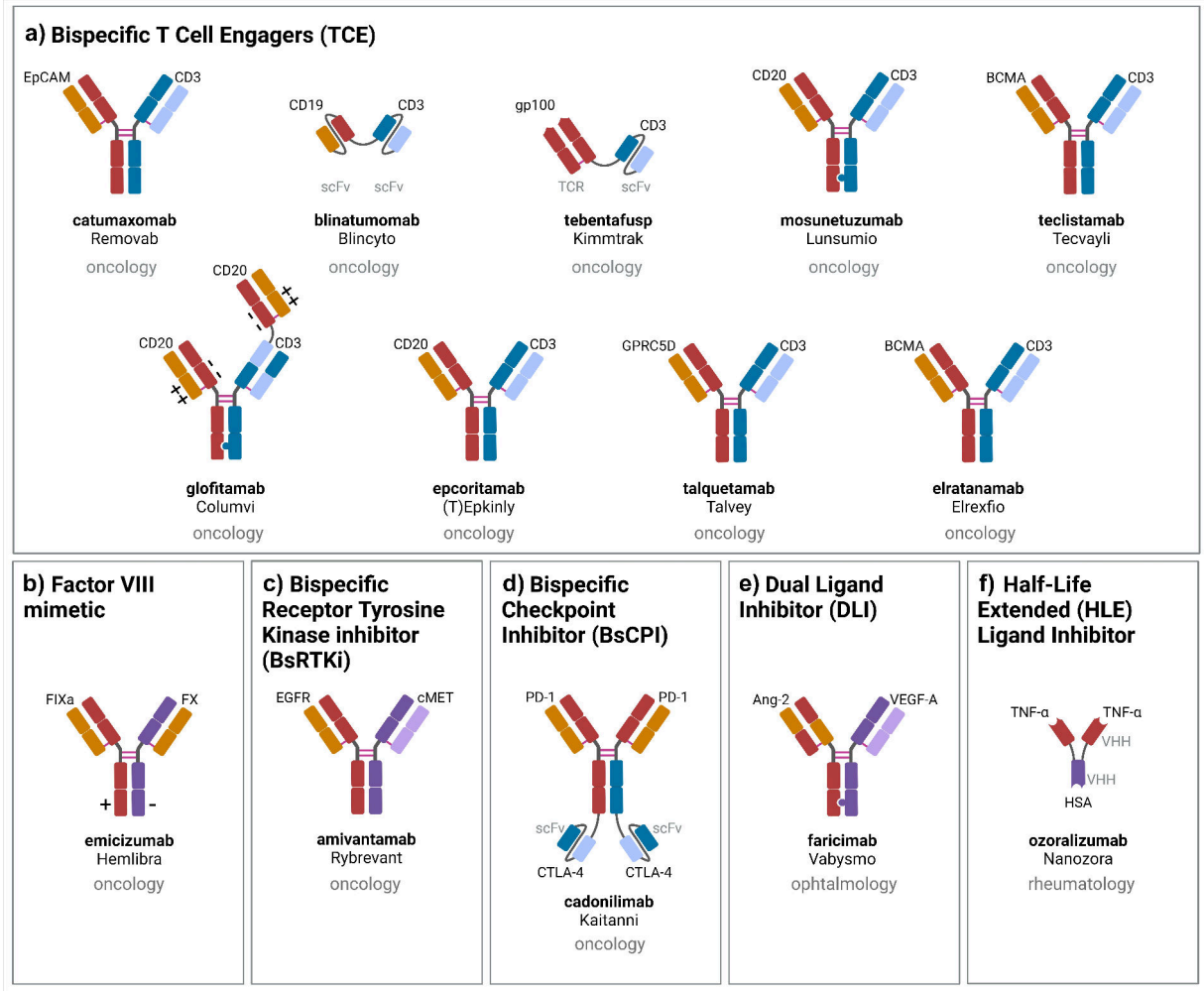

Figure 2. Schematic representation, indication and mechanism of action of approved bsAbs: a) T cell engagers (TCE), b) factor VIII mimetic, dual signaling inhibition: c) bispecific receptor tyrosine kinase (RTK) inhibitor (BsRtki), d) bispecific checkpoint inhibitor (BsCPI), e) dual ligand inhibitor (DLI), f) half-life extended (HLE) ligand inhibitor. Created with Biorender.com.

glofitamab[53] and epcoritamab[44] for the treatment of R/R DLBCL, and 3) the BCMA/CD3ε TCEs teclistamab[43] and elranatamab,[47] and GPRC5D/CD3ε talquetamab,[45] for the treatment of R/R multiple myeloma. While generally T cell engagement for the treatment of solid tumors appears to be more challenging,[63] the soluble gp100-peptideMHC/CD3ε -specific TCR-scFv fusion tebentafusp was the first TCE to be approved for the treatment of uveal melanoma, providing evidence for use outside of hematological tumors.

Hemophilia A is a hereditary bleeding disorder characterized by the lack of blood coagulation Factor VIII. While recombinant Factor VIII can be administered to patients, this is related to challenges such as Factor VIII production, short half-life with frequent administration and the development of neutralizing antibodies.[64] For this purpose, Chugai designed and optimized the IXa/X bsAb emicizumab so that it mimics the function of blood coagulation Factor VIII by bringing the enzyme Factor IXa and the substrate Factor X into close proximity while exhibiting IgG-like extended pharmacokinetics[49,50] (Figure 2b).

Monospecific receptor tyrosine kinase blocking mAbs, such as anti-EGFR cetuximab and panitumumab or anti-HER2 trastuzumab and pertuzumab, have revolutionized cancer therapy.[65] While there has been little progress in targeting additional RTKs, EGFR/c-Met bsAb amivantamab, a first bsAb targeting two RTKs simultaneously, was recently approved for a specific subset of NSCLC patients with EGFR exon 20 insertion mutations.[12,13] In addition to its dual signaling inhibitor function, both via blocking the ligand binding sites and via receptor downregulation, amivantamab also contains an afucosylated Fc portion to mediate enhanced antibody-dependent cellular toxicity (ADCC) for NK cell and macrophage/monocyte engagement[42] (Figure 2c).

During the past decade, approved immune checkpoint inhibitory antibodies, including those targeting PD-1 (nivolumab, pembrolizumab, cemiplimab), PD-L1 (atezolizumab, avelumab, durvalumab), and CTLA-4 (ipilimumab, tremelimumab), have revolutionized the field of cancer therapy and established cancer immunotherapy.[66] Based on this experience, the dual PD-1/CTLA-4 checkpoint inhibitory bsAb cadonilimab was designed with the goal of specifically, and ideally simultaneously, binding and inhibiting PD-1 and CTLA-4 on antigen-specific T cells to overcome checkpoint inhibition[54] (Figure 2d).

The pro-angiogenic ligands VEGF-A and Ang-2 contribute to vision loss by fostering retinal angiogenesis and destabilizing blood vessels causing leakiness and subsequent edema and

inflammation.[67,68] Faricimab was specifically designed to block VEGF-A and Ang-2 in the eye to interfere with angiogenesis, stabilize vessels and reduce leakage and inflammation[52,69] (Figure 2e). In order to minimize peripheral activity and abolish FcγR engagement, it was designed with an engineered Fc portion with Triple A FcRn and P329G LALA mutations.[52]

Notably, bispecificity is a major benefit when considering intraocular administration. For the TNF ligand inhibitor ozoralizumab, it should be noted that functionally, this nanobody construct functions like a monospecific antibody blocking TNF, with the second single domain specificity solely required to enable IgG-like pharmacokinetics by binding to HSA in the absence of an Fc portion, enabling FcRn recycling[41] (Figure 2f).

Outlook for the future

In this decade, 11 bsAbs have already been approved, and the approval of additional bsAbs with medical practice-changing potential can be expected in the coming years. In oncology, the development of differentiated dual RTK signaling inhibitors with bsAb co-targeting different cell surface receptors remains an area of active and advanced clinical research. Selected examples are: EGFR/LGR5 like petosemtamab,[70] HER2/HER3 like zenocutuzumab[71] or bi-paratopic bsAbs targeting HER2 like zanidatamab[72] which is currently under regulatory review in the US.[73–75] Another very important area to watch in this context is the use of bsAbs for the generation of bispecific antibody-drug conjugates (bsADCs),with several bsADCs being investigated in advanced clinical trials,[76–78] including bi-paratopic monospecific bsAbs targeting HER2 like zanidatamab zovodotin (ZW49) or c-MET with REGN5093.[79]

The development of TCEs for the treatment of different hematological malignancies will remain a major area of research in the field of synthetic immunity approaches, as this class of therapeutics already has proven its benefit. To date, the asymmetric 1 + 1 TCEs odronextamab (CD20/CD3ε)[80] and linvoseltamab (BCMA/CD3ε) based on Regeneron's VelociBi technology are currently under regulatory review that may result in approval in 2024, and various additional TCEs are in advanced clinical development in NHL, multiple myeloma and AML.[75] Importantly, emerging data support the idea that TCEs may in the future also find broader application in solid tumors. In fact, recently promising clinical data have been published for Amgen's 1 + 1 DLL3/CD3ε FcBiTE tarlatamab for the treatment of R/R small cell lung cancer,[81,82] which is currently under regulatory review, and for Xencor/Amgen's 2 + 1 STEAP1/CD3ε XmAb xaluritamig for the treatment of R/R prostate cancer.[83,84] These data support the view that solid tumor targets that are sufficiently tumor specific to achieve potent anti-tumor efficacy while limiting on-target off-tumor toxicity are available. In this context, tumor activation mechanisms like protease activation aim to increase the therapeutic window of solid tumor-directed TCEs.[85–89] Based on the mechanism of action of TCEs that provide the TCR signal 1 to T cells, rapid clinical adoption of CD28- or 4-1BB/CD137-targeted costimulatory bsAbs to provide the signal 2 to T cells, resulting in sustained and more durable T cell responses,[90,91] is now occurring.

In the field of boosting endogenous or preexisting immunity, another major area of research remains the development of dual-targeted checkpoint inhibitory bsAbs targeting, for example, PD-1 and CTLA-4[92,93] or LAG-3 (tebotelimab).[94] Several of these dual checkpoint inhibitors are currently in advanced clinical trials and results will show whether they are superior in terms of efficacy and/or safety compared to the respective combinations of PD-1/PD-L1 mAbs with CTLA-4 or LAG-3 mAbs. Notably, the dual-targeted PD-1/VEGF inhibitory bsAb ivonescimab is currently under regulatory review by the National Medicinal Product Administration in China for treatment of NSCLC.[75,95]

Finally, given the versatility of bsAbs and the potential to mediate completely novel MOAs, the field of bsAbs is poised to see novel emerging approaches and candidates enter the clinic, hopefully providing pivotal data in the years to come, both in oncology and in non-oncology indications, including applications in infection/virology, autoimmunity, metabolism, neurology and ophthalmology. These novel concepts include different approaches as described recently,[5] including the development of: 1) effector cell engagers different from TCEs, engaging, e.g., myeloid, NK or γδ-T cells,[96–98] 2) *in situ* assembly concepts to specifically activate bsAbs on dual target-expressing cells[99,100] or in the tumor microenvironment,[101] 3) PROTAC-like approaches resulting in internalization and degradation of membrane proteins,[102] 4) antibody-based cytokine mimetics to trigger cytokine receptors,[103,104] and 5) unique solutions for delivery of bsAbs beyond barriers such as the blood-brain-barrier,[105] which may have applications for the treatment of neurodegenerative and other diseases.[106]

Disclosure statement

MS declares employment and patents with Roche, CK declares employment, patents/royalties and stock ownership with Roche.

Funding

The author(s) reported there is no funding associated with the work featured in this article.

ORCID

Marlena Surowka http://orcid.org/0009-0007-2113-9692
Christian Klein http://orcid.org/0000-0001-7594-7280

References

1. Labrijn AF, Janmaat ML, Reichert JM, Parren P. Bispecific antibodies: a mechanistic review of the pipeline. Nat Rev Drug Discov. 2019;18(8):585–608. doi:10.1038/s41573-019-0028-1. PMID: 31175342.
2. Brinkmann U, Kontermann RE. The making of bispecific antibodies. MAbs. 2017;9(2):182–212. doi:10.1080/19420862.2016.1268307. PMID: 28071970.
3. Brinkmann U, Kontermann RE. Bispecific antibodies. Science. 2021;372(6545):916–17. doi:10.1126/science.abg1209. PMID: 34045345.
4. Kontermann RE, Brinkmann U. Bispecific antibodies. Drug Discov Today. 2015;20(7):838–47. doi:10.1016/j.drudis.2015.02.008. PMID: 25728220.

5. Klein C, Brinkmann U, Reichert JM, Kontermann RE. The present and future of bispecific antibodies for cancer therapy. Nat Rev Drug Discov. 2024. in press. doi:10.1038/s41573-024-00896-6.
6. Seimetz D, Lindhofer H, Bokemeyer C. Development and approval of the trifunctional antibody catumaxomab (anti-EpCAM×anti-CD3) as a targeted cancer immunotherapy. Cancer Treat Rev. 2010;36(6):458–67. doi:10.1016/j.ctrv.2010.03.001. PMID: 20347527.
7. Sanford M. Blinatumomab: first global approval. Drugs. 2015;75 (3):321–27. doi:10.1007/s40265-015-0356-3. PMID: 25637301.
8. Bargou R, Leo E, Zugmaier G, Klinger M, Goebeler M, Knop S, Noppeney R, Viardot A, Hess G, Schuler M. et al. Tumor regression in cancer patients by very low doses of a T cell–engaging antibody. Science. 2008;321(5891):974–77. doi:10.1126/science.1158545. PMID: 18703743.
9. Kantarjian H, Stein A, Gokbuget N, Fielding AK, Schuh AC, Ribera JM, Wei A, Dombret H, Foa R, Bassan R. et al. Blinatumomab versus chemotherapy for advanced acute lymphoblastic leukemia. N Engl J Med. 2017;376(9):836–47. doi:10.1056/NEJMoa1609783. PMID: 28249141.
10. Scott LJ, Kim ES. Emicizumab-kxwh: First Global Approval. Drugs. 2018;78(2):269–74. doi:10.1007/s40265-018-0861-2. PMID: 29357074.
11. Mahlangu J, Oldenburg J, Paz-Priel I, Negrier C, Niggli M, Mancuso ME, Schmitt C, Jimenez-Yuste V, Kempton C, Dhalluin C. et al. Emicizumab prophylaxis in patients who have hemophilia a without inhibitors. N Engl J Med. 2018;379 (9):811–22. doi:10.1056/NEJMoa1803550. PMID: 30157389.
12. Syed YY. Amivantamab: First Approval. Drugs. 2021;81 (11):1349–53. doi:10.1007/s40265-021-01561-7. PMID: 34292533.
13. Zhou C, Tang KJ, Cho BC, Liu B, Paz-Ares L, Cheng S, Kitazono S, Thiagarajan M, Goldman JW, Sabari JK. et al. Amivantamab plus chemotherapy in NSCLC with EGFR Exon 20 insertions. N Engl J Med. 2023;389(22):2039–51. doi:10.1056/NEJMoa2306441. PMID: 37870976.
14. Dhillon S. Tebentafusp: First Approval. Drugs. 2022;82(6):703–10. doi:10.1007/s40265-022-01704-4. PMID: 35364798.
15. Nathan P, Hassel JC, Rutkowski P, Baurain JF, Butler MO, Schlaak M, Sullivan RJ, Ochsenreither S, Dummer R, Kirkwood JM. et al. Overall survival benefit with Tebentafusp in metastatic uveal melanoma. N Engl J Med. 2021;385 (13):1196–206. doi:10.1056/NEJMoa2103485. PMID: 34551229.
16. Kang C. Mosunetuzumab: First Approval. Drugs. 2022;82 (11):1229–34. doi:10.1007/s40265-022-01749-5. PMID: 35947358.
17. Budde LE, Sehn LH, Matasar M, Schuster SJ, Assouline S, Giri P, Kuruvilla J, Canales M, Dietrich S, Fay K. et al. Safety and efficacy of mosunetuzumab, a bispecific antibody, in patients with relapsed or refractory follicular lymphoma: a single-arm, multicentre, phase 2 study. Lancet Oncol. 2022;23:1055–65. doi:10.1016/S1470-2045(22)00335-7. PMID: 35803286.
18. Keam SJ. Cadonilimab: First Approval. Drugs. 2022;82 (12):1333–39. doi:10.1007/s40265-022-01761-9. PMID: 35986837.
19. Frentzas S, Gan HK, Cosman R, Coward J, Tran B, Millward M, Zhou Y, Wang W, Xia D, Wang ZM. et al. A phase 1a/1b first-in-human study (COMPASSION-01) evaluating cadonilimab in patients with advanced solid tumors. Cell Rep Med. 2023;4 (11):101242. doi:10.1016/j.xcrm.2023.101242. PMID: 37852261.
20. Kang C. Teclistamab: First Approval. Drugs. 2022;82(16):1613–19. doi:10.1007/s40265-022-01793-1. PMID: 36352205.
21. Hindie E. Teclistamab in Relapsed or Refractory Multiple Myeloma. N Engl J Med. 2022;387:1721. doi:10.1056/NEJMc2211969. PMID: 36322859.
22. Shirley M. Glofitamab: First Approval. Drugs. 2023;83(10):935–41. doi:10.1007/s40265-023-01894-5. PMID: 37285013.
23. Dickinson MJ, Carlo-Stella C, Morschhauser F, Bachy E, Corradini P, Iacoboni G, Khan C, Wrobel T, Offner F, Trneny M. et al. Glofitamab for relapsed or refractory diffuse large B-Cell lymphoma. N Engl J Med. 2022;387(24):2220–31. doi:10.1056/NEJMoa2206913. PMID: 36507690.
24. Frampton JE. Epcoritamab: First Approval. Drugs. 2023;83 (14):1331–40. doi:10.1007/s40265-023-01930-4. PMID: 37597091.
25. Thieblemont C, Phillips T, Ghesquieres H, Cheah CY, Clausen MR, Cunningham D, Do YR, Feldman T, Gasiorowski R, Jurczak W. et al. Epcoritamab, a Novel, Subcutaneous CD3xCD20 Bispecific T-Cell–Engaging Antibody, in Relapsed or Refractory Large B-Cell Lymphoma: Dose Expansion in a Phase I/II Trial. JCO. 2022;41(12):2238–47. doi:10.1200/JCO.22.01725. PMID: 36548927.
26. Chari A, Minnema MC, Berdeja JG, Oriol A, van de Donk N, Rodriguez-Otero P, Askari E, Mateos MV, Costa LJ, Caers J. et al. Talquetamab, a T-Cell–Redirecting GPRC5D Bispecific Antibody for Multiple Myeloma. N Engl J Med. 2022;387(24):2232–44. doi:10.1056/NEJMoa2204591. PMID: 36507686.
27. Keam SJ. Talquetamab: First Approval. Drugs. 2023;83 (15):1439–45. doi:10.1007/s40265-023-01945-x. PMID: 37792138.
28. Lesokhin AM, Tomasson MH, Arnulf B, Bahlis NJ, Miles Prince H, Niesvizky R, Rodríguez-Otero P, Martinez-Lopez J, Koehne G, Touzeau C. et al. Elranatamab in relapsed or refractory multiple myeloma: phase 2 MagnetisMM-3 trial results. Nat Med. 2023;29 (9):2259–67. doi:10.1038/s41591-023-02528-9. PMID: 37582952.
29. Dhillon S. Elranatamab: First Approval. Drugs. 2023;83 (17):1621–27. doi:10.1007/s40265-023-01954-w. PMID: 37924427.
30. Heier JS, Khanani AM, Quezada Ruiz C, Basu K, Ferrone PJ, Brittain C, Figueroa MS, Lin H, Holz FG, Patel V. et al. Efficacy, durability, and safety of intravitreal faricimab up to every 16 weeks for neovascular age-related macular degeneration (TENAYA and LUCERNE): two randomised, double-masked, phase 3, non-inferiority trials. Lancet. 2022;399(10326):729–40. doi:10.1016/S0140-6736(22)00010-1. PMID: 35085502.
31. Shirley M. Faricimab: First Approval. Drugs. 2022;82(7):825–30. doi:10.1007/s40265-022-01713-3. PMID: 35474059.
32. Wykoff CC, Abreu F, Adamis AP, Basu K, Eichenbaum DA, Haskova Z, Lin H, Loewenstein A, Mohan S, Pearce IA. et al. Efficacy, durability, and safety of intravitreal faricimab with extended dosing up to every 16 weeks in patients with diabetic macular oedema (YOSEMITE and RHINE): two randomised, double-masked, phase 3 trials. Lancet. 2022;399(10326):741–55. doi:10.1016/S0140-6736(22)00018-6. PMID: 35085503.
33. Hattenbach LO, Abreu F, Arrisi P, Basu K, Danzig CJ, Guymer R, Haskova Z, Heier JS, Kotecha A, Liu Y. et al. BALATON and COMINO: phase III randomized clinical trials of Faricimab for retinal vein occlusion: study design and rationale. Ophthalmol Sci. 2023;3:100302. doi:10.1016/j.xops.2023.100302. PMID: 37810589.
34. Tanaka Y, Kawanishi M, Nakanishi M, Yamasaki H, Takeuchi T. Efficacy and safety of the anti-TNF multivalent NANOBODY® compound ozoralizumab in patients with rheumatoid arthritis and an inadequate response to methotrexate: a 52-week result of a phase II/III study (OHZORA trial). Mod Rheumatol. 2023;33 (5):883–90. doi:10.1093/mr/roac119. PMID: 36197757.
35. Tanaka Y, Kawanishi M, Nakanishi M, Yamasaki H, Takeuchi T. Efficacy and safety of anti-TNF multivalent NANOBODY® compound 'ozoralizumab' without methotrexate co-administration in patients with active rheumatoid arthritis: a 52-week result of phase III, randomised, open-label trial (NATSUZORA trial). Mod Rheumatol. 2023;33(5):875–82. doi:10.1093/mr/roac126. PMID: 36201360.
36. Keam SJ. Ozoralizumab: first approval. Drugs. 2023;83(1):87–92. doi:10.1007/s40265-022-01821-0. PMID: 36509938.
37. Dreier T, Baeuerle PA, Fichtner I, Grun M, Schlereth B, Lorenczewski G, Kufer P, Lutterbuse R, Riethmuller G, Gjorstrup P. et al. T cell costimulus-independent and very efficacious inhibition of tumor growth in mice bearing subcutaneous or leukemic human B cell lymphoma xenografts by a CD19-/CD3-bispecific single-chain antibody construct. J Immunol. 2003;170 (8):4397–402. doi:10.4049/jimmunol.170.8.4397. PMID: 12682277.
38. Kufer P, Lutterbuse R, Baeuerle PA. A revival of bispecific antibodies. Trends Biotechnol. 2004;22:238–44. doi:10.1016/j.tibtech.2004.03.006. PMID: 15109810.

39. Berman DM, Bell JI. Redirecting polyclonal T cells against cancer with soluble T cell receptors. Clin Cancer Res. 2022;29(4):697–704. doi:10.1158/1078-0432.CCR-22-0028. PMID: 36255733.
40. Liddy N, Bossi G, Adams KJ, Lissina A, Mahon TM, Hassan NJ, Gavarret J, Bianchi FC, Pumphrey NJ, Ladell K. et al. Monoclonal TCR-redirected tumor cell killing. Nat Med. 2012;18(6):980–87. doi:10.1038/nm.2764. PMID: 22561687.
41. Ishiwatari-Ogata C, Kyuuma M, Ogata H, Yamakawa M, Iwata K, Ochi M, Hori M, Miyata N, Fujii FY. Ozoralizumab, a humanized anti-TNFα NANOBODY® compound, exhibits efficacy not only at the onset of Arthritis in a human TNF transgenic mouse but also during secondary failure of administration of an Anti-TNFα IgG. Front Immunol. 2022;13:853008. doi:10.3389/fimmu.2022.853008. PMID: 35273620.
42. Neijssen J, Cardoso RMF, Chevalier KM, Wiegman L, Valerius T, Anderson GM, Moores SL, Schuurman J, Parren P, Strohl WR. et al. Discovery of amivantamab (JNJ-61186372), a bispecific antibody targeting EGFR and MET. J Biol Chem. 2021;296:100641. doi:10.1016/j.jbc.2021.100641. PMID: 33839159.
43. Pillarisetti K, Powers G, Luistro L, Babich A, Baldwin E, Li Y, Zhang X, Mendonca M, Majewski N, Nanjunda R. et al. Teclistamab is an active T cell–redirecting bispecific antibody against B-cell maturation antigen for multiple myeloma. Blood Adv. 2020;4(18):4538–49. doi:10.1182/bloodadvances.2020002393. PMID: 32956453.
44. Engelberts PJ, Hiemstra IH, de Jong B, Schuurhuis DH, Meesters J, Beltran Hernandez I, Oostindie SC, Neijssen J, van den Brink EN, Horbach GJ. et al. DuoBody-CD3xCD20 induces potent T-cell-mediated killing of malignant B cells in preclinical models and provides opportunities for subcutaneous dosing. EBioMedicine. 2020;52:102625. doi:10.1016/j.ebiom.2019.102625. PMID: 31981978.
45. Verkleij CPM, Broekmans MEC, van Duin M, Frerichs KA, Kuiper R, de Jonge AV, Kaiser M, Morgan G, Axel A, Boominathan R. et al. Preclinical activity and determinants of response of the GPRC5DxCD3 bispecific antibody talquetamab in multiple myeloma. Blood Adv. 2021;5:2196–215. doi:10.1182/bloodadvances.2020003805. PMID: 33890981.
46. Strop P, Ho WH, Boustany LM, Abdiche YN, Lindquist KC, Farias SE, Rickert M, Appah CT, Pascua E, Radcliffe T. et al. Generating bispecific human IgG1 and IgG2 antibodies from any antibody pair. J Mol Biol. 2012;420:204–19. doi:10.1016/j.jmb.2012.04.020. PMID: 22543237.
47. Panowski SH, Kuo TC, Zhang Y, Chen A, Geng T, Aschenbrenner L, Kamperschroer C, Pascua E, Chen W, Delaria K. et al. Preclinical efficacy and safety comparison of CD3 bispecific and ADC modalities targeting BCMA for the treatment of multiple myeloma. Mol Cancer Ther. 2019;18:2008–20. doi:10.1158/1535-7163.MCT-19-0007. PMID: 31434693.
48. Igawa T. Next generation antibody therapeutics using bispecific antibody technology. Yakugaku Zasshi. 2017;137:831–36. doi:10.1248/yakushi.16-00252-3. PMID: 28674296.
49. Kitazawa T, Igawa T, Sampei Z, Muto A, Kojima T, Soeda T, Yoshihashi K, Okuyama-Nishida Y, Saito H, Tsunoda H. et al. A bispecific antibody to factors IXa and X restores factor VIII hemostatic activity in a hemophilia a model. Nat Med. 2012;18:1570–74. doi:10.1038/nm.2942. PMID: 23023498.
50. Sampei Z, Igawa T, Soeda T, Okuyama-Nishida Y, Moriyama C, Wakabayashi T, Tanaka E, Muto A, Kojima T, Kitazawa T. et al. Identification and multidimensional optimization of an asymmetric bispecific IgG antibody mimicking the function of factor VIII cofactor activity. PloS One. 2013;8(2):e57479. doi:10.1371/journal.pone.0057479. PMID: 23468998.
51. Sun LL, Ellerman D, Mathieu M, Hristopoulos M, Chen X, Li Y, Yan X, Clark R, Reyes A, Stefanich E. et al. Anti-CD20/CD3 T cell–dependent bispecific antibody for the treatment of B cell malignancies. Sci Transl Med. 2015;7(287):287ra270. doi:10.1126/scitranslmed.aaa4802. PMID: 25972002.
52. Regula JT, Lundh von Leithner P, Foxton R, Barathi VA, Gemmy Cheung CM, Bo Tun SB, Wey YS, Iwata D, Dostalek M, Moelleken J. et al. Targeting key angiogenic pathways with a bispecific CrossMAb optimized for neovascular eye diseases. EMBO Mol Med. 2017;9(7):985. doi:10.15252/emmm.201707895. PMID: 28533211.
53. Bacac M, Colombetti S, Herter S, Sam J, Perro M, Chen S, Bianchi R, Richard M, Schoenle A, Nicolini V. et al. CD20-TCB with obinutuzumab pretreatment as next-generation treatment of hematologic malignancies. Clin Cancer Res. 2018;24:4785–97. doi:10.1158/1078-0432.CCR-18-0455. PMID: 29716920.
54. Pang X, Huang Z, Zhong T, Zhang P, Wang ZM, Xia M, Li B. Cadonilimab, a tetravalent PD-1/CTLA-4 bispecific antibody with trans-binding and enhanced target binding avidity. MAbs. 2023;15(1):2180794. doi:10.1080/19420862.2023.2180794. PMID: 36872527.
55. Gramer MJ, van den Bremer ET, van Kampen MD, Kundu A, Kopfmann P, Etter E, Stinehelfer D, Long J, Lannom T, Noordergraaf EH. et al. Production of stable bispecific IgG1 by controlled Fab-arm exchange: scalability from bench to large-scale manufacturing by application of standard approaches. MAbs. 2013;5(6):962–73. doi:10.4161/mabs.26233. PMID: 23995617.
56. Labrijn AF, Meesters JI, de Goeij BE, van den Bremer ET, Neijssen J, van Kampen MD, Strumane K, Verploegen S, Kundu A, Gramer MJ. et al. Efficient generation of stable bispecific IgG1 by controlled Fab-arm exchange. Proc Natl Acad Sci U S A. 2013;110:5145–50. doi:10.1073/pnas.1220145110. PMID: 23479652.
57. Ridgway JB, Presta LG, Carter P. 'Knobs-into-holes' engineering of antibody CH3 domains for heavy chain heterodimerization. Protein Eng. 1996;9(7):617–21. doi:10.1093/protein/9.7.617. PMID: 8844834.
58. Zhu Z, Presta LG, Zapata G, Carter P. Remodeling domain interfaces to enhance heterodimer formation. Protein Sci. 1997;6:781–88. doi:10.1002/pro.5560060404. PMID: 9098887.
59. Regula JT, Imhof-Jung S, Molhoj M, Benz J, Ehler A, Bujotzek A, Schaefer W, Klein C. Variable heavy–variable light domain and Fab-arm CrossMabs with charged residue exchanges to enforce correct light chain assembly. Protein Eng Des Sel. 2018;31(7–8):289–99. doi:10.1093/protein/gzy021. PMID: 30169707.
60. Schaefer W, Regula JT, Bahner M, Schanzer J, Croasdale R, Durr H, Gassner C, Georges G, Kettenberger H, Imhof-Jung S. et al. Immunoglobulin domain crossover as a generic approach for the production of bispecific IgG antibodies. Proc Natl Acad Sci U S A. 2011;108:11187–92. doi:10.1073/pnas.1019002108. PMID: 21690412.
61. Surowka M, Schaefer W, Klein C. Ten Years in the making: application of CrossMab technology for the development of therapeutic bispecific antibodies and antibody fusion proteins. MAbs. 2021;13(1):1967714. doi:10.1080/19420862.2021.1967714. PMID: 34491877.
62. van de Donk N, Zweegman S. T-cell-engaging bispecific antibodies in cancer. Lancet. 2023;402(10396):142–58. doi:10.1016/S0140-6736(23)00521-4. PMID: 37271153.
63. Arvedson T, Bailis JM, Britten CD, Klinger M, Nagorsen D, Coxon A, Egen JG, Martin F. Targeting solid tumors with bispecific T cell engager immune therapy. Annu Rev Cancer Biol. 2022;6(1):17–34. doi:10.1146/annurev-cancerbio-070620-104325. PMID: WOS:000789891800002.
64. Lenting PJ, Denis CV, Christophe OD. Emicizumab, a bispecific antibody recognizing coagulation factors IX and X: how does it actually compare to factor VIII? Blood. 2017;130(23):2463–68. doi:10.1182/blood-2017-08-801662. PMID: 29042366.
65. Fauvel B, Yasri A. Antibodies directed against receptor tyrosine kinases: current and future strategies to fight cancer. MAbs. 2014;6(4):838–51. doi:10.4161/mabs.29089. PMID: 24859229.
66. Sharma P, Goswami S, Raychaudhuri D, Siddiqui BA, Singh P, Nagarajan A, Liu J, Subudhi SK, Poon C, Gant KL. et al. Immune checkpoint therapy—current perspectives and future directions. Cell. 2023;186(8):1652–69. doi:10.1016/j.cell.2023.03.006. PMID: 37059068.

67. Cao Y, Langer R, Ferrara N. Targeting angiogenesis in oncology, ophthalmology and beyond. Nat Rev Drug Discov. 2023;22(6):476–95. doi:10.1038/s41573-023-00671-z. PMID: 37041221.
68. Sharma A, Kumar N, Kuppermann BD, Bandello F, Loewenstein A. Faricimab: expanding horizon beyond VEGF. Eye (Lond). 2020;34(5):802–04. doi:10.1038/s41433-019-0670-1. PMID: 31695160.
69. Foxton RH, Uhles S, Gruner S, Revelant F, Ullmer C. Efficacy of simultaneous VEGF-A/ANG-2 neutralization in suppressing spontaneous choroidal neovascularization. EMBO Mol Med. 2019;11(5). doi:10.15252/emmm.201810204. PMID: 31040126.
70. Herpers B, Eppink B, James MI, Cortina C, Canellas-Socias A, Boj SF, Hernando-Momblona X, Glodzik D, Roovers RC, van de Wetering M. et al. Functional patient-derived organoid screenings identify MCLA-158 as a therapeutic EGFR × LGR5 bispecific antibody with efficacy in epithelial tumors. Nat Cancer. 2022;3(4):418–36. doi:10.1038/s43018-022-00359-0. PMID: 35469014.
71. Schram AM, Odintsov I, Espinosa-Cotton M, Khodos I, Sisso WJ, Mattar MS, Lui AJW, Vojnic M, Shameem SH, Chauhan T. et al. Zenocutuzumab, a HER2xHER3 Bispecific Antibody, Is Effective Therapy for Tumors Driven by NRG1 Gene Rearrangements. Cancer Discov. 2022;12:1233–47. doi:10.1158/2159-8290.CD-21-1119. PMID: 35135829.
72. Weisser NE, Sanches M, Escobar-Cabrera E, O'Toole J, Whalen E, Chan PWY, Wickman G, Abraham L, Choi K, Harbourne B. et al. An anti-HER2 biparatopic antibody that induces unique HER2 clustering and complement-dependent cytotoxicity. Nat Commun. 2023;14(1):1394. doi:10.1038/s41467-023-37029-3. PMID: 36914633.
73. Meric-Bernstam F, Beeram M, Hamilton E, Oh DY, Hanna DL, Kang YK, Elimova E, Chaves J, Goodwin R, Lee J. et al. Zanidatamab, a novel bispecific antibody, for the treatment of locally advanced or metastatic HER2-expressing or HER2-amplified cancers: a phase 1, dose-escalation and expansion study. Lancet Oncol. 2022;23:1558–70. doi:10.1016/S1470-2045(22)00621-0. PMID: 36400106.
74. Harding JJ, Fan J, Oh DY, Choi HJ, Kim JW, Chang HM, Bao L, Sun HC, Macarulla T, Xie F. et al. Zanidatamab for HER2-amplified, unresectable, locally advanced or metastatic biliary tract cancer (HERIZON-BTC-01): a multicentre, single-arm, phase 2b study. Lancet Oncol. 2023;24:772–82. doi:10.1016/S1470-2045(23)00242-5. PMID: 37276871.
75. Crescioli S, Kaplon H, Chenoweth A, Wang L, Visweswaraiah J, Reichert JM. Antibodies to watch in 2024. MAbs. 2024;16(1):2297450. doi:10.1080/19420862.2023.2297450. PMID: 38178784.
76. Dumontet C, Reichert JM, Senter PD, Lambert JM, Beck A. Antibody–drug conjugates come of age in oncology. Nat Rev Drug Discov. 2023;22(8):641–61. doi:10.1038/s41573-023-00709-2. PMID: 37308581.
77. Tsuchikama K, Anami Y, Ha SYY, Yamazaki CM. Exploring the next generation of antibody-drug conjugates. Nat Rev Clin Oncol. 2024. doi:10.1038/s41571-023-00850-2. PMID: 38191923.
78. Gu Y, Wang Z, Wang Y. Bispecific antibody drug conjugates: Making 1+1>2. Acta Pharm Sin B. 2024. doi:10.1016/j.apsb.2024.01.009.
79. Perez Bay AE, Faulkner D, DaSilva JO, Young TM, Yang K, Giurleo JT, Ma D, Delfino FJ, Olson WC, Thurston G. et al. A bispecific METxMET antibody–drug conjugate with cleavable linker is processed in recycling and late endosomes. Mol Cancer Ther. 2023;22(3):357–70. doi:10.1158/1535-7163.MCT-22-0414. PMID: 36861363.
80. Bannerji R, Arnason JE, Advani RH, Brown JR, Allan JN, Ansell SM, Barnes JA, O'Brien SM, Chavez JC, Duell J. et al. Odronextamab, a human CD20×CD3 bispecific antibody in patients with CD20-positive B-cell malignancies (ELM-1): results from the relapsed or refractory non-Hodgkin lymphoma cohort in a single-arm, multicentre, phase 1 trial. Lancet Haematol. 2022;9(5):e327–39. doi:10.1016/S2352-3026(22)00072-2. PMID: 35366963.
81. Ahn MJ, Cho BC, Felip E, Korantzis I, Ohashi K, Majem M, Juan-Vidal O, Handzhiev S, Izumi H, Lee JS. et al. Tarlatamab for patients with Previously treated small-cell lung cancer. N Engl J Med. 2023;389(22):2063–75. doi:10.1056/NEJMoa2307980. PMID: 37861218.
82. Paz-Ares L, Champiat S, Lai WV, Izumi H, Govindan R, Boyer M, Hummel HD, Borghaei H, Johnson ML, Steeghs N. et al. Tarlatamab, a first-in-class DLL3-targeted bispecific T cell engager, in recurrent small-cell lung cancer: an open-label, phase 1 study. JCO. 2023;41(16):2893–903. doi:10.1200/JCO.22.02823. PMID: 36689692.
83. Kelly WK, Danila DC, Lin CC, Lee JL, Matsubara N, Ward PJ, Armstrong AJ, Pook D, Kim M, Dorff TB. et al. Xaluritamig, a STEAP1 × CD3 XmAb 2+1 immune therapy for metastatic castration-resistant prostate cancer: results from dose exploration in a first-in-human study. Cancer Discov. 2023;14(1):OF1–14. doi:10.1158/2159-8290.CD-23-0964. PMID: 37861461.
84. Nolan-Stevaux O, Li C, Liang L, Zhan J, Estrada J, Osgood T, Li F, Zhang H, Case R, Murawsky CM. et al. AMG 509 (Xaluritamig), an Anti-STEAP1 XmAb 2+1 T-cell Redirecting Immune Therapy with Avidity-Dependent Activity Against Prostate Cancer. Cancer Discov. 2023. doi:10.1158/2159-8290.CD-23-0984. PMID: 37861452.
85. Panchal A, Seto P, Wall R, Hillier BJ, Zhu Y, Krakow J, Datt A, Pongo E, Bagheri A, Chen TT. et al. COBRA™: a highly potent conditionally active T cell engager engineered for the treatment of solid tumors. MAbs. 2020;12(1):1792130. doi:10.1080/19420862.2020.1792130. PMID: 32684124.
86. Geiger M, Stubenrauch KG, Sam J, Richter WF, Jordan G, Eckmann J, Hage C, Nicolini V, Freimoser-Grundschober A, Ritter M. et al. Protease-activation using anti-idiotypic masks enables tumor specificity of a folate receptor 1-T cell bispecific antibody. Nat Commun. 2020;11(1):3196. doi:10.1038/s41467-020-16838-w. PMID: 32581215.
87. Dettling DE, Kwok E, Quach L, Datt A, Degenhardt JD, Panchal A, Seto P, Krakow JL, Wall R, Hillier BJ. et al. Regression of EGFR positive established solid tumors in mice with the conditionally active T cell engager TAK-186. J Immunother Cancer. 2022;10(6):e004336. doi:10.1136/jitc-2021-004336. PMID: 35728872.
88. Boustany LM, LaPorte SL, Wong L, White C, Vinod V, Shen J, Yu W, Koditek D, Winter MB, Moore SJ. et al. A probody T cell–engaging bispecific antibody targeting EGFR and CD3 inhibits colon cancer growth with limited toxicity. Cancer Res. 2022;82(22):4288–98. doi:10.1158/0008-5472.CAN-21-2483. PMID: 36112781.
89. Cattaruzza F, Nazeer A, To M, Hammond M, Koski C, Liu LY, Pete Yeung V, Rennerfeldt DA, Henkensiefken A, Fox M. et al. Precision-activated T-cell engagers targeting HER2 or EGFR and CD3 mitigate on-target, off-tumor toxicity for immunotherapy in solid tumors. Nat Cancer. 2023;4(4):485–501. doi:10.1038/s43018-023-00536-9. PMID: 36997747.
90. Claus C, Ferrara C, Xu W, Sam J, Lang S, Uhlenbrock F, Albrecht R, Herter S, Schlenker R, Husser T. et al. Tumor-targeted 4-1BB agonists for combination with T cell bispecific antibodies as off-the-shelf therapy. Sci Transl Med. 2019;11(496):11. doi:10.1126/scitranslmed.aav5989. PMID: 31189721.
91. Skokos D, Waite JC, Haber L, Crawford A, Hermann A, Ullman E, Slim R, Godin S, Ajithdoss D, Ye X. et al. A class of costimulatory CD28-bispecific antibodies that enhance the antitumor activity of CD3-bispecific antibodies. Sci Transl Med. 2020;12(525):12. doi:10.1126/scitranslmed.aaw7888. PMID: 31915305.
92. Berezhnoy A, Sumrow BJ, Stahl K, Shah K, Liu D, Li J, Hao SS, De Costa A, Kaul S, Bendell J. et al. Development and preliminary clinical activity of PD-1-Guided CTLA-4 blocking bispecific DART molecule. Cell Rep Med. 2020;1:100163. doi:10.1016/j.xcrm.2020.100163. PMID: 33377134.
93. Dovedi SJ, Elder MJ, Yang C, Sitnikova SI, Irving L, Hansen A, Hair J, Jones DC, Hasani S, Wang B. et al. Design and efficacy of a monovalent bispecific PD-1/CTLA4 antibody that enhances CTLA4 blockade on PD-1(+) activated T cells. Cancer Discov. 2021;11(5):1100–17. doi:10.1158/2159-8290.CD-20-1445. PMID: 33419761.

94. Luke JJ, Patel MR, Blumenschein GR, Hamilton E, Chmielowski B, Ulahannan SV, Connolly RM, Santa-Maria CA, Wang J, Bahadur SW. et al. The PD-1- and LAG-3-targeting bispecific molecule tebotelimab in solid tumors and hematologic cancers: a phase 1 trial. Nat Med. 2023;29(11):2814–24. doi:10.1038/s41591-023-02593-0. PMID: 37857711.
95. Wang L, Luo Y, Ren S, Zhang Z, Xiong A, Su C, Zhou J, Yu X, Hu Y, Zhang X. et al. A phase 1b study of ivonescimab, a programmed cell death protein-1 and vascular endothelial growth factor bispecific antibody, as first- or second-line therapy for advanced or metastatic immunotherapy-naive NSCLC. J Thorac Oncol. 2023. doi:10.1016/j.jtho.2023.10.014. PMID: 37879536.
96. Whalen KA, Rakhra K, Mehta NK, Steinle A, Michaelson JS, Baeuerle PA. Engaging natural killer cells for cancer therapy via NKG2D, CD16A and other receptors. MAbs. 2023;15(1):2208697. doi:10.1080/19420862.2023.2208697. PMID: 37165468.
97. Mensurado S, Blanco-Dominguez R, Silva-Santos B. The emerging roles of γδ T cells in cancer immunotherapy. Nat Rev Clin Oncol. 2023;20(3):178–91. doi:10.1038/s41571-022-00722-1. PMID: 36624304.
98. Sewnath CA, Behrens LM, van Egmond M. Targeting myeloid cells with bispecific antibodies as novel immunotherapies of cancer. Expert Opin Biol Th. 2022;22(8):983–95. doi:10.1080/14712598.2022.2098675. PMID: WOS:000828289800001.
99. Dickopf S, Buldun C, Vasic V, Georges G, Hage C, Mayer K, Forster M, Wessels U, Stubenrauch KG, Benz J. et al. Prodrug-Activating Chain Exchange (PACE) converts targeted prodrug derivatives to functional bi- or multispecific antibodies. Biol Chem. 2022;403:495–508. doi:10.1515/hsz-2021-0401. PMID: 35073465.
100. Banaszek A, Bumm TGP, Nowotny B, Geis M, Jacob K, Wolfl M, Trebing J, Kucka K, Kouhestani D, Gogishvili T. et al. On-target restoration of a split T cell-engaging antibody for precision immunotherapy. Nat Commun. 2019;10(1):5387. doi:10.1038/s41467-019-13196-0. PMID: 31772172.
101. Lucchi R, Bentanachs J, Oller-Salvia B. The masking game: design of activatable antibodies and mimetics for selective therapeutics and cell control. ACS Cent Sci. 2021;7(5):724–38. doi:10.1021/acscentsci.0c01448. PMID: 34079893.
102. Wells JA, Kumru K. Extracellular targeted protein degradation: an emerging modality for drug discovery. Nat Rev Drug Discov. 2023;23(2):126–40. doi:10.1038/s41573-023-00833-z. PMID: 38062152.
103. Yen M, Ren J, Liu Q, Glassman CR, Sheahan TP, Picton LK, Moreira FR, Rustagi A, Jude KM, Zhao X. et al. Facile discovery of surrogate cytokine agonists. Cell. 2022;185(8):1414–30 e1419. doi:10.1016/j.cell.2022.02.025. PMID: 35325595.
104. Harris KE, Lorentsen KJ, Malik-Chaudhry HK, Loughlin K, Basappa HM, Hartstein S, Ahmil G, Allen NS, Avanzino BC, Balasubramani A. et al. A bispecific antibody agonist of the IL-2 heterodimeric receptor preferentially promotes in vivo expansion of CD8 and NK cells. Sci Rep. 2021;11(1):10592. doi:10.1038/s41598-021-90096-8. PMID: 34011961.
105. Zhao P, Zhang N, An Z. Engineering antibody and protein therapeutics to cross the blood–brain barrier. Antib Ther. 2022;5(4):311–31. doi:10.1093/abt/tbac028. PMID: 36540309.
106. Grimm HP, Schumacher V, Schäfer M, Imhof-Jung S, Freskgård PO, Brady K, Hofmann C, Rüger P, Schlothauer T, Göpfert U. et al. Delivery of the Brainshuttle™ amyloid-beta antibody fusion trontinemab to non-human primate brain and projected efficacious dose regimens in humans. MAbs. 2023;15(1):2261509. doi:10.1080/19420862.2023.2261509. PMID: WOS:001084988100001.